



Universidad de Concepción  
Dirección de Postgrado  
Facultad de Ciencias Físicas y Matemáticas  
Programa de Doctorado en Ciencias Aplicadas  
con Mención en Ingeniería Matemática

**MÉTODOS DE ELEMENTOS FINITOS MIXTOS PARA PROBLEMAS  
ACOPLADOS NO LINEALES EN MEDIOS POROSOS Y FLUJOS  
NO ISOTÉRMICOS**

**(MIXED FINITE ELEMENT METHODS FOR NONLINEAR COUPLED  
PROBLEMS IN POROUS MEDIA AND NON-ISOTHERMAL FLOWS)**

Tesis para optar al grado de Doctor en Ciencias  
Aplicadas con mención en Ingeniería Matemática

SERGIO ANDRÉS CAUCAO PAILLÁN  
CONCEPCIÓN-CHILE  
2017

Profesor Guía: Gabriel N. Gatica Pérez  
CI<sup>2</sup>MA y Departamento de Ingeniería Matemática  
Universidad de Concepción, Chile

Cotutor: Ricardo Oyarzúa Vargas  
GIMNAP–Departamento de Matemática y CI<sup>2</sup>MA  
Universidad del Bío-Bío y Universidad de Concepción, Chile

# Mixed Finite Element Methods for Nonlinear Coupled Problems in Porous Media and Non-Isothermal Flows

Sergio Andrés Caucao Paillán

**Directores de Tesis:** Gabriel N. Gatica, Universidad de Concepción, Chile.

Ricardo Oyarzúa, Universidad del Bío-Bío, Chile.

**Director de Programa:** Raimund Bürger, Universidad de Concepción, Chile.

## COMISIÓN EVALUADORA

Prof. Marco Discacciati, Loughborough University, UK.

Prof. Serge Nicaise, Université de Valenciennes et du Hainaut Cambrésis, France.

Prof. Markus Sarkis, Worcester Polytechnic Institute, USA.

Prof. Ivan Yotov, University of Pittsburgh, USA.

## COMISIÓN EXAMINADORA

Firma: \_\_\_\_\_

Prof. Eligio Colmenares, Universidad del Bío-Bío, Chillán, Chile.

Firma: \_\_\_\_\_

Prof. Thomas Führer, Pontificia Universidad Católica de Chile, Chile.

Firma: \_\_\_\_\_

Prof. Gabriel N. Gatica, Universidad de Concepción, Chile.

Firma: \_\_\_\_\_

Prof. Ricardo Oyarzúa, Universidad del Bío-Bío, Concepción, Chile.

Firma: \_\_\_\_\_

Prof. Manuel Solano, Universidad de Concepción, Chile.

Calificación: \_\_\_\_\_

Concepción, 29 de Diciembre de 2017

---

## Abstract

---

The aim of this thesis is to analyse, develop and implement several mathematical and numerical techniques, based on mixed finite element methods and fixed-point strategies, with the purpose of establishing the solvability of linear and non-linear problems arising in the context of fluid mechanics, more precisely, coupled problems in porous media and non-isothermal flows.

We firstly derive an augmented fully-mixed finite element method for the coupling of fluid flow with porous media flow. The flows are governed by the Navier–Stokes equations (with nonlinear viscosity) and linear Darcy equations, respectively, and the transmission conditions are given by mass conservation, balance of normal forces, and the Beavers–Joseph–Saffman law. We apply dual-mixed formulations in both domains, and the nonlinearity involved in the Navier–Stokes region is handled by setting the strain and vorticity tensors as auxiliary unknowns. In turn, since the transmission conditions become essential, they are imposed weakly, which yields the introduction of the traces of the porous media pressure and the fluid velocity as the associated Lagrange multipliers. Furthermore, since the convective term in the fluid forces the velocity to live in a smaller space than usual, we augment the variational formulation with suitable Galerkin redundant terms. The resulting augmented scheme is then written equivalently as a fixed point equation, so that the well-known Schauder and Banach theorems, combined with classical results on bijective monotone operators, are applied to prove the unique solvability of the continuous and discrete systems. We also derive a reliable and efficient residual-based a posteriori error estimator for the coupled problem.

Next, we discuss the analysis of a mixed finite element method for the coupling problem of Navier–Stokes/Darcy–Forchheimer with constant density and viscosity. We consider the standard mixed formulation in the Navier–Stokes domain and the dual-mixed one in the Darcy–Forchheimer region, which yields the introduction of the trace of the porous medium pressure as a suitable Lagrange multiplier. The well-posedness of the problem is achieved combining a fixed point strategy, classical results on nonlinear monotone operators and the well-known Schauder and Banach theorems. In particular, we employ Bernardi–Raugel and Raviart–Thomas elements for the velocities, and piecewise constant elements for the pressures and the Lagrange multiplier. We show stability, convergence, and a priori error estimates for the associated Galerkin scheme.

Finally, we close this thesis with the a priori and a posteriori error analysis of an augmented fully-mixed finite element method for the non-isothermal Oldroyd–Stokes problem. For convenience of the analysis, the strain, the vorticity, and the stress tensors are introduced as further unknowns (besides the polymeric part of the extra-stress tensor, the velocity, the pressure, and the temperature of the fluid). This allows to join the polymeric and solvent viscosities in an adimensional viscosity, and to eliminate the polymeric part of the extra-stress tensor and the pressure from the system, which,

together with the solvent part of the extra-stress tensor, are easily recovered later on through suitable postprocessing formulae. In this way, a fully mixed approach is applied, in which the heat flux vector is incorporated as an additional unknown as well. Furthermore, since the convective term in the heat equation forces both the velocity and the temperature to live in a smaller space than usual, we augment the variational formulation by using suitable Galerkin redundant terms. We prove solvability of both the continuous and discrete problems, with its corresponding a priori estimate. Regarding the a posteriori error analysis, two reliable and efficient residual-based estimators are derived.

For all the problems described above, several numerical experiments are provided which illustrate the good performance of the proposed methods and confirm the theoretical results of convergence as well as reliability and efficiency of the respective a posteriori error estimators.

El objetivo de esta tesis es analizar, desarrollar e implementar diversas técnicas matemáticas y numéricas, basadas en métodos de elementos finitos mixtos y estrategias de punto fijo, con el propósito de establecer la solubilidad de problemas lineales y no lineales que surgen en el contexto de la mecánica de fluidos, más precisamente, problemas acoplados en medios porosos y flujos no isotérmicos.

En primer lugar, derivamos un método de elementos finitos completamente mixto aumentado para el acoplamiento de fluidos con flujo en medio poroso. Los flujos son modelados por las ecuaciones de Navier–Stokes (con viscosidad no lineal) y las ecuaciones de Darcy lineal, respectivamente, y las condiciones de transmisión están dadas por la conservación de masa, el balance de fuerzas normales, y por la ley de Beavers–Joseph–Saffman. Aplicamos formulaciones dual-mixtas en ambos dominios, y la no linealidad en la región de Navier–Stokes es controlada introduciendo los tensores de pequeñas deformaciones y vorticidad como incógnitas auxiliares. A su vez, ya que las condiciones de transmisión son esenciales, ellas son impuestas débilmente, lo cual motiva la introducción de las trazas de la presión en el medio poroso y de la velocidad del fluido como multiplicadores de Lagrange. Además, ya que el término convectivo en el fluido fuerza a la velocidad a vivir en un espacio más pequeño que el usual, aumentamos la formulación variacional con adecuados términos de Galerkin. El resultante esquema aumentado es escrito equivalentemente como una ecuación de punto fijo, de modo que los teoremas de Schauder y Banach, combinados con resultados clásicos de operadores monótonos biyectivos, son aplicados para probar la unicidad de los problemas continuo y discreto. Además, obtuvimos un estimador de error a posteriori confiable y eficiente para el problema acoplado.

Luego, abordamos el análisis de un método de elementos finitos mixto para el problema acoplado de Navier–Stokes/Darcy–Forchheimer con densidad y viscosidad constantes. Consideramos la formulación mixta standard en el dominio Navier–Stokes y la dual-mixta en la región Darcy–Forchheimer, lo cual motiva la introducción de la traza de la presión en el medio poroso como un multiplicador de Lagrange. La solubilidad del problema se obtiene combinando una estrategia de punto fijo, resultados clásicos de operadores monótonos no lineales y los teoremas de Schauder y Banach. En particular, empleamos elementos de Bernardi–Raugel y Raviart–Thomas para las velocidades, y elementos constantes a trozos para las presiones y el multiplicador de Lagrange. Mostramos estabilidad, convergencia, y estimaciones de error a priori para el esquema de Galerkin asociado.

Finalmente, cerramos esta tesis con el análisis de error a priori y a posteriori de un método de elementos finitos completamente mixto aumentado para el problema de Oldroyd–Stokes no isotérmico. Por conveniencia del análisis, el tensor de pequeñas deformaciones, la vorticidad, y el esfuerzo son introducidos como incógnitas adicionales (además de la parte polimérica del tensor de extra-esfuerzo, la velocidad, la presión, y la temperatura del fluido). Esto permite unir las viscosidades polimérica y

solvente en una viscosidad adimensional, y eliminar del sistema la parte polimérica del tensor de extra-esfuerzo y la presión, las que, junto con la parte solvente del tensor de extra-esfuerzo, son fácilmente recuperadas a través de una fórmula de postproceso. En este sentido, una aproximación completamente mixta es aplicada, en la cual el vector de flujo de calor es incorporado como una incógnita adicional. Además, ya que el término convectivo en la ecuación de calor fuerza tanto a la velocidad como a la temperatura a vivir en un espacio más pequeño que el usual, aumentamos la formulación variacional usando adecuados términos de Galerkin. Demostramos solubilidad de los problemas continuo y discreto, con su estimación a priori correspondiente. Con respecto al análisis de error a posteriori, se derivan dos estimadores confiables y eficientes de tipo residual.

Para todos los problemas descritos anteriormente se proporcionan varios experimentos numéricos que ilustran el buen desempeño de los métodos propuestos, y que confirman los resultados teóricos de convergencia así como de confiabilidad y eficiencia de los estimadores de error a posteriori respectivos.

---

## Agradecimientos

---

En primer lugar, agradezco a mi pareja, Marcela Valdés, quién siempre ha estado a mi lado y apoyado en los momentos complejos. A mi hijo, Alonso Caucao, quién llegó a mi vida como una motivación para terminar con éxito mis estudios doctorales. A mis padres, Pablo Caucao y María Paillán, quienes con el ejemplo me enseñaron los valores y el sentido de responsabilidad necesarios para culminar esta etapa. A mis hermanos, Paulo, Carlos y Cecilia, a los que periódicamente visitaba en Osorno y que en cada viaje me apoyaban a seguir adelante.

A mi tutor de tesis, el profesor Gabriel N. Gatica, por todo el tiempo, correcciones y consejos dados en estos años de formación doctoral. Su calidad como docente, investigador y persona, indudablemente han influenciado y motivado a concluir de buena manera este trabajo.

A mi co-tutor de tesis, el profesor Ricardo Oyarzúa, quien me inició en el mundo del análisis numérico cuando cursaba mis estudios de magister y durante mi formación doctoral continuó apoyándome y motivando a crecer en el mundo de la investigación matemática.

Al profesor Marco Discacciati, por las reuniones de trabajo, su hospitalidad y por todas las gestiones que realizó durante mi estadía de investigación en la Loughborough University, United Kingdom.

A todos y cada uno de mis amigos y compañeros del doctorado, en particular a: Paulo Zúñiga, Iván Velásquez, Eduardo de los Santos, Ramiro Rebolledo y Patrick Vega, con los que pasé horas y días estudiando, compartiendo y debatiendo ideas.

Al personal administrativo y docentes del Departamento de Ingeniería Matemática de la Universidad de Concepción. En particular al profesor Raimund Bürger, por sus consejos, gestiones y dedicación como director del programa de doctorado.

Al Centro de Investigación en Ingeniería Matemática (CI<sup>2</sup>MA) de la Universidad de Concepción, por brindarme el espacio, la comodidad y las condiciones óptimas para trabajar durante mis estudios. Al personal administrativo que lo compone: Lorena Carrasco, Angelina Fritz, Jorge Muñoz, Iván Tobar y Jacqueline Freire.

Finalmente, no por eso menos importante, a la Comisión Nacional de Investigación y Tecnología (CONICYT) del gobierno de Chile por brindarme financiamiento total durante los cuatro años de formación doctoral. Gracias a este financiamiento, pude dedicarme de manera exclusiva al trabajo de mi tesis. A la dirección de postgrado de la Universidad de Concepción, por el financiamiento para participar en congresos y cursos de Inglés.

Sergio Andrés Caucao Paillán

---

# Contents

---

|   |             |
|---|-------------|
| <b>Abstract</b>   | <b>iii</b>  |
| <b>Resumen</b>  | <b>v</b>    |
| <b>Agradecimientos</b>  | <b>vii</b>  |
| <b>Contents</b>   | <b>viii</b> |
| <b>List of Tables</b>   | <b>xii</b>  |
| <b>List of Figures</b>  | <b>xiv</b>  |
| <b>Introduction</b>   | <b>1</b>    |
| <b>Introducción</b>   | <b>6</b>    |
| <b>1 A fully-mixed finite element method for the Navier–Stokes/Darcy coupled problem with nonlinear viscosity</b> | <b>10</b>   |
| 1.1 Introduction . . . . .  | 10          |
| 1.2 The continuous formulation . . . . .  | 12          |
| 1.2.1 The model problem . . . . .   | 12          |
| 1.2.2 The augmented fully-mixed variational formulation . . . . .   | 14          |
| 1.3 Analysis of the continuous formulation . . . . .  | 18          |
| 1.3.1 Preliminaries . . . . .   | 18          |
| 1.3.2 A fixed point approach . . . . .  | 20          |
| 1.3.3 Solvability analysis of the fixed point equation . . . . .  | 25          |
| 1.4 The Galerkin scheme . . . . .   | 27          |
| 1.4.1 Discrete setting . . . . .  | 27          |



|          |  |           |
|----------|--|-----------|
| 1.4.2    | Well-posedness of the discrete problem . . . . .   | 29        |
| 1.5      | A priori error estimate . . . . .  | 31        |
| 1.5.1    | Preliminaries . . . . .  | 32        |
| 1.5.2    | The main result . . . . .  | 33        |
| 1.6      | Particular choices of discrete spaces . . . . .  | 36        |
| 1.6.1    | Raviart–Thomas elements in 2D . . . . .  | 36        |
| 1.6.2    | Raviart–Thomas elements in 3D . . . . .  | 37        |
| 1.7      | Numerical results . . . . .  | 38        |
| <b>2</b> | <b>A posteriori error analysis of a fully-mixed formulation for the Navier–Stokes/Darcy coupled problem with nonlinear viscosity</b> | <b>46</b> |
| 2.1      | Introduction . . . . .   | 46        |
| 2.2      | The Navier–Stokes/Darcy coupled problem . . . . .  | 48        |
| 2.2.1    | The model problem . . . . .  | 48        |
| 2.2.2    | The fully-mixed variational formulation . . . . .  | 49        |
| 2.2.3    | The fully-mixed finite element method . . . . .  | 52        |
| 2.3      | A residual-based a posteriori error estimator . . . . .  | 54        |
| 2.3.1    | Preliminaries . . . . .  | 54        |
| 2.3.2    | The main result . . . . .  | 58        |
| 2.3.3    | Reliability of $\Theta$ . . . . .  | 59        |
| 2.3.4    | Efficiency of $\Theta$ . . . . .   | 65        |
| 2.4      | Numerical results . . . . .  | 69        |
| <b>3</b> | <b>A conforming mixed finite element method for the Navier–Stokes/Darcy–Forchheimer coupled problem</b>                              | <b>79</b> |
| 3.1      | Introduction . . . . .   | 79        |
| 3.2      | The continuous formulation . . . . .   | 81        |
| 3.2.1    | The model problem . . . . .  | 81        |
| 3.2.2    | The variational formulation . . . . .  | 82        |
| 3.2.3    | Stability properties . . . . .   | 85        |
| 3.3      | Analysis of the continuous formulation . . . . .   | 86        |
| 3.3.1    | Preliminaries . . . . .  | 86        |
| 3.3.2    | A fixed-point approach . . . . .   | 90        |

|          |  |            |
|----------|--|------------|
| 3.3.3    | Well-definiteness of $\mathbf{T}$  | 90         |
| 3.3.4    | Solvability analysis of the fixed-point equation   | 94         |
| 3.4      | The Galerkin scheme  | 96         |
| 3.4.1    | Discrete setting   | 96         |
| 3.4.2    | Well-posedness of the discrete problem   | 98         |
| 3.5      | A priori error analysis  | 104        |
| 3.6      | Numerical results  | 107        |
| <b>4</b> | <b>Analysis of an augmented fully-mixed formulation for the non-isothermal Oldroyd–Stokes problem</b>                    | <b>117</b> |
| 4.1      | Introduction   | 117        |
| 4.2      | The continuous formulation   | 119        |
| 4.2.1    | The model problem  | 119        |
| 4.2.2    | The augmented fully-mixed variational formulation  | 121        |
| 4.3      | Analysis of the continuous formulation   | 124        |
| 4.3.1    | The fixed-point approach   | 124        |
| 4.3.2    | Well-posedness of the uncoupled problems   | 125        |
| 4.3.3    | Solvability analysis of the fixed-point equation   | 128        |
| 4.4      | The Galerkin scheme  | 131        |
| 4.4.1    | Discrete setting   | 131        |
| 4.4.2    | Solvability analysis   | 133        |
| 4.4.3    | Convergence of the Galerkin scheme   | 134        |
| 4.5      | Numerical results  | 139        |
| <b>5</b> | <b>A posteriori error analysis of an augmented fully-mixed formulation for the non-isothermal Oldroyd–Stokes problem</b> | <b>149</b> |
| 5.1      | Introduction   | 149        |
| 5.2      | The non-isothermal Oldroyd–Stokes problem  | 151        |
| 5.2.1    | The model problem  | 151        |
| 5.2.2    | The fully-mixed variational formulation  | 152        |
| 5.2.3    | The fully-mixed finite element method  | 154        |
| 5.3      | A posteriori error analysis: the 2D-case   | 155        |
| 5.3.1    | Preliminaries  | 155        |

|  |  |            |
|--|--|------------|
| 5.3.2                                  | The main result . . . . .                                  | 157        |
| 5.3.3                                  | A general a posteriori error estimate . . . . .            | 158        |
| 5.3.4                                  | Reliability of the a posteriori error estimators . . . . . | 161        |
| 5.3.5                                  | Efficiency of the a posteriori error estimators . . . . .  | 164        |
| 5.4                                    | A posteriori error analysis: the 3D-case . . . . .         | 167        |
| 5.5                                    | Numerical results . . . . .                                | 169        |
| <b>Conclusions and future works</b>    |  | <b>179</b> |
| <b>Conclusiones y trabajos futuros</b> |  | <b>182</b> |
| <b>References</b>                      |  | <b>185</b> |

---

## List of Tables

---

|     |  |     |
|-----|--|-----|
| 1.1 | EXAMPLE 1, Degrees of freedom, mesh sizes, errors, convergence history and Newton iteration count for the augmented finite element formulation. . . . .  | 41  |
| 1.2 | EXAMPLE 2, Degrees of freedom, mesh sizes, errors, convergence history and Newton iteration count for the augmented finite element formulation. . . . .  | 41  |
| 1.3 | EXAMPLE 2, Behaviour of the iterative Newton's method with respect to the viscosity $\mu$ , considering a Carreau law with parameters $\alpha_1 = 0.5$ and $\beta = 1$ . . . . .               | 42  |
| 1.4 | EXAMPLE 3, Degrees of freedom, mesh sizes, errors, convergence history and Newton iteration count for the augmented finite element formulation. . . . .  | 42  |
| 2.1 | EXAMPLE 1, quasi-uniform scheme. . . . .   | 73  |
| 2.2 | EXAMPLE 2, quasi-uniform scheme. . . . .   | 73  |
| 2.3 | EXAMPLE 2, adaptive scheme. . . . .  | 74  |
| 2.4 | EXAMPLE 3, quasi-uniform scheme. . . . .   | 75  |
| 2.5 | EXAMPLE 3, adaptive scheme. . . . .  | 76  |
| 3.1 | EXAMPLE 1, Degrees of freedom, mesh sizes, errors, convergence history and Newton iteration count for the approximation of the Navier–Stokes/Darcy–Forchheimer problem with $F = 1$ . . . . .  | 111 |
| 3.2 | EXAMPLE 2, Degrees of freedom, mesh sizes, errors, convergence history and Newton iteration count for the approximation of the Navier–Stokes/Darcy–Forchheimer problem with $F = 1$ . . . . .  | 112 |
| 3.3 | EXAMPLE 3, Convergence behavior of the iterative method (3.104) with respect to the Forchheimer number $F$ . . . . .   | 112 |
| 3.4 | EXAMPLE 3, Degrees of freedom, mesh sizes, errors, convergence history and Newton iteration count for the approximation of the Navier–Stokes/Darcy–Forchheimer problem with $F = 10$ . . . . . | 113 |

|     |   |     |
|-----|---|-----|
| 4.1 | EXAMPLE 1, Degrees of freedom, mesh sizes, errors, rates of convergence, and number of iterations for the fully-mixed $\mathbb{P}_0 - \mathbb{RT}_0 - \mathbb{P}_0 - \mathbf{P}_1 - \mathbf{RT}_0 - \mathbf{P}_1$ approximation of the non-isothermal Oldroyd–Stokes equations (* errors divided by $\epsilon = 0.01$ ). . . . .  | 141 |
| 4.2 | EXAMPLE 1, Degrees of freedom, mesh sizes, errors, rates of convergence, and number of iterations for the fully-mixed $\mathbb{P}_1 - \mathbb{RT}_1 - \mathbb{P}_1 - \mathbf{P}_2 - \mathbf{RT}_1 - \mathbf{P}_2$ approximation of the non-isothermal Oldroyd–Stokes equations (* errors divided by $\epsilon = 0.01$ ). . . . .  | 142 |
| 4.3 | EXAMPLE 2, Degrees of freedom, mesh sizes, errors, rates of convergence, and number of iterations for the fully-mixed $\mathbb{P}_0 - \mathbb{RT}_0 - \mathbb{P}_0 - \mathbf{P}_1 - \mathbf{RT}_0 - \mathbf{P}_1$ approximation of the non-isothermal Oldroyd–Stokes equations (* errors divided by $\epsilon = 0.01$ ). . . . .  | 142 |
| 4.4 | EXAMPLE 2, Degrees of freedom, mesh sizes, errors, rates of convergence, and number of iterations for the fully-mixed $\mathbb{P}_1 - \mathbb{RT}_1 - \mathbb{P}_1 - \mathbf{P}_2 - \mathbf{RT}_1 - \mathbf{P}_2$ approximation of the non-isothermal Oldroyd–Stokes equations (* errors divided by $\epsilon = 0.01$ ). . . . .  | 143 |
| 4.5 | EXAMPLE 3, Degrees of freedom, mesh sizes, errors, rates of convergence, and number of iterations for the fully-mixed $\mathbb{P}_0 - \mathbb{RT}_0 - \mathbb{P}_0 - \mathbf{P}_1 - \mathbf{RT}_0 - \mathbf{P}_1$ approximations of the non-isothermal Oldroyd–Stokes equations (* errors divided by $\epsilon = 0.01$ ). . . . . | 143 |
| 4.6 | EXAMPLE 4, Degrees of freedom, mesh sizes, errors, rates of convergence, and number of iterations for the fully-mixed $\mathbb{P}_0 - \mathbb{RT}_0 - \mathbb{P}_0 - \mathbf{P}_1 - \mathbf{RT}_0 - \mathbf{P}_1$ approximations of the non-isothermal Oldroyd–Stokes equations (* errors divided by $\epsilon = 0.01$ ). . . . . | 144 |
| 5.1 | EXAMPLE 1, $\mathbb{P}_0 - \mathbb{RT}_0 - \mathbb{P}_0 - \mathbf{P}_1 - \mathbf{RT}_0 - \mathbf{P}_1$ scheme with quasi-uniform refinement.  | 172 |
| 5.2 | EXAMPLE 1, $\mathbb{P}_1 - \mathbb{RT}_1 - \mathbb{P}_1 - \mathbf{P}_2 - \mathbf{RT}_1 - \mathbf{P}_2$ scheme with quasi-uniform refinement.  | 172 |
| 5.3 | EXAMPLE 2, $\mathbb{P}_0 - \mathbb{RT}_0 - \mathbb{P}_0 - \mathbf{P}_1 - \mathbf{RT}_0 - \mathbf{P}_1$ scheme with quasi-uniform refinement.  | 173 |
| 5.4 | EXAMPLE 2, $\mathbb{P}_0 - \mathbb{RT}_0 - \mathbb{P}_0 - \mathbf{P}_1 - \mathbf{RT}_0 - \mathbf{P}_1$ scheme with adaptive refinement via $\Theta_1$ .   | 173 |
| 5.5 | EXAMPLE 2, $\mathbb{P}_0 - \mathbb{RT}_0 - \mathbb{P}_0 - \mathbf{P}_1 - \mathbf{RT}_0 - \mathbf{P}_1$ scheme with adaptive refinement via $\Theta_2$ .   | 174 |
| 5.6 | EXAMPLE 3, $\mathbb{P}_0 - \mathbb{RT}_0 - \mathbb{P}_0 - \mathbf{P}_1 - \mathbf{RT}_0 - \mathbf{P}_1$ scheme with quasi-uniform refinement.  | 175 |
| 5.7 | EXAMPLE 3, $\mathbb{P}_0 - \mathbb{RT}_0 - \mathbb{P}_0 - \mathbf{P}_1 - \mathbf{RT}_0 - \mathbf{P}_1$ scheme with adaptive refinement via $\Theta_1$ .   | 175 |

---

## List of Figures

---

|     |  |     |
|-----|--|-----|
| 1.1 | Sketch of a 2D geometry of our Navier–Stokes/Darcy model . . . . .   | 13  |
| 1.2 | Example 1: Approximated spectral norm of the stress tensor components and the strain tensor (top panels), skew-symmetric part of the Navier–Stokes velocity gradient, Navier–Stokes pressure field, and Darcy pressure field (centre panels), and geometry configuration and velocity components on the whole domain (bottom row). . . . . | 43  |
| 1.3 | Example 2: Approximated spectral norm of the stress tensor components and the strain tensor (top panels), skew-symmetric part of the Navier–Stokes velocity gradient, Navier–Stokes pressure field, and Darcy pressure field (centre panels), and geometry configuration and velocity components on the whole domain (bottom row). . . . . | 44  |
| 1.4 | Example 3: Approximated spectral norm of the stress tensor components and the strain tensor (top panels), skew-symmetric part of the Navier–Stokes velocity gradient, Navier–Stokes pressure field, and Darcy pressure field (centre panels), and geometry configuration and velocity components on the whole domain (bottom row). . . . . | 45  |
| 2.1 | Sketch of a 2D geometry of our Navier–Stokes/Darcy model . . . . .   | 48  |
| 2.2 | Example 2, $e(\mathbf{t}, \underline{\varphi}, p_D)$ vs. $N$ for quasi-uniform/adaptive schemes. . . . .   | 75  |
| 2.3 | Example 2, adapted meshes with 588, 1019, 9680, 31110, 112409, and 447000 degrees of freedom. . . . .  | 77  |
| 2.4 | Example 3, $e(\mathbf{t}, \underline{\varphi}, p_D)$ vs. $N$ for quasi-uniform/adaptive schemes. . . . .   | 77  |
| 2.5 | Example 3, adapted meshes with 1037, 2092, 18993, 64472, 237874, and 915408 degrees of freedom. . . . .  | 78  |
| 3.1 | Sketch of a 2D geometry of our Navier–Stokes/Darcy–Forchheimer model . . . . .   | 81  |
| 3.2 | Example 1: Velocity components (top panels), velocity streamlines and pressure field in the whole domain (bottom panels). . . . .  | 114 |
| 3.3 | Example 2: Velocity components (top panels), velocity streamlines and pressure field in the whole domain (bottom panels). . . . .  | 115 |
| 3.4 | Example 3: Velocity components (top panels), velocity streamlines and pressure field in the whole domain (bottom panels). . . . .  | 116 |

|     |  |     |
|-----|--|-----|
| 4.1 | Example 1: $\mathbb{P}_0 - \mathbb{RT}_0 - \mathbb{P}_0 - \mathbf{P}_1 - \mathbf{RT}_0 - \mathbf{P}_1$ approximated spectral norm of strain tensor and the stress tensor components (top panels), velocity and heat flux vector components (centre panels), and temperature and pressure fields, and polymeric part of the extra-stress tensor component (bottom row). . . . .   | 145 |
| 4.2 | Example 2: $\mathbb{P}_0 - \mathbb{RT}_0 - \mathbb{P}_0 - \mathbf{P}_1 - \mathbf{RT}_0 - \mathbf{P}_1$ approximation of some components of the approximate solutions. . . . .  | 146 |
| 4.3 | Example 3: $\mathbb{P}_0 - \mathbb{RT}_0 - \mathbb{P}_0 - \mathbf{P}_1 - \mathbf{RT}_0 - \mathbf{P}_1$ approximation of the strain tensor component, approximated spectral norm of the stress tensor component, and vorticity streamlines (top panels), velocity streamlines, heat flux streamlines, and temperature field (centre panels), and pressure field, polymeric part and solvent part of the extra-stress tensor component (bottom row). . . . . | 147 |
| 4.4 | Example 4: $\mathbb{P}_0 - \mathbb{RT}_0 - \mathbb{P}_0 - \mathbf{P}_1 - \mathbf{RT}_0 - \mathbf{P}_1$ approximation of some components of the approximate solutions. . . . .  | 148 |
| 5.1 | Example 2, $\mathbf{e}$ vs. $\mathbf{N}$ for quasi-uniform/adaptive schemes. . . . .   | 176 |
| 5.2 | Example 2, approximated spectral norm of the stress tensor component, velocity streamlines, and pressure field (top panels), heat flux streamlines, temperature field, and polymeric part of the extra-stress tensor component (bottom panels). . . . .  | 176 |
| 5.3 | Example 2, three snapshots of adapted meshes according to the indicators $\Theta_1$ and $\Theta_2$ (top and bottom panels, respectively). . . . .  | 177 |
| 5.4 | Example 3, $\mathbf{e}$ vs. $\mathbf{N}$ for quasi-uniform/adaptive scheme via $\Theta_1$ . . . . .  | 177 |
| 5.5 | Example 3, approximated spectral norm of the stress tensor component, velocity streamlines, and pressure field (top panels), heat flux streamlines, temperature field, and polymeric part of the extra-stress tensor component (bottom panels). . . . .  | 178 |
| 5.6 | Example 3, three snapshots of adapted meshes according to the indicators $\Theta_1$ . . . . .  | 178 |

---

## Introduction

---

The modelling of natural phenomena arising from processes described by using continuum mechanics, as well as the design of appropriate numerical methods to approximate the solution of the corresponding systems of partial differential equations, is still a field of research that keeps an important part of the scientific community dedicated to the area of numerical analysis very active. In particular, physical phenomena such as: flows in porous media appearing in petroleum extraction, groundwater system in karst aquifers, reservoir wellbore, industrial filtrations, internal ventilation of a motorcycle helmet, the penetration of air into lungs, blood motion in tumors and microvessels can be modelled by the coupling of incompressible viscous fluids (described by the Navier–Stokes or Stokes equations) with flow in a porous medium (described by the Darcy–Forchheimer or Darcy model). In turn, some applications in the field of engineering such as: design of heat exchangers and chemical reactors, cooling processes and polymer processing, can be modelled by non-isothermal incompressible viscoelastic fluids (described by the coupling of Stokes-type equation for Oldroyd or Giesekus viscoelasticity with the heat equation). Many of these natural phenomena involve linear and nonlinear couplings, for which suitable numerical approximations of the stress, pseudostress, velocity, pressure, temperature, and other fields are usually required.

In general, the equations that describe these models are difficult to solve analytically, therefore, the resolution and computational simulation of these problems, in a precise and efficient way, is indispensable. In these types of scenarios, mixed finite element methods are very appropriate since, in addition to the original unknowns, they allow us to calculate directly other variables of physical interest such as vorticity, strain tensor of small deformations, gradient of velocity or heat-flux vector (see, e.g., [91, 116, 115, 23, 25, 24, 30, 28, 52, 51, 50]), to name a few. In particular, for the Navier–Stokes/Darcy–Forchheimer (or Navier–Stokes/Darcy, Stokes/Darcy) coupled problem, in literature we can find a significant amount of works related to this topic (see [11, 40, 43, 45, 63, 64, 65, 27, 92, 94, 96] and the references therein), which include for example formulations for the stress and velocity in the region modelled by the Navier–Stokes (or Stokes) equations. These are characterized by the advantage (with respect to the standard velocity-pressure formulation) that the auxiliary variables of interest are calculated directly, without apply any type of post-process of the system solution, which usually produces a major loss in accuracy.

In addition, other mathematical techniques like as fixed-point strategies and augmented mixed finite element methods by means of suitable Galerkin redundant terms (see, e.g., [2, 26, 27, 28, 29, 30, 88, 93]), allow us to derive and analyse new variational formulations and numerical schemes that lead to the numerical solution of a wide range of problems that arise in fluid mechanics. We emphasize that one of the advantages presented by the augmented methods is, on the one hand, greatly simplify the



continuous and discrete analysis, and on the other hand, allow us to employ standard finite elements spaces for the numerical approximations of the unknowns of interest.

According to the above, the aim of this thesis is to employ and develop several mathematical and numerical techniques, typical of the mixed finite element methods and Galerkin schemes, with the purpose of analyse the solvability of some linear and nonlinear problems (modelled by systems of partial differential equations) that arise in fluid mechanics, more precisely, coupled problems in porous media and non-isothermal flows, namely the Navier–Stokes/Darcy, Navier–Stokes/Darcy–Forchheimer coupled problem and the non-isothermal Oldroyd–Stokes problem. For the problems to be considered in this thesis, we are interested in:

- Establishing well-posed models for an appropriate analysis of the problem.
- Developing suitable variational formulations in order to establish existence and uniqueness of the continuous solution of the problem.
- Establishing the corresponding Galerkin scheme and employ suitable finite element spaces.
- Analysing the solvability of the Galerkin scheme and establish the corresponding stability and convergence results.
- Deriving a posteriori error estimators in order to establish adaptive methods that allow us to improve the precision of the numerical approximations, specially under the presence of singularities or high gradients of the solution.
- Validating the theoretical results through essays and illustrative numerical simulations, which include academic and application-oriented examples.

The present work is organized as follows. In **Chapter 1**, we extend the results obtained in [88] to the coupled nonlinear Navier–Stokes and linear Darcy problem with constant density and variable viscosity in the fluid region. To this end, we consider a similar approach to the one presented in [28] for the Navier–Stokes domain. Next, we define the nonlinear stress tensor as in [30] and subsequently eliminate the pressure unknown using the incompressibility condition. The transmission conditions consisting of mass conservation, balance of normal forces, and the Beavers–Joseph–Saffman law are imposed weakly, which results in additional Lagrange multipliers: the traces of the porous media pressure and the fluid velocity on the interface. We consider dual-mixed formulations in both domains. In addition, similarly to [91, 88], and in order to handle the nonlinearity in the fluid, the strain and vorticity tensors are introduced as additional unknowns. Furthermore, the difficulty that the fluid velocity lives now in  $H^1$  instead of  $L^2$  as usual, is resolved as in [28] by augmenting the variational formulation with suitable Galerkin redundant terms. The resulting augmented variational system of equations is then re-ordered so that it shows a twofold saddle point structure. This continuous problem is rewritten as a fixed point operator equation, so that the well-known Schauder and Banach theorems, combined with classical results on bijective monotone operators, are applied to prove the unique solvability of the continuous and discrete systems. The contents of this chapter gave rise to the following paper:

- [40] S. CAUCAO, G.N. GATICA, R. OYARZÚA, AND I. ŠEBESTOVÁ, *A fully-mixed finite element method for the Navier–Stokes/Darcy coupled problem with nonlinear viscosity*. **Journal of Numerical Mathematics**, vol. 25, 2, pp. 55–88, (2017).

In **Chapter 2**, we develop an a posteriori error analysis for the model problem studied in Chapter 1. More precisely, we derive a reliable and efficient a posteriori error estimator, which allows us to establish appropriate adaptive methods to guarantee greater precision of the numerical approximations, and mainly the convergence of the Galerkin scheme in situations in which there are singularities or high gradients of the solution. The finite elements considered are piecewise constants, Raviart–Thomas elements of lowest order, continuous piecewise linear elements, and piecewise constants for the strain, stress, velocity, and vorticity in the fluid, respectively, whereas Raviart–Thomas elements of lowest order for the velocity, piecewise constants for the pressure, and continuous piecewise linear elements for the traces, are considered in the porous medium. The proof of reliability of the estimator relies on a global inf-sup condition, suitable Helmholtz decompositions in the fluid and the porous medium, the local approximation properties of the Clément and Raviart–Thomas operators. In turn, inverse inequalities, the localization technique based on bubble functions, and known results from previous works are the main tools yielding the efficiency estimate. The contents of this chapter gave rise to the following paper:

- [38] S. CAUCAO, G.N. GATICA, AND R. OYARZÚA, *A posteriori error analysis of a fully-mixed formulation for the Navier–Stokes/Darcy coupled problem with nonlinear viscosity*. **Computer Methods in Applied Mechanics and Engineering**, vol. 315, pp. 943–971, (2017).

In **Chapter 3**, we extend the result obtained in [65, 92, 94] to the Navier–Stokes/Darcy–Forchheimer coupled problem with constant density and viscosity. We consider the standard velocity-pressure formulation for the Navier–Stokes equation and unlike [65], in the porous medium we consider the Darcy–Forchheimer equation in its dual-mixed formulation. In this way, we obtain the velocity and the pressure of the fluid in both media as the main unknowns of the coupled system. Since one of the interface conditions becomes essential, we proceed similarly to [124, 92] and incorporate the trace of the porous medium pressure as an additional unknown. The well-posedness and uniqueness of both the continuous and discrete formulation is proved employing a fixed-point argument and classical results on nonlinear monotone operators (see [144, 145]). In particular, we consider Bernardi–Raugel elements for the velocity in the free fluid region, Raviart–Thomas elements of lowest order for the filtration velocity in the porous media, piecewise constants with null mean value for the pressures, and piecewise constants elements for the Lagrange multiplier on the interface. This chapter is constituted by the following preprint:

- [36] S. CAUCAO, M. DISCACCIATI, G.N. GATICA, AND R. OYARZÚA, *A conforming mixed finite element method for the Navier–Stokes/Darcy–Forchheimer coupled problem*. Preprint 2017-29, Centro de Investigación en Ingeniería Matemática (CI<sup>2</sup>MA), Universidad de Concepción, Chile, 2017.

In **Chapter 4**, we develop and analyse a new mixed formulation for the Oldroyd–Stokes problem for non-isothermal viscoelastic fluids. To that end, unlike to [56] and [73], and in order to obtain a new fully-mixed formulation of this coupled problem, we first introduce the strain tensor as a new unknown, which allows us, on one hand, to eliminate the polymeric part of the extra-stress tensor from the system and compute it as a simple post-process of the solution, and on the other hand, to join the

polymeric and solvent viscosities in an adimensional viscosity. In addition, similarly to Chapter 1 and for convenience of the analysis, we also consider the stress and vorticity tensors as auxiliary unknowns, thanks to which the pressure can be eliminated from the system and approximated later on by a postprocessing formula. In turn, for deriving the mixed formulation of the heat equation we proceed similarly to [73] (see also [51, 52]) and set the heat-flux vector as a further unknown. Furthermore, the difficulty given by the fact that the fluid velocity and the temperature lives in  $H^1$  instead of  $L^2$  as usual, is resolved as in [51, 52] by augmenting the variational formulation with suitable Galerkin redundant terms. Then, following [51] and [2], we prove solvability of both the continuous and discrete problems, with its corresponding a priori estimate. This chapter is constituted by the following preprint:

- [37] S. CAUCAO, G.N. GATICA, AND R. OYARZÚA, *Analysis of an augmented fully-mixed formulation for the non-isothermal Oldroyd–Stokes problem*. Preprint 2017-21, Centro de Investigación en Ingeniería Matemática (CI<sup>2</sup>MA), Universidad de Concepción, Chile, 2017.

Finally, in **Chapter 5**, we develop an a posteriori error analysis for the variational formulation described in Chapter 4. More precisely, we proceed similarly to [3, 54, 53, 97], and develop two reliable and efficient residual-based a posteriori error estimators. This means that our analysis begins by applying the uniform ellipticity for the bilinear form defining the continuous formulation. Next, similarly to Chapter 2, we apply suitable Helmholtz decompositions, local approximation properties of the Clément and Raviart–Thomas interpolants, and others known estimates, to prove the reliability of a residual-based estimator. In turn, some of the main tools used to prove the efficiency of the estimators are inverse inequalities and localization techniques based on bubble functions. Alternatively, a second reliable and efficient residual-based a posteriori error estimator not making use of any Helmholtz decomposition is also proposed. This chapter is constituted by the following preprint:

- [39] S. CAUCAO, G.N. GATICA, AND R. OYARZÚA, *A posteriori error analysis of an augmented fully-mixed formulation for the non-isothermal Oldroyd–Stokes problem*. Preprint 2017-25, Centro de Investigación en Ingeniería Matemática (CI<sup>2</sup>MA), Universidad de Concepción, Chile, 2017.

Throughout the five chapters of this thesis, the theoretical results such as: orders of convergence, reliability and efficiency of the corresponding residual-based a posteriori error estimators, are illustrated through several numerical examples, which also highlight the good performance of the proposed discrete schemes and the associated adaptive algorithms. The computational implementations were obtained using the free access software for finite elements **FreeFemm ++** and the illustrator **ParaView**.

## Preliminary notations

Let  $\mathcal{O} \subseteq \mathbb{R}^n$ ,  $n \in \{2, 3\}$ , denote a bounded domain with Lipschitz boundary  $\Gamma = \bar{\Gamma}_D \cup \bar{\Gamma}_N$ , with  $\Gamma_D \cap \Gamma_N = \emptyset$  and  $|\Gamma_D|, |\Gamma_N| > 0$ , and denote by  $\mathbf{n}$  the outward unit normal vector on  $\Gamma$ . For  $s \geq 0$  and  $p \in [1, +\infty]$ , we define by  $L^p(\mathcal{O})$  and  $W^{s,p}(\mathcal{O})$  the usual Lebesgue and Sobolev spaces endowed with the norms  $\|\cdot\|_{L^p(\mathcal{O})}$  and  $\|\cdot\|_{W^{s,p}(\mathcal{O})}$ , respectively. Note that  $W^{0,p}(\mathcal{O}) = L^p(\mathcal{O})$ . If  $p = 2$ , we write  $H^s(\mathcal{O})$  in place of  $W^{s,2}(\mathcal{O})$ , and denote the corresponding Lebesgue and Sobolev norms by  $\|\cdot\|_{0,\mathcal{O}}$  and  $\|\cdot\|_{s,\mathcal{O}}$ , respectively, and the seminorm by  $|\cdot|_{s,\mathcal{O}}$ . In addition, we denote by  $W^{\frac{1}{q},p}(\Gamma)$  the trace

space of  $W^{1,p}(\mathcal{O})$  and  $W^{-\frac{1}{q},q}(\Gamma)$  the dual space of  $W^{\frac{1}{q},p}(\Gamma)$  endowed with the norms  $\|\cdot\|_{\frac{1}{q},p;\Gamma}$  and  $\|\cdot\|_{-\frac{1}{q},q;\Gamma}$ , respectively, where  $p, q \in (1, +\infty)$  with  $1/p + 1/q = 1$ . By  $\mathbf{M}$  and  $\mathbb{M}$  we will denote the corresponding vectorial and tensorial counterparts of the generic scalar functional space  $M$ , and  $\|\cdot\|$ , with no subscripts, will stand for the natural norm of either an element or an operator in any product functional space. In turn, for any vector fields  $\mathbf{v} = (v_i)_{i=1,n}$  and  $\mathbf{w} = (w_i)_{i=1,n}$ , we set the gradient, divergence, and tensor product operators, as

$$\nabla \mathbf{v} := \left( \frac{\partial v_i}{\partial x_j} \right)_{i,j=1,n}, \quad \operatorname{div} \mathbf{v} := \sum_{j=1}^n \frac{\partial v_j}{\partial x_j}, \quad \text{and} \quad \mathbf{v} \otimes \mathbf{w} := (v_i w_j)_{i,j=1,n}.$$

Furthermore, for any tensor fields  $\boldsymbol{\tau} = (\tau_{ij})_{i,j=1,n}$  and  $\boldsymbol{\zeta} = (\zeta_{ij})_{i,j=1,n}$ , we let  $\mathbf{div} \boldsymbol{\tau}$  be the divergence operator  $\operatorname{div}$  acting along the rows of  $\boldsymbol{\tau}$ , and define the transpose, the trace, the tensor inner product, and the deviatoric tensor, respectively, as

$$\boldsymbol{\tau}^t := (\tau_{ji})_{i,j=1,n}, \quad \operatorname{tr}(\boldsymbol{\tau}) := \sum_{i=1}^n \tau_{ii}, \quad \boldsymbol{\tau} : \boldsymbol{\zeta} := \sum_{i,j=1}^n \tau_{ij} \zeta_{ij}, \quad \text{and} \quad \boldsymbol{\tau}^d := \boldsymbol{\tau} - \frac{1}{n} \operatorname{tr}(\boldsymbol{\tau}) \mathbb{I},$$

where  $\mathbb{I}$  is the identity matrix in  $\mathbb{R}^{n \times n}$ . In what follows, when no confusion arises,  $|\cdot|$  will denote the Euclidean norm in  $\mathbb{R}^n$  or  $\mathbb{R}^{n \times n}$ . Additionally, we recall that

$$\mathbb{H}(\mathbf{div}; \mathcal{O}) := \left\{ \boldsymbol{\tau} \in \mathbb{L}^2(\mathcal{O}) : \mathbf{div} \boldsymbol{\tau} \in \mathbb{L}^2(\mathcal{O}) \right\},$$

equipped with the usual norm

$$\|\boldsymbol{\tau}\|_{\mathbf{div}; \mathcal{O}}^2 := \|\boldsymbol{\tau}\|_{0, \mathcal{O}}^2 + \|\mathbf{div} \boldsymbol{\tau}\|_{0, \mathcal{O}}^2,$$

is a standard Hilbert space in the realm of mixed problems. On the other hand, the following symbol for the  $L^2(\Gamma)$  inner product

$$\langle \xi, \lambda \rangle_{\Gamma} := \int_{\Gamma} \xi \lambda \quad \forall \xi, \lambda \in L^2(\Gamma),$$

will also be employed for their respective extension as the duality parity between  $W^{-\frac{1}{q},q}(\Gamma)$  and  $W^{\frac{1}{q},p}(\Gamma)$ . Furthermore, given an integer  $k \geq 0$  and a set  $S \subseteq \mathbb{R}^n$ ,  $P_k(S)$  denotes the space of polynomial functions on  $S$  of degree  $\leq k$ . In addition, and coherently with previous notations, we set  $\mathbf{P}_k(S) := [P_k(S)]^n$  and  $\mathbb{P}_k(S) := [P_k(S)]^{n \times n}$ . Finally, we end this section by mentioning that, throughout the rest of the paper, we employ  $\mathbf{0}$  to denote a generic null vector (or tensor), and use  $C$  and  $c$ , with or without subscripts, bars, tildes or hats, to denote generic constants independent of the discretization parameters, which may take different values at different places.

El modelamiento de fenómenos naturales asociados a procesos descritos a través de la mecánica de medios continuos, así como el diseño de métodos numéricos apropiados para aproximar la solución de los sistemas de ecuaciones diferenciales parciales correspondientes, sigue siendo un campo de investigación que mantiene muy activa a una parte importante de la comunidad científica dedicada al área del análisis numérico. En particular, fenómenos físicos tales como: flujos en medios porosos que aparecen en la extracción de petróleo, sistema de aguas subterráneas en los acuíferos kársticos, pozo de reserva de petróleo, filtraciones industriales, ventilación interna de un casco de motocicleta, ingreso del aire en los pulmones, el movimiento de la sangre en tumores y vasos sanguíneos, pueden ser modelados por el acoplamiento de fluidos viscosos incompresibles (descritos por las ecuaciones de Navier–Stokes o Stokes) con flujo en un medio poroso (descrito por el modelo de Darcy–Forchheimer o Darcy). A su vez, algunas aplicaciones en el campo de la ingeniería tales como: diseño de intercambiadores de calor y reactores químicos, procesos de enfriamiento y procesamiento de polímeros, pueden ser modelados por fluidos viscoelásticos incompresibles no isotérmicos (descritos por el acoplamiento de la ecuación de tipo Stokes para la viscoelasticidad de Oldroyd o Giesekus con la ecuación del calor). Muchos de estos fenómenos naturales involucran acoplamientos lineales y no lineales, para los cuales por lo general se requieren aproximaciones numéricas adecuadas del esfuerzo, pseudo-esfuerzo, la velocidad, la presión, la temperatura, entre otros campos.

En general, las ecuaciones que describen estos modelos son difíciles de resolver analíticamente, por lo cual, la resolución y simulación computacional de estos problemas, de manera precisa y eficiente se hace indispensable. En este tipo de escenarios, los métodos de elementos finitos mixtos resultan muy apropiados ya que, además de las incógnitas originales, ellos permiten calcular de manera directa otras variables de interés físico tales como la vorticidad, tensor de pequeñas deformaciones, gradiente de la velocidad o el vector de flujo de calor (ver, por ejemplo [91, 116, 115, 23, 25, 24, 30, 28, 52, 51, 50]), por nombrar algunas. En particular, para el problema acoplado de Navier–Stokes/Darcy–Forchheimer (o Navier–Stokes/Darcy, Stokes/Darcy), en la literatura podemos encontrar una cantidad importante de trabajos relacionados a este tema (ver [11, 40, 43, 45, 63, 64, 65, 27, 92, 94, 96] y sus referencias), incluyendo por ejemplo formulaciones para el esfuerzo y la velocidad en la región modelada por las ecuaciones de Navier–Stokes (o Stokes). Estas se caracterizan por la ventaja (con respecto a las formulaciones velocidad-presión estándar) de que las variables auxiliares de interés se calculan directamente, sin la necesidad de aplicar ningún tipo de post-proceso de la solución del sistema, que por lo general produce una pérdida importante en la precisión.

Además, otras técnicas matemáticas tales como estrategias de punto fijo y métodos de elementos finitos mixtos aumentados con términos de Galerkin adecuados (ver por ejemplo [2, 26, 27, 28, 29,

[30, 88, 93]), permiten derivar y analizar nuevas formulaciones variacionales y esquemas numéricos que conducen a la solución numérica de una amplia gama de problemas que surgen en la mecánica de fluidos. Destacamos que una de las ventajas que presentan los métodos aumentados es, por un lado, simplificar enormemente el análisis continuo y discreto, y por otro lado, permitir emplear espacios de elementos finitos estándar para las aproximaciones numéricas de las incógnitas de interés.

Acorde a lo expuesto anteriormente, el objetivo de esta tesis es emplear y desarrollar diversos aspectos matemáticos y numéricos, propios de los métodos de elementos finitos mixtos y esquemas de Galerkin, con el propósito de analizar la solubilidad de algunos problemas lineales y no lineales (modelados por sistemas de ecuaciones diferenciales parciales) que surgen en la mecánica de fluidos, más precisamente, problemas acoplados en medios porosos y flujos no isotérmicos, a saber, problemas acoplados de Navier–Stokes/Darcy, Navier–Stokes/Darcy–Forchheimer y el problema de Oldroyd–Stokes no isotérmico. Para los problemas a considerar dentro del desarrollo de esta tesis, estamos interesados en:

- ☐ Establecer modelos bien planteados para un análisis apropiado del problema.
- ☐ Desarrollar formulaciones variacionales apropiadas para establecer existencia y unicidad de la solución continua del problema.
- ☐ Establecer el esquema de Galerkin correspondiente y emplear espacios de elementos finitos apropiados.
- ☐ Analizar la solubilidad del esquema de Galerkin y establecer los resultados de estabilidad y convergencia correspondientes.
- ☐ Derivar estimadores de error a posteriori para establecer métodos adaptativos que permitan mejorar la precisión de las aproximaciones numéricas, principalmente bajo la presencia de singularidades o altos gradientes de la solución.
- ☐ Validar los resultados teóricos a través de ensayos y simulaciones numéricas ilustrativas, que incluyan ejemplos académicos y orientados a aplicaciones.

El presente trabajo se organiza de la siguiente manera. En el **Capítulo 1**, extendemos los resultados obtenidos en [88] al problema no lineal acoplado de Navier–Stokes y Darcy lineal con densidad constante y viscosidad variable en la región del fluido. Para este fin, consideramos un enfoque similar al presentado en [28] para el dominio de Navier–Stokes. Luego, definimos el tensor de esfuerzo no lineal como en [30] y eliminamos la presión usando la condición de incompresibilidad. Las condiciones de transmisión dadas por la conservación de masa, equilibrio de fuerzas normales, y la ley de Beavers–Joseph–Saffman son impuestas débilmente, lo cual resulta en multiplicadores de Lagrange dados por: las trazas de la presión en el medio poroso y la velocidad del fluido sobre la interfaz. Consideramos formulaciones dual-mixta en ambos dominios. Además, de manera similar a [91, 88], y para controlar la no linealidad en el fluido, el tensor de pequeñas deformaciones y la vorticidad son introducidas como incógnitas adicionales. Además, la dificultad de que la velocidad del fluido viva ahora en  $H^1$  en lugar de  $L^2$  como es usual, es resuelto como en [28] aumentando la formulación variacional con adecuados términos de Galerkin. El sistema aumentado se reordena para que muestre una estructura de doble punto de silla. Este problema continuo se reescribe como una ecuación de punto fijo, de modo que los teoremas de Schauder y Banach, combinados con resultados clásicos de operadores monótonos biyectivos, son

aplicados para probar la unicidad de los problemas continuo y discreto. Esta investigación dio origen a la siguiente publicación:

- [40] S. CAUCAO, G.N. GATICA, R. OYARZÚA, AND I. ŠEBESTOVÁ, *A fully-mixed finite element method for the Navier–Stokes/Darcy coupled problem with nonlinear viscosity*. **Journal of Numerical Mathematics**, vol. 25, 2, pp. 55–88, (2017).

En el **Capítulo 2**, desarrollamos un análisis de error a posteriori para el modelo estudiado en el Capítulo 1. En este trabajo se deriva un estimador de error a posteriori, confiable y eficiente, el cual permite establecer métodos adaptativos apropiados para garantizar mayor precisión de las aproximaciones numéricas, y principalmente la convergencia del esquema de Galerkin en situaciones en las que hay presencia de singularidades o bien altos gradientes de la solución. Los elementos finitos considerados son elementos constantes a trozos, elementos de Raviart–Thomas de bajo orden, elementos lineales continuos a trozos, y elementos constantes a trozos en el fluido para aproximar el tensor de pequeñas deformaciones, esfuerzo, velocidad, y vorticidad, respectivamente, mientras que espacios de Raviart–Thomas de bajo orden y elementos constantes a trozos para la velocidad y presión, junto con elementos lineales continuos a trozos para las trazas, constituyen opciones factibles en el medio poroso. En la demostración de confiabilidad del estimador se utilizan descomposiciones de Helmholtz y propiedades de aproximación local de los interpolantes de Clément y Raviart–Thomas. Por otro lado, algunas de las principales herramientas utilizadas para demostrar la eficiencia del estimador son desigualdades inversas y técnicas de localización basadas en funciones burbujas. Esta investigación dio origen a la siguiente publicación:

- [38] S. CAUCAO, G.N. GATICA, AND R. OYARZÚA, *A posteriori error analysis of a fully-mixed formulation for the Navier–Stokes/Darcy coupled problem with nonlinear viscosity*. **Computer Methods in Applied Mechanics and Engineering**, vol. 315, pp. 943–971, (2017).

En el **Capítulo 3**, extendemos los resultados obtenidos en [65, 92, 94] al problema acoplado de Navier–Stokes/Darcy–Forchheimer con densidad y viscosidad constante. Consideramos la formulación velocidad-presión estándar para la ecuación de Navier–Stokes y a diferencia de [65], en el medio poroso consideramos la ecuación de Darcy–Forchheimer en su formulación dual-mixta. De este modo, obtenemos la velocidad y la presión del fluido en ambos medios como las incógnitas principales del sistema acoplado. Dado que una de las condiciones de interfaz es esencial, procedemos de manera similar a [124, 92] e incorporamos la traza de la presión en el medio poroso como una incógnita adicional. Demostramos que las formulaciones continua y discreta están bien puestas empleando un argumento de punto fijo y resultados clásicos en operadores monótonos no lineales (ver [144, 145]). En particular, consideramos los elementos de Bernardi–Raugel para la velocidad en la región del fluido, elementos de Raviart–Thomas de bajo orden para la velocidad de filtración en el medio poroso, constantes a trozos con medida nula para las presiones, y elementos constantes a trozos para el multiplicador de Lagrange sobre la interfaz. Este capítulo está constituido por la siguiente pre-publicación:

- [36] S. CAUCAO, M. DISCACCIATI, G.N. GATICA, AND R. OYARZÚA, *A conforming mixed finite element method for the Navier–Stokes/Darcy–Forchheimer coupled problem*. Preprint 2017-29, Centro de Investigación en Ingeniería Matemática (CI<sup>2</sup>MA), Universidad de Concepción, Chile, 2017.



En el **Capítulo 4**, derivamos y analizamos una nueva formulación mixta para el problema de Oldroyd–Stokes para fluidos viscoelásticos no isotérmicos. Para ello, a diferencia de [56] y [73], y para obtener una nueva formulación completamente mixta de este problema acoplado, primero introducimos el tensor de pequeñas deformaciones como una nueva incógnita, lo cual nos permite, por un lado, eliminar la parte polimérica del tensor de extra-esfuerzo del sistema y recuperarlo por un simple post-proceso de la solución, y por otro lado, unir las viscosidades polimérica y solvente en una viscosidad adimensional. Además, de manera similar al Capítulo 1 y por conveniencia del análisis, también consideramos los tensores de esfuerzo y vorticidad como incógnitas auxiliares, gracias a lo cual la presión puede ser eliminada del sistema y luego aproximada con una fórmula de postprocesamiento. A su vez, para derivar la formulación mixta de la ecuación de calor procedemos de manera similar a [73] (ver también [51, 52]) e incluimos el vector de flujo de calor como una incógnita adicional. Además, la dificultad de que la velocidad del fluido y la temperatura vivan en  $H^1$  en lugar de  $L^2$  como es usual, es resuelta como en [51, 52] aumentando la formulación variacional con adecuados términos de Galerkin. Entonces, siguiendo [51] y [2], demostramos solubilidad de los problemas continuo y discreto, con su estimación a priori correspondiente. Este capítulo está constituido por la siguiente pre-publicación:

- [37] S. CAUCAO, G.N. GATICA, AND R. OYARZÚA, *Analysis of an augmented fully-mixed formulation for the non-isothermal Oldroyd–Stokes problem*. Preprint 2017-21, Centro de Investigación en Ingeniería Matemática (CI<sup>2</sup>MA), Universidad de Concepción, Chile, 2017.

Finalmente, en el **Capítulo 5** desarrollamos un análisis de error a posteriori para la formulación variacional descrita en el Capítulo 4. Más precisamente, procedemos de manera similar a [3, 54, 53, 97], y desarrollamos dos estimadores de error a posteriori confiables y eficientes basados en residuos. Esto significa que nuestro análisis comienza con la elipticidad uniforme de las formas bilineales de las formulaciones continuas. Luego, de manera similar al Capítulo 2, aplicamos adecuadas descomposiciones de Helmholtz, propiedades de aproximación local de los operadores de Clément y Raviart–Thomas, y otras estimaciones conocidas, para demostrar la confiabilidad del estimador. A su vez, algunas de las principales herramientas utilizadas para demostrar la eficiencia de los estimadores son desigualdades inversas y técnicas de localización basadas en funciones burbujas. Además, se propone un estimador de error a posteriori alternativo (también confiable y eficiente) basado en residuos, donde la descomposición de Helmholtz no es utilizada en la demostración de la confiabilidad. Este capítulo está constituido por la siguiente pre-publicación:

- [39] S. CAUCAO, G.N. GATICA, AND R. OYARZÚA, *A posteriori error analysis of an augmented fully-mixed formulation for the non-isothermal Oldroyd–Stokes problem*. Preprint 2017-25, Centro de Investigación en Ingeniería Matemática (CI<sup>2</sup>MA), Universidad de Concepción, Chile, 2017.

A lo largo de los cinco capítulos que conforman esta tesis, los resultados teóricos como: órdenes de convergencia, confiabilidad y eficiencia de los estimadores de error a posteriori de tipo residual correspondientes, son ilustrados a través de varios ejemplos numéricos, que destacan el buen desempeño de los esquemas discretos propuestos y los algoritmos adaptativos asociados. Las implementaciones computacionales se obtuvieron empleando el software para elementos finitos de acceso libre FreeFem++ y el ilustrador ParaView.



# CHAPTER 1

---

## A fully-mixed finite element method for the Navier–Stokes/Darcy coupled problem with nonlinear viscosity

---

In this chapter we analyse an augmented mixed finite element method for the coupling of fluid flow with porous media flow. The flows are governed by the Navier–Stokes equations (with nonlinear viscosity) and the linear Darcy model, respectively, and the transmission conditions are given by mass conservation, balance of normal forces, and the Beavers–Joseph–Saffman law.

### 1.1 Introduction

The coupling of fluid flow, governed by the Navier–Stokes equations, and porous media flow, governed by the Darcy equations, has been intensively studied in recent decades (see, e.g., [11, 22, 32, 45, 65, 66, 101, 152]) for the steady-state case and [42, 43] for the time dependent case. Applications include the interaction between surface and subsurface flows, modelling of blood flow, and others. In particular, a discontinuous Galerkin (DG) discretization for this coupled problem has been introduced and analyzed in [101]. The approach there considers diverse combinations of techniques, including the usual nonsymmetric, symmetric and incomplete interior penalty discretizations of the Laplacian in both media, and the upwind Lesaint–Raviart discretization of the convective term in the free fluid domain. In turn, in [11] the authors extend previous results on the Stokes–Darcy coupling (see [63] and [64]) and introduce an iterative subdomain method employing the velocity-pressure formulation for the Navier–Stokes equation and the primal one for the Darcy equation. More recently, a conforming mixed method for the coupled system has been introduced and analyzed in [65]. This work, which extends the previous results from [92], utilize the velocity-pressure formulation for the Navier–Stokes equation and the dual-mixed approach in the Darcy region, which yields the introduction of the trace of the porous medium pressure as a suitable Lagrange multiplier.

Now, in the context of incompressible fluid flows, the utilization of pseudostress- and stress-based formulations has gained considerable attention during the last decades due to the fact that, on one hand, it allows to unify the analysis for Newtonian and non-Newtonian flows, and on the other hand, besides the original unknowns, they yield direct approximations of several other quantities of physical interest (see, for instance [91, 116, 115, 23, 25, 24, 30, 28]). More precisely, the pseudostress-velocity formulation has been studied in [23] and [24] for the Stokes and Navier–Stokes equations, respectively, whereas

the pseudostress-pressure-velocity formulation has been introduced and analysed in [25] for both, the Stokes and Navier–Stokes equations as well. While the latter formulation leads to a larger algebraic system, a hybridization technique can be used, however, to eliminate the pseudostress unknowns and, hence, to reduce its size. It is worth noting that, in the case of the Navier–Stokes problem, the methods proposed in [24] and [25] are quasi-optimal. More recently, a new dual-mixed method for the Navier–Stokes equations, which introduces a nonlinear stress-like quantity that connects the stress and the convective term as a primary unknown together with the velocity and its gradient, has been proposed and analysed in [116]. The main advantage of this idea is that it allows for a unified analysis of Newtonian and non-Newtonian fluids. Moreover, the skew symmetry of the nonlinear terms is preserved, and therefore the classical theory for the mixed methods extends easily to that setting. On the other hand, it turns out that natural finite element candidates do not fulfill Babuška–Brezzi conditions for the associated discrete scheme and consequently construction of special finite elements is required.

The idea of a stress augmentation by the convective term has been later modified by connecting the pseudostress with the convective term in [30], where a new augmented mixed finite element method for the Navier–Stokes problem is proposed and analysed. The main unknowns are comprised only of the velocity and the aforementioned nonlinear pseudostress in this case. However, depending on the needs of the user, further variables of interest, such as velocity gradient, vorticity, and pressure, can be easily recovered by means of a simple postprocess of the solution, and without the necessity of performing numerical differentiation at the discrete level. In order to guarantee the well-posedness of the resulting variational formulation, certain Galerkin least-square terms arising from the constitutive and equilibrium equations, and the Dirichlet boundary condition are introduced. The idea of the augmented variational formulations goes back to [78] and later has been used for different kind of problems (see, e.g., [68, 79, 20, 77]). In order to prove well-posedness of both the continuous and discrete problems in [30], it suffices to apply the Lax–Milgram and Banach fixed point theorems, which means, in particular, that no discrete inf-sup conditions are required there. As a consequence, arbitrary finite element subspaces of corresponding continuous spaces can be used. Moreover, unlike previous results on stress-like methods for the Navier–Stokes problem (see e.g. [24, 25]), the method in [30] is optimally convergent. The results of [30] have been further extended in [28] to the Navier–Stokes equations with constant density and variable viscosity. In particular, the analysis in [28] focuses in developing a mixed finite element approach for those quasi-Newtonian fluids whose viscosity is a nonlinear function of the magnitude of the gradient of velocity. Another application of the idea of introducing the aforementioned nonlinear pseudostress has been done in [50] for the Boussinesq problem. In turn, in the context of stabilized methods, we can refer to [35], where two three-field (deviatoric stress-velocity-pressure) subgrid-scale type formulations of the Navier–Stokes problem with nonlinear viscosity has been studied. This approach allows to employ the same interpolation for all unknowns even in the convection-dominant case.

The purpose of this chapter is to extend the results obtained in [88] to the coupled nonlinear Navier–Stokes and linear Darcy problem with constant density and variable viscosity in the fluid region. To this end, we consider a similar approach to the one presented in [28] for the Navier–Stokes domain, which means that we aim to obtain an optimally convergent method, and allow the possibility of calculating additional variables of interest. Unlike [28], in our model the viscosity depends nonlinearly only on the strain tensor, not on the whole gradient of the velocity, which adds an additional difficulty

to the analysis since the symmetry of the stress must be taken into account. We overcome this drawback by imposing the symmetry weakly, which yields the vorticity of the fluid as the corresponding Lagrange multiplier. We define the nonlinear stress tensor as in [30] and subsequently eliminate the pressure unknown using the incompressibility condition. The transmission conditions consisting of mass conservation, balance of normal forces, and the Beavers–Joseph–Saffman law are imposed weakly, which results in additional Lagrange multipliers: the traces of the porous media pressure and the fluid velocity on the interface. We consider dual-mixed formulations in both domains. In addition, similarly to [91, 88], and in order to handle the nonlinearity in the fluid, the strain tensor is introduced as an additional unknown. Furthermore, the difficulty that the fluid velocity lives now in  $H^1$  instead of  $L^2$  as usual, is resolved as in [28] by augmenting the variational formulation with residuals arising from the constitutive and equilibrium equations for the fluid flow, and the formulas for the strain and vorticity tensors. The resulting augmented variational system of equations is then re-ordered so that it shows a twofold saddle point structure. This continuous problem is rewritten as a fixed point operator equation, which is shown first to be well-defined thanks to the generalized Babuška–Brezzi theory developed in [88] (see also [84]), and whose unique solvability is then established by applying the same arguments utilized in [28]. Proceeding in a similar fashion we can conclude the well-posedness of the corresponding Galerkin scheme. We point out here that our approach differs from previous works on the Navier–Stokes/Darcy coupling since all of them consider a simplified model with constant viscosity (see e.g. [11, 22, 32]), and hence the present work constitutes the first contribution dealing with both a stress-based mixed formulation in the fluid and a nonlinear viscosity.

The rest of the chapter is organized as follows. In Section 1.2 we introduce the continuous problem and identify the twofold saddle point structure of the corresponding variational system. The augmented fully-mixed variational formulation is then derived in Section 1.3, and, under the assumption that the data are sufficiently small, its well-posedness is proved there by combining fixed point theorems with the generalized Babuška–Brezzi theory. Next, hypotheses on the finite element spaces aiming to ensure the well-posedness of the corresponding Galerkin scheme are established in Section 1.4, and the discrete analogue of the theory applied to the continuous case is employed here for the respective proof. In turn, the associated a priori error estimate is derived in Section 1.5, whereas particular choices of discrete subspaces satisfying the hypotheses from Section 1.4 together with the rates of convergence of the Galerkin schemes, are specified in Section 1.6. Finally, we illustrate the accuracy of the augmented mixed finite element method with some numerical examples in Section 1.7.

## 1.2 The continuous formulation

In this section we introduce the model problem and derive the corresponding weak formulation.

### 1.2.1 The model problem

In order to describe the geometry under consideration we let  $\Omega_S$  and  $\Omega_D$  be bounded and simply connected open polyhedral domains in  $\mathbb{R}^n$ , such that  $\Omega_S \cap \Omega_D = \emptyset$  and  $\partial\Omega_S \cap \partial\Omega_D = \Sigma \neq \emptyset$ . Then, we let  $\Gamma_S := \partial\Omega_S \setminus \bar{\Sigma}$ ,  $\Gamma_D := \partial\Omega_D \setminus \bar{\Sigma}$ , and denote by  $\mathbf{n}$  the unit normal vector on the boundaries, which is chosen pointing outward from  $\Omega := \Omega_S \cup \Sigma \cup \Omega_D$  and  $\Omega_S$  (and hence inward to  $\Omega_D$  when seen

on  $\Sigma$ ). On  $\Sigma$  we also consider unit tangent vectors, which are given by  $\mathbf{t} = \mathbf{t}_1$  when  $n = 2$  (see Fig. 1.1 below) and by  $\{\mathbf{t}_1, \mathbf{t}_2\}$  when  $n = 3$ . The problem we are interested in consists of the movement of an incompressible quasi-Newtonian viscous fluid that occupies  $\Omega_S$  and that flows towards and from  $\Omega_D$  through  $\Sigma$ , where  $\Omega_D$  is saturated with the same fluid. The mathematical model is defined by two separate groups of equations and by a set of coupling terms. In  $\Omega_S$ , the governing equations are those of the Navier–Stokes problem with constant density and variable viscosity, which are written in the following nonstandard stress–velocity–pressure formulation:

$$\begin{aligned} \boldsymbol{\sigma}_S &= \mu(|\mathbf{e}(\mathbf{u}_S)|)\mathbf{e}(\mathbf{u}_S) - (\mathbf{u}_S \otimes \mathbf{u}_S) - p_S \mathbb{I} \quad \text{in } \Omega_S, & \operatorname{div} \mathbf{u}_S &= 0 \quad \text{in } \Omega_S, \\ -\operatorname{div} \boldsymbol{\sigma}_S &= \mathbf{f}_S \quad \text{in } \Omega_S, & \mathbf{u}_S &= \mathbf{0} \quad \text{on } \Gamma_S, \end{aligned} \quad (1.1)$$

where  $\boldsymbol{\sigma}_S$  is the nonlinear stress tensor,  $\mathbf{u}_S$  is the velocity,  $p_S$  is the pressure,  $\mu : \mathbb{R}^+ \rightarrow \mathbb{R}^+$  is the nonlinear kinematic viscosity,  $\mathbf{e}(\mathbf{u}_S) := \frac{1}{2}\{\nabla \mathbf{u}_S + (\nabla \mathbf{u}_S)^t\}$  is the strain tensor (or symmetric part of the velocity gradient) and  $\mathbf{f}_S \in \mathbf{L}^2(\Omega_S)$  is a known volume force.

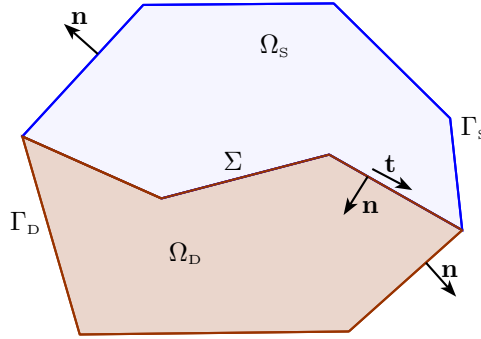


Figure 1.1: Sketch of a 2D geometry of our Navier–Stokes/Darcy model

Furthermore, we assume that  $\mu$  is of class  $C^1$ , and that there exist constants  $\mu_1, \mu_2 > 0$ , such that

$$\mu_1 \leq \mu(s) \leq \mu_2 \quad \text{and} \quad \mu_1 \leq \mu(s) + s\mu'(s) \leq \mu_2 \quad \forall s \geq 0, \quad (1.2)$$

which, according to the result provided in [98, Theorem 3.8], implies Lipschitz continuity and strong monotonicity of the nonlinear operator induced by  $\mu$ . This fact will be used later on in Section 1.3. In addition, it is easy to see that the forthcoming analysis also applies to the slightly more general case of a viscosity function acting on  $\Omega \times \mathbb{R}^+$ , that is  $\mu : \Omega \times \mathbb{R}^+ \rightarrow \mathbb{R}$ . Some examples of nonlinear  $\mu$  are the following:

$$\mu(s) := 2 + \frac{1}{1+s} \quad \text{and} \quad \mu(s) := \alpha_0 + \alpha_1(1+s^2)^{(\beta-2)/2}, \quad (1.3)$$

where  $\alpha_0, \alpha_1 > 0$  and  $\beta \in [1, 2]$ . The first example is basically academic but the second one corresponds to a particular case of the well-known Carreau law in fluid mechanics. It is easy to see that they both satisfy (1.2) with  $(\mu_1, \mu_2) = (2, 3)$  and  $(\mu_1, \mu_2) = (\alpha_0, \alpha_0 + \alpha_1)$ , respectively.

Now, in order to derive our fully-mixed formulation, we first observe, owing to the fact that  $\operatorname{tr} \mathbf{e}(\mathbf{u}_S) = \operatorname{div} \mathbf{u}_S$ , that the first two equations in (1.1) are equivalent to

$$\boldsymbol{\sigma}_S = \mu(|\mathbf{e}(\mathbf{u}_S)|)\mathbf{e}(\mathbf{u}_S) - (\mathbf{u}_S \otimes \mathbf{u}_S) - p_S \mathbb{I} \quad \text{and} \quad p_S = -\frac{1}{n} \operatorname{tr}(\boldsymbol{\sigma}_S + (\mathbf{u}_S \otimes \mathbf{u}_S)) \quad \text{in } \Omega_S, \quad (1.4)$$

and hence, eliminating the pressure  $p_S$  (which anyway can be approximated later on by the postprocessed formula suggested by the second equation of (1.4)), the Navier–Stokes problem (1.1) can be rewritten as

$$\boldsymbol{\sigma}_S^d = \mu(|\mathbf{e}(\mathbf{u}_S)|)\mathbf{e}(\mathbf{u}_S) - (\mathbf{u}_S \otimes \mathbf{u}_S)^d \quad \text{in } \Omega_S, \quad -\operatorname{div} \boldsymbol{\sigma}_S = \mathbf{f}_S \quad \text{in } \Omega_S, \quad \mathbf{u}_S = \mathbf{0} \quad \text{on } \Gamma_S. \quad (1.5)$$

Next, in order to handle the nonlinearity in  $\boldsymbol{\sigma}_S$  given by the term  $\mu(|\mathbf{e}(\mathbf{u}_S)|)\mathbf{e}(\mathbf{u}_S)$ , and employ the corresponding integration by parts formula, we adopt the approach from [91] (see also [89]) and introduce the additional unknowns

$$\mathbf{t}_S := \mathbf{e}(\mathbf{u}_S) \quad \text{and} \quad \boldsymbol{\rho}_S := \frac{1}{2} \{ \nabla \mathbf{u}_S - (\nabla \mathbf{u}_S)^t \} \quad \text{in } \Omega_S, \quad (1.6)$$

where  $\boldsymbol{\rho}_S$  is the vorticity (or skew-symmetric part of the velocity gradient). In this way, instead of (1.5), in the sequel we consider the set of equations with unknowns  $\mathbf{t}_S$ ,  $\mathbf{u}_S$ ,  $\boldsymbol{\sigma}_S$  and  $\boldsymbol{\rho}_S$ , given by

$$\begin{aligned} \mathbf{t}_S &= \nabla \mathbf{u}_S - \boldsymbol{\rho}_S \quad \text{in } \Omega_S, & \boldsymbol{\sigma}_S^d &= \mu(|\mathbf{t}_S|)\mathbf{t}_S - (\mathbf{u}_S \otimes \mathbf{u}_S)^d \quad \text{in } \Omega_S, \\ -\operatorname{div} \boldsymbol{\sigma}_S &= \mathbf{f}_S \quad \text{in } \Omega_S, & \mathbf{u}_S &= \mathbf{0} \quad \text{on } \Gamma_S, \end{aligned} \quad (1.7)$$

where both  $\mathbf{t}_S$  and  $\boldsymbol{\sigma}_S$  are symmetric tensors, and  $\operatorname{tr}(\mathbf{t}_S) = 0$  holds in  $\Omega_S$ .

On the other hand, in  $\Omega_D$  we consider the linearized Darcy model with homogeneous Neumann boundary condition on  $\Gamma_D$ :

$$\mathbf{u}_D = -\mathbf{K} \nabla p_D \quad \text{in } \Omega_D, \quad \operatorname{div} \mathbf{u}_D = f_D \quad \text{in } \Omega_D, \quad \mathbf{u}_D \cdot \mathbf{n} = 0 \quad \text{on } \Gamma_D, \quad (1.8)$$

where  $\mathbf{u}_D$  and  $p_D$  denote the velocity and pressure, respectively,  $f_D \in L^2(\Omega_D)$  is a source term satisfying  $\int_{\Omega_D} f_D = 0$ , and  $\mathbf{K} \in [L^\infty(\Omega_D)]^{n \times n}$  is a positive definite symmetric tensor describing the permeability of  $\Omega_D$  divided by a constant approximation of the viscosity, satisfying with  $C_{\mathbf{K}} > 0$

$$\mathbf{w} \cdot \mathbf{K}^{-1}(\mathbf{x}) \mathbf{w} \geq C_{\mathbf{K}} |\mathbf{w}|^2, \quad (1.9)$$

for almost all  $\mathbf{x} \in \Omega_D$ , and for all  $\mathbf{w} \in \mathbb{R}^n$ . Finally, the transmission conditions on  $\Sigma$  are given by

$$\mathbf{u}_S \cdot \mathbf{n} = \mathbf{u}_D \cdot \mathbf{n} \quad \text{on } \Sigma, \quad \boldsymbol{\sigma}_S \mathbf{n} + \sum_{l=1}^{n-1} \omega_l^{-1} (\mathbf{u}_S \cdot \mathbf{t}_l) \mathbf{t}_l = -p_D \mathbf{n} \quad \text{on } \Sigma, \quad (1.10)$$

where  $\{\omega_1, \dots, \omega_{n-1}\}$  is a set of positive frictional constants that can be determined experimentally. The first equation in (1.10) corresponds to mass conservation on  $\Sigma$ , whereas the second one establishes the balance of normal forces and a Beavers–Joseph–Saffman law.

### 1.2.2 The augmented fully-mixed variational formulation

In this section we proceed analogously to [88] (see also [93]) and derive a weak formulation of the coupled problem given by (1.7), (1.8), and (1.10). To this end, let us first introduce further notations and definitions. In what follows, given  $\star \in \{S, D\}$ ,  $u, v \in L^2(\Omega_\star)$ ,  $\mathbf{u}, \mathbf{v} \in \mathbf{L}^2(\Omega_\star)$ , and  $\boldsymbol{\sigma}, \boldsymbol{\tau} \in \mathbb{L}^2(\Omega_\star)$ , we set

$$(u, v)_\star := \int_{\Omega_\star} uv, \quad (\mathbf{u}, \mathbf{v})_\star := \int_{\Omega_\star} \mathbf{u} \cdot \mathbf{v}, \quad \text{and} \quad (\boldsymbol{\sigma}, \boldsymbol{\tau})_\star := \int_{\Omega_\star} \boldsymbol{\sigma} : \boldsymbol{\tau}.$$

In addition, we let  $\mathbb{L}_{\text{sym}}^2(\Omega_S)$  and  $\mathbb{L}_{\text{skew}}^2(\Omega_S)$  be the subspaces of symmetric and skew-symmetric tensors of  $\mathbb{L}^2(\Omega_S)$ , respectively, that is

$$\begin{aligned}\mathbb{L}_{\text{sym}}^2(\Omega_S) &:= \{\mathbf{r}_S \in \mathbb{L}^2(\Omega_S) : \mathbf{r}_S^t = \mathbf{r}_S\}, \\ \mathbb{L}_{\text{skew}}^2(\Omega_S) &:= \{\boldsymbol{\eta}_S \in \mathbb{L}^2(\Omega_S) : \boldsymbol{\eta}_S^t = -\boldsymbol{\eta}_S\}.\end{aligned}$$

Furthermore, we need to define the spaces

$$\begin{aligned}\mathbf{H}_0(\text{div}; \Omega_D) &:= \{\mathbf{v}_D \in \mathbf{H}(\text{div}; \Omega_D) : \mathbf{v}_D \cdot \mathbf{n} = 0 \text{ on } \Gamma_D\}, \\ \mathbb{L}_{\text{tr}}^2(\Omega_S) &:= \{\mathbf{r}_S \in \mathbb{L}_{\text{sym}}^2(\Omega_S) : \text{tr } \mathbf{r}_S = 0\},\end{aligned}$$

and the space of traces  $\mathbf{H}_{00}^{1/2}(\Sigma) := [H_{00}^{1/2}(\Sigma)]^n$ , where

$$H_{00}^{1/2}(\Sigma) := \{v|_{\Sigma} : v \in H^1(\Omega_S), \quad v = 0 \text{ on } \Gamma_S\}.$$

Observe that, if  $E_{0,S} : H^{1/2}(\Sigma) \rightarrow L^2(\partial\Omega_S)$  is the extension operator defined by

$$E_{0,S}(\psi) := \begin{cases} \psi & \text{on } \Sigma \\ 0 & \text{on } \Gamma_S \end{cases} \quad \forall \psi \in H^{1/2}(\Sigma),$$

we have that

$$H_{00}^{1/2}(\Sigma) = \left\{ \psi \in H^{1/2}(\Sigma) : E_{0,S}(\psi) \in H^{1/2}(\partial\Omega_S) \right\},$$

endowed with the norm  $\|\psi\|_{1/2,00,\Sigma} := \|E_{0,S}(\psi)\|_{1/2,\partial\Omega_S}$ . The dual space of  $\mathbf{H}_{00}^{1/2}(\Sigma)$  is denoted by  $\mathbf{H}_{00}^{-1/2}(\Sigma)$ .

Now, we proceed with the derivation of our weak formulation. We begin by introducing two additional unknowns on the coupling boundary

$$\boldsymbol{\varphi} := -\mathbf{u}_S|_{\Sigma} \in \mathbf{H}_{00}^{1/2}(\Sigma) \quad \text{and} \quad \lambda := p_D|_{\Sigma} \in H^{1/2}(\Sigma).$$

Then, to derive the weak formulation of the coupled system (1.7)–(1.8)–(1.10) we proceed similarly to [88] (see also [27, 93]), that is, we test the first equations of (1.7) and (1.8) with arbitrary  $\boldsymbol{\tau}_S \in \mathbb{H}(\text{div}; \Omega_S)$  and  $\mathbf{v}_D \in \mathbf{H}_0(\text{div}; \Omega_D)$ , respectively, integrate by parts, utilize the identity  $(\mathbf{t}_S, \boldsymbol{\tau}_S)_S = (\mathbf{t}_S, \boldsymbol{\tau}_S^d)_S$  (which follows from the fact that  $\mathbf{t}_S : \mathbb{I} = \text{tr } \mathbf{t}_S = 0$ ), and impose the remaining equations weakly, as well as the symmetry of  $\boldsymbol{\sigma}_S$ , to obtain the variational problem: Find  $\mathbf{t}_S \in \mathbb{L}_{\text{tr}}^2(\Omega_S)$ ,  $\boldsymbol{\sigma}_S \in \mathbb{H}(\text{div}; \Omega_S)$ ,  $\boldsymbol{\rho}_S \in \mathbb{L}_{\text{skew}}^2(\Omega_S)$ ,  $\mathbf{u}_D \in \mathbf{H}_0(\text{div}; \Omega_D)$ ,  $\boldsymbol{\varphi} \in \mathbf{H}_{00}^{1/2}(\Sigma)$ ,  $\lambda \in H^{1/2}(\Sigma)$ ,  $p_D \in L^2(\Omega_D)$  and  $\mathbf{u}_S$  in a suitable space (to be specified below), such that

$$\begin{aligned}(\mathbf{t}_S, \boldsymbol{\tau}_S^d)_S + (\text{div } \boldsymbol{\tau}_S, \mathbf{u}_S)_S + \langle \boldsymbol{\tau}_S \mathbf{n}, \boldsymbol{\varphi} \rangle_{\Sigma} + (\boldsymbol{\tau}_S, \boldsymbol{\rho}_S)_S &= 0, \\ (\mathbf{K}^{-1} \mathbf{u}_D, \mathbf{v}_D)_D - (\text{div } \mathbf{v}_D, p_D)_D - \langle \mathbf{v}_D \cdot \mathbf{n}, \lambda \rangle_{\Sigma} &= 0, \\ (\mu(|\mathbf{t}_S|) \mathbf{t}_S, \mathbf{r}_S)_S - (\mathbf{r}_S, \boldsymbol{\sigma}_S^d)_S - ((\mathbf{u}_S \otimes \mathbf{u}_S)^d, \mathbf{r}_S)_S &= 0, \\ -(\text{div } \boldsymbol{\sigma}_S, \mathbf{v}_S)_S &= (\mathbf{f}_S, \mathbf{v}_S)_S, \\ (\text{div } \mathbf{u}_D, q_D)_D &= (f_D, q_D)_D, \\ (\boldsymbol{\sigma}_S, \boldsymbol{\eta}_S)_S &= 0, \\ -\langle \boldsymbol{\varphi} \cdot \mathbf{n}, \xi \rangle_{\Sigma} - \langle \mathbf{u}_D \cdot \mathbf{n}, \xi \rangle_{\Sigma} &= 0, \\ \langle \boldsymbol{\sigma}_S \mathbf{n}, \boldsymbol{\psi} \rangle_{\Sigma} - \langle \boldsymbol{\varphi}, \boldsymbol{\psi} \rangle_{\mathbf{t},\Sigma} + \langle \boldsymbol{\psi} \cdot \mathbf{n}, \lambda \rangle_{\Sigma} &= 0,\end{aligned} \tag{1.11}$$

for all  $\mathbf{r}_S \in \mathbb{L}_{\text{tr}}^2(\Omega_S)$ ,  $\boldsymbol{\tau}_S \in \mathbb{H}(\mathbf{div}; \Omega_S)$ ,  $\boldsymbol{\eta}_S \in \mathbb{L}_{\text{skew}}^2(\Omega_S)$ ,  $\mathbf{v}_D \in \mathbf{H}_0(\text{div}; \Omega_D)$ ,  $\boldsymbol{\psi} \in \mathbf{H}_{00}^{1/2}(\Sigma)$ ,  $\xi \in H^{1/2}(\Sigma)$ ,  $q_D \in L^2(\Omega_D)$  and  $\mathbf{v}_S \in \mathbf{L}^2(\Omega_S)$ , where

$$\langle \boldsymbol{\varphi}, \boldsymbol{\psi} \rangle_{\mathbf{t}, \Sigma} := \sum_{l=1}^{n-1} \omega_l^{-1} \langle \boldsymbol{\varphi} \cdot \mathbf{t}_l, \boldsymbol{\psi} \cdot \mathbf{t}_l \rangle_{\Sigma}.$$

Notice that the third term in the third equation of the foregoing system requires  $\mathbf{u}_S$  to live in a smaller space than  $\mathbf{L}^2(\Omega_S)$ . In fact, by applying the Cauchy–Schwarz and Hölder inequalities and then the continuous injection  $\mathbf{i}_c$  of  $\mathbf{H}^1(\Omega_S)$  into  $\mathbf{L}^4(\Omega_S)$  (see e.g. [1, Theorem 6.3] or [139, Theorem 1.3.5]), we find that there holds

$$\left| ((\mathbf{u}_S \otimes \mathbf{w}_S)^d, \mathbf{r}_S)_S \right| \leq \|\mathbf{u}_S\|_{\mathbf{L}^4(\Omega_S)} \|\mathbf{w}_S\|_{\mathbf{L}^4(\Omega_S)} \|\mathbf{r}_S\|_{0, \Omega_S} \leq \|\mathbf{i}_c\|^2 \|\mathbf{u}_S\|_{1, \Omega_S} \|\mathbf{w}_S\|_{1, \Omega_S} \|\mathbf{r}_S\|_{0, \Omega_S}, \quad (1.12)$$

for all  $\mathbf{u}_S, \mathbf{w}_S \in \mathbf{H}^1(\Omega_S)$  and  $\mathbf{r}_S \in \mathbf{L}^2(\Omega_S)$ . According to this, we propose to look for the unknown  $\mathbf{u}_S$  in  $\mathbf{H}_{\Gamma_S}^1(\Omega_S)$  and to restrict the set of corresponding test functions  $\mathbf{v}_S$  to the same space, where

$$\mathbf{H}_{\Gamma_S}^1(\Omega_S) := \{\mathbf{v}_S \in \mathbf{H}^1(\Omega_S) : \mathbf{v}_S|_{\Gamma_S} = \mathbf{0}\}.$$

Next, analogously to [88], it is not difficult to see that the system (1.11) is not uniquely solvable since, given any solution  $(\mathbf{t}_S, \boldsymbol{\sigma}_S, \boldsymbol{\rho}_S, \mathbf{u}_D, \boldsymbol{\varphi}, \lambda, p_D, \mathbf{u}_S)$  in the indicated spaces, and given any constant  $c \in \mathbb{R}$ , the vector defined by  $(\mathbf{t}_S, \boldsymbol{\sigma}_S - c\mathbb{I}, \boldsymbol{\rho}_S, \mathbf{u}_D, \boldsymbol{\varphi}, \lambda + c, p_D + c, \mathbf{u}_S)$  also becomes a solution. As a consequence of the above, from now on we require the Darcy pressure  $p_D$  to be in  $L_0^2(\Omega_D)$ , where

$$L_0^2(\Omega_D) := \left\{ q \in L^2(\Omega_D) : (q, 1)_D = 0 \right\}.$$

In turn, due to the decomposition  $L^2(\Omega_D) = L_0^2(\Omega_D) \oplus \mathbb{R}$ , the boundary conditions  $\mathbf{u}_D \cdot \mathbf{n} = 0$  on  $\Gamma_D$  and  $\mathbf{u}_S = \mathbf{0}$  on  $\Gamma_S$ , the first transmission condition in (1.10), and the fact that  $\int_{\Omega_D} f_D = 0$ , guarantee that the fifth equation of (1.11) is equivalent to requiring it for all  $q_D \in L_0^2(\Omega_D)$ .

On the other hand, for convenience of the subsequent analysis, we consider the decomposition (see, for instance, [19], [81])

$$\mathbb{H}(\mathbf{div}; \Omega_S) = \mathbb{H}_0(\mathbf{div}; \Omega_S) \oplus \mathbb{R}\mathbb{I}, \quad (1.13)$$

where

$$\mathbb{H}_0(\mathbf{div}; \Omega_S) := \left\{ \boldsymbol{\tau} \in \mathbb{H}(\mathbf{div}; \Omega_S) : (\text{tr } \boldsymbol{\tau}, 1)_S = 0 \right\},$$

and redefine the stress tensor as  $\boldsymbol{\sigma}_S := \boldsymbol{\sigma}_S + l\mathbb{I}$ , with the new unknowns  $\boldsymbol{\sigma}_S \in \mathbb{H}_0(\mathbf{div}; \Omega_S)$  and  $l \in \mathbb{R}$ . In this way the first and last equations of (1.11) are rewritten, equivalently, as

$$\begin{aligned} (\mathbf{t}_S, \boldsymbol{\tau}_S^d)_S + (\mathbf{div } \boldsymbol{\tau}_S, \mathbf{u}_S)_S + \langle \boldsymbol{\tau}_S \mathbf{n}, \boldsymbol{\varphi} \rangle_{\Sigma} + (\boldsymbol{\tau}_S, \boldsymbol{\rho}_S)_S &= 0 \quad \forall \boldsymbol{\tau}_S \in \mathbb{H}_0(\mathbf{div}; \Omega_S), \\ j \langle \boldsymbol{\varphi} \cdot \mathbf{n}, 1 \rangle_{\Sigma} &= 0 \quad \forall j \in \mathbb{R}, \\ \langle \boldsymbol{\sigma}_S \mathbf{n}, \boldsymbol{\psi} \rangle_{\Sigma} - \langle \boldsymbol{\varphi}, \boldsymbol{\psi} \rangle_{\mathbf{t}, \Sigma} + \langle \boldsymbol{\psi} \cdot \mathbf{n}, \lambda \rangle_{\Sigma} + l \langle \boldsymbol{\psi} \cdot \mathbf{n}, 1 \rangle_{\Sigma} &= 0 \quad \forall \boldsymbol{\psi} \in \mathbf{H}_{00}^{1/2}(\Sigma). \end{aligned} \quad (1.14)$$

Finally, with the choice of the corresponding space for  $\mathbf{u}_S$ , and in order to be able to analyze the present variational formulation of (1.7), (1.8), and (1.10), we augment the resulting system through

the incorporation of the following redundant Galerkin-type terms:

$$\begin{aligned}
\kappa_1 (\boldsymbol{\sigma}_S^d - \mu(|\mathbf{t}_S|)\mathbf{t}_S + (\mathbf{u}_S \otimes \mathbf{u}_S)^d, \boldsymbol{\tau}_S^d)_S &= 0 \quad \forall \boldsymbol{\tau}_S \in \mathbb{H}_0(\mathbf{div}; \Omega_S), \\
\kappa_2 (\mathbf{div} \boldsymbol{\sigma}_S, \mathbf{div} \boldsymbol{\tau}_S)_S &= -\kappa_2 (\mathbf{f}_S, \mathbf{div} \boldsymbol{\tau}_S)_S \quad \forall \boldsymbol{\tau}_S \in \mathbb{H}_0(\mathbf{div}; \Omega_S), \\
\kappa_3 (\mathbf{e}(\mathbf{u}_S) - \mathbf{t}_S, \mathbf{e}(\mathbf{v}_S))_S &= 0 \quad \forall \mathbf{v}_S \in \mathbf{H}_{\Gamma_S}^1(\Omega_S), \\
\kappa_4 \left( \boldsymbol{\rho}_S - \frac{1}{2} (\nabla \mathbf{u}_S - (\nabla \mathbf{u}_S)^t), \boldsymbol{\eta}_S \right)_S &= 0 \quad \forall \boldsymbol{\eta}_S \in \mathbb{L}_{\text{skew}}^2(\Omega_S),
\end{aligned} \tag{1.15}$$

where  $\kappa_1, \kappa_2, \kappa_3$ , and  $\kappa_4$  are positive parameters to be specified later. Notice that the foregoing terms are nothing but consistent expressions, though tested differently from (1.11), arising from the equilibrium and constitutive equations, the relation between the strain tensor and  $\mathbf{t}_S$ , and the definition of the vorticity in terms of the velocity gradient. It is easy to see that each solution of the original system is also a solution of the resulting augmented one, and hence by solving the latter we find all the solutions of the former.

Now, it is clear that there are many different ways of ordering the augmented mixed variational formulation described above, but for the sake of the subsequent analysis we proceed as in [88] (see also [93, 27]), and adopt one leading to a doubly-mixed structure. To that end, we group the spaces, unknowns, and test functions as follows:

$$\begin{aligned}
\mathbf{X} &:= \mathbb{L}_{\text{tr}}^2(\Omega_S) \times \mathbb{H}_0(\mathbf{div}; \Omega_S) \times \mathbf{H}_{\Gamma_S}^1(\Omega_S) \times \mathbb{L}_{\text{skew}}^2(\Omega_S) \times \mathbf{H}_0(\text{div}; \Omega_D), \quad \mathbf{M} := \mathbf{H}_{00}^{1/2}(\Sigma) \times H^{1/2}(\Sigma), \\
\mathbb{X} &:= \mathbf{X} \times \mathbf{M}, \quad \text{and} \quad \mathbb{M} := L_0^2(\Omega_D) \times \mathbb{R},
\end{aligned}$$

$$\begin{aligned}
\underline{\mathbf{t}} &:= (\mathbf{t}_S, \boldsymbol{\sigma}_S, \mathbf{u}_S, \boldsymbol{\rho}_S, \mathbf{u}_D) \in \mathbf{X}, \quad \underline{\boldsymbol{\varphi}} := (\boldsymbol{\varphi}, \lambda) \in \mathbf{M}, \quad \underline{\mathbf{p}} := (p_D, l) \in \mathbb{M}, \\
\underline{\mathbf{r}} &:= (\mathbf{r}_S, \boldsymbol{\tau}_S, \mathbf{v}_S, \boldsymbol{\eta}_S, \mathbf{v}_D) \in \mathbf{X}, \quad \underline{\boldsymbol{\psi}} := (\boldsymbol{\psi}, \xi) \in \mathbf{M}, \quad \underline{\mathbf{q}} := (q_D, j) \in \mathbb{M},
\end{aligned}$$

where  $\mathbf{X}$ ,  $\mathbf{M}$ ,  $\mathbb{X}$ , and  $\mathbb{M}$  are respectively endowed with the norms

$$\|\underline{\mathbf{r}}\|_{\mathbf{X}} := \|\mathbf{r}_S\|_{0, \Omega_S} + \|\boldsymbol{\tau}_S\|_{\text{div}, \Omega_S} + \|\mathbf{v}_S\|_{1, \Omega_S} + \|\boldsymbol{\eta}_S\|_{0, \Omega_S} + \|\mathbf{v}_D\|_{\text{div}, \Omega_D},$$

$$\|\underline{\boldsymbol{\psi}}\|_{\mathbf{M}} := \|\boldsymbol{\psi}\|_{1/2, 00, \Sigma} + \|\xi\|_{1/2, \Sigma}, \quad \|(\underline{\mathbf{r}}, \underline{\boldsymbol{\psi}})\|_{\mathbb{X}} := \|\underline{\mathbf{r}}\|_{\mathbf{X}} + \|\underline{\boldsymbol{\psi}}\|_{\mathbf{M}} \quad \text{and} \quad \|\underline{\mathbf{q}}\|_{\mathbb{M}} := \|q_D\|_{0, \Omega_D} + |j|.$$

Hence, the augmented fully-mixed variational formulation for the system (1.11) with the new equations (1.14) and (1.15) reads: Find  $((\underline{\mathbf{t}}, \underline{\boldsymbol{\varphi}}), \underline{\mathbf{p}}) \in \mathbb{X} \times \mathbb{M}$  such that

$$\begin{aligned}
[\mathbf{A}(\mathbf{u}_S)(\underline{\mathbf{t}}, \underline{\boldsymbol{\varphi}}), (\underline{\mathbf{r}}, \underline{\boldsymbol{\psi}})] + [\mathbf{B}(\underline{\mathbf{r}}, \underline{\boldsymbol{\psi}}), \underline{\mathbf{p}}] &= [\mathbf{F}, (\underline{\mathbf{r}}, \underline{\boldsymbol{\psi}})] \quad \forall (\underline{\mathbf{r}}, \underline{\boldsymbol{\psi}}) \in \mathbb{X}, \\
[\mathbf{B}(\underline{\mathbf{t}}, \underline{\boldsymbol{\varphi}}), \underline{\mathbf{q}}] &= [\mathbf{G}, \underline{\mathbf{q}}] \quad \forall \underline{\mathbf{q}} \in \mathbb{M},
\end{aligned} \tag{1.16}$$

where

$$[\mathbf{F}, (\underline{\mathbf{r}}, \underline{\boldsymbol{\psi}})] := [F, \underline{\mathbf{r}}] \quad \text{and} \quad [\mathbf{G}, \underline{\mathbf{q}}] := [G, q_D], \tag{1.17}$$

with

$$[F, \underline{\mathbf{r}}] := -\kappa_2 (\mathbf{f}_S, \mathbf{div} \boldsymbol{\tau}_S)_S + (\mathbf{f}_S, \mathbf{v}_S)_S \quad \text{and} \quad [G, q_D] := -(f_D, q_D)_D.$$

In addition, given  $\mathbf{z}_S \in \mathbf{H}_{\Gamma_S}^1(\Omega_S)$ , the operator  $\mathbf{A}(\mathbf{z}_S) : \mathbb{X} \rightarrow \mathbb{X}'$  is defined by

$$[\mathbf{A}(\mathbf{z}_S)(\underline{\mathbf{t}}, \underline{\boldsymbol{\varphi}}), (\underline{\mathbf{r}}, \underline{\boldsymbol{\psi}})] := [a(\mathbf{z})(\underline{\mathbf{t}}), \underline{\mathbf{r}}] + [b(\underline{\mathbf{t}}), \underline{\boldsymbol{\psi}}] + [b(\underline{\mathbf{r}}), \underline{\boldsymbol{\varphi}}] - [c(\underline{\boldsymbol{\varphi}}), \underline{\boldsymbol{\psi}}], \tag{1.18}$$



with

$$\begin{aligned}
[a(\mathbf{z}_S)(\underline{\mathbf{t}}), \underline{\mathbf{r}}] &:= [a_1(\underline{\mathbf{t}}), \underline{\mathbf{r}}] + [a_2(\mathbf{z}_S)(\underline{\mathbf{t}}), \underline{\mathbf{r}}], \\
[a_1(\underline{\mathbf{t}}), \underline{\mathbf{r}}] &:= (\mu(|\mathbf{t}_S|)\mathbf{t}_S, \mathbf{r}_S)_S - (\mathbf{r}_S, \boldsymbol{\sigma}_S^d)_S + (\mathbf{t}_S, \boldsymbol{\tau}_S^d)_S + \kappa_1(\boldsymbol{\sigma}_S^d - \mu(|\mathbf{t}_S|)\mathbf{t}_S, \boldsymbol{\tau}_S^d)_S \\
&\quad + \kappa_2(\mathbf{div} \boldsymbol{\sigma}_S, \mathbf{div} \boldsymbol{\tau}_S)_S + (\mathbf{div} \boldsymbol{\tau}_S, \mathbf{u}_S)_S - (\mathbf{div} \boldsymbol{\sigma}_S, \mathbf{v}_S)_S \\
&\quad + (\boldsymbol{\tau}_S, \boldsymbol{\rho}_S)_S - (\boldsymbol{\sigma}_S, \boldsymbol{\eta}_S)_S + \kappa_3(\mathbf{e}(\mathbf{u}_S) - \mathbf{t}_S, \mathbf{e}(\mathbf{v}_S))_S \\
&\quad + \kappa_4 \left( \boldsymbol{\rho}_S - \frac{1}{2}(\nabla \mathbf{u}_S - (\nabla \mathbf{u}_S)^t), \boldsymbol{\eta}_S \right)_S + (\mathbf{K}^{-1} \mathbf{u}_D, \mathbf{v}_D)_D, \\
[a_2(\mathbf{z}_S)(\underline{\mathbf{t}}), \underline{\mathbf{r}}] &:= ((\mathbf{z}_S \otimes \mathbf{u}_S)^d, \kappa_1 \boldsymbol{\tau}^d - \mathbf{r}_S)_S, \\
[b(\underline{\mathbf{r}}), \underline{\boldsymbol{\psi}}] &:= \langle \boldsymbol{\tau}_S \mathbf{n}, \boldsymbol{\psi} \rangle_\Sigma - \langle \mathbf{v}_D \cdot \mathbf{n}, \xi \rangle_\Sigma, \\
[c(\underline{\boldsymbol{\varphi}}), \underline{\boldsymbol{\psi}}] &:= \langle \boldsymbol{\varphi} \cdot \mathbf{n}, \xi \rangle_\Sigma - \langle \boldsymbol{\psi} \cdot \mathbf{n}, \lambda \rangle_\Sigma + \langle \boldsymbol{\varphi}, \boldsymbol{\psi} \rangle_{\mathbf{t}, \Sigma},
\end{aligned} \tag{1.19}$$

whereas  $\mathbf{B} : \mathbb{X} \rightarrow \mathbb{M}'$  is given by

$$[\mathbf{B}(\underline{\mathbf{r}}, \underline{\boldsymbol{\psi}}), \underline{\mathbf{q}}] := [B_1(\underline{\mathbf{r}}), q_D] + [B_2(\underline{\boldsymbol{\psi}}), j], \tag{1.20}$$

with

$$[B_1(\underline{\mathbf{r}}), q_D] := -(\mathbf{div} \mathbf{v}_D, q_D)_D \quad \text{and} \quad [B_2(\underline{\boldsymbol{\psi}}), j] := j \langle \boldsymbol{\psi} \cdot \mathbf{n}, 1 \rangle_\Sigma.$$

In all the terms above,  $[\cdot, \cdot]$  denotes the duality pairing induced by the corresponding operators.

### 1.3 Analysis of the continuous formulation

In this section we analyse the well-posedness of problem (1.16) by means of a fixed point argument and a result on the solvability of twofold saddle point problems. To that end we first collect some previous results and notations that will serve for the forthcoming analysis.

#### 1.3.1 Preliminaries

We begin by recalling the following theorem to be employed next.

**Theorem 1.1.** *Let  $X_1, M_1$ , and  $M$  be Hilbert spaces, set  $X := X_1 \times M_1$ , and let  $X'_1, M'_1, M'$ , and  $X' := X'_1 \times M'_1$ , be their respective duals. Let  $A_1 : X_1 \rightarrow X'_1$  be a nonlinear operator, and  $S : M_1 \rightarrow M'_1$ ,  $B_1 : X_1 \rightarrow M'_1$ , and  $B : X \rightarrow M'$  be linear bounded operators. We also let  $B'_1 : M_1 \rightarrow X'_1$  and  $B' : M \rightarrow X'$  be the corresponding adjoints and define the nonlinear operator  $A : X \rightarrow X'$ , as:*

$$[A(\mathbf{s}, \boldsymbol{\phi}), (\mathbf{r}, \boldsymbol{\psi})] := [A_1(\mathbf{s}), \mathbf{r}] + [B'_1(\boldsymbol{\phi}), \mathbf{r}] + [B_1(\mathbf{s}), \boldsymbol{\psi}] - [S(\boldsymbol{\phi}), \boldsymbol{\psi}] \quad \forall (\mathbf{s}, \boldsymbol{\phi}), (\mathbf{r}, \boldsymbol{\psi}) \in X. \tag{1.21}$$

Finally, we let  $V$  be the kernel of  $B$ , that is

$$V := \{(\mathbf{r}, \boldsymbol{\psi}) \in X : [B(\mathbf{r}, \boldsymbol{\psi}), q] = 0 \quad \forall q \in M\},$$

and let  $\tilde{X}_1$  and  $\tilde{M}_1$  be subspaces of  $X_1$  and  $M_1$ , respectively, such that  $V = \tilde{X}_1 \times \tilde{M}_1$ .

Assume that

- (i)  $A_1|_{\tilde{X}_1} : \tilde{X}_1 \rightarrow \tilde{X}_1'$  is Lipschitz continuous and strongly monotone, that is, there exist constants  $\gamma, \alpha > 0$  such that

$$\|A_1(\mathbf{s}) - A_1(\mathbf{r})\|_{\tilde{X}_1'} \leq \gamma \|\mathbf{s} - \mathbf{r}\|_{X_1} \quad \forall \mathbf{s}, \mathbf{r} \in \tilde{X}_1$$

and

$$[A_1(\mathbf{s}) - A_1(\mathbf{r}), \mathbf{s} - \mathbf{r}] \geq \alpha \|\mathbf{s} - \mathbf{r}\|_{X_1}^2 \quad \forall \mathbf{s}, \mathbf{r} \in \tilde{X}_1.$$

- (ii) For each pair  $(\mathbf{r}, \mathbf{r}^\perp) \in \tilde{X}_1 \times \tilde{X}_1^\perp$  there holds the pseudolinear property

$$A_1(\mathbf{r} + \mathbf{r}^\perp) = A_1(\mathbf{r}) + A_1(\mathbf{r}^\perp).$$

- (iii)  $S$  is positive semi-definite on  $\tilde{M}_1$ , that is,

$$[S(\boldsymbol{\psi}), \boldsymbol{\psi}] \geq 0 \quad \forall \boldsymbol{\psi} \in \tilde{M}_1.$$

- (iv)  $B_1$  satisfies an inf-sup condition on  $\tilde{X}_1 \times \tilde{M}_1$ , that is, there exists  $\beta_1 > 0$  such that

$$\sup_{\substack{\mathbf{r} \in \tilde{X}_1 \\ \mathbf{r} \neq \mathbf{0}}} \frac{[B_1(\mathbf{r}), \boldsymbol{\psi}]}{\|\mathbf{r}\|_{X_1}} \geq \beta_1 \|\boldsymbol{\psi}\|_{M_1} \quad \forall \boldsymbol{\psi} \in \tilde{M}_1.$$

- (v)  $B$  satisfies an inf-sup condition on  $X \times M$ , that is, there exists  $\beta > 0$  such that

$$\sup_{\substack{(\mathbf{r}, \boldsymbol{\psi}) \in X \\ (\mathbf{r}, \boldsymbol{\psi}) \neq \mathbf{0}}} \frac{[B(\mathbf{r}, \boldsymbol{\psi}), q]}{\|(\mathbf{r}, \boldsymbol{\psi})\|_X} \geq \beta \|q\|_M \quad \forall q \in M.$$

Then, there exists a unique  $((\mathbf{t}, \boldsymbol{\varphi}), p) \in X \times M$ , such that

$$\begin{aligned} [A(\mathbf{t}, \boldsymbol{\varphi}), (\mathbf{r}, \boldsymbol{\psi})] + [B'(p), (\mathbf{r}, \boldsymbol{\psi})] &= [F, (\mathbf{r}, \boldsymbol{\psi})] \quad \forall (\mathbf{r}, \boldsymbol{\psi}) \in X, \\ [B(\mathbf{t}, \boldsymbol{\varphi}), q] &= [G, q] \quad \forall q \in M. \end{aligned} \tag{1.22}$$

Moreover, there exists  $C > 0$ , depending only on  $\alpha, \gamma, \beta_1, \beta, \|S\|$ , and  $\|B_1\|$  such that

$$\|((\mathbf{t}, \boldsymbol{\varphi}), p)\|_{X \times M} \leq C \{\|F\|_{X'} + \|G\|_{M'}\}.$$

*Proof.* See [88, Theorem 3.1]. □

Next, we recall that for each  $\mathbf{r}, \mathbf{s} \in \mathbb{L}^2(\Omega)$  (see [98, Theorem 3.8] for details) there holds

$$\|\mu(|\mathbf{r}|)\mathbf{r} - \mu(|\mathbf{s}|)\mathbf{s}\|_{0, \Omega} \leq L_\mu \|\mathbf{r} - \mathbf{s}\|_{0, \Omega}, \tag{1.23}$$

$$\int_{\Omega} \{\mu(|\mathbf{r}|)\mathbf{r} - \mu(|\mathbf{s}|)\mathbf{s}\} : (\mathbf{r} - \mathbf{s}) \geq \mu_1 \|\mathbf{r} - \mathbf{s}\|_{0, \Omega}^2, \tag{1.24}$$

where  $L_\mu := \max\{\mu_2, 2\mu_2 - \mu_1\}$ , with  $\mu_1$  and  $\mu_2$  being the bounds of  $\mu$  given in (1.2).

### 1.3.2 A fixed point approach

We begin the solvability analysis of (1.16) by defining the operator  $\mathbf{T} : \mathbf{H}_{\Gamma_S}^1(\Omega_S) \rightarrow \mathbf{H}_{\Gamma_S}^1(\Omega_S)$  by

$$\mathbf{T}(\mathbf{z}_S) := \mathbf{u}_S \quad \forall \mathbf{z}_S \in \mathbf{H}_{\Gamma_S}^1(\Omega_S), \quad (1.25)$$

where  $\mathbf{u}_S$  is the third component of  $\mathbf{t} \in \mathbf{X}$ , which in turn is the first component of the unique solution (to be confirmed below) of the nonlinear problem: Find  $((\mathbf{t}, \underline{\varphi}), \mathbf{p}) \in \mathbb{X} \times \mathbb{M}$ , such that

$$\begin{aligned} [\mathbf{A}(\mathbf{z}_S)(\mathbf{t}, \underline{\varphi}), (\mathbf{r}, \underline{\psi})] + [\mathbf{B}(\mathbf{r}, \underline{\psi}), \mathbf{p}] &= [\mathbf{F}, (\mathbf{r}, \underline{\psi})] \quad \forall (\mathbf{r}, \underline{\psi}) \in \mathbb{X}, \\ [\mathbf{B}(\mathbf{t}, \underline{\varphi}), \mathbf{q}] &= [\mathbf{G}, \mathbf{q}] \quad \forall \mathbf{q} \in \mathbb{M}. \end{aligned} \quad (1.26)$$

It follows that  $((\mathbf{t}, \underline{\varphi}), \mathbf{p}) \in \mathbb{X} \times \mathbb{M}$  is a solution of (1.16) if and only if  $\mathbf{u}_S \in \mathbf{H}_{\Gamma_S}^1(\Omega_S)$  satisfies

$$\mathbf{T}(\mathbf{u}_S) = \mathbf{u}_S. \quad (1.27)$$

However, we remark in advance that the definition of  $\mathbf{T}$  will make sense only in a closed ball of  $\mathbf{H}_{\Gamma_S}^1(\Omega_S)$ . Now, it is clear that problem (1.26) has the same structure as the one in Theorem 1.1. Therefore, in what follows we apply this result to establish the well-posedness of (1.26), equivalently the well-definiteness of  $\mathbf{T}$ . To that end, we first observe that the kernel of the operator  $\mathbf{B}$  (cf. (1.20)) can be written, equivalently, as

$$\mathbb{V} := \{(\mathbf{r}, \underline{\psi}) \in \mathbb{X} : [\mathbf{B}(\mathbf{r}, \underline{\psi}), \mathbf{q}] = 0 \quad \forall \mathbf{q} \in \mathbb{M}\} = \tilde{\mathbf{X}} \times \tilde{\mathbf{M}},$$

where

$$\tilde{\mathbf{X}} = \mathbb{L}_{\text{tr}}^2(\Omega_S) \times \mathbb{H}_0(\mathbf{div}; \Omega_S) \times \mathbf{H}_{\Gamma_S}^1(\Omega_S) \times \mathbb{L}_{\text{skew}}^2(\Omega_S) \times \tilde{\mathbf{H}}_0(\mathbf{div}; \Omega_D)$$

and

$$\tilde{\mathbf{M}} = \tilde{\mathbf{H}}_{00}^{1/2}(\Sigma) \times H^{1/2}(\Sigma),$$

with

$$\tilde{\mathbf{H}}_0(\mathbf{div}; \Omega_D) := \{\mathbf{v}_D \in \mathbf{H}_0(\mathbf{div}; \Omega_D) : \mathbf{div}(\mathbf{v}_D) \in P_0(\Omega_D)\}$$

and

$$\tilde{\mathbf{H}}_{00}^{1/2}(\Sigma) := \left\{ \boldsymbol{\psi} \in \mathbf{H}_{00}^{1/2}(\Sigma) : \langle \boldsymbol{\psi} \cdot \mathbf{n}, 1 \rangle_\Sigma = 0 \right\}.$$

At this point we recall, for later use, that there exist positive constants  $c_1(\Omega_S)$ ,  $C_{\text{div}}$ , and  $C_{K_o}$ , such that (see, [19, Proposition 3.1, Chapter IV], [93, Lemma 3.2], and [19, 100], respectively, for details)

$$c_1(\Omega_S) \|\boldsymbol{\tau}_S\|_{0, \Omega_S}^2 \leq \|\boldsymbol{\tau}_S^d\|_{0, \Omega_S}^2 + \|\mathbf{div} \boldsymbol{\tau}_S\|_{0, \Omega_S}^2 \quad \forall \boldsymbol{\tau}_S \in \mathbb{H}_0(\mathbf{div}; \Omega_S), \quad (1.28)$$

$$\|\mathbf{v}_D\|_{0, \Omega_D}^2 \geq C_{\text{div}} \|\mathbf{v}_D\|_{\mathbf{div}, \Omega_D}^2 \quad \forall \mathbf{v}_D \in \tilde{\mathbf{H}}_0(\mathbf{div}; \Omega_D), \quad (1.29)$$

and

$$\|\mathbf{e}(\mathbf{v}_S)\|_{0, \Omega_S}^2 \geq C_{K_o} \|\mathbf{v}_S\|_{1, \Omega_S}^2 \quad \forall \mathbf{v}_S \in \mathbf{H}_{\Gamma_S}^1(\Omega_S), \quad (1.30)$$

where, in particular, (1.30) is known as Korn's inequality. Regarding this result, we notice that in general  $C_{K_o}$  is unknown. However, for the numerical results reported below in Section 1.7 we employ a heuristic approximation of this constant.

In what follows, and through the verification of the hypotheses of Theorem 1.1, we provide sufficient conditions under which the operator  $\mathbf{T}$  is well-defined. We begin with the Lipschitz-continuity and strong-monotonicity of  $a(\mathbf{z}_S)(\cdot)$  for a given  $\mathbf{z}_S \in \mathbf{H}_{\Gamma_S}^1(\Omega)$ .

**Lemma 1.2.** *Assume that*

$$\kappa_1 \in \left(0, \frac{2\delta_1\mu_1}{L_\mu}\right), \quad \kappa_3 \in \left(0, 2\delta_2\left(\mu_1 - \frac{\kappa_1 L_\mu}{2\delta_1}\right)\right) \quad \text{and} \quad \kappa_4 \in \left(0, 2\delta_3 C_{K_0} \kappa_3 \left(1 - \frac{\delta_2}{2}\right)\right),$$

with  $\delta_1 \in \left(0, \frac{2}{L_\mu}\right)$ ,  $\delta_2 \in (0, 2)$ ,  $\delta_3 \in (0, 2)$ , and that  $\kappa_2 > 0$ . Then, there exists  $r_0 > 0$  such that for each  $r \in (0, r_0)$ , the nonlinear operator  $a(\mathbf{z}_S)(\cdot)$  is strongly-monotone on  $\tilde{\mathbf{X}}$  and Lipschitz-continuous on  $\mathbf{X}$ , for each  $\mathbf{z}_S \in \mathbf{H}_{\Gamma_S}^1(\Omega_S)$  such that  $\|\mathbf{z}_S\|_{1,\Omega_S} \leq r$ , with respective constants  $\alpha(\Omega) > 0$  and  $\gamma(\Omega) > 0$ , independent of  $\mathbf{z}_S$ .

*Proof.* Let  $\mathbf{z}_S \in \mathbf{H}_{\Gamma_S}^1(\Omega_S)$  such that  $\|\mathbf{z}_S\|_{1,\Omega_S} \leq r$ , with  $r \in (0, r_0)$  and  $r_0$  to be defined below. We first observe that  $a_1$  and  $a_2(\mathbf{z}_S)$ , and consequently  $a(\mathbf{z}_S)$  (cf. (1.19)), are Lipschitz-continuous. In fact, using the Cauchy–Schwarz inequality, and the Lipschitz-continuity of the operator induced by  $\mu$  (cf. (1.23)), we deduce from (1.19) that  $a_1$  is Lipschitz continuous with a positive constant  $L_{a_1}$ , depending on  $L_\mu$ , and the parameters  $\kappa_i, i \in \{1, \dots, 4\}$ , that is

$$\|a_1(\underline{\mathbf{t}}) - a_1(\underline{\mathbf{r}})\|_{\mathbf{X}'} \leq L_{a_1} \|\underline{\mathbf{t}} - \underline{\mathbf{r}}\|_{\mathbf{X}} \quad \forall \underline{\mathbf{t}}, \underline{\mathbf{r}} \in \mathbf{X}. \quad (1.31)$$

In addition, from (1.12) and (1.19) we easily obtain that

$$\begin{aligned} |[a_2(\mathbf{z}_S)(\underline{\mathbf{t}}), \underline{\mathbf{r}}]| &\leq (\kappa_1^2 + 1)^{1/2} \|\mathbf{z}_S\|_{\mathbf{L}^4(\Omega_S)} \|\mathbf{u}_S\|_{\mathbf{L}^4(\Omega_S)} \|\underline{\mathbf{r}}\|_{\mathbf{X}} \\ &\leq c_2(\Omega_S) (\kappa_1^2 + 1)^{1/2} \|\mathbf{z}_S\|_{1,\Omega_S} \|\underline{\mathbf{t}}\|_{\mathbf{X}} \|\underline{\mathbf{r}}\|_{\mathbf{X}} \quad \forall \underline{\mathbf{t}}, \underline{\mathbf{r}} \in \mathbf{X}, \end{aligned} \quad (1.32)$$

which, together with the linearity of  $a_2(\mathbf{z}_S)$ , and the Lipschitz-continuity of  $a_1$ , implies that

$$\begin{aligned} \|a(\mathbf{z}_S)(\underline{\mathbf{t}}) - a(\mathbf{z}_S)(\underline{\mathbf{r}})\|_{\mathbf{X}'} &\leq (L_{a_1} + c_2(\Omega_S) (\kappa_1^2 + 1)^{1/2} \|\mathbf{z}_S\|_{1,\Omega_S}) \|\underline{\mathbf{t}} - \underline{\mathbf{r}}\|_{\mathbf{X}} \\ &\leq \gamma(\Omega) \|\underline{\mathbf{t}} - \underline{\mathbf{r}}\|_{\mathbf{X}} \quad \forall \underline{\mathbf{t}}, \underline{\mathbf{r}} \in \mathbf{X}, \end{aligned} \quad (1.33)$$

with  $\gamma(\Omega) := L_{a_1} + c_2(\Omega_S) (\kappa_1^2 + 1)^{1/2} r$ . Now, for the strong monotonicity of  $a(\mathbf{z}_S)$ , we observe from the definition of  $a_1$  (cf. (1.18)) that it readily follows that

$$\begin{aligned} [a_1(\underline{\mathbf{t}}) - a_1(\underline{\mathbf{r}}), \underline{\mathbf{t}} - \underline{\mathbf{r}}] &= (\mu(|\mathbf{t}_S|)\mathbf{t}_S - \mu(|\mathbf{r}_S|)\mathbf{r}_S, \mathbf{t}_S - \mathbf{r}_S)_S + \kappa_1 \|(\boldsymbol{\sigma}_S - \boldsymbol{\tau}_S)^d\|_{0,\Omega_S}^2 \\ &\quad - \kappa_1 (\mu(|\mathbf{t}_S|)\mathbf{t}_S - \mu(|\mathbf{r}_S|)\mathbf{r}_S, (\boldsymbol{\sigma}_S - \boldsymbol{\tau}_S)^d)_S + \kappa_2 \|\mathbf{div}(\boldsymbol{\sigma}_S - \boldsymbol{\tau}_S)\|_{0,\Omega_S}^2 \\ &\quad + \kappa_3 \|\mathbf{e}(\mathbf{u}_S - \mathbf{v}_S)\|_{0,\Omega_S}^2 - \kappa_3 (\mathbf{t}_S - \mathbf{r}_S, \mathbf{e}(\mathbf{u}_S - \mathbf{v}_S))_S + \kappa_4 \|\boldsymbol{\rho}_S - \boldsymbol{\eta}_S\|_{0,\Omega_S}^2 \\ &\quad - \frac{1}{2} \kappa_4 (\nabla(\mathbf{u}_S - \mathbf{v}_S) - (\nabla(\mathbf{u}_S - \mathbf{v}_S))^t, \boldsymbol{\rho}_S - \boldsymbol{\eta}_S)_S + (\mathbf{K}^{-1}(\mathbf{u}_D - \mathbf{v}_D), \mathbf{u}_D - \mathbf{v}_D)_D. \end{aligned}$$

Hence, we proceed similarly to the proof of [28, Lemma 3.4], utilize the Cauchy–Schwarz and Young’s inequalities, and apply (1.9), (1.23) and (1.24) to obtain that for any  $\delta_1, \delta_2, \delta_3 > 0$ , and for all  $\underline{\mathbf{t}}, \underline{\mathbf{r}} \in \tilde{\mathbf{X}}$ , there holds

$$\begin{aligned} [a_1(\underline{\mathbf{t}}) - a_1(\underline{\mathbf{r}}), \underline{\mathbf{t}} - \underline{\mathbf{r}}] &\geq \mu_1 \|\mathbf{t}_S - \mathbf{r}_S\|_{0,\Omega_S}^2 + \kappa_1 \|(\boldsymbol{\sigma}_S - \boldsymbol{\tau}_S)^d\|_{0,\Omega_S}^2 \\ &\quad - \frac{\kappa_1 L_\mu}{2} \left\{ \frac{1}{\delta_1} \|\mathbf{t}_S - \mathbf{r}_S\|_{0,\Omega_S}^2 + \delta_1 \|(\boldsymbol{\sigma}_S - \boldsymbol{\tau}_S)^d\|_{0,\Omega_S}^2 \right\} \\ &\quad + \kappa_2 \|\mathbf{div}(\boldsymbol{\sigma}_S - \boldsymbol{\tau}_S)\|_{0,\Omega_S}^2 + \kappa_3 \|\mathbf{e}(\mathbf{u}_S - \mathbf{v}_S)\|_{0,\Omega_S}^2 \\ &\quad - \frac{\kappa_3}{2} \left\{ \frac{1}{\delta_2} \|\mathbf{t}_S - \mathbf{r}_S\|_{0,\Omega_S}^2 + \delta_2 \|\mathbf{e}(\mathbf{u}_S - \mathbf{v}_S)\|_{0,\Omega_S}^2 \right\} + \kappa_4 \|\boldsymbol{\rho}_S - \boldsymbol{\eta}_S\|_{0,\Omega_S}^2 \\ &\quad - \frac{\kappa_4}{2} \left\{ \frac{1}{\delta_3} \|\mathbf{u}_S - \mathbf{v}_S\|_{1,\Omega_S}^2 + \delta_3 \|\boldsymbol{\rho}_S - \boldsymbol{\eta}_S\|_{0,\Omega_S}^2 \right\} + C_{\mathbf{K}} \|\mathbf{u}_D - \mathbf{v}_D\|_{0,\Omega_D}^2, \end{aligned}$$

which, together with (1.29) and Korn's inequality (1.30), implies

$$\begin{aligned}
[a_1(\underline{\mathbf{t}}) - a_1(\underline{\mathbf{r}}), \underline{\mathbf{t}} - \underline{\mathbf{r}}] &\geq \left\{ \left( \mu_1 - \frac{\kappa_1 L_\mu}{2\delta_1} \right) - \frac{\kappa_3}{2\delta_2} \right\} \|\underline{\mathbf{t}}_S - \underline{\mathbf{r}}_S\|_{0,\Omega_S}^2 \\
&\quad + \kappa_1 \left( 1 - \frac{\delta_1 L_\mu}{2} \right) \|(\boldsymbol{\sigma}_S - \boldsymbol{\tau}_S)^d\|_{0,\Omega_S}^2 + \kappa_2 \|\mathbf{div}(\boldsymbol{\sigma}_S - \boldsymbol{\tau}_S)\|_{0,\Omega_S}^2 \\
&\quad + \left\{ C_{Ko}\kappa_3 \left( 1 - \frac{\delta_2}{2} \right) - \frac{\kappa_4}{2\delta_3} \right\} \|\underline{\mathbf{u}}_S - \underline{\mathbf{v}}_S\|_{1,\Omega_S}^2 \\
&\quad + \kappa_4 \left( 1 - \frac{\delta_3}{2} \right) \|\underline{\boldsymbol{\rho}}_S - \underline{\boldsymbol{\eta}}_S\|_{0,\Omega_S}^2 + C_{\mathbf{K}} C_{\text{div}} \|\underline{\mathbf{u}}_D - \underline{\mathbf{v}}_D\|_{\text{div},\Omega_D}^2.
\end{aligned} \tag{1.34}$$

Then, assuming the stipulated hypotheses on  $\delta_1, \kappa_1, \kappa_3, \delta_2, \delta_3, \kappa_4$ , and  $\kappa_2$ , and applying the inequality (1.28), we can define the positive constants

$$\begin{aligned}
\alpha_1(\Omega_S) &:= \left( \mu_1 - \frac{\kappa_1 L_\mu}{2\delta_1} \right) - \frac{\kappa_3}{2\delta_2}, & \alpha_2(\Omega_S) &:= \min \left\{ \kappa_1 \left( 1 - \frac{\delta_1 L_\mu}{2} \right), \frac{\kappa_2}{2} \right\}, \\
\alpha_3(\Omega_S) &:= \min \left\{ \alpha_2(\Omega_S) c_1(\Omega_S), \frac{\kappa_2}{2} \right\}, & \alpha_4(\Omega_S) &:= C_{Ko}\kappa_3 \left( 1 - \frac{\delta_2}{2} \right) - \frac{\kappa_4}{2\delta_3}, \\
\alpha_5(\Omega_S) &:= \kappa_4 \left( 1 - \frac{\delta_3}{2} \right), & \alpha_6(\Omega_D) &:= C_{\mathbf{K}} C_{\text{div}},
\end{aligned}$$

which allow us to deduce from (1.34) that

$$[a_1(\underline{\mathbf{t}}) - a_1(\underline{\mathbf{r}}), \underline{\mathbf{t}} - \underline{\mathbf{r}}] \geq \alpha_0(\Omega) \|\underline{\mathbf{t}} - \underline{\mathbf{r}}\|_{\tilde{\mathbf{X}}}^2 \quad \forall \underline{\mathbf{t}}, \underline{\mathbf{r}} \in \tilde{\mathbf{X}}, \tag{1.35}$$

where

$$\alpha_0(\Omega) := \min \left\{ \min_{i \in \{1, \dots, 5\}} \{\alpha_i(\Omega_S)\}, \alpha_6(\Omega_D) \right\} \tag{1.36}$$

is the strong monotonicity constant of  $a_1$ . Moreover, according to the definition of  $a(\mathbf{z}_S)$  (cf. (1.19)), and combining (1.32) and (1.35), we obtain

$$[a(\mathbf{z}_S)(\underline{\mathbf{t}}) - a(\mathbf{z}_S)(\underline{\mathbf{r}}), \underline{\mathbf{t}} - \underline{\mathbf{r}}] \geq \left\{ \alpha_0(\Omega) - c_2(\Omega_S)(\kappa_1^2 + 1)^{1/2} \|\mathbf{z}_S\|_{1,\Omega_S} \right\} \|\underline{\mathbf{t}} - \underline{\mathbf{r}}\|_{\tilde{\mathbf{X}}}^2,$$

for all  $\underline{\mathbf{t}}, \underline{\mathbf{r}} \in \tilde{\mathbf{X}}$ . Consequently, by requiring  $\|\mathbf{z}_S\|_{1,\Omega_S} \leq r_0$ , with

$$r_0 := \frac{\alpha_0(\Omega)}{2c_2(\Omega_S)(\kappa_1^2 + 1)^{1/2}}, \tag{1.37}$$

the strong monotonicity of  $a(\mathbf{z}_S)$  is ensured with a constant  $\alpha(\Omega) := \frac{\alpha_0(\Omega)}{2}$  independent of  $\mathbf{z}_S$ , that is

$$[a(\mathbf{z}_S)(\underline{\mathbf{t}}) - a(\mathbf{z}_S)(\underline{\mathbf{r}}), \underline{\mathbf{t}} - \underline{\mathbf{r}}] \geq \frac{\alpha_0(\Omega)}{2} \|\underline{\mathbf{t}} - \underline{\mathbf{r}}\|_{\tilde{\mathbf{X}}}^2 \quad \forall \underline{\mathbf{t}}, \underline{\mathbf{r}} \in \tilde{\mathbf{X}}. \tag{1.38}$$

□

At this point we remark that the condition  $\|\mathbf{z}_S\|_{1,\Omega_S} \leq r_0$  imposed in the above proof, with  $r_0$  given by (1.37), does not actually have a physical meaning, but only constitutes a condition guaranteeing that  $a(\mathbf{z}_S)$  is strongly monotone independently of  $\mathbf{z}_S$  in the closed ball of  $\mathbf{H}_{\Gamma_S}^1(\Omega_S)$  with center at the null function and radius  $r_0$ .

We continue with the pseudolinearity of  $a(\mathbf{z}_S)(\cdot)$  (cf. (1.19)).

**Lemma 1.3.** *Given  $\mathbf{z}_S \in \mathbf{H}_{\Gamma_S}^1(\Omega_S)$ , for each pair  $(\underline{\mathbf{t}}, \underline{\mathbf{t}}^\perp) \in \tilde{\mathbf{X}} \times \tilde{\mathbf{X}}^\perp$  there holds*

$$a(\mathbf{z}_S)(\underline{\mathbf{t}} + \underline{\mathbf{t}}^\perp) = a(\mathbf{z}_S)(\underline{\mathbf{t}}) + a(\mathbf{z}_S)(\underline{\mathbf{t}}^\perp). \quad (1.39)$$

*Proof.* Let  $\mathbf{z}_S \in \mathbf{H}_{\Gamma_S}^1(\Omega_S)$ . We first decompose  $\mathbf{X}$  as  $\mathbf{X} = \mathbf{X}^l \times \mathbf{X}^r$ , with  $\mathbf{X}^l := \mathbb{L}_{\text{tr}}^2(\Omega_S)$  and  $\mathbf{X}^r := \mathbb{H}_0(\mathbf{div}; \Omega_S) \times \mathbf{H}_{\Gamma_S}^1(\Omega_S) \times \mathbb{L}_{\text{skew}}^2(\Omega_S) \times \mathbf{H}_0(\mathbf{div}; \Omega_D)$ . In addition, since  $\mathbf{B}$  (cf. (1.20)) does not depend on the variable from  $\mathbf{X}^l$ , we easily obtain that  $\tilde{\mathbf{X}} = \mathbf{X}^l \times \tilde{\mathbf{X}}^r$ , with

$$\tilde{\mathbf{X}}^r := \mathbb{H}_0(\mathbf{div}; \Omega_S) \times \mathbf{H}_{\Gamma_S}^1(\Omega_S) \times \mathbb{L}_{\text{skew}}^2(\Omega_S) \times \tilde{\mathbf{H}}_0(\mathbf{div}; \Omega_D) \subseteq \mathbf{X}^r,$$

which yields  $\tilde{\mathbf{X}}^\perp = \{\mathbf{0}\} \times (\tilde{\mathbf{X}}^r)^\perp$ . In turn, given  $\underline{\mathbf{s}} = (\mathbf{0}, \underline{\mathbf{s}}^r)$ , with  $\underline{\mathbf{s}}^r = (\boldsymbol{\sigma}_S, \mathbf{u}_S, \boldsymbol{\rho}_S, \mathbf{u}_D) \in \mathbf{X}^r$  and  $\underline{\mathbf{r}} = (\mathbf{r}_S, \boldsymbol{\tau}_S, \mathbf{v}_S, \boldsymbol{\eta}_S, \mathbf{v}_D) \in \mathbf{X}$ , there holds

$$\begin{aligned} [a(\mathbf{z}_S)(\underline{\mathbf{s}}), \underline{\mathbf{r}}] = & -(\mathbf{r}_S, \boldsymbol{\sigma}_S^d)_S + \kappa_1(\boldsymbol{\sigma}_S^d, \boldsymbol{\tau}_S^d)_S + \kappa_2(\mathbf{div} \boldsymbol{\sigma}_S, \mathbf{div} \boldsymbol{\tau}_S)_S + (\mathbf{div} \boldsymbol{\tau}_S, \mathbf{u}_S)_S - (\mathbf{div} \boldsymbol{\sigma}_S, \mathbf{v}_S)_S \\ & + (\boldsymbol{\tau}_S, \boldsymbol{\rho}_S)_S - (\boldsymbol{\sigma}_S, \boldsymbol{\eta}_S)_S + \kappa_3(\mathbf{e}(\mathbf{u}_S), \mathbf{e}(\mathbf{v}_S))_S + \kappa_4 \left( \boldsymbol{\rho}_S - \frac{1}{2}(\nabla \mathbf{u}_S - (\nabla \mathbf{u}_S)^t), \boldsymbol{\eta}_S \right)_S \\ & + (\mathbf{K}^{-1} \mathbf{u}_D, \mathbf{v}_D)_D + ((\mathbf{z} \otimes \mathbf{u}_S)^d, \kappa_1 \boldsymbol{\tau}_S^d - \mathbf{r}_S)_S, \end{aligned}$$

which shows that  $a(\mathbf{z}_S)$  is linear in  $\{\mathbf{0}\} \times \mathbf{X}^r$ . Similarly, from the definition of  $a(\mathbf{z}_S)$ , we also find that for each  $\underline{\mathbf{t}} := (\underline{\mathbf{t}}^l, \underline{\mathbf{t}}^r) \in \mathbf{X} = \mathbf{X}^l \times \mathbf{X}^r$  and for each  $\underline{\mathbf{r}} \in \mathbf{X}$ , there holds

$$[a(\mathbf{z}_S)(\mathbf{0}, \underline{\mathbf{t}}^r) + a(\mathbf{z}_S)(\underline{\mathbf{t}}^l, \mathbf{0}), \underline{\mathbf{r}}] = [a(\mathbf{z}_S)(\underline{\mathbf{t}}), \underline{\mathbf{r}}].$$

According to the previous analysis, it readily follows that  $a(\mathbf{z}_S)$  satisfies (1.39).  $\square$

Now, we establish the positive semi-definiteness of  $c$  (cf. (1.19)).

**Lemma 1.4.** *There holds*

$$[c(\underline{\boldsymbol{\psi}}), \underline{\boldsymbol{\psi}}] \geq 0 \quad \forall \underline{\boldsymbol{\psi}} \in \mathbf{M}. \quad (1.40)$$

*Proof.* From the definition of operator  $c$ , it readily follows that

$$[c(\underline{\boldsymbol{\psi}}), \underline{\boldsymbol{\psi}}] := \sum_{l=1}^{n-1} \omega_l^{-1} \|\boldsymbol{\psi} \cdot \mathbf{t}_l\|_{0,\Sigma}^2 \geq 0 \quad \forall \underline{\boldsymbol{\psi}} \in \mathbf{M}, \quad (1.41)$$

which clearly confirms that  $c$  is positive semi-definite.  $\square$

We end the verification of the hypotheses of Theorem 1.1 with the corresponding inf-sup conditions for the bilinear forms  $b$  and  $\mathbf{B}$  (cf. (1.19) and (1.20), respectively).

**Lemma 1.5.** *There exist positive constants  $\beta_1$  and  $\beta$ , such that*

$$\sup_{\substack{\underline{\mathbf{r}} \in \tilde{\mathbf{X}} \\ \underline{\mathbf{r}} \neq \mathbf{0}}} \frac{[b(\underline{\mathbf{r}}), \underline{\boldsymbol{\psi}}]}{\|\underline{\mathbf{r}}\|_{\mathbf{X}}} \geq \beta_1 \|\underline{\boldsymbol{\psi}}\|_{\mathbf{M}} \quad \forall \underline{\boldsymbol{\psi}} \in \tilde{\mathbf{M}} \quad (1.42)$$

and

$$\sup_{\substack{(\underline{\mathbf{r}}, \underline{\boldsymbol{\psi}}) \in \mathbb{X} \\ (\underline{\mathbf{r}}, \underline{\boldsymbol{\psi}}) \neq \mathbf{0}}} \frac{[\mathbf{B}(\underline{\mathbf{r}}, \underline{\boldsymbol{\psi}}), \underline{\mathbf{q}}]}{\|(\underline{\mathbf{r}}, \underline{\boldsymbol{\psi}})\|_{\mathbb{X}}} \geq \beta \|\underline{\mathbf{q}}\|_{\mathbb{M}} \quad \forall \underline{\mathbf{q}} \in \mathbb{M}. \quad (1.43)$$

*Proof.* For the proof of (1.42) we refer the reader to [88, Lemma 4.3] whereas a slight modification of [87, Lemma 4.3] implies (1.43). We omit further details.  $\square$

We are now in position of establishing the well-posedness of (1.26) (equivalently the well-definiteness of  $\mathbf{T}$ ).

**Lemma 1.6.** *Let  $r \in (0, r_0)$ , with  $r_0$  given by (1.37). Assume that*

$$\kappa_1 \in \left(0, \frac{2\delta_1\mu_1}{L_\mu}\right), \quad \kappa_3 \in \left(0, 2\delta_2\left(\mu_1 - \frac{\kappa_1 L_\mu}{2\delta_1}\right)\right) \quad \text{and} \quad \kappa_4 \in \left(0, 2\delta_3 C_{K_0} \kappa_3 \left(1 - \frac{\delta_2}{2}\right)\right),$$

*with  $\delta_1 \in \left(0, \frac{2}{L_\mu}\right)$ ,  $\delta_2 \in (0, 2)$ ,  $\delta_3 \in (0, 2)$ , and that  $\kappa_2 > 0$ . Then, the problem (1.26) has a unique solution for each  $\mathbf{z}_S \in \mathbf{H}_{\Gamma_S}^1(\Omega_S)$ , such that  $\|\mathbf{z}_S\|_{1,\Omega_S} \leq r$ . Moreover, there exists a constant  $c_{\mathbf{T}} > 0$ , independent of  $\mathbf{z}_S$  and the data  $\mathbf{f}_S$  and  $f_D$ , such that there holds*

$$\|\mathbf{T}(\mathbf{z}_S)\|_{1,\Omega_S} = \|\mathbf{u}_S\|_{1,\Omega_S} \leq \|((\mathbf{t}, \underline{\varphi}), \mathbf{p})\|_{\mathbb{X} \times \mathbb{M}} \leq c_{\mathbf{T}} \left\{ \|\mathbf{f}_S\|_{0,\Omega_S} + \|f_D\|_{0,\Omega_D} \right\}. \quad (1.44)$$

*Proof.* Given  $\mathbf{z}_S \in \mathbf{H}_{\Gamma_S}^1(\Omega_S)$ , such that  $\|\mathbf{z}_S\|_{1,\Omega_S} \leq r$ , the well-posedness of (1.26) follows from Lemmas 1.2 – 1.5, and a straightforward application of Theorem 1.1. Now, concerning the estimate (1.44), we first deduce from the definitions of  $\mathbf{F}$  and  $\mathbf{G}$  (cf. (1.17)), and from the Cauchy–Schwarz and Young’s inequalities, that there exist constants  $c_{\mathbf{F}} > 0$  and  $c_{\mathbf{G}} > 0$ , such that

$$\|\mathbf{F}\|_{\mathbb{X}'} \leq c_{\mathbf{F}} \|\mathbf{f}_S\|_{0,\Omega_S} \quad \text{and} \quad \|\mathbf{G}\|_{\mathbb{M}'} \leq c_{\mathbf{G}} \|f_D\|_{0,\Omega_D}. \quad (1.45)$$

This fact and Theorem 1.1 imply the estimate

$$\|((\mathbf{t}, \underline{\varphi}), \mathbf{p})\|_{\mathbb{X} \times \mathbb{M}} \leq c_{\mathbf{T}} \left\{ \|\mathbf{f}_S\|_{0,\Omega_S} + \|f_D\|_{0,\Omega_D} \right\},$$

with  $c_{\mathbf{T}}$  independent of  $\mathbf{z}_S$ , which implies (1.44) and concludes the proof.  $\square$

We end this section by remarking that the constant  $\alpha_0(\Omega)$  yielding the strong monotonicity of both  $a_1$  and  $a(\mathbf{z}_S)$  can be maximized by taking the parameters  $\delta_1, \kappa_1, \delta_2, \kappa_3, \delta_3$ , and  $\kappa_4$  as the middle points of their feasible ranges, and by choosing  $\kappa_2$  so that it maximizes the minimum defining  $\alpha_2(\Omega_S)$ . More precisely, we simply take

$$\begin{aligned} \delta_1 &= \frac{1}{L_\mu}, \quad \kappa_1 = \frac{\delta_1 \mu_1}{L_\mu} = \frac{\mu_1}{L_\mu^2}, \quad \delta_2 = 1, \quad \kappa_3 = \delta_2 \left( \mu_1 - \frac{\kappa_1 L_\mu}{2\delta_1} \right) = \frac{\mu_1}{2}, \quad \delta_3 = 1, \\ \kappa_4 &= \delta_3 C_{K_0} \kappa_3 \left( 1 - \frac{\delta_2}{2} \right) = C_{K_0} \frac{\mu_1}{4}, \quad \text{and} \quad \kappa_2 = 2\kappa_1 \left( 1 - \frac{\delta_1 L_\mu}{2} \right) = \frac{\mu_1}{L_\mu^2}, \end{aligned} \quad (1.46)$$

which yields

$$\begin{aligned} \alpha_1(\Omega_S) &= \frac{\mu_1}{4}, \quad \alpha_2(\Omega_S) = \frac{\mu_1}{2L_\mu^2}, \quad \alpha_3(\Omega_S) = \min\{c_1(\Omega_S), 1\} \frac{\mu_1}{2L_\mu^2}, \\ \alpha_4(\Omega_S) &= C_{K_0} \frac{\mu_1}{8}, \quad \alpha_5(\Omega_S) = C_{K_0} \frac{\mu_1}{8}, \quad \alpha_6(\Omega_D) = C_{\mathbf{K}} C_{\text{div}}, \end{aligned}$$

and hence

$$\alpha_0(\Omega) = \min \left\{ \min \left\{ C_{K_0}, 1 \right\} \frac{\mu_1}{8}, \min \left\{ c_1(\Omega_S), 1 \right\} \frac{\mu_1}{2L_\mu^2}, C_{\mathbf{K}} C_{\text{div}} \right\}.$$

The explicit values of the stabilization parameters  $\kappa_i$ ,  $i \in \{1, \dots, 4\}$ , given in (1.46), will be employed in Section 1.7 for the corresponding numerical experiments.

### 1.3.3 Solvability analysis of the fixed point equation

In this section we proceed analogously to [28, Section 3.3] and establish existence of a fixed point of the operator  $\mathbf{T}$  (cf. (1.25)) by means of the well known Schauder fixed point theorem. The uniqueness can then be established by means of the Banach fixed point theorem by utilizing the same estimates derived for the existence.

We begin by recalling the first of the aforementioned results (see, e.g. [47, Theorem 9.12-1(b)]).

**Theorem 1.7.** *Let  $W$  be a closed and convex subset of a Banach space  $X$ , and let  $T : W \rightarrow W$  be a continuous mapping such that  $\overline{T(W)}$  is compact. Then  $T$  has at least one fixed point.*

The verification of the hypotheses of Theorem 1.7 is provided next.

**Lemma 1.8.** *Let  $r \in (0, r_0)$ , with  $r_0$  given by (1.37), let  $W_r$  be the closed ball defined by  $W_r := \{\mathbf{z}_S \in \mathbf{H}_{\Gamma_S}^1(\Omega_S) : \|\mathbf{z}_S\|_{1,\Omega_S} \leq r\}$ , and assume that the data satisfy*

$$c_{\mathbf{T}} \left\{ \|\mathbf{f}_S\|_{0,\Omega_S} + \|f_D\|_{0,\Omega_D} \right\} \leq r, \quad (1.47)$$

with  $c_{\mathbf{T}}$  the positive constant satisfying (1.51). Then there holds  $\mathbf{T}(W_r) \subseteq W_r$ .

*Proof.* It is a straightforward consequence of Lemma 1.6.  $\square$

We continue with the following result providing an estimate needed to derive next the required continuity and compactness properties of the operator  $\mathbf{T}$  (cf. (1.25)).

**Lemma 1.9.** *Let  $r \in (0, r_0)$ , with  $r_0$  given by (1.37), and let  $W_r := \{\mathbf{z}_S \in \mathbf{H}_{\Gamma_S}^1(\Omega_S) : \|\mathbf{z}_S\|_{1,\Omega_S} \leq r\}$ . Then there exists a positive constant  $C_{\mathbf{T}}$ , depending on  $\kappa_1$ ,  $\|\mathbf{i}_c\|$ , and  $\alpha_0(\Omega)$  (cf. (1.36)), such that*

$$\|\mathbf{T}(\mathbf{z}_S) - \mathbf{T}(\tilde{\mathbf{z}}_S)\|_{1,\Omega_S} \leq C_{\mathbf{T}} \|\mathbf{T}(\tilde{\mathbf{z}}_S)\|_{1,\Omega_S} \|\mathbf{z}_S - \tilde{\mathbf{z}}_S\|_{L^4(\Omega_S)} \quad \forall \mathbf{z}_S, \tilde{\mathbf{z}}_S \in W_r. \quad (1.48)$$

*Proof.* Given  $r$  as indicated and  $\mathbf{z}_S, \tilde{\mathbf{z}}_S \in W_r$ , we let  $\mathbf{u}_S = \mathbf{T}(\mathbf{z}_S)$  and  $\tilde{\mathbf{u}}_S = \mathbf{T}(\tilde{\mathbf{z}}_S)$ . According to the definition of  $\mathbf{T}$  (cf. (1.25)), it follows that

$$\begin{aligned} [\mathbf{A}(\mathbf{z}_S)(\mathbf{t}, \underline{\varphi}), (\mathbf{r}, \underline{\psi})] + [\mathbf{B}(\mathbf{r}, \underline{\psi}), \mathbf{p}] &= [\mathbf{F}, (\mathbf{r}, \underline{\psi})] \quad \forall (\mathbf{r}, \underline{\psi}) \in \mathbb{X}, \\ [\mathbf{B}(\mathbf{t}, \underline{\varphi}), \mathbf{q}] &= [\mathbf{G}, \mathbf{q}] \quad \forall \mathbf{q} \in \mathbb{M}, \end{aligned}$$

and

$$\begin{aligned} [\mathbf{A}(\tilde{\mathbf{z}}_S)(\tilde{\mathbf{t}}, \tilde{\underline{\varphi}}), (\mathbf{r}, \underline{\psi})] + [\mathbf{B}(\mathbf{r}, \underline{\psi}), \tilde{\mathbf{p}}] &= [\mathbf{F}, (\mathbf{r}, \underline{\psi})] \quad \forall (\mathbf{r}, \underline{\psi}) \in \mathbb{X}, \\ [\mathbf{B}(\tilde{\mathbf{t}}, \tilde{\underline{\varphi}}), \mathbf{q}] &= [\mathbf{G}, \mathbf{q}] \quad \forall \mathbf{q} \in \mathbb{M}. \end{aligned}$$

Then, recalling the definition of  $\mathbf{A}$ ,  $\mathbf{B}$ ,  $\mathbf{F}$  and  $\mathbf{G}$ , in (1.18), (1.20) and (1.17), respectively, we subtract both problems to obtain

$$\begin{aligned} [(a_1 + a_2(\mathbf{z}_S))(\mathbf{t}) - (a_1 + a_2(\tilde{\mathbf{z}}_S))(\tilde{\mathbf{t}}), \mathbf{r}] + [b(\mathbf{r}), \underline{\varphi} - \tilde{\underline{\varphi}}] + [B_1(\mathbf{r}), p_D - \tilde{p}_D] &= 0, \\ [b(\mathbf{t} - \tilde{\mathbf{t}}), \underline{\psi}] - [c(\underline{\varphi} - \tilde{\underline{\varphi}}), \underline{\psi}] + [B_2(\underline{\psi}), l - \tilde{l}] &= 0, \\ [B_1(\mathbf{t} - \tilde{\mathbf{t}}), q_D] &= 0, \\ [B_2(\underline{\varphi} - \tilde{\underline{\varphi}}), j] &= 0, \end{aligned}$$



for all  $(\underline{\mathbf{r}}, \underline{\psi}, q_D, j) \in \mathbf{X} \times \mathbf{M} \times L_0^2(\Omega_D) \times \mathbb{R}$ . In particular, taking  $\underline{\mathbf{r}} = \underline{\mathbf{t}} - \tilde{\underline{\mathbf{t}}}$ ,  $\underline{\psi} = \underline{\varphi} - \tilde{\underline{\varphi}}$ ,  $q_D = p_D - \tilde{p}_D$  and  $j = l - \tilde{l}$  in the latter system, we get

$$[(a_1 + a_2(\mathbf{z}_S))(\underline{\mathbf{t}}) - (a_1 + a_2(\tilde{\mathbf{z}}_S))(\tilde{\underline{\mathbf{t}}}), \underline{\mathbf{t}} - \tilde{\underline{\mathbf{t}}}] = -[c(\underline{\varphi} - \tilde{\underline{\varphi}}), \underline{\varphi} - \tilde{\underline{\varphi}}]. \quad (1.49)$$

Hence, adding and subtracting  $a_2(\mathbf{z}_S)(\tilde{\underline{\mathbf{t}}})$  in the second term on the left hand side of (1.49), and using the strong monotonicity of  $a(\mathbf{z}_S) = a_1 + a_2(\mathbf{z}_S)$  (cf. (1.38)), and the fact that  $c$  is positive semi-definite (cf. (1.40)), it follows that

$$\frac{\alpha_0(\Omega)}{2} \|\underline{\mathbf{t}} - \tilde{\underline{\mathbf{t}}}\|_{\mathbf{X}}^2 \leq [a_2(\tilde{\mathbf{z}}_S - \mathbf{z}_S)(\tilde{\underline{\mathbf{t}}}), \underline{\mathbf{t}} - \tilde{\underline{\mathbf{t}}}].$$

In this way, by applying the first inequality in (1.32) and then bounding  $\|\tilde{\mathbf{u}}_S\|_{\mathbf{L}^4(\Omega_S)}$  by  $\|\mathbf{i}_c\| \|\tilde{\mathbf{u}}_S\|_{1, \Omega_S}$ , we deduce that

$$\|\underline{\mathbf{t}} - \tilde{\underline{\mathbf{t}}}\|_{\mathbf{X}} \leq \frac{2(\kappa_1^2 + 1)^{1/2} \|\mathbf{i}_c\|}{\alpha_0(\Omega)} \|\tilde{\mathbf{u}}_S\|_{1, \Omega_S} \|\mathbf{z}_S - \tilde{\mathbf{z}}_S\|_{\mathbf{L}^4(\Omega_S)},$$

which implies (1.48) with

$$C_{\mathbf{T}} := \frac{2(\kappa_1^2 + 1)^{1/2} \|\mathbf{i}_c\|}{\alpha_0(\Omega)}, \quad (1.50)$$

thus completing the proof.  $\square$

Owing to the above analysis, we establish now the announced properties of the operator  $\mathbf{T}$ .

**Lemma 1.10.** *Given  $r \in (0, r_0)$ , with  $r_0$  defined by (1.37), we let  $W_r := \{\mathbf{z}_S \in \mathbf{H}_{\Gamma_S}^1(\Omega_S) : \|\mathbf{z}_S\|_{1, \Omega_S} \leq r\}$ , and assume that the data  $\mathbf{f}_S$  and  $f_D$  satisfy (1.47). Then,  $\mathbf{T} : W_r \rightarrow W_r$  is continuous and  $\overline{\mathbf{T}(W_r)}$  is compact.*

*Proof.* The required result follows straightforwardly from estimate (1.48) and the compactness of  $\mathbf{i}_c : \mathbf{H}^1(\Omega_S) \rightarrow \mathbf{L}^4(\Omega_S)$ . We omit further details and refer to [28, Lemma 3.8].  $\square$

We are now in position of establishing the main result of this section.

**Theorem 1.11.** *Suppose that the parameters  $\kappa_i$ ,  $i \in \{1, \dots, 4\}$ , satisfy the conditions required by Lemma 1.6. In addition, given  $r \in (0, r_0)$ , with  $r_0$  defined by (1.37), we let  $W_r := \{\mathbf{z}_S \in \mathbf{H}_{\Gamma_S}^1(\Omega_S) : \|\mathbf{z}_S\|_{1, \Omega_S} \leq r\}$ , and assume that the data  $\mathbf{f}_S$  and  $f_D$  satisfy (1.47). Then, the augmented fully-mixed formulation (1.16) has a unique solution  $((\underline{\mathbf{t}}, \underline{\varphi}), \underline{\mathbf{p}}) \in \mathbf{X} \times \mathbf{M}$  with  $\mathbf{u}_S \in W_r$ , and there holds*

$$\|((\underline{\mathbf{t}}, \underline{\varphi}), \underline{\mathbf{p}})\|_{\mathbf{X} \times \mathbf{M}} \leq c_{\mathbf{T}} \left\{ \|\mathbf{f}_S\|_{0, \Omega_S} + \|f_D\|_{0, \Omega_D} \right\}. \quad (1.51)$$

*Proof.* The equivalence between (1.16) and the fixed point equation (1.27), together with Lemmas 1.8 and 1.10, confirm the existence of solution of (1.16) as a direct application of the Schauder fixed point Theorem 1.7. In addition, it is clear that the estimate (1.51) follows straightforwardly from (1.44). On the other hand, using the estimate (1.48), the continuity of the compact injection  $\mathbf{i}_c$ , and the definitions of  $C_{\mathbf{T}}$  (cf. (1.50)) and  $r_0$  (cf. (1.37)), we easily obtain

$$\|\mathbf{T}(\mathbf{z}_S) - \mathbf{T}(\tilde{\mathbf{z}}_S)\|_{1, \Omega_S} \leq \frac{r}{r_0} \|\mathbf{z}_S - \tilde{\mathbf{z}}_S\|_{1, \Omega_S},$$

which, thanks to the Banach fixed point Theorem, implies that the solution is actually unique.  $\square$

We end this section by remarking, similarly as we did for one of the hypotheses of Lemma 1.2 right after its proof, that condition (1.47), rather than having a physical meaning, is an assumption ensuring existence and uniqueness of solution of problem (1.16), which is consistent with the classical results for the Navier–Stokes equation ([100, Chapter IV, Section 2]), as well as with recent results for the Navier–Stokes/Darcy coupled problem ([11, 65]).

## 1.4 The Galerkin scheme

In this section we introduce the Galerkin scheme of problem (1.16) and analyse its well-posedness by establishing suitable assumptions on the finite element subspaces involved.

### 1.4.1 Discrete setting

We first introduce a set of arbitrary discrete subspaces, namely

$$\begin{aligned} L_h^2(\Omega_\star) &\subset L^2(\Omega_\star), \quad \mathbf{H}_h(\Omega_\star) \subset \mathbf{H}(\mathbf{div}; \Omega_\star), \quad \star \in \{\mathbf{S}, \mathbf{D}\}, \\ \mathbf{H}_h^1(\Omega_\mathbf{S}) &\subset \mathbf{H}^1(\Omega_\mathbf{S}), \quad \mathbb{L}_{\text{skew},h}^2(\Omega_\mathbf{S}) \subset \mathbb{L}_{\text{skew}}^2(\Omega_\mathbf{S}), \quad \Lambda_h^\mathbf{S}(\Sigma) \subset H_{00}^{1/2}(\Sigma), \quad \Lambda_h^\mathbf{D}(\Sigma) \subset H^{1/2}(\Sigma), \end{aligned} \quad (1.52)$$

and set

$$\begin{aligned} \mathbb{H}_h(\Omega_\mathbf{S}) &:= \{\boldsymbol{\tau}_\mathbf{S} \in \mathbb{H}(\mathbf{div}; \Omega_\mathbf{S}) : \mathbf{c}^\mathbf{t} \boldsymbol{\tau} \in \mathbf{H}_h(\Omega_\mathbf{S}) \quad \forall \mathbf{c} \in \mathbb{R}^n\}, \\ \mathbb{H}_{h,0}(\Omega_\mathbf{S}) &:= \mathbb{H}_h(\Omega_\mathbf{S}) \cap \mathbb{H}_0(\mathbf{div}; \Omega_\mathbf{S}), \\ \mathbf{H}_{h,\Gamma_\mathbf{S}}^1(\Omega_\mathbf{S}) &:= \mathbf{H}_h^1(\Omega_\mathbf{S}) \cap \mathbf{H}_{\Gamma_\mathbf{S}}^1(\Omega_\mathbf{S}), \\ \mathbf{H}_{h,0}(\Omega_\mathbf{D}) &:= \mathbf{H}_h(\Omega_\mathbf{D}) \cap \mathbf{H}_0(\mathbf{div}; \Omega_\mathbf{D}), \\ \mathbb{L}_{\text{tr},h}^2(\Omega_\mathbf{S}) &:= [L_h^2(\Omega_\mathbf{S})]^{n \times n} \cap \mathbb{L}_{\text{tr}}^2(\Omega_\mathbf{S}), \\ L_{h,0}^2(\Omega_\mathbf{D}) &:= L_h^2(\Omega_\mathbf{D}) \cap L_0^2(\Omega_\mathbf{D}), \\ \Lambda_h^\mathbf{S}(\Sigma) &:= [\Lambda_h^\mathbf{S}(\Sigma)]^n. \end{aligned} \quad (1.53)$$

Then, defining the global spaces, unknowns, and test functions as follows

$$\begin{aligned} \mathbf{X}_h &:= \mathbb{L}_{\text{tr},h}^2(\Omega_\mathbf{S}) \times \mathbb{H}_{h,0}(\Omega_\mathbf{S}) \times \mathbf{H}_{h,\Gamma_\mathbf{S}}^1(\Omega_\mathbf{S}) \times \mathbb{L}_{\text{skew},h}^2(\Omega_\mathbf{S}) \times \mathbf{H}_{h,0}(\Omega_\mathbf{D}), \\ \mathbf{M}_h &:= \Lambda_h^\mathbf{S}(\Sigma) \times \Lambda_h^\mathbf{D}(\Sigma), \quad \mathbb{X}_h := \mathbf{X}_h \times \mathbf{M}_h, \quad \mathbb{M}_h := L_{h,0}^2(\Omega_\mathbf{D}) \times \mathbb{R}, \\ \underline{\mathbf{t}}_h &:= (\mathbf{t}_{\mathbf{S},h}, \boldsymbol{\sigma}_{\mathbf{S},h}, \mathbf{u}_{\mathbf{S},h}, \boldsymbol{\rho}_{\mathbf{S},h}, \mathbf{u}_{\mathbf{D},h}) \in \mathbf{X}_h, \quad \underline{\boldsymbol{\varphi}}_h := (\boldsymbol{\varphi}_h, \lambda_h) \in \mathbf{M}_h, \\ \underline{\mathbf{r}}_h &:= (\mathbf{r}_{\mathbf{S},h}, \boldsymbol{\tau}_{\mathbf{S},h}, \mathbf{v}_{\mathbf{S},h}, \boldsymbol{\eta}_{\mathbf{S},h}, \mathbf{v}_{\mathbf{D},h}) \in \mathbf{X}_h, \quad \underline{\boldsymbol{\psi}}_h := (\boldsymbol{\psi}_h, \xi_h) \in \mathbf{M}_h, \\ \underline{\mathbf{p}}_h &:= (p_{\mathbf{D},h}, l_h) \in \mathbb{M}_h, \quad \text{and} \quad \underline{\mathbf{q}}_h := (q_{\mathbf{D},h}, j_h) \in \mathbb{M}_h, \end{aligned} \quad (1.54)$$

the Galerkin scheme associated with problem (1.16) reads: Find  $((\underline{\mathbf{t}}_h, \underline{\boldsymbol{\varphi}}_h), \underline{\mathbf{p}}_h) \in \mathbb{X}_h \times \mathbb{M}_h$  such that

$$\begin{aligned} [\mathbf{A}(\mathbf{u}_{\mathbf{S},h})(\underline{\mathbf{t}}_h, \underline{\boldsymbol{\varphi}}_h), (\underline{\mathbf{r}}_h, \underline{\boldsymbol{\psi}}_h)] + [\mathbf{B}(\underline{\mathbf{r}}_h, \underline{\boldsymbol{\psi}}_h), \underline{\mathbf{p}}_h] &= [\mathbf{F}, (\underline{\mathbf{r}}_h, \underline{\boldsymbol{\psi}}_h)] \quad \forall (\underline{\mathbf{r}}_h, \underline{\boldsymbol{\psi}}_h) \in \mathbb{X}_h, \\ [\mathbf{B}(\underline{\mathbf{t}}_h, \underline{\boldsymbol{\varphi}}_h), \underline{\mathbf{q}}_h] &= [\mathbf{G}, \underline{\mathbf{q}}_h] \quad \forall \underline{\mathbf{q}}_h \in \mathbb{M}_h. \end{aligned} \quad (1.55)$$

Now, we proceed similarly to [93] and [88] (see also [27]), and derive suitable hypotheses on the spaces (1.52) ensuring the well-posedness of problem (1.55). We begin by noticing that, in order to have meaningful spaces  $\mathbb{H}_{h,0}(\Omega_S)$  and  $L_{h,0}^2(\Omega_D)$ , we need to be able to eliminate multiples of the identity matrix and constant polynomials from  $\mathbb{H}_h(\Omega_S)$  and  $L_h^2(\Omega_D)$ , respectively. This requirement is certainly satisfied if we assume:

**(H.0)**  $[P_0(\Omega_S)]^n \subseteq \mathbf{H}_h(\Omega_S)$  and  $P_0(\Omega_D) \subseteq L_h^2(\Omega_D)$ , where  $P_0(\Omega_S)$  and  $P_0(\Omega_D)$  are the spaces of constant polynomials on  $\Omega_S$  and  $\Omega_D$ , respectively. In particular, it follows that  $\mathbb{I} \in \mathbb{H}_h(\Omega_S)$  for all  $h$ , and hence there holds the decomposition

$$\mathbb{H}_h(\Omega_S) = \mathbb{H}_{h,0}(\Omega_S) \oplus P_0(\Omega_S)\mathbb{I}. \quad (1.56)$$

Next, we look at the discrete kernel of  $\mathbf{B}$ , which is given by

$$\mathbb{V}_h := \left\{ (\mathbf{r}_h, \underline{\psi}_h) \in \mathbb{X}_h : \quad [\mathbf{B}(\mathbf{r}_h, \underline{\psi}_h), \underline{\mathbf{q}}_h] = 0 \quad \forall \underline{\mathbf{q}}_h \in \mathbb{M}_h \right\}.$$

In order to have a more explicit definition of  $\mathbb{V}_h$ , we introduce the following assumption:

**(H.1)**  $\operatorname{div} \mathbf{H}_h(\Omega_D) \subseteq L_h^2(\Omega_D)$ .

Then, owing to **(H.1)** and recalling the definition of  $\mathbf{B}$  (cf. (1.20)), it follows that  $\mathbb{V}_h = \tilde{\mathbf{X}}_h \times \tilde{\mathbf{M}}_h$ , where

$$\tilde{\mathbf{X}}_h = \mathbb{L}_{\operatorname{tr},h}^2(\Omega_S) \times \mathbb{H}_{h,0}(\Omega_S) \times \mathbf{H}_{h,\Gamma_S}^1(\Omega_S) \times \mathbb{L}_{\operatorname{skew},h}^2(\Omega_S) \times \tilde{\mathbf{H}}_{h,0}(\Omega_D)$$

and

$$\tilde{\mathbf{M}}_h = \tilde{\Lambda}_h^S(\Sigma) \times \Lambda_h^D(\Sigma),$$

with

$$\tilde{\mathbf{H}}_{h,0}(\Omega_D) := \left\{ \mathbf{v}_{D,h} \in \mathbf{H}_{h,0}(\Omega_D) : \quad \operatorname{div}(\mathbf{v}_{D,h}) \in P_0(\Omega_D) \right\},$$

and

$$\tilde{\Lambda}_h^S(\Sigma) := \left\{ \psi_h \in \Lambda_h^S(\Sigma) : \quad \langle \psi_h \cdot \mathbf{n}, 1 \rangle_\Sigma = 0 \right\}. \quad (1.57)$$

In particular, it readily follows that  $\mathbb{V}_h \subseteq \mathbb{V}$ .

On the other hand, for the subsequent analysis we need to ensure the discrete version of the inf-sup conditions (1.42) and (1.43) of  $b$  and  $\mathbf{B}$  (cf. (1.20)), respectively, namely the existence of constants  $\tilde{\beta}_1, \tilde{\beta} > 0$ , independent of  $h$ , such that

$$\sup_{\substack{\mathbf{r}_h \in \tilde{\mathbf{X}}_h \\ \mathbf{r}_h \neq \mathbf{0}}} \frac{[b(\mathbf{r}_h), \underline{\psi}_h]}{\|\mathbf{r}_h\|_{\mathbf{X}}} \geq \tilde{\beta}_1 \|\underline{\psi}_h\|_{\mathbf{M}} \quad \forall \underline{\psi}_h \in \tilde{\mathbf{M}}_h, \quad (1.58)$$

and

$$\sup_{\substack{(\mathbf{r}_h, \underline{\psi}_h) \in \mathbb{X}_h \\ (\mathbf{r}_h, \underline{\psi}_h) \neq \mathbf{0}}} \frac{[\mathbf{B}(\mathbf{r}_h, \underline{\psi}_h), \underline{\mathbf{q}}_h]}{\|(\mathbf{r}_h, \underline{\psi}_h)\|_{\mathbb{X}}} \geq \tilde{\beta} \|\underline{\mathbf{q}}_h\|_{\mathbb{M}} \quad \forall \underline{\mathbf{q}}_h \in \mathbb{M}_h. \quad (1.59)$$

For (1.58) we apply the same diagonal argument utilized in [88, Section 5.2] (see also [93, Lemma 3.8]) to deduce that  $b$  satisfies the discrete inf-sup condition (1.58) if and only if the following hypothesis holds:

(H.2) There exist  $\widehat{\beta}_S, \widehat{\beta}_D > 0$ , independent of  $h$ , such that

$$\sup_{\substack{\boldsymbol{\tau}_{S,h} \in \mathbb{H}_h(\Omega_S) \\ \boldsymbol{\tau}_{S,h} \neq \mathbf{0}}} \frac{\langle \boldsymbol{\tau}_{S,h} \mathbf{n}, \boldsymbol{\psi}_h \rangle_\Sigma}{\|\boldsymbol{\tau}_{S,h}\|_{\text{div}, \Omega_S}} \geq \widehat{\beta}_S \|\boldsymbol{\psi}_h\|_{1/2, 00, \Sigma} \quad \forall \boldsymbol{\psi}_h \in \tilde{\Lambda}_h^S(\Sigma), \quad (1.60)$$

$$\sup_{\substack{\mathbf{v}_{D,h} \in \mathbf{H}_{h,0}(\Omega_D) \\ \mathbf{v}_{D,h} \neq \mathbf{0}}} \frac{\langle \mathbf{v}_{D,h} \mathbf{n}, \boldsymbol{\xi}_h \rangle_\Sigma}{\|\mathbf{v}_{D,h}\|_{\text{div}, \Omega_D}} \geq \widehat{\beta}_D \|\boldsymbol{\xi}_h\|_{1/2, \Sigma} \quad \forall \boldsymbol{\xi}_h \in \Lambda_h^D(\Sigma). \quad (1.61)$$

Similarly, employing the same arguments in [88, Section 5.2] we obtain that  $\mathbf{B}$  satisfies the discrete inf-sup condition (1.59) provided that the following hypothesis holds

(H.3) There exist  $\tilde{\beta}_D > 0$ , independent of  $h$ , and  $\boldsymbol{\psi}_0 \in \mathbf{H}_{00}^{1/2}(\Sigma)$ , such that

$$\boldsymbol{\psi}_0 \in \Lambda_h^S(\Sigma) \quad \forall h \quad \text{and} \quad \langle \boldsymbol{\psi}_0 \cdot \mathbf{n}, 1 \rangle_\Sigma \neq 0, \quad (1.62)$$

$$\sup_{\substack{\mathbf{v}_{D,h} \in \mathbf{H}_{h,0}(\Omega_D) \\ \mathbf{v}_{D,h} \neq \mathbf{0}}} \frac{(\text{div } \mathbf{v}_{D,h}, q_{D,h})_D}{\|\mathbf{v}_{D,h}\|_{\text{div}, \Omega_D}} \geq \tilde{\beta}_D \|q_{D,h}\|_{0, \Omega_D} \quad \forall q_{D,h} \in L_{h,0}^2(\Omega_D). \quad (1.63)$$

### 1.4.2 Well-posedness of the discrete problem

In what follows, we assume that hypotheses (H.0), (H.1), (H.2), and (H.3) hold, and, analogously to the analysis of the continuous problem, apply a fixed point argument to prove the well-posedness of the Galerkin scheme (1.55). To that end, we let  $\mathbf{T}_h : \mathbf{H}_{h,\Gamma_S}^1(\Omega_S) \rightarrow \mathbf{H}_{h,\Gamma_S}^1(\Omega_S)$  be the discrete operator defined by

$$\mathbf{T}_h(\mathbf{z}_{S,h}) := \mathbf{u}_{S,h} \quad \forall \mathbf{z}_{S,h} \in \mathbf{H}_{h,\Gamma_S}^1(\Omega_S), \quad (1.64)$$

where  $\mathbf{u}_{S,h}$  is the third component of  $\mathbf{t}_h$ , which in turn is the first component of the unique solution (to be confirmed below) of the discrete nonlinear problem: Find  $((\mathbf{t}_h, \underline{\boldsymbol{\varphi}}_h), \mathbf{p}_h) \in \mathbb{X}_h \times \mathbb{M}_h$  such that

$$\begin{aligned} [\mathbf{A}(\mathbf{z}_h)(\mathbf{t}_h, \underline{\boldsymbol{\varphi}}_h), (\mathbf{r}_h, \underline{\boldsymbol{\psi}}_h)] + [\mathbf{B}(\mathbf{r}_h, \underline{\boldsymbol{\psi}}_h), \mathbf{p}_h] &= [\mathbf{F}, (\mathbf{r}_h, \underline{\boldsymbol{\psi}}_h)] \quad \forall (\mathbf{r}_h, \underline{\boldsymbol{\psi}}_h) \in \mathbb{X}_h, \\ [\mathbf{B}(\mathbf{t}_h, \underline{\boldsymbol{\varphi}}_h), \mathbf{q}_h] &= [\mathbf{G}, \mathbf{q}_h] \quad \forall \mathbf{q}_h \in \mathbb{M}_h. \end{aligned} \quad (1.65)$$

Then, similarly as for the continuous case, the Galerkin scheme (1.55) can be rewritten, equivalently, as the fixed point problem: Find  $\mathbf{u}_{S,h} \in \mathbf{H}_{h,\Gamma_S}^1(\Omega_S)$  such that

$$\mathbf{T}_h(\mathbf{u}_{S,h}) = \mathbf{u}_{S,h}. \quad (1.66)$$

Now, in order to prove the well-posedness of problem (1.55), or equivalently the well-definiteness of operator  $\mathbf{T}_h$  (cf. (1.64)), we will require the following discrete version of Theorem 1.1 (cf. [88, Theorem 3.3]).

**Theorem 1.12.** *In addition to the spaces and operators defined in Theorem 1.1, let  $X_{1,h}, M_{1,h}$ , and  $M_h$  be finite dimensional subspaces of  $X_1, M_1$ , and  $M$ , respectively, and let  $X_h := X_{1,h} \times M_{1,h} \subseteq X := X_1 \times M_1$ . In turn, let  $V_h$  be the discrete kernel of  $B$ , that is,*

$$V_h := \left\{ (\mathbf{r}_h, \boldsymbol{\psi}_h) \in X_h : \quad [B(\mathbf{r}_h, \boldsymbol{\psi}_h), q_h] = 0 \quad \forall q_h \in M_h \right\},$$

and let  $\tilde{X}_{1,h}$  and  $\tilde{M}_{1,h}$  be subspaces of  $X_{1,h}$  and  $M_{1,h}$  respectively, such that  $V_h = \tilde{X}_{1,h} \times \tilde{M}_{1,h}$ . Assume that

- (i)  $A_1|_{\tilde{X}_{1,h}} : \tilde{X}_{1,h} \rightarrow \tilde{X}'_{1,h}$  is Lipschitz continuous and strongly monotone, that is, there exist constants  $\gamma_h, \alpha_h > 0$  such that

$$\|A_1(\mathbf{s}_h) - A_1(\mathbf{r}_h)\|_{\tilde{X}'_{1,h}} \leq \gamma_h \|\mathbf{s}_h - \mathbf{r}_h\|_{X_1} \quad \forall \mathbf{s}_h, \mathbf{r}_h \in \tilde{X}_{1,h}$$

and

$$[A_1(\mathbf{s}_h) - A_1(\mathbf{r}_h), \mathbf{s}_h - \mathbf{r}_h] \geq \alpha_h \|\mathbf{s}_h - \mathbf{r}_h\|_{X_1}^2 \quad \forall \mathbf{s}_h, \mathbf{r}_h \in \tilde{X}_{1,h}.$$

- (ii) For each pair  $(\mathbf{r}_h, \mathbf{r}_h^\perp) \in \tilde{X}_{1,h} \times \tilde{X}_{1,h}^\perp$  there holds the pseudolinear property

$$A_1(\mathbf{r}_h + \mathbf{r}_h^\perp) = A_1(\mathbf{r}_h) + A_1(\mathbf{r}_h^\perp).$$

- (iii)  $S$  is positive semi-definite on  $\tilde{M}_{1,h}$ , that is,

$$[S(\boldsymbol{\psi}_h), \boldsymbol{\psi}_h] \geq 0 \quad \forall \boldsymbol{\psi}_h \in \tilde{M}_{1,h}.$$

- (iv)  $B_1$  satisfies an inf-sup condition on  $\tilde{X}_{1,h} \times \tilde{M}_{1,h}$ , that is, there exists  $\beta_{1,h} > 0$  such that

$$\sup_{\substack{\mathbf{r}_h \in \tilde{X}_{1,h} \\ \mathbf{r}_h \neq \mathbf{0}}} \frac{[B_1(\mathbf{r}_h), \boldsymbol{\psi}_h]}{\|\mathbf{r}_h\|_{X_1}} \geq \beta_{1,h} \|\boldsymbol{\psi}_h\|_{M_{1,h}} \quad \forall \boldsymbol{\psi}_h \in \tilde{M}_{1,h}.$$

- (v)  $B$  satisfies an inf-sup condition on  $X_h \times M_h$ , that is, there exists  $\beta_h > 0$  such that

$$\sup_{\substack{(\mathbf{r}_h, \boldsymbol{\psi}_h) \in X_h \\ (\mathbf{r}_h, \boldsymbol{\psi}_h) \neq \mathbf{0}}} \frac{[B(\mathbf{r}_h, \boldsymbol{\psi}_h), q_h]}{\|(\mathbf{r}_h, \boldsymbol{\psi}_h)\|_X} \geq \beta_h \|q_h\|_M \quad \forall q_h \in M_h.$$

Then, there exists a unique  $((\mathbf{t}_h, \boldsymbol{\varphi}_h), p_h) \in X_h \times M_h$ , such that

$$\begin{aligned} [A(\mathbf{t}_h, \boldsymbol{\varphi}_h), (\mathbf{r}_h, \boldsymbol{\psi}_h)] + [B'(p_h), (\mathbf{r}_h, \boldsymbol{\psi}_h)] &= [F, (\mathbf{r}_h, \boldsymbol{\psi}_h)] \quad \forall (\mathbf{r}_h, \boldsymbol{\psi}_h) \in X_h, \\ [B(\mathbf{t}_h, \boldsymbol{\varphi}_h), q_h] &= [G, q_h] \quad \forall q_h \in M_h. \end{aligned} \tag{1.67}$$

Moreover, there exists  $C_h > 0$ , depending only on  $\alpha_h, \gamma_h, \beta_{1,h}, \beta_h, \|S\|$ , and  $\|B_1\|$  such that

$$\|((\mathbf{t}_h, \boldsymbol{\varphi}_h), p_h)\|_{X \times M} \leq C_h \left\{ \|F\|_{X_h} \|X'_h\| + \|G\|_{M_h} \|M'_h\| \right\}.$$

The following lemma establishes the well-definiteness of operator  $\mathbf{T}_h$  (cf. (1.64)).

**Lemma 1.13.** Assume that hypotheses (H.0), (H.1), (H.2), and (H.3) hold. Assume further that  $\kappa_i, i \in \{1, \dots, 4\}$  satisfy the conditions required by Lemma 1.6. Then, for each  $r \in (0, r_0)$ , with  $r_0$  given by (1.37), the problem (1.65) has a unique solution  $((\mathbf{t}_h, \boldsymbol{\varphi}_h), \mathbf{p}_h) \in \mathbb{X} \times \mathbb{M}$  for each  $\mathbf{z}_{S,h} \in \mathbf{H}_{h,\Gamma_S}^1(\Omega_S)$  such that  $\|\mathbf{z}_{S,h}\|_{1,\Omega_S} \leq r$ . Moreover, there exists a constant  $\tilde{c}_{\mathbf{T}} > 0$ , independent of  $\mathbf{z}_{S,h}$  and the data  $\mathbf{f}_S$  and  $f_D$ , such that there holds

$$\|\mathbf{T}_h(\mathbf{z}_{S,h})\|_{1,\Omega_S} \leq \|((\mathbf{t}_h, \boldsymbol{\varphi}_h), \mathbf{p}_h)\|_{\mathbb{X} \times \mathbb{M}} \leq \tilde{c}_{\mathbf{T}} \left\{ \|\mathbf{f}_S\|_{0,\Omega_S} + \|f_D\|_{0,\Omega_D} \right\}. \tag{1.68}$$

*Proof.* Let  $\mathbf{z}_{S,h} \in \mathbf{H}_{h,\Gamma_S}^1(\Omega_S)$  such that  $\|\mathbf{z}_{S,h}\|_{1,\Omega_S} \leq r$ . Recalling that  $\mathbb{X}_h \subseteq \mathbb{X}$ ,  $\mathbb{M}_h \subseteq \mathbb{M}$  (cf. (1.54)) and  $\mathbb{V}_h \subseteq \mathbb{V}$ , a straightforward application of Lemmas 1.2, 1.3 and 1.4, implies, respectively, that hypotheses (i), (ii) and (iii) in Theorem 1.12, hold. In turn, as already discussed in Section 1.4.1, the inf-sup conditions (iv) and (v) follow from hypotheses (H.2) and (H.3), respectively. Therefore, according to the above, a direct application of Theorem 1.12 allows us to conclude that there exists a unique  $((\underline{\mathbf{t}}_h, \underline{\boldsymbol{\varphi}}_h), \underline{\mathbf{p}}_h) \in \mathbb{X}_h \times \mathbb{M}_h$  solution to (1.65), which satisfies

$$\|((\underline{\mathbf{t}}_h, \underline{\boldsymbol{\varphi}}_h), \underline{\mathbf{p}}_h)\|_{\mathbb{X} \times \mathbb{M}} \leq \tilde{c}_{\mathbf{T}} \left\{ \|\mathbf{f}_S\|_{0,\Omega_S} + \|f_D\|_{0,\Omega_D} \right\},$$

with  $\tilde{c}_{\mathbf{T}}$  independent of  $\mathbf{z}_{S,h}$  and  $h$ .  $\square$

We are now in position of establishing the well-posedness of (1.55).

**Theorem 1.14.** *Assume that hypotheses (H.0), (H.1), (H.2), and (H.3) hold. Assume further that  $\kappa_i$ ,  $i \in \{1, \dots, 4\}$  satisfy the conditions required by Lemma 1.6. In addition, given  $r \in (0, r_0)$ , with  $r_0$  defined by (1.37), let  $W_r^h := \left\{ \mathbf{z}_{S,h} \in \mathbf{H}_{h,\Gamma_S}^1(\Omega_S) : \|\mathbf{z}_{S,h}\|_{1,\Omega_S} \leq r \right\}$ , and assume that the data  $\mathbf{f}_S$  and  $f_D$  satisfy*

$$\tilde{c}_{\mathbf{T}} \left\{ \|\mathbf{f}_S\|_{0,\Omega_S} + \|f_D\|_{0,\Omega_D} \right\} \leq r, \quad (1.69)$$

*with  $\tilde{c}_{\mathbf{T}} > 0$  the constant in (1.68). Then, there exists a unique  $((\underline{\mathbf{t}}_h, \underline{\boldsymbol{\varphi}}_h), \underline{\mathbf{p}}_h) \in \mathbb{X}_h \times \mathbb{M}_h$  solution to (1.55), which satisfies  $\mathbf{u}_{S,h} \in W_r^h$  and*

$$\|((\underline{\mathbf{t}}_h, \underline{\boldsymbol{\varphi}}_h), \underline{\mathbf{p}}_h)\|_{\mathbb{X} \times \mathbb{M}} \leq \tilde{c}_{\mathbf{T}} \left\{ \|\mathbf{f}_S\|_{0,\Omega_S} + \|f_D\|_{0,\Omega_D} \right\}. \quad (1.70)$$

*Proof.* We first observe, owing to (1.68), that the assumption (1.69) guarantees that  $\mathbf{T}_h(W_r^h) \subseteq W_r^h$ . Next, proceeding analogously to the proof of Lemma 1.9, that is, applying the strong monotonicity of  $a(\mathbf{z}_{S,h}) : \mathbf{X}_h \rightarrow \mathbf{X}'_h$  for each  $\mathbf{z}_{S,h} \in W_r^h$ , and using again the boundedness of the compact injection  $\mathbf{i}_c$ , we find that

$$\|\mathbf{T}_h(\mathbf{z}_{S,h}) - \mathbf{T}_h(\tilde{\mathbf{z}}_{S,h})\|_{1,\Omega_S} \leq C_{\mathbf{T}} \|\mathbf{i}_c\| \|\mathbf{T}_h(\tilde{\mathbf{z}}_{S,h})\|_{1,\Omega_S} \|\mathbf{z}_{S,h} - \tilde{\mathbf{z}}_{S,h}\|_{1,\Omega_S} \quad \forall \mathbf{z}_{S,h}, \tilde{\mathbf{z}}_{S,h} \in W_r^h,$$

which, together with (1.50), (1.68), (1.69), and the definition of  $r_0$  (cf. (1.37)), implies

$$\|\mathbf{T}_h(\mathbf{z}_{S,h}) - \mathbf{T}_h(\tilde{\mathbf{z}}_{S,h})\|_{1,\Omega_S} \leq \frac{r}{r_0} \|\mathbf{z}_{S,h} - \tilde{\mathbf{z}}_{S,h}\|_{1,\Omega_S} \quad \forall \mathbf{z}_{S,h}, \tilde{\mathbf{z}}_{S,h} \in W_r^h,$$

thus confirming that  $\mathbf{T}_h : W_r^h \rightarrow W_r^h$  is a contraction mapping. Then, the Banach fixed point Theorem and the equivalence between (1.55) and (1.66) imply the well-posedness of (1.55). In turn, the a priori estimate (1.70) follows directly from (1.68).  $\square$

## 1.5 A priori error estimate

In this section, we derive an a priori error estimate for the Galerkin scheme (1.55). To that end, we first establish some preliminary results that will be utilized in our subsequent analysis.

### 1.5.1 Preliminaries

We begin with the following Strang-type lemma,

**Lemma 1.15.** *Let  $X$  and  $M$  be Hilbert spaces,  $F \in (X \times M)' := X' \times M'$ , and  $P : X \times M \rightarrow X' \times M'$  a nonlinear operator. In addition, let  $\{X_n\}_{n \in N}$  and  $\{M_n\}_{n \in N}$  be sequences of finite dimensional subspaces of  $X$  and  $M$ , respectively, and for each  $n \in N$  consider a nonlinear operator  $P_n : X_n \times M_n \rightarrow (X_n \times M_n)' := X'_n \times M'_n$  and a functional  $F_n \in X'_n \times M'_n$ . Assume that the family  $\{P\} \cup \{P_n\}_{n \in N}$  is uniformly Lipschitz continuous with constant  $C_{LC} > 0$ . Moreover, assume that  $P_n$  has a hemi-continuous first-order Gâteaux derivative  $\mathcal{D}P_n(\vec{s})(\cdot, \cdot)$ , for all  $\vec{s} \in X \times M$ , which satisfies the global inf-sup condition*

$$C_G \|\vec{s}_n\| \leq \sup_{\substack{\vec{r}_n \in X_n \times M_n \\ \vec{r}_n \neq \mathbf{0}}} \frac{\mathcal{D}P_n(\vec{s})(\vec{s}_n, \vec{r}_n)}{\|\vec{r}_n\|} \quad \forall \vec{s}_n \in X_n \times M_n, \quad (1.71)$$

with a constant  $C_G > 0$  independent of  $\vec{s}$ . Furthermore, let  $\vec{t} := ((\mathbf{t}, \varphi), \mathbf{p}) \in X \times M$  and  $\vec{t}_n := ((\mathbf{t}_n, \varphi_n), p_n) \in X_n \times M_n$  be such that

$$[P(\vec{t}), \vec{r}] = [F, \vec{r}] \quad \forall \vec{r} := ((\mathbf{r}, \psi), \mathbf{q}) \in X \times M \quad (1.72)$$

and

$$[P_n(\vec{t}_n), \vec{r}_n] = [F_n, \vec{r}_n] \quad \forall \vec{r}_n := ((\mathbf{r}_n, \psi_n), \mathbf{q}_n) \in X_n \times M_n. \quad (1.73)$$

Then for each  $n \in N$ , there holds

$$\begin{aligned} \|\vec{t} - \vec{t}_n\| \leq & C_{ST} \left\{ \sup_{\substack{\vec{r}_n \in X_n \times M_n \\ \vec{r}_n \neq \mathbf{0}}} \frac{|[F, \vec{r}_n] - [F_n, \vec{r}_n]|}{\|\vec{r}_n\|} \right. \\ & \left. + \inf_{\substack{\vec{s}_n \in X_n \times M_n \\ \vec{s}_n \neq \mathbf{0}}} \left( \|\vec{t} - \vec{s}_n\| + \sup_{\substack{\vec{r}_n \in X_n \times M_n \\ \vec{r}_n \neq \mathbf{0}}} \frac{|[P(\vec{s}_n), \vec{r}_n] - [P_n(\vec{s}_n), \vec{r}_n]|}{\|\vec{r}_n\|} \right) \right\}, \end{aligned} \quad (1.74)$$

with  $C_{ST} := C_G^{-1} \max\{1, C_G + C_{LC}\}$ .

*Proof.* We proceed as in the proof of [84, Theorem 3.3] (see also [88, Theorem 3.5]). In fact, given  $\vec{t}_n, \vec{s}_n \in X_n \times M_n$ , we first observe that the hemi-continuity of  $\mathcal{D}P_n$  implies that there exists  $\mu_0 \in (0, 1)$ , such that

$$\begin{aligned} [P_n(\vec{t}_n), \vec{r}_n] - [P_n(\vec{s}_n), \vec{r}_n] &= \int_0^1 \mathcal{D}P_n(\mu \vec{t}_n + (1 - \mu) \vec{s}_n)(\vec{t}_n - \vec{s}_n, \vec{r}_n) d\mu \\ &= \mathcal{D}P_n(\mu_0 \vec{t}_n + (1 - \mu_0) \vec{s}_n)(\vec{t}_n - \vec{s}_n, \vec{r}_n), \end{aligned}$$

and hence, by taking  $\vec{s} = \mu_0 \vec{t}_n + (1 - \mu_0) \vec{s}_n$  in (1.71), we find that

$$\|\vec{t}_n - \vec{s}_n\| \leq C_G^{-1} \sup_{\substack{\vec{r}_n \in X_n \times M_n \\ \vec{r}_n \neq \mathbf{0}}} \frac{[P_n(\vec{t}_n), \vec{r}_n] - [P_n(\vec{s}_n), \vec{r}_n]}{\|\vec{r}_n\|}. \quad (1.75)$$

In turn, using (1.72) and (1.73), and adding and subtracting appropriate terms, we easily obtain

$$[P_n(\vec{t}_n), \vec{r}_n] - [P_n(\vec{s}_n), \vec{r}_n] = [F_n, \vec{r}_n] - [F, \vec{r}_n] + [P(\vec{t}), \vec{r}_n] - [P(\vec{s}_n), \vec{r}_n] + [P(\vec{s}_n), \vec{r}_n] - [P_n(\vec{s}_n), \vec{r}_n],$$

which, together with the Lipschitz continuity of  $P$ , implies

$$\left| [P_n(\vec{\mathbf{t}}_n), \vec{\mathbf{r}}_n] - [P_n(\vec{\mathbf{s}}_n), \vec{\mathbf{r}}_n] \right| \leq \left| [F, \vec{\mathbf{r}}_n] - [F_n, \vec{\mathbf{r}}_n] \right| + C_{\text{LC}} \|\vec{\mathbf{t}} - \vec{\mathbf{s}}_n\| \|\vec{\mathbf{r}}_n\| + \left| [P(\vec{\mathbf{s}}_n), \vec{\mathbf{r}}_n] - [P_n(\vec{\mathbf{s}}_n), \vec{\mathbf{r}}_n] \right|, \quad (1.76)$$

for all  $\vec{\mathbf{s}}_n \in X_n \times M_n$ . In this way, from (1.75), (1.76) and the triangle inequality we readily obtain (1.74), which concludes the proof.  $\square$

In addition, we will require the following linear version of Theorem 1.12.

**Theorem 1.16.** *Consider the notations and definitions given in Theorem 1.12. Assume that*

- (i)  $A_1|_{X_{1,h}} : X_{1,h} \rightarrow X'_{1,h}$  is linear, bounded and  $\tilde{X}_{1,h}$ -elliptic, that is, there exist  $\gamma_h, \alpha_h > 0$ , such that

$$\|A_1(\mathbf{r}_h)\|_{X'_{1,h}} \leq \gamma_h \|\mathbf{r}_h\|_{X_1} \quad \forall \mathbf{r}_h \in \tilde{X}_{1,h},$$

and

$$[A_1(\mathbf{r}_h), \mathbf{r}_h] \geq \alpha_h \|\mathbf{r}_h\|_{X_1}^2 \quad \forall \mathbf{r}_h \in \tilde{X}_{1,h}.$$

- (ii) The conditions (iii)-(v) from Theorem 1.12 are satisfied.

Then, there exists a unique  $((\mathbf{t}_h, \boldsymbol{\varphi}_h), p_h) \in X \times M$  solution of (1.67). Moreover, there exists  $C_h > 0$ , depending only on  $\alpha_h, \gamma_h, \beta_{1,h}, \beta_h, \|S\|$  and  $\|B_1\|$ , such that

$$\|((\mathbf{t}_h, \boldsymbol{\varphi}_h), p_h)\|_{X \times M} \leq C_h \{ \|F|_{X_h}\|_{X'_h} + \|G|_{M_h}\|_{M'_h} \}. \quad (1.77)$$

*Proof.* It reduces to verify the hypotheses of Theorem 1.12. We omit further details  $\square$

We observe here that (1.77) is equivalent to the global inf-sup condition

$$\|((\mathbf{s}_h, \boldsymbol{\psi}_h), \rho_h)\|_{X \times M} \leq C_h \sup_{((\mathbf{r}, \boldsymbol{\psi}), q) \in X_h \times M_h \setminus \mathbf{0}} \frac{[A(\mathbf{s}_h, \phi_h), (\mathbf{r}, \boldsymbol{\psi})] + [B'(\rho_h), (\mathbf{r}, \boldsymbol{\psi})] + [B(\mathbf{s}_h, \phi_h), q]}{\|((\mathbf{r}, \boldsymbol{\psi}), q)\|_{X \times M}}, \quad (1.78)$$

for all  $((\mathbf{s}_h, \boldsymbol{\psi}_h), \rho_h) \in X_h \times M_h$ .

### 1.5.2 The main result

In what follows, we establish the corresponding a priori error estimate of our Galerkin scheme (1.55). To that end, and for the sake of simplicity, hereafter we denote by  $\vec{\mathbf{t}} := ((\underline{\mathbf{t}}, \underline{\boldsymbol{\varphi}}), \underline{\mathbf{p}}) \in \mathbb{X} \times \mathbb{M}$  and  $\vec{\mathbf{t}}_h := ((\underline{\mathbf{t}}_h, \underline{\boldsymbol{\varphi}}_h), \underline{\mathbf{p}}_h) \in \mathbb{X}_h \times \mathbb{M}_h$  the solutions of problems (1.16) and (1.55), respectively. In turn, we let  $\mathbf{P} : \mathbb{X} \times \mathbb{M} \rightarrow (\mathbb{X} \times \mathbb{M})' := \mathbb{X}' \times \mathbb{M}'$  and  $\mathbf{P}_h : \mathbb{X}_h \times \mathbb{M}_h \rightarrow (\mathbb{X}_h \times \mathbb{M}_h)' := \mathbb{X}'_h \times \mathbb{M}'_h$ , be the nonlinear operators obtained after adding on the left hand side of (1.16) and (1.55), respectively, that is

$$\begin{aligned} [\mathbf{P}(\vec{\mathbf{s}}), \vec{\mathbf{r}}] &:= [(a_1 + a_2(\mathbf{u}_S))(\underline{\mathbf{s}}), \underline{\mathbf{r}}] + [b(\underline{\mathbf{s}}), \underline{\boldsymbol{\psi}}] + [b(\underline{\mathbf{r}}), \underline{\boldsymbol{\phi}}] - [c(\underline{\boldsymbol{\phi}}), \underline{\boldsymbol{\psi}}] \\ &\quad + [\mathbf{B}(\underline{\mathbf{r}}, \underline{\boldsymbol{\psi}}), \underline{\mathbf{m}}] + [\mathbf{B}(\underline{\mathbf{s}}, \underline{\boldsymbol{\phi}}), \underline{\mathbf{q}}], \end{aligned} \quad (1.79)$$



and

$$\begin{aligned} [\mathbf{P}_h(\vec{\mathbf{s}}_h), \vec{\mathbf{r}}_h] &:= [(a_1 + a_2(\mathbf{u}_{S,h}))(\underline{\mathbf{s}}_h), \underline{\mathbf{r}}_h] + [b(\underline{\mathbf{s}}_h), \underline{\boldsymbol{\psi}}_h] + [b(\underline{\mathbf{r}}_h), \underline{\boldsymbol{\phi}}_h] - [c(\underline{\boldsymbol{\phi}}_h), \underline{\boldsymbol{\psi}}_h] \\ &\quad + [\mathbf{B}(\underline{\mathbf{r}}_h, \underline{\boldsymbol{\psi}}_h), \underline{\mathbf{m}}_h] + [\mathbf{B}(\underline{\mathbf{s}}_h, \underline{\boldsymbol{\phi}}_h), \underline{\mathbf{q}}_h], \end{aligned} \quad (1.80)$$

for all  $\vec{\mathbf{s}} = ((\underline{\mathbf{s}}, \underline{\boldsymbol{\phi}}), \underline{\mathbf{m}})$ ,  $\vec{\mathbf{r}} = ((\underline{\mathbf{r}}, \underline{\boldsymbol{\psi}}), \underline{\mathbf{q}}) \in \mathbb{X} \times \mathbb{M}$  and  $\vec{\mathbf{s}}_h = ((\underline{\mathbf{s}}_h, \underline{\boldsymbol{\phi}}_h), \underline{\mathbf{m}}_h)$ ,  $\vec{\mathbf{r}}_h = ((\underline{\mathbf{r}}_h, \underline{\boldsymbol{\psi}}_h), \underline{\mathbf{q}}_h) \in \mathbb{X}_h \times \mathbb{M}_h$ , respectively, where  $\mathbf{u}_S \in W_r$  and  $\mathbf{u}_{S,h} \in W_r^h$  are the velocity solutions of (1.16) and (1.55), respectively.

According to the above, and denoting by  $\mathcal{F} := (\mathbf{F}, \mathbf{G}) \in \mathbb{X}' \times \mathbb{M}'$ , it follows that

$$[\mathbf{P}(\vec{\mathbf{t}}), \vec{\mathbf{r}}] = [\mathcal{F}, \vec{\mathbf{r}}] \quad \forall \vec{\mathbf{r}} := ((\underline{\mathbf{r}}, \underline{\boldsymbol{\psi}}), \underline{\mathbf{q}}) \in \mathbb{X} \times \mathbb{M} \quad (1.81)$$

and

$$[\mathbf{P}_h(\vec{\mathbf{t}}_h), \vec{\mathbf{r}}_h] = [\mathcal{F}, \vec{\mathbf{r}}_h] \quad \forall \vec{\mathbf{r}}_h := ((\underline{\mathbf{r}}_h, \underline{\boldsymbol{\psi}}_h), \underline{\mathbf{q}}_h) \in \mathbb{X}_h \times \mathbb{M}_h. \quad (1.82)$$

Next, since the Lipschitz-continuity of  $a_1$  (cf. (1.31)) holds at the continuous and discrete levels with the same constant, as well as the continuity of  $a_2$ ,  $b$ ,  $c$  and  $\mathbf{B}$ , we observe that the family  $\{\mathbf{P}\} \cup \{\mathbf{P}_h\}_{h>0}$  is uniformly Lipschitz-continuous with constant denoted from now on by  $C_{LC} > 0$ .

On the other hand, owing to the fact that  $\mu$  is assumed to be of class  $C^1$  (cf. (1.2)), it is not difficult to see that  $a_1 : \mathbf{X} \rightarrow \mathbf{X}'$  has hemi-continuous first order Gâteaux derivative  $\mathcal{D}a_1 : \mathbf{X} \rightarrow \mathcal{L}(\mathbf{X}, \mathbf{X}')$ , which in particular implies that for any  $\underline{\mathbf{s}}, \underline{\mathbf{r}} \in \mathbf{X}$ , the mapping  $\mathbb{R} \ni \mu \rightarrow \mathcal{D}a_1(\underline{\mathbf{s}} + \mu \underline{\mathbf{r}})(\underline{\mathbf{r}})(\cdot) \in \mathbf{X}'$  is continuous. Moreover, we have the following lemma.

**Lemma 1.17.** *For any  $\underline{\mathbf{s}} \in \mathbf{X}$ , the Gâteaux derivative  $\mathcal{D}a_1(\underline{\mathbf{s}})$  constitutes a bounded bilinear form on  $\mathbf{X} \times \mathbf{X}$  that becomes elliptic on  $\tilde{\mathbf{X}} \times \tilde{\mathbf{X}}$ , with boundedness and ellipticity constants  $L_{a_1}$  (cf. (1.31)) and  $\alpha_0(\Omega)$  (cf. (1.36)), respectively.*

*Proof.* Given  $\underline{\mathbf{s}} \in \mathbf{X}$ , the Gâteaux derivative  $\mathcal{D}a_1(\underline{\mathbf{s}})$  is the operator in  $\mathcal{L}(\mathbf{X}, \mathbf{X}')$  (equivalently, the bilinear form on  $\mathbf{X} \times \mathbf{X}$ ) defined by

$$\mathcal{D}a_1(\underline{\mathbf{s}})(\underline{\mathbf{r}}, \hat{\underline{\mathbf{r}}}) := \lim_{\epsilon \rightarrow 0} \frac{[a_1(\underline{\mathbf{s}} + \epsilon \underline{\mathbf{r}}), \hat{\underline{\mathbf{r}}}] - [a_1(\underline{\mathbf{s}}), \hat{\underline{\mathbf{r}}}]}{\epsilon} \quad \forall \underline{\mathbf{r}}, \hat{\underline{\mathbf{r}}} \in \mathbf{X}.$$

The rest of the proof follows as in [84, Lemma 3.1] by employing the properties (1.31), (1.35) and the continuity of the mapping  $\mathbb{R} \ni \mu \rightarrow \mathcal{D}a_1(\underline{\mathbf{s}} + \mu \underline{\mathbf{r}})(\underline{\mathbf{r}})(\cdot) \in \mathbf{X}'$ . We omit further details.  $\square$

Now, due to the hemi-continuity of the first order Gâteaux derivative  $\mathcal{D}a_1$ , and since the operators defining  $\mathbf{P}_h$  (besides  $a_1$ ) are linear, we easily obtain that, given  $\vec{\mathbf{s}} = ((\underline{\mathbf{s}}, \underline{\boldsymbol{\phi}}), \underline{\mathbf{m}}) \in \mathbb{X} \times \mathbb{M}$ , the Gâteaux derivative of  $\mathbf{P}_h$  at  $\vec{\mathbf{s}}$  is obtained by replacing  $[a_1(\underline{\mathbf{t}}_h), \underline{\mathbf{r}}_h]$  in (1.80) by  $\mathcal{D}a_1(\underline{\mathbf{s}})(\underline{\mathbf{t}}_h, \underline{\mathbf{r}}_h)$ , that is

$$\begin{aligned} \mathcal{D}\mathbf{P}_h(\vec{\mathbf{s}})(\vec{\mathbf{t}}_h, \vec{\mathbf{r}}_h) &:= \mathcal{D}a_1(\underline{\mathbf{s}})(\underline{\mathbf{t}}_h, \underline{\mathbf{r}}_h) + [a_2(\mathbf{u}_{S,h})(\underline{\mathbf{t}}_h), \underline{\mathbf{r}}_h] + [b(\underline{\mathbf{t}}_h), \underline{\boldsymbol{\psi}}_h] + [b(\underline{\mathbf{r}}_h), \underline{\boldsymbol{\varphi}}_h] \\ &\quad - [c(\underline{\boldsymbol{\varphi}}_h), \underline{\boldsymbol{\psi}}_h] + [\mathbf{B}(\underline{\mathbf{r}}_h, \underline{\boldsymbol{\psi}}_h), \underline{\mathbf{p}}_h] + [\mathbf{B}(\underline{\mathbf{t}}_h, \underline{\boldsymbol{\varphi}}_h), \underline{\mathbf{q}}_h], \end{aligned} \quad (1.83)$$

for all  $\vec{\mathbf{t}}_h := ((\underline{\mathbf{t}}_h, \underline{\boldsymbol{\varphi}}_h), \underline{\mathbf{p}}_h)$ ,  $\vec{\mathbf{r}}_h := ((\underline{\mathbf{r}}_h, \underline{\boldsymbol{\psi}}_h), \underline{\mathbf{q}}_h) \in \mathbb{X}_h \times \mathbb{M}_h$ , which, according to Lemma 1.17, becomes a bounded bilinear form on  $(\mathbb{X}_h \times \mathbb{M}_h) \times (\mathbb{X}_h \times \mathbb{M}_h)$ . Moreover, since  $c$  is positive-semidefinite, and assuming for a moment that (H.0), (H.1), (H.2) and (H.3) hold, we obtain that the conditions (iii)–(v) in Theorem 1.12 are verified, and as a result, having in mind Lemma 1.17, the bilinear form  $\mathcal{D}\mathbf{P}_h(\vec{\mathbf{s}})(\cdot, \cdot)$

satisfies the hypotheses of Theorem 1.16. Moreover, in virtue of (1.78), there holds the global inf-sup condition

$$C_G \|\vec{s}_h\| \leq \sup_{\substack{\vec{r}_h \in \mathbb{X}_h \times \mathbb{M}_h \\ \vec{r}_h \neq \mathbf{0}}} \frac{\mathcal{DP}_h(\vec{s})(\vec{s}_h, \vec{r}_h)}{\|\vec{r}_h\|} \quad \forall \vec{s}_h \in \mathbb{X}_h \times \mathbb{M}_h. \quad (1.84)$$

According to the foregoing analysis, it follows that the family of operators  $\{\mathbf{P}\} \cup \{\mathbf{P}_h\}_{h>0}$  satisfy the hypotheses of Lemma 1.15, and consequently we can establish now the main result of this section.

**Theorem 1.18.** *Assume that the hypotheses (H.0), (H.1), (H.2) and (H.3), as well as the conditions on  $\kappa_i, i \in \{1, \dots, 4\}$  required by Lemma 1.6, hold. Let  $r \in (0, r_0)$ , with  $r_0$  defined by (1.37) and assume further that the data  $\mathbf{f}_S$  and  $f_D$  satisfy*

$$c_T \left\{ \|\mathbf{f}_S\|_{0, \Omega_S} + \|f_D\|_{0, \Omega_D} \right\} \leq \frac{r}{\alpha_0(\Omega) C_{ST}}, \quad (1.85)$$

with  $c_T$  and  $\alpha_0(\Omega)$  being the positive constants satisfying (1.51) and (1.36), respectively. In addition, let  $\vec{\mathbf{t}} := ((\underline{\mathbf{t}}, \underline{\varphi}), \underline{\mathbf{p}}) \in \mathbb{X} \times \mathbb{M}$  with  $\mathbf{u}_S \in W_r$ , and  $\vec{\mathbf{t}}_h := ((\underline{\mathbf{t}}_h, \underline{\varphi}_h), \underline{\mathbf{p}}_h) \in \mathbb{X}_h \times \mathbb{M}_h$  with  $\mathbf{u}_{S,h} \in W_r^h$  be the unique solutions of problems (1.16) and (1.55), respectively. Then there exists a positive constant  $C > 0$ , depending only on  $\alpha_0(\Omega)$  and  $C_{ST}$ , such that

$$\|\vec{\mathbf{t}} - \vec{\mathbf{t}}_h\|_{\mathbb{X} \times \mathbb{M}} \leq C \text{dist}(\vec{\mathbf{t}}, \mathbb{X}_h \times \mathbb{M}_h). \quad (1.86)$$

*Proof.* From the Strang-type estimate (1.74) and from (1.81) and (1.82), we first obtain

$$\|\vec{\mathbf{t}} - \vec{\mathbf{t}}_h\|_{\mathbb{X} \times \mathbb{M}} \leq C_{ST} \inf_{\vec{s}_h \in \mathbb{X}_h \times \mathbb{M}_h} \left\{ \|\vec{\mathbf{t}} - \vec{s}_h\|_{\mathbb{X} \times \mathbb{M}} + \sup_{\substack{\vec{r}_h \in \mathbb{X}_h \times \mathbb{M}_h \\ \vec{r}_h \neq \mathbf{0}}} \frac{|\mathbf{P}(\vec{s}_h), \vec{r}_h| - |\mathbf{P}_h(\vec{s}_h), \vec{r}_h|}{\|\vec{r}_h\|_{\mathbb{X} \times \mathbb{M}}} \right\}. \quad (1.87)$$

In turn, utilizing the definition of  $\mathbf{P}$  and  $\mathbf{P}_h$  (resp. (1.79) and (1.80)), applying the estimate (1.32), adding and subtracting  $\vec{\mathbf{t}}$ , and bounding both  $\|\mathbf{u}_S\|_{1, \Omega_S}$  and  $\|\mathbf{u}_{S,h}\|_{1, \Omega_S}$  by  $r_0 = \frac{\alpha_0(\Omega)}{2c_2(\Omega_S)(\kappa_1^2+1)^{1/2}}$ , we find that

$$\begin{aligned} & \left| |\mathbf{P}(\vec{s}_h), \vec{r}_h| - |\mathbf{P}_h(\vec{s}_h), \vec{r}_h| \right| = \left| [a_2(\mathbf{u}_S - \mathbf{u}_{S,h})(\vec{s}_h), \vec{r}_h] \right| \\ & \leq c_2(\Omega_S)(\kappa_1^2 + 1)^{1/2} \|\mathbf{u}_S - \mathbf{u}_{S,h}\|_{1, \Omega_S} \left\{ \|\vec{\mathbf{t}} - \vec{s}_h\|_{\mathbb{X} \times \mathbb{M}} + \|\vec{\mathbf{t}}\|_{\mathbb{X} \times \mathbb{M}} \right\} \|\vec{r}_h\|_{\mathbb{X} \times \mathbb{M}} \\ & \leq \left\{ 2c_2(\Omega_S)(\kappa_1^2 + 1)^{1/2} r_0 \|\vec{\mathbf{t}} - \vec{s}_h\|_{\mathbb{X} \times \mathbb{M}} + c_2(\Omega_S)(\kappa_1^2 + 1)^{1/2} \|\vec{\mathbf{t}}\|_{\mathbb{X} \times \mathbb{M}} \|\mathbf{u}_S - \mathbf{u}_{S,h}\|_{1, \Omega_S} \right\} \|\vec{r}_h\|_{\mathbb{X} \times \mathbb{M}} \\ & = \left\{ \alpha_0(\Omega) \|\vec{\mathbf{t}} - \vec{s}_h\|_{\mathbb{X} \times \mathbb{M}} + c_2(\Omega_S)(\kappa_1^2 + 1)^{1/2} \|\vec{\mathbf{t}}\|_{\mathbb{X} \times \mathbb{M}} \|\mathbf{u}_S - \mathbf{u}_{S,h}\|_{1, \Omega_S} \right\} \|\vec{r}_h\|_{\mathbb{X} \times \mathbb{M}}, \end{aligned}$$

which, substituted back into (1.87), taking infimum, and using that  $\|\mathbf{u}_S - \mathbf{u}_{S,h}\|_{1, \Omega_S} \leq \|\vec{\mathbf{t}} - \vec{\mathbf{t}}_h\|_{\mathbb{X} \times \mathbb{M}}$ , yields

$$\|\vec{\mathbf{t}} - \vec{\mathbf{t}}_h\|_{\mathbb{X} \times \mathbb{M}} \leq C_{ST} \{1 + \alpha_0(\Omega)\} \text{dist}(\vec{\mathbf{t}}, \mathbb{X}_h \times \mathbb{M}_h) + C_{ST} c_2(\Omega_S)(\kappa_1^2 + 1)^{1/2} \|\vec{\mathbf{t}}\|_{\mathbb{X} \times \mathbb{M}} \|\vec{\mathbf{t}} - \vec{\mathbf{t}}_h\|_{\mathbb{X} \times \mathbb{M}}. \quad (1.88)$$

Finally, recalling from (1.51) that  $\|\vec{\mathbf{t}}\|_{\mathbb{X} \times \mathbb{M}} \leq c_T \left\{ \|\mathbf{f}_S\|_{0, \Omega_S} + \|f_D\|_{0, \Omega_D} \right\}$ , and employing assumption (1.85), we obtain that

$$C_{ST} c_2(\Omega_S)(\kappa_1^2 + 1)^{1/2} \|\vec{\mathbf{t}}\|_{\mathbb{X} \times \mathbb{M}} \leq \frac{1}{2}, \quad (1.89)$$

which, together with (1.88), implies (1.86) with  $C = 2C_{ST}\{1 + \alpha_0(\Omega)\}$ , thus ending the proof.  $\square$

## 1.6 Particular choices of discrete spaces

We now introduce specific discrete spaces satisfying hypotheses **(H.0)**, **(H.1)**, **(H.2)**, and **(H.3)** in 2D and 3D. To this end, we let  $\mathcal{T}_h^S$  and  $\mathcal{T}_h^D$  be respective triangulations of the domains  $\Omega_S$  and  $\Omega_D$ , which are formed by shape-regular triangles (in  $\mathbb{R}^2$ ) or tetrahedra (in  $\mathbb{R}^3$ ) of diameter  $h_T$ , and assume that they match in  $\Sigma$  so that  $\mathcal{T}_h^S \cup \mathcal{T}_h^D$  is a triangulation of  $\Omega_S \cup \Sigma \cup \Omega_D$ . We also let  $\Sigma_h$  be the partition of  $\Sigma$  inherited from  $\mathcal{T}_h^S$  (or  $\mathcal{T}_h^D$ ). Then, given an integer  $k \geq 0$ , we set for each  $T \in \mathcal{T}_h^S \cup \mathcal{T}_h^D$  the local Raviart–Thomas space of order  $k$  as

$$\mathbf{RT}_k(T) := \mathbf{P}_k(T) \oplus P_k(T)\mathbf{x},$$

where  $\mathbf{x} := (x_1, \dots, x_n)^\top$  is a generic vector of  $\mathbb{R}^n$ .

### 1.6.1 Raviart–Thomas elements in 2D

We define the discrete subspaces in (1.52) as follows:

$$\begin{aligned} L_h^2(\Omega_\star) &:= \{q_h \in L^2(\Omega_\star) : q_h|_T \in P_k(T) \quad \forall T \in \mathcal{T}_h^\star\}, \quad \star \in \{S, D\}, \\ \mathbf{H}_h(\Omega_\star) &:= \{\tau_h \in \mathbf{H}(\text{div}; \Omega_\star) : \tau_h|_T \in \mathbf{RT}_k(T) \quad \forall T \in \mathcal{T}_h^\star\}, \quad \star \in \{S, D\}, \\ \mathbf{H}_h^1(\Omega_S) &:= \{\mathbf{v}_h \in [\mathcal{C}(\overline{\Omega}_S)]^2 : \mathbf{v}_h|_T \in \mathbf{P}_{k+1}(T) \quad \forall T \in \mathcal{T}_h^S\}, \\ \mathbb{L}_{\text{tr},h}^2(\Omega_S) &:= \{\mathbf{r}_h \in \mathbb{L}_{\text{tr}}^2(\Omega_S) : \mathbf{r}_h|_T \in \mathbb{P}_k(T) \quad \forall T \in \mathcal{T}_h^S\}, \\ \mathbb{L}_{\text{skew},h}^2(\Omega_S) &:= \{\boldsymbol{\eta}_h \in \mathbb{L}_{\text{skew}}^2(\Omega_S) : \boldsymbol{\eta}_h|_T \in \mathbb{P}_k(T) \quad \forall T \in \mathcal{T}_h^S\}. \end{aligned} \tag{1.90}$$

In addition, in order to introduce the particular subspaces  $\Lambda_h^S(\Sigma)$  and  $\Lambda_h^D(\Sigma)$ , we follow the simplest approach suggested in [93] and [126]. To this end, we first assume, without loss of generality, that the number of edges of  $\Sigma_h$  is even. Then, we let  $\Sigma_{2h}$  be the partition of  $\Sigma$  arising by joining pairs of adjacent edges of  $\Sigma_h$ . Note that, since  $\Sigma_h$  is inherited from the interior triangulations, it is automatically of bounded variation (that is, the ratio of lengths of adjacent edges is bounded) and, therefore, so is  $\Sigma_{2h}$ . Now, if the number of edges of  $\Sigma_h$  is odd, we simply reduce it to the even case by joining any pair of two adjacent elements, and then construct  $\Sigma_{2h}$  from this reduced partition. In this way, denoting by  $x_0$  and  $x_N$  the extreme points of  $\Sigma$ , we set

$$\begin{aligned} \Lambda_h^S(\Sigma) &:= \{\psi_h \in \mathcal{C}(\Sigma) : \psi_h|_e \in P_{k+1}(e) \quad \forall \text{ edge } e \in \Sigma_{2h}, \quad \psi_h(x_0) = \psi_h(x_N) = 0\}, \\ \Lambda_h^D(\Sigma) &:= \{\xi_h \in \mathcal{C}(\Sigma) : \xi_h|_e \in P_{k+1}(e) \quad \forall \text{ edge } e \in \Sigma_{2h}\}. \end{aligned} \tag{1.91}$$

Then, we define the global spaces  $\mathbb{X}_h$  and  $\mathbb{M}_h$  (cf. (1.54)) by combining (1.53), (1.54), (1.90) and (1.91). Now, concerning hypotheses **(H.0)**–**(H.3)**, we start mentioning that **(H.0)** and **(H.1)** are straightforward from the definitions in (1.90). In turn, it is well known that the discrete inf-sup condition (1.63) in **(H.3)** holds (see for instance [19, Chapter IV] or [81, Section 4.2]). In addition, the existence of  $\boldsymbol{\psi}_0 \in \mathbf{H}_{00}^{1/2}(\Sigma)$  satisfying (1.62) follows as explained in [93, Section 2.5] or [96, Section 3.2]. Finally, the inf-sup conditions (1.60) and (1.61) in **(H.2)** can be derived by combining the results in [93, Section 2.5] and [126, Theorem A.1]. We omit further details and refer the reader to [88, Section 5.3.1] for the verification of these inf-sup conditions.

According to the above, we conclude that the Galerkin scheme (1.55) defined with the spaces in (1.90) is well posed. Moreover, by employing the approximations properties of the finite element subspaces involved (see, e.g. [19, 81, 100, 112]), and the a priori estimate (1.86), we can easily obtain the following result.

**Theorem 1.19.** *Assume that the hypotheses of Theorem 1.18 hold. Let  $\vec{\mathbf{t}} := ((\underline{\mathbf{t}}, \underline{\varphi}), \underline{\mathbf{p}}) \in \mathbb{X} \times \mathbb{M}$  with  $\mathbf{u}_S \in W_r$  and  $\vec{\mathbf{t}}_h := ((\underline{\mathbf{t}}_h, \underline{\varphi}_h), \underline{\mathbf{p}}_h) \in \mathbb{X}_h \times \mathbb{M}_h$  with  $\mathbf{u}_{S,h} \in W_r^h$  be the unique solutions of the problems (1.16) and (1.55), respectively. Assume further that there exists  $\delta > 0$ , such that  $\mathbf{t}_S \in \mathbb{H}^\delta(\Omega_S)$ ,  $\boldsymbol{\sigma}_S \in \mathbb{H}^\delta(\Omega_S)$ ,  $\operatorname{div} \boldsymbol{\sigma}_S \in \mathbf{H}^\delta(\Omega_S)$ ,  $\mathbf{u}_S \in \mathbf{H}^{1+\delta}(\Omega_S)$ ,  $\varphi \in \mathbf{H}^{1/2+\delta}(\Sigma)$ ,  $\boldsymbol{\rho}_S \in \mathbb{H}^\delta(\Omega_S)$ ,  $\mathbf{u}_D \in \mathbf{H}^\delta(\Omega_D)$ , and  $\operatorname{div} \mathbf{u}_D \in H^\delta(\Omega_D)$ . Then,  $p_D \in H^{1+\delta}(\Omega_D)$ ,  $\lambda \in H^{1/2+\delta}(\Sigma)$ , and there exists  $C > 0$ , independent of  $h$ , such that*

$$\begin{aligned} \|\vec{\mathbf{t}} - \vec{\mathbf{t}}_h\|_{\mathbb{X} \times \mathbb{M}} &\leq C h^{\min\{\delta, k+1\}} \left\{ \|\mathbf{t}_S\|_{\delta, \Omega_S} + \|\boldsymbol{\sigma}_S\|_{\delta, \Omega_S} + \|\operatorname{div} \boldsymbol{\sigma}_S\|_{\delta, \Omega_S} + \|\mathbf{u}_S\|_{1+\delta, \Omega_S} \right. \\ &\quad \left. + \|\boldsymbol{\rho}_S\|_{\delta, \Omega_S} + \|\mathbf{u}_D\|_{\delta, \Omega_D} + \|\operatorname{div} \mathbf{u}_D\|_{\delta, \Omega_D} + \|p_D\|_{1+\delta, \Omega_D} \right\}. \end{aligned}$$

*Proof.* From the second equation of (1.11), we readily obtain that  $\nabla p_D = -\mathbf{K}^{-1} \mathbf{u}_D$ , which implies that  $p_D \in H^{1+\delta}(\Omega_D)$ , whence  $\lambda = p_D|_\Sigma \in H^{1/2+\delta}(\Sigma)$ . The rest of the proof follows from the a priori estimate (1.86), the approximation properties of the discrete spaces involved and the fact that, owing to the trace theorems in  $\Omega_S$  and  $\Omega_D$ , respectively, there holds

$$\|\varphi\|_{1/2+\delta, \Sigma} \leq c \|\mathbf{u}_S\|_{1+\delta, \Omega_S} \quad \text{and} \quad \|\lambda\|_{1/2+\delta, \Sigma} \leq c \|p_D\|_{1+\delta, \Omega_D}.$$

□

### 1.6.2 Raviart–Thomas elements in 3D

Let us now consider the discrete spaces:

$$\begin{aligned} L_h^2(\Omega_\star) &:= \{q_h \in L^2(\Omega_\star) : q_h|_T \in P_k(T) \quad \forall T \in \mathcal{T}_h^\star\}, \quad \star \in \{S, D\}, \\ \mathbf{H}_h(\Omega_\star) &:= \{\tau_h \in \mathbf{H}(\operatorname{div}; \Omega_\star) : \tau_h|_T \in \mathbf{RT}_k(T) \quad \forall T \in \mathcal{T}_h^\star\}, \quad \star \in \{S, D\}, \\ \mathbf{H}_h^1(\Omega_S) &:= \{\mathbf{v}_h \in [\mathcal{C}(\overline{\Omega_S})]^3 : \mathbf{v}_h|_T \in \mathbf{P}_{k+1}(T) \quad \forall T \in \mathcal{T}_h^S\}, \\ \mathbb{L}_{\operatorname{tr}, h}^2(\Omega_S) &:= \{\mathbf{r}_h \in \mathbb{L}_{\operatorname{tr}}^2(\Omega_S) : \mathbf{r}_h|_T \in \mathbb{P}_k(T) \quad \forall T \in \mathcal{T}_h^S\}, \\ \mathbb{L}_{\operatorname{skew}, h}^2(\Omega_S) &:= \{\boldsymbol{\eta}_h \in \mathbb{L}_{\operatorname{skew}}^2(\Omega_S) : \boldsymbol{\eta}_h|_T \in \mathbb{P}_k(T) \quad \forall T \in \mathcal{T}_h^S\}. \end{aligned} \tag{1.92}$$

Now, in order to define the discrete spaces for the unknowns on the interface  $\Sigma$ , we introduce an independent triangulation  $\Sigma_{\hat{h}}$  of  $\Sigma$ , by triangles  $K$  of diameter  $\hat{h}$ , and define  $\hat{h}_\Sigma := \max\{\hat{h}_K : K \in \Sigma_{\hat{h}}\}$ . Then, denoting by  $\partial\Sigma$  the polygonal boundary of  $\Sigma$ , we define

$$\begin{aligned} \Lambda_h^S(\Sigma) &:= \{\psi_h \in \mathcal{C}(\Sigma) : \psi_h|_K \in P_{k+1}(K) \quad \forall K \in \Sigma_{\hat{h}}, \quad \psi_h = 0 \quad \text{on} \quad \partial K\}, \\ \Lambda_h^D(\Sigma) &:= \{\xi_h \in \mathcal{C}(\Sigma) : \xi_h|_K \in P_{k+1}(K) \quad \forall K \in \Sigma_{\hat{h}}\}. \end{aligned} \tag{1.93}$$

In this way, we define the global spaces  $\mathbb{X}_h$  and  $\mathbb{M}_h$  by combining (1.53), (1.54), (1.92), and (1.93).

Now, for the verification of hypotheses **(H.0)**–**(H.3)** we first observe that applying the same arguments as for the 2D case, it follows that **(H.0)**, **(H.1)** and **(H.3)** hold. However, for the inf-sup

conditions in **(H.2)** we need to proceed differently and apply [86, Lemma 7.5]. More precisely, utilizing [86, Lemma 7.5] we conclude that there exists  $C_0 \in (0, 1)$  such that for each pair  $(h_\Sigma, \widehat{h}_\Sigma)$  verifying  $h_\Sigma \leq C_0 \widehat{h}_\Sigma$ , the inf-sup conditions (1.60) and (1.61) hold.

Having verified hypotheses **(H.0)**–**(H.3)** we conclude that the Galerkin scheme (1.55) defined with the spaces in (1.92) is well posed. In addition, owing again to the approximations properties of the finite element subspaces involved (see, e.g. [19, 81, 100, 112]), and the a priori estimate (1.86), the following result holds.

**Theorem 1.20.** *Assume that the hypotheses of Theorem 1.18 hold. Let  $\vec{\mathbf{t}} := ((\mathbf{t}, \underline{\varphi}), \mathbf{p}) \in \mathbb{X} \times \mathbb{M}$  with  $\mathbf{u}_S \in W_r$  and  $\vec{\mathbf{t}}_h := ((\mathbf{t}_h, \underline{\varphi}_h), \mathbf{p}_h) \in \mathbb{X}_h \times \mathbb{M}_h$  with  $\mathbf{u}_{S,h} \in W_r^h$  be the unique solutions of the problems (1.16) and (1.55), respectively. Assume further that there exists  $\delta > 0$ , such that  $\mathbf{t}_S \in \mathbb{H}^\delta(\Omega_S)$ ,  $\boldsymbol{\sigma}_S \in \mathbb{H}^\delta(\Omega_S)$ ,  $\mathbf{div} \boldsymbol{\sigma}_S \in \mathbf{H}^\delta(\Omega_S)$ ,  $\mathbf{u}_S \in \mathbf{H}^{1+\delta}(\Omega_S)$ ,  $\varphi \in \mathbf{H}^{1/2+\delta}(\Sigma)$ ,  $\boldsymbol{\rho}_S \in \mathbb{H}^\delta(\Omega_S)$ ,  $\mathbf{u}_D \in \mathbf{H}^\delta(\Omega_D)$ , and  $\mathbf{div} \mathbf{u}_D \in H^\delta(\Omega_D)$ . Then,  $p_D \in H^{1+\delta}(\Omega_D)$ ,  $\lambda \in H^{1/2+\delta}(\Sigma)$ , and there exists  $C > 0$ , independent of  $h$ , such that*

$$\begin{aligned} \|\vec{\mathbf{t}} - \vec{\mathbf{t}}_h\|_{\mathbb{X} \times \mathbb{M}} \leq C h^{\min\{\delta, k+1\}} \Big\{ & \|\mathbf{t}_S\|_{\delta, \Omega_S} + \|\boldsymbol{\sigma}_S\|_{\delta, \Omega_S} + \|\mathbf{div} \boldsymbol{\sigma}_S\|_{\delta, \Omega_S} + \|\mathbf{u}_S\|_{1+\delta, \Omega_S} \\ & + \|\boldsymbol{\rho}_S\|_{\delta, \Omega_S} + \|\mathbf{u}_D\|_{\delta, \Omega_D} + \|\mathbf{div} \mathbf{u}_D\|_{\delta, \Omega_D} + \|p_D\|_{1+\delta, \Omega_D} \Big\}. \end{aligned}$$

## 1.7 Numerical results

In this section we present three examples illustrating the performance of our augmented mixed finite element scheme (1.55), and confirming the rates of convergence provided by Theorem 1.19. Our implementation is based on a FreeFem++ code (see [111]), in conjunction with the direct linear solver UMFPACK (see [62]). Regarding the implementation of the Newton iterative method, the iterations are terminated once the relative error of the entire coefficient vectors between two consecutive iterates is sufficiently small, i.e.,

$$\frac{\|\text{coeff}^{m+1} - \text{coeff}^m\|_{l^2}}{\|\text{coeff}^{m+1}\|_{l^2}} \leq \text{tol},$$

where  $\|\cdot\|_{l^2}$  is the standard  $l^2$ -norm in  $\mathbb{R}^N$ , with  $N$  denoting the total number of degrees of freedom defining the finite element subspaces  $\mathbb{L}_{\text{tr},h}^2(\Omega_S)$ ,  $\mathbb{H}_{h,0}(\Omega_S)$ ,  $\mathbf{H}_{h,\Gamma_S}^1(\Omega_S)$ ,  $\mathbb{L}_{\text{skew},h}^2(\Omega_S)$ ,  $\mathbf{H}_{h,0}(\Omega_D)$ ,  $\boldsymbol{\Lambda}_h^S(\Sigma)$ ,  $\boldsymbol{\Lambda}_h^D(\Sigma)$ , and  $L_{h,0}^2(\Omega_D)$ , and  $\text{tol}$  is a fixed tolerance to be specified for each example. As usual, the individual errors are denoted by:

$$\begin{aligned} \mathbf{e}(\mathbf{t}_S) &:= \|\mathbf{t}_S - \mathbf{t}_{S,h}\|_{0, \Omega_S}, & \mathbf{e}(\boldsymbol{\sigma}_S) &:= \|\boldsymbol{\sigma}_S - \boldsymbol{\sigma}_{S,h}\|_{\mathbf{div}, \Omega_S}, & \mathbf{e}(\mathbf{u}_S) &:= \|\mathbf{u}_S - \mathbf{u}_{S,h}\|_{1, \Omega_S}, \\ \mathbf{e}(\boldsymbol{\rho}_S) &:= \|\boldsymbol{\rho}_S - \boldsymbol{\rho}_{S,h}\|_{0, \Omega_S}, & \mathbf{e}(p_S) &:= \|p_S - p_{S,h}\|_{0, \Omega_S}, & \mathbf{e}(\mathbf{u}_D) &:= \|\mathbf{u}_D - \mathbf{u}_{D,h}\|_{\mathbf{div}, \Omega_D}, \\ \mathbf{e}(p_D) &:= \|p_D - p_{D,h}\|_{0, \Omega_D}, & \mathbf{e}(\varphi) &:= \|\varphi - \varphi_h\|_{1/2, 0, \Sigma}, & \mathbf{e}(\lambda) &:= \|\lambda - \lambda_h\|_{1/2, \Sigma}. \end{aligned}$$

where  $p_{S,h}$  is the postprocessed pressure given by

$$p_{S,h} := -\frac{1}{n} \text{tr}(\boldsymbol{\sigma}_{S,h} + (\mathbf{u}_{S,h} \otimes \mathbf{u}_{S,h})) - l_h \quad \text{in } \Omega_S.$$

In addition, we define the experimental rates of convergence

$$r(\diamond) := \frac{\log(\mathbf{e}(\diamond)/\widehat{\mathbf{e}}(\diamond))}{\log(h/\widehat{h})} \quad \text{for each } \diamond \in \{\mathbf{t}_S, \boldsymbol{\sigma}_S, \mathbf{u}_S, \boldsymbol{\rho}_S, p_S, \mathbf{u}_D, p_D, \varphi, \lambda\},$$

where  $\mathbf{e}$  and  $\widehat{\mathbf{e}}$  denote errors computed on two consecutive meshes of sizes  $h$  and  $\widehat{h}$ , respectively.

The examples to be considered in this section are described next. In all of them we choose  $\mathbf{K} = \mathbb{I}$ ,  $\omega = 1$ , and according to (1.46), the stabilization parameters are taken as  $\kappa_1 = \mu_1/L_\mu^2$ , with  $L_\mu := \max\{\mu_2, 2\mu_2 - \mu_1\}$ ,  $\kappa_2 = \kappa_1$ ,  $\kappa_3 = \mu_1/2$ , and  $\kappa_4 = C_{\text{Ko}}\mu_1/4$ . In this regard, and since  $C_{\text{Ko}}$  is not known for  $\mathbf{H}_{\Gamma_S}^1(\Omega_S)$ , in what follows we propose a heuristic approximation of this constant by observing first from (1.30) that  $C_{\text{Ko}}$  can be defined as

$$C_{\text{Ko}} := \inf_{\substack{\mathbf{v}_S \in \mathbf{H}_{\Gamma_S}^1(\Omega_S) \\ \mathbf{v}_S \neq \mathbf{0}}} \frac{\|\mathbf{e}(\mathbf{v}_S)\|_{0,\Omega_S}^2}{\|\mathbf{v}_S\|_{1,\Omega_S}^2}.$$

Then, noting that certainly  $\mathbf{H}_0^1(\Omega_S) \subseteq \mathbf{H}_{\Gamma_S}^1(\Omega_S)$ , and recalling from [128, Theorem 10.1] (see also [114, eq. (2.11)]) that

$$\frac{1}{2} \leq \frac{\|\mathbf{e}(\mathbf{v}_S)\|_{0,\Omega_S}^2}{\|\mathbf{v}_S\|_{1,\Omega_S}^2} \quad \forall \mathbf{v}_S \in \mathbf{H}_0^1(\Omega_S), \mathbf{v}_S \neq \mathbf{0},$$

we readily deduce that

$$C_{\text{Ko}} \leq \widetilde{C}_{\text{Ko}} := \inf_{\substack{\mathbf{v}_S \in \mathbf{H}_0^1(\Omega_S) \\ \mathbf{v}_S \neq \mathbf{0}}} \frac{\|\mathbf{e}(\mathbf{v}_S)\|_{0,\Omega_S}^2}{\|\mathbf{v}_S\|_{1,\Omega_S}^2} \quad \text{and} \quad \frac{1}{2} \leq \widetilde{C}_{\text{Ko}},$$

which suggests to choose this lower bound of  $\widetilde{C}_{\text{Ko}}$ , that is  $1/2$ , as the required approximation of  $C_{\text{Ko}}$ . In addition, the conditions  $\int_{\Omega_S} \text{tr } \boldsymbol{\sigma}_S = 0$  and  $\int_{\Omega_D} p_D = 0$  are imposed via a penalization strategy.

In our first example we consider a porous unit square, coupled with a semi-disk-shaped fluid domain, i.e.,  $\Omega_D := (-0.5, 0.5)^2$  and  $\Omega_S := \{(x_1, x_2) : x_1^2 + (x_2 - 0.5)^2 < 0.25, x_2 > 0.5\}$  (see bottom left panel of Figure 1.2). In this case, we set the nonlinear viscosity to

$$\mu(s) := 2 + \frac{1}{1+s} \quad \text{for } s \geq 0.$$

The data  $\mathbf{f}_S$  and  $f_D$  are chosen so that the exact solution in the tombstone-shaped domain  $\Omega$  is given by the smooth functions

$$p_S(\mathbf{x}) = \sin(\pi x_1) \sin(\pi x_2), \quad \mathbf{u}_S(\mathbf{x}) = -\mathbf{curl}(\cos(\pi x_1) \cos(\pi x_2)),$$

for all  $\mathbf{x} := (x_1, x_2) \in \Omega_S$ , and

$$p_D(\mathbf{x}) = \sin(\pi x_1) \sin(\pi x_2) \quad \forall \mathbf{x} := (x_1, x_2) \in \Omega_D,$$

where  $\mathbf{curl}(v) := \left( \frac{\partial v}{\partial x_2}, -\frac{\partial v}{\partial x_1} \right)^t$  for any sufficiently smooth function  $v$ . Notice that this solution satisfies  $\mathbf{u}_S \cdot \mathbf{n} = \mathbf{u}_D \cdot \mathbf{n}$  on  $\Sigma$  and the boundary condition  $\mathbf{u}_D \cdot \mathbf{n} = 0$  on  $\Gamma_D$ . However, the Dirichlet boundary condition for the Navier–Stokes velocity on  $\Gamma_S$  is non-homogeneous. Then, we need to modify accordingly the functional  $\mathbf{F}$  (cf. (1.17)), as follows

$$[\mathbf{F}, (\underline{\mathbf{r}}, \underline{\psi})] := -\kappa_2(\mathbf{f}_S, \mathbf{div} \boldsymbol{\tau}_S)_S + (\mathbf{f}_S, \mathbf{v}_S)_S + \langle \boldsymbol{\tau}_S \mathbf{n}, \mathbf{g} \rangle_{\Gamma_S} \quad \forall (\underline{\mathbf{r}}, \underline{\psi}) \in \mathbb{X},$$

where  $\mathbf{g} := \mathbf{u}_S|_{\Gamma_S} \in \mathbf{H}^{1/2}(\Gamma_S)$ .

In our second example we consider the regions  $\Omega_S := (0, 1)^2$  and  $\Omega_D := (0, 1) \times (-1, 0)$ . The viscosity follows a Carreau law (cf. (1.3)), that is

$$\mu(s) := \alpha_0 + \alpha_1(1 + s^2)^{(\beta-2)/2} \quad \text{for } s \geq 0,$$

and the data  $\mathbf{f}_S$  and  $f_D$  are chosen so that the exact solution is given by

$$p_S(\mathbf{x}) = x_1^2 - x_2^2, \quad \mathbf{u}_S(\mathbf{x}) = \mathbf{curl}(x_1(x_1 - 1)(x_2 - 1)\sin(\pi x_1)\sin(\pi x_2))$$

for all  $\mathbf{x} := (x_1, x_2) \in \Omega_S$ , and

$$p_D(\mathbf{x}) = \cos(\pi x_1) \cos(\pi x_2) \quad \forall \mathbf{x} := (x_1, x_2) \in \Omega_D.$$

Finally, in Example 3 we consider  $\Omega_S := (0, 1)^2$  and let  $\Omega_D$  be the  $L$ -shaped domain given by  $(-1, 1)^2 \setminus \overline{\Omega}_S$ . The viscosity follows a Carreau law with  $\alpha_0 = 0.5$ ,  $\alpha_1 = 0.5$ , and  $\beta = 1.5$ , that is

$$\mu(s) := 0.5 + 0.5(1 + s^2)^{-1/4} \quad \text{for } s \geq 0.$$

The data  $\mathbf{f}_S$  and  $f_D$  are chosen so that the exact solution is given by

$$p_S(\mathbf{x}) = \cos(\pi x_1) \cos(\pi x_2), \quad \mathbf{u}_S(\mathbf{x}) = \mathbf{curl}(\sin(\pi x_1) \sin(\pi x_2))$$

for all  $\mathbf{x} := (x_1, x_2) \in \Omega_S$ , and

$$p_D(\mathbf{x}) = \cos(\pi x_1) \cos(\pi x_2) \quad \forall \mathbf{x} := (x_1, x_2) \in \Omega_D.$$

In Tables 1.1, 1.2 and 1.4 we summarize the convergence history for a sequence of quasi-uniform triangulations, considering the finite element spaces introduced in Section 1.6.1 with  $k = 0$ , and solving the nonlinear problem with a tolerance  $\text{tol} = 1E - 6$ , which required around five Newton iterations. In Table 1.2 it has been considered  $\alpha_0 = 0.5$ ,  $\alpha_1 = 0.5$ , and  $\beta = 1$  in the Carreau law. We observe that the rate of convergence  $O(h^{k+1})$  predicted by Theorem 1.19 (when  $\delta = k + 1$ ) is attained in all the variables (with  $k = 0$ ). Next, in Table 1.3 we present the behaviour of the iterative method and CPU time applied to Example 2, considering a decreasing parameter  $\alpha_0$  and different mesh sizes. We observe there that the number of iterations remains bounded even for small values of  $\alpha_0$ . In addition, although the CPU time increases for small values of  $h_S$ , it also remains bounded as  $\alpha_0$  decreases. In addition, some components of the approximate solutions for the three examples are displayed in Figures 1.2, 1.3 and 1.4. All the figures were obtained with 785349, 1470527 and 2190236 degrees of freedom for the Examples 1, 2, and 3, respectively. In particular, we can observe in Figure 1.2 that the second components of  $\mathbf{u}_S$  and  $\mathbf{u}_D$  coincide on  $\Sigma$  as expected, and hence, the continuity of the normal components of the velocities on  $\Sigma$  is preserved. Moreover, it can be seen that the pressure is continuous in the whole domain and preserves the sinusoidal behaviour. Next, similarly to Figure 1.2, in Figure 1.3 we can also observe the continuity of the normal components of the velocities on  $\Sigma$  since their second components coincide on the interface.

| dof    | $h_S$ | $e(t_S)$ | $r(t_S)$ | $e(\sigma_S)$ | $r(\sigma_S)$ | $e(u_S)$ | $r(u_S)$ | $e(\rho_S)$ | $r(\rho_S)$ | $e(p_S)$ | $r(p_S)$ |
|--------|-------|----------|----------|---------------|---------------|----------|----------|-------------|-------------|----------|----------|
| 859    | 0.191 | 0.415    | –        | 4.675         | –             | 0.931    | –        | 1.206       | –           | 0.624    | –        |
| 3205   | 0.091 | 0.206    | 1.054    | 2.472         | 0.958         | 0.471    | 0.946    | 0.705       | 0.807       | 0.341    | 0.908    |
| 12542  | 0.049 | 0.104    | 0.994    | 1.280         | 0.964         | 0.239    | 1.037    | 0.354       | 1.009       | 0.153    | 1.174    |
| 50281  | 0.024 | 0.048    | 1.100    | 0.639         | 0.991         | 0.114    | 1.058    | 0.168       | 1.063       | 0.069    | 1.142    |
| 198922 | 0.013 | 0.025    | 0.970    | 0.349         | 0.889         | 0.058    | 1.021    | 0.088       | 0.947       | 0.036    | 0.935    |
| 785349 | 0.008 | 0.013    | 0.979    | 0.174         | 1.009         | 0.029    | 1.002    | 0.045       | 0.973       | 0.018    | 0.987    |

| dof    | $h_D$ | $e(u_D)$ | $r(u_D)$ | $e(p_D)$ | $r(p_D)$ | $e(\varphi)$ | $r(\varphi)$ | $e(\lambda)$ | $r(\lambda)$ | iter |
|--------|-------|----------|----------|----------|----------|--------------|--------------|--------------|--------------|------|
| 859    | 0.190 | 1.186    | –        | 0.059    | –        | 1.067        | –            | 0.203        | –            | 5    |
| 3205   | 0.098 | 0.605    | 1.033    | 0.030    | 1.034    | 0.557        | 0.937        | 0.098        | 1.056        | 5    |
| 12542  | 0.054 | 0.305    | 1.007    | 0.015    | 1.007    | 0.270        | 1.044        | 0.048        | 1.032        | 5    |
| 50281  | 0.025 | 0.152    | 1.015    | 0.008    | 1.015    | 0.134        | 1.008        | 0.024        | 0.978        | 5    |
| 198922 | 0.015 | 0.076    | 1.002    | 0.004    | 1.003    | 0.067        | 0.997        | 0.012        | 1.025        | 5    |
| 785349 | 0.007 | 0.038    | 1.007    | 0.002    | 1.007    | 0.034        | 1.003        | 0.006        | 1.003        | 5    |

Table 1.1: EXAMPLE 1, Degrees of freedom, mesh sizes, errors, convergence history and Newton iteration count for the augmented finite element formulation.

| dof     | $h_S$ | $e(t_S)$ | $r(t_S)$ | $e(\sigma_S)$ | $r(\sigma_S)$ | $e(u_S)$ | $r(u_S)$ | $e(\rho_S)$ | $r(\rho_S)$ | $e(p_S)$ | $r(p_S)$ |
|---------|-------|----------|----------|---------------|---------------|----------|----------|-------------|-------------|----------|----------|
| 1595    | 0.196 | 0.241    | –        | 1.055         | –             | 0.510    | –        | 0.643       | –           | 0.123    | –        |
| 5975    | 0.100 | 0.116    | 1.101    | 0.550         | 0.981         | 0.251    | 1.068    | 0.375       | 0.812       | 0.060    | 1.084    |
| 23486   | 0.049 | 0.056    | 1.071    | 0.269         | 1.046         | 0.120    | 1.076    | 0.184       | 1.038       | 0.030    | 1.028    |
| 93248   | 0.025 | 0.028    | 0.989    | 0.137         | 0.978         | 0.061    | 0.988    | 0.101       | 0.876       | 0.015    | 1.002    |
| 373093  | 0.014 | 0.014    | 1.026    | 0.067         | 1.025         | 0.030    | 1.003    | 0.050       | 1.000       | 0.007    | 1.067    |
| 1470527 | 0.007 | 0.007    | 1.064    | 0.033         | 1.022         | 0.015    | 1.047    | 0.026       | 0.983       | 0.003    | 1.110    |

| dof     | $h_D$ | $e(u_D)$ | $r(u_D)$ | $e(p_D)$ | $r(p_D)$ | $e(\varphi)$ | $r(\varphi)$ | $e(\lambda)$ | $r(\lambda)$ | iter |
|---------|-------|----------|----------|----------|----------|--------------|--------------|--------------|--------------|------|
| 1595    | 0.190 | 1.221    | –        | 0.061    | –        | 0.511        | –            | 0.220        | –            | 5    |
| 5975    | 0.095 | 0.600    | 1.087    | 0.030    | 1.097    | 0.214        | 1.258        | 0.100        | 1.133        | 5    |
| 23486   | 0.048 | 0.303    | 1.003    | 0.015    | 1.002    | 0.103        | 1.053        | 0.049        | 1.018        | 5    |
| 93248   | 0.026 | 0.152    | 1.007    | 0.008    | 1.007    | 0.055        | 0.903        | 0.025        | 1.007        | 5    |
| 373093  | 0.014 | 0.076    | 1.001    | 0.004    | 1.001    | 0.027        | 1.053        | 0.012        | 1.007        | 5    |
| 1470527 | 0.007 | 0.038    | 1.004    | 0.002    | 1.003    | 0.014        | 0.935        | 0.006        | 0.980        | 5    |

Table 1.2: EXAMPLE 2, Degrees of freedom, mesh sizes, errors, convergence history and Newton iteration count for the augmented finite element formulation.



| $\alpha_0$ | $h_S = 0.1964$ | cpu[s] | $h_S = 0.0997$ | cpu[s] | $h_S = 0.0487$ | cpu[s]  |
|------------|----------------|--------|----------------|--------|----------------|---------|
| 1          | 4              | 1.3648 | 4              | 3.0490 | 4              | 8.9298  |
| 1/2        | 5              | 1.4532 | 5              | 3.6315 | 5              | 10.9285 |
| 1/4        | 5              | 1.4801 | 5              | 3.8027 | 5              | 10.5086 |
| 1/8        | 6              | 1.7455 | 5              | 3.6785 | 5              | 10.1666 |
| 1/16       | 6              | 1.8367 | 6              | 4.3328 | 6              | 12.0209 |
| 1/32       | 6              | 1.7321 | 6              | 4.3937 | 6              | 12.0770 |
| 1/64       | 7              | 1.9799 | 7              | 4.8938 | 6              | 12.1350 |
| 1/128      | 7              | 1.9292 | 7              | 4.9459 | 7              | 13.6913 |

| $\alpha_0$ | $h_S = 0.0250$ | cpu[s]  | $h_S = 0.0136$ | cpu[s]    | $h_S = 0.0072$ | cpu[s]     |
|------------|----------------|---------|----------------|-----------|----------------|------------|
| 1          | 4              | 36.1339 | 4              | 1400.5835 | 4              | 19934.6071 |
| 1/2        | 5              | 43.7478 | 5              | 1217.9274 | 5              | 24872.5168 |
| 1/4        | 5              | 43.9839 | 5              | 371.6146  | 5              | 22011.6552 |
| 1/8        | 5              | 43.0072 | 5              | 357.1378  | 5              | 4284.1578  |
| 1/16       | 6              | 50.0509 | 6              | 392.7867  | 6              | 2313.1802  |
| 1/32       | 6              | 50.3200 | 6              | 393.5295  | 6              | 2269.6475  |
| 1/64       | 6              | 57.2579 | 6              | 399.4585  | 6              | 2282.7094  |
| 1/128      | 6              | 51.0813 | 6              | 405.1886  | 6              | 2297.5849  |

Table 1.3: EXAMPLE 2, Behaviour of the iterative Newton's method with respect to the viscosity  $\mu$ , considering a Carreau law with parameters  $\alpha_1 = 0.5$  and  $\beta = 1$ .

| dof     | $h_S$ | $e(\mathbf{t}_S)$ | $r(\mathbf{t}_S)$ | $e(\boldsymbol{\sigma}_S)$ | $r(\boldsymbol{\sigma}_S)$ | $e(\mathbf{u}_S)$ | $r(\mathbf{u}_S)$ | $e(\boldsymbol{\rho}_S)$ | $r(\boldsymbol{\rho}_S)$ | $e(p_S)$ | $r(p_S)$ |
|---------|-------|-------------------|-------------------|----------------------------|----------------------------|-------------------|-------------------|--------------------------|--------------------------|----------|----------|
| 2317    | 0.196 | 0.856             | —                 | 3.729                      | —                          | 1.556             | —                 | 2.991                    | —                        | 0.625    | —        |
| 8754    | 0.099 | 0.452             | 0.962             | 1.958                      | 0.972                      | 0.787             | 1.028             | 1.806                    | 0.761                    | 0.357    | 0.846    |
| 34744   | 0.049 | 0.209             | 1.127             | 0.962                      | 1.038                      | 0.388             | 1.032             | 0.961                    | 0.920                    | 0.150    | 1.264    |
| 138089  | 0.025 | 0.106             | 0.981             | 0.482                      | 1.000                      | 0.195             | 0.999             | 0.486                    | 0.989                    | 0.076    | 0.984    |
| 552690  | 0.014 | 0.052             | 1.019             | 0.241                      | 1.001                      | 0.096             | 1.014             | 0.249                    | 0.965                    | 0.037    | 1.031    |
| 2190236 | 0.007 | 0.024             | 1.133             | 0.119                      | 1.032                      | 0.047             | 1.051             | 0.122                    | 1.044                    | 0.018    | 1.083    |

| dof     | $h_D$ | $e(\mathbf{u}_D)$ | $r(\mathbf{u}_D)$ | $e(p_D)$ | $r(p_D)$ | $e(\boldsymbol{\varphi})$ | $r(\boldsymbol{\varphi})$ | $e(\lambda)$ | $r(\lambda)$ | iter |
|---------|-------|-------------------|-------------------|----------|----------|---------------------------|---------------------------|--------------|--------------|------|
| 2317    | 0.217 | 2.151             | —                 | 0.123    | —        | 1.480                     | —                         | 0.523        | —            | 5    |
| 8754    | 0.103 | 1.088             | 1.024             | 0.055    | 1.213    | 0.789                     | 0.908                     | 0.218        | 1.260        | 5    |
| 34744   | 0.059 | 0.539             | 1.013             | 0.027    | 1.036    | 0.399                     | 0.985                     | 0.095        | 1.202        | 5    |
| 138089  | 0.029 | 0.271             | 1.000             | 0.014    | 1.002    | 0.188                     | 1.082                     | 0.053        | 0.853        | 5    |
| 552690  | 0.016 | 0.135             | 0.999             | 0.007    | 1.000    | 0.093                     | 1.014                     | 0.027        | 0.977        | 5    |
| 2190236 | 0.008 | 0.068             | 1.003             | 0.003    | 1.000    | 0.047                     | 0.993                     | 0.012        | 0.975        | 5    |

Table 1.4: EXAMPLE 3, Degrees of freedom, mesh sizes, errors, convergence history and Newton iteration count for the augmented finite element formulation.

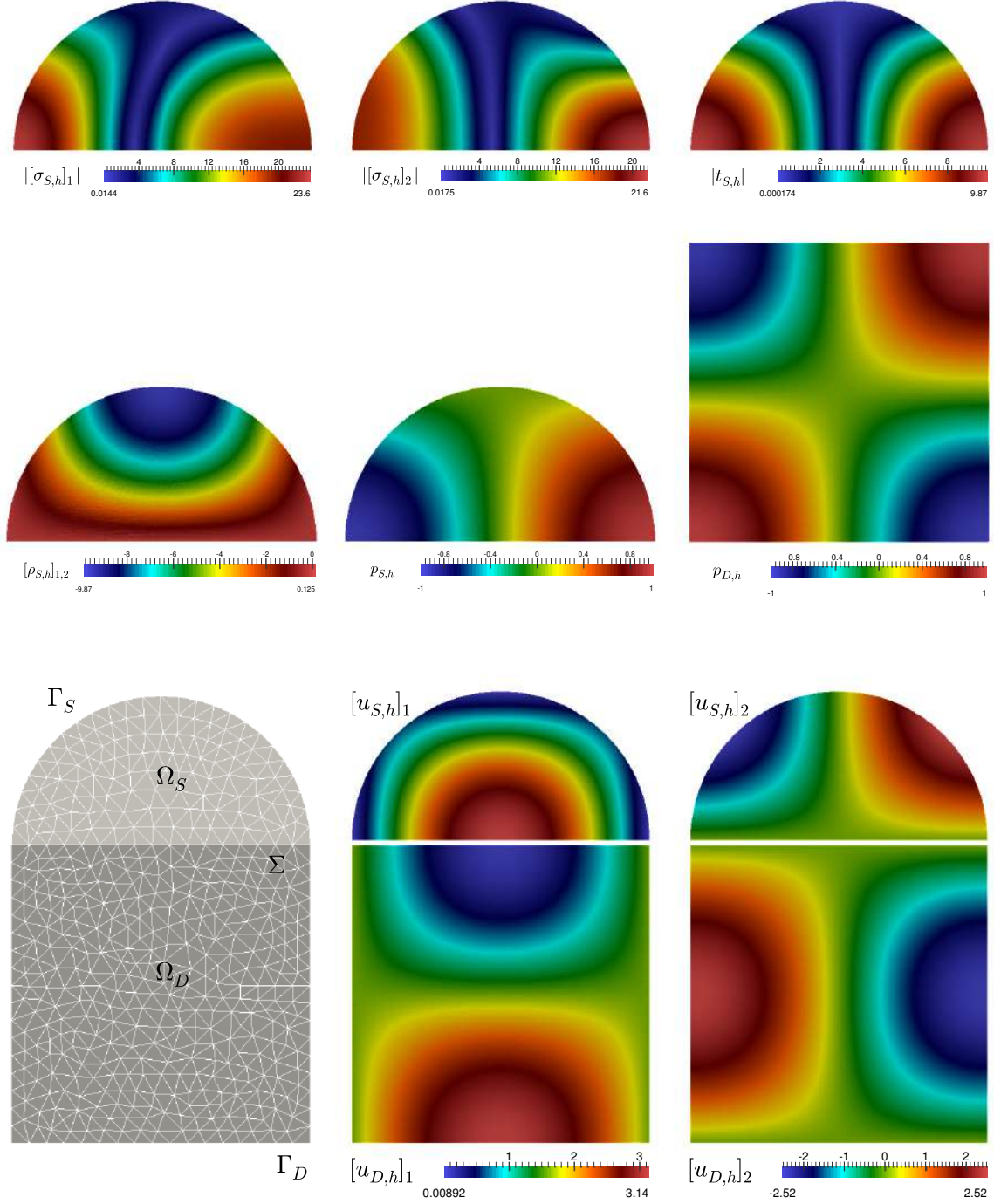


Figure 1.2: Example 1: Approximated spectral norm of the stress tensor components and the strain tensor (top panels), skew-symmetric part of the Navier–Stokes velocity gradient, Navier–Stokes pressure field, and Darcy pressure field (centre panels), and geometry configuration and velocity components on the whole domain (bottom row).

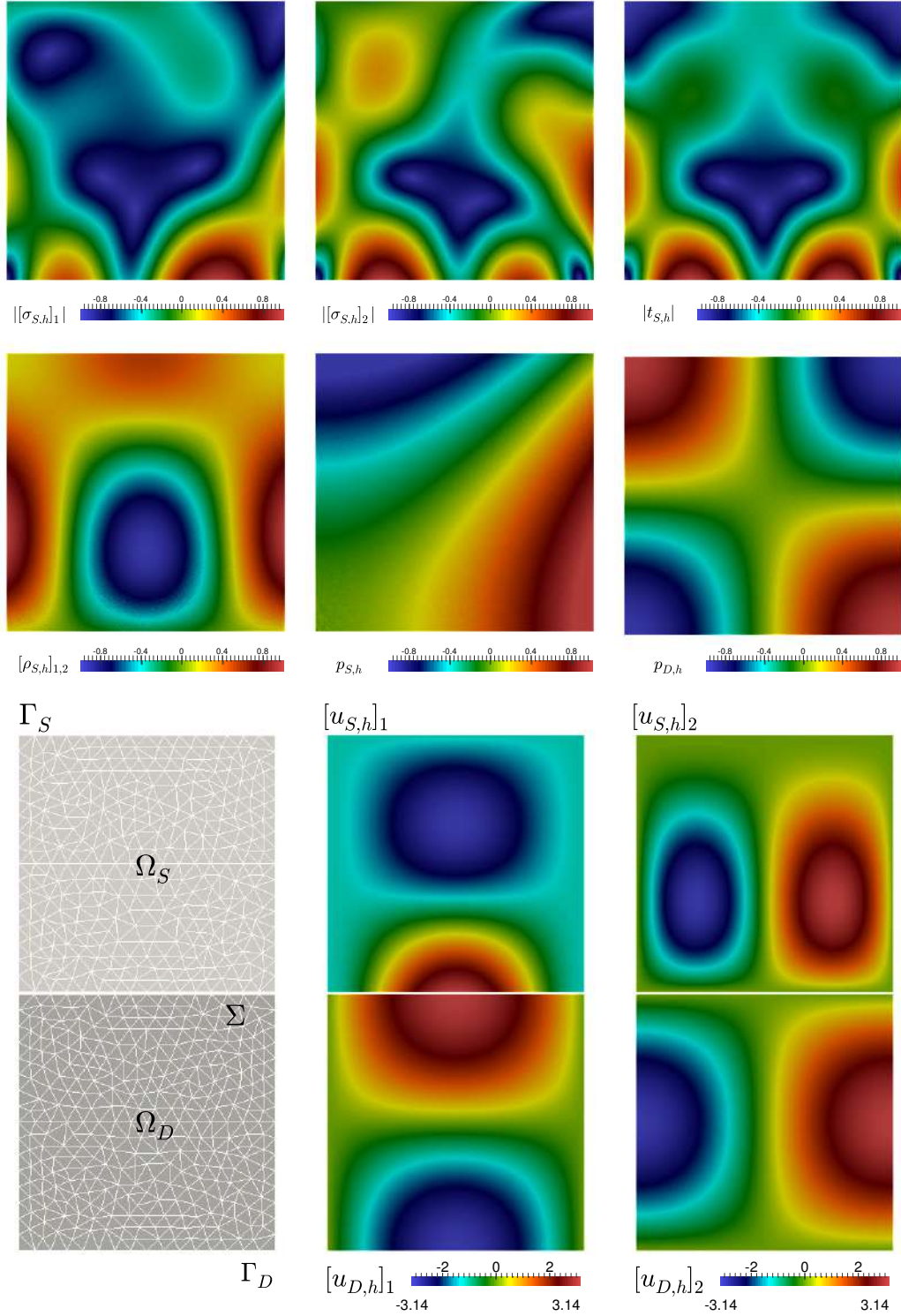


Figure 1.3: Example 2: Approximated spectral norm of the stress tensor components and the strain tensor (top panels), skew-symmetric part of the Navier–Stokes velocity gradient, Navier–Stokes pressure field, and Darcy pressure field (centre panels), and geometry configuration and velocity components on the whole domain (bottom row).

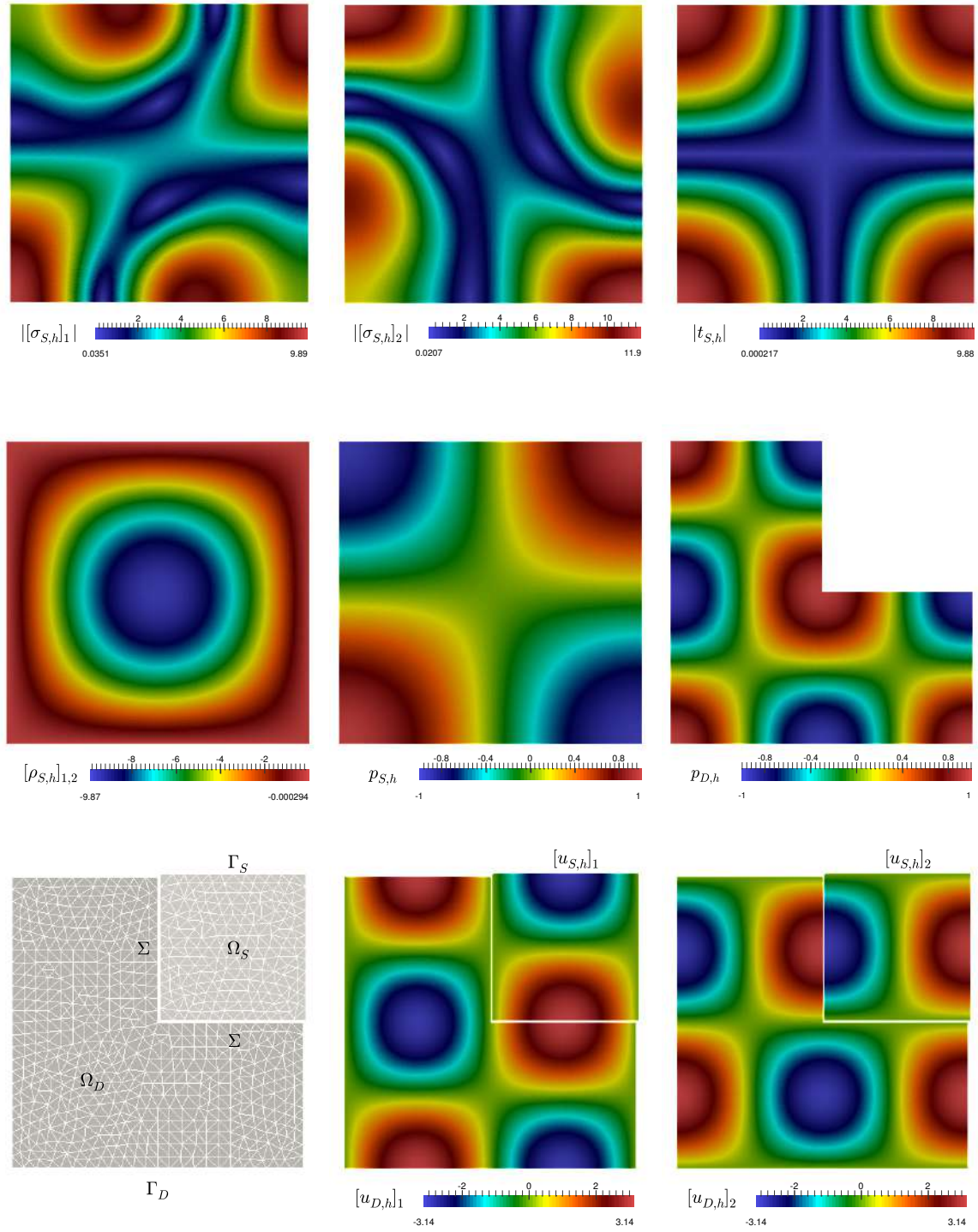


Figure 1.4: Example 3: Approximated spectral norm of the stress tensor components and the strain tensor (top panels), skew-symmetric part of the Navier–Stokes velocity gradient, Navier–Stokes pressure field, and Darcy pressure field (centre panels), and geometry configuration and velocity components on the whole domain (bottom row).



## CHAPTER 2

---

### A posteriori error analysis of a fully-mixed formulation for the Navier–Stokes/Darcy coupled problem with nonlinear viscosity

---

In this chapter we develop an a posteriori error analysis for the coupled problem studied in Chapter 1. We derive a reliable and efficient residual-based a posteriori error estimator to establish adaptive methods allowing to improve the accuracy of the numerical approximations, mainly under presence of singularities or high gradients of the solution.

#### 2.1 Introduction

Over the last decades, a wide range of numerical methods capturing the behaviour of a free fluid flow interacting with a porous medium have been proposed. The reason of such an interest by the numerical analysis community relies on the fact that, in industry, engineering sciences and several other disciplines, several interesting phenomena can be described under the framework of this kind of interaction problems. In particular, for specific applications we refer to flow in vuggy porous media appearing in petroleum extraction (see, e.g. [6], [7]), groundwater system in karst aquifers (see, e.g. [74], [129]), reservoir wellbore (see, e.g. [8]), industrial filtrations (see, e.g. [110], [132]), topology optimization (see, e.g. [107]), and blood motion in tumors and microvessels (see, e.g. [138], [146]). One of the most popular models utilized to describe the aforementioned interaction is the Navier–Stokes/Darcy (or Stokes/Darcy) model, which consists in a set of differential equations where the Navier–Stokes (or Stokes) problem is coupled with the Darcy model through a set of coupling equations acting on a common interface given by mass conservation, balance of normal forces, and the so called Beavers–Joseph–Saffman condition. In [11, 40, 43, 45, 63, 64, 65, 27, 92, 94, 96], and in the references therein, we can find a large list of contributions devoted to numerically approximate the solution of this interaction problem, including primal and mixed conforming formulations, as well as nonconforming methods.

In Chapter 1, it has been introduced and analyzed a new augmented-mixed finite element method for the Navier–Stokes/Darcy coupled problem with nonlinear viscosity. The formulation there considers dual-mixed formulations in both domains, and in order to deal with the nonlinear viscosity, the strain tensor and the vorticity are introduced as auxiliary unknowns. In turn, since the transmission conditions become essential, they are imposed weakly, which yields the introduction of the traces of the

porous media pressure and the fluid velocity as associated Lagrange multipliers. Furthermore, since the convective term in the fluid forces the velocity to live in a smaller space than usual, similarly to [28] and [30], the variational formulation is augmented with suitable Galerkin type terms arising from the constitutive and equilibrium equations of the Navier–Stokes model, as well as from the relations defining the strain and vorticity tensors. The resulting augmented variational system of equations is then suitably ordered so that it exhibits a twofold saddle point structure, which is similar to the one analyzed in [88] for the Stokes–Darcy coupled problem with nonlinear viscosity. The formulation is then written equivalently as a fixed point equation, and the well-known Schauder and Banach theorems, as well as the abstract theory developed in [88], which is based on classical results on bijective monotone operators, are applied to prove the unique solvability of the continuous and discrete systems. A feasible choice of finite element subspaces for the formulation introduced in Chapter 1 is given by piecewise constants, Raviart–Thomas spaces of lowest order, continuous piecewise linear elements, and piecewise constants for the strain, Cauchy stress, velocity, and vorticity in the fluid, respectively, whereas Raviart–Thomas spaces of lowest order and piecewise constants for the velocity and pressure, together with continuous piecewise linear elements for the Lagrange multipliers, can be utilized in the Darcy region. Optimal a priori error estimates were also derived.

Now, it is well known that under the eventual presence of singularities, as well as when dealing with nonlinear problems, as in the present case, most of the standard Galerkin procedures such as finite element and mixed finite element methods inevitably lose accuracy, and hence one usually tries to recover it by applying an adaptive algorithm based on a posteriori error estimates. In this direction, and particularly for the coupling of fluid flows with porous media flows, we refer to [10, 27, 44, 58, 59, 95, 96, 108, 127, 133, 151] where different contributions addressing this interesting issue, most of them devoted to the Stokes–Darcy coupled problem, can be found. Up to the authors’ knowledge, the first work dealing with adaptive algorithms for the Navier–Stokes/Darcy coupling is [108], where an a posteriori error estimator for a discontinuous Galerkin approximation of this coupled problem with constant parameters is proposed.

According to the above discussion, and in order to complement the study started in Chapter 1 for the Navier–Stokes/Darcy equations with variable viscosity, in this chapter we proceed similarly to [95, 96] and [27], and develop an a posteriori error analysis for the finite element method studied in Chapter 1. More precisely, assuming a smallness condition on the data, we derive a reliable and efficient residual-based a posteriori error estimator for the three dimensional version of the augmented-mixed method introduced in Chapter 1. The global inf-sup condition, a suitable Helmholtz decomposition recently provided in [82], and the approximation properties of the Clemené and Raviart–Thomas operators, among others, are the main tools yielding the reliability. In turn, the efficiency estimate is consequence of standard arguments such as inverse inequalities, the localization technique based on bubble functions, and other known results to be specified later on in Section 2.3.4. The rest of this chapter is organized as follows. In Section 2.2 we recall from Chapter 1 the model problem and its continuous and discrete augmented fully-mixed variational formulations. In Section 2.3, we derive the a posteriori error estimator. The reliability analysis is carried out in Section 2.3.3, whereas in Section 2.3.4 we provide the efficiency analysis. Finally, some numerical results confirming the reliability and efficiency of the a posteriori error estimator and showing the good performance of the associated adaptive algorithm for the fully-mixed finite element method, are presented in Section 2.4.

## 2.2 The Navier–Stokes/Darcy coupled problem

In this section we recall from Chapter 1 the Navier–Stokes/Darcy model, its fully-mixed variational formulation, the associated Galerkin scheme, and the main results concerning the corresponding solvability analysis.

### 2.2.1 The model problem

In order to describe the geometry under consideration we let  $\Omega_S$  and  $\Omega_D$  be bounded and simply connected open polyhedral domains in  $\mathbb{R}^n$ , such that  $\Omega_S \cap \Omega_D = \emptyset$  and  $\partial\Omega_S \cap \partial\Omega_D = \Sigma \neq \emptyset$ . Then, we let  $\Gamma_S := \partial\Omega_S \setminus \bar{\Sigma}$ ,  $\Gamma_D := \partial\Omega_D \setminus \bar{\Sigma}$ , and denote by  $\mathbf{n}$  the unit normal vector on the boundaries, which is chosen pointing outward from  $\Omega := \Omega_S \cup \Sigma \cup \Omega_D$  and  $\Omega_S$  (and hence inward to  $\Omega_D$  when seen on  $\Sigma$ ). On  $\Sigma$  we also consider unit tangent vectors, which are given by  $\mathbf{t} = \mathbf{t}_1$  when  $n = 2$  (see Fig. 2.1 below) and by  $\{\mathbf{t}_1, \mathbf{t}_2\}$  when  $n = 3$ . The problem we are interested in consists of the movement of an incompressible quasi-Newtonian viscous fluid occupying  $\Omega_S$  which flows towards and from a porous medium  $\Omega_D$  through  $\Sigma$ , where  $\Omega_D$  is saturated with the same fluid. The mathematical model is defined by two separate groups of equations and by a set of coupling terms. In  $\Omega_S$ , the governing equations are those of the Navier–Stokes problem with constant density and variable viscosity, which are written in the following nonstandard stress-velocity-pressure formulation:

$$\begin{aligned} \boldsymbol{\sigma}_S &= \mu(|\mathbf{e}(\mathbf{u}_S)|)\mathbf{e}(\mathbf{u}_S) - (\mathbf{u}_S \otimes \mathbf{u}_S) - p_S \mathbb{I} \quad \text{in } \Omega_S, & \operatorname{div} \mathbf{u}_S &= 0 \quad \text{in } \Omega_S, \\ -\operatorname{div} \boldsymbol{\sigma}_S &= \mathbf{f}_S \quad \text{in } \Omega_S, & \mathbf{u}_S &= \mathbf{0} \quad \text{on } \Gamma_S, \end{aligned} \quad (2.1)$$

where  $\boldsymbol{\sigma}_S$  is the nonlinear stress tensor,  $\mathbf{u}_S$  is the velocity,  $p_S$  is the pressure,  $\mu : \mathbb{R}^+ \rightarrow \mathbb{R}^+$  is the nonlinear kinematic viscosity,  $\mathbf{e}(\mathbf{u}_S) := \frac{1}{2}\{\nabla \mathbf{u}_S + (\nabla \mathbf{u}_S)^t\}$  is the strain tensor (or symmetric part of the velocity gradient) and  $\mathbf{f}_S \in \mathbf{L}^2(\Omega_S)$  is a known volume force.

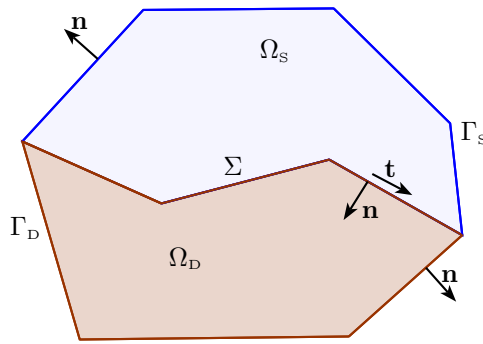


Figure 2.1: Sketch of a 2D geometry of our Navier–Stokes/Darcy model

Furthermore, we assume that  $\mu$  is of class  $\mathcal{C}^1$ , and that there exist constants  $\mu_1, \mu_2 > 0$ , such that

$$\mu_1 \leq \mu(s) \leq \mu_2 \quad \text{and} \quad \mu_1 \leq \mu(s) + s\mu'(s) \leq \mu_2 \quad \forall s \geq 0, \quad (2.2)$$

which, according to the results provided in [98, Theorem 3.8], implies Lipschitz continuity of the nonlinear operator induced by  $\mu$ . This fact will be used later on in Sections 2.3.3 and 2.3.4. In

addition, it is easy to see that the forthcoming analysis also applies to the slightly more general case of a viscosity function acting on  $\Omega \times \mathbb{R}^+$ , that is  $\mu : \Omega \times \mathbb{R}^+ \rightarrow \mathbb{R}$ . Some examples of nonlinear  $\mu$  are the following:

$$\mu(s) := 2 + \frac{1}{1+s} \quad \text{and} \quad \mu(s) := \alpha_0 + \alpha_1(1+s^2)^{(\beta-2)/2}, \quad (2.3)$$

where  $\alpha_0, \alpha_1 > 0$  and  $\beta \in [1, 2]$ . The first example is basically academic but the second one corresponds to a particular case of the well-known Carreau law in fluid mechanics. It is easy to see that they both satisfy (2.2) with  $(\mu_1, \mu_2) = (2, 3)$  and  $(\mu_1, \mu_2) = (\alpha_0, \alpha_0 + \alpha_1)$ , respectively.

Next, we adopt the approach from [40] (see also [91, 89]) and introduce the additional unknowns  $\mathbf{t}_S := \mathbf{e}(\mathbf{u}_S)$  and  $\boldsymbol{\rho}_S := \frac{1}{2}(\nabla \mathbf{u}_S - (\nabla \mathbf{u}_S)^t)$ , where  $\boldsymbol{\rho}_S$  is the vorticity (or skew-symmetric part of the velocity gradient). In this way, we observe that the equations in (2.1) can be rewritten equivalently as

$$\begin{aligned} \mathbf{t}_S &= \nabla \mathbf{u}_S - \boldsymbol{\rho}_S \quad \text{in } \Omega_S, \quad \boldsymbol{\sigma}_S^d = \mu(|\mathbf{t}_S|)\mathbf{t}_S - (\mathbf{u}_S \otimes \mathbf{u}_S)^d \quad \text{in } \Omega_S, \\ -\operatorname{div} \boldsymbol{\sigma}_S &= \mathbf{f}_S \quad \text{in } \Omega_S, \quad p_S = -\frac{1}{n} \operatorname{tr}(\boldsymbol{\sigma}_S + (\mathbf{u}_S \otimes \mathbf{u}_S)) \quad \text{in } \Omega_S, \quad \mathbf{u}_S = \mathbf{0} \quad \text{on } \Gamma_S. \end{aligned} \quad (2.4)$$

Note that the fourth equation in (2.4) allows us to eliminate the pressure  $p_S$  from the system and compute it as a simple post-process of the solution.

On the other hand, in  $\Omega_D$  we consider the linearized Darcy model with homogeneous Neumann boundary condition on  $\Gamma_D$ :

$$\mathbf{u}_D = -\mathbf{K} \nabla p_D \quad \text{in } \Omega_D, \quad \operatorname{div} \mathbf{u}_D = f_D \quad \text{in } \Omega_D, \quad \mathbf{u}_D \cdot \mathbf{n} = 0 \quad \text{on } \Gamma_D, \quad (2.5)$$

where  $\mathbf{u}_D$  and  $p_D$  denote the velocity and pressure, respectively,  $f_D \in L^2(\Omega_D)$  is a source term satisfying  $\int_{\Omega_D} f_D = 0$ , and  $\mathbf{K} \in [L^\infty(\Omega_D)]^{n \times n}$  is a positive definite symmetric tensor describing the permeability of  $\Omega_D$  divided by a constant approximation of the viscosity.

Finally, the transmission conditions are given by

$$\mathbf{u}_S \cdot \mathbf{n} = \mathbf{u}_D \cdot \mathbf{n} \quad \text{and} \quad \boldsymbol{\sigma}_S \mathbf{n} + \sum_{l=1}^{n-1} \omega_l^{-1} (\mathbf{u}_S \cdot \mathbf{t}_l) \mathbf{t}_l = -p_D \mathbf{n} \quad \text{on } \Sigma, \quad (2.6)$$

where  $\{\omega_1, \dots, \omega_{n-1}\}$  is a set of positive frictional constants that can be determined experimentally. The first equation in (2.6) corresponds to mass conservation on  $\Sigma$ , whereas the second one establishes the balance of normal forces and a Beavers–Joseph–Saffman law.

### 2.2.2 The fully-mixed variational formulation

In this section we introduce the weak formulation derived in Chapter 1 for the coupled problem given by (2.4), (2.5), and (2.6). To this end, let us first introduce further notations and definitions. In what follows, given  $\star \in \{S, D\}$ ,  $u, v \in L^2(\Omega_\star)$ ,  $\mathbf{u}, \mathbf{v} \in \mathbf{L}^2(\Omega_\star)$ , and  $\boldsymbol{\sigma}, \boldsymbol{\tau} \in \mathbb{L}^2(\Omega_\star)$ , we set

$$(u, v)_\star := \int_{\Omega_\star} uv, \quad (\mathbf{u}, \mathbf{v})_\star := \int_{\Omega_\star} \mathbf{u} \cdot \mathbf{v}, \quad \text{and} \quad (\boldsymbol{\sigma}, \boldsymbol{\tau})_\star := \int_{\Omega_\star} \boldsymbol{\sigma} : \boldsymbol{\tau}.$$



In addition, we let  $\mathbb{L}_{\text{sym}}^2(\Omega_S)$  and  $\mathbb{L}_{\text{skew}}^2(\Omega_S)$  be the subspaces of symmetric and skew-symmetric tensors of  $\mathbb{L}^2(\Omega_S)$ , respectively, that is

$$\begin{aligned}\mathbb{L}_{\text{sym}}^2(\Omega_S) &:= \left\{ \mathbf{r}_S \in \mathbb{L}^2(\Omega_S) : \mathbf{r}_S^t = \mathbf{r}_S \right\}, \\ \mathbb{L}_{\text{skew}}^2(\Omega_S) &:= \left\{ \boldsymbol{\eta}_S \in \mathbb{L}^2(\Omega_S) : \boldsymbol{\eta}_S^t = -\boldsymbol{\eta}_S \right\}.\end{aligned}$$

Furthermore, we define the spaces

$$\begin{aligned}\mathbf{H}_0(\text{div}; \Omega_D) &:= \left\{ \mathbf{v}_D \in \mathbf{H}(\text{div}; \Omega_D) : \mathbf{v}_D \cdot \mathbf{n} = 0 \text{ on } \Gamma_D \right\}, \\ \mathbb{L}_{\text{tr}}^2(\Omega_S) &:= \left\{ \mathbf{r}_S \in \mathbb{L}_{\text{sym}}^2(\Omega_S) : \text{tr } \mathbf{r}_S = 0 \right\}, \\ \mathbf{H}_{\Gamma_S}^1(\Omega_S) &:= \left\{ v_S \in H^1(\Omega_S) : v_S = 0 \text{ on } \Gamma_S \right\}, \quad \mathbf{H}_{\Gamma_S}^1(\Omega_S) := [\mathbf{H}_{\Gamma_S}^1(\Omega_S)]^n,\end{aligned}$$

and the space of traces

$$\mathbf{H}_{00}^{1/2}(\Sigma) := \left\{ v|_{\Sigma} : v \in \mathbf{H}_{\Gamma_S}^1(\Omega_S) \right\}, \quad \mathbf{H}_{00}^{1/2}(\Sigma) := [\mathbf{H}_{00}^{1/2}(\Sigma)]^n.$$

Equivalently, if  $E_{0,S} : H^{1/2}(\Sigma) \rightarrow L^2(\partial\Omega_S)$  is the extension operator defined by

$$E_{0,S}(\psi) := \begin{cases} \psi & \text{on } \Sigma \\ 0 & \text{on } \Gamma_S \end{cases} \quad \forall \psi \in H^{1/2}(\Sigma),$$

we have that

$$\mathbf{H}_{00}^{1/2}(\Sigma) = \left\{ \psi \in H^{1/2}(\Sigma) : E_{0,S}(\psi) \in H^{1/2}(\partial\Omega_S) \right\},$$

which is endowed with the norm  $\|\psi\|_{1/2,00,\Sigma} := \|E_{0,S}(\psi)\|_{1/2,\partial\Omega_S}$ . In addition,  $\|\cdot\|_{1/2,00,\Sigma}$  also stands for the corresponding product norm of  $\mathbf{H}_{00}^{1/2}(\Sigma)$ . In turn,  $\mathbf{H}_{00}^{-1/2}(\Sigma)$  and  $\mathbf{H}_{00}^{-1/2}(\Sigma)$  are the dual spaces of  $\mathbf{H}_{00}^{1/2}(\Sigma)$  and  $\mathbf{H}_{00}^{1/2}(\Sigma)$ , respectively, with norms denoted in both cases by  $\|\cdot\|_{-1/2,00,\Sigma}$ .

Now, in order to deduce our variational system we need to add two auxiliary unknowns on the coupling boundary

$$\boldsymbol{\varphi} := -\mathbf{u}_S|_{\Sigma} \in \mathbf{H}_{00}^{1/2}(\Sigma) \quad \text{and} \quad \lambda := p_D|_{\Sigma} \in H^{1/2}(\Sigma).$$

In this way, our variational system will be written in terms of the unknowns  $\underline{\mathbf{t}} := (\mathbf{t}_S, \boldsymbol{\sigma}_S, \mathbf{u}_S, \boldsymbol{\rho}_S, \mathbf{u}_D)$ ,  $\underline{\boldsymbol{\varphi}} := (\boldsymbol{\varphi}, \lambda)$  and  $p_D$ . Let us recall from [40, Section 2.3] that, given any constant  $c \in \mathbb{R}$ , the vector defined by  $((\mathbf{t}_S, \boldsymbol{\sigma}_S - c\mathbb{I}, \mathbf{u}_S, \boldsymbol{\rho}_S, \mathbf{u}_D), (\boldsymbol{\varphi}, \lambda + c), p_D + c)$  also becomes a solution of the problem defined below. Hence, in order to ensure uniqueness of solution, we will require the Darcy pressure  $p_D$  to live in  $L_0^2(\Omega_D)$ , where

$$L_0^2(\Omega_D) := \left\{ q \in L^2(\Omega_D) : (q, 1)_D = 0 \right\}.$$

Then, defining the spaces

$$\begin{aligned}\mathbf{X} &:= \mathbb{L}_{\text{tr}}^2(\Omega_S) \times \mathbb{H}(\mathbf{div}; \Omega_S) \times \mathbf{H}_{\Gamma_S}^1(\Omega_S) \times \mathbb{L}_{\text{skew}}^2(\Omega_S) \times \mathbf{H}_0(\text{div}; \Omega_D), \\ \mathbf{M} &:= \mathbf{H}_{00}^{1/2}(\Sigma) \times H^{1/2}(\Sigma), \quad \mathbb{X} := \mathbf{X} \times \mathbf{M}, \quad \text{and} \quad \mathbb{M} := L_0^2(\Omega_D),\end{aligned}$$

with  $\mathbf{X}$ ,  $\mathbf{M}$ ,  $\mathbb{X}$  and  $\mathbb{X} \times \mathbb{M}$  endowed with the product norms

$$\begin{aligned}\|\underline{\mathbf{r}}\|_{\mathbf{X}} &:= \|\mathbf{r}_S\|_{0,\Omega_S} + \|\boldsymbol{\tau}_S\|_{\mathbf{div},\Omega_S} + \|\mathbf{v}_S\|_{1,\Omega_S} + \|\boldsymbol{\eta}_S\|_{0,\Omega_S} + \|\mathbf{v}_D\|_{\text{div},\Omega_D}, \\ \|\underline{\boldsymbol{\psi}}\|_{\mathbf{M}} &:= \|\boldsymbol{\psi}\|_{1/2,00,\Sigma} + \|\xi\|_{1/2,\Sigma}, \quad \|(\underline{\mathbf{r}}, \underline{\boldsymbol{\psi}})\|_{\mathbb{X}} := \|\underline{\mathbf{r}}\|_{\mathbf{X}} + \|\underline{\boldsymbol{\psi}}\|_{\mathbf{M}}, \\ \|((\underline{\mathbf{r}}, \underline{\boldsymbol{\psi}}), q_D)\|_{\mathbb{X} \times \mathbb{M}} &:= \|(\underline{\mathbf{r}}, \underline{\boldsymbol{\psi}})\|_{\mathbb{X}} + \|q_D\|_{0,\Omega},\end{aligned}$$

as explained in [40, Section 2.2], we arrive at the following modified variational formulation for (2.4), (2.5), and (2.6): Find  $((\underline{\mathbf{t}}, \underline{\boldsymbol{\varphi}}), p_D) \in \mathbb{X} \times \mathbb{M}$  such that

$$\begin{aligned} [\mathbf{A}(\mathbf{u}_S)(\underline{\mathbf{t}}, \underline{\boldsymbol{\varphi}}), (\underline{\mathbf{r}}, \underline{\boldsymbol{\psi}})] + [\mathbf{B}(\underline{\mathbf{r}}, \underline{\boldsymbol{\psi}}), p_D] &= [\mathbf{F}, (\underline{\mathbf{r}}, \underline{\boldsymbol{\psi}})] \quad \forall (\underline{\mathbf{r}}, \underline{\boldsymbol{\psi}}) \in \mathbb{X}, \\ [\mathbf{B}(\underline{\mathbf{t}}, \underline{\boldsymbol{\varphi}}), q_D] &= [\mathbf{G}, q_D] \quad \forall q_D \in \mathbb{M}, \end{aligned} \quad (2.7)$$

where, given  $\mathbf{z}_S \in \mathbf{H}_{\Gamma_S}^1(\Omega_S)$ , the operator  $\mathbf{A}(\mathbf{z}_S) : \mathbb{X} \rightarrow \mathbb{X}'$  is defined by

$$[\mathbf{A}(\mathbf{z}_S)(\underline{\mathbf{t}}, \underline{\boldsymbol{\varphi}}), (\underline{\mathbf{r}}, \underline{\boldsymbol{\psi}})] := [a(\mathbf{z}_S)(\underline{\mathbf{t}}), \underline{\mathbf{r}}] + [b(\underline{\mathbf{t}}), \underline{\boldsymbol{\psi}}] + [b(\underline{\mathbf{r}}), \underline{\boldsymbol{\varphi}}] - [c(\underline{\boldsymbol{\varphi}}), \underline{\boldsymbol{\psi}}], \quad (2.8)$$

with

$$\begin{aligned} [a(\mathbf{z}_S)(\underline{\mathbf{t}}), \underline{\mathbf{r}}] &:= [a_1(\underline{\mathbf{t}}), \underline{\mathbf{r}}] + [a_2(\mathbf{z}_S)(\underline{\mathbf{t}}), \underline{\mathbf{r}}], \\ [a_1(\underline{\mathbf{t}}), \underline{\mathbf{r}}] &:= (\mu(|\mathbf{t}_S|)\mathbf{t}_S, \mathbf{r}_S)_S - (\mathbf{r}_S, \boldsymbol{\sigma}_S^d)_S + (\mathbf{t}_S, \boldsymbol{\tau}_S^d)_S + \kappa_1(\boldsymbol{\sigma}_S^d - \mu(|\mathbf{t}_S|)\mathbf{t}_S, \boldsymbol{\tau}_S^d)_S \\ &\quad + \kappa_2(\mathbf{div} \boldsymbol{\sigma}_S, \mathbf{div} \boldsymbol{\tau}_S)_S + (\mathbf{div} \boldsymbol{\tau}_S, \mathbf{u}_S)_S - (\mathbf{div} \boldsymbol{\sigma}_S, \mathbf{v}_S)_S \\ &\quad + (\boldsymbol{\tau}_S, \boldsymbol{\rho}_S)_S - (\boldsymbol{\sigma}_S, \boldsymbol{\eta}_S)_S + \kappa_3(\mathbf{e}(\mathbf{u}_S) - \mathbf{t}_S, \mathbf{e}(\mathbf{v}_S))_S \\ &\quad + \kappa_4 \left( \boldsymbol{\rho}_S - \frac{1}{2}(\nabla \mathbf{u}_S - (\nabla \mathbf{u}_S)^t), \boldsymbol{\eta}_S \right)_S + (\mathbf{K}^{-1} \mathbf{u}_D, \mathbf{v}_D)_D, \\ [a_2(\mathbf{z}_S)(\underline{\mathbf{t}}), \underline{\mathbf{r}}] &:= ((\mathbf{z}_S \otimes \mathbf{u}_S)^d, \kappa_1 \boldsymbol{\tau}^d - \mathbf{r}_S)_S, \\ [b(\underline{\mathbf{r}}), \underline{\boldsymbol{\psi}}] &:= \langle \boldsymbol{\tau}_S \mathbf{n}, \boldsymbol{\psi} \rangle_\Sigma - \langle \mathbf{v}_D \cdot \mathbf{n}, \xi \rangle_\Sigma, \\ [c(\underline{\boldsymbol{\varphi}}), \underline{\boldsymbol{\psi}}] &:= \langle \boldsymbol{\varphi} \cdot \mathbf{n}, \xi \rangle_\Sigma - \langle \boldsymbol{\psi} \cdot \mathbf{n}, \lambda \rangle_\Sigma + \sum_{l=1}^{n-1} \omega_l^{-1} \langle \boldsymbol{\varphi} \cdot \mathbf{t}_l, \boldsymbol{\psi} \cdot \mathbf{t}_l \rangle_\Sigma, \end{aligned} \quad (2.9)$$

whereas the operator  $\mathbf{B} : \mathbb{X} \rightarrow \mathbb{M}'$  and the functionals  $\mathbf{F} : \mathbb{X} \rightarrow \mathbb{R}$  and  $\mathbf{G} : \mathbb{M} \rightarrow \mathbb{R}$  are given by

$$[\mathbf{B}(\underline{\mathbf{r}}, \underline{\boldsymbol{\psi}}), q_D] := -(\mathbf{div} \mathbf{v}_D, q_D)_D, \quad (2.10)$$

and

$$[\mathbf{F}, (\underline{\mathbf{r}}, \underline{\boldsymbol{\psi}})] := -\kappa_2(\mathbf{f}_S, \mathbf{div} \boldsymbol{\tau}_S)_S + (\mathbf{f}_S, \mathbf{v}_S)_S \quad \text{and} \quad [\mathbf{G}, q_D] := -(f_D, q_D)_D. \quad (2.11)$$

In all the foregoing terms,  $[\cdot, \cdot]$  denotes the duality pairing induced by the corresponding operators and  $\kappa_i$ ,  $i \in \{1, \dots, 4\}$ , are positive parameters to be specified below in Theorem 2.1.

Furthermore, we notice from (2.9) that, owing to the Cauchy–Schwarz and Hölder’s inequalities, and the continuous injection  $\mathbf{i}_c$  of  $\mathbf{H}^1(\Omega_S)$  into  $\mathbf{L}^4(\Omega_S)$  (see e.g. [1, Theorem 6.3] or [139, Theorem 1.3.5]), there holds

$$|[a_2(\mathbf{z}_S)(\underline{\mathbf{t}}), \underline{\mathbf{r}}]| \leq c_2(\Omega_S)(\kappa_1^2 + 1)^{1/2} \|\mathbf{z}_S\|_{1, \Omega_S} \|\mathbf{u}_S\|_{1, \Omega_S} \|\underline{\mathbf{r}}\|_{\mathbf{X}} \quad \forall \underline{\mathbf{t}}, \underline{\mathbf{r}} \in \mathbf{X}, \quad (2.12)$$

where  $c_2(\Omega_S) := \|\mathbf{i}_c\|^2$ . Additionally, we observe that (2.7) is equivalent to the variational formulation defined in [40, Section 2.2], in which  $\boldsymbol{\sigma}_S$  is decomposed as  $\boldsymbol{\sigma}_S = \boldsymbol{\sigma} + l\mathbb{I}$ , with  $\boldsymbol{\sigma} \in \mathbb{H}_0(\mathbf{div}; \Omega_S)$  and  $l \in \mathbb{R}$ , where

$$\mathbb{H}_0(\mathbf{div}; \Omega_S) := \left\{ \boldsymbol{\tau} \in \mathbb{H}(\mathbf{div}; \Omega_S) : (\text{tr } \boldsymbol{\tau}, 1)_S = 0 \right\}.$$

The following result taken from [40] establishes the well-posedness of (2.7).

**Theorem 2.1.** *Assume that*

$$\kappa_1 \in \left(0, \frac{2\delta_1\mu_1}{L_\mu}\right), \quad \kappa_2 > 0, \quad \kappa_3 \in \left(0, 2\delta_2 \left(\mu_1 - \frac{\kappa_1 L_\mu}{2\delta_1}\right)\right), \quad \text{and} \quad \kappa_4 \in \left(0, 2\delta_3 C_{\text{Ko}} \kappa_3 \left(1 - \frac{\delta_2}{2}\right)\right),$$

with  $L_\mu := \max\{\mu_2, 2\mu_2 - \mu_1\}$ ,  $C_{\text{Ko}}$  the Korn's constant given by [40, eq. (3.10)],  $\delta_1 \in \left(0, \frac{2}{L_\mu}\right)$ ,  $\delta_2 \in (0, 2)$ , and  $\delta_3 \in (0, 2)$ . In addition, given  $r \in (0, r_0)$ , with

$$r_0 := \frac{\alpha_0(\Omega)}{2c_2(\Omega_S)(\kappa_1^2 + 1)^{1/2}}, \quad (2.13)$$

where  $c_2(\Omega_S)$  is the constant in (2.12) and  $\alpha_0(\Omega)$  is the strong monotonicity constant of the nonlinear operator  $a$  (see [40, eq. (3.16)]), we let  $W_r := \left\{\mathbf{z}_S \in \mathbf{H}_{\Gamma_S}^1(\Omega_S) : \|\mathbf{z}_S\|_{1,\Omega_S} \leq r\right\}$ , and assume that the data  $\mathbf{f}_S$  and  $f_D$  satisfy

$$c_{\mathbf{T}} \left\{ \|\mathbf{f}_S\|_{0,\Omega_S} + \|f_D\|_{0,\Omega_D} \right\} \leq r, \quad (2.14)$$

where  $c_{\mathbf{T}}$  is the positive constant, independent of the data, provided by [40, Lemma 3.6]. Then, the augmented fully-mixed formulation (2.7) has a unique solution  $((\underline{\mathbf{t}}, \underline{\boldsymbol{\varphi}}), p_D) \in \mathbb{X} \times \mathbb{M}$  with  $\mathbf{u}_S \in W_r$ , which satisfies

$$\|((\underline{\mathbf{t}}, \underline{\boldsymbol{\varphi}}), p_D)\|_{\mathbb{X} \times \mathbb{M}} \leq c_{\mathbf{T}} \left\{ \|\mathbf{f}_S\|_{0,\Omega_S} + \|f_D\|_{0,\Omega_D} \right\}. \quad (2.15)$$

*Proof.* See [40, Theorem 3.11] for details.  $\square$

### 2.2.3 The fully-mixed finite element method

Here, for clarity of exposition of the a posteriori error estimator to be defined next in Section 2.3, we restrict ourselves to the particular case provided in [40, Section 6.2] with  $k = 0$  and introduce a Galerkin scheme for the 3D version of (2.7). To that end we let  $\mathcal{T}_h^S$  and  $\mathcal{T}_h^D$  be respective triangulations of the domains  $\Omega_S$  and  $\Omega_D$ , which are formed by shape-regular tetrahedra  $T$  of diameter  $h_T$ , and assume that they match in  $\Sigma$  so that  $\mathcal{T}_h^S \cup \mathcal{T}_h^D$  is a triangulation of  $\Omega := \Omega_S \cup \Sigma \cup \Omega_D$ . Then, for each  $T \in \mathcal{T}_h^S \cup \mathcal{T}_h^D$  we set the local Raviart–Thomas space of lowest order,

$$\text{RT}_0(T) := \mathbf{P}_0(T) + P_0(T)\mathbf{x},$$

where  $\mathbf{x}$  is a generic vector in  $\mathbb{R}^3$ . We also let  $\Sigma_h$  be the partition of  $\Sigma$  inherited from  $\mathcal{T}_h^S$  (or  $\mathcal{T}_h^D$ ), which is formed by triangles  $e$  of diameter  $h_e$ , and set  $h_\Sigma := \max\{h_e : e \in \Sigma_h\}$ . Furthermore, we introduce the following discrete subspaces

$$\begin{aligned} \mathbb{L}_h^2(\Omega_\star) &:= \{q_h \in L^2(\Omega_\star) : q_h|_T \in P_0(T) \quad \forall T \in \mathcal{T}_h^\star\}, \quad \star \in \{S, D\}, \\ \mathbf{H}_h(\Omega_\star) &:= \{\tau_h \in \mathbf{H}(\text{div}; \Omega_\star) : \tau_h|_T \in \text{RT}_0(T) \quad \forall T \in \mathcal{T}_h^\star\}, \quad \star \in \{S, D\}, \\ \mathbf{H}_h^1(\Omega_S) &:= \{\mathbf{v}_h \in [\mathcal{C}(\overline{\Omega_S})]^3 : \mathbf{v}_h|_T \in \mathbf{P}_1(T) \quad \forall T \in \mathcal{T}_h^S\}, \\ \mathbb{L}_{\text{tr},h}^2(\Omega_S) &:= \{\mathbf{r}_h \in \mathbb{L}_{\text{tr}}^2(\Omega_S) : \mathbf{r}_h|_T \in \mathbb{P}_0(T) \quad \forall T \in \mathcal{T}_h^S\}, \\ \mathbb{L}_{\text{skew},h}^2(\Omega_S) &:= \{\boldsymbol{\eta}_h \in \mathbb{L}_{\text{skew}}^2(\Omega_S) : \boldsymbol{\eta}_h|_T \in \mathbb{P}_0(T) \quad \forall T \in \mathcal{T}_h^S\}. \end{aligned}$$

In turn, in order to define the discrete spaces for the unknowns on the interface  $\Sigma$ , we introduce an independent triangulation  $\widehat{\Sigma}_h$  of  $\Sigma$ , by triangles  $\widehat{e}$  of diameter  $h_{\widehat{e}}$ , and define the associated meshsize  $h_{\widehat{\Sigma}} := \max\{h_{\widehat{e}} : \widehat{e} \in \widehat{\Sigma}_h\}$ . Then, denoting by  $\partial\Sigma$  the polygonal boundary of  $\Sigma$ , we define

$$\begin{aligned}\Lambda_h^S(\Sigma) &:= \left\{ \psi_h \in \mathcal{C}(\Sigma) : \quad \psi_h|_{\widehat{e}} \in P_1(\widehat{e}) \quad \forall \widehat{e} \in \widehat{\Sigma}_h, \quad \psi_h = 0 \quad \text{on} \quad \partial\Sigma \right\}, \\ \Lambda_h^D(\Sigma) &:= \left\{ \xi_h \in \mathcal{C}(\Sigma) : \quad \xi_h|_{\widehat{e}} \in P_1(\widehat{e}) \quad \forall \widehat{e} \in \widehat{\Sigma}_h \right\}.\end{aligned}\tag{2.16}$$

Employing the above notations, we set

$$\begin{aligned}\mathbb{H}_h(\Omega_S) &:= \left\{ \boldsymbol{\tau}_S \in \mathbb{H}(\mathbf{div}; \Omega_S) : \quad \mathbf{c}^t \boldsymbol{\tau} \in \mathbf{H}_h(\Omega_S) \quad \forall \mathbf{c} \in \mathbb{R}^3 \right\}, \\ \mathbb{H}_{h,0}(\Omega_S) &:= \mathbb{H}_h(\Omega_S) \cap \mathbb{H}_0(\mathbf{div}; \Omega_S), \\ \mathbf{H}_{h,\Gamma_S}^1(\Omega_S) &:= \mathbf{H}_h^1(\Omega_S) \cap \mathbf{H}_{\Gamma_S}^1(\Omega_S), \\ \mathbf{H}_{h,0}(\Omega_D) &:= \mathbf{H}_h(\Omega_D) \cap \mathbf{H}_0(\mathbf{div}; \Omega_D), \\ L_{h,0}^2(\Omega_D) &:= L_h^2(\Omega_D) \cap L_0^2(\Omega_D), \\ \Lambda_h^S(\Sigma) &:= [\Lambda_h^S(\Sigma)]^3.\end{aligned}$$

Then, defining the global spaces, unknowns, and test functions as follows

$$\begin{aligned}\mathbf{X}_h &:= \mathbb{L}_{\text{tr},h}^2(\Omega_S) \times \mathbb{H}_{h,0}(\Omega_S) \times \mathbf{H}_{h,\Gamma_S}^1(\Omega_S) \times \mathbb{L}_{\text{skew},h}^2(\Omega_S) \times \mathbf{H}_{h,0}(\Omega_D), \\ \mathbf{M}_h &:= \Lambda_h^S(\Sigma) \times \Lambda_h^D(\Sigma), \quad \mathbb{X}_h := \mathbf{X}_h \times \mathbf{M}_h, \quad \mathbb{M}_h := L_{h,0}^2(\Omega_D), \\ \underline{\mathbf{t}}_h &:= (\mathbf{t}_{S,h}, \boldsymbol{\sigma}_{S,h}, \mathbf{u}_{S,h}, \boldsymbol{\rho}_{S,h}, \mathbf{u}_{D,h}) \in \mathbf{X}_h, \quad \underline{\boldsymbol{\varphi}}_h := (\boldsymbol{\varphi}_h, \lambda_h) \in \mathbf{M}_h, \\ \underline{\mathbf{r}}_h &:= (\mathbf{r}_{S,h}, \boldsymbol{\tau}_{S,h}, \mathbf{v}_{S,h}, \boldsymbol{\eta}_{S,h}, \mathbf{v}_{D,h}) \in \mathbf{X}_h, \quad \underline{\boldsymbol{\psi}}_h := (\boldsymbol{\psi}_h, \xi_h) \in \mathbf{M}_h, \\ p_{D,h} &\in \mathbb{M}_h, \quad \text{and} \quad q_{D,h} \in \mathbb{M}_h,\end{aligned}$$

the Galerkin scheme for problem (2.7) reads: Find  $((\underline{\mathbf{t}}_h, \underline{\boldsymbol{\varphi}}_h), p_{D,h}) \in \mathbb{X}_h \times \mathbb{M}_h$  such that

$$\begin{aligned}[\mathbf{A}(\mathbf{u}_{S,h})(\underline{\mathbf{t}}_h, \underline{\boldsymbol{\varphi}}_h), (\underline{\mathbf{r}}_h, \underline{\boldsymbol{\psi}}_h)] + [\mathbf{B}(\underline{\mathbf{r}}_h, \underline{\boldsymbol{\psi}}_h), p_{D,h}] &= [\mathbf{F}, (\underline{\mathbf{r}}_h, \underline{\boldsymbol{\psi}}_h)] \quad \forall (\underline{\mathbf{r}}_h, \underline{\boldsymbol{\psi}}_h) \in \mathbb{X}_h, \\ [\mathbf{B}(\underline{\mathbf{t}}_h, \underline{\boldsymbol{\varphi}}_h), q_{D,h}] &= [\mathbf{G}, q_{D,h}] \quad \forall q_{D,h} \in \mathbb{M}_h.\end{aligned}\tag{2.17}$$

The following theorem, also taken from [40], provides the well-posedness of (2.17), the associated Céa estimate, and the corresponding theoretical rate of convergence.

**Theorem 2.2.** *Assume that the conditions on  $\kappa_i, i \in \{1, \dots, 4\}$ , required by Theorem 2.1 hold. In addition, given  $r \in (0, r_0)$ , with  $r_0$  defined by (2.13), we let*

$$W_r^h := \left\{ \mathbf{z}_{S,h} \in \mathbf{H}_{h,\Gamma_S}^1(\Omega_S) : \quad \|\mathbf{z}_{S,h}\|_{1,\Omega_S} \leq r \right\},$$

and assume that the data  $\mathbf{f}_S$  and  $f_D$  satisfy

$$\tilde{\mathbf{c}}_{\mathbf{T}} \{ \|\mathbf{f}_S\|_{0,\Omega_S} + \|f_D\|_{0,\Omega_D} \} \leq r,\tag{2.18}$$

where  $\tilde{c}_{\mathbf{T}}$  is the positive constant, independent of the data, provided by [40, Lemma 4.2]. Then there exists a constant  $C_0 > 0$  such that, whenever  $h_{\Sigma} \leq C_0 h_{\widehat{\Sigma}}$ , there exists a unique  $((\underline{\mathbf{t}}_h, \underline{\boldsymbol{\varphi}}_h), p_{D,h}) \in \mathbb{X}_h \times \mathbb{M}_h$  solution to problem (2.17) with  $\mathbf{u}_{S,h} \in W_r^h$ . In addition, there holds

$$\|((\underline{\mathbf{t}}_h, \underline{\boldsymbol{\varphi}}_h), p_{D,h})\|_{\mathbb{X} \times \mathbb{M}} \leq \tilde{c}_{\mathbf{T}} \left\{ \|\mathbf{f}_S\|_{0,\Omega_S} + \|f_D\|_{0,\Omega_D} \right\}, \quad (2.19)$$

and there exists  $C_1 > 0$ , independent of  $h$ ,  $h_{\Sigma}$ , and  $h_{\widehat{\Sigma}}$ , such that

$$\|((\underline{\mathbf{t}}, \underline{\boldsymbol{\varphi}}), p_D) - ((\underline{\mathbf{t}}_h, \underline{\boldsymbol{\varphi}}_h), p_{D,h})\|_{\mathbb{X} \times \mathbb{M}} \leq C_1 \text{dist}(((\underline{\mathbf{t}}, \underline{\boldsymbol{\varphi}}), p_D), \mathbb{X}_h \times \mathbb{M}_h).$$

Assume further that there exists  $\delta > 0$  such that  $\mathbf{t}_S \in \mathbb{H}^{\delta}(\Omega_S)$ ,  $\boldsymbol{\sigma}_S \in \mathbb{H}^{\delta}(\Omega_S)$ ,  $\mathbf{div} \boldsymbol{\sigma}_S \in \mathbf{H}^{\delta}(\Omega_S)$ ,  $\mathbf{u}_S \in \mathbf{H}^{1+\delta}(\Omega_S)$ ,  $\boldsymbol{\varphi} \in \mathbf{H}^{1/2+\delta}(\Sigma)$ ,  $\boldsymbol{\rho}_S \in \mathbb{H}^{\delta}(\Omega_S)$ ,  $\mathbf{u}_D \in \mathbf{H}^{\delta}(\Omega_D)$ , and  $\text{div} \mathbf{u}_D \in \mathbf{H}^{\delta}(\Omega_D)$ . Then  $p_D \in H^{1+\delta}(\Omega_D)$ ,  $\lambda \in H^{1/2+\delta}(\Sigma)$ , and there exists  $C_2 > 0$ , independent of  $h$ ,  $h_{\Sigma}$ , and  $h_{\widehat{\Sigma}}$ , such that

$$\begin{aligned} \|((\underline{\mathbf{t}}, \underline{\boldsymbol{\varphi}}), p_D) - ((\underline{\mathbf{t}}_h, \underline{\boldsymbol{\varphi}}_h), p_{D,h})\|_{\mathbb{X} \times \mathbb{M}} &\leq C_2 h^{\delta} \left\{ \|\mathbf{t}_S\|_{\delta,\Omega_S} + \|\boldsymbol{\sigma}_S\|_{\delta,\Omega_S} + \|\mathbf{div} \boldsymbol{\sigma}_S\|_{\delta,\Omega_S} + \|\mathbf{u}_S\|_{1+\delta,\Omega_S} \right. \\ &\quad \left. + \|\boldsymbol{\rho}_S\|_{\delta,\Omega_S} + \|\mathbf{u}_D\|_{\delta,\Omega_D} + \|\text{div} \mathbf{u}_D\|_{\delta,\Omega_D} + \|p_D\|_{1+\delta,\Omega_D} \right\}. \end{aligned}$$

*Proof.* We refer the reader to [40, Theorems 4.3, 5.4, and 6.2] for details.  $\square$

We end this section by pointing out that the assumption  $h_{\Sigma} \leq C_0 h_{\widehat{\Sigma}}$  required in Theorem 2.2 is needed to prove the discrete inf-sup condition for the bilinear form  $b$  (cf. (2.9)). We omit further details about this issue and refer the reader to [86, Lemma 7.5] for more details.

## 2.3 A residual-based a posteriori error estimator

In this section we derive a reliable and efficient residual-based *a posteriori* error estimator for the three dimensional Galerkin scheme (2.17). The corresponding a posteriori error analysis for the 2D case should be quite straightforward. We remark in advance that most of the proofs here make extensive use of estimates already available in the literature. In particular, we apply results from [82, 80, 89, 93, 97], among others.

### 2.3.1 Preliminaries

We begin by introducing further notations and definitions. First, given  $T \in \mathcal{T}_h^S \cup \mathcal{T}_h^D$ , we let  $\mathcal{E}(T)$  be the set of faces of  $T$ , and denote by  $\mathcal{E}_h$  the set of all faces of  $\mathcal{T}_h^S \cup \mathcal{T}_h^D$ , subdivided as follows:

$$\mathcal{E}_h = \mathcal{E}_h(\Gamma_S) \cup \mathcal{E}_h(\Gamma_D) \cup \mathcal{E}_h(\Omega_S) \cup \mathcal{E}_h(\Omega_D) \cup \mathcal{E}_h(\Sigma),$$

where  $\mathcal{E}_h(\Gamma_{\star}) := \{e \in \mathcal{E}_h : e \subseteq \Gamma_{\star}\}$ ,  $\mathcal{E}_h(\Omega_{\star}) := \{e \in \mathcal{E}_h : e \subseteq \Omega_{\star}\}$ , for  $\star \in \{S, D\}$ , and the faces of  $\mathcal{E}_h(\Sigma)$  are exactly those forming the previously defined partition  $\Sigma_h$ , that is  $\mathcal{E}_h(\Sigma) := \{e \in \mathcal{E}_h : e \subseteq \Sigma\}$ . Also, for each  $e \in \mathcal{E}_h(\Omega_{\star})$  we fix a unit normal  $\mathbf{n}_e$ , and then, given  $\mathbf{v} = (v_1, v_2, v_3)^t \in \mathbf{L}^2(\Omega)$  and  $\boldsymbol{\tau} := (\tau_{ij})_{3 \times 3} \in \mathbb{L}^2(\Omega)$  such that  $\mathbf{v}|_T \in \mathbf{C}(T)$  and  $\boldsymbol{\tau}|_T \in \mathbb{C}(T)$  on each  $T \in \mathcal{T}_h$ , we let  $\llbracket \mathbf{v} \times \mathbf{n}_e \rrbracket$  and  $\llbracket \boldsymbol{\tau} \times \mathbf{n}_e \rrbracket$  be the corresponding jumps of the tangential traces across  $e$ . In other words,  $\llbracket \mathbf{v} \times \mathbf{n}_e \rrbracket := (\mathbf{v}|_T - \mathbf{v}|_{T'})|_e \times \mathbf{n}_e$

and  $[\boldsymbol{\tau} \times \mathbf{n}_e] := (\boldsymbol{\tau}|_T - \boldsymbol{\tau}|_{T'})|_e \times \mathbf{n}_e$ , respectively, where  $T$  and  $T'$  are the elements of  $\mathcal{T}_h^\star$  having  $e$  as a common face and

$$\boldsymbol{\tau} \times \mathbf{n}_e := \begin{pmatrix} (\tau_{11}, \tau_{12}, \tau_{13}) \times \mathbf{n}_e \\ (\tau_{21}, \tau_{22}, \tau_{23}) \times \mathbf{n}_e \\ (\tau_{31}, \tau_{32}, \tau_{33}) \times \mathbf{n}_e \end{pmatrix}.$$

From now on, when no confusion arises, we simply write  $\mathbf{n}$  instead of  $\mathbf{n}_e$ . In the sequel we will also make use of the following differential operators:

$$\operatorname{curl}(\mathbf{v}) = \nabla \times \mathbf{v} := \left( \frac{\partial v_3}{\partial x_2} - \frac{\partial v_2}{\partial x_3}, \frac{\partial v_1}{\partial x_3} - \frac{\partial v_3}{\partial x_1}, \frac{\partial v_2}{\partial x_1} - \frac{\partial v_1}{\partial x_2} \right)$$

and

$$\underline{\operatorname{curl}}(\boldsymbol{\tau}) := \begin{pmatrix} \operatorname{curl}(\tau_{11}, \tau_{12}, \tau_{13}) \\ \operatorname{curl}(\tau_{21}, \tau_{22}, \tau_{23}) \\ \operatorname{curl}(\tau_{31}, \tau_{32}, \tau_{33}) \end{pmatrix}.$$

In turn, the tangential curl operator  $\mathbf{curl}_s : \mathbf{H}^{1/2}(\Sigma) \rightarrow \mathcal{L}(\mathbf{H}^{-1/2}(\Sigma))$ , with  $\mathcal{L}(\mathbf{H}^{-1/2}(\Sigma))$  denoting the tangential vector fields of order  $-1/2$ , will also be needed. This operator which can be defined by  $\mathbf{curl}_s(\xi) = \nabla \xi \times \mathbf{n}$  for any sufficiently smooth function  $\xi$ , is linear and continuous (see [21, Propositions 3.4 and 3.6] for details). A tensor version of  $\mathbf{curl}_s$ , say  $\underline{\operatorname{curl}}_s : \mathbf{H}^{1/2}(\Sigma) \rightarrow \mathcal{L}(\mathbf{H}^{-1/2}(\Sigma))$ , which is defined component-wise by  $\mathbf{curl}_s$ , will be also utilized.

Let us now recall the main properties of the Raviart–Thomas interpolator of lowest order (see [19, 81, 100]) and the Cl  ment operator onto the space of continuous piecewise linear functions [49]. We begin with the aforementioned Raviart–Thomas operator  $\Pi_h^\star : \mathbf{H}^1(\Omega_\star) \rightarrow \mathbf{H}_h(\Omega_\star)$  (recall the definition of  $\mathbf{H}_h(\Omega_\star)$  in Section 2.2.3),  $\star \in \{S, D\}$ , which is characterized by the identity

$$\int_e \Pi_h^\star \mathbf{v} \cdot \mathbf{n} = \int_e \mathbf{v} \cdot \mathbf{n} \quad \forall \text{ face } e \text{ of } \mathcal{T}_h^\star. \quad (2.20)$$

As a consequence of (2.20), there holds

$$\operatorname{div}(\Pi_h^\star \mathbf{v}) = \mathcal{P}_h^\star(\operatorname{div} \mathbf{v}), \quad (2.21)$$

where  $\mathcal{P}_h^\star$  is the  $L^2(\Omega_\star)$ -orthogonal projector onto the piecewise constant functions on  $\Omega_\star$ . A tensor version of  $\Pi_h^\star$ , say  $\mathbf{\Pi}_h^\star : \mathbb{H}^1(\Omega_\star) \rightarrow \mathbb{H}_h(\Omega_\star)$ , which is defined row-wise by  $\Pi_h^\star$ , and a vector version of  $\mathcal{P}_h^\star$ , say  $\mathbf{P}_h^\star$ , which is the  $L^2(\Omega_\star)$ -orthogonal projector onto the piecewise constant vectors on  $\Omega_\star$ , might also be required. The local approximation properties of  $\Pi_h^\star$  (and hence of  $\mathbf{\Pi}_h^\star$ ) are established in the following lemma. For the corresponding proof we refer to [19] (see also [81]).

**Lemma 2.3.** *For each  $\star \in \{S, D\}$  there exist constants  $c_1, c_2 > 0$ , independent of  $h$ , such that for all  $\mathbf{v} \in \mathbf{H}^1(\Omega_\star)$  there hold*

$$\|\mathbf{v} - \Pi_h^\star \mathbf{v}\|_{0,T} \leq c_1 h_T \|\mathbf{v}\|_{1,T} \quad \forall T \in \mathcal{T}_h^\star,$$

and

$$\|\mathbf{v} \cdot \mathbf{n} - \Pi_h^\star \mathbf{v} \cdot \mathbf{n}\|_{0,e} \leq c_2 h_e^{1/2} \|\mathbf{v}\|_{1,T_e} \quad \forall \text{ face } e \text{ of } \mathcal{T}_h^\star,$$

where  $T_e$  is a tetrahedron of  $\mathcal{T}_h^\star$  containing  $e$  on its boundary.

In turn, the Clément operator  $I_h^* : \mathbf{H}^1(\Omega_\star) \rightarrow \mathbf{H}_h^1(\Omega_\star)$ , with

$$\mathbf{H}_h^1(\Omega_\star) := \left\{ v \in \mathcal{C}(\overline{\Omega}_\star) : v|_T \in P_1(T) \quad \forall T \in \mathcal{T}_h^\star \right\},$$

approximates optimally non-smooth functions by continuous piecewise linear functions. The local approximation properties of this operator are established in the following lemma (see [49]).

**Lemma 2.4.** *For each  $\star \in \{\mathbf{S}, \mathbf{D}\}$  there exist constants  $c_3, c_4 > 0$ , independent of  $h$ , such that for all  $v \in \mathbf{H}^1(\Omega_\star)$  there holds*

$$\|v - I_h^\star v\|_{0,T} \leq c_3 h_T \|v\|_{1,\Delta_\star(T)} \quad \forall T \in \mathcal{T}_h^\star,$$

and

$$\|v - I_h^\star v\|_{0,e} \leq c_4 h_e^{1/2} \|v\|_{1,\Delta_\star(e)} \quad \forall e \in \mathcal{E}_h,$$

where

$$\Delta_\star(T) := \cup \left\{ T' \in \mathcal{T}_h^\star : T' \cap T \neq \emptyset \right\} \quad \text{and} \quad \Delta_\star(e) := \cup \left\{ T' \in \mathcal{T}_h^\star : T' \cap e \neq \emptyset \right\}.$$

In what follows, a vector version of  $I_h^\star$ , say  $\mathbf{I}_h^\star : \mathbf{H}^1(\Omega_\star) \rightarrow \mathbf{H}_h^1(\Omega_\star)$ , which is defined component-wise by  $I_h^\star$ , will be needed as well.

For the forthcoming analysis we will also utilize a couple of results providing stable Helmholtz decompositions for  $\mathbb{H}(\mathbf{div}; \Omega_\mathbf{S})$  and  $\mathbf{H}_0(\mathbf{div}; \Omega_\mathbf{D})$ . In this regard, we remark in advance that the decomposition for  $\mathbf{H}_0(\mathbf{div}; \Omega_\mathbf{D})$  will require the boundary  $\Gamma_\mathbf{D}$  to lie in a “convex part” of  $\Omega_\mathbf{D}$ , which means that there exists a convex domain containing  $\Omega_\mathbf{D}$ , and whose boundary contains  $\Gamma_\mathbf{D}$ . More precisely, we have the following lemma.

**Lemma 2.5.**

a) *For each  $\boldsymbol{\tau}_\mathbf{S} \in \mathbb{H}(\mathbf{div}; \Omega_\mathbf{S})$  there exist  $\boldsymbol{\eta} \in \mathbf{H}^2(\Omega_\mathbf{S})$  and  $\boldsymbol{\chi} \in \mathbb{H}^1(\Omega_\mathbf{S})$  such that*

$$\boldsymbol{\tau}_\mathbf{S} = \nabla \boldsymbol{\eta} + \underline{\text{curl}} \boldsymbol{\chi} \quad \text{in } \Omega_\mathbf{S} \quad \text{and} \quad \|\boldsymbol{\eta}\|_{2,\Omega_\mathbf{S}} + \|\boldsymbol{\chi}\|_{1,\Omega_\mathbf{S}} \leq C_\mathbf{S} \|\boldsymbol{\tau}_\mathbf{S}\|_{\mathbf{div},\Omega_\mathbf{S}}, \quad (2.22)$$

where  $C_\mathbf{S}$  is a positive constant independent of all the foregoing variables.

b) *Assume that there exists a convex domain  $\Xi$  such that  $\Omega_\mathbf{D} \subseteq \Xi$  and  $\Gamma_\mathbf{D} \subseteq \partial\Xi$ . Then, given  $\mathbf{v}_\mathbf{D} \in \mathbf{H}_0(\mathbf{div}; \Omega_\mathbf{D})$  there exist  $w \in \mathbf{H}^2(\Omega_\mathbf{D})$  and  $\boldsymbol{\beta} \in \mathbf{H}_{\Gamma_\mathbf{D}}^1(\Omega_\mathbf{D})$  such that*

$$\mathbf{v}_\mathbf{D} = \nabla w + \text{curl} \boldsymbol{\beta} \quad \text{in } \Omega_\mathbf{D} \quad \text{and} \quad \|w\|_{2,\Omega_\mathbf{D}} + \|\boldsymbol{\beta}\|_{1,\Omega_\mathbf{D}} \leq C_\mathbf{D} \|\mathbf{v}_\mathbf{D}\|_{\mathbf{div},\Omega_\mathbf{D}}, \quad (2.23)$$

where  $C_\mathbf{D}$  is a positive constant independent of all the foregoing variables, and

$$\mathbf{H}_{\Gamma_\mathbf{D}}^1(\Omega_\mathbf{D}) := \left\{ \boldsymbol{\beta} \in \mathbf{H}^1(\Omega_\mathbf{D}) : \boldsymbol{\beta}|_{\Gamma_\mathbf{D}} \in \mathbf{P}_0(\Gamma_\mathbf{D}) \right\}.$$

*Proof.* See [82, Theorems 3.1 and 3.2]. □

We end this section with a lemma providing estimates in terms of local quantities for the  $\mathbf{H}_{00}^{-1/2}(\Sigma)$  and  $\mathbf{H}^{-1/2}(\Sigma)$  norms of functions in particular subspaces of  $\mathbf{L}^2(\Sigma)$  and  $\mathbf{H}^{-1/2}(\Sigma) \cap \mathbf{L}^2(\Sigma)$ , respectively.

More precisely, having in mind the definitions of  $\Lambda_h^S(\Sigma)$  and  $\Lambda_h^D(\Sigma)$  (cf. (2.16)), which are subspaces of  $H_{00}^{1/2}(\Sigma)$  and  $H^{1/2}(\Sigma)$ , respectively, we introduce the orthogonal-type spaces

$$\Lambda_h^{S,\perp}(\Sigma) := \left\{ \lambda \in L^2(\Sigma) : \langle \lambda, \psi_h \rangle_\Sigma = 0 \quad \forall \psi_h \in \Lambda_h^S(\Sigma) \right\} \quad (2.24)$$

and

$$\Lambda_h^{D,\perp}(\Sigma) := \left\{ \lambda \in H^{-1/2}(\Sigma) \cap L^2(\Sigma) : \langle \lambda, \xi_h \rangle_\Sigma = 0 \quad \forall \xi_h \in \Lambda_h^D(\Sigma) \right\}. \quad (2.25)$$

Then, the announced lemma is stated as follows.

**Lemma 2.6.** *Assume that for each  $e \in \Sigma_h$  there exists  $\widehat{e} \in \widehat{\Sigma}_h$  such that  $e \subseteq \widehat{e}$  and  $h_{\widehat{e}} \leq C_1 h_e$ , with a constant  $C_1 > 0$  independent of  $h_\Sigma$  and  $h_{\widehat{\Sigma}}$ . Then, there exists  $C > 0$ , independent of the aforementioned meshsizes, such that*

$$\|\lambda\|_{-1/2,00,\Sigma}^2 \leq C \sum_{e \in \Sigma_h} h_e \|\lambda\|_{0,e}^2 \quad \forall \lambda \in \Lambda_h^{S,\perp}(\Sigma), \quad (2.26)$$

and

$$\|\lambda\|_{-1/2,\Sigma}^2 \leq C \sum_{e \in \Sigma_h} h_e \|\lambda\|_{0,e}^2 \quad \forall \lambda \in \Lambda_h^{D,\perp}(\Sigma). \quad (2.27)$$

*Proof.* Given  $\lambda \in \Lambda_h^{S,\perp}(\Sigma)$ , we first observe that  $\lambda \in H_{00}^{-1/2}(\Sigma)$  and that

$$\|\lambda\|_{-1/2,00,\Sigma} = \sup_{\substack{\xi \in H_{00}^{1/2}(\Sigma) \\ \xi \neq 0}} \frac{\langle \lambda, \xi \rangle_\Sigma}{\|\xi\|_{1/2,00,\Sigma}} \leq \sup_{\substack{v \in H_{\Gamma_S}^1(\Omega_S) \\ v \neq 0}} \frac{\langle \lambda, v \rangle_\Sigma}{\|v\|_{1,\Omega_S}}. \quad (2.28)$$

Next, we let  $\widehat{\mathcal{T}}_h^S$  be a regular triangulation of the domain  $\Omega_S$  which coincides with  $\widehat{\Sigma}_h$  on  $\Sigma$ , and let

$$\widehat{I}_h : H^1(\Omega_S) \rightarrow \widehat{Y}_h := \left\{ v \in \mathcal{C}(\overline{\Omega_S}) : v|_T \in P_1(T) \quad \forall T \in \widehat{\mathcal{T}}_h^S \right\}$$

be the usual Clément operator (see Section 2.3.1). Then, since  $\widehat{I}_h(v)|_\Sigma \in \Lambda_h^S(\Sigma) \quad \forall v \in H_{\Gamma_S}^1(\Omega_S)$ , it follows from (2.24), (2.28), and the Cauchy–Schwarz inequality, that

$$\|\lambda\|_{-1/2,00,\Sigma} \leq \sup_{\substack{v \in H_{\Gamma_S}^1(\Omega_S) \\ v \neq 0}} \frac{\langle \lambda, v - \widehat{I}_h(v) \rangle_\Sigma}{\|v\|_{1,\Omega_S}} \leq \sup_{\substack{v \in H_{\Gamma_S}^1(\Omega_S) \\ v \neq 0}} \frac{\sum_{e \in \Sigma_h} \|\lambda\|_{0,e} \|v - \widehat{I}_h(v)\|_{0,\widehat{e}}}{\|v\|_{1,\Omega_S}}, \quad (2.29)$$

where we also use that  $\|v - \widehat{I}_h(v)\|_{0,e} \leq \|v - \widehat{I}_h(v)\|_{0,\widehat{e}}$ . In turn, applying the second approximation property from Lemma 2.4, the estimate  $h_{\widehat{e}} \leq C_1 h_e$ , and the fact that the number of triangles of the macro-elements  $\Delta(\widehat{e})$  are uniformly bounded, we find that

$$\begin{aligned} \sum_{e \in \Sigma_h} \|\lambda\|_{0,e} \|v - \widehat{I}_h(v)\|_{0,\widehat{e}} &\leq \sum_{e \in \Sigma_h} h_{\widehat{e}}^{1/2} \|\lambda\|_{0,e} \|v\|_{1,\Delta(\widehat{e})} \\ &\leq \left\{ \sum_{e \in \Sigma_h} h_{\widehat{e}} \|\lambda\|_{0,e}^2 \right\}^{1/2} \left\{ \sum_{e \in \Sigma_h} \|v\|_{1,\Delta(\widehat{e})}^2 \right\}^{1/2} \leq C \left\{ \sum_{e \in \Sigma_h} h_e \|\lambda\|_{0,e}^2 \right\}^{1/2} \|v\|_{1,\Omega_S}, \end{aligned}$$

which, replaced back into (2.29), gives (2.26). The proof of (2.27), being similar to that of (2.26), is omitted.  $\square$



### 2.3.2 The main result

In what follows we assume that the hypotheses of Theorem 2.1, Theorem 2.2, and Lemma 2.6, hold and let  $\vec{\mathbf{t}} := ((\mathbf{t}, \boldsymbol{\varphi}), p_D) \in \mathbb{X} \times \mathbb{M}$  and  $\vec{\mathbf{t}}_h := ((\mathbf{t}_h, \boldsymbol{\varphi}_h), p_{D,h}) \in \mathbb{X}_h \times \mathbb{M}_h$  be the unique solutions of problems (2.7) and (2.17), respectively. Then, our global *a posteriori* error estimator is defined by:

$$\Theta := \left\{ \sum_{T \in \mathcal{T}_h^S} \Theta_{S,T}^2 + \sum_{T \in \mathcal{T}_h^D} \Theta_{D,T}^2 \right\}^{1/2}, \quad (2.30)$$

where the local error indicators  $\Theta_{S,T}^2$  (with  $T \in \mathcal{T}_h^S$ ) and  $\Theta_{D,T}^2$  (with  $T \in \mathcal{T}_h^D$ ) are given by

$$\begin{aligned} \Theta_{S,T}^2 := & \|\mathbf{f}_S + \mathbf{div} \boldsymbol{\sigma}_{S,h}\|_{0,T}^2 + \|\mathbf{f}_S - \mathbf{P}_h^S(\mathbf{f}_S)\|_{0,T}^2 + \left\| \boldsymbol{\rho}_{S,h} - \frac{1}{2} (\nabla \mathbf{u}_{S,h} - (\nabla \mathbf{u}_{S,h})^t) \right\|_{0,T}^2 \\ & + \|\mathbf{e}(\mathbf{u}_{S,h}) - \mathbf{t}_{S,h}\|_{0,T}^2 + \|\boldsymbol{\sigma}_{S,h} - \boldsymbol{\sigma}_{S,h}^t\|_{0,T}^2 + \left\| \boldsymbol{\sigma}_{S,h}^d - \mu(|\mathbf{t}_{S,h}|) \mathbf{t}_{S,h} + (\mathbf{u}_{S,h} \otimes \mathbf{u}_{S,h})^d \right\|_{0,T}^2 \\ & + h_T^2 \|\nabla \mathbf{u}_{S,h} - (\mathbf{t}_{S,h} + \boldsymbol{\rho}_{S,h})\|_{0,T}^2 + h_T^2 \|\underline{\mathbf{curl}}(\mathbf{t}_{S,h} + \boldsymbol{\rho}_{S,h})\|_{0,T}^2 \\ & + \sum_{e \in \mathcal{E}(T) \cap \mathcal{E}_h(\Omega_S)} h_e \|\llbracket (\mathbf{t}_{S,h} + \boldsymbol{\rho}_{S,h}) \times \mathbf{n} \rrbracket\|_{0,e}^2 + \sum_{e \in \mathcal{E}(T) \cap \mathcal{E}_h(\Gamma_S)} h_e \|(\mathbf{t}_{S,h} + \boldsymbol{\rho}_{S,h}) \times \mathbf{n}\|_{0,e}^2 \\ & + \sum_{e \in \mathcal{E}(T) \cap \mathcal{E}_h(\Sigma)} \left\{ h_e \|(\mathbf{t}_{S,h} + \boldsymbol{\rho}_{S,h}) \times \mathbf{n} + \underline{\mathbf{curl}}_s \boldsymbol{\varphi}_h\|_{0,e}^2 + h_e \|\boldsymbol{\varphi}_h + \mathbf{u}_{S,h}\|_{0,e}^2 \right\} \\ & + \sum_{e \in \mathcal{E}(T) \cap \mathcal{E}_h(\Sigma)} h_e \left\| \boldsymbol{\sigma}_{S,h} \mathbf{n} - \sum_{l=1}^2 \omega_l^{-1} (\boldsymbol{\varphi}_h \cdot \mathbf{t}_l) \mathbf{t}_l + \lambda_h \mathbf{n} \right\|_{0,e}^2, \end{aligned} \quad (2.31)$$

and

$$\begin{aligned} \Theta_{D,T}^2 := & \|f_D - \mathbf{div} \mathbf{u}_{D,h}\|_{0,T}^2 + h_T^2 \|\mathbf{K}^{-1} \mathbf{u}_{D,h}\|_{0,T}^2 + h_T^2 \|\mathbf{curl}(\mathbf{K}^{-1} \mathbf{u}_{D,h})\|_{0,T}^2 \\ & + \sum_{e \in \mathcal{E}(T) \cap \mathcal{E}_h(\Omega_D)} h_e \|\llbracket \mathbf{K}^{-1} \mathbf{u}_{D,h} \times \mathbf{n} \rrbracket\|_{0,e}^2 + \sum_{e \in \mathcal{E}(T) \cap \mathcal{E}_h(\Gamma_D)} h_e \|\mathbf{K}^{-1} \mathbf{u}_{D,h} \times \mathbf{n}\|_{0,e}^2 \\ & + \sum_{e \in \mathcal{E}(T) \cap \mathcal{E}_h(\Sigma)} \left\{ h_e \|\mathbf{K}^{-1} \mathbf{u}_{D,h} \times \mathbf{n} + \underline{\mathbf{curl}}_s \lambda_h\|_{0,e}^2 + h_e \|p_{D,h} - \lambda_h\|_{0,e}^2 + h_e \|\mathbf{u}_{D,h} \cdot \mathbf{n} + \boldsymbol{\varphi}_h \cdot \mathbf{n}\|_{0,e}^2 \right\}. \end{aligned} \quad (2.32)$$

The main goal of the present Section 2.3 is to establish, under suitable assumptions, the existence of positive constants  $C_{\text{rel}}$  and  $C_{\text{eff}}$ , independent of the meshsizes and the continuous and discrete solutions, such that

$$C_{\text{eff}} \Theta + \text{h.o.t.} \leq \|\vec{\mathbf{t}} - \vec{\mathbf{t}}_h\|_{\mathbb{X} \times \mathbb{M}} \leq C_{\text{rel}} \Theta, \quad (2.33)$$

where h.o.t. stands, eventually, for one or several terms of higher order.

The upper and lower bounds in (2.33), which are known as the reliability and efficiency of  $\Theta$ , are derived below in Sections 2.3.3 and 2.3.4, respectively.

### 2.3.3 Reliability of $\Theta$

Proceeding analogously to [40, Section 5.2], we first let  $\mathbf{P} : \mathbb{X} \times \mathbb{M} \rightarrow (\mathbb{X} \times \mathbb{M})' := \mathbb{X}' \times \mathbb{M}'$  and  $\mathbf{P}_h : \mathbb{X}_h \times \mathbb{M}_h \rightarrow (\mathbb{X}_h \times \mathbb{M}_h)' := \mathbb{X}_h' \times \mathbb{M}_h'$  be the nonlinear operators suggested by the left hand sides of (2.7) and (2.17) with the given velocity solutions  $\mathbf{u}_S \in W_r$  and  $\mathbf{u}_{S,h} \in W_r^h$ , that is

$$\begin{aligned} [\mathbf{P}(\vec{\mathbf{s}}), \vec{\mathbf{r}}] &:= [(a_1 + a_2(\mathbf{u}_S))(\underline{\mathbf{s}}), \underline{\mathbf{r}}] + [b(\underline{\mathbf{s}}), \underline{\boldsymbol{\psi}}] + [b(\underline{\mathbf{r}}), \underline{\boldsymbol{\phi}}] - [c(\underline{\boldsymbol{\phi}}), \underline{\boldsymbol{\psi}}] \\ &\quad + [\mathbf{B}(\underline{\mathbf{r}}, \underline{\boldsymbol{\psi}}), r_D] + [\mathbf{B}(\underline{\mathbf{s}}, \underline{\boldsymbol{\phi}}), q_D], \end{aligned} \quad (2.34)$$

for all  $\vec{\mathbf{s}} = ((\underline{\mathbf{s}}, \underline{\boldsymbol{\phi}}), r_D)$ ,  $\vec{\mathbf{r}} = ((\underline{\mathbf{r}}, \underline{\boldsymbol{\psi}}), q_D) \in \mathbb{X} \times \mathbb{M}$ , and

$$\begin{aligned} [\mathbf{P}_h(\vec{\mathbf{s}}_h), \vec{\mathbf{r}}_h] &:= [(a_1 + a_2(\mathbf{u}_{S,h}))(\underline{\mathbf{s}}_h), \underline{\mathbf{r}}_h] + [b(\underline{\mathbf{s}}_h), \underline{\boldsymbol{\psi}}_h] + [b(\underline{\mathbf{r}}_h), \underline{\boldsymbol{\phi}}_h] - [c(\underline{\boldsymbol{\phi}}_h), \underline{\boldsymbol{\psi}}_h] \\ &\quad + [\mathbf{B}(\underline{\mathbf{r}}_h, \underline{\boldsymbol{\psi}}_h), r_{D,h}] + [\mathbf{B}(\underline{\mathbf{s}}_h, \underline{\boldsymbol{\phi}}_h), q_{D,h}], \end{aligned} \quad (2.35)$$

for all  $\vec{\mathbf{s}}_h = ((\underline{\mathbf{s}}_h, \underline{\boldsymbol{\phi}}_h), r_{D,h})$ ,  $\vec{\mathbf{r}}_h = ((\underline{\mathbf{r}}_h, \underline{\boldsymbol{\psi}}_h), q_{D,h}) \in \mathbb{X}_h \times \mathbb{M}_h$ . Then, setting  $\mathcal{F} := (\mathbf{F}, \mathbf{G}) \in \mathbb{X}' \times \mathbb{M}'$ , it is clear from (2.7) and (2.17) that  $\mathbf{P}$  and  $\mathbf{P}_h$  satisfy

$$[\mathbf{P}(\vec{\mathbf{t}}), \vec{\mathbf{r}}] = [\mathcal{F}, \vec{\mathbf{r}}] \quad \forall \vec{\mathbf{r}} \in \mathbb{X} \times \mathbb{M} \quad (2.36)$$

and

$$[\mathbf{P}_h(\vec{\mathbf{t}}_h), \vec{\mathbf{r}}_h] = [\mathcal{F}, \vec{\mathbf{r}}_h] \quad \forall \vec{\mathbf{r}}_h \in \mathbb{X}_h \times \mathbb{M}_h, \quad (2.37)$$

respectively. In addition, since  $\mu$  is assumed to be of class  $C^1$  (cf. (2.2)), we find, as explained in [40, Section 5.2], that  $a_1$  (cf. (2.9)) has hemi-continuous first order Gâteaux derivative  $\mathcal{D}a_1 : \mathbf{X} \rightarrow \mathcal{L}(\mathbf{X}, \mathbf{X}')$ . In this way, the Gâteaux derivative of  $\mathbf{P}$  at  $\vec{\mathbf{s}}$  is obtained by replacing  $[a_1(\cdot), \cdot]$  in (2.34) by  $\mathcal{D}a_1(\vec{\mathbf{s}})(\cdot, \cdot)$  (see [40, Lemma 5.3] for details), that is

$$\begin{aligned} \mathcal{D}\mathbf{P}(\vec{\mathbf{s}})(\vec{\mathbf{t}}, \vec{\mathbf{r}}) &:= \mathcal{D}a_1(\underline{\mathbf{s}})(\underline{\mathbf{t}}, \underline{\mathbf{r}}) + [a_2(\mathbf{u}_S)(\underline{\mathbf{t}}), \underline{\mathbf{r}}] + [b(\underline{\mathbf{t}}), \underline{\boldsymbol{\psi}}] + [b(\underline{\mathbf{r}}), \underline{\boldsymbol{\phi}}] - [c(\underline{\boldsymbol{\phi}}), \underline{\boldsymbol{\psi}}] \\ &\quad + [\mathbf{B}(\underline{\mathbf{r}}, \underline{\boldsymbol{\psi}}), p_D] + [\mathbf{B}(\underline{\mathbf{t}}, \underline{\boldsymbol{\phi}}), q_D], \end{aligned}$$

for all  $\vec{\mathbf{t}} = ((\underline{\mathbf{t}}, \underline{\boldsymbol{\phi}}), p_D)$ ,  $\vec{\mathbf{r}} = ((\underline{\mathbf{r}}, \underline{\boldsymbol{\psi}}), q_D) \in \mathbb{X} \times \mathbb{M}$ , which, according to [40, Lemma 5.3], becomes a uniformly bounded (with respect to  $\vec{\mathbf{s}}$ ) bilinear form on  $(\mathbb{X} \times \mathbb{M}) \times (\mathbb{X} \times \mathbb{M})$ . Moreover, thanks to the assumptions on  $\kappa_i$ ,  $i \in \{1, \dots, 4\}$ , required by Theorem 2.1, recalling that  $c$  is positive-semidefinite, employing the continuous version of [40, Theorem 5.2], and proceeding again as in [40, Section 5.2], we deduce the existence of a positive constant  $C_{\mathbf{P}}$ , independent of  $\vec{\mathbf{s}}$  and the continuous and discrete solutions, such that the following global inf-sup condition holds

$$C_{\mathbf{P}} \|\vec{\boldsymbol{\zeta}}\|_{\mathbb{X} \times \mathbb{M}} \leq \sup_{\substack{\vec{\mathbf{r}} \in \mathbb{X} \times \mathbb{M} \\ \vec{\mathbf{r}} \neq \mathbf{0}}} \frac{\mathcal{D}\mathbf{P}(\vec{\mathbf{s}})(\vec{\boldsymbol{\zeta}}, \vec{\mathbf{r}})}{\|\vec{\mathbf{r}}\|_{\mathbb{X} \times \mathbb{M}}} \quad \forall \vec{\boldsymbol{\zeta}} \in \mathbb{X} \times \mathbb{M}. \quad (2.38)$$

We are now in position of establishing the following preliminary a posteriori error estimate.

**Theorem 2.7.** *Given  $r \in (0, r_0)$ , with  $r_0$  defined by (2.13), assume that the data  $\mathbf{f}_S$  and  $f_D$  satisfy*

$$\tilde{c}_{\mathbf{T}} \left\{ \|\mathbf{f}_S\|_{0, \Omega_S} + \|f_D\|_{0, \Omega_D} \right\} \leq \frac{C_{\mathbf{P}} r}{\alpha_0(\Omega)}, \quad (2.39)$$

where  $\tilde{c}_{\mathbf{T}}$  and  $\alpha_0(\Omega)$  are the positive constants, independent of the data, provided by [40, Lemma 4.2 and eq. (3.16)], and  $C_{\mathbf{P}}$  is given above in (2.38). Then, there holds

$$\|\vec{\mathbf{t}} - \vec{\mathbf{t}}_h\|_{\mathbb{X} \times \mathbb{M}} \leq \frac{2}{C_{\mathbf{P}}} \|\mathbf{R}\|_{(\mathbb{X} \times \mathbb{M})'}, \quad (2.40)$$

where  $\mathbf{R} : \mathbb{X} \times \mathbb{M} \rightarrow \mathbb{R}$  is the residual functional given by  $\mathbf{R}(\vec{\mathbf{r}}) := [\mathcal{F} - \mathbf{P}_h(\vec{\mathbf{t}}_h), \vec{\mathbf{r}}]$   $\forall \vec{\mathbf{r}} \in \mathbb{X} \times \mathbb{M}$ , which satisfies

$$\mathbf{R}(\vec{\mathbf{r}}_h) = 0 \quad \forall \vec{\mathbf{r}}_h \in \mathbb{X}_h \times \mathbb{M}_h. \quad (2.41)$$

*Proof.* Since  $\vec{\mathbf{t}}$  and  $\vec{\mathbf{t}}_h$  belong to  $\mathbb{X} \times \mathbb{M}$ , a straightforward application of the mean value theorem yields the existence of a convex combination of  $\vec{\mathbf{t}}$  and  $\vec{\mathbf{t}}_h$ , say  $\vec{\mathbf{s}}_h \in \mathbb{X} \times \mathbb{M}$ , such that (see for instance the proof of [97, Lemma 3.5])

$$\mathcal{D}\mathbf{P}(\vec{\mathbf{s}}_h)(\vec{\mathbf{t}} - \vec{\mathbf{t}}_h, \vec{\mathbf{r}}) = [\mathbf{P}(\vec{\mathbf{t}}) - \mathbf{P}(\vec{\mathbf{t}}_h), \vec{\mathbf{r}}] \quad \forall \vec{\mathbf{r}} \in \mathbb{X} \times \mathbb{M}.$$

Then, using that  $[\mathbf{P}(\vec{\mathbf{t}}), \vec{\mathbf{r}}] = [\mathcal{F}, \vec{\mathbf{r}}]$  (cf. (2.36)), and adding and subtracting  $[\mathbf{P}_h(\vec{\mathbf{t}}_h), \vec{\mathbf{r}}]$ , it readily follows from the foregoing identity that

$$\mathcal{D}\mathbf{P}(\vec{\mathbf{s}}_h)(\vec{\mathbf{t}} - \vec{\mathbf{t}}_h, \vec{\mathbf{r}}) = \mathbf{R}(\vec{\mathbf{r}}) + [\mathbf{P}_h(\vec{\mathbf{t}}_h) - \mathbf{P}(\vec{\mathbf{t}}_h), \vec{\mathbf{r}}] \quad \forall \vec{\mathbf{r}} \in \mathbb{X} \times \mathbb{M}. \quad (2.42)$$

In turn, applying (2.38) with  $\vec{\mathbf{s}} = \vec{\mathbf{s}}_h$  and  $\vec{\boldsymbol{\zeta}} = \vec{\mathbf{t}} - \vec{\mathbf{t}}_h$ , and employing (2.42), we deduce after minor algebraic manipulations that

$$C_{\mathbf{P}} \|\vec{\mathbf{t}} - \vec{\mathbf{t}}_h\|_{\mathbb{X} \times \mathbb{M}} \leq \|\mathbf{R}\|_{(\mathbb{X} \times \mathbb{M})'} + \sup_{\substack{\vec{\mathbf{r}} \in \mathbb{X} \times \mathbb{M} \\ \vec{\mathbf{r}} \neq \mathbf{0}}} \frac{[\mathbf{P}_h(\vec{\mathbf{t}}_h) - \mathbf{P}(\vec{\mathbf{t}}_h), \vec{\mathbf{r}}]}{\|\vec{\mathbf{r}}\|_{\mathbb{X} \times \mathbb{M}}}. \quad (2.43)$$

Next, according to the definitions of  $\mathbf{P}$  and  $\mathbf{P}_h$  (cf. (2.34) - (2.35)), and using the estimates (2.12) and (2.19), and the definition of  $r_0$  (cf. (2.13)), we obtain

$$\begin{aligned} \left| [\mathbf{P}_h(\vec{\mathbf{t}}_h) - \mathbf{P}(\vec{\mathbf{t}}_h), \vec{\mathbf{r}}] \right| &= \left| [a_2(\mathbf{u}_{S,h} - \mathbf{u}_S)(\vec{\mathbf{t}}_h), \vec{\mathbf{r}}] \right| \\ &\leq c_2(\Omega_S) (\kappa_1^2 + 1)^{1/2} \|\mathbf{u}_{S,h}\|_{1,\Omega_S} \|\mathbf{u}_S - \mathbf{u}_{S,h}\|_{1,\Omega_S} \|\vec{\mathbf{r}}\|_{\mathbf{X}} \\ &\leq c_2(\Omega_S) (\kappa_1^2 + 1)^{1/2} \|\vec{\mathbf{t}}_h\|_{\mathbb{X} \times \mathbb{M}} \|\vec{\mathbf{t}} - \vec{\mathbf{t}}_h\|_{\mathbb{X} \times \mathbb{M}} \|\vec{\mathbf{r}}\|_{\mathbf{X}} \\ &\leq \frac{\alpha_0(\Omega)}{2r_0} \tilde{c}_{\mathbf{T}} \left\{ \|\mathbf{f}_S\|_{0,\Omega_S} + \|\mathbf{f}_D\|_{0,\Omega_D} \right\} \|\vec{\mathbf{t}} - \vec{\mathbf{t}}_h\|_{\mathbb{X} \times \mathbb{M}} \|\vec{\mathbf{r}}\|_{\mathbf{X}}, \end{aligned}$$

which, thanks to the assumption (2.39) and the fact that  $\frac{r}{r_0} \leq 1$ , yields

$$\left| [\mathbf{P}_h(\vec{\mathbf{t}}_h) - \mathbf{P}(\vec{\mathbf{t}}_h), \vec{\mathbf{r}}] \right| \leq \frac{C_{\mathbf{P}}}{2} \|\vec{\mathbf{t}} - \vec{\mathbf{t}}_h\|_{\mathbb{X} \times \mathbb{M}} \|\vec{\mathbf{r}}\|_{\mathbf{X}}.$$

Thus, replacing this estimate back into (2.43) we arrive at (2.40). Finally, the fact that  $\mathbf{R}$  vanishes in  $\mathbb{X}_h \times \mathbb{M}_h$ , that is (2.41), follows straightforwardly from (2.37).  $\square$

According to the upper bound (2.40) provided by the previous lemma, it only remains now to estimate  $\|\mathbf{R}\|_{(\mathbb{X} \times \mathbb{M})'}$ . To this end, we first observe that the functional  $\mathbf{R}$  can be decomposed as

$$\mathbf{R}(\vec{\mathbf{r}}) := \mathbf{R}_1(\boldsymbol{\tau}_S) + \mathbf{R}_2(\mathbf{v}_S) + \mathbf{R}_3(\boldsymbol{\eta}_S) + \mathbf{R}_4(\mathbf{r}_S) + \mathbf{R}_5(\mathbf{v}_D) + \mathbf{R}_6(q_D) + \mathbf{R}_7(\boldsymbol{\psi}) + \mathbf{R}_8(\boldsymbol{\xi})$$

for all  $\vec{\mathbf{r}} = ((\underline{\mathbf{r}}, \underline{\boldsymbol{\psi}}), q_D) \in \mathbb{X} \times \mathbb{M}$ , where

$$\begin{aligned}
R_1(\boldsymbol{\tau}_S) &:= -\kappa_2(\mathbf{f}_S + \mathbf{div} \boldsymbol{\sigma}_{S,h}, \mathbf{div} \boldsymbol{\tau}_S)_S - \kappa_1(\boldsymbol{\sigma}_{S,h}^d - \mu(|\mathbf{t}_{S,h}|)\mathbf{t}_{S,h} + (\mathbf{u}_{S,h} \otimes \mathbf{u}_{S,h})^d, \boldsymbol{\tau}_S^d)_S \\
&\quad - (\mathbf{t}_{S,h}, \boldsymbol{\tau}_S^d)_S - (\boldsymbol{\tau}_S, \boldsymbol{\rho}_{S,h})_S - (\mathbf{div} \boldsymbol{\tau}_S, \mathbf{u}_{S,h})_S - \langle \boldsymbol{\tau}_S \mathbf{n}, \boldsymbol{\varphi}_h \rangle_\Sigma, \\
R_2(\mathbf{v}_S) &:= (\mathbf{f}_S + \mathbf{div} \boldsymbol{\sigma}_{S,h}, \mathbf{v}_S)_S - \kappa_3(\mathbf{e}(\mathbf{u}_{S,h}) - \mathbf{t}_{S,h}, \mathbf{e}(\mathbf{v}_S))_S, \\
R_3(\boldsymbol{\eta}_S) &:= (\boldsymbol{\sigma}_{S,h}, \boldsymbol{\eta}_S)_S - \kappa_4 \left( \boldsymbol{\rho}_{S,h} - \frac{1}{2} (\nabla \mathbf{u}_{S,h} - (\nabla \mathbf{u}_{S,h})^t), \boldsymbol{\eta}_S \right)_S, \\
R_4(\mathbf{r}_S) &:= (\boldsymbol{\sigma}_{S,h}^d - \mu(|\mathbf{t}_{S,h}|)\mathbf{t}_{S,h} + (\mathbf{u}_{S,h} \otimes \mathbf{u}_{S,h})^d, \mathbf{r}_S)_S, \\
R_5(\mathbf{v}_D) &:= -(\mathbf{K}^{-1} \mathbf{u}_{D,h}, \mathbf{v}_D)_D + (\mathbf{div} \mathbf{v}_D, p_{D,h})_D + \langle \mathbf{v}_D \cdot \mathbf{n}, \lambda_h \rangle_\Sigma, \\
R_6(q_D) &:= -(f_D - \mathbf{div} \mathbf{u}_{D,h}, q_D)_D, \\
R_7(\boldsymbol{\psi}) &:= -\langle \boldsymbol{\sigma}_{S,h} \mathbf{n}, \boldsymbol{\psi} \rangle_\Sigma + \sum_{l=1}^2 \omega_l^{-1} \langle \boldsymbol{\varphi} \cdot \mathbf{t}_l, \boldsymbol{\psi} \cdot \mathbf{t}_l \rangle_\Sigma - \langle \boldsymbol{\psi} \cdot \mathbf{n}, \lambda_h \rangle_\Sigma, \\
R_8(\xi) &:= \langle \boldsymbol{\varphi}_h \cdot \mathbf{n}, \xi \rangle_\Sigma + \langle \mathbf{u}_{D,h} \cdot \mathbf{n}, \xi \rangle_\Sigma.
\end{aligned}$$

In this way, it follows that

$$\begin{aligned}
\|\mathbf{R}\|_{(\mathbb{X} \times \mathbb{M})'} &\leq \left\{ \|\mathbf{R}_1\|_{\mathbb{H}(\mathbf{div}; \Omega_S)'} + \|\mathbf{R}_2\|_{\mathbf{H}_{\Gamma_S}^1(\Omega_S)'} + \|\mathbf{R}_3\|_{\mathbb{L}_{\text{skew}}^2(\Omega_S)'} + \|\mathbf{R}_4\|_{\mathbb{L}_{\text{tr}}^2(\Omega_S)'} \right. \\
&\quad \left. + \|\mathbf{R}_5\|_{\mathbf{H}_0(\mathbf{div}; \Omega_D)'} + \|\mathbf{R}_6\|_{\mathbb{L}_0^2(\Omega_D)'} + \|\mathbf{R}_7\|_{\mathbf{H}_{00}^{-1/2}(\Sigma)} + \|\mathbf{R}_8\|_{\mathbf{H}^{-1/2}(\Sigma)} \right\}, \tag{2.44}
\end{aligned}$$

and hence our next purpose is to derive suitable upper bounds for each one of the terms on the right hand side of (2.44). We start with the following lemma, which is a direct consequence of the Cauchy–Schwarz inequality.

**Lemma 2.8.** *There exist  $C_2, C_3 > 0$ , independent of the meshsizes, such that*

$$\|\mathbf{R}_2\|_{\mathbf{H}_{\Gamma_S}^1(\Omega_S)'} \leq C_2 \left\{ \sum_{T \in \mathcal{T}_h^S} \|\mathbf{f}_S + \mathbf{div} \boldsymbol{\sigma}_{S,h}\|_{0,T}^2 + \|\mathbf{e}(\mathbf{u}_{S,h}) - \mathbf{t}_{S,h}\|_{0,T}^2 \right\}^{1/2}$$

and

$$\|\mathbf{R}_3\|_{\mathbb{L}_{\text{skew}}^2(\Omega_S)'} \leq C_3 \left\{ \sum_{T \in \mathcal{T}_h^S} \|\boldsymbol{\sigma}_{S,h} - \boldsymbol{\sigma}_{S,h}^t\|_{0,T}^2 + \left\| \boldsymbol{\rho}_{S,h} - \frac{1}{2} (\nabla \mathbf{u}_{S,h} - (\nabla \mathbf{u}_{S,h})^t) \right\|_{0,T}^2 \right\}^{1/2}.$$

In addition, there holds

$$\|\mathbf{R}_4\|_{\mathbb{L}_{\text{tr}}^2(\Omega_S)'} \leq \left\{ \sum_{T \in \mathcal{T}_h^S} \left\| \boldsymbol{\sigma}_{S,h}^d - \mu(|\mathbf{t}_{S,h}|)\mathbf{t}_{S,h} + (\mathbf{u}_{S,h} \otimes \mathbf{u}_{S,h})^d \right\|_{0,T}^2 \right\}^{1/2}$$

and

$$\|\mathbf{R}_6\|_{\mathbb{L}_0^2(\Omega_D)'} \leq \left\{ \sum_{T \in \mathcal{T}_h^D} \|f_D - \mathbf{div} \mathbf{u}_{D,h}\|_{0,T}^2 \right\}^{1/2}.$$

Next, we derive the upper bounds for  $R_7$  and  $R_8$ , the functionals acting on the interface  $\Sigma$ .

**Lemma 2.9.** *There exist  $C_7, C_8 > 0$ , independent of the meshsizes, such that*

$$\|R_7\|_{\mathbf{H}_{00}^{-1/2}(\Sigma)} \leq C_7 \left\{ \sum_{e \in \mathcal{E}_h(\Sigma)} h_e \left\| \sigma_{S,h} \mathbf{n} - \sum_{l=1}^2 \omega_l^{-1} (\varphi_h \cdot \mathbf{t}_l) \mathbf{t}_l + \lambda_h \mathbf{n} \right\|_{0,e}^2 \right\}^{1/2}, \quad (2.45)$$

and

$$\|R_8\|_{H^{-1/2}(\Sigma)} \leq C_8 \left\{ \sum_{e \in \mathcal{E}_h(\Sigma)} h_e \left\| \mathbf{u}_{D,h} \cdot \mathbf{n} + \varphi_h \cdot \mathbf{n} \right\|_{0,e}^2 \right\}^{1/2}. \quad (2.46)$$

*Proof.* It is clear from the definition of  $R_7$  that

$$R_7(\psi) = - \left\langle \sigma_{S,h} \mathbf{n} - \sum_{l=1}^2 \omega_l^{-1} (\varphi_h \cdot \mathbf{t}_l) \mathbf{t}_l + \lambda_h \mathbf{n}, \psi \right\rangle_{\Sigma} \quad \forall \psi \in \mathbf{H}_{00}^{1/2}(\Sigma),$$

which certainly yields

$$\|R_7\|_{\mathbf{H}_{00}^{-1/2}(\Sigma)} = \left\| \sigma_{S,h} \mathbf{n} - \sum_{l=1}^2 \omega_l^{-1} (\varphi_h \cdot \mathbf{t}_l) \mathbf{t}_l + \lambda_h \mathbf{n} \right\|_{-1/2,00,\Sigma}. \quad (2.47)$$

Then, taking  $\psi_h \in \Lambda_h^S(\Sigma)$  and then  $(\mathbf{r}_h, \underline{\psi}_h) = (\mathbf{0}, (\psi_h, 0)) \in \mathbb{X}_h$  in the first equation of (2.17), we deduce that

$$\left\langle \sigma_{S,h} \mathbf{n} - \sum_{l=1}^2 \omega_l^{-1} (\varphi_h \cdot \mathbf{t}_l) \mathbf{t}_l + \lambda_h \mathbf{n}, \psi_h \right\rangle_{\Sigma} = 0 \quad \forall \psi_h \in \Lambda_h^S(\Sigma),$$

which says that each component of  $\sigma_{S,h} \mathbf{n} - \sum_{l=1}^2 \omega_l^{-1} (\varphi_h \cdot \mathbf{t}_l) \mathbf{t}_l + \lambda_h \mathbf{n}$  belongs to  $\Lambda_h^{S,\perp}(\Sigma)$  (cf. (2.24)). In this way, (2.45) follows from (2.47) and a direct component-wise application of (2.26) (cf. Lemma 2.6). In turn, the proof of (2.46) proceeds analogously by noting now that  $\mathbf{u}_{D,h} \cdot \mathbf{n} + \varphi_h \cdot \mathbf{n} \in \Lambda_h^{D,\perp}(\Sigma)$  (cf. (2.25)), and then by applying (2.27) (cf. Lemma 2.6).  $\square$

Our next goal is to derive the upper bound for  $R_1$ , for which, given  $\tau_S \in \mathbb{H}(\mathbf{div}; \Omega_S)$ , we consider its Helmholtz decomposition provided by part a) of Lemma 2.5. More precisely, we let  $\boldsymbol{\eta} \in \mathbf{H}^2(\Omega_S)$  and  $\boldsymbol{\chi} \in \mathbb{H}^1(\Omega_S)$  be such that  $\tau_S = \nabla \boldsymbol{\eta} + \mathbf{curl} \boldsymbol{\chi}$  in  $\Omega_S$ , and

$$\|\boldsymbol{\eta}\|_{2,\Omega_S} + \|\boldsymbol{\chi}\|_{1,\Omega_S} \leq C_S \|\tau_S\|_{\mathbf{div},\Omega_S}. \quad (2.48)$$

Then, defining  $\tau_{S,h} := \Pi_h^S(\nabla \boldsymbol{\eta}) + \mathbf{curl}(\mathbf{I}_h^S \boldsymbol{\chi}) \in \mathbb{H}_h(\Omega_S)$  (cf. Section 2.3.1), which can be seen as a discrete Helmholtz decomposition of  $\tau_{S,h}$ , and applying from (2.41) that  $R_1(\tau_{S,h}) = 0$ , we can write

$$R_1(\tau_S) = R_1(\tau_S - \tau_{S,h}) = R_1(\nabla \boldsymbol{\eta} - \Pi_h^S(\nabla \boldsymbol{\eta})) + R_1(\mathbf{curl}(\boldsymbol{\chi} - \mathbf{I}_h^S \boldsymbol{\chi})).$$

Consequently, we now require to bound the expressions on the right hand side of the foregoing equation, which is provided by the following two lemmas.

**Lemma 2.10.** *There exists  $C > 0$ , independent of the meshsizes, such that for each  $\boldsymbol{\eta} \in \mathbf{H}^2(\Omega_S)$  there holds*

$$|\mathbf{R}_1(\nabla \boldsymbol{\eta} - \boldsymbol{\Pi}_h^S(\nabla \boldsymbol{\eta}))| \leq C \left\{ \sum_{T \in \mathcal{T}_h^S} \widehat{\Theta}_{1,T}^2 \right\}^{1/2} \|\boldsymbol{\eta}\|_{2,\Omega}, \quad (2.49)$$

where

$$\begin{aligned} \widehat{\Theta}_{1,T}^2 &= h_T^2 \left\| \boldsymbol{\sigma}_{S,h}^d - \mu(|\mathbf{t}_{S,h}|) \mathbf{t}_{S,h} + (\mathbf{u}_{S,h} \otimes \mathbf{u}_{S,h})^d \right\|_{0,T}^2 + \|\mathbf{f}_S - \mathbf{P}_h^S(\mathbf{f}_S)\|_{0,T}^2 \\ &+ h_T^2 \left\| \nabla \mathbf{u}_{S,h} - (\mathbf{t}_{S,h} + \boldsymbol{\rho}_{S,h}) \right\|_{0,T}^2 + \sum_{e \in \mathcal{E}(T) \cap \mathcal{E}_h(\Sigma)} h_e \|\boldsymbol{\varphi}_h + \mathbf{u}_{S,h}\|_{0,e}^2. \end{aligned} \quad (2.50)$$

*Proof.* It follows almost straightforwardly from a slight modification of the proof of [97, Lemma 3.10] (see also [93, Lemma 3.6]). We omit further details.  $\square$

**Lemma 2.11.** *There exists  $C > 0$ , independent of the meshsizes, such that for each  $\boldsymbol{\chi} \in \mathbf{H}^1(\Omega_S)$  there holds*

$$|\mathbf{R}_1(\underline{\mathbf{curl}}(\boldsymbol{\chi} - \mathbf{I}_h^S \boldsymbol{\chi}))| \leq C \left\{ \sum_{T \in \mathcal{T}_h^S} \widehat{\Theta}_{2,T}^2 \right\}^{1/2} \|\boldsymbol{\chi}\|_{1,\Omega_S}, \quad (2.51)$$

where

$$\begin{aligned} \widehat{\Theta}_{2,T}^2 &= \left\| \boldsymbol{\sigma}_{S,h}^d - \mu(|\mathbf{t}_{S,h}|) \mathbf{t}_{S,h} + (\mathbf{u}_{S,h} \otimes \mathbf{u}_{S,h})^d \right\|_{0,T}^2 + h_T^2 \left\| \underline{\mathbf{curl}}(\mathbf{t}_{S,h} + \boldsymbol{\rho}_{S,h}) \right\|_{0,T}^2 \\ &+ \sum_{e \in \mathcal{E}(T) \cap \mathcal{E}_h(\Omega_S)} h_e \left\| [(\mathbf{t}_{S,h} + \boldsymbol{\rho}_{S,h}) \times \mathbf{n}] \right\|_{0,e}^2 + \sum_{e \in \mathcal{E}(T) \cap \mathcal{E}_h(\Gamma_S)} h_e \left\| (\mathbf{t}_{S,h} + \boldsymbol{\rho}_{S,h}) \times \mathbf{n} \right\|_{0,e}^2 \\ &+ \sum_{e \in \mathcal{E}(T) \cap \mathcal{E}_h(\Sigma)} h_e \left\| (\mathbf{t}_{S,h} + \boldsymbol{\rho}_{S,h}) \times \mathbf{n} + \underline{\mathbf{curl}}_s \boldsymbol{\varphi}_h \right\|_{0,e}^2. \end{aligned} \quad (2.52)$$

*Proof.* Given  $\boldsymbol{\chi} \in \mathbf{H}^1(\Omega_S)$ , we first notice from the definition of  $\mathbf{R}_1$  that there holds

$$\mathbf{R}_1(\underline{\mathbf{curl}}(\boldsymbol{\chi} - \mathbf{I}_h^S \boldsymbol{\chi})) = \widetilde{\mathbf{T}}_1(\boldsymbol{\chi}) + \widehat{\mathbf{T}}_1(\boldsymbol{\chi}),$$

where

$$\widetilde{\mathbf{T}}_1(\boldsymbol{\chi}) := -\kappa_1(\boldsymbol{\sigma}_{S,h}^d - \mu(|\mathbf{t}_{S,h}|) \mathbf{t}_{S,h} + (\mathbf{u}_{S,h} \otimes \mathbf{u}_{S,h})^d, \underline{\mathbf{curl}}(\boldsymbol{\chi} - \mathbf{I}_h^S \boldsymbol{\chi}))_S,$$

and, denoting  $\boldsymbol{\zeta}_h := \mathbf{t}_{S,h} + \boldsymbol{\rho}_{S,h}$ ,

$$\widehat{\mathbf{T}}_1(\boldsymbol{\chi}) := -(\boldsymbol{\zeta}_h, \underline{\mathbf{curl}}(\boldsymbol{\chi} - \mathbf{I}_h^S \boldsymbol{\chi}))_S - \langle \underline{\mathbf{curl}}(\boldsymbol{\chi} - \mathbf{I}_h^S \boldsymbol{\chi}) \mathbf{n}, \boldsymbol{\varphi}_h \rangle_\Sigma.$$

For estimating  $\widetilde{\mathbf{T}}_1(\boldsymbol{\chi})$  we proceed as in the proof of [97, Lemma 3.9] and apply the boundedness of  $\mathbf{I}_h^S : \mathbf{H}^1(\Omega_S) \rightarrow \mathbf{H}^1(\Omega_S)$  ([69, Lemma 1.127, pag. 69]), as well as the Cauchy-Schwarz and triangle inequalities, to obtain

$$|\widetilde{\mathbf{T}}_1(\boldsymbol{\chi})| \leq C \left\{ \sum_{T \in \mathcal{T}_h^S} \left\| \boldsymbol{\sigma}_{S,h}^d - \mu(|\mathbf{t}_{S,h}|) \mathbf{t}_{S,h} + (\mathbf{u}_{S,h} \otimes \mathbf{u}_{S,h})^d \right\|_{0,T}^2 \right\}^{1/2} \|\boldsymbol{\chi}\|_{1,\Omega_S}. \quad (2.53)$$

Next, for  $\widehat{\mathbf{T}}_1(\boldsymbol{\chi})$  we first apply the identities from [100, Chapter I, eq. (2.17) and Theorem 2.11] to deduce that

$$\langle \underline{\mathbf{curl}}(\boldsymbol{\chi} - \mathbf{I}_h^S \boldsymbol{\chi}) \mathbf{n}, \boldsymbol{\varphi}_h \rangle_\Sigma = \langle \underline{\mathbf{curl}}_s \boldsymbol{\varphi}_h, \boldsymbol{\chi} - \mathbf{I}_h^S \boldsymbol{\chi} \rangle_\Sigma = \sum_{e \in \mathcal{E}_h(\Sigma)} \int_e \underline{\mathbf{curl}}_s \boldsymbol{\varphi}_h : (\boldsymbol{\chi} - \mathbf{I}_h^S \boldsymbol{\chi}). \quad (2.54)$$

Then, analogously to the proof of [97, Lemma 3.9], we integrate by parts  $(\boldsymbol{\zeta}_h, \underline{\mathbf{curl}}(\boldsymbol{\chi} - \mathbf{I}_h^S \boldsymbol{\chi}))_S$  on each  $T \in \mathcal{T}_h^S$ , and add (2.54) to the resulting expression, to obtain

$$\begin{aligned} \widehat{\mathbf{T}}_1(\boldsymbol{\chi}) = & - \sum_{T \in \mathcal{T}_h^S} \int_T \underline{\mathbf{curl}} \boldsymbol{\zeta}_h : (\boldsymbol{\chi} - \mathbf{I}_h^S \boldsymbol{\chi}) - \sum_{e \in \mathcal{E}_h(\Omega_S)} \int_e \llbracket \boldsymbol{\zeta}_h \times \mathbf{n} \rrbracket : (\boldsymbol{\chi} - \mathbf{I}_h^S \boldsymbol{\chi}) \\ & - \sum_{e \in \mathcal{E}_h(\Gamma_S)} \int_e \boldsymbol{\zeta}_h \times \mathbf{n} : (\boldsymbol{\chi} - \mathbf{I}_h^S \boldsymbol{\chi}) - \sum_{e \in \mathcal{E}_h(\Sigma)} \int_e (\boldsymbol{\zeta}_h \times \mathbf{n} + \underline{\mathbf{curl}}_s \boldsymbol{\varphi}_h) : (\boldsymbol{\chi} - \mathbf{I}_h^S \boldsymbol{\chi}). \end{aligned} \quad (2.55)$$

In this way, applying the Cauchy–Schwarz inequality, the approximation properties of the Clément interpolator  $\mathbf{I}_h^S$  (cf. Lemma 2.4) and the fact that the number of triangles of the macro-elements  $\Delta_S(T)$  and  $\Delta_S(e)$  are uniformly bounded, we deduce from (2.55) that

$$\begin{aligned} |\widehat{\mathbf{T}}_1(\boldsymbol{\chi})| \leq & \sum_{T \in \mathcal{T}_h^S} \left\{ h_T^2 \|\underline{\mathbf{curl}}(\boldsymbol{\zeta}_h)\|_{0,T}^2 + \sum_{e \in \mathcal{E}(T) \cap \mathcal{E}_h(\Omega_S)} h_e \|\llbracket \boldsymbol{\zeta}_h \times \mathbf{n} \rrbracket\|_{0,e}^2 \right. \\ & \left. + \sum_{e \in \mathcal{E}(T) \cap \mathcal{E}_h(\Gamma_S)} h_e \|\boldsymbol{\zeta}_h \times \mathbf{n}\|_{0,e}^2 + \sum_{e \in \mathcal{E}(T) \cap \mathcal{E}_h(\Sigma)} h_e \|\boldsymbol{\zeta}_h \times \mathbf{n} + \underline{\mathbf{curl}}_s \boldsymbol{\varphi}_h\|_{0,e}^2 \right\}^{1/2} \|\boldsymbol{\chi}\|_{1,\Omega_S}, \end{aligned} \quad (2.56)$$

which together with (2.53) implies (2.51) and concludes the proof.  $\square$

As a direct consequence of Lemmas 2.10 and 2.11, and the stability estimate (2.48) for the Helmholtz decomposition, we obtain the following upper bound for  $\|\mathbf{R}_1\|_{\mathbb{H}(\mathbf{div};\Omega_S)'}.$

**Lemma 2.12.** *There exists  $C_1 > 0$ , independent of the meshsizes, such that*

$$\|\mathbf{R}_1\|_{\mathbb{H}(\mathbf{div};\Omega_S)'} \leq C_1 \left\{ \sum_{T \in \mathcal{T}_h^S} \widehat{\Theta}_{S,T}^2 \right\}^{1/2},$$

where

$$\widehat{\Theta}_{S,T}^2 = \widehat{\Theta}_{1,T}^2 + \widehat{\Theta}_{2,T}^2 - h_T^2 \left\| \boldsymbol{\sigma}_{S,h}^d - \mu(|\mathbf{t}_{S,h}|) \mathbf{t}_{S,h} + (\mathbf{u}_{S,h} \otimes \mathbf{u}_{S,h})^d \right\|_{0,T}^2,$$

that is

$$\begin{aligned} \widehat{\Theta}_{S,T}^2 := & \|\mathbf{f}_S - \mathbf{P}_h^S(\mathbf{f}_S)\|_{0,T}^2 + \left\| \boldsymbol{\sigma}_{S,h}^d - \mu(|\mathbf{t}_{S,h}|) \mathbf{t}_{S,h} + (\mathbf{u}_{S,h} \otimes \mathbf{u}_{S,h})^d \right\|_{0,T}^2 \\ & + h_T^2 \|\nabla \mathbf{u}_{S,h} - (\mathbf{t}_{S,h} + \boldsymbol{\rho}_{S,h})\|_{0,T}^2 + h_T^2 \|\underline{\mathbf{curl}}(\mathbf{t}_{S,h} + \boldsymbol{\rho}_{S,h})\|_{0,T}^2 \\ & + \sum_{e \in \mathcal{E}(T) \cap \mathcal{E}_h(\Omega_S)} h_e \|\llbracket (\mathbf{t}_{S,h} + \boldsymbol{\rho}_{S,h}) \times \mathbf{n} \rrbracket\|_{0,e}^2 + \sum_{e \in \mathcal{E}(T) \cap \mathcal{E}_h(\Gamma_S)} h_e \|(\mathbf{t}_{S,h} + \boldsymbol{\rho}_{S,h}) \times \mathbf{n}\|_{0,e}^2 \\ & + \sum_{e \in \mathcal{E}(T) \cap \mathcal{E}_h(\Sigma)} \left\{ h_e \|(\mathbf{t}_{S,h} + \boldsymbol{\rho}_{S,h}) \times \mathbf{n} + \underline{\mathbf{curl}}_s \boldsymbol{\varphi}_h\|_{0,e}^2 + h_e \|\boldsymbol{\varphi}_h + \mathbf{u}_{S,h}\|_{0,e}^2 \right\}. \end{aligned}$$

*Proof.* It suffices to see that the first term defining  $\widehat{\Theta}_{1,T}^2$  (cf. (2.50) in Lemma 2.10) is dominated by the first term defining  $\widehat{\Theta}_{2,T}^2$  (cf. (2.52) in Lemma 2.11), which explains the subtraction of the former in the original definition of  $\widehat{\Theta}_{S,T}^2$ .  $\square$

Finally, the corresponding estimate for  $R_5$  is given by the following lemma.

**Lemma 2.13.** *Assume that there exists a convex domain  $\Xi$  such that  $\Omega_D \subseteq \Xi$  and  $\Gamma_D \subseteq \partial\Xi$ . Then there exists  $C_5 > 0$ , independent of the meshsizes, such that*

$$\|R_5\|_{\mathbf{H}_0(\text{div}; \Omega_D)'} \leq C_5 \left\{ \sum_{T \in \mathcal{T}_h^D} \widehat{\Theta}_{D,T}^2 \right\}^{1/2},$$

where

$$\begin{aligned} \widehat{\Theta}_{D,T}^2 &:= h_T^2 \|\mathbf{K}^{-1} \mathbf{u}_{D,h}\|_{0,T}^2 + h_T^2 \|\text{curl}(\mathbf{K}^{-1} \mathbf{u}_{D,h})\|_{0,T}^2 \\ &+ \sum_{e \in \mathcal{E}(T) \cap \mathcal{E}_h(\Omega_D)} h_e \|\llbracket \mathbf{K}^{-1} \mathbf{u}_{D,h} \times \mathbf{n} \rrbracket\|_{0,e}^2 + \sum_{e \in \mathcal{E}(T) \cap \mathcal{E}_h(\Gamma_D)} h_e \|\mathbf{K}^{-1} \mathbf{u}_{D,h} \times \mathbf{n}\|_{0,e}^2 \\ &+ \sum_{e \in \mathcal{E}(T) \cap \mathcal{E}_h(\Sigma)} \left\{ h_e \|\mathbf{K}^{-1} \mathbf{u}_{D,h} \times \mathbf{n} + \mathbf{curl}_s \lambda_h\|_{0,e}^2 + h_e \|p_{D,h} - \lambda_h\|_{0,e}^2 \right\}. \end{aligned}$$

*Proof.* The result follows analogously to the proof of Lemmas 2.10, 2.11, and 2.12, taking into account now the Helmholtz decomposition provided by part b) of Lemma 2.5, the fact that  $R_5(\mathbf{v}_{D,h}) = 0 \forall \mathbf{v}_{D,h} \in \mathbf{H}_{h,0}(\Omega_D)$  (which also follows from (2.41)), and the analogue of the integration by parts formula (2.54), which here becomes

$$\langle \text{curl} \phi \cdot \mathbf{n}, \lambda_h \rangle_\Sigma = \langle \mathbf{curl}_s \lambda_h, \phi \rangle_\Sigma \quad \forall \phi \in H^1(\Omega_D),$$

where  $\mathbf{curl}_s$  is the operator defined in Section 2.3.1. Additionally we refer to [93, Lemma 3.9] for the proof of the 2D version of this lemma. We omit further details.  $\square$

We end this section by concluding that the reliability of  $\Theta$ , that is the upper bound in (2.33), is a straightforward consequence of Lemmas 2.8, 2.9, 2.12, and 2.13.

### 2.3.4 Efficiency of $\Theta$

We now aim to establish the lower bound in (2.33). For this purpose, we will make extensive use of the original system of equations given by (2.4)–(2.5)–(2.6), which is recovered from the augmented-mixed continuous formulation (2.7) by choosing suitable test functions and integrating by parts backwardly the corresponding equations.

We begin the derivation of the efficiency estimates with the following result.



**Lemma 2.14.** *There hold*

$$\begin{aligned}\|\mathbf{f}_S - \mathbf{P}_h^S(\mathbf{f}_S)\|_{0,T} &\leq 2\|\boldsymbol{\sigma}_S - \boldsymbol{\sigma}_{S,h}\|_{\text{div},T} \quad \forall T \in \mathcal{T}_h^S, \\ \|\mathbf{f}_S + \text{div} \boldsymbol{\sigma}_{S,h}\|_{0,T} &\leq \|\boldsymbol{\sigma}_S - \boldsymbol{\sigma}_{S,h}\|_{\text{div},T} \quad \forall T \in \mathcal{T}_h^S, \\ \|f_D - \text{div} \mathbf{u}_{D,h}\|_{0,T} &\leq \|\mathbf{u}_D - \mathbf{u}_{D,h}\|_{\text{div},T} \quad \forall T \in \mathcal{T}_h^D,\end{aligned}$$

and there exist constants  $c_i > 0$ ,  $i \in \{1, \dots, 4\}$ , independent of the meshsizes, such that

$$\begin{aligned}\|\boldsymbol{\sigma}_{S,h} - \boldsymbol{\sigma}_{S,h}^t\|_{0,T} &\leq c_1 \|\boldsymbol{\sigma}_S - \boldsymbol{\sigma}_{S,h}\|_{0,T} \quad \forall T \in \mathcal{T}_h^S, \\ \|\mathbf{e}(\mathbf{u}_{S,h}) - \mathbf{t}_{S,h}\|_{0,T} &\leq c_2 \left\{ \|\mathbf{u}_S - \mathbf{u}_{S,h}\|_{1,T} + \|\mathbf{t}_S - \mathbf{t}_{S,h}\|_{0,T} \right\} \quad \forall T \in \mathcal{T}_h^S, \\ \left\| \boldsymbol{\rho}_{S,h} - \frac{1}{2} (\nabla \mathbf{u}_{S,h} - (\nabla \mathbf{u}_{S,h})^t) \right\|_{0,T} &\leq c_3 \left\{ \|\boldsymbol{\rho}_S - \boldsymbol{\rho}_{S,h}\|_{0,T} + \|\mathbf{u}_S - \mathbf{u}_{S,h}\|_{1,T} \right\} \quad \forall T \in \mathcal{T}_h^S,\end{aligned}$$

and

$$\left\| \nabla \mathbf{u}_{S,h} - (\mathbf{t}_{S,h} + \boldsymbol{\rho}_{S,h}) \right\|_{0,T} \leq c_4 \left\{ \|\mathbf{u}_S - \mathbf{u}_{S,h}\|_{1,T} + \|\mathbf{t}_S - \mathbf{t}_{S,h}\|_{0,T} + \|\boldsymbol{\rho}_S - \boldsymbol{\rho}_{S,h}\|_{0,T} \right\} \quad \forall T \in \mathcal{T}_h^S.$$

*Proof.* It suffices to recall that  $\mathbf{f}_S = -\text{div} \boldsymbol{\sigma}_S$ ,  $f_D = \text{div} \mathbf{u}_D$ ,  $\mathbf{t}_S = \mathbf{e}(\mathbf{u}_S)$ ,  $\boldsymbol{\rho}_S = \frac{1}{2} (\nabla \mathbf{u}_S - (\nabla \mathbf{u}_S)^t)$ , and  $\boldsymbol{\sigma}_S = \boldsymbol{\sigma}_S^t$ . In particular, for the first estimate we refer to [97, Lemma 3.13]. Further details are omitted.  $\square$

Now we turn to provide the corresponding estimates for the rest of terms defining  $\Theta_S$  and  $\Theta_D$ . To do that, we proceed similarly as in [93], [97], and [83] and apply some known results based on inverse inequalities (see [47]) and the localization technique (see [150]) based on tetrahedron-bubble and face-bubble functions. In particular, the following lemma provides local efficiency estimates for several terms on  $\Sigma$ .

**Lemma 2.15.** *There exist constants  $c_i > 0$ ,  $i \in \{5, 6, 7, 8\}$ , independent of the meshsizes, such that*

- a)  $h_e \|p_{D,h} - \lambda_h\|_{0,e}^2 \leq c_5 \left\{ \|p_D - p_{D,h}\|_{0,T_e}^2 + h_T^2 \|\mathbf{u}_D - \mathbf{u}_{D,h}\|_{0,T_e}^2 + h_e \|\lambda - \lambda_h\|_{0,e}^2 \right\},$   
for all  $e \in \mathcal{E}_h(\Sigma)$ , where  $T_e$  is the tetrahedron of  $\mathcal{T}_h^D$  having  $e$  as a face,
- b)  $h_e \|\mathbf{u}_{D,h} \cdot \mathbf{n} + \boldsymbol{\varphi}_h \cdot \mathbf{n}\|_{0,e}^2 \leq c_6 \left\{ \|\mathbf{u}_D - \mathbf{u}_{D,h}\|_{0,T_e}^2 + h_T^2 \|\text{div}(\mathbf{u}_D - \mathbf{u}_{D,h})\|_{0,T_e}^2 + h_e \|\boldsymbol{\varphi} - \boldsymbol{\varphi}_h\|_{0,e}^2 \right\},$   
for all  $e \in \mathcal{E}_h(\Sigma)$ , where  $T_e$  is the tetrahedron of  $\mathcal{T}_h^D$  having  $e$  as a face,
- c) 
$$h_e \left\| \boldsymbol{\sigma}_{S,h} \mathbf{n} - \sum_{l=1}^2 \omega_l^{-1} (\boldsymbol{\varphi}_h \cdot \mathbf{t}_l) \mathbf{t}_l + \lambda_h \mathbf{n} \right\|_{0,e}^2$$
  
$$\leq c_7 \left\{ \|\boldsymbol{\sigma}_S - \boldsymbol{\sigma}_{S,h}\|_{0,T_e}^2 + h_T^2 \|\text{div}(\boldsymbol{\sigma}_S - \boldsymbol{\sigma}_{S,h})\|_{0,T_e}^2 + h_e \|\boldsymbol{\varphi} - \boldsymbol{\varphi}_h\|_{0,e}^2 + h_e \|\lambda - \lambda_h\|_{0,e}^2 \right\},$$
  
for all  $e \in \mathcal{E}_h(\Sigma)$ , where  $T_e$  is the tetrahedron of  $\mathcal{T}_h^S$  having  $e$  as a face,
- d)  $h_e \|\mathbf{u}_{S,h} + \boldsymbol{\varphi}_h\|_{0,e}^2 \leq c_8 \left\{ \|\mathbf{u}_S - \mathbf{u}_{S,h}\|_{0,T_e}^2 + h_T^2 \|\mathbf{u}_S - \mathbf{u}_{S,h}\|_{1,T_e}^2 + h_e \|\boldsymbol{\varphi} - \boldsymbol{\varphi}_h\|_{0,e}^2 \right\},$   
for all  $e \in \mathcal{E}_h(\Sigma)$ , where  $T_e$  is the tetrahedron of  $\mathcal{T}_h^S$  having  $e$  as a face.

*Proof.* We notice that all the estimates here can be easily obtained by adapting the proofs of their two-dimensional counterparts. In fact, the estimate in a) can be easily obtained after a slight modification of [10, Lemma 4.12], whereas the proofs of b), c), and d) readily follow from [93, Lemmas 3.15, 3.16 and 3.17], respectively.  $\square$

The sixth residual expression defining  $\Theta_{S,T}^2$  (cf. (2.31)), that is the one containing the nonlinear operator and the convective term, as well as the rest of terms acting on  $\Sigma$ , are estimated now.

**Lemma 2.16.** *There exist  $c_i > 0$ ,  $i \in \{9, 10, 11\}$ , independent of the meshsizes, such that*

$$\begin{aligned} \text{a)} \quad & \left\| \boldsymbol{\sigma}_{S,h}^d - \mu(|\mathbf{t}_{S,h}|) \mathbf{t}_{S,h} + (\mathbf{u}_{S,h} \otimes \mathbf{u}_{S,h})^d \right\|_{0,\Omega_S} \\ & \leq c_9 \left\{ \|\boldsymbol{\sigma}_S - \boldsymbol{\sigma}_{S,h}\|_{0,\Omega_S} + \|\mathbf{t}_S - \mathbf{t}_{S,h}\|_{0,\Omega_S} + \|\mathbf{u}_S - \mathbf{u}_{S,h}\|_{1,\Omega_S} \right\}. \\ \text{b)} \quad & \sum_{e \in \mathcal{E}_h(\Sigma)} h_e \left\| (\mathbf{t}_{S,h} + \boldsymbol{\rho}_{S,h}) \times \mathbf{n} + \underline{\mathbf{curl}}_s \boldsymbol{\varphi}_h \right\|_{0,e}^2 \\ & \leq c_{10} \left\{ \sum_{e \in \mathcal{E}_h(\Sigma)} \left( \|\mathbf{t}_S - \mathbf{t}_{S,h}\|_{0,T_e}^2 + \|\boldsymbol{\rho}_S - \boldsymbol{\rho}_{S,h}\|_{0,T_e}^2 \right) + \|\boldsymbol{\varphi} - \boldsymbol{\varphi}_h\|_{1/2,\Sigma}^2 \right\}, \end{aligned}$$

and

$$\text{c)} \quad \sum_{e \in \mathcal{E}_h(\Sigma)} h_e \left\| \mathbf{K}^{-1} \mathbf{u}_{D,h} \times \mathbf{n} + \underline{\mathbf{curl}}_s \lambda_h \right\|_{0,e}^2 \leq c_{11} \left\{ \sum_{e \in \mathcal{E}_h(\Sigma)} \|\mathbf{u}_D - \mathbf{u}_{D,h}\|_{0,T_e}^2 + \|\lambda - \lambda_h\|_{1/2,\Sigma}^2 \right\},$$

where, given  $e \in \mathcal{E}_h(\Sigma)$ ,  $T_e$  is the tetrahedron of  $\mathcal{T}_h^D$  having  $e$  as a face.

*Proof.* The efficiency estimate a) follows exactly as in the first part of the proof of [97, Theorem 3.12]. Indeed, after introducing the identity  $\boldsymbol{\sigma}_S^d - \mu(|\mathbf{t}_S|) \mathbf{t}_S + (\mathbf{u}_S \otimes \mathbf{u}_S)^d = 0$ , the rest of the proof reduces to employ the Lipschitz-continuity of the nonlinear operator induced by  $\mu$  (cf. [91, Lemma 2.1]), the compact imbedding  $\mathbf{i}_c : \mathbf{H}^1(\Omega_S) \rightarrow \mathbf{L}^4(\Omega_S)$ , and the fact that  $\|\mathbf{u}_S\|_{1,\Omega_S}$  and  $\|\mathbf{u}_{S,h}\|_{1,\Omega_S}$  are both bounded by  $r$ , thus obtaining

$$\|\mu(|\mathbf{t}_S|) \mathbf{t}_S - \mu(|\mathbf{t}_{S,h}|) \mathbf{t}_{S,h}\|_{0,\Omega_S} \leq L_\mu \|\mathbf{t}_S - \mathbf{t}_{S,h}\|_{0,\Omega_S}$$

and

$$\begin{aligned} \|\mathbf{u}_S \otimes \mathbf{u}_S - \mathbf{u}_{S,h} \otimes \mathbf{u}_{S,h}\|_{0,\Omega_S} & \leq \|(\mathbf{u}_S - \mathbf{u}_{S,h}) \otimes \mathbf{u}_S\|_{0,\Omega_S} + \|\mathbf{u}_{S,h} \otimes (\mathbf{u}_S - \mathbf{u}_{S,h})\|_{0,\Omega_S} \\ & \leq \|\mathbf{i}_c\|^2 \left\{ \|\mathbf{u}_S\|_{1,\Omega_S} + \|\mathbf{u}_{S,h}\|_{1,\Omega_S} \right\} \|\mathbf{u}_S - \mathbf{u}_{S,h}\|_{1,\Omega_S} \leq 2\|\mathbf{i}_c\|^2 r \|\mathbf{u}_S - \mathbf{u}_{S,h}\|_{1,\Omega_S}. \end{aligned}$$

Further details are omitted. In turn, the proofs of b) and c) follow after a straightforward adaptation of that of [85, Lemma 20], and recalling from [21, Proposition 3.6] that the operators  $\underline{\mathbf{curl}}_s$  and  $\mathbf{curl}_s$  are bounded.  $\square$

We observe here that b) and c) are the only non-local efficiency bounds obtained so far. However, the following lemma shows that local estimates can still be derived for these terms under additional regularity assumptions on  $\boldsymbol{\varphi}$  and  $\lambda$ .

**Lemma 2.17.** *Assume that  $\boldsymbol{\varphi}|_e \in \mathbf{H}^1(e)$  and  $\lambda|_e \in \mathbf{H}^1(e)$ , for each  $e \in \mathcal{E}_h(\Sigma)$ . Then there exist  $c_{12}, c_{13} > 0$ , independent of the meshsizes, such that for each  $e \in \mathcal{E}_h(\Sigma)$  there hold*

$$\begin{aligned} & h_e \left\| (\mathbf{t}_{S,h} + \boldsymbol{\rho}_{S,h}) \times \mathbf{n} + \underline{\mathbf{curl}}_s \boldsymbol{\varphi}_h \right\|_{0,e}^2 \\ & \leq c_{12} \left\{ \|\mathbf{t}_S - \mathbf{t}_{S,h}\|_{0,T}^2 + \|\boldsymbol{\rho}_S - \boldsymbol{\rho}_{S,h}\|_{0,T}^2 + h_e \|\underline{\mathbf{curl}}_s(\boldsymbol{\varphi} - \boldsymbol{\varphi}_h)\|_{0,e}^2 \right\} \end{aligned} \quad (2.57)$$

and

$$h_e \left\| \mathbf{K}^{-1} \mathbf{u}_{D,h} \times \mathbf{n} + \underline{\mathbf{curl}}_s \lambda_h \right\|_{0,e}^2 \leq c_{13} \left\{ \|\mathbf{u}_D - \mathbf{u}_{D,h}\|_{0,T_e}^2 + h_e \|\underline{\mathbf{curl}}_s(\lambda - \lambda_h)\|_{0,e}^2 \right\}, \quad (2.58)$$

where  $T_e$  is the tetrahedron of  $\mathcal{T}_h^S$  (respectively  $\mathcal{T}_h^D$ ) having  $e$  as a face.

*Proof.* The proof of both estimates follow exactly as in the proof of [85, Lemma 21]. We omit further details.  $\square$

Finally, the following lemma provides the corresponding upper bounds for the remaining terms defining  $\Theta_{S,T}^2$  and  $\Theta_{D,T}^2$ . In particular, in order to deal with those involving  $\mathbf{K}^{-1}$ , we assume from now on that  $\mathbf{K}^{-1} \mathbf{u}_{D,h}$  is polynomial on each  $T \in \mathcal{T}_h^D$ . Otherwise, assuming suitable regularity hypotheses and proceeding similarly as in [41, Section 6.2], higher order terms are obtained, which explains the expression h.o.t. in the lower bound of (2.33).

**Lemma 2.18.** *There exist positive constants  $c_i$ ,  $i \in \{14, \dots, 20\}$ , independent of the meshsizes, such that*

- a)  $h_T^2 \|\mathbf{K}^{-1} \mathbf{u}_{D,h}\|_{0,T}^2 \leq c_{14} \left\{ \|p_D - p_{D,h}\|_{0,T}^2 + h_T^2 \|\mathbf{u}_D - \mathbf{u}_{D,h}\|_{0,T}^2 \right\} \quad \forall T \in \mathcal{T}_h^D,$
- b)  $h_T^2 \|\underline{\mathbf{curl}}(\mathbf{K}^{-1} \mathbf{u}_{D,h})\|_{0,T}^2 \leq c_{15} \|\mathbf{u}_D - \mathbf{u}_{D,h}\|_{0,T}^2 \quad \forall T \in \mathcal{T}_h^D,$
- c)  $h_e \left\| \llbracket \mathbf{K}^{-1} \mathbf{u}_{D,h} \times \mathbf{n} \rrbracket \right\|_{0,e}^2 \leq c_{16} \|\mathbf{u}_D - \mathbf{u}_{D,h}\|_{0,\omega_e}^2$   
for all  $e \in \mathcal{E}_h(\Omega_D)$ , where the set  $\omega_e$  is given by  $\omega_e := \cup \{T' \in \mathcal{T}_h^D : e \in \mathcal{E}(T')\}$ ,
- d)  $h_e \left\| \mathbf{K}^{-1} \mathbf{u}_{D,h} \times \mathbf{n} \right\|_{0,e}^2 \leq c_{17} \|\mathbf{u}_D - \mathbf{u}_{D,h}\|_{0,T_e}^2$   
for all  $e \in \mathcal{E}_h(\Gamma_D)$ , where  $T_e$  is the tetrahedron of  $\mathcal{T}_h^D$  having  $e$  as a face,
- e)  $h_T^2 \|\underline{\mathbf{curl}}(\mathbf{t}_{S,h} + \boldsymbol{\rho}_{S,h})\|_{0,T}^2 \leq c_{18} \left\{ \|\mathbf{t}_S - \mathbf{t}_{S,h}\|_{0,T}^2 + \|\boldsymbol{\rho}_S - \boldsymbol{\rho}_{S,h}\|_{0,T}^2 \right\} \quad \forall T \in \mathcal{T}_h^S,$
- f)  $h_e \left\| \llbracket (\mathbf{t}_{S,h} + \boldsymbol{\rho}_{S,h}) \times \mathbf{n} \rrbracket \right\|_{0,e}^2 \leq c_{19} \left\{ \|\mathbf{t}_S - \mathbf{t}_{S,h}\|_{0,\omega_e}^2 + \|\boldsymbol{\rho}_S - \boldsymbol{\rho}_{S,h}\|_{0,\omega_e}^2 \right\}$   
for all  $e \in \mathcal{E}_h(\Omega_S)$ , where the set  $\omega_e$  is given by  $\omega_e := \cup \{T' \in \mathcal{T}_h^S : e \in \mathcal{E}(T')\}$ ,
- g)  $h_e \left\| (\mathbf{t}_{S,h} + \boldsymbol{\rho}_{S,h}) \times \mathbf{n} \right\|_{0,e}^2 \leq c_{20} \left\{ \|\mathbf{t}_S - \mathbf{t}_{S,h}\|_{0,T_e}^2 + \|\boldsymbol{\rho}_S - \boldsymbol{\rho}_{S,h}\|_{0,T_e}^2 \right\}$   
for all  $e \in \mathcal{E}_h(\Gamma_S)$ , where  $T_e$  is the tetrahedron of  $\mathcal{T}_h^S$  having  $e$  as a face.

*Proof.* For a) we refer to [34, Lemma 6.3] or alternatively [15, Lemma 4.3] (see also [90, Lemma 4.9]). In turn, noting that

$$\underline{\mathbf{curl}}(\mathbf{K}^{-1} \mathbf{u}_D) = -\underline{\mathbf{curl}}(\nabla p_D) = \mathbf{0} \quad \text{and} \quad \underline{\mathbf{curl}}(\mathbf{t}_S + \boldsymbol{\rho}_S) = \underline{\mathbf{curl}}(\nabla \mathbf{u}_S) = \mathbf{0},$$

we find that the proofs of b) and e) are direct consequences of [83, Lemma 4.9]. Similarly, the proofs of c), d), f) and g) follow after a straightforward application of [83, Lemma 4.10] (see also [34, Lemma 6.2] and [15, Lemma 4.4]).  $\square$

We end this section by observing that the required efficiency of the *a posteriori* error estimator  $\Theta$  (cf. lower bound in (2.33)) is a direct consequence of Lemmas 2.14, 2.16, 2.18, and 2.15. In particular, the terms  $h_e \|\lambda - \lambda_h\|_{0,e}^2$  and  $h_e \|\varphi - \varphi_h\|_{0,e}^2$  appearing in Lemma 2.15 (items a) – d)), are bounded as follows:

$$\sum_{e \in \mathcal{E}_h(\Sigma)} h_e \|\lambda - \lambda_h\|_{0,e}^2 \leq h \|\lambda - \lambda_h\|_{0,\Sigma}^2 \leq C h \|\lambda - \lambda_h\|_{1/2,\Sigma}^2,$$

and

$$\sum_{e \in \mathcal{E}_h(\Sigma)} h_e \|\varphi - \varphi_h\|_{0,e}^2 \leq h \|\varphi - \varphi_h\|_{0,\Sigma}^2 \leq C h \|\varphi - \varphi_h\|_{1/2,00,\Sigma}^2.$$

## 2.4 Numerical results

We now turn to the implementation of some numerical tests that confirm the predicted reliability and efficiency of the proposed *a posteriori* error estimator. For the sake of simplicity, here we restrict ourselves to the two-dimensional case. To do that we remark that the 2D version of the *a posteriori* error indicators  $\Theta_S$  and  $\Theta_D$  described in (2.31) and (2.32) are defined exactly as their 3D counterparts, considering where appropriate (with  $\mathbf{v} := (v_1, v_2)^t$  and  $\boldsymbol{\tau} := (\tau_{ij})_{2 \times 2}$ ),  $\mathbf{v} \cdot \mathbf{t}$  and  $\boldsymbol{\tau} \mathbf{t}$  instead of  $\mathbf{v} \times \mathbf{n}$  and  $\boldsymbol{\tau} \times \mathbf{n}$ ,

$$\text{rot } \mathbf{v} := \frac{\partial v_2}{\partial x_1} - \frac{\partial v_1}{\partial x_2}, \quad \text{and} \quad \mathbf{rot } \boldsymbol{\tau} := \left( \frac{\partial \tau_{12}}{\partial x_1} - \frac{\partial \tau_{11}}{\partial x_2}, \frac{\partial \tau_{22}}{\partial x_1} - \frac{\partial \tau_{21}}{\partial x_2} \right)^t,$$

instead of  $\text{curl } \mathbf{v}$  and  $\mathbf{curl } \boldsymbol{\tau}$ , and  $\frac{d\varphi_h}{ds}$  and  $\frac{d\lambda_h}{ds}$  instead of  $\mathbf{curl}_s \varphi_h$  and  $\mathbf{curl}_s \lambda_h$ , respectively, where  $\frac{d\varphi_h}{ds}$  and  $\frac{d\lambda_h}{ds}$  stand for the tangential derivatives of  $\varphi_h$  and  $\lambda_h$ , respectively, along  $\Sigma$ .

Our implementation is based on a FreeFem++ code (see [111]), in conjunction with the direct linear solver UMFPACK (see [62]). Regarding the implementation of the Newton iterative method, the iterations are terminated once the relative error of the entire coefficient vectors between two consecutive iterates is sufficiently small, i.e.,

$$\frac{\|\text{coeff}^{m+1} - \text{coeff}^m\|_{l^2}}{\|\text{coeff}^{m+1}\|_{l^2}} \leq \text{tol},$$

where  $\|\cdot\|_{l^2}$  is the standard  $l^2$ -norm in  $\mathbb{R}^N$ , with  $N$  denoting the total number of degrees of freedom defining the finite element subspaces  $\mathbb{L}_{\text{tr},h}^2(\Omega_S)$ ,  $\mathbb{H}_h(\Omega_S)$ ,  $\mathbf{H}_{h,\Gamma_S}^1(\Omega_S)$ ,  $\mathbb{L}_{\text{skew},h}^2(\Omega_S)$ ,  $\mathbf{H}_{h,0}(\Omega_D)$ ,  $\boldsymbol{\Lambda}_h^S(\Sigma)$ ,  $\boldsymbol{\Lambda}_h^D(\Sigma)$ , and  $\mathbb{L}_{h,0}^2(\Omega_D)$ , and  $\text{tol}$  is a fixed tolerance to be specified later. As usual, the individual errors are denoted by:

$$\begin{aligned} e(\mathbf{t}_S) &:= \|\mathbf{t}_S - \mathbf{t}_{S,h}\|_{0,\Omega_S}, & e(\boldsymbol{\sigma}_S) &:= \|\boldsymbol{\sigma}_S - \boldsymbol{\sigma}_{S,h}\|_{\text{div},\Omega_S}, & e(\mathbf{u}_S) &:= \|\mathbf{u}_S - \mathbf{u}_{S,h}\|_{1,\Omega_S}, \\ e(\boldsymbol{\rho}_S) &:= \|\boldsymbol{\rho}_S - \boldsymbol{\rho}_{S,h}\|_{0,\Omega_S}, & e(p_S) &:= \|p_S - p_{S,h}\|_{0,\Omega_S}, & e(\mathbf{u}_D) &:= \|\mathbf{u}_D - \mathbf{u}_{D,h}\|_{\text{div},\Omega_D}, \\ e(p_D) &:= \|p_D - p_{D,h}\|_{0,\Omega_D}, & e(\varphi) &:= \|\varphi - \varphi_h\|_{1/2,00,\Sigma}, & e(\lambda) &:= \|\lambda - \lambda_h\|_{1/2,\Sigma}, \end{aligned}$$

where  $p_{S,h}$  is the postprocessed pressure given by

$$p_{S,h} := -\frac{1}{2} \text{tr}(\boldsymbol{\sigma}_{S,h} + (\mathbf{u}_{S,h} \otimes \mathbf{u}_{S,h})) \quad \text{in } \Omega_S.$$

In turn, the global error is computed as

$$\mathbf{e}(\vec{\mathbf{t}}) := \left\{ \mathbf{e}(\mathbf{t}_S)^2 + \mathbf{e}(\boldsymbol{\sigma}_S)^2 + \mathbf{e}(\mathbf{u}_S)^2 + \mathbf{e}(\boldsymbol{\rho}_S)^2 + \mathbf{e}(\mathbf{u}_D)^2 + \mathbf{e}(p_D)^2 + \mathbf{e}(\boldsymbol{\varphi})^2 + \mathbf{e}(\lambda)^2 \right\}^{1/2},$$

whereas the effectivity index with respect to  $\Theta$  is given by

$$\text{eff}(\Theta) := \frac{\mathbf{e}(\vec{\mathbf{t}})}{\Theta}.$$

In addition, we define the experimental rates of convergence

$$r(\diamond) := \frac{\log(\mathbf{e}(\diamond)/\mathbf{e}'(\diamond))}{\log(h/h')} \quad \text{for each } \diamond \in \{\mathbf{t}_S, \boldsymbol{\sigma}_S, \mathbf{u}_S, \boldsymbol{\rho}_S, p_S, \mathbf{u}_D, p_D, \boldsymbol{\varphi}, \lambda, \vec{\mathbf{t}}\},$$

where  $\mathbf{e}$  and  $\mathbf{e}'$  denote errors computed on two consecutive meshes of sizes  $h$  and  $h'$ , respectively. However, when the adaptive algorithm is applied (see details below), the expression  $\log(h/h')$  appearing in the computation of the above rates is replaced by  $-\frac{1}{2} \log(N/N')$ , where  $N$  and  $N'$  denote the corresponding degrees of freedom of each triangulation.

The examples to be considered in this section are described next. In all of them we choose  $\mathbf{K} = \mathbb{I}$ ,  $\omega_1 = 1$ , and according to [40, eq. (3.26) in Section 3.2], the stabilization parameters are taken as  $\kappa_1 = \mu_1/L_\mu^2$ , with  $L_\mu := \max\{\mu_2, 2\mu_2 - \mu_1\}$ ,  $\kappa_2 = \kappa_1$ ,  $\kappa_3 = \mu_1/2$ , and  $\kappa_4 = C_{K_0}\mu_1/4$ . Since the Korn inequality constant is not known when considering mixed boundary conditions,  $C_{K_0}$  is taken here heuristically as 0.5 (see [40, Section 7] for details). In addition, the tolerance  $\text{tol}$  is taken as  $1E-6$  in all the examples.

Example 1 is used to corroborate the reliability and efficiency of the a posteriori error estimator  $\Theta$ , whereas Examples 2 and 3 are utilized to illustrate the behaviour of the associated adaptive algorithm, which applies the following procedure from [149]:

- (1) Start with a coarse mesh  $\mathcal{T}_h := \mathcal{T}_h^S \cup \mathcal{T}_h^D$ .
- (2) Solve the discrete problem (2.17) for the current mesh  $\mathcal{T}_h$ .
- (3) Compute  $\Theta_T := \Theta_{\star,T}$  for each triangle  $T \in \mathcal{T}_h^\star$ ,  $\star \in \{S, D\}$ .
- (4) Check the stopping criterion and decide whether to finish or go to next step.
- (5) Use blue-green refinement on those  $T' \in \mathcal{T}_h$  whose indicator  $\Theta_{T'}$  satisfies

$$\Theta_{T'} \geq \frac{1}{2} \max_{T \in \mathcal{T}_h} \left\{ \Theta_T : T \in \mathcal{T}_h \right\}$$

- (6) Define resulting meshes as current meshes  $\mathcal{T}_h^S$  and  $\mathcal{T}_h^D$ , and go to step 2.

In Example 1 we consider the regions  $\Omega_S := \{(x_1, x_2) : (x_1 - 0.5)^2 + (x_2 - 1)^2 < 0.25, x_2 > 1\}$  and  $\Omega_D := (0, 1)^2$ . In this case, we set the nonlinear viscosity to

$$\mu(s) := 2 + \frac{1}{1+s} \quad \text{for } s \geq 0.$$

The data  $\mathbf{f}_S$  and  $f_D$  are chosen so that the exact solution in the tombstone-shaped domain  $\Omega$  is given by the smooth functions

$$p_S(\mathbf{x}) = \cos(\pi x_1) \cos(\pi x_2), \quad \mathbf{u}_S(\mathbf{x}) = -\text{curl}(\sin(\pi x_1) \sin(\pi x_2)),$$

for all  $\mathbf{x} := (x_1, x_2) \in \Omega_S$ , and

$$p_D(\mathbf{x}) = \cos(\pi x_1) \cos(\pi x_2) \quad \forall \mathbf{x} := (x_1, x_2) \in \Omega_D,$$

where  $\text{curl}(q) := \left(\frac{\partial q}{\partial x_2}, -\frac{\partial q}{\partial x_1}\right)^t$  for any sufficiently smooth function  $q$ . Notice that this solution satisfies  $\mathbf{u}_S \cdot \mathbf{n} = \mathbf{u}_D \cdot \mathbf{n}$  on  $\Sigma$  and the boundary condition  $\mathbf{u}_D \cdot \mathbf{n} = 0$  on  $\Gamma_D$ . However, the Dirichlet boundary condition for the Navier–Stokes velocity on  $\Gamma_S$  is non-homogeneous. Then, we need to modify accordingly the functional  $\mathbf{F}$  (cf. (2.11)), as follows

$$[\mathbf{F}, (\underline{\mathbf{r}}, \underline{\psi})] := -\kappa_2(\mathbf{f}_S, \mathbf{div} \boldsymbol{\tau}_S)_S + (\mathbf{f}_S, \mathbf{v}_S)_S + \langle \boldsymbol{\tau}_S \mathbf{n}, \mathbf{g} \rangle_{\Gamma_S} \quad \forall (\underline{\mathbf{r}}, \underline{\psi}) \in \mathbb{X},$$

where  $\mathbf{g} := \mathbf{u}_S|_{\Gamma_S} \in \mathbf{H}^{1/2}(\Gamma_S)$ .

In Example 2 we consider the inverted L-shaped domain  $\Omega = \Omega_S \cup \Omega_D$ , where  $\Omega_S = (0, 1)^2$  and  $\Omega_D := (-1, 1) \times (-1, 0)$ , representing a fluid channel on top of a porous basin. The viscosity follows a Carreau law with  $\alpha_0 = 0.5$ ,  $\alpha_1 = 0.5$ , and  $\beta = 1.5$ , that is

$$\mu(s) := 0.5 + 0.5(1 + s^2)^{-1/4} \quad \text{for } s \geq 0,$$

and the data  $\mathbf{f}_S$  and  $f_D$  are chosen so that the exact solution is given by

$$p_S(\mathbf{x}) = \cos(\pi x_1) \cos(\pi x_2), \quad \mathbf{u}_S(\mathbf{x}) = \mathbf{curl} \left( x_1^2(x_1 - 1)^2 x_2^2(x_2 - 1)^2 \right),$$

for all  $\mathbf{x} := (x_1, x_2) \in \Omega_S$ , and

$$p_D(\mathbf{x}) = \frac{(x_1^2 - 1)^2 x_2^2 (x_2 + 1)^2}{(x_1 + 0.01)^2 + (y - 0.01)^2} \quad \forall \mathbf{x} := (x_1, x_2) \in \Omega_D.$$

Notice that the Darcy velocity and pressure exhibit high gradients near the origin.

Finally, in Example 3 we consider  $\Omega_D := (-1, 0)^2$  and let  $\Omega_S$  be the L-shaped domain given by  $(-1, 1)^2 \setminus \overline{\Omega_D}$ , which yields a porous medium partially surrounded by a fluid. The viscosity follows again a Carreau law (cf. (2.3)) with  $\alpha_0 = 0.5$ ,  $\alpha_1 = 0.5$ , and  $\beta = 1$ , that is

$$\mu(s) := 0.5 + 0.5(1 + s^2)^{-1/2} \quad \text{for } s \geq 0,$$

and the data  $\mathbf{f}_S$  and  $f_D$  are chosen so that the exact solution is given by

$$p_S(\mathbf{x}) = \frac{1}{100(x_1^2 + x_2^2) + 0.01}, \quad \mathbf{u}_S(\mathbf{x}) = \text{curl} \left( 0.1(x_2^2 - 1)^2 \sin^2(\pi x_1) \right),$$

for all  $\mathbf{x} := (x_1, x_2) \in \Omega_S$ , and

$$p_D(\mathbf{x}) = \cos(\pi x_1) \cos(\pi x_2) \quad \forall \mathbf{x} := (x_1, x_2) \in \Omega_D.$$

Note that the fluid pressure  $p_S$  has high gradients around the origin.

Concerning a priori regularity estimates for the Navier–Stokes problem on polygonal domains, which can be used to explain the singularities of the manufactured solutions of the examples, we refer in particular to [61], where the corresponding results are derived first for the Stokes system, and then extended to the nonlinear case through a linearization procedure. Related contributions for general elliptic problems in non-smooth domains can be found in the classical references [105] and [106].

In Table 2.1 we summarize the convergence history of the fully-mixed finite element method (2.17), as applied to Example 1, for a sequence of quasi-uniform triangulations of the domain, considering the finite element spaces introduced in Section 2.2.3, and solving the nonlinear problem with around five Newton iterations. We observe there, looking at the corresponding experimental rates of convergence, that the  $O(h)$  predicted by Theorem 2.2 (here  $\delta = 1$ ) is attained in all the unknowns. In addition, we notice that the effectivity index  $\text{eff}(\Theta)$  remains always in a neighbourhood of 0.98, which illustrates the reliability and efficiency of  $\Theta$  in the case of a regular solution.

Next, in Tables 2.2, 2.3, 2.4, and 2.5, we provide the convergence history of the quasi-uniform and adaptive schemes, as applied to Examples 2 and 3, solving the nonlinear problem with around three and six Newton iterations, respectively. We observe that the errors of the adaptive procedure decrease faster than those obtained by the quasi-uniform ones, which is confirmed by the global experimental rates of convergence provided there. This fact is also illustrated in Figures 2.2 and 2.4 where we display the total errors  $\mathbf{e}(\mathbf{t}, \underline{\varphi}, p_D)$  vs. the number of degrees of freedom  $N$  for both refinements. As shown by the values of  $\mathbf{r}(\mathbf{t}, \underline{\varphi}, p_D)$ , the adaptive method is able to keep the quasi-optimal rate of convergence  $O(h)$  for the total error. Furthermore, the effectivity indexes remain bounded from above and below, which confirms the reliability and efficiency of  $\Theta$  in these cases of non-smooth solutions. Intermediate meshes obtained with the adaptive refinements are displayed in Figures 2.3 and 2.5. Note that the method is able to recognize the region with high gradients in Examples 2 and 3.

| dof    | $h_S$  | $e(t_S)$ | $r(t_S)$ | $e(\sigma_S)$ | $r(\sigma_S)$ | $e(u_S)$ | $r(u_S)$ | $e(\rho_S)$ | $r(\rho_S)$ |
|--------|--------|----------|----------|---------------|---------------|----------|----------|-------------|-------------|
| 854    | 0.1905 | 0.5866   | –        | 4.6754        | –             | 0.9306   | –        | 1.7056      | –           |
| 3195   | 0.0911 | 0.2909   | 1.0633   | 2.4721        | 0.9660        | 0.4707   | 1.0332   | 0.9970      | 0.8139      |
| 12543  | 0.0486 | 0.1460   | 1.0085   | 1.2793        | 0.9634        | 0.2381   | 0.9968   | 0.5015      | 1.0050      |
| 50188  | 0.0242 | 0.0679   | 1.1031   | 0.6398        | 0.9995        | 0.1142   | 1.0593   | 0.2371      | 1.0804      |
| 198838 | 0.0129 | 0.0352   | 0.9553   | 0.3493        | 0.8791        | 0.0580   | 0.9843   | 0.1256      | 0.9231      |
| 783886 | 0.0068 | 0.0179   | 0.9822   | 0.1742        | 1.0143        | 0.0294   | 0.9912   | 0.0639      | 0.9862      |

| dof    | $h_S$  | $h_D$  | $e(p_S)$ | $r(p_S)$ | $e(u_D)$ | $r(u_D)$ | $e(p_D)$ | $r(p_D)$ |
|--------|--------|--------|----------|----------|----------|----------|----------|----------|
| 854    | 0.1905 | 0.1901 | 0.6240   | –        | 1.2480   | –        | 0.0619   | –        |
| 3195   | 0.0911 | 0.0966 | 0.3409   | 0.9165   | 0.6004   | 1.1092   | 0.0296   | 1.1159   |
| 12543  | 0.0486 | 0.0573 | 0.1470   | 1.2302   | 0.3035   | 0.9975   | 0.0150   | 0.9962   |
| 50188  | 0.0242 | 0.0259 | 0.0686   | 1.0987   | 0.1516   | 1.0018   | 0.0075   | 1.0023   |
| 198838 | 0.0129 | 0.0135 | 0.0364   | 0.9227   | 0.0756   | 1.0106   | 0.0037   | 1.0105   |
| 783886 | 0.0068 | 0.0070 | 0.0183   | 1.0003   | 0.0382   | 0.9945   | 0.0019   | 0.9935   |

| dof    | $\hat{h}$ | $e(\varphi)$ | $r(\varphi)$ | $e(\lambda)$ | $r(\lambda)$ | $e(\vec{t})$ | $r(\vec{t})$ | $\Theta$ | $\text{eff}(\Theta)$ | iter |
|--------|-----------|--------------|--------------|--------------|--------------|--------------|--------------|----------|----------------------|------|
| 854    | 1/4       | 1.0668       | –            | 0.2038       | –            | 5.3590       | –            | 5.5271   | 0.9696               | 5    |
| 3195   | 1/8       | 0.5573       | 0.9844       | 0.0980       | 1.1090       | 2.8448       | 0.9600       | 2.9156   | 0.9757               | 5    |
| 12543  | 1/16      | 0.2710       | 1.0545       | 0.0479       | 1.0485       | 1.4609       | 0.9746       | 1.4804   | 0.9868               | 5    |
| 50188  | 1/32      | 0.1345       | 1.0104       | 0.0243       | 0.9767       | 0.7245       | 1.0116       | 0.7312   | 0.9908               | 5    |
| 198838 | 1/64      | 0.0675       | 1.0025       | 0.0119       | 1.0336       | 0.3909       | 0.8963       | 0.3938   | 0.9926               | 5    |
| 783886 | 1/128     | 0.0336       | 1.0168       | 0.0064       | 0.9157       | 0.1956       | 1.0098       | 0.1967   | 0.9940               | 5    |

Table 2.1: EXAMPLE 1, quasi-uniform scheme.

| dof    | $h_S$  | $h_D$  | $e(t_S)$ | $e(\sigma_S)$ | $e(u_S)$ | $e(\rho_S)$ | $e(p_S)$ | $e(u_D)$ | $e(p_D)$ |
|--------|--------|--------|----------|---------------|----------|-------------|----------|----------|----------|
| 588    | 0.2926 | 0.3297 | 0.2022   | 0.5672        | 0.1893   | 0.3651      | 0.1754   | 39.9583  | 0.4761   |
| 1931   | 0.1964 | 0.1901 | 0.1811   | 0.3955        | 0.2030   | 0.3665      | 0.1092   | 73.9004  | 0.4069   |
| 7317   | 0.0997 | 0.1000 | 0.0724   | 0.1796        | 0.0814   | 0.1344      | 0.0572   | 59.6887  | 0.1433   |
| 28860  | 0.0487 | 0.0534 | 0.0172   | 0.0726        | 0.0068   | 0.0425      | 0.0172   | 76.9741  | 0.0140   |
| 115506 | 0.0250 | 0.0263 | 0.0084   | 0.0363        | 0.0034   | 0.0206      | 0.0082   | 66.9770  | 0.0055   |
| 459154 | 0.0136 | 0.0147 | 0.0042   | 0.0181        | 0.0015   | 0.0106      | 0.0041   | 54.0296  | 0.0028   |

| dof    | $\hat{h}$ | $e(\varphi)$ | $e(\lambda)$ | $e(\vec{t})$ | $r(\vec{t})$ | $\Theta$ | $\text{eff}(\Theta)$ | iter |
|--------|-----------|--------------|--------------|--------------|--------------|----------|----------------------|------|
| 588    | 1/2       | 0.2161       | 0.8872       | 39.9782      | –            | 40.2227  | 0.9939               | 4    |
| 1931   | 1/4       | 0.2601       | 1.2136       | 73.9144      | –            | 74.0108  | 0.9987               | 4    |
| 7317   | 1/8       | 0.0931       | 0.6470       | 59.6930      | 0.3208       | 59.7396  | 0.9992               | 4    |
| 28860  | 1/16      | 0.0092       | 0.1010       | 76.9742      | –            | 76.9937  | 0.9997               | 3    |
| 115506 | 1/32      | 0.0057       | 0.0485       | 66.9770      | 0.2006       | 66.9905  | 0.9998               | 3    |
| 459154 | 1/64      | 0.0029       | 0.0320       | 54.0296      | 0.3113       | 54.0370  | 0.9999               | 3    |

Table 2.2: EXAMPLE 2, quasi-uniform scheme.



| dof    | $e(\mathbf{t}_S)$ | $e(\boldsymbol{\sigma}_S)$ | $e(\mathbf{u}_S)$ | $e(\boldsymbol{\rho}_S)$ | $e(p_S)$ | $e(\mathbf{u}_D)$ | $e(p_D)$ |
|--------|-------------------|----------------------------|-------------------|--------------------------|----------|-------------------|----------|
| 588    | 0.2022            | 0.5672                     | 0.1893            | 0.3651                   | 0.1754   | 39.9583           | 0.4761   |
| 784    | 0.1505            | 0.5215                     | 0.1347            | 0.2404                   | 0.1385   | 65.1904           | 0.1957   |
| 1019   | 0.1031            | 0.4988                     | 0.0802            | 0.1297                   | 0.1271   | 73.1960           | 0.0295   |
| 1431   | 0.0996            | 0.4973                     | 0.0889            | 0.0982                   | 0.1536   | 55.1764           | 0.0284   |
| 2111   | 0.0991            | 0.4995                     | 0.0891            | 0.0863                   | 0.1419   | 29.5771           | 0.0283   |
| 3185   | 0.0994            | 0.5011                     | 0.0890            | 0.0805                   | 0.1364   | 12.6187           | 0.0282   |
| 5555   | 0.0999            | 0.5028                     | 0.0893            | 0.0777                   | 0.1493   | 7.1633            | 0.0280   |
| 9680   | 0.0996            | 0.5023                     | 0.0887            | 0.0848                   | 0.1481   | 5.2107            | 0.0208   |
| 17147  | 0.0916            | 0.3984                     | 0.0628            | 0.1351                   | 0.1290   | 3.8253            | 0.0152   |
| 31110  | 0.0691            | 0.3124                     | 0.0398            | 0.1078                   | 0.0935   | 2.8216            | 0.0124   |
| 59678  | 0.0490            | 0.1961                     | 0.0197            | 0.0866                   | 0.0536   | 2.0190            | 0.0076   |
| 112409 | 0.0394            | 0.1672                     | 0.0165            | 0.0653                   | 0.0484   | 1.4593            | 0.0063   |
| 221370 | 0.0245            | 0.1003                     | 0.0084            | 0.0389                   | 0.0271   | 1.0402            | 0.0038   |
| 427000 | 0.0206            | 0.0870                     | 0.0068            | 0.0327                   | 0.0226   | 0.7425            | 0.0032   |

| dof    | $e(\boldsymbol{\varphi})$ | $e(\lambda)$ | $e(\vec{\mathbf{t}})$ | $\mathbf{r}(\vec{\mathbf{t}})$ | $\Theta$ | $\text{eff}(\Theta)$ | iter |
|--------|---------------------------|--------------|-----------------------|--------------------------------|----------|----------------------|------|
| 588    | 0.2161                    | 0.8872       | 39.9782               | —                              | 40.2227  | 0.9939               | 4    |
| 784    | 0.1439                    | 0.8114       | 65.1987               | —                              | 65.2262  | 0.9996               | 4    |
| 1019   | 0.0634                    | 0.1014       | 73.1980               | —                              | 73.2245  | 0.9996               | 3    |
| 1431   | 0.0504                    | 0.0475       | 55.1790               | 1.6645                         | 55.2056  | 0.9995               | 3    |
| 2111   | 0.0444                    | 0.0201       | 29.5818               | 3.2070                         | 29.6221  | 0.9986               | 3    |
| 3185   | 0.0428                    | 0.0155       | 12.6297               | 4.1387                         | 12.7177  | 0.9931               | 3    |
| 5555   | 0.0416                    | 0.0152       | 7.1828                | 2.0292                         | 7.3110   | 0.9825               | 3    |
| 9680   | 0.0459                    | 0.0130       | 5.2375                | 1.1374                         | 5.3244   | 0.9837               | 3    |
| 17147  | 0.0479                    | 0.0118       | 3.8503                | 1.0763                         | 3.9225   | 0.9816               | 3    |
| 31110  | 0.0255                    | 0.0060       | 2.8422                | 1.0192                         | 2.8947   | 0.9819               | 3    |
| 59678  | 0.0217                    | 0.0039       | 2.0312                | 1.0314                         | 2.0692   | 0.9816               | 3    |
| 112409 | 0.0136                    | 0.0021       | 1.4710                | 1.0192                         | 1.4982   | 0.9818               | 3    |
| 221370 | 0.0085                    | 0.0012       | 1.0461                | 1.0059                         | 1.0651   | 0.9822               | 3    |
| 427000 | 0.0072                    | 0.0006       | 0.7487                | 1.0184                         | 0.7625   | 0.9819               | 3    |

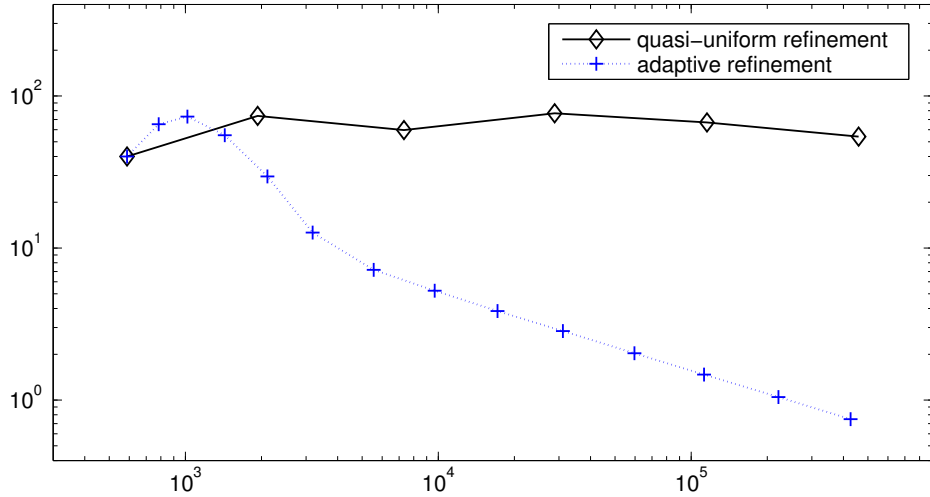
Table 2.3: EXAMPLE 2, adaptive scheme.

| dof    | $h_S$  | $h_D$  | $e(\mathbf{t}_S)$ | $e(\boldsymbol{\sigma}_S)$ | $e(\mathbf{u}_S)$ | $e(\boldsymbol{\rho}_S)$ | $e(p_S)$ | $e(\mathbf{u}_D)$ | $e(p_D)$ |
|--------|--------|--------|-------------------|----------------------------|-------------------|--------------------------|----------|-------------------|----------|
| 1037   | 0.3529 | 0.3019 | 1.2001            | 19.6901                    | 2.6722            | 2.8717                   | 0.6257   | 2.1914            | 0.1139   |
| 3664   | 0.1947 | 0.1964 | 2.1724            | 58.3515                    | 4.5117            | 3.3283                   | 1.1404   | 1.2395            | 0.0657   |
| 13956  | 0.0960 | 0.1025 | 2.4894            | 114.3013                   | 5.8122            | 4.1176                   | 1.0524   | 0.6207            | 0.0314   |
| 55663  | 0.0520 | 0.0495 | 1.7729            | 94.6633                    | 3.2125            | 2.7450                   | 0.8685   | 0.3093            | 0.0153   |
| 220100 | 0.0293 | 0.0260 | 0.8835            | 51.4952                    | 1.0053            | 1.4521                   | 0.5310   | 0.1513            | 0.0075   |
| 879198 | 0.0145 | 0.0143 | 0.5353            | 33.8233                    | 0.3295            | 1.2531                   | 0.3642   | 0.0759            | 0.0037   |

| dof    | $\hat{h}$ | $e(\boldsymbol{\varphi})$ | $e(\lambda)$ | $e(\vec{\mathbf{t}})$ | $\mathbf{r}(\vec{\mathbf{t}})$ | $\Theta$ | $\text{eff}(\Theta)$ | iter |
|--------|-----------|---------------------------|--------------|-----------------------|--------------------------------|----------|----------------------|------|
| 1037   | 1/2       | 1.3033                    | 0.9173       | 20.2949               | —                              | 20.6086  | 0.9848               | 5    |
| 3664   | 1/4       | 2.0423                    | 0.6667       | 58.7129               | —                              | 58.7574  | 0.9992               | 5    |
| 13956  | 1/8       | 2.4754                    | 0.4053       | 114.5792              | —                              | 114.5746 | 1.0000               | 5    |
| 55663  | 1/16      | 1.8369                    | 0.2100       | 94.7926               | 0.2741                         | 94.7881  | 1.0000               | 5    |
| 220100 | 1/32      | 0.7827                    | 0.0855       | 51.5392               | 0.8865                         | 51.5419  | 0.9999               | 5    |
| 879198 | 1/64      | 0.5891                    | 0.0577       | 33.8576               | 0.6068                         | 33.8559  | 1.0000               | 5    |

Table 2.4: EXAMPLE 3, quasi-uniform scheme.

Figure 2.2: Example 2,  $e(\mathbf{t}, \underline{\boldsymbol{\varphi}}, p_D)$  vs.  $N$  for quasi-uniform/adaptive schemes.

| dof    | $e(\mathbf{t}_S)$ | $e(\boldsymbol{\sigma}_S)$ | $e(\mathbf{u}_S)$ | $e(\boldsymbol{\rho}_S)$ | $e(p_S)$ | $e(\mathbf{u}_D)$ | $e(p_D)$ |
|--------|-------------------|----------------------------|-------------------|--------------------------|----------|-------------------|----------|
| 1037   | 1.2001            | 19.6901                    | 2.6722            | 2.8717                   | 0.6257   | 2.1914            | 0.1139   |
| 1579   | 3.0393            | 98.1488                    | 6.1149            | 4.8488                   | 1.2574   | 1.9106            | 0.0933   |
| 2092   | 2.0017            | 84.5704                    | 2.9416            | 2.9343                   | 1.0256   | 1.8860            | 0.0929   |
| 2766   | 0.7046            | 42.4930                    | 0.8777            | 1.4751                   | 0.3717   | 1.8982            | 0.0936   |
| 4748   | 0.5235            | 16.4829                    | 0.7695            | 1.4233                   | 0.2375   | 1.9012            | 0.0938   |
| 9936   | 0.4928            | 8.2112                     | 0.7622            | 1.4148                   | 0.2143   | 1.5623            | 0.0779   |
| 18993  | 0.3580            | 5.6827                     | 0.5430            | 1.0980                   | 0.1401   | 1.0019            | 0.0495   |
| 33974  | 0.2681            | 4.2302                     | 0.3972            | 0.9634                   | 0.1096   | 0.7945            | 0.0395   |
| 64472  | 0.1785            | 3.0476                     | 0.2581            | 0.7001                   | 0.0752   | 0.5697            | 0.0282   |
| 122011 | 0.1438            | 2.2169                     | 0.2111            | 0.5401                   | 0.0643   | 0.4319            | 0.0215   |
| 237874 | 0.0928            | 1.5864                     | 0.1340            | 0.3908                   | 0.0407   | 0.3042            | 0.0151   |
| 460024 | 0.0708            | 1.1390                     | 0.1038            | 0.3028                   | 0.0301   | 0.2232            | 0.0111   |
| 915408 | 0.0456            | 0.8086                     | 0.0667            | 0.2074                   | 0.0201   | 0.1567            | 0.0078   |

| dof    | $e(\boldsymbol{\varphi})$ | $e(\lambda)$ | $e(\vec{\mathbf{t}})$ | $\mathbf{r}(\vec{\mathbf{t}})$ | $\Theta$ | $\text{eff}(\Theta)$ | iter |
|--------|---------------------------|--------------|-----------------------|--------------------------------|----------|----------------------|------|
| 1037   | 1.3033                    | 0.9173       | 20.2949               | —                              | 20.6086  | 0.9848               | 5    |
| 1579   | 5.6381                    | 1.0470       | 98.6908               | —                              | 98.8258  | 0.9986               | 5    |
| 2092   | 3.5592                    | 0.5382       | 84.7936               | 1.0790                         | 84.8825  | 0.9990               | 5    |
| 2766   | 0.6262                    | 0.4790       | 42.5832               | 4.9324                         | 42.6743  | 0.9979               | 5    |
| 4748   | 0.4162                    | 0.4813       | 16.6915               | 3.4667                         | 16.9205  | 0.9865               | 5    |
| 9936   | 0.3749                    | 0.4612       | 8.5469                | 1.8128                         | 8.7791   | 0.9736               | 5    |
| 18993  | 0.3330                    | 0.2994       | 5.9270                | 1.1300                         | 6.1023   | 0.9713               | 5    |
| 33974  | 0.2066                    | 0.2053       | 4.4464                | 0.9885                         | 4.5652   | 0.9740               | 5    |
| 64472  | 0.1455                    | 0.1665       | 3.2017                | 1.0252                         | 3.3074   | 0.9680               | 5    |
| 122011 | 0.1153                    | 0.1202       | 2.3423                | 0.9799                         | 2.4071   | 0.9731               | 5    |
| 237874 | 0.0839                    | 0.0852       | 1.6742                | 1.0060                         | 1.7299   | 0.9678               | 5    |
| 460024 | 0.0552                    | 0.0664       | 1.2092                | 0.9865                         | 1.2446   | 0.9716               | 5    |
| 915408 | 0.0436                    | 0.0463       | 0.8556                | 1.0055                         | 0.8850   | 0.9668               | 5    |

Table 2.5: EXAMPLE 3, adaptive scheme.

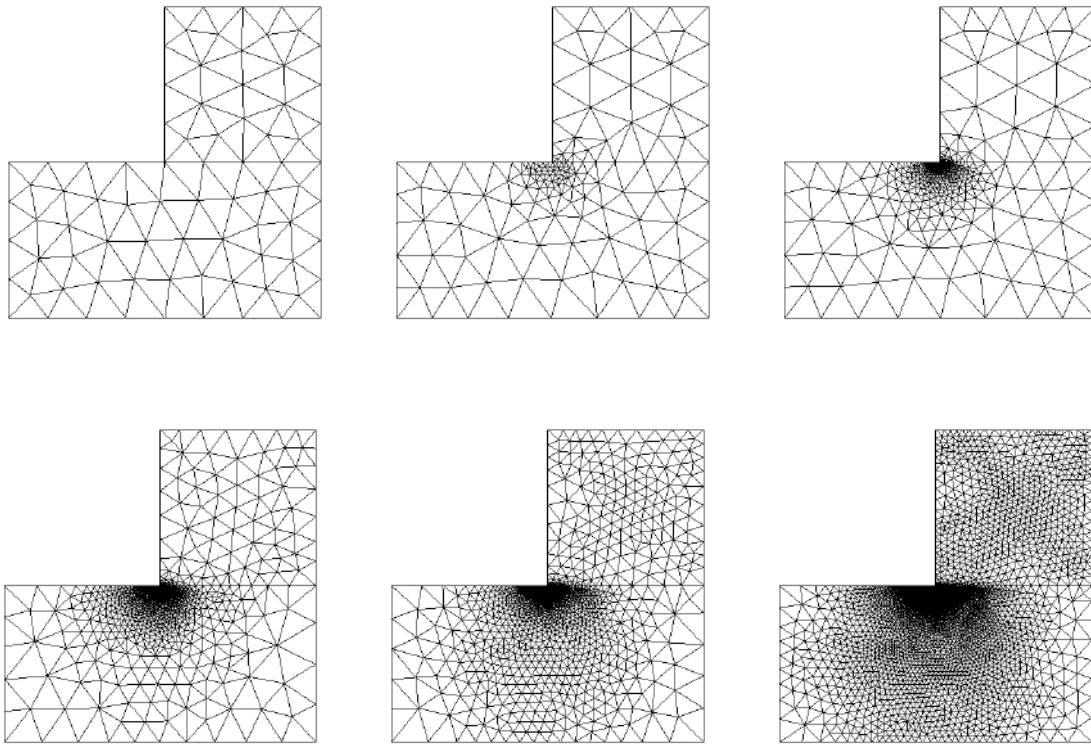


Figure 2.3: Example 2, adapted meshes with 588, 1019, 9680, 31110, 112409, and 447000 degrees of freedom.

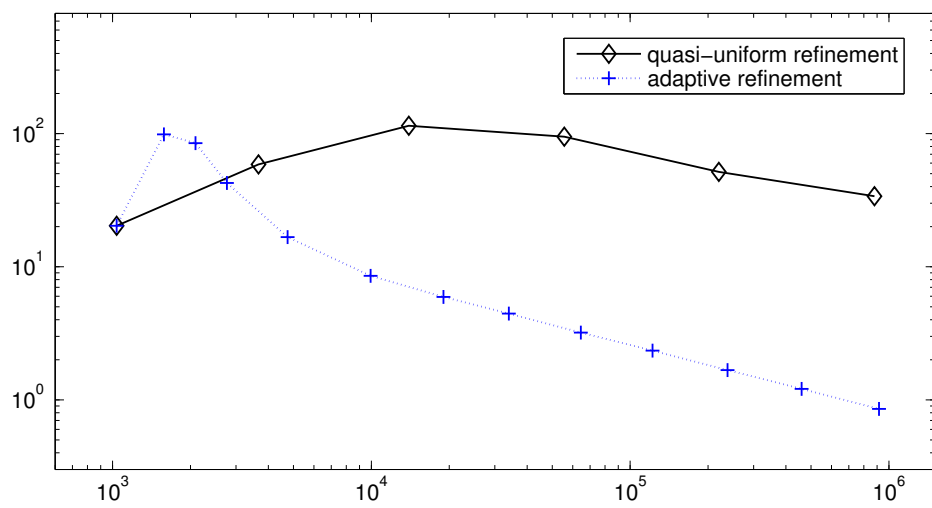


Figure 2.4: Example 3,  $e(\underline{t}, \underline{\varphi}, p_D)$  vs.  $N$  for quasi-uniform/adaptive schemes.

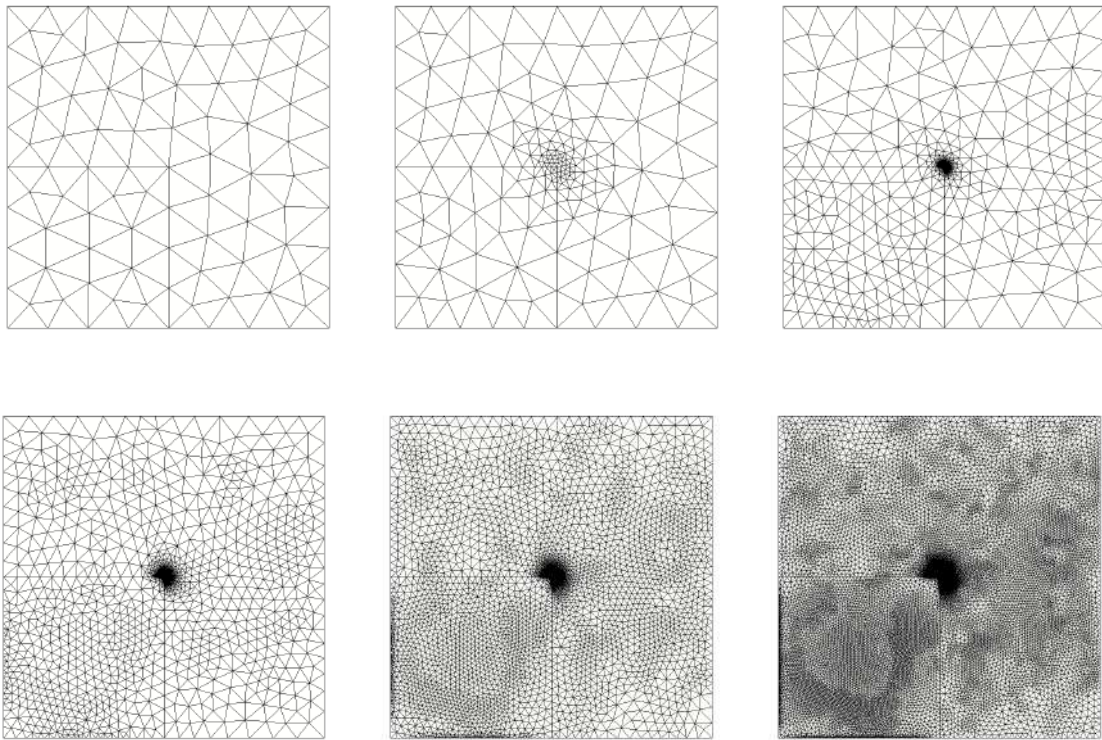


Figure 2.5: Example 3, adapted meshes with 1037, 2092, 18993, 64472, 237874, and 915408 degrees of freedom.

## CHAPTER 3

---

### A conforming mixed finite element method for the Navier–Stokes/Darcy–Forchheimer coupled problem

---

In this chapter we analyse a mixed finite element method for the Navier–Stokes/Darcy–Forchheimer coupled problem with constant density and viscosity. We consider the standard velocity-pressure formulation for the Navier–Stokes equation and in the porous medium we consider the Darcy–Forchheimer equation in its dual-mixed formulation.

#### 3.1 Introduction

The modelling and numerical simulation of incompressible fluid flows in regions partially occupied by porous media has become a very active research area during the last decades, mostly due to its relevance in the fields of natural sciences and engineering branches. In particular, these kind of phenomena can be found in several applications such as in vuggy porous media appearing in petroleum extraction (see, e.g., [7],[6]), groundwater system in karst aquifers (see, e.g., [74], [129]), reservoir wellbore (see, e.g., [5, 8]), internal ventilation of a motorcycle helmet (see, e.g., [31, 48]), and blood motion in tumors and microvessels (see, e.g., [138], [146]), to name a few. One of the most popular models utilised to describe the aforementioned interaction is the Navier–Stokes/Darcy–Forchheimer (or Navier–Stokes/Darcy, Stokes/Darcy) model, which consists in a set of differential equations where the Navier–Stokes (or Stokes) problem is coupled with the Darcy–Forchheimer (or Darcy) model through a set of coupling equations acting on a common interface, which are given by mass conservation, balance of normal forces, and the so called Beavers–Joseph–Saffman condition. In [64, 63, 43, 92, 11, 94, 93, 96, 65, 40], and in the references therein, we can find a large list of contributions devoted to numerically approximate the solution of this interaction problem, including primal and mixed conforming formulations, as well as nonconforming methods. At this point we remark that the Navier–Stokes/Darcy–Forchheimer model is considered when the fluid velocity is higher and the porosity is nonuniform, which holds when the kinematic forces dominates over viscous forces. We refer the reader to [9, 102, 135, 142] for the derivation and analysis of the Darcy–Forchheimer equations.

Up to the authors’ knowledge, one of the first works in analysing the coupling of Navier–Stokes and Darcy–Forchheimer equations is [5]. In that work, the authors study the coupling of a 2D reservoir model with a 1.5D vertical wellbore model, both written in axisymmetric form. The physical problems

are described by the Darcy–Forchheimer and the compressible Navier–Stokes equations, respectively, together with an exhaustive energy equation. Later on, motivated by the study of the internal ventilation of a motorcycle helmet, a penalization approach was introduced and analysed in [48]. In particular, the authors consider the velocity and pressure in the whole domain as the main unknowns of the system, and the corresponding Galerkin approximation employs piecewise quadratic elements and piecewise linear for the velocity and pressure, respectively. Notice that this method is applied to both 2D and 3D domains. More recently, in [147] a 3D discrete dynamical system was derived from the generalized Navier–Stokes equations for incompressible flow with nonlinear drag forces (represented by Forchheimer terms) in porous media via a Galerkin procedure. We observe that this method can be employed in subgrid-scale models of synthetic-velocity form for large-eddy simulation of turbulent flow through porous media.

Furthermore, and concerning simpler related models, we highlight that a conforming mixed method for the Stokes–Darcy coupled problem has been introduced and analysed in [92]. In this work, the velocity-pressure formulation in the Stokes equation and the dual-mixed approach in the Darcy region is considered, which yields the introduction of the trace of the porous medium pressure as a suitable Lagrange multiplier. Later on, it was shown in [94] that the use of any pair of stable Stokes and Darcy elements guarantees the well-posedness of the corresponding Stokes–Darcy Galerkin scheme. More recently, in [65] the authors extend the results from [92] to the Navier–Stokes/Darcy coupled problem. Since this coupled system is nonlinear (due to the convective term in the free fluid region), the analysis of the continuous problem begins with the linearisation of the Oseen problem in the free fluid domain. This simplified model is then studied by means of the classical Babuška–Brezzi theory, similarly as it was done for the Stokes–Darcy coupling in [92]. Then, a fixed-point strategy based on the aforementioned linearisation is associate to the nonlinear coupling, which allows to establish existence and uniqueness of solution thanks to Schauder’s and Banach’s fixed point theorems, respectively.

According to the above bibliographic discussion, in this chapter we aim to extend the results obtained in [65, 92, 94] to the Navier–Stokes/Darcy–Forchheimer coupled problem. We consider the standard velocity-pressure formulation for the Navier–Stokes equation and unlike [65], in the porous medium we consider the Darcy–Forchheimer equation in its dual-mixed formulation. In this way, we obtain the velocity and the pressure of the fluid in both media as the main unknowns of the coupled system. Since one of the interface conditions becomes essential, we proceed similarly to [65, 92] and incorporate the trace of the porous medium pressure as an additional unknown. The well-posedness of both the continuous and discrete formulations is proved, employing a fixed-point argument and classical results on nonlinear monotone operators (see [144, 145]). In particular, for the continuous formulation, under a smallness data assumption, we prove existence and uniqueness of solution by means of a fixed-point strategy where the Schauder (for existence) and Banach (for uniqueness) fixed-point theorems are employed. Using similar arguments (but applying Brower’s fixed-point theorem instead of Schauder’s for the existence result) we prove the well-posedness of the discrete problem for a specific choice of discrete space. More precisely, we consider Bernardi–Raugel elements for the velocity in the free fluid region, Raviart–Thomas elements of lowest order for the filtration velocity in the porous media, piecewise constants with null mean value for the pressures, and piecewise constant elements for the Lagrange multiplier on the interface.

The rest of this chapter is organised as follows. In Section 3.2 we introduce the model problem and

derive the variational formulation. Next, in Section 3.3, we establish that our variational formulation is well posed. The corresponding Galerkin scheme is introduced and analysed in Section 3.4. In Section 3.5 we derive the corresponding Céa's estimate and a sub-optimal rate of convergence. Finally, several numerical examples illustrating the performance of the method, confirming the theoretical sub-optimal order of convergence and suggesting an optimal rate of convergence, are reported in Section 3.6.

## 3.2 The continuous formulation

In this section we introduce the model problem and derive the corresponding weak formulation. For simplicity of exposition we set the problem in  $\mathbb{R}^2$ . However, our study can be extended to the 3D case with few modifications, which we will be pointed out appropriately in the paper.

### 3.2.1 The model problem

In order to describe the geometry, we let  $\Omega_S$  and  $\Omega_D$  be two bounded and simply connected polygonal domains in  $\mathbb{R}^2$  such that  $\partial\Omega_S \cap \partial\Omega_D = \Sigma \neq \emptyset$  and  $\Omega_S \cap \Omega_D = \emptyset$ . Then, let  $\Gamma_S := \partial\Omega_S \setminus \bar{\Sigma}$ ,  $\Gamma_D := \partial\Omega_D \setminus \bar{\Sigma}$ , and denote by  $\mathbf{n}$  the unit normal vector on the boundaries, which is chosen pointing outward from  $\Omega := \Omega_S \cup \Sigma \cup \Omega_D$  and  $\Omega_S$  (and hence inward to  $\Omega_D$  when seen on  $\Sigma$ ). On  $\Sigma$  we also consider a unit tangent vector  $\mathbf{t}$  (see Figure 3.1 below). The problem we are interested in consists of the movement of an incompressible viscous fluid occupying  $\Omega_S$  which flows towards and from a porous medium  $\Omega_D$  through  $\Sigma$ , where  $\Omega_D$  is saturated with the same fluid. The mathematical model is defined by two separate groups of equations and by a set of coupling terms. In the free fluid domain  $\Omega_S$ , the motion of the fluid can be described by the incompressible Navier–Stokes equations:

$$\begin{aligned} \boldsymbol{\sigma}_S &= -p_S \mathbb{I} + 2\mu \mathbf{e}(\mathbf{u}_S) \quad \text{in } \Omega_S, & -\operatorname{div} \boldsymbol{\sigma}_S + \rho(\nabla \mathbf{u}_S) \mathbf{u}_S &= \mathbf{f}_S \quad \text{in } \Omega_S, \\ \operatorname{div} \mathbf{u}_S &= 0 \quad \text{in } \Omega_S, & \mathbf{u}_S &= \mathbf{0} \quad \text{on } \Gamma_S, \end{aligned} \tag{3.1}$$

where the unknowns are the fluid velocity  $\mathbf{u}_S$ , the pressure  $p_S$ , and the Cauchy stress tensor  $\boldsymbol{\sigma}_S$ . In addition,  $\mathbf{e}(\mathbf{u}_S) := \frac{1}{2} \left\{ \nabla \mathbf{u}_S + (\nabla \mathbf{u}_S)^t \right\}$  stands for the strain tensor of small deformations,  $\mu$  is the viscosity of the fluid,  $\rho$  is the density, and  $\mathbf{f}_S \in \mathbf{L}^2(\Omega_S)$  is a given external force.

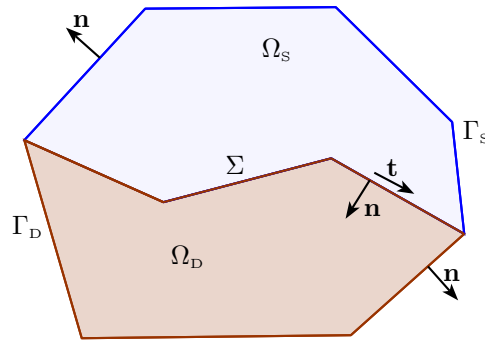


Figure 3.1: Sketch of a 2D geometry of our Navier–Stokes/Darcy–Forchheimer model



In the porous medium  $\Omega_D$  we consider a nonlinear version of the Darcy problem to approximate the velocity  $\mathbf{u}_D$  and the pressure  $p_D$ , which is considered when the fluid velocity is higher and the porosity is nonuniform. More precisely, we consider the Darcy–Forchheimer equations [142, 135]:

$$\frac{\mu}{\rho} \mathbf{K}^{-1} \mathbf{u}_D + \frac{F}{\rho} |\mathbf{u}_D| \mathbf{u}_D + \nabla p_D = \mathbf{f}_D \quad \text{in } \Omega_D, \quad \operatorname{div} \mathbf{u}_D = g_D \quad \text{in } \Omega_D, \quad \mathbf{u}_D \cdot \mathbf{n} = 0 \quad \text{on } \Gamma_D, \quad (3.2)$$

where  $F$  represents the Forchheimer number of the porous medium, and  $\mathbf{K} \in \mathbb{L}^\infty(\Omega_D)$  is a symmetric tensor in  $\Omega_D$  representing the intrinsic permeability  $\kappa$  of the porous medium divided by the viscosity  $\mu$  of the fluid. Throughout the paper we assume that there exists  $C_{\mathbf{K}} > 0$  such that

$$\mathbf{w} \cdot \mathbf{K}^{-1}(\mathbf{x}) \mathbf{w} \geq C_{\mathbf{K}} |\mathbf{w}|^2, \quad (3.3)$$

for almost all  $\mathbf{x} \in \Omega_D$ , and for all  $\mathbf{w} \in \mathbb{R}^2$ . In turn, as will be explained below,  $\mathbf{f}_D$  and  $g_D$  are given functions in  $\mathbf{L}^{3/2}(\Omega_D)$  and  $L^2(\Omega_D)$ , respectively. In addition, according to the compressibility conditions, the boundary conditions on  $\mathbf{u}_D$  and  $\mathbf{u}_S$ , and the principle of mass conservation (cf. (3.4) below),  $g_D$  must satisfy the compatibility condition:

$$\int_{\Omega_D} g_D = 0.$$

Finally, the transmission conditions that couple the Navier–Stokes and the Darcy–Forchheimer models through the interface  $\Sigma$  are given by

$$\mathbf{u}_S \cdot \mathbf{n} = \mathbf{u}_D \cdot \mathbf{n} \quad \text{on } \Sigma \quad \text{and} \quad \boldsymbol{\sigma}_S \mathbf{n} + \frac{\alpha_d \mu}{\sqrt{\mathbf{t} \cdot \boldsymbol{\kappa} \mathbf{t}}} (\mathbf{u}_S \cdot \mathbf{t}) \mathbf{t} = -p_D \mathbf{n} \quad \text{on } \Sigma, \quad (3.4)$$

where  $\alpha_d$  is a dimensionless positive constant which depends only on the geometrical characteristics of the porous medium and usually assumes values between 0.8 and 1.2 (see [16, 48]). The first condition in (3.4) is a consequence of the incompressibility of the fluid and of the conservation of mass across  $\Sigma$ . The second transmission condition on  $\Sigma$  can be decomposed, at least formally, into its normal and tangential components as follows:

$$(\boldsymbol{\sigma}_S \mathbf{n}) \cdot \mathbf{n} = -p_D \quad \text{and} \quad (\boldsymbol{\sigma}_S \mathbf{n}) \cdot \mathbf{t} = -\frac{\alpha_d \mu}{\sqrt{\mathbf{t} \cdot \boldsymbol{\kappa} \mathbf{t}}} (\mathbf{u}_S \cdot \mathbf{t}) \quad \text{on } \Sigma. \quad (3.5)$$

The first equation in (3.5) corresponds to the balance of normal forces, whereas the second one is known as the Beavers–Joseph–Saffman condition, which establishes that the slip velocity along  $\Sigma$  is proportional to the shear stress long  $\Sigma$ . We refer the reader to [12, Section 3.2] (see also [143, 117]) for further details on the choice of this interface condition.

### 3.2.2 The variational formulation

In this section we proceed analogously to [92, Section 2] and derive a weak formulation of the coupled problem given by (3.1), (3.2), and (3.4). To this end, let us first introduce further notations and definitions. In what follows, given  $\star \in \{S, D\}$ , we set

$$(p, q)_\star := \int_{\Omega_\star} p q, \quad (\mathbf{u}, \mathbf{v})_\star := \int_{\Omega_\star} \mathbf{u} \cdot \mathbf{v}, \quad \text{and} \quad (\boldsymbol{\sigma}, \boldsymbol{\tau})_\star := \int_{\Omega_\star} \boldsymbol{\sigma} : \boldsymbol{\tau},$$

where, given two arbitrary tensors  $\boldsymbol{\sigma}$  and  $\boldsymbol{\tau}$ ,  $\boldsymbol{\sigma} : \boldsymbol{\tau} = \text{tr}(\boldsymbol{\sigma}^t \boldsymbol{\tau}) = \sum_{i,j=1}^2 \sigma_{ij} \tau_{ij}$ . Furthermore, in the sequel we will employ the following Banach space,

$$\mathbf{H}^3(\text{div}; \Omega_D) := \left\{ \mathbf{v}_D \in \mathbf{L}^3(\Omega_D) : \quad \text{div } \mathbf{v}_D \in L^2(\Omega_D) \right\},$$

endowed with the norm

$$\|\mathbf{v}_D\|_{\mathbf{H}^3(\text{div}; \Omega_D)} := \left( \|\mathbf{v}_D\|_{\mathbf{L}^3(\Omega_D)}^3 + \|\text{div } \mathbf{v}_D\|_{0, \Omega_D}^3 \right)^{1/3},$$

and the following subspaces of  $\mathbf{H}^1(\Omega_S)$  and  $\mathbf{H}^3(\text{div}; \Omega_D)$ , respectively

$$\begin{aligned} \mathbf{H}_{\Gamma_S}^1(\Omega_S) &:= \left\{ \mathbf{v}_S \in \mathbf{H}^1(\Omega_S) : \quad \mathbf{v}_S = \mathbf{0} \quad \text{on } \Gamma_S \right\}, \\ \mathbf{H}_{\Gamma_D}^3(\text{div}; \Omega_D) &:= \left\{ \mathbf{v}_D \in \mathbf{H}^3(\text{div}; \Omega_D) : \quad \mathbf{v}_D \cdot \mathbf{n} = 0 \quad \text{on } \Gamma_D \right\}. \end{aligned}$$

Notice that  $\mathbf{H}^3(\text{div}; \Omega_D) = \mathbf{H}(\text{div}; \Omega_D) \cap \mathbf{L}^3(\Omega_D)$ , which guarantees that  $\mathbf{v}_D \cdot \mathbf{n}$  is well defined for  $\mathbf{v}_D \in \mathbf{H}_{\Gamma_D}^3(\text{div}; \Omega_D)$ .

To begin with the derivation of our variational formulation for the Navier–Stokes/Darcy–Forchheimer problem we first proceed similarly to [65, 92] and test the second equation of (3.1) by  $\mathbf{v}_S \in \mathbf{H}_{\Gamma_S}^1(\Omega_S)$ , integrate by parts and utilize the second equation of (3.4) to obtain

$$\begin{aligned} 2\mu(\mathbf{e}(\mathbf{u}_S), \mathbf{e}(\mathbf{v}_S))_S + \left\langle \frac{\alpha_d \mu}{\sqrt{\mathbf{t} \cdot \boldsymbol{\kappa} \mathbf{t}}} \mathbf{u}_S \cdot \mathbf{t}, \mathbf{v}_S \cdot \mathbf{t} \right\rangle_{\Sigma} + \rho((\nabla \mathbf{u}_S) \mathbf{u}_S, \mathbf{v}_S)_S \\ - (p_S, \text{div } \mathbf{v}_S)_S + \langle \mathbf{v}_S \cdot \mathbf{n}, \lambda \rangle_{\Sigma} = (\mathbf{f}, \mathbf{v}_S)_S, \end{aligned} \quad (3.6)$$

for all  $\mathbf{v}_S \in \mathbf{H}_{\Gamma_S}^1(\Omega_S)$ , where  $\lambda$  is a further unknown representing the trace of the porous medium pressure on  $\Sigma$ , that is  $\lambda = p_D|_{\Gamma}$ . The corresponding space of  $\lambda$  will be specified next. In turn, we incorporate the incompressibility condition  $\text{div } \mathbf{u}_S = 0$  in  $\Omega_S$  weakly as follows

$$(q_S, \text{div } \mathbf{u}_S)_S = 0 \quad \forall q_S \in L^2(\Omega_S). \quad (3.7)$$

Next, we multiply the first equation of (3.2) by  $\mathbf{v}_D \in \mathbf{H}_{\Gamma_D}^3(\text{div}; \Omega_D)$  and integrate by parts to obtain

$$\frac{\mu}{\rho}(\mathbf{K}^{-1} \mathbf{u}_D, \mathbf{v}_D)_D + \frac{F}{\rho}(|\mathbf{u}_D| \mathbf{u}_D, \mathbf{v}_D)_D - (p_D, \text{div } \mathbf{v}_D)_D - \langle \mathbf{v}_D \cdot \mathbf{n}, \lambda \rangle_{\Sigma} = (\mathbf{f}_D, \mathbf{v}_D)_D, \quad (3.8)$$

for all  $\mathbf{v}_D \in \mathbf{H}_{\Gamma_D}^3(\text{div}; \Omega_D)$ . Observe that if  $\mathbf{u}_D \in \mathbf{H}^3(\text{div}; \Omega_D)$  and  $p_D \in L^2(\Omega_D)$ , then  $|\mathbf{u}_D| \mathbf{u}_D \cdot \mathbf{v}_D \in L^1(\Omega_D)$  and  $p_D \text{div } \mathbf{v}_D \in L^1(\Omega_D)$ , and hence the second and third terms of (3.8) are well defined, which justifies the introduction of the spaces  $\mathbf{H}^3(\text{div}; \Omega_D)$  for the derivation of our weak formulation. On the other hand, we observe that for each  $\mathbf{v}_D \in \mathbf{H}^3(\text{div}; \Omega_D)$ , the normal trace  $\mathbf{v}_D \cdot \mathbf{n} : \mathbf{H}^3(\text{div}; \Omega_D) \rightarrow W^{-\frac{1}{3}, 3}(\partial \Omega_D)$  is well defined and continuous. In fact, since  $W^{1, \frac{3}{2}}(\Omega_D)$  is continuously embedded into  $L^2(\Omega_D)$  then for each  $\xi \in W^{\frac{1}{3}, \frac{3}{2}}(\partial \Omega_D)$  the quantity

$$\langle \mathbf{v}_D \cdot \mathbf{n}, \xi \rangle_{\partial \Omega_D} := \int_{\Omega_D} \mathbf{v}_D \cdot \nabla \tilde{\gamma}_0^{-1}(\xi) + \int_{\Omega_D} \tilde{\gamma}_0^{-1}(\xi) \text{div } \mathbf{v}_D,$$

is well defined, where  $\langle \cdot, \cdot \rangle_{\partial \Omega_D}$  stands for the duality pairing between  $W^{-\frac{1}{3}, 3}(\partial \Omega_D)$  and  $W^{\frac{1}{3}, \frac{3}{2}}(\partial \Omega_D)$ , and  $\tilde{\gamma}_0^{-1}$  is the right inverse of the well known trace operator  $\gamma_0 : W^{1, \frac{3}{2}}(\Omega_D) \rightarrow W^{\frac{1}{3}, \frac{3}{2}}(\partial \Omega_D)$ . Furthermore,

as will be explained next at the end of Section 3.3.1,  $\mathbf{v}_D \cdot \mathbf{n}|_\Sigma \in W^{-\frac{1}{3},3}(\Sigma)$ , which suggests to set  $W^{\frac{1}{3},\frac{3}{2}}(\Sigma)$  as the appropriate space for the unknown  $\lambda$ , that is

$$\lambda = p_D|_\Sigma \in W^{\frac{1}{3},\frac{3}{2}}(\Sigma).$$

Note that, in principle, the space for  $p_D$  does not allow enough regularity for the trace  $\lambda$  to exist. However, the solution of (3.2) has the pressure in  $W^{1,\frac{3}{2}}(\Omega_D) \cap L^2(\Omega_D)$ .

Finally, we impose the second equation of (3.2) and the first equation of (3.4) weakly as follows

$$(q_D, \operatorname{div} \mathbf{u}_D)_D = (g_D, q_D)_D \quad \forall q_D \in L^2(\Omega_D), \quad (3.9)$$

and

$$\langle \mathbf{u}_S \cdot \mathbf{n} - \mathbf{u}_D \cdot \mathbf{n}, \xi \rangle_\Sigma = 0 \quad \forall \xi \in W^{\frac{1}{3},\frac{3}{2}}(\Sigma). \quad (3.10)$$

As a consequence of the above, we write  $\Omega := \Omega_S \cup \Sigma \cup \Omega_D$ , and define  $p := p_S \chi_S + p_D \chi_D$ , with  $\chi_\star$  being the characteristic function:

$$\chi_\star := \begin{cases} 1 & \text{in } \Omega_\star, \\ 0 & \text{in } \Omega \setminus \overline{\Omega_\star}, \end{cases}$$

for  $\star \in \{S, D\}$ , to obtain the variational problem: Find  $\mathbf{u}_S \in \mathbf{H}_{\Gamma_S}^1(\Omega_S)$ ,  $p \in L^2(\Omega)$ ,  $\mathbf{u}_D \in \mathbf{H}_{\Gamma_D}^3(\operatorname{div}; \Omega_D)$  and  $\lambda \in W^{\frac{1}{3},\frac{3}{2}}(\Sigma)$  such that (3.6)–(3.10) hold.

Now, let us observe that if  $(\mathbf{u}_S, \mathbf{u}_D, p, \lambda)$  is a solution of the resulting variational problem, then for all  $c \in \mathbb{R}$ ,  $(\mathbf{u}_S, \mathbf{u}_D, p + c, \lambda + c)$  is also a solution. Then, we avoid the non-uniqueness of (3.6)–(3.10) by requiring from now on that  $p \in L_0^2(\Omega)$ , where

$$L_0^2(\Omega) := \left\{ q \in L^2(\Omega) : \int_\Omega q = 0 \right\}.$$

In this way, we group the spaces and unknowns as follows:

$$\begin{aligned} \mathbf{H} &:= \mathbf{H}_{\Gamma_S}^1(\Omega_S) \times \mathbf{H}_{\Gamma_D}^3(\operatorname{div}; \Omega_D), & \mathbf{Q} &:= L_0^2(\Omega) \times W^{\frac{1}{3},\frac{3}{2}}(\Sigma), \\ \mathbf{u} &:= (\mathbf{u}_S, \mathbf{u}_D) \in \mathbf{H}, & (p, \lambda) &\in \mathbf{Q}, \end{aligned}$$

and propose the mixed variational formulation: Find  $(\mathbf{u}, (p, \lambda)) \in \mathbf{H} \times \mathbf{Q}$ , such that

$$\begin{aligned} [\mathbf{a}(\mathbf{u}_S)(\mathbf{u}), \mathbf{v}] + [\mathbf{b}(\mathbf{v}), (p, \lambda)] &= [\mathbf{f}, \mathbf{v}] \quad \forall \mathbf{v} := (\mathbf{v}_S, \mathbf{v}_D) \in \mathbf{H}, \\ [\mathbf{b}(\mathbf{u}), (q, \xi)] &= [\mathbf{g}, (q, \xi)] \quad \forall (q, \xi) \in \mathbf{Q}, \end{aligned} \quad (3.11)$$

where, given  $\mathbf{w}_S \in \mathbf{H}_{\Gamma_S}^1(\Omega_S)$ , the operator  $\mathbf{a}(\mathbf{w}_S) : \mathbf{H} \rightarrow \mathbf{H}'$  is defined by

$$[\mathbf{a}(\mathbf{w}_S)(\mathbf{u}), \mathbf{v}] := [\mathcal{A}_S(\mathbf{u}_S), \mathbf{v}_S] + [\mathcal{B}_S(\mathbf{w}_S)(\mathbf{u}_S), \mathbf{v}_S] + [\mathcal{A}_D(\mathbf{u}_D), \mathbf{v}_D], \quad (3.12)$$

with

$$\begin{aligned} [\mathcal{A}_S(\mathbf{u}_S), \mathbf{v}_S] &:= 2\mu(\mathbf{e}(\mathbf{u}_S), \mathbf{e}(\mathbf{v}_S))_S + \left\langle \frac{\alpha_d \mu}{\sqrt{\mathbf{t} \cdot \boldsymbol{\kappa} \mathbf{t}}} \mathbf{u}_S \cdot \mathbf{t}, \mathbf{v}_S \cdot \mathbf{t} \right\rangle_\Sigma, \\ [\mathcal{B}_S(\mathbf{w}_S)(\mathbf{u}_S), \mathbf{v}_S] &:= \rho((\nabla \mathbf{u}_S) \mathbf{w}_S, \mathbf{v}_S)_S, \\ [\mathcal{A}_D(\mathbf{u}_D), \mathbf{v}_D] &:= \frac{\mu}{\rho} (\mathbf{K}^{-1} \mathbf{u}_D, \mathbf{v}_D)_D + \frac{F}{\rho} (|\mathbf{u}_D| \mathbf{u}_D, \mathbf{v}_D)_D, \end{aligned} \quad (3.13)$$

whereas the operator  $\mathbf{b} : \mathbf{H} \rightarrow \mathbf{Q}'$  is given by

$$[\mathbf{b}(\mathbf{v}), (q, \xi)] := -(\operatorname{div} \mathbf{v}_S, q)_S - (\operatorname{div} \mathbf{v}_D, q)_D + \langle \mathbf{v}_S \cdot \mathbf{n} - \mathbf{v}_D \cdot \mathbf{n}, \xi \rangle_\Sigma. \quad (3.14)$$

In turn, the functionals  $\mathbf{f}$  and  $\mathbf{g}$  are defined by

$$[\mathbf{f}, \mathbf{v}] := (\mathbf{f}_S, \mathbf{v}_S)_S + (\mathbf{f}_D, \mathbf{v}_D)_D \quad \text{and} \quad [\mathbf{g}, (q, \xi)] := -(g_D, q)_D. \quad (3.15)$$

In all the terms above,  $[\cdot, \cdot]$  denotes the duality pairing induced by the corresponding operators.

### 3.2.3 Stability properties

Let us now discuss the stability properties of the operators in (3.13) and (3.14). We begin by observing that the operators  $\mathcal{A}_S$ ,  $\mathcal{B}_S$  and  $\mathbf{b}$  are continuous:

$$\begin{aligned} |[\mathcal{A}_S(\mathbf{u}_S), \mathbf{v}_S]| &\leq C_{\mathcal{A}_S} \|\mathbf{u}_S\|_{1, \Omega_S} \|\mathbf{v}_S\|_{1, \Omega_S}, \\ |[\mathcal{B}_S(\mathbf{w}_S)(\mathbf{u}_S), \mathbf{v}_S]| &\leq \rho C_S^2 \|\mathbf{w}_S\|_{1, \Omega_S} \|\mathbf{u}_S\|_{1, \Omega_S} \|\mathbf{v}_S\|_{1, \Omega_S}, \\ |[\mathbf{b}(\mathbf{v}), (q, \xi)]| &\leq C_{\mathbf{b}} \|\mathbf{v}\|_{\mathbf{H}}(q, \xi) \|_{\mathbf{Q}}, \end{aligned} \quad (3.16)$$

where  $C_S$  is the continuity constant of the Sobolev embedding from  $H^1(\Omega_S)$  into  $L^4(\Omega_S)$ . In turn, from the definition of  $\mathcal{A}_D$  (cf. (3.13)), (3.3), and the triangle and Hölder inequalities, we obtain that there exists  $L_{\mathcal{A}_D} > 0$ , depending only on  $\mu, \rho, F, \mathbf{K}$ , and  $\Omega_D$ , such that

$$\begin{aligned} &\|\mathcal{A}_D(\mathbf{u}_D) - \mathcal{A}_D(\mathbf{v}_D)\|_{(\mathbf{H}^3(\operatorname{div}; \Omega_D))'} \\ &\leq L_{\mathcal{A}_D} \left\{ \|\mathbf{u}_D - \mathbf{v}_D\|_{\mathbf{H}^3(\operatorname{div}; \Omega_D)} + \|\mathbf{u}_D - \mathbf{v}_D\|_{\mathbf{H}^3(\operatorname{div}; \Omega_D)} \left( \|\mathbf{u}_D\|_{\mathbf{H}^3(\operatorname{div}; \Omega_D)} + \|\mathbf{v}_D\|_{\mathbf{H}^3(\operatorname{div}; \Omega_D)} \right) \right\}, \end{aligned} \quad (3.17)$$

for all  $\mathbf{u}_D, \mathbf{v}_D \in \mathbf{H}^3(\operatorname{div}; \Omega_D)$ . In addition, using the Cauchy–Schwarz and Young inequalities, it is not difficult to see that  $\mathbf{f}$  and  $\mathbf{g}$  are bounded, that is, there exist constants  $c_{\mathbf{f}}, c_{\mathbf{g}} > 0$ , such that

$$\|\mathbf{f}\|_{\mathbf{H}'} \leq c_{\mathbf{f}} \left\{ \|\mathbf{f}_S\|_{0, \Omega_S} + \|\mathbf{f}_D\|_{\mathbf{L}^{3/2}(\Omega_D)} \right\} \quad (3.18)$$

and

$$\|\mathbf{g}\|_{\mathbf{Q}'} \leq c_{\mathbf{g}} \|g_D\|_{0, \Omega_D}, \quad (3.19)$$

which confirm the announced smoothness of  $\mathbf{f}_D$ . On the other hand, from the well known Korn and Poincaré inequalities (see, e.g., [81]), we easily obtain that there exists a constant  $\alpha_S > 0$ , depending only on  $\Omega_S$ , such that

$$[\mathcal{A}_S(\mathbf{v}_S), \mathbf{v}_S] \geq 2\mu\alpha_S \|\mathbf{v}_S\|_{1, \Omega_S}^2 \quad \forall \mathbf{v}_S \in \mathbf{H}_{\Gamma_S}^1(\Omega_S). \quad (3.20)$$

In turn, integrating by parts and assuming that  $\operatorname{div} \mathbf{w}_S = 0$  in  $\Omega_S$ , similarly to [65, eq. (29)], we obtain

$$[\mathcal{B}_S(\mathbf{w}_S)(\mathbf{v}_S), \mathbf{v}_S] = \frac{\rho}{2} \int_{\Sigma} (\mathbf{w}_S \cdot \mathbf{n}) |\mathbf{v}_S|^2 \quad \forall \mathbf{w}_S, \mathbf{v}_S \in \mathbf{H}_{\Gamma_S}^1(\Omega_S). \quad (3.21)$$

Finally, from the definition of  $\mathcal{A}_D$  (cf. (3.13)) and the inequality (3.3), we deduce that for a fixed  $\mathbf{t}_D \in \mathbf{L}^3(\Omega_D)$ , there holds

$$\begin{aligned} &[\mathcal{A}_D(\mathbf{u}_D + \mathbf{t}_D) - \mathcal{A}_D(\mathbf{v}_D + \mathbf{t}_D), \mathbf{u}_D - \mathbf{v}_D] \\ &\geq \frac{\mu}{\rho} C_{\mathbf{K}} \|\mathbf{u}_D - \mathbf{v}_D\|_{0, \Omega_D}^2 + \frac{F}{\rho} (|\mathbf{u}_D + \mathbf{t}_D|(\mathbf{u}_D + \mathbf{t}_D) - |\mathbf{v}_D + \mathbf{t}_D|(\mathbf{v}_D + \mathbf{t}_D), \mathbf{u}_D - \mathbf{v}_D)_D, \end{aligned} \quad (3.22)$$

for all  $\mathbf{u}_D, \mathbf{v}_D \in \mathbf{L}^3(\Omega_D)$ . Then, thanks to [103, Lemma 5.1], there exist  $C_D > 0$ , depending only on  $\Omega_D$ , such that

$$(|\mathbf{u}_D + \mathbf{t}_D|(\mathbf{u}_D + \mathbf{t}_D) - |\mathbf{v}_D + \mathbf{t}_D|(\mathbf{v}_D + \mathbf{t}_D), \mathbf{u}_D - \mathbf{v}_D)_D \geq C_D \|\mathbf{u}_D - \mathbf{v}_D\|_{\mathbf{L}^3(\Omega_D)}^3,$$

which, together with (3.22), and neglecting the first term on the right hand side of (3.22), yields

$$[\mathcal{A}_D(\mathbf{u}_D + \mathbf{t}_D) - \mathcal{A}_D(\mathbf{v}_D + \mathbf{t}_D), \mathbf{u}_D - \mathbf{v}_D] \geq \alpha_D \|\mathbf{u}_D - \mathbf{v}_D\|_{\mathbf{L}^3(\Omega_D)}^3 \quad \forall \mathbf{u}_D, \mathbf{v}_D \in \mathbf{L}^3(\Omega_D), \quad (3.23)$$

with  $\alpha_D = \frac{FC_D}{\rho}$ .

### 3.3 Analysis of the continuous formulation

In this section we analyse the well-posedness of problem (3.11) by means of a fixed-point argument and classical results on nonlinear monotone operators. To that end we first collect some preliminaries results and notations that will serve for the forthcoming analysis.

#### 3.3.1 Preliminaries

First we introduce some definitions that will be utilized next. To this end we let  $X$  and  $Y$  be reflexive Banach spaces. Then, we say that a nonlinear operator  $T : X \rightarrow Y$  is bounded if  $T(S)$  is bounded for each bounded set  $S \subseteq X$ . In addition, we say that a nonlinear operator  $T : X \rightarrow X'$  is of *type M* if  $u_n \rightharpoonup u$ ,  $Tu_n \rightharpoonup f$  and  $\limsup [Tu_n, u_n] \leq f(u)$  imply  $Tu = f$ . In turn, we say that  $T$  is coercive if

$$\frac{[Tu, u]}{\|u\|} \rightarrow \infty \quad \text{as} \quad \|u\| \rightarrow \infty.$$

Now, we establish the following abstract result taken from [144, Proposition 2.3], which has been adapted to our context where the nonlinear operator is defined on a product space  $X = X_1 \times X_2$ , with  $X_1$  and  $X_2$  depending on parameters  $p_1$  and  $p_2$ , respectively, in place of an space  $X$  depending on a parameter  $p$ .

**Theorem 3.1.** *Let  $X_1, X_2$  and  $Y$  be separable and reflexive Banach spaces, being  $X_1$  and  $X_2$  uniformly convex, set  $X = X_1 \times X_2$ , and let  $X'_1, X'_2, Y'$ , and  $X' := X'_1 \times X'_2$ , be their respective duals. Let  $a : X \rightarrow X'$  be a nonlinear operator and  $b : X \rightarrow Y'$  be a linear bounded operator. In turn, we denote by  $V$  the kernel of  $b$ , that is,*

$$V := \left\{ v \in X : [b(v), q] = 0 \quad \forall q \in Y' \right\}.$$

*Assume that*

- (i)  *$a$  is hemi-continuous, that is, for each  $u, v \in X$ , the real mapping*

$$J : \mathbb{R} \rightarrow \mathbb{R}, \quad t \rightarrow J(t) = [a(u + tv), v]$$

*is continuous.*

(ii) there exist constants  $\gamma > 0$  and  $p_1, p_2 \geq 2$ , such that

$$\|a(u) - a(v)\|_{X'} \leq \gamma \sum_{j=1}^2 \left\{ \|u_j - v_j\|_{X_j} + \|u_j - v_j\|_{X_j} \left( \|u_j\|_{X_j} + \|v_j\|_{X_j} \right)^{p_j-2} \right\},$$

for all  $u = (u_1, u_2), v = (v_1, v_2) \in X$ .

(iii) for fixed  $t \in X \setminus V$ , the operator  $a(\cdot + t) : V \rightarrow V'$  is strictly monotone in the following sense: there exist  $\alpha > 0$  and  $p_1, p_2 \geq 2$ , such that

$$[a(u + t) - a(v + t), u - v] \geq \alpha \left\{ \|u_1 - v_1\|_{X_1}^{p_1} + \|u_2 - v_2\|_{X_2}^{p_2} \right\},$$

for all  $u = (u_1, u_2), v = (v_1, v_2) \in V$ .

(iv) there exists  $\beta > 0$  such that

$$\sup_{\substack{v \in X \\ v \neq 0}} \frac{[b(v), q]}{\|v\|_X} \geq \beta \|q\|_{Y'} \quad \forall q \in Y'.$$

Then, for each  $(f, g) \in X' \times Y'$  there exists a unique  $(u, p) \in X \times Y$  such that

$$\begin{aligned} [a(u), v] + [b(v), p] &= [f, v] \quad \forall v \in X, \\ [b(u), q] &= [g, q] \quad \forall q \in Y'. \end{aligned} \tag{3.24}$$

Moreover, there exists  $C > 0$ , depending only on  $\alpha, \gamma, \beta, p_1$ , and  $p_2$ , such that

$$\|(u, p)\|_{X \times Y} \leq C \mathcal{M}(f, g), \tag{3.25}$$

where

$$\mathcal{M}(f, g) := \max \left\{ \mathcal{N}(f, g)^{\frac{1}{p_1-1}}, \mathcal{N}(f, g)^{\frac{1}{p_2-1}}, \mathcal{N}(f, g), \mathcal{N}(f, g)^{\frac{p_1-1}{p_2-1}}, \mathcal{N}(f, g)^{\frac{p_2-1}{p_1-1}} \right\},$$

and

$$\mathcal{N}(f, g) := \|f\|_{X'} + \|g\|_{Y'} + \|g\|_{Y'}^{p_1-1} + \|g\|_{Y'}^{p_2-1} + \|a(0)\|_{X'}.$$

*Proof.* We begin by noting that hypothesis (iv) establishes, equivalently, that  $b$  is surjective. Then, given  $g \in Y'$  there exists a unique  $u_g \in X \setminus V$  such that (see [125, Lemma A.1] for details):

$$b(u_g) = g \quad \text{and} \quad \|u_g\|_X \leq \frac{1}{\beta} \|g\|_{Y'}. \tag{3.26}$$

Then, given this  $u_g$  in  $X \setminus V$  satisfying (3.26), we observe that problem (3.24) with  $v \in V$  leads to: find  $\tilde{u} \in V$ , such that

$$[a_g(\tilde{u}), v] := [a(\tilde{u} + u_g), v] = [f, v] \quad \forall v \in V, \tag{3.27}$$

which suggests to define later on  $u$  as  $\tilde{u} + u_g$ . In this way, since  $f - a(u) \in {}^\circ V$  and hypothesis (iv) also guarantees that the adjoint operator  $b'$  is an isomorphism from  $Y$  into  ${}^\circ V$ , we deduce that there exists a unique  $p \in Y$  such that  $b'(p) = f - a(u)$  and

$$\|p\|_Y \leq \frac{1}{\beta} \|b'(p)\|_X \leq \frac{1}{\beta} \left\{ \|f\|_{X'} + \|a(u)\|_{X'} \right\}. \tag{3.28}$$

Therefore to prove that problem (3.24) is well posed, in what follows we prove equivalently that  $a_g(\cdot) = a(\cdot + u_g)$  is bijective on  $V$ . We begin by observing that the injectivity of the operator  $a_g(\cdot)$  follows straightforwardly from hypothesis (iii). In addition, from hypotheses (i) and (iii) and [145, Chapter II, Lemma 2.1] it can be readily seen that  $a_g(\cdot)$  is an operator of *type M*. Now, given  $v = (v_1, v_2) \in V$ , and denoting by  $u_j^g$ ,  $j = 1, 2$ , the components of  $u_g$ , we observe that, owing to (ii), (iii) and using the inequality  $(a + b)^q \leq C(q)(a^q + b^q)$ , with  $C(q)$  depending only on  $q$ , which is valid for all  $q \in [0, +\infty)$  and  $a, b \geq 0$  [6, Lemma 2.2], there hold

$$\begin{aligned} \|a_g(v)\|_{X'} &\leq \|a_g(v) - a_g(0)\|_{X'} + \|a_g(0)\|_{X'} = \|a(v + u_g) - a(u_g)\|_{X'} + \|a(u_g)\|_{X'} \\ &\leq \gamma \sum_{j=1}^2 \left\{ \|v_j\|_{X_j} + \|v_j\|_{X_j} \left( \|v_j + u_j^g\|_{X_j} + \|u_j^g\|_{X_j} \right)^{p_j-2} \right\} + \|a(u_g)\|_{X'} \\ &\leq C \sum_{j=1}^2 \left\{ \|v_j\|_{X_j} + \|v_j\|_{X_j}^{p_j-1} + \|v_j\|_{X_j} \|u_j^g\|_{X_j}^{p_j-2} \right\} + \|a(u_g)\|_{X'} \\ &\leq C \left( 1 + \|v_1\|_{X_1}^{p_1-2} + \|v_2\|_{X_2}^{p_2-2} + \|u_1^g\|_{X_1}^{p_1-2} + \|u_2^g\|_{X_2}^{p_2-2} \right) \|v\|_X + \|a(u_g)\|_{X'}, \end{aligned}$$

and

$$\begin{aligned} \frac{[a_g(v), v]}{\|v\|_X} &= \frac{[a(v + u_g) - a(0 + u_g), v]}{\|v\|_X} + \frac{[a(u_g), v]}{\|v\|_X} \geq \alpha \frac{\left\{ \|v_1\|_{X_1}^{p_1} + \|v_2\|_{X_2}^{p_2} \right\}}{\|v\|_X} - \|a(u_g)\|_{X'} \\ &\geq C \min \left\{ \|v\|_X^{p_1-1}, \|v\|_X^{p_2-1} \right\} - \|a(u_g)\|_{X'}, \end{aligned}$$

which clearly show that  $a_g$  is bounded and coercive on  $V$ , respectively. In this way, by applying [145, Chapter II, Corollary 2.2] it can be readily seen that  $a_g$  is surjective on  $V$ . Having verified the bijectivity of  $a_g$  on  $V$  we deduce that problem (3.27) is well-posed, or equivalently (3.24) admits a unique solution  $(u, p) = (\tilde{u} + u_g, p) \in X \times Y$ . Now, in order to obtain (3.25), we proceed similarly to [144, Proposition 2.3]. In fact, taking  $v = \tilde{u} \in V$  in (3.27), we have

$$[a(\tilde{u} + u_g) - a(0 + u_g), \tilde{u}] = [f, \tilde{u}] - [a(u_g), \tilde{u}].$$

Then, combining hypothesis (ii) – (iii) and (3.26), it is clear that

$$\begin{aligned} \alpha \left\{ \|\tilde{u}_1\|_{X_1}^{p_1} + \|\tilde{u}_2\|_{X_2}^{p_2} \right\} &\leq \left\{ \|f\|_{X'} + \|a(u_g)\|_{X'} \right\} \|\tilde{u}\|_X \\ &\leq c_1 \left\{ \|f\|_{X'} + \|g\|_{Y'} + \|g\|_{Y'}^{p_1-1} + \|g\|_{Y'}^{p_2-1} + \|a(0)\|_{X'} \right\} \|\tilde{u}\|_X, \end{aligned}$$

with  $c_1 > 0$  depending only on  $\gamma, \beta, p_1$ , and  $p_2$ , which yields

$$\|\tilde{u}\|_X \leq 2 \max \left\{ \left( \frac{2c_1}{\alpha} \mathcal{N}(f, g) \right)^{\frac{1}{p_1-1}}, \left( \frac{2c_1}{\alpha} \mathcal{N}(f, g) \right)^{\frac{1}{p_2-1}} \right\}, \quad (3.29)$$

where  $\mathcal{N}(f, g) := \|f\|_{X'} + \|g\|_{Y'} + \|g\|_{Y'}^{p_1-1} + \|g\|_{Y'}^{p_2-1} + \|a(0)\|_{X'}$ . In this way, due to  $u = \tilde{u} + u_g$ , combining (3.26) and (3.29), we conclude that

$$\|u\|_X \leq \|\tilde{u}\|_X + \|u_g\|_X \leq c_2 \max \left\{ \mathcal{N}(f, g)^{\frac{1}{p_1-1}}, \mathcal{N}(f, g)^{\frac{1}{p_2-1}} \right\}, \quad (3.30)$$

with  $c_2 > 0$  depending only on  $\alpha, \gamma, \beta, p_1$ , and  $p_2$ . On the other hand, from (3.28) and using again (ii), we deduce that

$$\|p\|_Y \leq c_3 \left\{ \|f\|_{X'} + \|u\|_X + \|u_1\|_{X_1}^{p_1-1} + \|u_2\|_{X_2}^{p_2-1} + \|a(0)\|_{X'} \right\}, \quad (3.31)$$

with  $c_3 > 0$  depending only on  $\gamma$  and  $\beta$ . Then, (3.30) and (3.31) conclude the proof.  $\square$

We remark that when  $p_1 = p_2 = 2$  and  $\|a(0)\|_{X'}$  is equal to zero, the previous analysis leads to the classical estimate

$$\|(u, p)\|_{X \times Y} \leq C \left\{ \|f\|_{X'} + \|g\|_{Y'} \right\},$$

with  $C > 0$ , depending only on  $\alpha, \gamma$ , and  $\beta$ .

Now, we follow [70, Appendix A] (see also [96, 65]) to recall some preliminary results concerning boundary conditions and extension operators. We start by recalling that, given  $\mathbf{v}_D \in \mathbf{H}_{\Gamma_D}^3(\text{div}; \Omega_D)$ , the boundary condition  $\mathbf{v}_D \cdot \mathbf{n} = 0$  on  $\Gamma_D$  means

$$\langle \mathbf{v}_D \cdot \mathbf{n}, E_{0,D}(\xi) \rangle_{\partial\Omega_D} = 0 \quad \forall \xi \in W^{\frac{1}{3}, \frac{3}{2}}(\Gamma_D),$$

where  $E_{0,D} : W^{\frac{1}{3}, \frac{3}{2}}(\Gamma_D) \rightarrow W^{\frac{1}{3}, \frac{3}{2}}(\partial\Omega_D)$  is the extension operator defined by

$$E_{0,D}(\xi) := \begin{cases} \xi & \text{on } \Gamma_D \\ 0 & \text{on } \Sigma \end{cases} \quad \forall \xi \in W^{\frac{1}{3}, \frac{3}{2}}(\Gamma_D),$$

We observe that according to [105, Theorem 1.5.2.3], the operator  $E_{0,D}$  is well defined. In turn, similarly to [70, eq. (A.6)] we can identify the restriction of  $\mathbf{v}_D \cdot \mathbf{n}$  to  $\Sigma$  with an element of  $W^{-\frac{1}{3}, 3}(\Sigma)$ , namely

$$\langle \mathbf{v}_D \cdot \mathbf{n}, \xi \rangle_{\Sigma} := \langle \mathbf{v}_D \cdot \mathbf{n}, E_{\Sigma}(\xi) \rangle_{\partial\Omega_D} \quad \forall \xi \in W^{\frac{1}{3}, \frac{3}{2}}(\Sigma), \quad (3.32)$$

where  $E_{\Sigma} : W^{\frac{1}{3}, \frac{3}{2}}(\Sigma) \rightarrow W^{\frac{1}{3}, \frac{3}{2}}(\partial\Omega_D)$  is any bounded extension operator. In addition, analogously to the proof of [70, Lemma A.2] one can show that for all  $\psi \in W^{\frac{1}{3}, \frac{3}{2}}(\partial\Omega_D)$ , there exist unique elements  $\psi_{\Sigma} \in W^{\frac{1}{3}, \frac{3}{2}}(\Sigma)$  and  $\psi_{\Gamma_D} \in W^{\frac{1}{3}, \frac{3}{2}}(\Gamma_D)$  such that

$$\psi = E_{\Sigma}(\psi_{\Sigma}) + E_{0,D}(\psi_{\Gamma_D}), \quad (3.33)$$

and there exist  $C_1, C_2 > 0$ , such that

$$C_1 \left\{ \|\psi_{\Sigma}\|_{\frac{1}{3}, \frac{3}{2}; \Sigma} + \|\psi_{\Gamma_D}\|_{\frac{1}{3}, \frac{3}{2}; \Gamma_D} \right\} \leq \|\psi\|_{\frac{1}{3}, \frac{3}{2}; \partial\Omega_D} \leq C_2 \left\{ \|\psi_{\Sigma}\|_{\frac{1}{3}, \frac{3}{2}; \Sigma} + \|\psi_{\Gamma_D}\|_{\frac{1}{3}, \frac{3}{2}; \Gamma_D} \right\}. \quad (3.34)$$

In fact, although [70, Lemma A.2] is derived for  $W^{1-\frac{1}{p}, p}(\partial\Omega_D)$  with  $p \geq 2$ , using a slight modification of [103, Section 2] one can easily extend the analysis to the case  $p > 1$ . Finally, we observe that, since  $H^{1/2}(\partial\Omega_S)$  is continuously embedded into  $L^p(\partial\Omega_S)$  with  $p > 1$ , and the trace operator is continuous, the following inequality holds:

$$\|\mathbf{v}_S\|_{\mathbf{L}^p(\Sigma)} \leq \|\mathbf{v}_S\|_{\mathbf{L}^p(\partial\Omega_S)} \leq C_s \|\mathbf{v}_S\|_{1/2, \partial\Omega_S} \leq C_s C_{\text{tr}} \|\mathbf{v}_S\|_{1, \Omega_S} \quad \forall \mathbf{v}_S \in \mathbf{H}_{\Gamma_S}^1(\Omega_S), \quad (3.35)$$

where  $C_s$  is the continuity constant of the Sobolev embedding from  $H^{1/2}(\partial\Omega_S)$  into  $L^p(\partial\Omega_S)$ , and  $C_{\text{tr}}$  is the norm of the usual trace operator from  $H^1(\Omega_S)$  into  $H^{1/2}(\partial\Omega_S)$ .



### 3.3.2 A fixed-point approach

We begin the solvability analysis of (3.11) by defining the operator  $\mathbf{T} : \mathbf{H}_{\Gamma_S}^1(\Omega_S) \rightarrow \mathbf{H}_{\Gamma_S}^1(\Omega_S)$  by

$$\mathbf{T}(\mathbf{w}_S) := \mathbf{u}_S \quad \forall \mathbf{w}_S \in \mathbf{H}_{\Gamma_S}^1(\Omega_S), \quad (3.36)$$

where  $\mathbf{u} := (\mathbf{u}_S, \mathbf{u}_D) \in \mathbf{H}$  is the first component of the unique solution (to be confirmed below) of the nonlinear problem: Find  $(\mathbf{u}, (p, \lambda)) \in \mathbf{H} \times \mathbf{Q}$ , such that

$$\begin{aligned} [\mathbf{a}(\mathbf{w}_S)(\mathbf{u}), \mathbf{v}] + [\mathbf{b}(\mathbf{v}), (p, \lambda)] &= [\mathbf{f}, \mathbf{v}] \quad \forall \mathbf{v} \in \mathbf{H}, \\ [\mathbf{b}(\mathbf{u}), (q, \xi)] &= [\mathbf{g}, (q, \xi)] \quad \forall (q, \xi) \in \mathbf{Q}. \end{aligned} \quad (3.37)$$

Hence, it is not difficult to see that  $(\mathbf{u}, (p, \lambda)) \in \mathbf{H} \times \mathbf{Q}$  is a solution of (3.11) if and only if  $\mathbf{u}_S \in \mathbf{H}_{\Gamma_S}^1(\Omega_S)$  satisfies:  $\mathbf{u}_S \in \mathbf{H}_{\Gamma_S}^1(\Omega_S)$  and  $\mathbf{T}(\mathbf{u}_S) = \mathbf{u}_S$ . In this way, in what follows we focus on proving that  $\mathbf{T}$  possesses a unique fixed-point. However, we remark in advance that the definition of  $\mathbf{T}$  will make sense only in a closed ball of  $\mathbf{H}_{\Gamma_S}^1(\Omega_S)$ . Before continuing with the solvability analysis of (3.11), we first provide the hypotheses under which operator  $\mathbf{T}$  is well defined.

### 3.3.3 Well-definiteness of $\mathbf{T}$

Given  $\mathbf{w}_S \in \mathbf{H}_{\Gamma_S}^1(\Omega_S)$ , it is clear that problem (3.37) has the same structure of the one in Theorem 3.1. Therefore, in what follows we apply this result to establish the well-posedness of (3.37), or equivalently, the well-definiteness of  $\mathbf{T}$ . We begin by observing that, thanks to the uniform convexity and separability of  $L^p(\Omega)$  for  $p \in (1, +\infty)$ , each space defining  $\mathbf{H}$  and  $\mathbf{Q}$  shares the same properties, which implies that  $\mathbf{H}$  and  $\mathbf{Q}$  are uniformly convex and separable as well.

We continue with the required continuity property of  $\mathbf{a}(\mathbf{w}_S)$  for each  $\mathbf{w}_S \in \mathbf{H}_{\Gamma_S}^1(\Omega_S)$ .

**Lemma 3.2.** *Given  $\mathbf{w}_S \in \mathbf{H}_{\Gamma_S}^1(\Omega_S)$ , the operator  $\mathbf{a}(\mathbf{w}_S)$  is hemi-continuous in  $\mathbf{H}$ .*

*Proof.* For fixed  $\mathbf{w}_S \in \mathbf{H}_{\Gamma_S}^1(\Omega_S)$ ,  $\mathbf{u} = (\mathbf{u}_S, \mathbf{u}_D)$ , and  $\mathbf{v} = (\mathbf{v}_S, \mathbf{v}_D) \in \mathbf{H}$ , we introduce the real function  $\mathcal{J} : \mathbb{R} \rightarrow \mathbb{R}$  defined by

$$\begin{aligned} \mathcal{J}(t) &:= [\mathbf{a}(\mathbf{w}_S)(\mathbf{u} + t\mathbf{v}), \mathbf{v}] = [\mathcal{A}_S(\mathbf{u}_S + t\mathbf{v}_S), \mathbf{v}_S] \\ &\quad + [\mathcal{B}_S(\mathbf{w}_S)(\mathbf{u}_S + t\mathbf{v}_S), \mathbf{v}_S] + [\mathcal{A}_D(\mathbf{u}_D + t\mathbf{v}_D), \mathbf{v}_D]. \end{aligned}$$

Then, the hemi-continuity of  $\mathbf{a}(\mathbf{w}_S)$ , that is the continuity of  $\mathcal{J}$ , follows straightforwardly from the linearity and continuity of  $\mathcal{A}_S$  and  $\mathcal{B}_S(\mathbf{w}_S)$  and from [102, Proposition 3]. We omit further details.  $\square$

We continue our analysis with the verification of hypothesis (ii) of Theorem 3.1.

**Lemma 3.3.** *Let  $\mathbf{w}_S \in \mathbf{H}_{\Gamma_S}^1(\Omega_S)$ . Then, there exists  $\gamma > 0$ , depending on  $C_{\mathcal{A}_S}$  and  $L_{\mathcal{A}_D}$  (cf. (3.16), (3.17)), such that*

$$\begin{aligned} \|\mathbf{a}(\mathbf{w}_S)(\mathbf{u}) - \mathbf{a}(\mathbf{w}_S)(\mathbf{v})\|_{\mathbf{H}'} &\leq \gamma \left\{ (1 + \|\mathbf{w}_S\|_{1, \Omega_S}) \|\mathbf{u}_S - \mathbf{v}_S\|_{1, \Omega_S} + \|\mathbf{u}_D - \mathbf{v}_D\|_{\mathbf{H}^3(\text{div}; \Omega_D)} \right. \\ &\quad \left. + \|\mathbf{u}_D - \mathbf{v}_D\|_{\mathbf{H}^3(\text{div}; \Omega_D)} \left( \|\mathbf{u}_D\|_{\mathbf{H}^3(\text{div}; \Omega_D)} + \|\mathbf{v}_D\|_{\mathbf{H}^3(\text{div}; \Omega_D)} \right) \right\}, \end{aligned}$$

for all  $\mathbf{u} = (\mathbf{u}_S, \mathbf{u}_D), \mathbf{v} = (\mathbf{v}_S, \mathbf{v}_D) \in \mathbf{H}$ .

*Proof.* The result follows straightforwardly from the definition of  $\mathbf{a}(\mathbf{w}_S)$  (cf. (3.12)), the triangle inequality, and the stability properties (3.16) and (3.17). We omit further details.  $\square$

Now, let us look at the kernel of the operator  $\mathbf{b}$ , that is

$$\mathbf{V} := \left\{ \mathbf{v} \in \mathbf{H} : [\mathbf{b}(\mathbf{v}), (q, \xi)] = 0 \quad \forall (q, \xi) \in \mathbf{Q} \right\}. \quad (3.38)$$

According to the definition of  $\mathbf{b}$  (cf. (3.14)), we observe that  $\mathbf{v} = (\mathbf{v}_S, \mathbf{v}_D) \in \mathbf{V}$  if and only if

$$(\operatorname{div} \mathbf{v}_S, q)_S + (\operatorname{div} \mathbf{v}_D, q)_D = 0 \quad \forall q \in L_0^2(\Omega)$$

and

$$\langle \mathbf{v}_S \cdot \mathbf{n} - \mathbf{v}_D \cdot \mathbf{n}, \xi \rangle_\Sigma = 0 \quad \forall \xi \in W^{\frac{1}{3}, \frac{3}{2}}(\Sigma).$$

In this way, noting that  $L^2(\Omega) = L_0^2(\Omega) \oplus \mathbb{R}$ , and taking  $\xi \in \mathbb{R}$  in the latter equation, we deduce that

$$(\operatorname{div} \mathbf{v}_S, q)_S + (\operatorname{div} \mathbf{v}_D, q)_D = 0 \quad \forall q \in L^2(\Omega),$$

which implies

$$\operatorname{div} \mathbf{v}_S = 0 \quad \text{in } \Omega_S \quad \text{and} \quad \operatorname{div} \mathbf{v}_D = 0 \quad \text{in } \Omega_D. \quad (3.39)$$

In the following result we provide the assumptions under which operator  $\mathbf{a}(\mathbf{w}_S)$  satisfies hypothesis (iii) of Theorem 3.1.

**Lemma 3.4.** *Let  $\mathbf{w}_S \in \mathbf{H}_{\Gamma_S}^1(\Omega_S)$  such that  $\operatorname{div} \mathbf{w}_S = 0$  in  $\Omega_S$  and*

$$\|\mathbf{w}_S \cdot \mathbf{n}\|_{0, \Sigma} \leq \frac{2\mu\alpha_S}{\rho C_{\operatorname{tr}}^2 C_S^2}. \quad (3.40)$$

*Then, for each  $\mathbf{t} \in \mathbf{H} \setminus \mathbf{V}$ , the nonlinear operator  $\mathbf{a}(\mathbf{w}_S)(\cdot + \mathbf{t})$  is strictly monotone on  $\mathbf{V}$  (cf. (3.38)).*

*Proof.* Let  $\mathbf{t} := (\mathbf{t}_S, \mathbf{t}_D) \in \mathbf{H} \setminus \mathbf{V}$  fixed, and let  $\mathbf{w}_S \in \mathbf{H}_{\Gamma_S}^1(\Omega_S)$  as indicated. Then, according to (3.12), the linearity of  $\mathcal{A}_S$  and  $\mathcal{B}_S(\mathbf{w}_S)$ , the identity (3.39) and the stabilities properties (3.20) and (3.23), we find that

$$\begin{aligned} [\mathbf{a}(\mathbf{w}_S)(\mathbf{u} + \mathbf{t}) - \mathbf{a}(\mathbf{w}_S)(\mathbf{v} + \mathbf{t}), \mathbf{u} - \mathbf{v}] &\geq 2\mu\alpha_S \|\mathbf{u}_S - \mathbf{v}_S\|_{1, \Omega_S}^2 \\ &+ \alpha_D \|\mathbf{u}_D - \mathbf{v}_D\|_{\mathbf{H}^3(\operatorname{div}; \Omega_D)}^3 + [\mathcal{B}_S(\mathbf{w}_S)(\mathbf{u}_S - \mathbf{v}_S), \mathbf{u}_S - \mathbf{v}_S], \end{aligned}$$

for all  $\mathbf{u}, \mathbf{v} \in \mathbf{V}$ . In addition, similarly to [65, Lemma 2], we deduce from (3.21), applying Cauchy–Schwarz’s inequality and (3.35) with  $p = 4$ , that

$$\left| [\mathcal{B}_S(\mathbf{w}_S)(\mathbf{u}_S - \mathbf{v}_S), \mathbf{u}_S - \mathbf{v}_S] \right| \leq \frac{\rho C_{\operatorname{tr}}^2 C_S^2}{2} \|\mathbf{w}_S \cdot \mathbf{n}\|_{0, \Sigma} \|\mathbf{u}_S - \mathbf{v}_S\|_{1, \Omega_S}^2,$$

which implies

$$\begin{aligned} &[\mathbf{a}(\mathbf{w}_S)(\mathbf{u} + \mathbf{t}) - \mathbf{a}(\mathbf{w}_S)(\mathbf{v} + \mathbf{t}), \mathbf{u} - \mathbf{v}] \\ &\geq \left\{ 2\mu\alpha_S - \frac{\rho C_{\operatorname{tr}}^2 C_S^2}{2} \|\mathbf{w}_S \cdot \mathbf{n}\|_{0, \Sigma} \right\} \|\mathbf{u}_S - \mathbf{v}_S\|_{1, \Omega_S}^2 + \alpha_D \|\mathbf{u}_D - \mathbf{v}_D\|_{\mathbf{H}^3(\operatorname{div}; \Omega_D)}^3. \end{aligned}$$

Consequently, the hypothesis (3.40) and the foregoing inequality imply

$$[\mathbf{a}(\mathbf{w}_S)(\mathbf{u} + \mathbf{t}) - \mathbf{a}(\mathbf{w}_S)(\mathbf{v} + \mathbf{t}), \mathbf{u} - \mathbf{v}] \geq \alpha(\Omega) \left\{ \|\mathbf{u}_S - \mathbf{v}_S\|_{1, \Omega_S}^2 + \|\mathbf{u}_D - \mathbf{v}_D\|_{\mathbf{H}^3(\operatorname{div}; \Omega_D)}^3 \right\},$$

for all  $\mathbf{u}, \mathbf{v} \in \mathbf{V}$ , with  $\alpha(\Omega) := \min \{ \mu\alpha_S, \alpha_D \}$  independent of  $\mathbf{w}_S$ .  $\square$

We remark that, similarly to the strict monotonicity of  $\mathbf{a}(\mathbf{w}_S)(\cdot + \mathbf{t})$  on  $\mathbf{V}$  with  $\mathbf{t} \in \mathbf{H} \setminus \mathbf{V}$  fixed, using (3.23) with  $\mathbf{t}_D = \mathbf{0} \in \mathbf{L}^3(\Omega_D)$ , we deduce that

$$[\mathbf{a}(\mathbf{w}_S)(\mathbf{u}) - \mathbf{a}(\mathbf{w}_S)(\mathbf{v}), \mathbf{u} - \mathbf{v}] \geq \alpha(\Omega) \left\{ \|\mathbf{u}_S - \mathbf{v}_S\|_{1,\Omega_S}^2 + \|\mathbf{u}_D - \mathbf{v}_D\|_{\mathbf{H}^3(\text{div}; \Omega_D)}^3 \right\}, \quad (3.41)$$

for all  $\mathbf{u}, \mathbf{v} \in \mathbf{H}$  with  $\text{div}(\mathbf{u}_D - \mathbf{v}_D) = 0$  in  $\Omega_D$ .

We end the verification of the hypotheses of Theorem 3.1 by proving the continuous inf-sup condition for  $\mathbf{b}$ . To that end, we adapt the proof of [92, Lemma 2.1] to the present case, using similar results from [96, Lemma 3.3] and [65, Lemma 1] to handle the mixed boundary conditions on  $\partial\Omega_D$ .

**Lemma 3.5.** *There exists  $\beta > 0$  such that*

$$S(q, \xi) := \sup_{\substack{\mathbf{v} \in \mathbf{H} \\ \mathbf{v} \neq \mathbf{0}}} \frac{[\mathbf{b}(\mathbf{v}), (q, \xi)]}{\|\mathbf{v}\|_{\mathbf{H}}} \geq \beta \|(q, \xi)\|_{\mathbf{Q}} \quad \forall (q, \xi) \in \mathbf{Q}. \quad (3.42)$$

*Proof.* Let  $(q, \xi) \in \mathbf{Q}$ . Since  $q \in L_0^2(\Omega)$ , it is well known (see, e.g., [100, Corollary 2.4]) that there exists  $\mathbf{z} \in \mathbf{H}_0^1(\Omega)$  such that  $\text{div} \mathbf{z} = -q$  in  $\Omega$  and  $\|\mathbf{z}\|_{1,\Omega} \leq c\|q\|_{0,\Omega}$ . Setting  $\widehat{\mathbf{v}} := (\widehat{\mathbf{v}}_S, \widehat{\mathbf{v}}_D)$  with  $\widehat{\mathbf{v}}_\star = \mathbf{z}|_{\Omega_\star}$  for  $\star \in \{S, D\}$ , we find that  $\widehat{\mathbf{v}}_S \cdot \mathbf{n} = \widehat{\mathbf{v}}_D \cdot \mathbf{n}$  on  $\Sigma$ , and using the continuous embedding from  $H^1(\Omega_D)$  into  $L^3(\Omega_D)$ , we obtain  $\|\widehat{\mathbf{v}}\|_{\mathbf{H}} \leq \widehat{c}\|\mathbf{z}\|_{1,\Omega} \leq \widehat{c}\|q\|_{0,\Omega}$ , whence

$$S(q, \xi) \geq \frac{[\mathbf{b}(\widehat{\mathbf{v}}), (q, \xi)]}{\|\widehat{\mathbf{v}}\|_{\mathbf{H}}} = \frac{\|q\|_{0,\Omega}^2}{\|\widehat{\mathbf{v}}\|_{\mathbf{H}}} \geq c_1\|q\|_{0,\Omega}. \quad (3.43)$$

On the other hand, given  $\phi \in W^{-\frac{1}{3},3}(\Sigma)$ , we define  $\eta \in W^{-\frac{1}{3},3}(\partial\Omega_D)$  as

$$\langle \eta, \mu \rangle_{\partial\Omega_D} := \langle \phi, \mu \rangle_{\Sigma} \quad \forall \mu \in W^{\frac{1}{3},\frac{3}{2}}(\partial\Omega_D),$$

where  $\mu_\Sigma \in W^{\frac{1}{3},\frac{3}{2}}(\Sigma)$  is given by the decomposition (3.33). It is not difficult to see that

$$\langle \eta, E_{0,D}(\rho) \rangle_{\partial\Omega_D} = 0 \quad \forall \rho \in W^{\frac{1}{3},\frac{3}{2}}(\Gamma_D), \quad (3.44)$$

$$\langle \eta, E_\Sigma(\varphi) \rangle_{\partial\Omega_D} = \langle \phi, \varphi \rangle_{\Sigma} \quad \forall \varphi \in W^{\frac{1}{3},\frac{3}{2}}(\Sigma), \quad (3.45)$$

and

$$\|\eta\|_{-\frac{1}{3},3;\partial\Omega_D} \leq C\|\phi\|_{-\frac{1}{3},3;\Sigma}. \quad (3.46)$$

Next, we set  $\widetilde{\mathbf{v}}_D := \nabla z$  in  $\Omega_D$ , with  $z \in W^{1,3}(\Omega_D)$  being the unique solution of the boundary value problem (see [99] for details):

$$-\Delta z = -\frac{1}{|\Omega_D|} \langle \eta, 1 \rangle_{\partial\Omega_D} \quad \text{in } \Omega_D, \quad \nabla z \cdot \mathbf{n} = \eta \quad \text{on } \partial\Omega_D, \quad (z, 1)_D = 0.$$

It follows that  $\text{div} \widetilde{\mathbf{v}}_D = \frac{1}{|\Omega_D|} \langle \eta, 1 \rangle_{\partial\Omega_D} \in P_0(\Omega_D)$ ,  $\widetilde{\mathbf{v}}_D \cdot \mathbf{n} = \eta$  on  $\partial\Omega_D$ , and using (3.46) we find that

$$\|\widetilde{\mathbf{v}}_D\|_{\mathbf{H}^3(\text{div}; \Omega_D)} \leq c\|\eta\|_{-\frac{1}{3},3;\partial\Omega_D} \leq C\|\phi\|_{-\frac{1}{3},3;\Sigma}. \quad (3.47)$$

In addition, using (3.32), (3.44) and (3.45), we deduce that

$$\langle \widetilde{\mathbf{v}}_D \cdot \mathbf{n}, \xi \rangle_{\Sigma} = \langle \widetilde{\mathbf{v}}_D \cdot \mathbf{n}, E_\Sigma(\xi) \rangle_{\partial\Omega_D} = \langle \eta, E_\Sigma(\xi) \rangle_{\partial\Omega_D} = \langle \phi, \xi \rangle_{\Sigma},$$

and

$$\langle \tilde{\mathbf{v}}_D \cdot \mathbf{n}, E_{0,D}(\rho) \rangle_{\partial\Omega_D} = \langle \eta, E_{0,D}(\rho) \rangle_{\partial\Omega_D} = 0 \quad \forall \rho \in W^{\frac{1}{3}, \frac{3}{2}}(\Gamma_D).$$

The latter means that  $\tilde{\mathbf{v}}_D \in \mathbf{H}_{\Gamma_D}^3(\text{div}; \Omega_D)$ . In this way, defining  $\tilde{\mathbf{v}} := (\mathbf{0}, \tilde{\mathbf{v}}_D) \in \mathbf{H}$ , we obtain, thanks to (3.46) and (3.47), that

$$\begin{aligned} S(q, \xi) &\geq \frac{|\mathbf{b}(\tilde{\mathbf{v}}), (q, \xi)|}{\|\tilde{\mathbf{v}}\|_{\mathbf{H}}} = \frac{|\langle \phi, \xi \rangle_{\Sigma} + \frac{1}{|\Omega_D|} \langle \eta, 1 \rangle_{\partial\Omega_D} (q, 1)_D|}{\|\tilde{\mathbf{v}}_D\|_{\mathbf{H}^3(\text{div}; \Omega_D)}} \\ &\geq c_2 \frac{|\langle \phi, \xi \rangle_{\Sigma}|}{\|\phi\|_{-\frac{1}{3}, 3; \Sigma}} - c_3 \|q\|_{0, \Omega}, \end{aligned}$$

which, considering that  $\phi \in W^{-\frac{1}{3}, 3}(\Sigma)$  is arbitrary, yields

$$S(q, \xi) \geq c_2 \|\xi\|_{\frac{1}{3}, \frac{3}{2}; \Sigma} - c_3 \|q\|_{0, \Omega}. \quad (3.48)$$

Then, combining (3.43) and (3.48) we easily obtain that

$$S(q, \xi) \geq \frac{c_1 c_2}{c_1 + c_3} \|\xi\|_{\frac{1}{3}, \frac{3}{2}; \Sigma},$$

which, together with (3.43), completes the proof with  $\beta$  depending on  $c_1, c_2$  and  $c_3$ .  $\square$

We are now in position of establishing the well-definiteness of  $\mathbf{T}$ . To that end, and in order to simplify the subsequent analysis, given  $\mathbf{w}_S \in \mathbf{H}_{\Gamma_S}^1(\Omega_S)$  we first note that  $\|\mathbf{a}(\mathbf{w}_S)(\mathbf{0})\|_{\mathbf{H}'} = 0$ , and then, by considering  $p_1 = 2$  and  $p_2 = 3$  in Theorem 3.1, we introduce the following notation

$$\mathcal{M}(\mathbf{f}_S, \mathbf{f}_D, g_D) := \max \left\{ \mathcal{N}(\mathbf{f}_S, \mathbf{f}_D, g_D)^{1/2}, \mathcal{N}(\mathbf{f}_S, \mathbf{f}_D, g_D), \mathcal{N}(\mathbf{f}_S, \mathbf{f}_D, g_D)^2 \right\}, \quad (3.49)$$

with

$$\mathcal{N}(\mathbf{f}_S, \mathbf{f}_D, g_D) := \|\mathbf{f}_S\|_{0, \Omega_S} + \|\mathbf{f}_D\|_{\mathbf{L}^{3/2}(\Omega_D)} + \|g_D\|_{0, \Omega_D} + \|g_D\|_{0, \Omega_D}^2.$$

The main result of this section is established now.

**Theorem 3.6.** *Let  $\mathbf{w}_S \in \mathbf{H}_{\Gamma_S}^1(\Omega_S)$  such that  $\text{div } \mathbf{w}_S = 0$  in  $\Omega_S$  and*

$$\|\mathbf{w}_S \cdot \mathbf{n}\|_{0, \Sigma} \leq \frac{2\mu\alpha_S}{\rho C_{\text{tr}}^2 C_S^2},$$

*and let  $\mathbf{f}_S \in \mathbf{L}^2(\Omega_S)$ ,  $\mathbf{f}_D \in \mathbf{L}^{3/2}(\Omega_D)$  and  $g_D \in L^2(\Omega_D)$ . Then, (3.37) has a unique solution  $(\mathbf{u}, (p, \lambda)) \in \mathbf{H} \times \mathbf{Q}$ , with  $\mathbf{u} := (\mathbf{u}_S, \mathbf{u}_D)$ , which allows to define  $\mathbf{T}(\mathbf{w}_S) := \mathbf{u}_S$ . Moreover, there exists a constant  $c_{\mathbf{T}} > 0$ , independent of the solution, such that*

$$\|\mathbf{T}(\mathbf{w}_S)\|_{1, \Omega_S} = \|\mathbf{u}_S\|_{1, \Omega_S} \leq \|(\mathbf{u}, (p, \lambda))\|_{\mathbf{H} \times \mathbf{Q}} \leq c_{\mathbf{T}} \mathcal{M}(\mathbf{f}_S, \mathbf{f}_D, g_D). \quad (3.50)$$

*Proof.* It follows from Lemmas 3.4–3.5 and a straightforward application of Theorem 3.1. In turn, estimate (3.50) is a direct consequence of (3.25) (cf. Theorem 3.1) and (3.18) – (3.19).  $\square$

### 3.3.4 Solvability analysis of the fixed-point equation

In this section we proceed analogously to [65, Section 2.4] (see also [28, 40]) and establish the existence of a fixed-point of operator  $\mathbf{T}$  (cf. (3.36)) by means of the well known Schauder fixed-point theorem and a sufficiently small data assumption. In addition, under a more restrictive small data assumption, the uniqueness of solution is also established by means of the Banach fixed-point theorem. We begin by recalling the first of the aforementioned results (see, e.g., [47, Theorem 9.12-1(b)]).

**Theorem 3.7.** *Let  $W$  be a closed and convex subset of a Banach space  $X$ , and let  $T : W \rightarrow W$  be a continuous mapping such that  $\overline{T(W)}$  is compact. Then  $T$  has at least one fixed-point.*

The verification of the hypotheses of Theorem 3.7 is provided in what follows. To this aim, we start by introducing the set

$$\mathbf{W} := \left\{ \mathbf{v}_S \in \mathbf{H}_{\Gamma_S}^1(\Omega_S) : \quad \operatorname{div} \mathbf{v}_S = 0 \quad \text{in} \quad \Omega_S \quad \text{and} \quad \|\mathbf{v}_S\|_{1,\Omega_S} \leq c_{\mathbf{T}} \mathcal{M}(\mathbf{f}_S, \mathbf{f}_D, g_D) \right\}. \quad (3.51)$$

Then, assuming that (cf. (3.49)):

$$\mathcal{M}(\mathbf{f}_S, \mathbf{f}_D, g_D) \leq \frac{2\mu\alpha_S}{c_{\mathbf{T}} \rho C_{\text{tr}}^3 C_S^2}, \quad (3.52)$$

with  $c_{\mathbf{T}}$  the positive constant satisfying (3.50), it is not difficult to see that  $\mathbf{T}$  is well defined from  $\mathbf{W}$  to  $\mathbf{W}$ . In fact, given  $\mathbf{w}_S \in \mathbf{W}$ , from (3.52) we deduce that

$$\|\mathbf{w}_S \cdot \mathbf{n}\|_{0,\Sigma} \leq C_{\text{tr}} \|\mathbf{w}_S\|_{1,\Omega_S} \leq \frac{2\mu\alpha_S}{\rho C_{\text{tr}}^2 C_S^2}, \quad (3.53)$$

which together with Theorem 3.6 proves that  $\mathbf{T}$  is well defined. In this way, we obtain the following result.

**Lemma 3.8.** *Let  $\mathbf{W}$  be the closed ball defined by (3.51) and assume that the data satisfy (3.52). Then there holds  $\mathbf{T}(\mathbf{W}) \subseteq \mathbf{W}$ .*

We continue with the following result providing an estimate needed to derive next the required continuity and compactness properties of the operator  $\mathbf{T}$  (cf. (3.36)).

**Lemma 3.9.** *Let  $\mathbf{W}$  be the closed ball defined by (3.51) and assume that the data satisfy (3.52). Then,*

$$\|\mathbf{T}(\mathbf{w}_S) - \mathbf{T}(\tilde{\mathbf{w}}_S)\|_{1,\Omega_S} \leq \frac{\rho C_S}{\mu\alpha_S} \|\mathbf{T}(\tilde{\mathbf{w}}_S)\|_{1,\Omega_S} \|\mathbf{w}_S - \tilde{\mathbf{w}}_S\|_{\mathbf{L}^4(\Omega_S)} \quad \forall \mathbf{w}_S, \tilde{\mathbf{w}}_S \in \mathbf{W}. \quad (3.54)$$

*Proof.* Given  $\mathbf{w}_S, \tilde{\mathbf{w}}_S \in \mathbf{W}$ , we let  $\mathbf{u}_S := \mathbf{T}(\mathbf{w}_S)$  and  $\tilde{\mathbf{u}}_S := \mathbf{T}(\tilde{\mathbf{w}}_S)$ . According to the definition of  $\mathbf{T}$ , it follows that

$$\begin{aligned} [\mathbf{a}(\mathbf{w}_S)(\mathbf{u}), \mathbf{v}] + [\mathbf{b}(\mathbf{v}), (p, \lambda)] &= [\mathbf{f}, \mathbf{v}] \quad \forall \mathbf{v} \in \mathbf{H}, \\ [\mathbf{b}(\mathbf{u}), (q, \xi)] &= [\mathbf{g}, (q, \xi)] \quad \forall (q, \xi) \in \mathbf{Q}, \end{aligned}$$

and

$$\begin{aligned} [\mathbf{a}(\tilde{\mathbf{w}}_S)(\tilde{\mathbf{u}}), \mathbf{v}] + [\mathbf{b}(\mathbf{v}), (\tilde{p}, \tilde{\lambda})] &= [\mathbf{f}, \mathbf{v}] \quad \forall \mathbf{v} \in \mathbf{H}, \\ [\mathbf{b}(\tilde{\mathbf{u}}), (q, \xi)] &= [\mathbf{g}, (q, \xi)] \quad \forall (q, \xi) \in \mathbf{Q}. \end{aligned}$$

Then, recalling the definition of  $\mathbf{a}(\mathbf{w}_S)$  (cf. (3.12)) and subtracting both problems we obtain

$$\begin{aligned} [\mathbf{a}(\mathbf{w}_S)(\mathbf{u}) - \mathbf{a}(\tilde{\mathbf{w}}_S)(\tilde{\mathbf{u}}), \mathbf{v}] + [\mathbf{b}(\mathbf{v}), (p - \tilde{p}, \lambda - \tilde{\lambda})] &= 0 \\ [\mathbf{b}(\mathbf{u} - \tilde{\mathbf{u}}), (q, \xi)] &= 0 \end{aligned}$$

for all  $(\mathbf{v}, (q, \xi)) \in \mathbf{H} \times \mathbf{Q}$ . In particular, taking  $\mathbf{v} = \mathbf{u} - \tilde{\mathbf{u}}$ ,  $q = p - \tilde{p}$  and  $\xi = \lambda - \tilde{\lambda}$  in the latter system, the first equation becomes

$$[\mathbf{a}(\mathbf{w}_S)(\mathbf{u}) - \mathbf{a}(\tilde{\mathbf{w}}_S)(\tilde{\mathbf{u}}), \mathbf{u} - \tilde{\mathbf{u}}] = 0. \quad (3.55)$$

Hence, adding and subtracting  $\mathcal{B}_S(\mathbf{w}_S)(\tilde{\mathbf{u}}_S)$  in the second term of the left-hand side of (3.55), using the fact that  $\mathbf{u} - \tilde{\mathbf{u}} \in \mathbf{V}$  (cf. (3.39)), and the strict monotonicity of  $\mathbf{a}(\mathbf{w}_S)$  (cf. (3.41)), it follows that

$$\mu\alpha_S \|\mathbf{u}_S - \tilde{\mathbf{u}}_S\|_{1,\Omega_S}^2 \leq [\mathbf{a}(\mathbf{w}_S)(\mathbf{u}) - \mathbf{a}(\mathbf{w}_S)(\tilde{\mathbf{u}}), \mathbf{u} - \tilde{\mathbf{u}}] = [\mathcal{B}_S(\tilde{\mathbf{w}}_S - \mathbf{w}_S)(\tilde{\mathbf{u}}_S), \mathbf{u}_S - \tilde{\mathbf{u}}_S].$$

In this way, the continuity of  $\mathcal{B}_S$  (cf. (3.16)) gives from the foregoing equation

$$\mu\alpha_S \|\mathbf{u}_S - \tilde{\mathbf{u}}_S\|_{1,\Omega_S}^2 \leq \rho C_S \|\mathbf{w}_S - \tilde{\mathbf{w}}_S\|_{\mathbf{L}^4(\Omega_S)} \|\tilde{\mathbf{u}}_S\|_{1,\Omega_S} \|\mathbf{u}_S - \tilde{\mathbf{u}}_S\|_{1,\Omega_S},$$

which yields the result.  $\square$

Owing to the above analysis, we establish now the announced properties of the operator  $\mathbf{T}$ .

**Lemma 3.10.** *Assume that the estimate (3.52) holds. Then  $\mathbf{T}$  has at least one fixed-point in  $\mathbf{W}$ .*

*Proof.* The required result follows straightforwardly from estimate (3.54), the continuity of the Sobolev embedding from  $H^1(\Omega_S)$  into  $L^4(\Omega_S)$ , and the Schauder theorem. We omit further details and refer to [65, Lemma 5].  $\square$

Under a more restrictive assumption on the data, in what follows we prove that  $\mathbf{T}$  has exactly one fixed-point by means of the well-known Banach fixed-point theorem.

**Lemma 3.11.** *Let  $\mathbf{f}_S \in \mathbf{L}^2(\Omega_S)$ ,  $\mathbf{f}_D \in \mathbf{L}^{3/2}(\Omega_D)$  and  $g_D \in L^2(\Omega_D)$ , such that*

$$\mathcal{M}(\mathbf{f}_S, \mathbf{f}_D, g_D) < r, \quad (3.56)$$

where

$$r := \frac{\mu\alpha_S}{c_{\mathbf{T}}\rho} \min \left\{ \frac{1}{C_S^2}, \frac{2}{C_S^2 C_{\text{tr}}^3} \right\}.$$

Then,  $\mathbf{T}$  has a unique fixed-point.

*Proof.* The result follows straightforwardly from (3.54), the continuity of the compact injection from  $H^1(\Omega_S)$  into  $L^4(\Omega_S)$ , the fact that  $\mathbf{T}(\mathbf{W}) \subseteq \mathbf{W}$ , and the constraint (3.56).  $\square$

We are now in position of establishing the main result of this section.

**Theorem 3.12.** *Let  $\mathbf{f}_S \in \mathbf{L}^2(\Omega_S)$ ,  $\mathbf{f}_D \in \mathbf{L}^{3/2}(\Omega_D)$  and  $g_D \in L^2(\Omega_D)$ . Assume that (3.52) holds. Then the problem (3.11) admits a solution  $(\mathbf{u}, (p, \lambda)) \in \mathbf{H} \times \mathbf{Q}$ . In addition, if it is assumed that (3.56) holds, then the solution is unique. In any case, there exists a constant  $c_T > 0$  (cf. (3.50)), independent of the solution, such that*

$$\|(\mathbf{u}, (p, \lambda))\|_{\mathbf{H} \times \mathbf{Q}} \leq c_T \mathcal{M}(\mathbf{f}_S, \mathbf{f}_D, g_D). \quad (3.57)$$

*Proof.* The existence and uniqueness of solution of problem (3.11) follows by recalling the definition of operator  $\mathbf{T}$  and combining Lemmas 3.10 and 3.11. In addition, it is clear that the estimate (3.57) is consequence of (3.50).  $\square$

## 3.4 The Galerkin scheme

In this section we introduce the Galerkin scheme of problem (3.11) and analyse its well-posedness.

### 3.4.1 Discrete setting

Let  $\mathcal{T}_h^S$  and  $\mathcal{T}_h^D$  be respective triangulations of the domains  $\Omega_S$  and  $\Omega_D$  formed by shape-regular triangles of diameter  $h_T$  and denote by  $h_S$  and  $h_D$  their corresponding mesh sizes. Assume that they match on  $\Sigma$  so that  $\mathcal{T}_h := \mathcal{T}_h^S \cup \mathcal{T}_h^D$  is a triangulation of  $\Omega := \Omega_S \cup \Sigma \cup \Omega_D$ . Hereafter  $h := \max\{h_S, h_D\}$ . For each  $T \in \mathcal{T}_h^D$  we consider the local Raviart–Thomas space of the lowest order [140]:

$$\text{RT}_0(T) := \text{span}\{(1, 0), (0, 1), (x_1, x_2)\}.$$

In addition, for each  $T \in \mathcal{T}_h^S$  we denote by  $\text{BR}(T)$  the local Bernardi–Raugel space (see [17, 100]):

$$\text{BR}(T) := [\text{P}_1(T)]^2 \oplus \text{span}\{\eta_2 \eta_3 \mathbf{n}_1, \eta_1 \eta_3 \mathbf{n}_2, \eta_1 \eta_2 \mathbf{n}_3\},$$

where  $\{\eta_1, \eta_2, \eta_3\}$  are the barycentric coordinates of  $T$ , and  $\{\mathbf{n}_1, \mathbf{n}_2, \mathbf{n}_3\}$  are the unit outward normals to the opposite sides of the corresponding vertices of  $T$ . Hence, we define the following finite element subspaces:

$$\begin{aligned} \mathbf{H}_h(\Omega_S) &:= \left\{ \mathbf{v} \in \mathbf{H}^1(\Omega_S) : \quad \mathbf{v}|_T \in \text{BR}(T), \quad \forall T \in \mathcal{T}_h^S \right\}, \\ \mathbf{H}_h(\Omega_D) &:= \left\{ \mathbf{v} \in \mathbf{H}^3(\text{div}; \Omega_D) : \quad \mathbf{v}|_T \in \text{RT}_0(T), \quad \forall T \in \mathcal{T}_h^D \right\}, \\ L_h(\Omega) &:= \left\{ q \in L^2(\Omega) : \quad q|_T \in \text{P}_0(T), \quad \forall T \in \mathcal{T}_h \right\}. \end{aligned}$$

Then, the finite element subspaces for the velocities and pressure are, respectively,

$$\begin{aligned} \mathbf{H}_{h, \Gamma_S}(\Omega_S) &:= \mathbf{H}_h(\Omega_S) \cap \mathbf{H}_{\Gamma_S}^1(\Omega_S), \\ \mathbf{H}_{h, \Gamma_D}(\Omega_D) &:= \mathbf{H}_h(\Omega_D) \cap \mathbf{H}_{\Gamma_D}^3(\text{div}; \Omega_D), \\ L_{h, 0}(\Omega) &:= L_h(\Omega) \cap L_0^2(\Omega). \end{aligned}$$

Next, for introducing the finite element subspace of  $W^{\frac{1}{3}, \frac{3}{2}}(\Sigma)$ , we denote by  $\Sigma_h$  the partition of  $\Sigma$  inherited from  $\mathcal{T}_h^D$  (or  $\mathcal{T}_h^S$ ), which is formed by edges  $e$  of length  $h_e$ , and set  $h_\Sigma := \max\{h_e : e \in \Sigma_h\}$ . In turn, since the space  $\prod_{e \in \Sigma_h} W^{1-\frac{1}{p}, p}(e)$  coincides with  $W^{1-\frac{1}{p}, p}(\Sigma)$ , without extra conditions when

$1 < p < 2$  [105, Theorem 1.5.2.3-(a)] (see also [106, Proposition 1.4.3] and [104, Section 2] for the 3D case), it can be readily seen that a conforming finite element subspace for  $W^{\frac{1}{3}, \frac{3}{2}}(\Sigma)$  can be defined by

$$\Lambda_h(\Sigma) := \left\{ \xi_h : \Sigma \rightarrow \mathbb{R} : \quad \xi_h|_e \in P_0(e) \quad \forall \text{ edge } e \in \Sigma_h \right\}.$$

Notice that this space coincides with the set of discrete normal traces on  $\Sigma$  of  $\mathbf{H}_h(\Omega_D)$ . Notice also that since  $\mathcal{T}_h^S$  and  $\mathcal{T}_h^D$  match on  $\Sigma$ , there holds  $h_\Sigma \leq \min\{h_S, h_D\}$ .

In this way, grouping the unknowns and spaces as follows:

$$\begin{aligned} \mathbf{H}_h &:= \mathbf{H}_{h,\Gamma_S}(\Omega_S) \times \mathbf{H}_{h,\Gamma_D}(\Omega_D), \quad \mathbf{Q}_h := L_{h,0}(\Omega) \times \Lambda_h(\Sigma), \\ \mathbf{u}_h &:= (\mathbf{u}_{S,h}, \mathbf{u}_{D,h}) \in \mathbf{H}_h, \quad (p_h, \lambda_h) \in \mathbf{Q}_h, \end{aligned}$$

where  $p_h := p_{S,h}\chi_S + p_{D,h}\chi_D$ , our Galerkin scheme for (3.11) reads: Find  $(\mathbf{u}_h, (p_h, \lambda_h)) \in \mathbf{H}_h \times \mathbf{Q}_h$ , such that

$$\begin{aligned} [\mathbf{a}_h(\mathbf{u}_{S,h})(\mathbf{u}_h), \mathbf{v}_h] + [\mathbf{b}(\mathbf{v}_h), (p_h, \lambda_h)] &= [\mathbf{f}, \mathbf{v}_h] \quad \forall \mathbf{v}_h := (\mathbf{v}_{S,h}, \mathbf{v}_{D,h}) \in \mathbf{H}_h, \\ [\mathbf{b}(\mathbf{u}_h), (q_h, \xi_h)] &= [\mathbf{g}, (q_h, \xi_h)] \quad \forall (q_h, \xi_h) \in \mathbf{Q}_h. \end{aligned} \quad (3.58)$$

Here,  $\mathbf{a}_h(\mathbf{w}_{S,h}) : \mathbf{H}_h \rightarrow \mathbf{H}'_h$  is the discrete version of  $\mathbf{a}(\mathbf{w}_S)$  (with  $\mathbf{w}_{S,h} \in \mathbf{H}_{h,\Gamma_S}(\Omega_S)$  in place of  $\mathbf{w}_S \in \mathbf{H}_{\Gamma_S}^1(\Omega_S)$ ), which is defined by

$$[\mathbf{a}_h(\mathbf{w}_{S,h})(\mathbf{u}_h), \mathbf{v}_h] := [\mathcal{A}_S(\mathbf{u}_{S,h}), \mathbf{v}_{S,h}] + [\mathcal{B}_S^h(\mathbf{w}_{S,h})(\mathbf{u}_{S,h}), \mathbf{v}_{S,h}] + [\mathcal{A}_D(\mathbf{u}_{D,h}), \mathbf{v}_{D,h}], \quad (3.59)$$

where  $\mathcal{B}_S^h(\mathbf{w}_{S,h})$  is the well-known skew-symmetric convection form [148]:

$$[\mathcal{B}_S^h(\mathbf{w}_{S,h})(\mathbf{u}_{S,h}), \mathbf{v}_{S,h}] := \rho((\nabla \mathbf{u}_{S,h})\mathbf{w}_{S,h}, \mathbf{v}_{S,h})_S + \frac{\rho}{2}(\operatorname{div} \mathbf{w}_{S,h} \mathbf{u}_{S,h}, \mathbf{v}_{S,h})_S,$$

for all  $\mathbf{u}_{S,h}, \mathbf{v}_{S,h}, \mathbf{w}_{S,h} \in \mathbf{H}_{h,\Gamma_S}(\Omega_S)$ . Observe that integrating by parts, similarly to (3.21), there holds

$$[\mathcal{B}_S^h(\mathbf{w}_{S,h})(\mathbf{v}_{S,h}), \mathbf{v}_{S,h}] = \frac{\rho}{2} \int_{\Sigma} (\mathbf{w}_{S,h} \cdot \mathbf{n}) |\mathbf{v}_{S,h}|^2 \geq 0 \quad \forall \mathbf{w}_{S,h}, \mathbf{v}_{S,h} \in \mathbf{H}_{h,\Gamma_S}(\Omega_S). \quad (3.60)$$

Moreover, proceeding as for  $\mathcal{B}_S$  (cf. (3.16)), it is easy to see that for all  $\mathbf{w}_{S,h}, \mathbf{u}_{S,h}, \mathbf{v}_{S,h} \in \mathbf{H}_{h,\Gamma_S}(\Omega_S)$ , there holds

$$\left| [\mathcal{B}_S^h(\mathbf{w}_{S,h})(\mathbf{u}_{S,h}), \mathbf{v}_{S,h}] \right| \leq C_{\text{sk}} \|\mathbf{w}_{S,h}\|_{1,\Omega_S} \|\mathbf{u}_{S,h}\|_{1,\Omega_S} \|\mathbf{v}_{S,h}\|_{1,\Omega_S}, \quad (3.61)$$

with  $C_{\text{sk}} := \rho C_S^2 \left(1 + \frac{\sqrt{2}}{2}\right)$ .

Now, let  $\Pi_S : \mathbf{H}_{\Gamma_S}^1(\Omega_S) \rightarrow \mathbf{H}_{h,\Gamma_S}(\Omega_S)$  be the Bernardi–Raugel interpolation operator [17], which is linear and bounded with respect to the  $\mathbf{H}^1(\Omega_S)$ -norm. In this regard, we recall that, given  $\mathbf{v} \in \mathbf{H}_{\Gamma_S}^1(\Omega_S)$ , there holds

$$\int_e \Pi_S(\mathbf{v}) \cdot \mathbf{n} = \int_e \mathbf{v} \cdot \mathbf{n} \quad \text{for each edge } e \text{ of } \mathcal{T}_h^S, \quad (3.62)$$

and hence

$$(\operatorname{div} \Pi_S(\mathbf{v}), q_h)_S = (\operatorname{div} \mathbf{v}, q_h)_S \quad \forall q_h \in L_h(\Omega). \quad (3.63)$$

Equivalently, if  $\mathcal{P}_S$  denotes the  $L^2(\Omega_S)$ -orthogonal projection onto the restriction of  $L_h(\Omega)$  to  $\Omega_S$ , then the relation (3.63) can be written as

$$\mathcal{P}_S(\operatorname{div}(\Pi_S(\mathbf{v}))) = \mathcal{P}_S(\operatorname{div} \mathbf{v}) \quad \forall \mathbf{v} \in \mathbf{H}_{\Gamma_S}^1(\Omega_S). \quad (3.64)$$



On the other hand, let  $\Pi_D : \mathbf{H}^1(\Omega_D) \rightarrow \mathbf{H}_h(\Omega_D)$  be the well-known Raviart–Thomas interpolation operator. We recall that, given  $\mathbf{v} \in \mathbf{H}^1(\Omega_D)$ , this operator is characterized by

$$\int_e \Pi_D(\mathbf{v}) \cdot \mathbf{n} = \int_e \mathbf{v} \cdot \mathbf{n} \quad \text{for each edge } e \text{ of } \mathcal{T}_h^D, \quad (3.65)$$

which implies that

$$(\operatorname{div} \Pi_D(\mathbf{v}), q_h)_D = (\operatorname{div} \mathbf{v}, q_h)_D \quad \forall q_h \in L_h(\Omega). \quad (3.66)$$

Equivalently, if  $\mathcal{P}_D$  denotes the  $L^2(\Omega_D)$ -orthogonal projection onto the restriction of  $L_h(\Omega)$  to  $\Omega_D$ , then the relation (3.66) can be written as

$$\operatorname{div}(\Pi_D(\mathbf{v})) = \mathcal{P}_D(\operatorname{div} \mathbf{v}) \quad \forall \mathbf{v} \in \mathbf{H}^1(\Omega_D). \quad (3.67)$$

At this point we recall, according to [69, Sections 1.2.7 and 1.4.7] (see also [19, Chapter III.3.3]), that the Raviart–Thomas operator  $\Pi_D$  is also well defined for all  $\mathbf{v} \in \mathbf{V}^{\operatorname{div}}(\Omega_D) := \left\{ \mathbf{v} \in \mathbf{L}^p(\Omega_D) : \operatorname{div} \mathbf{v} \in L^s(\Omega_D) \right\}$ , with  $p > 2$  and  $s \geq q$ ,  $\frac{1}{q} = \frac{1}{p} + \frac{1}{n}$ , since the local space  $\mathbf{V}^{\operatorname{div}}(T)$  coincides with  $\mathbf{W}^{1,t}(T)$  when  $t > \frac{2n}{n+2}$ , for each  $T \in \mathcal{T}_h^D$ . In particular, considering  $n = 2$ ,  $p = 3$ , and  $s = 2$ , we deduce that  $\Pi_D$  can be applied to functions in  $\mathbf{H}^3(\operatorname{div}; \Omega_D)$ . We will use this fact later on in the proof of the discrete inf-sup condition of  $\mathbf{b}$ .

### 3.4.2 Well-posedness of the discrete problem

In this section, analogously to the analysis of the continuous problem, we apply a fixed-point argument to prove the well-posedness of the Galerkin scheme (3.58). To that end, we now let  $\mathbf{T}_h : \mathbf{H}_{h,\Gamma_S}(\Omega_S) \rightarrow \mathbf{H}_{h,\Gamma_S}(\Omega_S)$  be the discrete operator defined by

$$\mathbf{T}_h(\mathbf{w}_{S,h}) := \mathbf{u}_{S,h} \quad \forall \mathbf{w}_{S,h} \in \mathbf{H}_{h,\Gamma_S}(\Omega_S), \quad (3.68)$$

where  $\mathbf{u}_h := (\mathbf{u}_{S,h}, \mathbf{u}_{D,h}) \in \mathbf{H}_h$  is the first component of the unique solution (to be confirmed below) of the discrete nonlinear problem: Find  $(\mathbf{u}_h, (p_h, \lambda_h)) \in \mathbf{H}_h \times \mathbf{Q}_h$ , such that

$$\begin{aligned} [\mathbf{a}_h(\mathbf{w}_{S,h})(\mathbf{u}_h), \mathbf{v}_h] + [\mathbf{b}(\mathbf{v}_h), (p_h, \lambda_h)] &= [\mathbf{f}, \mathbf{v}_h] \quad \forall \mathbf{v}_h \in \mathbf{H}_h, \\ [\mathbf{b}(\mathbf{u}_h), (q_h, \xi_h)] &= [\mathbf{g}, (q_h, \xi_h)] \quad \forall (q_h, \xi_h) \in \mathbf{Q}_h. \end{aligned} \quad (3.69)$$

Then, similarly as for the continuous case, the Galerkin scheme (3.58) can be rewritten, equivalently, as the fixed-point problem: Find  $\mathbf{u}_{S,h} \in \mathbf{H}_{h,\Gamma_S}(\Omega_S)$  such that

$$\mathbf{T}_h(\mathbf{u}_{S,h}) = \mathbf{u}_{S,h}.$$

In this way, in what follows we focus on analysing the existence and uniqueness of such a fixed-point, for which we require the following discrete version of Theorem 3.1.

**Theorem 3.13.** *In addition to the spaces and operators defined in Theorem 3.1, let  $X_{1,h}$ ,  $X_{2,h}$  and  $Y_h$  be finite dimensional subspaces of  $X_1$ ,  $X_2$ , and  $Y$ , respectively, and set  $X_h = X_{1,h} \times X_{2,h} \subseteq X := X_1 \times X_2$ . In addition, let  $V_h$  be the discrete kernel of  $b$ , that is,*

$$V_h := \left\{ v_h \in X_h : [b(v_h), q_h] = 0 \quad \forall q_h \in Y_h \right\}.$$

Assume that

(i)  $a$  is hemi-continuous from  $X_h$  to  $X'_h$ , that is, for each  $u, v \in X_h$ , the real mapping

$$J : \mathbb{R} \rightarrow \mathbb{R}, \quad t \rightarrow J(t) = [a(u + tv), v]$$

is continuous.

(ii) there exist constants  $\tilde{\gamma} > 0$  and  $p_1, p_2 \geq 2$ , such that

$$\|a(u_h) - a(v_h)\|_{X'} \leq \tilde{\gamma} \sum_{j=1}^2 \left\{ \|u_{j,h} - v_{j,h}\|_{X_j} + \|u_{j,h} - v_{j,h}\|_{X_j} \left( \|u_{j,h}\|_{X_j} + \|v_{j,h}\|_{X_j} \right)^{p_j-2} \right\},$$

for all  $u_h = (u_{1,h}, u_{2,h}), v_h = (v_{1,h}, v_{2,h}) \in X_h$ .

(iii) for fixed  $t_h \in V_h^\perp \equiv X_h \setminus V_h$ , the operator  $a(\cdot + t_h) : V_h \rightarrow V'_h$  is strictly monotone, that is, there exists  $\tilde{\alpha} > 0$  and  $p_1, p_2 \geq 2$ , such that

$$[a(u_h + t_h) - a(v_h + t_h), u_h - v_h] \geq \tilde{\alpha} \left\{ \|u_{1,h} - v_{1,h}\|_{X_1}^{p_1} + \|u_{2,h} - v_{2,h}\|_{X_2}^{p_2} \right\},$$

for all  $u_h = (u_{1,h}, u_{2,h}), v_h = (v_{1,h}, v_{2,h}) \in V_h$ .

(iv) there exists  $\tilde{\beta} > 0$  such that

$$\sup_{\substack{v_h \in X_h \\ v_h \neq 0}} \frac{[b(v_h), q_h]}{\|v_h\|_X} \geq \tilde{\beta} \|q_h\|_Y \quad \forall q_h \in Y_h.$$

Then, for each  $(f, g) \in X' \times Y'$  there exists a unique  $(u_h, p_h) \in X_h \times Y_h$ , such that

$$\begin{aligned} [a(u_h), v_h] + [b(v_h), p_h] &= [f, v_h] \quad \forall v_h \in X_h, \\ [b(u_h), q_h] &= [g, q_h] \quad \forall q_h \in Y_h. \end{aligned}$$

Moreover, there exists  $\tilde{C} > 0$ , depending only on  $\tilde{\alpha}, \tilde{\gamma}, \tilde{\beta}, p_1$ , and  $p_2$ , such that

$$\|(u_h, p_h)\|_{X \times Y} \leq \tilde{C} \mathcal{M}(f, g),$$

where

$$\mathcal{M}(f, g) := \max \left\{ \mathcal{N}(f, g)^{\frac{1}{p_1-1}}, \mathcal{N}(f, g)^{\frac{1}{p_2-1}}, \mathcal{N}(f, g), \mathcal{N}(f, g)^{\frac{p_1-1}{p_2-1}}, \mathcal{N}(f, g)^{\frac{p_2-1}{p_1-1}} \right\},$$

and

$$\mathcal{N}(f, g) := \|f\|_{X'} + \|g\|_{Y'} + \|g\|_{Y'}^{p_1-1} + \|g\|_{Y'}^{p_2-1} + \|a(0)\|_{X'}.$$

*Proof.* It reduces to a simple application of Theorem 3.1 to the present discrete setting.  $\square$

Similarly to the analysis developed in Section 3.3.3, in what follows we provide suitable assumptions under which problem (3.69) is well posed or equivalently  $\mathbf{T}_h$  is well defined. For this purpose, we must verify that the operators defining the discrete problem (3.69) satisfy the hypotheses of Theorem 3.13. We begin with the hemi-continuity of  $\mathbf{a}_h$ .

**Lemma 3.14.** *Given  $\mathbf{w}_{S,h} \in \mathbf{H}_{h,\Gamma_S}^1(\Omega_S)$ , the operator  $\mathbf{a}_h(\mathbf{w}_{S,h})$  is hemi-continuous in  $\mathbf{H}_h$ .*

*Proof.* The proof follows analogously to the proof of Lemma 3.2, by using now the linearity and continuity of  $\mathcal{B}_S^h(\mathbf{w}_{S,h})$  (in addition to those of  $\mathcal{A}_S$ ).  $\square$

Now we verify that hypothesis (ii) of Theorem 3.13 holds.

**Lemma 3.15.** *Let  $\mathbf{w}_{S,h} \in \mathbf{H}_{h,\Gamma_S}(\Omega_S)$ . Then, there exists  $\tilde{\gamma} > 0$ , depending on  $C_{\mathcal{A}_S}$  and  $L_{\mathcal{A}_D}$  (cf. (3.16), (3.17)), such that*

$$\begin{aligned} \|\mathbf{a}_h(\mathbf{w}_{S,h})(\mathbf{u}_h) - \mathbf{a}_h(\mathbf{w}_{S,h})(\mathbf{v}_h)\|_{\mathbf{H}'} &\leq \tilde{\gamma} \left\{ (1 + \|\mathbf{w}_{S,h}\|_{1,\Omega_S}) \|\mathbf{u}_{S,h} - \mathbf{v}_{S,h}\|_{1,\Omega_S} + \|\mathbf{u}_{D,h} - \mathbf{v}_{D,h}\|_{\mathbf{H}^3(\text{div};\Omega_D)} \right. \\ &\quad \left. + \|\mathbf{u}_{D,h} - \mathbf{v}_{D,h}\|_{\mathbf{H}^3(\text{div};\Omega_D)} \left( \|\mathbf{u}_{D,h}\|_{\mathbf{H}^3(\text{div};\Omega_D)} + \|\mathbf{v}_{D,h}\|_{\mathbf{H}^3(\text{div};\Omega_D)} \right) \right\}, \end{aligned}$$

for all  $\mathbf{u}_h = (\mathbf{u}_{S,h}, \mathbf{u}_{D,h})$ ,  $\mathbf{v} = (\mathbf{v}_{S,h}, \mathbf{v}_{D,h}) \in \mathbf{H}$ .

*Proof.* Similarly to the continuous case, the result follows straightforwardly from the definition of  $\mathbf{a}_h(\mathbf{w}_{S,h})$  (cf. (3.59)), the triangle inequality, and the stability properties (3.16), (3.17) and (3.61). We omit further details.  $\square$

Now, we proceed to establish the strict monotonicity of  $\mathbf{a}_h(\mathbf{w}_{S,h})$  on the discrete kernel of  $\mathbf{b}$ :

$$\mathbf{V}_h := \left\{ \mathbf{v}_h := (\mathbf{v}_{S,h}, \mathbf{v}_{D,h}) \in \mathbf{H}_h : [\mathbf{b}(\mathbf{v}_h), (q_h, \xi_h)] = 0 \quad \forall (q_h, \xi_h) \in \mathbf{Q}_h \right\}, \quad (3.70)$$

for suitable  $\mathbf{w}_{S,h} \in \mathbf{H}_{h,\Gamma_S}(\Omega_S)$ . Observe that, similarly to the continuous case,  $\mathbf{v}_h \in \mathbf{V}_h$  if and only if

$$(\text{div } \mathbf{v}_{S,h}, q_h)_S + (\text{div } \mathbf{v}_{D,h}, q_h)_D = 0 \quad \forall q_h \in L_{h,0}(\Omega),$$

and

$$\langle \mathbf{v}_{S,h} \cdot \mathbf{n} - \mathbf{v}_{D,h} \cdot \mathbf{n}, \xi_h \rangle_\Sigma = 0 \quad \forall \xi_h \in \Lambda_h(\Sigma),$$

which, in particular, imply that

$$(\text{div } \mathbf{v}_{S,h}, q_h)_S = 0 \quad \forall q_h \in L_h(\Omega_S) \quad \text{and} \quad \text{div } \mathbf{v}_{D,h} = 0 \quad \text{in } \Omega_D, \quad (3.71)$$

where  $L_h(\Omega_S)$  is the set of functions of  $L_h(\Omega)$  restricted to  $\Omega_S$ . Then, the announced result is as follows.

**Lemma 3.16.** *Let  $\mathbf{w}_{S,h} \in \mathbf{H}_{h,\Gamma_S}(\Omega_S)$  such that*

$$\|\mathbf{w}_{S,h} \cdot \mathbf{n}\|_{0,\Sigma} \leq \frac{2\mu\alpha_S}{\rho C_{\text{tr}}^2 C_S^2}. \quad (3.72)$$

*Then, for fixed  $\mathbf{t}_h \in \mathbf{H}_h \setminus \mathbf{V}_h$ , the nonlinear operator  $\mathbf{a}_h(\mathbf{w}_{S,h})(\cdot + \mathbf{t}_h)$  is strictly monotone on  $\mathbf{V}_h$  (cf. (3.70)).*

*Proof.* The proof follows analogously to the proof of Lemma 3.4. Further details are omitted.  $\square$

We continue by adapting the results provided in [92, Section 4] to our domain and spaces configuration to prove that  $\mathbf{b}$  satisfies the corresponding discrete inf-sup condition. We start by establishing the following two preliminary lemmas.

**Lemma 3.17.** *There exists  $\tilde{C}_1 > 0$ , independent of  $h$ , such that for all  $(q_h, \xi_h) \in \mathbf{Q}_h$ , there holds*

$$S_h(q_h, \xi_h) := \sup_{\substack{\mathbf{v}_h \in \mathbf{H}_h \\ \mathbf{v}_h \neq \mathbf{0}}} \frac{[\mathbf{b}(\mathbf{v}_h), (q_h, \xi_h)]}{\|\mathbf{v}_h\|_{\mathbf{H}}} \geq \tilde{C}_1 \|\xi_h\|_{\frac{1}{3}, \frac{3}{2}; \Sigma} - \|q_h\|_{0, \Omega}. \quad (3.73)$$

*Proof.* Let  $\xi_h \in \Lambda_h(\Sigma) \subseteq W^{\frac{1}{3}, \frac{3}{2}}(\Sigma)$ ,  $\xi_h \neq 0$ . Since

$$\sup_{\substack{\tilde{\phi} \in W^{-\frac{1}{3}, 3}(\Sigma) \\ \tilde{\phi} \neq 0}} \frac{\langle \tilde{\phi}, \xi_h \rangle_{\Sigma}}{\|\tilde{\phi}\|_{-\frac{1}{3}, 3; \Sigma}} = \|\xi_h\|_{\frac{1}{3}, \frac{3}{2}; \Sigma},$$

we deduce that there exists  $\tilde{\phi} \in W^{-\frac{1}{3}, 3}(\Sigma) \setminus \{0\}$  such that

$$\langle \tilde{\phi}, \xi_h \rangle_{\Sigma} \geq \frac{1}{2} \|\tilde{\phi}\|_{-\frac{1}{3}, 3; \Sigma} \|\xi_h\|_{\frac{1}{3}, \frac{3}{2}; \Sigma}. \quad (3.74)$$

Next, exactly as we did in the proof of Lemma 3.5, we “extend”  $\tilde{\phi} \in W^{-\frac{1}{3}, 3}(\Sigma)$  to  $\eta \in W^{-\frac{1}{3}, 3}(\partial\Omega_D)$  by

$$\langle \eta, \mu \rangle_{\partial\Omega_D} := \langle \tilde{\phi}, \mu_{\Sigma} \rangle_{\Sigma} \quad \forall \mu \in W^{\frac{1}{3}, \frac{3}{2}}(\partial\Omega_D),$$

where  $\mu_{\Sigma} \in W^{\frac{1}{3}, \frac{3}{2}}(\Sigma)$  is given by the decomposition (3.33). Then, proceeding again as in the second part of the proof of Lemma 3.5, we find  $\tilde{\mathbf{v}}_D \in \mathbf{H}_{\Gamma_D}^3(\text{div}; \Omega_D)$  satisfying  $\tilde{\mathbf{v}}_D \cdot \mathbf{n} = \eta$  on  $\partial\Omega_D$ , and (cf. (3.47))

$$\|\tilde{\mathbf{v}}_D\|_{\mathbf{H}^3(\text{div}; \Omega_D)} \leq C \|\eta\|_{-\frac{1}{3}, 3; \partial\Omega_D} \leq C \|\tilde{\phi}\|_{-\frac{1}{3}, 3; \Sigma},$$

which, combined with (3.74), implies

$$\begin{aligned} \langle \tilde{\mathbf{v}}_D \cdot \mathbf{n}, \xi_h \rangle_{\Sigma} &:= \langle \tilde{\mathbf{v}}_D \cdot \mathbf{n}, E_{\Sigma}(\xi_h) \rangle_{\partial\Omega_D} = \langle \eta, E_{\Sigma}(\xi_h) \rangle_{\partial\Omega_D} = \langle \tilde{\phi}, \xi_h \rangle_{\Sigma} \\ &\geq \frac{1}{2C} \|\tilde{\mathbf{v}}_D\|_{\mathbf{H}^3(\text{div}; \Omega_D)} \|\xi_h\|_{\frac{1}{3}, \frac{3}{2}; \Sigma}. \end{aligned} \quad (3.75)$$

On the other hand, given  $\mathbf{v}_D \in \mathbf{H}^3(\text{div}; \Omega_D)$ , the properties of  $\Pi_D$  (cf. (3.65), (3.66)) and [72, Lemma 3.2] allow to establish that

$$\langle \mathbf{v}_D \cdot \mathbf{n}, \xi_h \rangle_{\Sigma} = \int_{\Sigma} (\Pi_D(\mathbf{v}_D) \cdot \mathbf{n}) \xi_h \quad \forall \xi_h \in \Lambda_h(\Sigma), \quad (3.76)$$

and

$$\|\Pi_D(\mathbf{v}_D)\|_{\mathbf{H}^3(\text{div}; \Omega_D)} \leq C_D \|\mathbf{v}_D\|_{\mathbf{H}^3(\text{div}; \Omega_D)}. \quad (3.77)$$

Thus, defining  $\tilde{\mathbf{v}}_{D,h} := \Pi_D(\tilde{\mathbf{v}}_D) \in \mathbf{H}_{h, \Gamma_D}(\Omega_D)$ , and then using (3.75), (3.76), and (3.77), we obtain

$$\frac{|\langle \tilde{\mathbf{v}}_{D,h} \cdot \mathbf{n}, \xi_h \rangle_{\Sigma}|}{\|\tilde{\mathbf{v}}_{D,h}\|_{\mathbf{H}^3(\text{div}; \Omega_D)}} \geq \frac{1}{C_D} \frac{|\langle \tilde{\mathbf{v}}_D \cdot \mathbf{n}, \xi_h \rangle_{\Sigma}|}{\|\tilde{\mathbf{v}}_D\|_{\mathbf{H}^3(\text{div}; \Omega_D)}} \geq \tilde{C}_1 \|\xi_h\|_{\frac{1}{3}, \frac{3}{2}; \Sigma}. \quad (3.78)$$

Finally, setting  $\tilde{\mathbf{v}}_h := (\mathbf{0}, \tilde{\mathbf{v}}_{D,h}) \in \mathbf{H}_h$ , we deduce that

$$\begin{aligned} S_h(q_h, \xi_h) &:= \sup_{\substack{\mathbf{v}_h \in \mathbf{H}_h \\ \mathbf{v}_h \neq \mathbf{0}}} \frac{[\mathbf{b}(\mathbf{v}_h), (q_h, \xi_h)]}{\|\mathbf{v}_h\|_{\mathbf{H}}} \geq \frac{|[\mathbf{b}(\tilde{\mathbf{v}}_h), (q_h, \xi_h)]|}{\|\tilde{\mathbf{v}}_h\|_{\mathbf{H}}} \\ &= \frac{|\langle \tilde{\mathbf{v}}_{D,h} \cdot \mathbf{n}, \xi_h \rangle_{\Sigma} - (\text{div } \tilde{\mathbf{v}}_{D,h}, q_h)_D|}{\|\tilde{\mathbf{v}}_{D,h}\|_{\mathbf{H}^3(\text{div}; \Omega_D)}} \geq \frac{|\langle \tilde{\mathbf{v}}_{D,h} \cdot \mathbf{n}, \xi_h \rangle_{\Sigma}|}{\|\tilde{\mathbf{v}}_{D,h}\|_{\mathbf{H}^3(\text{div}; \Omega_D)}} - \|q_h\|_{0, \Omega}, \end{aligned}$$

which, together with (3.78), imply (3.73) and complete the proof.  $\square$

**Lemma 3.18.** *There exists  $\tilde{C}_2 > 0$ , independent of  $h$ , such that for all  $(q_h, \xi_h) \in \mathbf{Q}_h$ , there holds*

$$S_h(q_h, \xi_h) := \sup_{\substack{\mathbf{v}_h \in \mathbf{H}_h \\ \mathbf{v}_h \neq \mathbf{0}}} \frac{[\mathbf{b}(\mathbf{v}_h), (q_h, \xi_h)]}{\|\mathbf{v}_h\|_{\mathbf{H}}} \geq \tilde{C}_2 \|q_h\|_{0,\Omega}. \quad (3.79)$$

*Proof.* The proof follows similarly to the first part of the proof of Lemma 3.5. In fact, given  $(q_h, \xi_h) \in \mathbf{Q}_h$  we recall that  $q_h \in L_0^2(\Omega)$  and apply again [100, Corollary 2.4] to deduce that there exists  $\mathbf{z} \in \mathbf{H}_0^1(\Omega)$  such that

$$\operatorname{div} \mathbf{z} = -q_h \quad \text{in } \Omega \quad \text{and} \quad \|\mathbf{z}\|_{1,\Omega} \leq c \|q_h\|_{0,\Omega}. \quad (3.80)$$

Then, we let  $\mathbf{z}_\star := \mathbf{z}|_{\Omega_\star}$  for  $\star \in \{S, D\}$  and observe that  $\mathbf{z}_S = \mathbf{z}_D$  on  $\Sigma$ , which implies that

$$(\mathbf{z}_S - \mathbf{z}_D) \cdot \mathbf{n} = 0 \quad \text{on } \Sigma.$$

Hence, defining  $\mathbf{z}_h := (\mathbf{z}_{S,h}, \mathbf{z}_{D,h})$ , with  $\mathbf{z}_{S,h} = \Pi_S(\mathbf{z}_S)$  and  $\mathbf{z}_{D,h} = \Pi_D(\mathbf{z}_D)$ , we observe from (3.62), (3.65), and the fact that  $\mathcal{T}_h^S$  and  $\mathcal{T}_h^D$  match on  $\Sigma$ , that

$$\langle (\mathbf{z}_{S,h} - \mathbf{z}_{D,h}) \cdot \mathbf{n}, \xi_h \rangle_\Sigma = \langle (\mathbf{z}_S - \mathbf{z}_D) \cdot \mathbf{n}, \xi_h \rangle_\Sigma = 0. \quad (3.81)$$

In addition, since  $\mathbf{z} = \mathbf{0}$  on  $\partial\Omega := \Gamma_S \cup \Gamma_D$ , it is clear that  $\mathbf{z}_h \in \mathbf{H}_h$ , and therefore, thanks to the continuity of  $\Pi_S$  and the estimate (3.77), we obtain that

$$\|\mathbf{z}_h\|_{\mathbf{H}} \leq C \|q_h\|_{0,\Omega}, \quad (3.82)$$

with  $C > 0$  independent of  $h$ . Finally, from the identities (3.64) and (3.67), it can be readily seen that

$$\operatorname{div} \mathbf{z}_h = -q_h \quad \text{in } \Omega, \quad (3.83)$$

which, together with (3.81) and (3.82), yield

$$\sup_{\substack{\mathbf{v}_h \in \mathbf{H}_h \\ \mathbf{v}_h \neq \mathbf{0}}} \frac{[\mathbf{b}(\mathbf{v}_h), (q_h, \xi_h)]}{\|\mathbf{v}_h\|_{\mathbf{H}}} \geq \frac{[\mathbf{b}(\mathbf{z}_h), (q_h, \xi_h)]}{\|\mathbf{z}_h\|_{\mathbf{H}}} \geq \frac{1}{C} \|q_h\|_{0,\Omega},$$

which concludes the proof.  $\square$

Owing to Lemmas 3.17 and 3.18, now we are in position of establishing the full discrete inf-sup condition of  $\mathbf{b}$ .

**Lemma 3.19.** *There exists  $\tilde{\beta} > 0$ , independent of  $h$ , such that for all  $(q_h, \xi_h) \in \mathbf{Q}_h$  there holds*

$$S_h(q_h, \xi_h) := \sup_{\substack{\mathbf{v}_h \in \mathbf{H}_h \\ \mathbf{v}_h \neq \mathbf{0}}} \frac{[\mathbf{b}(\mathbf{v}_h), (q_h, \xi_h)]}{\|\mathbf{v}_h\|_{\mathbf{H}}} \geq \tilde{\beta} \|(q_h, \xi_h)\|_{\mathbf{Q}}. \quad (3.84)$$

*Proof.* It follows straightforwardly from the estimates (3.73) and (3.79).  $\square$

The following result establishes the well-definiteness of operator  $\mathbf{T}_h$ .

**Theorem 3.20.** *Let  $\mathbf{w}_{S,h} \in \mathbf{H}_{h,\Gamma_S}(\Omega_S)$  such that*

$$\|\mathbf{w}_{S,h} \cdot \mathbf{n}\|_{0,\Sigma} \leq \frac{2\mu\alpha_S}{\rho C_{\text{tr}}^2 C_S^2}, \quad (3.85)$$

*and assume that  $\mathbf{f}_S \in \mathbf{L}^2(\Omega_S)$ ,  $\mathbf{f}_D \in \mathbf{L}^{3/2}(\Omega_D)$  and  $g_D \in L^2(\Omega_D)$ . Then there exists a unique  $\mathbf{u}_{S,h} \in \mathbf{H}_{h,\Gamma_S}(\Omega_S)$  such that  $\mathbf{T}_h(\mathbf{w}_{S,h}) = \mathbf{u}_{S,h}$ . Moreover, there exists a constant  $\tilde{c}_{\mathbf{T}} > 0$ , independent of the solution, such that*

$$\|\mathbf{T}_h(\mathbf{w}_{S,h})\|_{1,\Omega_S} = \|\mathbf{u}_{S,h}\|_{1,\Omega_S} \leq \|(\mathbf{u}_h, (p_h, \lambda_h))\|_{\mathbf{H} \times \mathbf{Q}} \leq \tilde{c}_{\mathbf{T}} \mathcal{M}(\mathbf{f}_S, \mathbf{f}_D, g_D). \quad (3.86)$$

*Proof.* Similarly to the continuous case, and noticing that the well-definiteness of  $\mathbf{T}_h$  is equivalent to the well-posedness of problem (3.69), the result is a direct consequence of Lemmas 3.14, 3.15, 3.16 and 3.19, and Theorem 3.13.  $\square$

Having verified the well-definiteness of operator  $\mathbf{T}_h$ , now we are in position of establishing the main result of this section, namely, the well-posedness of problem (3.58).

**Theorem 3.21.** *Let  $\mathbf{W}_h$  be the compact convex subset of  $\mathbf{H}_{h,\Gamma_S}^1(\Omega_S)$  defined by*

$$\mathbf{W}_h := \left\{ \mathbf{v}_{S,h} \in \mathbf{H}_{h,\Gamma_S}^1(\Omega_S) : \|\mathbf{v}_{S,h}\|_{1,\Omega_S} \leq \tilde{c}_{\mathbf{T}} \mathcal{M}(\mathbf{f}_S, \mathbf{f}_D, g_D) \right\}. \quad (3.87)$$

*Assume that the data  $\mathbf{f}_S, \mathbf{f}_D$ , and  $g_D$  satisfy*

$$\mathcal{M}(\mathbf{f}_S, \mathbf{f}_D, g_D) < \tilde{r}, \quad (3.88)$$

*where*

$$\tilde{r} := \frac{2\mu\alpha_S}{\tilde{c}_{\mathbf{T}}\rho} \min \left\{ \frac{1}{C_S^2(2+\sqrt{2})}, \frac{1}{C_s^2 C_{\text{tr}}^3} \right\},$$

*and  $\tilde{c}_{\mathbf{T}} > 0$  is the constant in (3.86). Then, there exists a unique  $(\mathbf{u}_h, (p_h, \lambda_h)) \in \mathbf{H}_h \times \mathbf{Q}_h$  solution to (3.58), which satisfies  $\mathbf{u}_{S,h} \in \mathbf{W}_h$  and*

$$\|(\mathbf{u}_h, (p_h, \lambda_h))\|_{\mathbf{H} \times \mathbf{Q}} \leq \tilde{c}_{\mathbf{T}} \mathcal{M}(\mathbf{f}_S, \mathbf{f}_D, g_D). \quad (3.89)$$

*Proof.* We first observe thanks to (3.86), that assumption (3.88) guarantees that  $\mathbf{T}_h(\mathbf{W}_h) \subseteq \mathbf{W}_h$ . Next, proceeding analogously to the proof of Lemma 3.9, the assumption (3.88) implies the estimate

$$\begin{aligned} \mu\alpha_S \|\mathbf{T}_h(\mathbf{w}_{S,h}) - \mathbf{T}_h(\tilde{\mathbf{w}}_{S,h})\|_{1,\Omega_S}^2 &\leq [\mathbf{a}_h(\mathbf{w}_{S,h})(\mathbf{u}_h) - \mathbf{a}_h(\mathbf{w}_{S,h})(\tilde{\mathbf{u}}_h), \mathbf{u}_h - \tilde{\mathbf{u}}_h] \\ &= [\mathcal{B}_S^h(\tilde{\mathbf{w}}_{S,h} - \mathbf{w}_{S,h})(\tilde{\mathbf{u}}_{S,h}), \mathbf{u}_{S,h} - \tilde{\mathbf{u}}_{S,h}], \end{aligned}$$

which, together with the continuity of  $\mathcal{B}_S^h$  (see (3.61)) leads to

$$\|\mathbf{T}_h(\mathbf{w}_{S,h}) - \mathbf{T}_h(\tilde{\mathbf{w}}_{S,h})\|_{1,\Omega_S} \leq \frac{\rho C_S^2(2+\sqrt{2})}{2\mu\alpha_S} \|\mathbf{T}_h(\tilde{\mathbf{w}}_{S,h})\|_{1,\Omega_S} \|\mathbf{w}_{S,h} - \tilde{\mathbf{w}}_{S,h}\|_{1,\Omega_S}, \quad (3.90)$$

thus proving the continuity of  $\mathbf{T}_h$ . Then, the existence result follows from the Brower fixed-point theorem. Moreover, from (3.90) and the fact that  $\mathbf{T}_h(\tilde{\mathbf{w}}_{S,h})$  belongs to  $\mathbf{W}_h$ , it is easy to see that  $\mathbf{T}_h$  is a contraction mapping if and only if (3.88) holds, which due to the Banach fixed-point theorem, implies the uniqueness of solution. In turn, the a priori estimate (3.89) follows directly from (3.86).  $\square$

### 3.5 A priori error analysis

Now we establish the corresponding Céa estimate and the theoretical rate of convergence of the Galerkin scheme (3.58). To that end, we first introduce some notations and state some previous results. We begin by defining the set

$$\mathbf{H}_h^{\mathbf{g}} := \left\{ \mathbf{v}_h := (\mathbf{v}_{S,h}, \mathbf{v}_{D,h}) \in \mathbf{H}_h : [\mathbf{b}(\mathbf{v}_h), (q_h, \xi_h)] = [\mathbf{g}, (q_h, \xi_h)] \quad \forall (q_h, \xi_h) \in \mathbf{Q}_h \right\},$$

which is clearly noempty, since (3.84) holds. Also, it is not difficult to see that, due to the inf-sup condition (3.84), the following inequality holds (cf. [81, Theorem 2.6], [144, Théorème 2.1]):

$$\inf_{\mathbf{v}_h \in \mathbf{H}_h^{\mathbf{g}}} \|\mathbf{u} - \mathbf{v}_h\|_{\mathbf{H}} \leq \left(1 + \frac{C_{\mathbf{b}}}{\beta}\right) \inf_{\mathbf{v}_h \in \mathbf{H}_h} \|\mathbf{u} - \mathbf{v}_h\|_{\mathbf{H}}. \quad (3.91)$$

In turn, in order to simplify the subsequent analysis, we write  $\mathbf{e}_{\mathbf{u}_S} = \mathbf{u}_S - \mathbf{u}_{S,h}$ ,  $\mathbf{e}_{\mathbf{u}_D} = \mathbf{u}_D - \mathbf{u}_{D,h}$ ,  $e_p = p - p_h$ , and  $e_\lambda = \lambda - \lambda_h$ . As usual, for a given  $\bar{\mathbf{v}}_h = (\bar{\mathbf{v}}_{S,h}, \bar{\mathbf{v}}_{D,h}) \in \mathbf{H}_h^{\mathbf{g}}$  and  $(\bar{q}_h, \bar{\xi}_h) \in \mathbf{Q}_h$ , we shall then decompose these errors into

$$\mathbf{e}_{\mathbf{u}_S} = \boldsymbol{\delta}_{\mathbf{u}_S} + \boldsymbol{\eta}_{\mathbf{u}_S}, \quad \mathbf{e}_{\mathbf{u}_D} = \boldsymbol{\delta}_{\mathbf{u}_D} + \boldsymbol{\eta}_{\mathbf{u}_D}, \quad e_p = \delta_p + \eta_p, \quad e_\lambda = \delta_\lambda + \eta_\lambda, \quad (3.92)$$

with

$$\begin{aligned} \boldsymbol{\delta}_{\mathbf{u}_S} &= \mathbf{u}_S - \bar{\mathbf{v}}_{S,h}, & \boldsymbol{\eta}_{\mathbf{u}_S} &= \bar{\mathbf{v}}_{S,h} - \mathbf{u}_{S,h}, & \boldsymbol{\delta}_{\mathbf{u}_D} &= \mathbf{u}_D - \bar{\mathbf{v}}_{D,h}, & \boldsymbol{\eta}_{\mathbf{u}_D} &= \bar{\mathbf{v}}_{D,h} - \mathbf{u}_{D,h}, \\ \delta_p &= p - \bar{q}_h, & \eta_p &= \bar{q}_h - p_h, & \delta_\lambda &= \lambda - \bar{\xi}_h, & \eta_\lambda &= \bar{\xi}_h - \lambda_h. \end{aligned} \quad (3.93)$$

Finally, since the exact solution  $\mathbf{u}_S \in \mathbf{H}_{\Gamma_S}^1(\Omega_S)$  satisfies  $\operatorname{div} \mathbf{u}_S = 0$  in  $\Omega_S$ , we have

$$[\mathcal{B}_S^h(\mathbf{u}_S)(\mathbf{u}_S), \mathbf{v}_{S,h}] = [\mathcal{B}_S(\mathbf{u}_S)(\mathbf{u}_S), \mathbf{v}_{S,h}] \quad \forall \mathbf{v}_{S,h} \in \mathbf{H}_{h,\Gamma_S}(\Omega_S).$$

Consequently, the following Galerkin orthogonality property holds:

$$\begin{aligned} & [\mathcal{A}_S(\mathbf{e}_{\mathbf{u}_S}), \mathbf{v}_{S,h}] + [\mathcal{B}_S^h(\mathbf{u}_S)(\mathbf{u}_S), \mathbf{v}_{S,h}] - [\mathcal{B}_S^h(\mathbf{u}_{S,h})(\mathbf{u}_{S,h}), \mathbf{v}_{S,h}] \\ & + [\mathcal{A}_D(\mathbf{u}_D) - \mathcal{A}_D(\mathbf{u}_{D,h}), \mathbf{v}_{D,h}] + [\mathbf{b}(\mathbf{v}_h), (e_p, e_\lambda)] = 0 \\ & [\mathbf{b}(\mathbf{e}_{\mathbf{u}_S}, \mathbf{e}_{\mathbf{u}_D}), (q_h, \xi_h)] = 0 \end{aligned} \quad (3.94)$$

for all  $\mathbf{v}_h := (\mathbf{v}_{S,h}, \mathbf{v}_{D,h}) \in \mathbf{H}_h$  and  $(q_h, \xi_h) \in \mathbf{Q}_h$ .

We now establish the main result of this section.

**Theorem 3.22.** *Let  $\mathbf{f}_S \in \mathbf{L}^2(\Omega_S)$ ,  $\mathbf{f}_D \in \mathbf{L}^{3/2}(\Omega_D)$  and  $g_D \in \mathbf{L}^2(\Omega_D)$ , such that*

$$\mathcal{M}(\mathbf{f}_S, \mathbf{f}_D, g_D) < \frac{1}{2} \min \{r, \tilde{r}\}, \quad (3.95)$$

where  $r$  and  $\tilde{r}$  are the constants defined in Lemma 3.11 and Theorem 3.21, respectively. Let  $(\mathbf{u}, (p, \lambda)) := ((\mathbf{u}_S, \mathbf{u}_D), (p, \lambda)) \in \mathbf{H} \times \mathbf{Q}$  and  $(\mathbf{u}_h, (p_h, \lambda_h)) := ((\mathbf{u}_{S,h}, \mathbf{u}_{D,h}), (p_h, \lambda_h)) \in \mathbf{H}_h \times \mathbf{Q}_h$  be the unique solutions of the continuous and discrete problems (3.11) and (3.58), respectively. Then there exists  $C > 0$ , independent of  $h$  and the continuous and discrete solutions, such that

$$\begin{aligned} & \|(\mathbf{u}, (p, \lambda)) - (\mathbf{u}_h, (p_h, \lambda_h))\|_{\mathbf{H} \times \mathbf{Q}} \\ & \leq C \max_{i \in \{2,3\}} \left\{ \left( \inf_{\mathbf{v}_h \in \mathbf{H}_h} \left( \|\mathbf{u} - \mathbf{v}_h\|_{\mathbf{H}} + \|\mathbf{u} - \mathbf{v}_h\|_{\mathbf{H}}^2 \right) + \inf_{(q_h, \xi_h) \in \mathbf{Q}_h} \|(p, \lambda) - (q_h, \xi_h)\|_{\mathbf{Q}} \right)^{\frac{1}{i-1}} \right\}. \end{aligned} \quad (3.96)$$

*Proof.* In what follows we adapt the proof of [65, Theorem 5] to the present case. To do that, we let  $\bar{\mathbf{v}}_h = (\bar{\mathbf{v}}_{S,h}, \bar{\mathbf{v}}_{D,h}) \in \mathbf{H}_h^{\mathbf{g}}$  and  $(\bar{q}_h, \bar{\xi}_h) \in \mathbf{Q}_h$ , and define  $\boldsymbol{\delta}_{\mathbf{u}_S}, \boldsymbol{\delta}_{\mathbf{u}_D}, \delta_p, \delta_\lambda, \boldsymbol{\eta}_{\mathbf{u}_S}, \boldsymbol{\eta}_{\mathbf{u}_D}, \eta_p$ , and  $\eta_\lambda$ , as in (3.93). In addition, we recall that thanks to assumption (3.95), it follows that  $\mathbf{u}_S \in \mathbf{W}$  and  $\mathbf{u}_{S,h} \in \mathbf{W}_h$  (cf. (3.51) and (3.87)), which implies (cf. Theorems 3.12 and 3.21):

$$\begin{aligned} \|\mathbf{u}_D\|_{\mathbf{H}^3(\text{div}; \Omega_D)}, \|\mathbf{u}_S\|_{1, \Omega_S} &\leq c_{\mathbf{T}} \mathcal{M}(\mathbf{f}_S, \mathbf{f}_D, g_D), \\ \|\mathbf{u}_{D,h}\|_{\mathbf{H}^3(\text{div}; \Omega_D)}, \|\mathbf{u}_{S,h}\|_{1, \Omega_S} &\leq \tilde{c}_{\mathbf{T}} \mathcal{M}(\mathbf{f}_S, \mathbf{f}_D, g_D). \end{aligned} \quad (3.97)$$

In turn, since  $\mathbf{u}_h, \bar{\mathbf{v}}_h \in \mathbf{H}_h^{\mathbf{g}}$ , we observe that

$$(\boldsymbol{\eta}_{\mathbf{u}_S}, \boldsymbol{\eta}_{\mathbf{u}_D}) := \bar{\mathbf{v}}_h - \mathbf{u}_h \in \mathbf{V}_h. \quad (3.98)$$

According to the above, we first note that for all  $\mathbf{v}_{S,h} \in \mathbf{H}_{h, \Gamma_S}(\Omega_S)$ , there holds

$$\begin{aligned} [\mathcal{B}_S^h(\mathbf{u}_S)(\mathbf{u}_S), \mathbf{v}_{S,h}] - [\mathcal{B}_S^h(\mathbf{u}_{S,h})(\mathbf{u}_{S,h}), \mathbf{v}_{S,h}] &= [\mathcal{B}_S^h(\mathbf{e}_{\mathbf{u}_S})(\mathbf{u}_S), \mathbf{v}_{S,h}] + [\mathcal{B}_S^h(\mathbf{u}_{S,h})(\mathbf{e}_{\mathbf{u}_S}), \mathbf{v}_{S,h}] \\ &= [\mathcal{B}_S^h(\mathbf{u}_{S,h})(\boldsymbol{\eta}_{\mathbf{u}_S}), \mathbf{v}_{S,h}] + \mathcal{R}(\mathbf{v}_{S,h}), \end{aligned} \quad (3.99)$$

with

$$\mathcal{R}(\mathbf{v}_{S,h}) = [\mathcal{B}_S^h(\mathbf{u}_{S,h})(\boldsymbol{\delta}_{\mathbf{u}_S}), \mathbf{v}_{S,h}] + [\mathcal{B}_S^h(\boldsymbol{\delta}_{\mathbf{u}_S})(\mathbf{u}_S), \mathbf{v}_{S,h}] + [\mathcal{B}_S^h(\boldsymbol{\eta}_{\mathbf{u}_S})(\mathbf{u}_S), \mathbf{v}_{S,h}].$$

Then, adding and subtracting suitable terms in the first equation of (3.94) with  $\mathbf{v}_h = (\boldsymbol{\eta}_{\mathbf{u}_S}, \boldsymbol{\eta}_{\mathbf{u}_D}) \in \mathbf{V}_h$  (cf. (3.98)), and observing that  $[\mathbf{b}(\boldsymbol{\eta}_{\mathbf{u}_S}, \boldsymbol{\eta}_{\mathbf{u}_D}), (\eta_p, \eta_\lambda)] = 0$ , we obtain

$$\begin{aligned} &[\mathbf{a}_h(\mathbf{u}_{S,h})(\bar{\mathbf{v}}_h) - \mathbf{a}_h(\mathbf{u}_{S,h})(\mathbf{u}_h), \bar{\mathbf{v}}_h - \mathbf{u}_h] \\ &= -[\mathcal{A}_S(\boldsymbol{\delta}_{\mathbf{u}_S}), \boldsymbol{\eta}_{\mathbf{u}_S}] - \mathcal{R}(\boldsymbol{\eta}_{\mathbf{u}_S}) - [\mathcal{A}_D(\mathbf{u}_D) - \mathcal{A}_D(\bar{\mathbf{v}}_{D,h}), \boldsymbol{\eta}_{\mathbf{u}_D}] - [\mathbf{b}(\boldsymbol{\eta}_{\mathbf{u}_S}, \boldsymbol{\eta}_{\mathbf{u}_D}), (\delta_p, \delta_\lambda)]. \end{aligned}$$

Hence, proceeding analogously to the proof of Lemma 3.4, using the continuity of  $\mathcal{A}_S$ ,  $\mathcal{B}_S^h$  and  $\mathbf{b}$  (cf. (3.16) and (3.61)), and inequality (3.17), we deduce that

$$\begin{aligned} &\mu \alpha_S \|\boldsymbol{\eta}_{\mathbf{u}_S}\|_{1, \Omega_S}^2 + \alpha_D \|\boldsymbol{\eta}_{\mathbf{u}_D}\|_{\mathbf{H}^3(\text{div}; \Omega_D)}^3 \\ &\leq \left\{ C_{\mathcal{A}_S} + C_{\text{sk}} \left( \|\mathbf{u}_{S,h}\|_{1, \Omega_S} + \|\mathbf{u}_S\|_{1, \Omega_S} \right) \right\} \|\boldsymbol{\delta}_{\mathbf{u}_S}\|_{1, \Omega_S} \|\boldsymbol{\eta}_{\mathbf{u}_S}\|_{1, \Omega_S} + C_{\text{sk}} \|\mathbf{u}_S\|_{1, \Omega_S} \|\boldsymbol{\eta}_{\mathbf{u}_S}\|_{1, \Omega_S}^2 \\ &\quad + L_{\mathcal{A}_D} \left\{ \left( 1 + 2 \|\mathbf{u}_D\|_{\mathbf{H}^3(\text{div}; \Omega_D)} \right) \|\boldsymbol{\delta}_{\mathbf{u}_D}\|_{\mathbf{H}^3(\text{div}; \Omega_D)} + \|\boldsymbol{\delta}_{\mathbf{u}_D}\|_{\mathbf{H}^3(\text{div}; \Omega_D)}^2 \right\} \|\boldsymbol{\eta}_{\mathbf{u}_D}\|_{\mathbf{H}^3(\text{div}; \Omega_D)} \\ &\quad + C_{\mathbf{b}} \|(\boldsymbol{\eta}_{\mathbf{u}_S}, \boldsymbol{\eta}_{\mathbf{u}_D})\|_{\mathbf{H}} \|(\delta_p, \delta_\lambda)\|_{\mathbf{Q}}, \end{aligned}$$

which, together with (3.97) and assumption (3.95), implies that there exists  $C > 0$ , depending only on parameters, data and other constants, all of them independent of  $h$ , such that

$$\|(\boldsymbol{\eta}_{\mathbf{u}_S}, \boldsymbol{\eta}_{\mathbf{u}_D})\|_{\mathbf{H}} \leq C \max_{i \in \{2,3\}} \left\{ \left( \|(\boldsymbol{\delta}_{\mathbf{u}_S}, \boldsymbol{\delta}_{\mathbf{u}_D})\|_{\mathbf{H}} + \|(\boldsymbol{\delta}_{\mathbf{u}_S}, \boldsymbol{\delta}_{\mathbf{u}_D})\|_{\mathbf{H}}^2 + \|(\delta_p, \delta_\lambda)\|_{\mathbf{Q}} \right)^{\frac{1}{i-1}} \right\}. \quad (3.100)$$

In this way, from (3.92), (3.100), and the triangle inequality, we obtain

$$\begin{aligned} \|(\mathbf{e}_{\mathbf{u}_S}, \mathbf{e}_{\mathbf{u}_D})\|_{\mathbf{H}} &\leq \|(\boldsymbol{\delta}_{\mathbf{u}_S}, \boldsymbol{\delta}_{\mathbf{u}_D})\|_{\mathbf{H}} + \|(\boldsymbol{\eta}_{\mathbf{u}_S}, \boldsymbol{\eta}_{\mathbf{u}_D})\|_{\mathbf{H}} \\ &\leq \tilde{C} \max_{i \in \{2,3\}} \left\{ \left( \|(\boldsymbol{\delta}_{\mathbf{u}_S}, \boldsymbol{\delta}_{\mathbf{u}_D})\|_{\mathbf{H}} + \|(\boldsymbol{\delta}_{\mathbf{u}_S}, \boldsymbol{\delta}_{\mathbf{u}_D})\|_{\mathbf{H}}^2 + \|(\delta_p, \delta_\lambda)\|_{\mathbf{Q}} \right)^{\frac{1}{i-1}} \right\}. \end{aligned} \quad (3.101)$$



In turn, to estimate  $e_p$  and  $e_\lambda$  we observe that from the discrete inf-sup condition (3.84), the first equation of (3.94), and the first equation of (3.99), there holds

$$\begin{aligned} \tilde{\beta} \|(\eta_p, \eta_\lambda)\|_{\mathbf{Q}} &\leq \sup_{\substack{\mathbf{v}_h \in \mathbf{H}_h \\ \mathbf{v}_h \neq \mathbf{0}}} \frac{[\mathbf{b}(\mathbf{v}_h), (\eta_p, \eta_\lambda)]}{\|\mathbf{v}_h\|_{\mathbf{H}}} = \sup_{\substack{\mathbf{v}_h \in \mathbf{H}_h \\ \mathbf{v}_h \neq \mathbf{0}}} \frac{[\mathbf{b}(\mathbf{v}_h), (e_p, e_\lambda)] - [\mathbf{b}(\mathbf{v}_h), (\delta_p, \delta_\lambda)]}{\|\mathbf{v}_h\|_{\mathbf{H}}} \\ &= \sup_{\substack{\mathbf{v}_h \in \mathbf{H}_h \\ \mathbf{v}_h \neq \mathbf{0}}} - \left\{ \frac{[\mathcal{A}_S(\mathbf{e}_{\mathbf{u}_S}), \mathbf{v}_{S,h}] + [\mathcal{B}_S^h(\mathbf{e}_{\mathbf{u}_S})(\mathbf{u}_S), \mathbf{v}_{S,h}] + [\mathcal{B}_S^h(\mathbf{u}_{S,h})(\mathbf{e}_{\mathbf{u}_S}), \mathbf{v}_{S,h}]}{\|\mathbf{v}_h\|_{\mathbf{H}}} \right. \\ &\quad \left. + \frac{[\mathcal{A}_D(\mathbf{u}_D) - \mathcal{A}_D(\mathbf{u}_{D,h}), \mathbf{v}_{D,h}] + [\mathbf{b}(\mathbf{v}_h), (\delta_p, \delta_\lambda)]}{\|\mathbf{v}_h\|_{\mathbf{H}}} \right\}. \end{aligned}$$

Then, the continuity of  $\mathcal{A}_S$ ,  $\mathcal{B}_S^h$ , and  $\mathbf{b}$  (cf. (3.16) and (3.61)), and the inequality (3.17), imply

$$\begin{aligned} \tilde{\beta} \|(\eta_p, \eta_\lambda)\|_{\mathbf{Q}} &\leq \left\{ C_{\mathcal{A}_S} + C_{\text{sk}} \left( \|\mathbf{u}_S\|_{1,\Omega_S} + \|\mathbf{u}_{S,h}\|_{1,\Omega_S} \right) \right\} \|\mathbf{e}_{\mathbf{u}_S}\|_{1,\Omega_S} \\ &\quad + L_{\mathcal{A}_D} \left\{ 1 + \|\mathbf{u}_D\|_{\mathbf{H}^3(\text{div};\Omega_D)} + \|\mathbf{u}_{D,h}\|_{\mathbf{H}^3(\text{div};\Omega_D)} \right\} \|\mathbf{e}_{\mathbf{u}_D}\|_{\mathbf{H}^3(\text{div};\Omega_D)} + C_{\mathbf{b}} \|(\delta_p, \delta_\lambda)\|_{\mathbf{Q}}, \end{aligned}$$

which, together with assumption (3.95), inequalities (3.97) and (3.101), yield

$$\|(\eta_p, \eta_\lambda)\|_{\mathbf{Q}} \leq c \max_{i \in \{2,3\}} \left\{ \left( \|(\delta_{\mathbf{u}_S}, \delta_{\mathbf{u}_D})\|_{\mathbf{H}} + \|(\delta_{\mathbf{u}_S}, \delta_{\mathbf{u}_D})\|_{\mathbf{H}}^2 + \|(\delta_p, \delta_\lambda)\|_{\mathbf{Q}} \right)^{\frac{1}{i-1}} \right\}.$$

Thus, from (3.92), the triangle inequality, and the foregoing bound, we obtain

$$\begin{aligned} \|(e_p, e_\lambda)\|_{\mathbf{Q}} &\leq \|(\delta_p, \delta_\lambda)\|_{\mathbf{Q}} + \|(\eta_p, \eta_\lambda)\|_{\mathbf{Q}} \\ &\leq \tilde{c} \max_{i \in \{2,3\}} \left\{ \left( \|(\delta_{\mathbf{u}_S}, \delta_{\mathbf{u}_D})\|_{\mathbf{H}} + \|(\delta_{\mathbf{u}_S}, \delta_{\mathbf{u}_D})\|_{\mathbf{H}}^2 + \|(\delta_p, \delta_\lambda)\|_{\mathbf{Q}} \right)^{\frac{1}{i-1}} \right\}, \end{aligned} \tag{3.102}$$

where  $\tilde{c} > 0$  is independent of  $h$ . Therefore, recalling that  $\bar{\mathbf{v}}_h \in \mathbf{H}_h^{\mathbf{g}}$  and  $(\bar{q}_h, \bar{\lambda}_h) \in \mathbf{Q}_h$  are arbitrary, (3.101) and (3.102) give

$$\begin{aligned} &\|((\mathbf{e}_{\mathbf{u}_S}, \mathbf{e}_{\mathbf{u}_D}), (e_p, e_\lambda))\|_{\mathbf{H} \times \mathbf{Q}} \\ &\leq C \max_{i \in \{2,3\}} \left\{ \left( \inf_{\mathbf{v}_h \in \mathbf{H}_h^{\mathbf{g}}} \left( \|\mathbf{u} - \mathbf{v}_h\|_{\mathbf{H}} + \|\mathbf{u} - \mathbf{v}_h\|_{\mathbf{H}}^2 \right) + \inf_{(q_h, \xi_h) \in \mathbf{Q}_h} \|(p, \lambda) - (q_h, \xi_h)\|_{\mathbf{Q}} \right)^{\frac{1}{i-1}} \right\}, \end{aligned}$$

which, together with (3.91), concludes the proof.  $\square$

Now, in order to provide the theoretical rate of convergence of the Galerkin scheme (3.58), we recall the approximation properties of the subspaces involved (see, e.g., [17, 69, 72, 81]). Note that each one of them is named after the unknown to which it is applied later on.

( $\mathbf{AP}_h^{\mathbf{u}_S}$ ) For each  $\mathbf{v}_S \in \mathbf{H}^2(\Omega_S)$ , there holds

$$\|\mathbf{v}_S - \Pi_S(\mathbf{v}_S)\|_{1,\Omega_S} \leq Ch \|\mathbf{v}_S\|_{2,\Omega_S}.$$

( $\mathbf{AP}_h^{\mathbf{u}_D}$ ) For each  $\mathbf{v}_D \in \mathbf{W}^{1,3}(\Omega_D)$  with  $\text{div } \mathbf{v}_D \in \mathbf{H}^1(\Omega_D)$ , there holds

$$\|\mathbf{v}_D - \Pi_D(\mathbf{v}_D)\|_{\mathbf{H}^3(\text{div};\Omega_D)} \leq Ch \left\{ \|\mathbf{v}_D\|_{1,3;\Omega_D} + \|\text{div } \mathbf{v}_D\|_{1,\Omega_D} \right\}.$$

( $\mathbf{AP}_h^p$ ) For each  $q \in H^1(\Omega) \cap L_0^2(\Omega)$ , there exists  $q_h \in L_{h,0}(\Omega)$  such that

$$\|q - q_h\|_{0,\Omega} \leq Ch\|q\|_{1,\Omega}.$$

( $\mathbf{AP}_h^\lambda$ ) For each  $\xi \in W^{1,\frac{3}{2}}(\Sigma)$ , there exists  $\xi_h \in \Lambda_h(\Sigma)$  such that

$$\|\xi - \xi_h\|_{\frac{1}{3},\frac{3}{2};\Sigma} \leq Ch^{2/3}\|\xi\|_{1,\frac{3}{2};\Sigma}.$$

We remark that the sub-optimal approximation property ( $\mathbf{AP}_h^\lambda$ ) follows from the fact that  $W^{\frac{1}{3},\frac{3}{2}}(\Sigma)$  is the interpolation space with index  $1/3$  between  $W^{1,\frac{3}{2}}(\Sigma)$  and  $L^{3/2}(\Sigma)$  (cf. [18, Corollary 3.2-(a)]), and from the estimate  $\|\xi - \xi_h\|_{L^{3/2}(\Sigma)} \leq Ch\|\xi\|_{1,\frac{3}{2};\Sigma}$ , which is valid for all  $\xi \in W^{1,\frac{3}{2}}(\Sigma)$  and  $\xi_h := \mathcal{P}_\Sigma(\xi)$ , with  $\mathcal{P}_\Sigma$  being the  $L^2(\Sigma)$ -orthogonal projection onto  $\Lambda_h(\Sigma)$  (cf. [69, Proposition 1.135]). In fact, given  $\xi \in W^{1,\frac{3}{2}}(\Sigma)$  there exists a constant  $C > 0$ , depending on  $\Sigma$ , such that

$$\|\xi - \xi_h\|_{\frac{1}{3},\frac{3}{2};\Sigma} \leq c\|\xi - \xi_h\|_{L^{3/2}(\Sigma)}^{1-1/3}\|\xi\|_{1,\frac{3}{2};\Sigma}^{1/3} \leq Ch^{2/3}\|\xi\|_{1,\frac{3}{2};\Sigma},$$

where we have used the fact that  $\xi_h$  is piecewise constant and then  $\|\xi - \xi_h\|_{1,\frac{3}{2};\Sigma} \leq c\|\xi\|_{1,\frac{3}{2};\Sigma}$ .

The following theorem provides the theoretical sub-optimal rate of convergence of the Galerkin scheme (3.58), under suitable regularity assumptions on the exact solution.

**Theorem 3.23.** *Let  $\mathbf{f}_S \in \mathbf{L}^2(\Omega_S)$ ,  $\mathbf{f}_D \in \mathbf{L}^{3/2}(\Omega_D)$  and  $g_D \in L^2(\Omega_D)$ , such that (3.95) holds. Let  $(\mathbf{u}, (p, \lambda)) := ((\mathbf{u}_S, \mathbf{u}_D), (p, \lambda)) \in \mathbf{H} \times \mathbf{Q}$  and  $(\mathbf{u}_h, (p_h, \lambda_h)) := ((\mathbf{u}_{S,h}, \mathbf{u}_{D,h}), (p_h, \lambda_h)) \in \mathbf{H}_h \times \mathbf{Q}_h$  be the unique solutions of the continuous and discrete problems (3.11) and (3.58), respectively, and assume that  $\mathbf{u}_S \in \mathbf{H}^2(\Omega_S)$ ,  $\mathbf{u}_D \in \mathbf{W}^{1,3}(\Omega_D)$ ,  $\operatorname{div} \mathbf{u}_D \in H^1(\Omega_D)$ ,  $p \in H^1(\Omega)$ , and  $\lambda \in W^{1,\frac{3}{2}}(\Sigma)$ . Then, there exists  $C > 0$ , independent of  $h$  and the continuous and discrete solutions, such that*

$$\begin{aligned} \|(\mathbf{u}, (p, \lambda)) - (\mathbf{u}_h, (p_h, \lambda_h))\|_{\mathbf{H} \times \mathbf{Q}} &\leq Ch^{1/3} \max_{i \in \{2,3\}} \left\{ \left( \|\mathbf{u}_S\|_{2,\Omega_S} + \|\mathbf{u}_D\|_{1,3;\Omega_D} + \|\operatorname{div} \mathbf{u}_D\|_{1,\Omega_D} \right. \right. \\ &\quad \left. \left. + \|\mathbf{u}_S\|_{2,\Omega_S}^2 + \|\mathbf{u}_D\|_{1,3;\Omega_D}^2 + \|\operatorname{div} \mathbf{u}_D\|_{1,\Omega_D}^2 + \|p\|_{1,\Omega} + \|\lambda\|_{1,\frac{3}{2};\Sigma} \right)^{\frac{1}{i-1}} \right\}. \end{aligned} \quad (3.103)$$

*Proof.* It suffices to apply Theorem 3.22 and the approximation properties of the discrete subspaces. We omit further details.  $\square$

## 3.6 Numerical results

In this section we present some examples illustrating the performance of our mixed finite element scheme (3.58) on a set of quasi-uniform triangulations of the corresponding domains. Our implementation is based on a FreeFem++ code [111], in conjunction with the direct linear solver UMFPACK [62].

In order to solve the nonlinear problem (3.58), given  $\mathbf{w}_D \in \mathbf{H}_{\Gamma_D}^3(\operatorname{div}; \Omega_D)$  we introduce the Gâteaux derivative associated to  $\mathcal{A}_D$  (cf. (3.13)), i.e.,

$$\mathcal{DA}_D(\mathbf{w}_D)(\mathbf{u}_D, \mathbf{v}_D) := \frac{\mu}{\rho} (\mathbf{K}^{-1} \mathbf{u}_D, \mathbf{v}_D)_D + \frac{F}{\rho} (|\mathbf{w}_D| \mathbf{u}_D, \mathbf{v}_D)_D + \frac{F}{\rho} \left( \frac{\mathbf{w}_D \cdot \mathbf{u}_D}{|\mathbf{w}_D|}, \mathbf{w}_D \cdot \mathbf{v}_D \right)_D,$$

for all  $\mathbf{u}_D, \mathbf{v}_D \in \mathbf{H}_{\Gamma_D}^3(\text{div}; \Omega_D)$ . In this way, we propose the Newton-type strategy: Given  $\mathbf{u}_h^0 = (\mathbf{u}_{S,h}^0, \mathbf{u}_{D,h}^0) \in \mathbf{H}_h$ ,  $p_h^0 \in L_{h,0}(\Omega)$  and  $\lambda_h^0 \in \Lambda_h(\Sigma)$ , for  $m \geq 1$ , find  $\mathbf{u}_h^m = (\mathbf{u}_{S,h}^m, \mathbf{u}_{D,h}^m) \in \mathbf{H}_h$ ,  $p_h^m \in L_{h,0}(\Omega)$  and  $\lambda_h^m \in \Lambda_h(\Sigma)$ , such that

$$\begin{aligned} & [\mathcal{A}_S(\mathbf{u}_{S,h}^m), \mathbf{v}_{S,h}] + [\mathcal{B}_S^h(\mathbf{u}_{S,h}^{m-1})(\mathbf{u}_{S,h}^m), \mathbf{v}_{S,h}] + [\mathcal{B}_S^h(\mathbf{u}_{S,h}^m)(\mathbf{u}_{S,h}^{m-1}), \mathbf{v}_{S,h}] + \mathcal{D}\mathcal{A}_D(\mathbf{u}_{D,h}^{m-1})(\mathbf{u}_{D,h}^m, \mathbf{v}_{D,h}) \\ & + [\mathbf{b}(\mathbf{v}_h), (p_h^m, \lambda_h^m)] = [\mathcal{B}_S^h(\mathbf{u}_{S,h}^{m-1})(\mathbf{u}_{S,h}^{m-1}), \mathbf{v}_{S,h}] + \frac{F}{\rho} \left( |\mathbf{u}_{D,h}^{m-1}| \mathbf{u}_{D,h}^{m-1}, \mathbf{v}_{D,h} \right)_D + [\mathbf{f}, \mathbf{v}_h] \\ & [\mathbf{b}(\mathbf{u}_h^m), (q_h, \xi_h)] = [\mathbf{g}, (q_h, \xi_h)] \end{aligned} \quad (3.104)$$

for all  $\mathbf{v}_h = (\mathbf{v}_{S,h}, \mathbf{v}_{D,h}) \in \mathbf{H}_h$  and  $(q_h, \xi_h) \in \mathbf{Q}_h$ .

In all the numerical experiments below, the iterations are terminated once the relative error of the entire coefficient vectors between two consecutive iterates is sufficiently small, i.e.,

$$\frac{\|\text{coeff}^{m+1} - \text{coeff}^m\|_{l^2}}{\|\text{coeff}^{m+1}\|_{l^2}} \leq \text{tol},$$

where  $\|\cdot\|_{l^2}$  is the standard  $l^2$ -norm in  $\mathbb{R}^N$ , with  $N$  denoting the total number of degrees of freedom defining the finite element subspaces  $\mathbf{H}_h$  and  $\mathbf{Q}_h$ , and  $\text{tol}$  is a fixed tolerance chosen as  $\text{tol} = 1E - 06$ . For each example shown below we simply take  $\mathbf{u}_h^0 = (\mathbf{0}, (0.1, 0))$  and  $(p_h^0, \lambda_h^0) = \mathbf{0}$  as initial guess. As usual, the individual errors are denoted by:

$$\mathbf{e}(\mathbf{u}_S) := \|\mathbf{u}_S - \mathbf{u}_{S,h}\|_{1,\Omega_S}, \quad \mathbf{e}(\mathbf{u}_D) := \|\mathbf{u}_D - \mathbf{u}_{D,h}\|_{\mathbf{H}^3(\text{div}; \Omega_D)},$$

$$\mathbf{e}(p_S) := \|p_S - p_{S,h}\|_{0,\Omega_S}, \quad \mathbf{e}(p_D) := \|p_D - p_{D,h}\|_{0,\Omega_D}, \quad \mathbf{e}(\lambda) := \|\lambda - \lambda_h\|_{L^{3/2}(\Sigma)}.$$

Notice that we considered  $\|\lambda - \lambda_h\|_{L^{3/2}(\Sigma)}$  in place of  $\|\lambda - \lambda_h\|_{\frac{1}{3}, \frac{3}{2}; \Sigma}$  because of the last norm is not computable. Notice also that  $\|\lambda - \lambda_h\|_{L^{3/2}(\Sigma)}$  satisfies the sub-optimal rate of convergence (3.103). Next, we define the experimental rates of convergence

$$\begin{aligned} r(\mathbf{u}_S) &:= \frac{\log(\mathbf{e}(\mathbf{u}_S)/\mathbf{e}'(\mathbf{u}_S))}{\log(h_S/h'_S)}, \quad r(\mathbf{u}_D) := \frac{\log(\mathbf{e}(\mathbf{u}_D)/\mathbf{e}'(\mathbf{u}_D))}{\log(h_D/h'_D)}, \\ r(p_S) &:= \frac{\log(\mathbf{e}(p_S)/\mathbf{e}'(p_S))}{\log(h_S/h'_S)}, \quad r(p_D) := \frac{\log(\mathbf{e}(p_D)/\mathbf{e}'(p_D))}{\log(h_D/h'_D)}, \quad r(\lambda) := \frac{\log(\mathbf{e}(\lambda)/\mathbf{e}'(\lambda))}{\log(h_\Sigma/h'_\Sigma)}, \end{aligned}$$

where  $h_\star$  and  $h'_\star$  ( $\star \in \{S, D, \Sigma\}$ ) denote two consecutive mesh sizes with their respective errors  $\mathbf{e}$  and  $\mathbf{e}'$ .

The examples to be considered in this section are described next. In all of them, for the sake of simplicity, we choose the parameters  $\mu = 1$ ,  $\rho = 1$ ,  $\alpha_d = 1$ ,  $\kappa = \mathbb{I}$ , and  $\mathbf{K} = \mathbb{I}$ . In addition, the condition  $\int_\Omega p_h = 0$  is imposed via a penalization strategy.

### Example 1: Tombstone-shaped domain without source in the porous media.

In our first example we consider a semi-disk-shaped fluid domain coupled with a porous unit square, i.e.,  $\Omega_S := \{(x_1, x_2) : x_1^2 + (x_2 - 0.5)^2 < 0.5^2, x_2 > 0.5\}$  and  $\Omega_D := (-0.5, 0.5)^2$ . We consider the Forchheimer number  $F = 1$  and the data  $\mathbf{f}_S, \mathbf{f}_D$ , and  $g_D$ , are adjusted so that the exact solution in the tombstone-shaped domain  $\Omega = \Omega_S \cup \Sigma \cup \Omega_D$  is given by the smooth functions

$$\begin{aligned}
\mathbf{u}_S(x_1, x_2) &= \begin{pmatrix} \pi \cos(\pi x_1) \sin(\pi x_2) \\ -\pi \sin(\pi x_1) \cos(\pi x_2) \end{pmatrix} \quad \text{in } \Omega_S, \\
\mathbf{u}_D(x_1, x_2) &= \begin{pmatrix} \pi \sin(\pi x_2) \exp(x_1) \\ \cos(\pi x_2) \exp(x_1) \end{pmatrix} \quad \text{in } \Omega_D, \\
p_\star(x_1, x_2) &= \sin(\pi x_1) \sin(\pi x_2) \quad \text{in } \Omega_\star, \quad \text{with } \star \in \{S, D\}.
\end{aligned}$$

Notice that the source of the porous media is  $g_D = 0$ . Notice also that this solution satisfies  $\mathbf{u}_S \cdot \mathbf{n} = \mathbf{u}_D \cdot \mathbf{n}$  on  $\Sigma$ . However, the Beavers–Joseph–Saffman condition (cf. (3.4)) is not satisfied, the Dirichlet boundary condition for the Navier–Stokes velocity on  $\Gamma_S$  and the Neumann boundary condition for the Darcy–Forchheimer velocity on  $\Gamma_D$  are both non-homogeneous. In this way, the right-hand side of the resulting system must be modified accordingly.

### Example 2: Rectangle domain with a Kovasznay solution.

In our second example we consider a rectangular domain  $\Omega = \Omega_S \cup \Sigma \cup \Omega_D$ , with  $\Omega_S := (-0.5, 1.5) \times (0, 0.5)$  and  $\Omega_D := (-0.5, 1.5) \times (-0.5, 0)$ . We consider the Forchheimer number  $F = 1$  and the data  $\mathbf{f}_S, \mathbf{f}_D$ , and  $g_D$ , are adjusted so that the exact solution in the rectangle domain  $\Omega$  is given by the smooth functions

$$\begin{aligned}
\mathbf{u}_S(x_1, x_2) &= \begin{pmatrix} 1 - \exp(\omega x_1) \cos(2\pi x_2) \\ \frac{\omega}{2\pi} \exp(\omega x_1) \sin(2\pi x_2) \end{pmatrix} \quad \text{in } \Omega_S, \\
\mathbf{u}_D(x_1, x_2) &= \begin{pmatrix} (x_1 + 0.5)(x_1 - 1.5) \exp(x_2) \\ (x_2 + 2)(2x_2 + 1) \exp(x_1) \end{pmatrix} \quad \text{in } \Omega_D, \\
p_\star(x_1, x_2) &= -\frac{1}{2} \exp(2\omega x_1) + p_0 \quad \text{in } \Omega_\star, \quad \text{with } \star \in \{S, D\},
\end{aligned}$$

and

$$\omega = \frac{-8\pi^2}{\mu^{-1} + \sqrt{\mu^{-1} + 16\pi^2}}.$$

The constant  $p_0$  is such that  $\int_\Omega p = 0$ . Notice that  $(\mathbf{u}_S, p_S)$  is the well known analytical solution for the Navier–Stokes problem obtained by Kovasznay in [121], which presents a boundary layer at  $\{-0.5\} \times (-0.5, 0.5)$ . Notice also that in this example both the conservation of mass and the Beavers–Joseph–Saffman boundary conditions (cf. (3.4)) are not satisfied and the right-hand side of the resulting system must be modified accordingly.

### Example 3: 2D helmet-shaped domain with different Forchheimer numbers.

In our last example we focus on the performance of the iterative method (3.104) with respect to the Forchheimer number  $F$ . To that end, and motivated by [31, Section 2], we consider a 2D helmet-shaped domain. More precisely, we consider the domain  $\Omega = \Omega_S \cup \Sigma \cup \Omega_D$ , where  $\Omega_D := (-1, 1) \times (-0.5, 0)$  and  $\Omega_S := (-1, -0.75) \times (0, 1.25) \cup \Omega_{S,1} \cup (-0.5, 0.5) \times (0, 0.25) \cup \Omega_{S,2} \cup (0.75, 1) \times (0, 1.25)$ , with

$$\Omega_{S,1} := \left\{ (x_1, x_2) : (x_1 + 0.5)^2 + (x_2 - 0.5)^2 > 0.25^2, -0.75 < x_1 < -0.5, x_2 > 0 \right\}$$

and

$$\Omega_{S,2} := \left\{ (x_1, x_2) : (x_1 - 0.5)^2 + (x_2 - 0.5)^2 > 0.25^2, 0.5 < x_1 < 0.75, x_2 > 0 \right\}.$$

The data  $\mathbf{f}_S$ ,  $\mathbf{f}_D$ , and  $g_D$ , are chosen so that the exact solution in the 2D helmet-shaped domain  $\Omega$  is given by the smooth functions

$$\begin{aligned} \mathbf{u}_S(x_1, x_2) &= \begin{pmatrix} -\sin(2\pi x_1) \cos(2\pi x_2) \\ \cos(2\pi x_1) \sin(2\pi x_2) \end{pmatrix} \quad \text{in } \Omega_S, \\ \mathbf{u}_D(x_1, x_2) &= \begin{pmatrix} \sin(2\pi x_1) \exp(x_2) \\ \sin(2\pi x_2) \exp(x_1) \end{pmatrix} \quad \text{in } \Omega_D, \\ p_\star(x_1, x_2) &= \sin(\pi x_1) \exp(x_2) + p_0 \quad \text{in } \Omega_\star, \quad \text{with } \star \in \{S, D\}. \end{aligned}$$

The constant  $p_0$  is such that  $\int_\Omega p = 0$ . Notice that, this solution satisfies  $\mathbf{u}_S \cdot \mathbf{n} = \mathbf{u}_D \cdot \mathbf{n}$  on  $\Sigma$  and  $\mathbf{u}_D \cdot \mathbf{n} = 0$  on  $\Gamma_D$ . However, the Beavers–Joseph–Saffman condition (cf. (3.4)) is not satisfied and the Dirichlet boundary condition for the Navier–Stokes velocity on  $\Gamma_S$  is non-homogeneous and therefore the right-hand side of the resulting system must be modified accordingly.

In Tables 3.1, 3.2 and 3.4 we summarise the convergence history for a sequence of quasi-uniform triangulations, considering the finite element spaces introduced in Section 3.4.1, and solving the nonlinear problem (3.104), which require around eight, six and nine Newton iterations for the Examples 1, 2 and 3, respectively. We observe that the sub-optimal rate of convergence  $O(h^{1/3})$  provided by Theorem 3.23 is attained in all the cases. Even more, the numerical result suggest that there exist a way to prove optimal rate of convergence  $O(h)$ . In Table 3.3 we show the behaviour of the iterative method (3.104) as a function of the Forchheimer number  $F$ , considering different mesh sizes  $h := \max\{h_S, h_D\}$ , and a tolerance  $\text{tol} = 1E - 06$ . Here we observe that the higher the parameter  $F$  the higher the number of iterations as it occurs also in the Newton method for the Navier–Stokes/Darcy–Forchheimer coupled problem. Notice also that when  $F = 0$  the Darcy–Forchheimer equations reduce to the classical linear Darcy equations and as expected the iterative Newton method (3.104) is faster.

On the other hand, the velocity components, velocity streamlines and pressure field in the whole domain of the approximate solutions for the three examples are displayed in Figures 3.2, 3.3, and 3.4. All the figures were obtained with 588445, 858658, and 883963 degrees of freedom for the Examples 1, 2, and 3, respectively. In particular, we can observe in Figure 3.2 that the second components of  $\mathbf{u}_S$  and  $\mathbf{u}_D$  coincide on  $\Sigma$  as expected, and hence, the continuity of the normal components of the velocities on  $\Sigma$  is preserved. In turn, we can see that the velocity streamlines are higher in the Darcy–Forchheimer domain. Moreover, it can be seen that the pressure is continuous in the whole domain and preserves the sinusoidal behaviour. Next, in Figure 3.3 we observe that the pressure presents a boundary layer at  $\{-0.5\} \times (-0.5, 0.5)$  as expected. Finally, similarly to Figure 3.2, in Figure 3.4 we can also observe the continuity of the normal components of the velocities on  $\Sigma$  since their second components coincide on the interface.

| $N$    | $h_S$      | $e(\mathbf{u}_S)$ | $r(\mathbf{u}_S)$ | $e(p_S)$ | $r(p_S)$ |
|--------|------------|-------------------|-------------------|----------|----------|
| 691    | 0.1915     | 0.4439            | –                 | 0.1588   | –        |
| 2491   | 0.0911     | 0.2293            | 0.8896            | 0.0725   | 1.0561   |
| 9562   | 0.0486     | 0.1188            | 1.0441            | 0.0382   | 1.0179   |
| 37815  | 0.0242     | 0.0531            | 1.1558            | 0.0175   | 1.1214   |
| 149693 | 0.0134     | 0.0288            | 1.0380            | 0.0094   | 1.0474   |
| 588445 | 0.0078     | 0.0147            | 1.2290            | 0.0048   | 1.2231   |
| $N$    | $h_D$      | $e(\mathbf{u}_D)$ | $r(\mathbf{u}_D)$ | $e(p_D)$ | $r(p_D)$ |
| 691    | 0.1901     | 0.3481            | –                 | 0.0643   | –        |
| 2491   | 0.0978     | 0.1678            | 1.0974            | 0.0305   | 1.1202   |
| 9562   | 0.0535     | 0.0856            | 1.1169            | 0.0151   | 1.1629   |
| 37815  | 0.0249     | 0.0427            | 0.9122            | 0.0075   | 0.9206   |
| 149693 | 0.0145     | 0.0214            | 1.2713            | 0.0037   | 1.2840   |
| 588445 | 0.0068     | 0.0107            | 0.9140            | 0.0019   | 0.9087   |
| $N$    | $h_\Sigma$ | $e(\lambda)$      | $r(\lambda)$      | iter     |          |
| 691    | 0.1250     | 0.0718            | –                 | 7        |          |
| 2491   | 0.0625     | 0.0352            | 1.0308            | 7        |          |
| 9562   | 0.0313     | 0.0175            | 1.0084            | 8        |          |
| 37815  | 0.0156     | 0.0087            | 1.0060            | 8        |          |
| 149693 | 0.0078     | 0.0043            | 1.0012            | 8        |          |
| 588445 | 0.0039     | 0.0022            | 1.0004            | 8        |          |

Table 3.1: EXAMPLE 1, Degrees of freedom, mesh sizes, errors, convergence history and Newton iteration count for the approximation of the Navier–Stokes/Darcy–Forchheimer problem with  $F = 1$ .

| $N$    | $h_S$  | $e(\mathbf{u}_S)$ | $r(\mathbf{u}_S)$ | $e(p_S)$ | $r(p_S)$ |
|--------|--------|-------------------|-------------------|----------|----------|
| 989    | 0.2001 | 10.3170           | –                 | 8.2614   | –        |
| 3880   | 0.0966 | 4.5495            | 1.1249            | 3.9855   | 1.0015   |
| 13888  | 0.0492 | 2.2051            | 1.0713            | 1.8753   | 1.1151   |
| 55727  | 0.0270 | 1.1168            | 1.1342            | 0.9489   | 1.1357   |
| 213833 | 0.0161 | 0.5456            | 1.3877            | 0.4746   | 1.3423   |
| 858658 | 0.0078 | 0.2769            | 0.9419            | 0.2404   | 0.9444   |

| $N$    | $h_D$  | $e(\mathbf{u}_D)$ | $r(\mathbf{u}_D)$ | $e(p_D)$ | $r(p_D)$ |
|--------|--------|-------------------|-------------------|----------|----------|
| 989    | 0.2001 | 0.4678            | –                 | 7.2964   | –        |
| 3880   | 0.0950 | 0.2249            | 0.9835            | 3.3197   | 1.0578   |
| 13888  | 0.0500 | 0.1145            | 1.0518            | 1.7322   | 1.0135   |
| 55727  | 0.0254 | 0.0569            | 1.0326            | 0.9133   | 0.9457   |
| 213833 | 0.0160 | 0.0278            | 1.5453            | 0.4353   | 1.5956   |
| 858658 | 0.0066 | 0.0141            | 0.7674            | 0.2295   | 0.7283   |

| $N$    | $h_\Sigma$ | $e(\lambda)$ | $r(\lambda)$ | iter |
|--------|------------|--------------|--------------|------|
| 989    | 0.1250     | 8.9940       | –            | 6    |
| 3880   | 0.0625     | 4.6538       | 0.9505       | 6    |
| 13888  | 0.0313     | 2.3459       | 0.9883       | 6    |
| 55727  | 0.0156     | 1.1788       | 0.9928       | 6    |
| 213833 | 0.0078     | 0.5962       | 0.9835       | 6    |
| 858658 | 0.0039     | 0.3078       | 0.9539       | 6    |

Table 3.2: EXAMPLE 2, Degrees of freedom, mesh sizes, errors, convergence history and Newton iteration count for the approximation of the Navier–Stokes/Darcy–Forchheimer problem with  $F = 1$ .

| $F$ | $h = 0.2001$ | $h = 0.1088$ | $h = 0.0494$ | $h = 0.0262$ | $h = 0.0146$ | $h = 0.0077$ |
|-----|--------------|--------------|--------------|--------------|--------------|--------------|
| 0   | 4            | 4            | 4            | 4            | 4            | 4            |
| 1   | 5            | 5            | 5            | 6            | 6            | 6            |
| 10  | 7            | 8            | 9            | 9            | 9            | 9            |
| 100 | 8            | 9            | 10           | 10           | 11           | 11           |

Table 3.3: EXAMPLE 3, Convergence behavior of the iterative method (3.104) with respect to the Forchheimer number  $F$ .

| $N$    | $h_S$  | $\mathbf{e}(\mathbf{u}_S)$ | $\mathbf{r}(\mathbf{u}_S)$ | $\mathbf{e}(p_S)$ | $\mathbf{r}(p_S)$ |
|--------|--------|----------------------------|----------------------------|-------------------|-------------------|
| 1007   | 0.1881 | 1.0274                     | –                          | 0.5355            | –                 |
| 3790   | 0.1088 | 0.5114                     | 1.2753                     | 0.2156            | 1.6636            |
| 14014  | 0.0481 | 0.2472                     | 0.8896                     | 0.0978            | 0.9668            |
| 55428  | 0.0254 | 0.1243                     | 1.0742                     | 0.0483            | 1.1028            |
| 214828 | 0.0137 | 0.0620                     | 1.1285                     | 0.0237            | 1.1564            |
| 883963 | 0.0077 | 0.0307                     | 1.2174                     | 0.0123            | 1.1392            |

| $N$    | $h_D$  | $\mathbf{e}(\mathbf{u}_D)$ | $\mathbf{r}(\mathbf{u}_D)$ | $\mathbf{e}(p_D)$ | $\mathbf{r}(p_D)$ |
|--------|--------|----------------------------|----------------------------|-------------------|-------------------|
| 1007   | 0.2001 | 1.2760                     | –                          | 0.1105            | –                 |
| 3790   | 0.0950 | 0.6135                     | 0.9837                     | 0.0385            | 1.4165            |
| 14014  | 0.0494 | 0.3115                     | 1.0366                     | 0.0150            | 1.4375            |
| 55428  | 0.0262 | 0.1566                     | 1.0813                     | 0.0067            | 1.2820            |
| 214828 | 0.0146 | 0.0784                     | 1.1839                     | 0.0033            | 1.2215            |
| 883963 | 0.0072 | 0.0393                     | 0.9815                     | 0.0016            | 0.9948            |

| $N$    | $h_\Sigma$ | $\mathbf{e}(\lambda)$ | $\mathbf{r}(\lambda)$ | iter |
|--------|------------|-----------------------|-----------------------|------|
| 1007   | 0.1250     | 0.1930                | –                     | 7    |
| 3790   | 0.0625     | 0.0704                | 1.4545                | 8    |
| 14014  | 0.0313     | 0.0296                | 1.2527                | 9    |
| 55428  | 0.0156     | 0.0141                | 1.0638                | 9    |
| 214828 | 0.0078     | 0.0070                | 1.0217                | 9    |
| 883963 | 0.0039     | 0.0035                | 1.0093                | 9    |

Table 3.4: EXAMPLE 3, Degrees of freedom, mesh sizes, errors, convergence history and Newton iteration count for the approximation of the Navier–Stokes/Darcy–Forchheimer problem with  $F = 10$ .



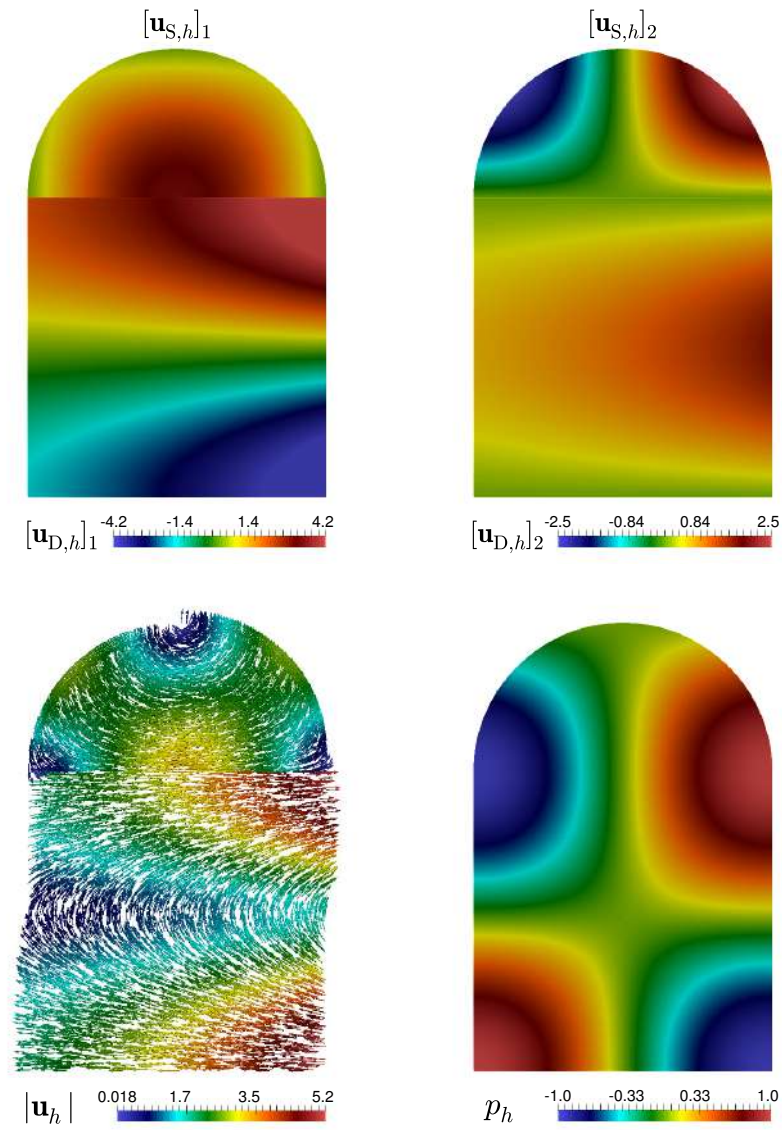


Figure 3.2: Example 1: Velocity components (top panels), velocity streamlines and pressure field in the whole domain (bottom panels).

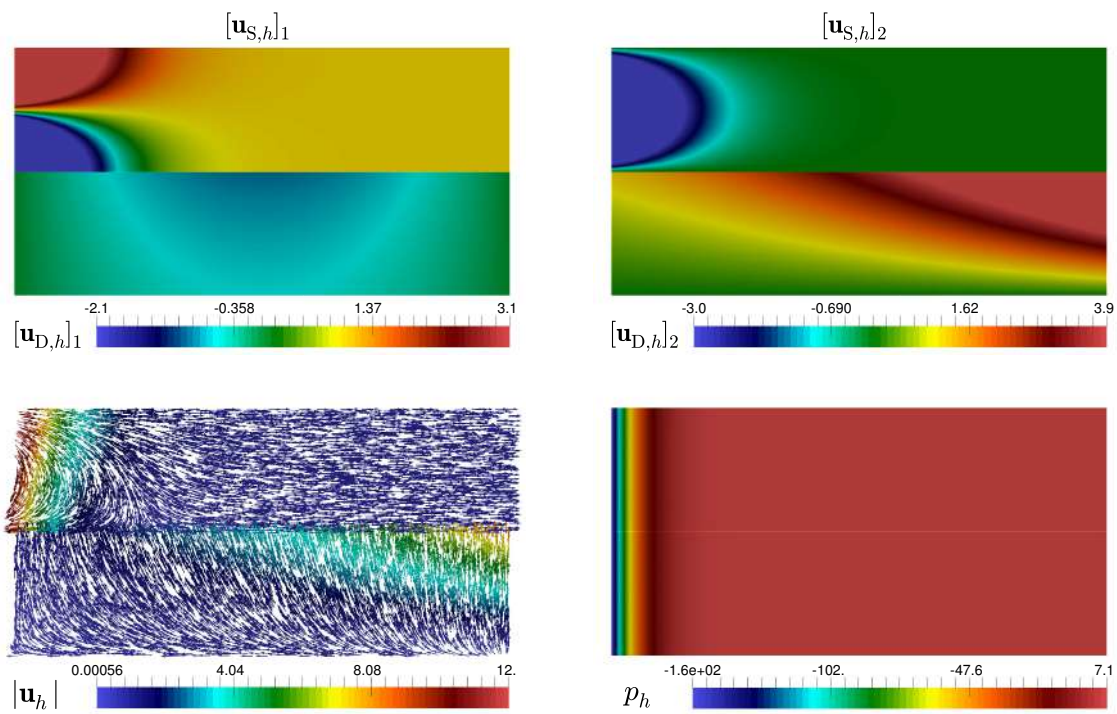


Figure 3.3: Example 2: Velocity components (top panels), velocity streamlines and pressure field in the whole domain (bottom panels).

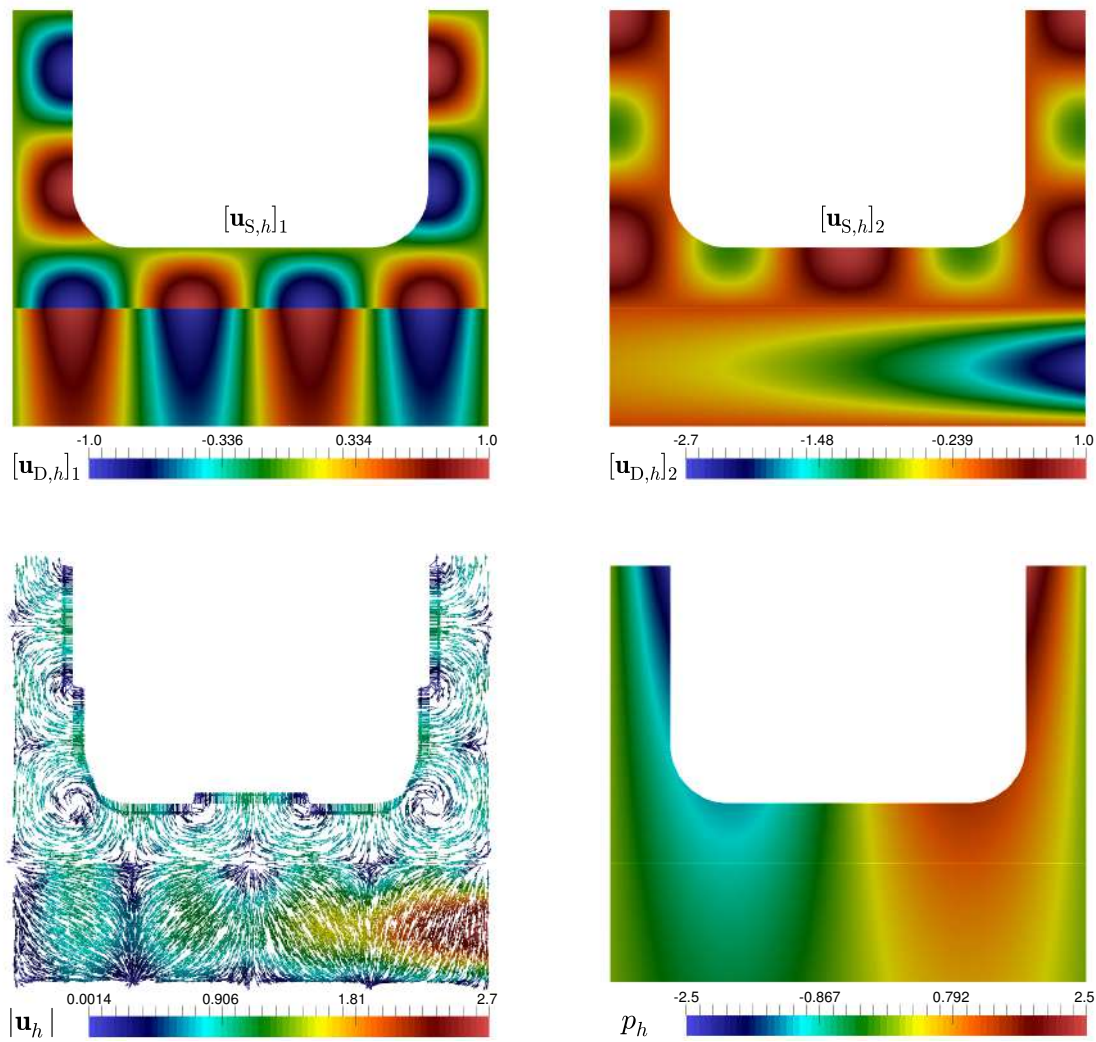


Figure 3.4: Example 3: Velocity components (top panels), velocity streamlines and pressure field in the whole domain (bottom panels).

## CHAPTER 4

---

### Analysis of an augmented fully-mixed formulation for the non-isothermal Oldroyd–Stokes problem

---

In this chapter we develop and analyse a new augmented-mixed finite element method to numerically approximate the flow patterns of a non-isothermal incompressible viscoelastic fluid described by the non-isothermal Oldroyd–Stokes equations.

#### 4.1 Introduction

The numerical simulation of viscoelastic fluid flows has become increasingly important for a variety of research areas in the fields of the natural sciences and engineering branches. This fact has been motivated by its diverse applications in industry such as design of heat exchangers and chemical reactors, cooling processes, and polymer processing (see, e.g., [113, 46, 120, 130]), to name a few. The complexity of the governing equations and the physical domains makes analysis of the mathematical models and the associated numerical methods especially difficult. Current efforts to model isothermal viscoelastic flows often revolve around the solution of the Stokes problem for the Oldroyd viscoelastic model (see, e.g., [14, 13, 33, 4], and the references therein). In particular, in [4] the authors analysed an extra stress-vorticity formulation and proved that this formulation satisfies an inf-sup condition and consequently, classical finite element spaces can be used for its approximation. We remark that, although most of the research on the viscoelastic fluid flows concerns isothermal cases, many flows of practical interest in polymeric melt processing are non-isothermal (see, e.g., [136, 123, 60, 118]). The combination of high viscosities of polymeric melts and high deformation rates results in the transformation of large amounts of mechanical energy into heat, and therefore in a temperature rise of the material. This phenomenon is, for instance, used in extruders where viscous dissipation is employed to enhance melting of the material (see [136] for details). This kind of fluid flows has motivated the introduction of the coupled problem between the Stokes equation for the Oldroyd viscoelastic model and the heat equation through a convective term and the viscosity of the fluid, thus arising the so called non-isothermal Oldroyd–Stokes problem.

Up to the authors' knowledge, [56] constitutes one of the first works in analysing a finite element discretization for the non-isothermal Oldroyd–Stokes equations. In that work, the authors provide a complete analysis of a mixed-primal formulation for the coupled problem, in which the main unknowns

are the polymeric part of the extra-stress tensor, the velocity, the pressure and the temperature of the fluid. The focus of this work is the discrete scheme, where by considering piecewise quadratic elements for the velocity and the temperature, continuous piecewise linear elements for the pressure, and discontinuous piecewise linear elements for the polymeric part of the extra-stress tensor, it is proved existence of at least one solution by using inverse inequalities of  $L^\infty$  into  $L^2$  and the Schaefer fixed-point theorem. In addition, the Galerkin scheme has optimal rates of convergence under a smallness assumption on the data. Later on, a new dual-mixed formulation was introduced and analysed in [73], where the solvent part of the extra-stress tensor, the vorticity, and the heat flux vector are set as further unknowns (besides the polymeric part of the extra-stress tensor, the velocity, the pressure and the temperature). The corresponding mixed finite element scheme employs Raviart–Thomas elements of lowest order plus bubble function for the solvent part of the extra-stress tensor, Raviart–Thomas elements of lowest order for the heat flux vector, continuous piecewise linear elements for the vorticity, and piecewise constants for the polymeric part of the extra-stress tensor, velocity, pressure and the temperature of the fluid. Existence of solution and convergence of the numerical scheme are proved and optimal error estimates are also provided by using inverse inequalities of  $L^\infty$  into  $L^2$ , smallness assumption on the data and the Schaefer fixed-point theorem. We remark that this formulation has properties analogous to finite volume methods, namely local conservation of momentum and mass.

The purpose of the present chapter is to contribute in the development of new numerical methods for the non-isothermal Oldroyd–Stokes problem. To that end, unlike to [56] and [73], and in order to obtain a new fully-mixed formulation of this coupled problem, we first introduce the strain tensor as a new unknown, which allows us, on one hand, to eliminate the polymeric part of the extra-stress tensor from the system and compute it as a simple post-process of the solution, and on the other hand, to join the polymeric and solvent viscosities in an adimensional viscosity. In addition, for convenience of the analysis we also consider the stress and vorticity tensors as auxiliary unknowns, thanks to which the pressure can be eliminated from the system and approximated later on by a postprocessing formula. In turn, for deriving the mixed formulation of the heat equation we proceed similarly to [73] (see also [51, 52]) and set the heat-flux vector as a further unknown. Furthermore, the difficulty given by the fact that the fluid velocity and the temperature lives in  $H^1$  instead of  $L^2$  as usual, is resolved as in [51, 52] by augmenting the variational formulation with suitable Galerkin type expressions arising from the constitutive and equilibrium equations, the relation defining the strain and vorticity tensors, and the Dirichlet boundary condition on the temperature. Then, following [51] and [2], we combine classical fixed-point arguments, suitable regularity assumptions on the decoupled problems, the Lax–Milgram lemma, the Sobolev embedding and Rellich–Kondrachov theorems, and sufficiently small data assumptions to establish existence and uniqueness of solution of the continuous problem. Similarly, the existence of solution of the discrete problem relies on the Brouwer fixed-point theorem and analogous arguments to those employed in the continuous analysis. Moreover, applying a Strang-type lemma valid for linear problems, we are able to derive the corresponding Céa estimate and to provide optimal a priori error bounds for the Galerkin solution. Finally, we point out that the main advantages of approximating the solution of the coupled system through this new approach include, on one hand, the fact that no discrete inf-sup conditions are required for the discrete analysis, and therefore arbitrary finite element subspaces can be employed, and on the other hand, the possibility of recovering by post-processing formulae the pressure, the polymeric part and solvent part of the extra-stress tensor in terms of the solution, conserving the same rates of convergence.

We have organised the contents of this chapter as follows. In Section 4.2 we introduce the model problem and derive the augmented fully-mixed variational formulation. Next, in Section 4.3 we establish the well-posedness of this continuous scheme by means of a fixed-point strategy and the Schauder and Banach fixed point theorems. The corresponding Galerkin system is introduced and analysed in Section 4.4, where the discrete analogue of the theory used in the continuous case is employed to prove existence of solution. In addition, a suitable Strang-type lemma is utilized here to derive the corresponding a priori error estimate and the resulting rates of convergence. Finally, in Section 4.5 we report several numerical essays illustrating the accuracy of our augmented fully-mixed finite element method.

## 4.2 The continuous formulation

In this section we introduce the model problem and derive the corresponding weak formulation.

### 4.2.1 The model problem

The non-isothermal Oldroyd–Stokes problem consists of a system of equations where the Stokes equation for the Oldroyd viscoelastic model introduced in [14], is coupled with the heat equation through a convective term and the viscosity of the fluid (cf. [56, 73]). More precisely, given a body force  $\mathbf{f}$ , and a heat source  $g$ , the aforementioned system of equations is given by

$$\begin{aligned} \boldsymbol{\sigma}_P - 2\mu_P(\theta)\mathbf{e}(\mathbf{u}) &= \mathbf{0} & \text{in } \Omega, \\ -\operatorname{div}(\boldsymbol{\sigma}_P + 2\epsilon\mu_N(\theta)\mathbf{e}(\mathbf{u})) + \nabla p &= \mathbf{f} & \text{in } \Omega, \\ \operatorname{div} \mathbf{u} &= 0 & \text{in } \Omega, \\ -\operatorname{div}(\kappa\nabla\theta) + \mathbf{u} \cdot \nabla\theta &= g & \text{in } \Omega, \\ \mathbf{u} &= \mathbf{0} & \text{on } \Gamma, \\ \theta &= \theta_D & \text{on } \Gamma_D, \\ \kappa\nabla\theta \cdot \mathbf{n} &= 0 & \text{on } \Gamma_N, \end{aligned} \tag{4.1}$$

where the unknowns are the polymeric part of the extra-stress tensor  $\boldsymbol{\sigma}_P$ , the velocity  $\mathbf{u}$ , the pressure  $p$ , and the temperature  $\theta$  of a fluid occupying the region  $\Omega$ . In addition,  $\mathbf{e}(\mathbf{u}) := \frac{1}{2}\{\nabla\mathbf{u} + (\nabla\mathbf{u})^t\}$  stands for the strain tensor of small deformations,  $\kappa$  is the thermal conductivity coefficient,  $\mu_P$  and  $\mu_N$  are the polymeric and solvent (or newtonian) viscosities, respectively, which are given by the following Arrhenius relationship:

$$\mu_P(\theta) = a_1 \exp\left(\frac{b_1}{\theta}\right), \quad \mu_N(\theta) = a_2 \exp\left(\frac{b_2}{\theta}\right), \tag{4.2}$$

where the coefficients  $a_1, b_1, a_2$ , and  $b_2$  are defined so that

$$0 < \mu_P(s) \leq 1, \quad 0 < \mu_N(s) \leq 1 \quad \forall s \geq 0. \tag{4.3}$$

Furthermore, we assume that both the polymeric and solvent viscosities are Lipschitz continuous and bounded from above and from below, that is,

$$|\mu_P(s) - \mu_P(t)| \leq L_{\mu_P}|s - t|, \quad |\mu_N(s) - \mu_N(t)| \leq L_{\mu_N}|s - t| \quad \forall s, t \geq 0, \tag{4.4}$$



and

$$\mu_{1,P} \leq \mu_P(s) \leq \mu_{2,P}, \quad \mu_{1,N} \leq \mu_N(s) \leq \mu_{2,N} \quad \forall s \geq 0. \quad (4.5)$$

Note that a small real parameter  $\epsilon > 0$  on the second equation of (4.1) is introduced to make the effect of the solvent viscosity much smaller than that of the polymeric part. Moreover, it is well known that uniqueness of a pressure solution of (4.1) (see, e.g., [134]) is ensured in the space

$$L_0^2(\Omega) := \left\{ q \in L^2(\Omega) : \int_{\Omega} q = 0 \right\}.$$

Now, in order to derive our augmented fully-mixed formulation we first need to rewrite (4.1) as a first-order system of equations. To this end, unlike to [56] and [73], we begin by introducing the strain tensor as an additional unknown  $\mathbf{t} := \mathbf{e}(\mathbf{u})$ , whence the polymeric and solvent parts of the extra-stress tensor can be written, respectively, as

$$\boldsymbol{\sigma}_P = 2\mu_P(\theta)\mathbf{t} \quad \text{and} \quad \boldsymbol{\sigma}_N = 2\epsilon\mu_N(\theta)\mathbf{t} \quad \text{in } \Omega. \quad (4.6)$$

Next, defining the dimensionless effective viscosity as in [73], that is

$$\mu(\theta) := 2\mu_P(\theta) + 2\epsilon\mu_N(\theta), \quad (4.7)$$

and adopting the approach from [91] (see also [89, 40, 26]), we introduce the auxiliary unknowns

$$\boldsymbol{\rho} := \nabla \mathbf{u} - \mathbf{e}(\mathbf{u}) \quad \text{and} \quad \boldsymbol{\sigma} := \mu(\theta)\mathbf{t} - p\mathbb{I} \quad \text{in } \Omega,$$

where  $\boldsymbol{\rho}$  is the vorticity (or skew-symmetric part of the velocity gradient). In this way, utilising the incompressibility condition  $\operatorname{div} \mathbf{u} = \operatorname{tr}(\mathbf{e}(\mathbf{u})) = 0$ , we find that the equations modelling the fluid in (4.1) can be rewritten, equivalently, as the set of equations with unknowns  $\mathbf{t}, \boldsymbol{\sigma}, \boldsymbol{\rho}$  and  $\mathbf{u}$ , given by

$$\begin{aligned} \mathbf{t} + \boldsymbol{\rho} &= \nabla \mathbf{u} \quad \text{in } \Omega, \quad \boldsymbol{\sigma}^d = \mu(\theta)\mathbf{t} \quad \text{in } \Omega, \quad -\operatorname{div} \boldsymbol{\sigma} = \mathbf{f} \quad \text{in } \Omega, \\ \mathbf{u} &= \mathbf{0} \quad \text{on } \Gamma, \quad p = -\frac{1}{n}\operatorname{tr} \boldsymbol{\sigma} \quad \text{in } \Omega, \quad \int_{\Omega} \operatorname{tr} \boldsymbol{\sigma} = 0, \end{aligned} \quad (4.8)$$

where both  $\mathbf{t}$  and  $\boldsymbol{\sigma}$  are symmetric tensors, and  $\operatorname{tr} \mathbf{t} = 0$  holds in  $\Omega$ . Note that the fifth equation in (4.8) allows us to eliminate the pressure  $p$  from the system (which anyway can be approximated later on by postprocessed), whereas the last equation takes care of the requirement that  $p \in L_0^2(\Omega)$ . In addition, it easy to see from (4.4) and (4.5) that the fluid viscosity  $\mu(\cdot)$  is Lipschitz continuous and bounded from above and from below, that is, there exist constants  $L_\mu > 0$  and  $\mu_1, \mu_2 > 0$ , such that

$$|\mu(s) - \mu(t)| \leq L_\mu |s - t| \quad \forall s, t \geq 0, \quad (4.9)$$

and

$$\mu_1 \leq \mu(s) \leq \mu_2 \quad \forall s \geq 0. \quad (4.10)$$

Similarly, for the convection-diffusion equation modelling the temperature of the fluid in (4.1), we adopt the approach from [73] (see also [51, 52]) and introduce as a further unknown the heat flux vector

$$\mathbf{p} := \kappa \nabla \theta - \theta \mathbf{u} \quad \text{in } \Omega,$$

so that, utilising the incompressibility condition  $\operatorname{div} \mathbf{u} = 0$  in  $\Omega$  and the homogenous Dirichlet boundary condition  $\mathbf{u} = \mathbf{0}$  on  $\Gamma$ , the remaining equations in the system (4.1) can be rewritten, equivalently, as

$$\begin{aligned} \kappa^{-1} \mathbf{p} + \kappa^{-1} \theta \mathbf{u} &= \nabla \theta \quad \text{in } \Omega, & -\operatorname{div} \mathbf{p} &= g \quad \text{in } \Omega, \\ \theta &= \theta_D \quad \text{on } \Gamma_D, & \mathbf{p} \cdot \mathbf{n} &= 0 \quad \text{on } \Gamma_N. \end{aligned} \quad (4.11)$$

We end this section emphasizing from (4.6) that we can recover the polymeric and solvent parts of the extra-stress tensor in terms of  $\theta$  and  $\mathbf{t}$ , whereas from the fifth equation of (4.8) we obtain the pressure in terms of  $\boldsymbol{\sigma}$ . Alternatively, from (4.6), (4.7), and the second equation of (4.8), we arrive at the identity

$$\boldsymbol{\sigma}_P + \boldsymbol{\sigma}_N = \boldsymbol{\sigma}^d \quad \text{in } \Omega, \quad (4.12)$$

from which each part of the extra stress can be computed in terms of  $\boldsymbol{\sigma}^d$  and the other part. The formulae provided by (4.6), (4.12), and the fifth equation of (4.8), will suggest in Section 4.5 suitable approximations of the polymeric and solvent parts of the extra-stress tensor, and the pressure (cf. (4.80)). They will all depend on the unique finite element solution of a Galerkin scheme to be introduced below (cf. (4.57)), and hence the same rates of convergence will be obtained.

#### 4.2.2 The augmented fully-mixed variational formulation

In this section we derive the weak formulation of the coupled system (4.8)–(4.11). We begin by recalling (see, e.g., [19, 81, 100]) that there holds

$$\mathbb{H}(\mathbf{div}; \Omega) = \mathbb{H}_0(\mathbf{div}; \Omega) \oplus \mathbb{R}\mathbb{I}, \quad (4.13)$$

where

$$\mathbb{H}_0(\mathbf{div}; \Omega) := \left\{ \boldsymbol{\tau} \in \mathbb{H}(\mathbf{div}; \Omega) : \int_{\Omega} \operatorname{tr} \boldsymbol{\tau} = 0 \right\}.$$

In this way, decomposing  $\boldsymbol{\tau} \in \mathbb{H}(\mathbf{div}; \Omega)$  as  $\boldsymbol{\tau} = \boldsymbol{\tau}_0 + c\mathbb{I}$ , with  $\boldsymbol{\tau}_0 \in \mathbb{H}_0(\mathbf{div}; \Omega)$  and  $c \in \mathbb{R}$ , noticing that  $\boldsymbol{\tau}^d = \boldsymbol{\tau}_0^d$  and  $\mathbf{div} \boldsymbol{\tau} = \mathbf{div} \boldsymbol{\tau}_0$ , and using the last equation of (4.8), we deduce that both  $\boldsymbol{\sigma}$  and  $\boldsymbol{\tau}$  can be considered hereafter in  $\mathbb{H}_0(\mathbf{div}; \Omega)$ . In addition, thanks to the incompressibility condition and the first equation of (4.8), we can look for the strain tensor  $\mathbf{t}$  in the space

$$\mathbb{L}_{\operatorname{tr}}^2(\Omega) := \left\{ \mathbf{r} \in \mathbb{L}^2(\Omega) : \mathbf{r}^t = \mathbf{r} \quad \text{and} \quad \operatorname{tr} \mathbf{r} = 0 \right\},$$

whereas the vorticity  $\boldsymbol{\rho}$  lives in

$$\mathbb{L}_{\operatorname{skew}}^2(\Omega) := \left\{ \boldsymbol{\eta} \in \mathbb{L}^2(\Omega) : \boldsymbol{\eta}^t = -\boldsymbol{\eta} \right\}.$$

In turn, the homogeneous Neumann boundary condition for  $\mathbf{p}$  on  $\Gamma_N$  (cf. fourth equation in (4.11)) suggests the introduction of the functional space

$$\mathbf{H}_{\Gamma_N}(\operatorname{div}; \Omega) := \left\{ \mathbf{q} \in \mathbf{H}(\operatorname{div}; \Omega) : \mathbf{q} \cdot \mathbf{n} = 0 \quad \text{on } \Gamma_N \right\}.$$

Hence, we begin the derivation of our weak formulation by testing the first equations of (4.8) and (4.11) with arbitrary  $\boldsymbol{\tau} \in \mathbb{H}_0(\mathbf{div}; \Omega)$  and  $\mathbf{q} \in \mathbf{H}_{\Gamma_N}(\operatorname{div}; \Omega)$ , respectively. Then, integrating by parts,



utilising the identity  $\mathbf{t} : \boldsymbol{\tau} = \mathbf{t} : \boldsymbol{\tau}^d$  (which follows from the fact that  $\mathbf{t} : \mathbb{I} = \text{tr } \mathbf{t} = 0$ ), and imposing the remaining equations weakly, which includes the symmetry of  $\boldsymbol{\sigma}$ , we arrive at the variational problem: Find  $\mathbf{t} \in \mathbb{L}_{\text{tr}}^2(\Omega)$ ,  $\boldsymbol{\sigma} \in \mathbb{H}_0(\text{div}; \Omega)$ ,  $\boldsymbol{\rho} \in \mathbb{L}_{\text{skew}}^2(\Omega)$ ,  $\mathbf{p} \in \mathbf{H}_{\Gamma_N}(\text{div}; \Omega)$ , and  $\mathbf{u}$ ,  $\theta$  in suitable spaces to be defined, such that

$$\begin{aligned} \int_{\Omega} \mu(\theta) \mathbf{t} : \mathbf{r} - \int_{\Omega} \boldsymbol{\sigma}^d : \mathbf{r} &= 0 & \forall \mathbf{r} \in \mathbb{L}_{\text{tr}}^2(\Omega), \\ \int_{\Omega} \mathbf{t} : \boldsymbol{\tau}^d + \int_{\Omega} \mathbf{u} \cdot \text{div } \boldsymbol{\tau} + \int_{\Omega} \boldsymbol{\rho} : \boldsymbol{\tau} &= 0 & \forall \boldsymbol{\tau} \in \mathbb{H}_0(\text{div}; \Omega), \\ - \int_{\Omega} \mathbf{v} \cdot \text{div } \boldsymbol{\sigma} - \int_{\Omega} \boldsymbol{\sigma} : \boldsymbol{\eta} &= \int_{\Omega} \mathbf{f} \cdot \mathbf{v} & \forall (\mathbf{v}, \boldsymbol{\eta}) \in \mathbf{L}^2(\Omega) \times \mathbb{L}_{\text{skew}}^2(\Omega), \\ \kappa^{-1} \int_{\Omega} \mathbf{p} \cdot \mathbf{q} + \int_{\Omega} \theta \text{div } \mathbf{q} + \kappa^{-1} \int_{\Omega} \theta \mathbf{u} \cdot \mathbf{q} &= \langle \mathbf{q} \cdot \mathbf{n}, \theta_D \rangle_{\Gamma_D} & \forall \mathbf{q} \in \mathbf{H}_{\Gamma_N}(\text{div}; \Omega), \\ - \int_{\Omega} \psi \text{div } \mathbf{p} &= \int_{\Omega} g \psi & \forall \psi \in L^2(\Omega). \end{aligned} \quad (4.14)$$

Before continuing we observe that the third term on the left-hand side of the fourth equation in (4.14) requires a suitable regularity for both unknowns  $\mathbf{u}$  and  $\theta$ . Indeed, by applying Cauchy–Schwarz and Hölder’s inequalities, and then the continuous injection  $\mathbf{i}$  of  $H^1(\Omega)$  into  $L^4(\Omega)$  (see, e.g., [1, Theorem 6.3] or [139, Theorem 1.3.5]), we find that there exist a positive constant  $c(\Omega) := \|\mathbf{i}\|^2$ , such that

$$\left| \int_{\Omega} \theta \mathbf{u} \cdot \mathbf{q} \right| \leq c(\Omega) \|\theta\|_{1,\Omega} \|\mathbf{u}\|_{1,\Omega} \|\mathbf{q}\|_{0,\Omega} \quad \forall \theta \in H^1(\Omega) \quad \forall \mathbf{u} \in \mathbf{H}^1(\Omega) \quad \forall \mathbf{q} \in \mathbf{L}^2(\Omega). \quad (4.15)$$

According to the above, and in order to be able to analyse the present variational formulation of the coupled system (4.8)–(4.11), we propose to seek  $\mathbf{u} \in \mathbf{H}_0^1(\Omega)$  and  $\theta \in H^1(\Omega)$ , and to restrict the set of corresponding test functions  $\mathbf{v}$  and  $\psi$  to the same space, respectively. In this way, similarly as in [51] (see also [52]), we augment (4.14) through the following redundant Galerkin terms arising from the constitutive and equilibrium equations, the relation between the strain tensor and  $\mathbf{t}$ , the definition of the vorticity in terms of the velocity gradient, and the Dirichlet boundary condition on the temperature:

$$\begin{aligned} \kappa_1 \int_{\Omega} \left\{ \boldsymbol{\sigma}^d - \mu(\theta) \mathbf{t} \right\} : \boldsymbol{\tau}^d &= 0 & \forall \boldsymbol{\tau} \in \mathbb{H}_0(\text{div}; \Omega), \\ \kappa_2 \int_{\Omega} \text{div } \boldsymbol{\sigma} \cdot \text{div } \boldsymbol{\tau} &= -\kappa_2 \int_{\Omega} \mathbf{f} \cdot \text{div } \boldsymbol{\tau} & \forall \boldsymbol{\tau} \in \mathbb{H}_0(\text{div}; \Omega), \\ \kappa_3 \int_{\Omega} \left\{ \mathbf{e}(\mathbf{u}) - \mathbf{t} \right\} : \mathbf{e}(\mathbf{v}) &= 0 & \forall \mathbf{v} \in \mathbf{H}_0^1(\Omega), \\ \kappa_4 \int_{\Omega} \left( \boldsymbol{\rho} - \left\{ \nabla \mathbf{u} - \mathbf{e}(\mathbf{u}) \right\} \right) : \boldsymbol{\eta} &= 0 & \forall \boldsymbol{\eta} \in \mathbb{L}_{\text{skew}}^2(\Omega), \end{aligned} \quad (4.16)$$

and

$$\begin{aligned} \kappa_5 \int_{\Omega} \left\{ \nabla \theta - \kappa^{-1} \mathbf{p} - \kappa^{-1} \theta \mathbf{u} \right\} \cdot \nabla \psi &= 0 & \forall \psi \in H^1(\Omega), \\ \kappa_6 \int_{\Omega} \text{div } \mathbf{p} \text{div } \mathbf{q} &= -\kappa_6 \int_{\Omega} g \text{div } \mathbf{q} & \forall \mathbf{q} \in \mathbf{H}_{\Gamma_N}(\text{div}; \Omega), \\ \kappa_7 \int_{\Gamma_D} \theta \psi &= \kappa_7 \int_{\Gamma_D} \theta_D \psi & \forall \psi \in H^1(\Omega), \end{aligned} \quad (4.17)$$

where  $(\kappa_1, \dots, \kappa_7)$  is a vector of positive parameters to be specified later.

At this point we remark that there are many different ways of ordering the augmented fully-mixed variational formulation described above, but for the sake of subsequent analysis we proceed as in [51, Section 3.1], and adopt one leading to an uncoupled structure. To that end, we start by grouping appropriately some of the unknowns and spaces as follows:

$$\underline{\mathbf{t}} := (\mathbf{t}, \boldsymbol{\sigma}, \boldsymbol{\rho}) \in \mathbb{H} := \mathbb{L}_{\text{tr}}^2(\Omega) \times \mathbb{H}_0(\text{div}; \Omega) \times \mathbb{L}_{\text{skew}}^2(\Omega),$$

where  $\mathbb{H}$  is endowed with the norm

$$\|\underline{\mathbf{r}}\|_{\mathbb{H}}^2 := \|\mathbf{r}\|_{0,\Omega}^2 + \|\boldsymbol{\tau}\|_{\text{div};\Omega}^2 + \|\boldsymbol{\eta}\|_{0,\Omega}^2 \quad \forall \underline{\mathbf{r}} := (\mathbf{r}, \boldsymbol{\tau}, \boldsymbol{\eta}) \in \mathbb{H}.$$

Hence, the augmented fully-mixed variational formulation for the non-isothermal Oldroyd–Stokes problem reads: Find  $(\underline{\mathbf{t}}, \mathbf{u}, \mathbf{p}, \theta) \in \mathbb{H} \times \mathbf{H}_0^1(\Omega) \times \mathbf{H}_{\Gamma_N}(\text{div}; \Omega) \times H^1(\Omega)$  such that

$$\begin{aligned} \mathbf{A}_\theta((\underline{\mathbf{t}}, \mathbf{u}), (\underline{\mathbf{r}}, \mathbf{v})) &= \mathbf{F}(\underline{\mathbf{r}}, \mathbf{v}) \quad \forall (\underline{\mathbf{r}}, \mathbf{v}) \in \mathbb{H} \times \mathbf{H}_0^1(\Omega), \\ \tilde{\mathbf{A}}((\mathbf{p}, \theta), (\mathbf{q}, \psi)) + \tilde{\mathbf{B}}_{\mathbf{u}}((\mathbf{p}, \theta), (\mathbf{q}, \psi)) &= \tilde{\mathbf{F}}(\mathbf{q}, \psi) \quad \forall (\mathbf{q}, \psi) \in \mathbf{H}_{\Gamma_N}(\text{div}; \Omega) \times H^1(\Omega), \end{aligned} \quad (4.18)$$

where, given  $\phi \in H^1(\Omega)$  and  $\mathbf{w} \in \mathbf{H}_0^1(\Omega)$ ,  $\mathbf{A}_\phi$ ,  $\tilde{\mathbf{A}}$ , and  $\tilde{\mathbf{B}}_{\mathbf{w}}$  are the bilinear forms defined, respectively, as

$$\begin{aligned} \mathbf{A}_\phi((\underline{\mathbf{t}}, \mathbf{u}), (\underline{\mathbf{r}}, \mathbf{v})) &:= \int_{\Omega} \mu(\phi) \mathbf{t} : \left\{ \mathbf{r} - \kappa_1 \boldsymbol{\tau}^{\text{d}} \right\} + \int_{\Omega} \boldsymbol{\sigma}^{\text{d}} : \left\{ \kappa_1 \boldsymbol{\tau}^{\text{d}} - \mathbf{r} \right\} + \int_{\Omega} \mathbf{t} : \boldsymbol{\tau}^{\text{d}} \\ &+ \int_{\Omega} \left\{ \mathbf{u} + \kappa_2 \text{div} \boldsymbol{\sigma} \right\} \cdot \text{div} \boldsymbol{\tau} - \int_{\Omega} \mathbf{v} \cdot \text{div} \boldsymbol{\sigma} + \int_{\Omega} \boldsymbol{\rho} : \boldsymbol{\tau} - \int_{\Omega} \boldsymbol{\sigma} : \boldsymbol{\eta} \\ &+ \kappa_3 \int_{\Omega} \left\{ \mathbf{e}(\mathbf{u}) - \mathbf{t} \right\} : \mathbf{e}(\mathbf{v}) + \kappa_4 \int_{\Omega} \left( \boldsymbol{\rho} - \left\{ \nabla \mathbf{u} - \mathbf{e}(\mathbf{u}) \right\} \right) : \boldsymbol{\eta}, \end{aligned} \quad (4.19)$$

$$\begin{aligned} \tilde{\mathbf{A}}((\mathbf{p}, \theta), (\mathbf{q}, \psi)) &:= \kappa^{-1} \int_{\Omega} \mathbf{p} \cdot \left\{ \mathbf{q} - \kappa_5 \nabla \psi \right\} + \int_{\Omega} \left\{ \theta + \kappa_6 \text{div} \mathbf{p} \right\} \text{div} \mathbf{q} - \int_{\Omega} \psi \text{div} \mathbf{p} \\ &+ \kappa_5 \int_{\Omega} \nabla \theta \cdot \nabla \psi + \kappa_7 \int_{\Gamma_D} \theta \psi, \end{aligned} \quad (4.20)$$

and

$$\tilde{\mathbf{B}}_{\mathbf{w}}((\mathbf{p}, \theta), (\mathbf{q}, \psi)) := \kappa^{-1} \int_{\Omega} \theta \mathbf{w} \cdot \left\{ \mathbf{q} - \kappa_5 \nabla \psi \right\}, \quad (4.21)$$

for all  $(\underline{\mathbf{t}}, \mathbf{u}), (\underline{\mathbf{r}}, \mathbf{v}) \in \mathbb{H} \times \mathbf{H}_0^1(\Omega)$  and for all  $(\mathbf{p}, \theta), (\mathbf{q}, \psi) \in \mathbf{H}_{\Gamma_N}(\text{div}; \Omega) \times H^1(\Omega)$ . In turn,  $\mathbf{F}$  and  $\tilde{\mathbf{F}}$  are the bounded linear functionals given by

$$\mathbf{F}(\underline{\mathbf{r}}, \mathbf{v}) := \int_{\Omega} \mathbf{f} \cdot \left\{ \mathbf{v} - \kappa_2 \text{div} \boldsymbol{\tau} \right\}, \quad (4.22)$$

for all  $(\underline{\mathbf{r}}, \mathbf{v}) \in \mathbb{H} \times \mathbf{H}_0^1(\Omega)$  and

$$\tilde{\mathbf{F}}(\mathbf{q}, \psi) := \langle \mathbf{q} \cdot \mathbf{n}, \theta_D \rangle_{\Gamma_D} + \int_{\Omega} g \left\{ \psi - \kappa_6 \text{div} \mathbf{q} \right\} + \kappa_7 \int_{\Gamma_D} \theta_D \psi, \quad (4.23)$$

for all  $(\mathbf{q}, \psi) \in \mathbf{H}_{\Gamma_N}(\text{div}; \Omega) \times H^1(\Omega)$ .

### 4.3 Analysis of the continuous formulation

In this section we proceed similarly as in [51] (see also [52, 2]) and utilise a fixed-point strategy to prove that problem (4.18) is well posed. More precisely, in Section 4.3.1 we rewrite (4.18) as an equivalent fixed-point equation in terms of an operator  $\mathbf{T}$ . Next in Section 4.3.2 we show that  $\mathbf{T}$  is well defined, and finally in Section 4.3.3 we apply the well known Schauder and Banach theorems to conclude that  $\mathbf{T}$  has a unique fixed point.

#### 4.3.1 The fixed-point approach

We start by defining the operator  $\mathbf{S} : H^1(\Omega) \rightarrow \mathbb{H} \times \mathbf{H}_0^1(\Omega)$  by

$$\mathbf{S}(\phi) := (\mathbf{S}_1(\phi), \mathbf{S}_2(\phi)) = (\underline{\mathbf{t}}, \mathbf{u}) \quad \forall \phi \in H^1(\Omega), \quad (4.24)$$

where  $\mathbf{S}_1(\phi) := (\mathbf{S}_1^t(\phi), \mathbf{S}_1^\sigma(\phi), \mathbf{S}_1^\rho(\phi))$  and  $(\underline{\mathbf{t}}, \mathbf{u})$  is the unique solution of the problem: Find  $(\underline{\mathbf{t}}, \mathbf{u}) \in \mathbb{H} \times \mathbf{H}_0^1(\Omega)$  such that

$$\mathbf{A}_\phi((\underline{\mathbf{t}}, \mathbf{u}), (\underline{\mathbf{r}}, \mathbf{v})) = \mathbf{F}(\underline{\mathbf{r}}, \mathbf{v}) \quad \forall (\underline{\mathbf{r}}, \mathbf{v}) \in \mathbb{H} \times \mathbf{H}_0^1(\Omega), \quad (4.25)$$

where the bilinear form  $\mathbf{A}_\phi$  is given by (4.19). In turn, the functional  $\mathbf{F}$  is defined exactly as in (4.22). In addition, we also introduce the operator  $\tilde{\mathbf{S}} : \mathbf{H}_0^1(\Omega) \rightarrow \mathbf{H}_{\Gamma_N}(\text{div}; \Omega) \times H^1(\Omega)$  defined as

$$\tilde{\mathbf{S}}(\mathbf{w}) := (\tilde{\mathbf{S}}_1(\mathbf{w}), \tilde{\mathbf{S}}_2(\mathbf{w})) = (\mathbf{p}, \theta) \quad \forall \mathbf{w} \in \mathbf{H}_0^1(\Omega), \quad (4.26)$$

where  $(\mathbf{p}, \theta)$  is the unique solution of the problem: Find  $(\mathbf{p}, \theta) \in \mathbf{H}_{\Gamma_N}(\text{div}; \Omega) \times H^1(\Omega)$  such that

$$\tilde{\mathbf{A}}((\mathbf{p}, \theta), (\mathbf{q}, \psi)) + \tilde{\mathbf{B}}_{\mathbf{w}}((\mathbf{p}, \theta), (\mathbf{q}, \psi)) = \tilde{\mathbf{F}}(\mathbf{q}, \psi) \quad \forall (\mathbf{q}, \psi) \in \mathbf{H}_{\Gamma_N}(\text{div}; \Omega) \times H^1(\Omega). \quad (4.27)$$

Here the bilinear form  $\tilde{\mathbf{A}}$  and the functional  $\tilde{\mathbf{F}}$  are defined exactly as in (4.20) and (4.23), respectively. In turn, the bilinear form  $\tilde{\mathbf{B}}_{\mathbf{w}}$  is given by (4.21). In this way, we define the operator  $\mathbf{T} : H^1(\Omega) \rightarrow H^1(\Omega)$  as

$$\mathbf{T}(\phi) := \tilde{\mathbf{S}}_2(\mathbf{S}_2(\phi)) \quad \forall \phi \in H^1(\Omega), \quad (4.28)$$

and realise that (4.18) can be rewritten as the fixed-point problem: Find  $\theta \in H^1(\Omega)$  such that

$$\mathbf{T}(\theta) = \theta. \quad (4.29)$$

This fact certainly requires that both operators  $\mathbf{S}$  and  $\tilde{\mathbf{S}}$  be well defined. In other words, we first need to analyse the well-posedness of the uncoupled problems (4.25) and (4.27). The next section is devoted to this matter.

We end this section by recalling, for later use, that there exist positive constants  $c_1(\Omega)$  and  $c_2(\Omega)$ , such that (see [81, Lemma 2.3] and [122, Theorem 5.11.2], respectively, for details)

$$c_1(\Omega) \|\boldsymbol{\tau}\|_{0,\Omega}^2 \leq \|\boldsymbol{\tau}^d\|_{0,\Omega}^2 + \|\mathbf{div} \boldsymbol{\tau}\|_{0,\Omega}^2 \quad \forall \boldsymbol{\tau} \in \mathbb{H}_0(\mathbf{div}; \Omega), \quad (4.30)$$

$$|\psi|_{1,\Omega} + \|\psi\|_{0,\Gamma_D} \geq c_2(\Omega) \|\psi\|_{1,\Omega} \quad \forall \psi \in H^1(\Omega), \quad (4.31)$$

and

$$\|\mathbf{e}(\mathbf{v})\|_{0,\Omega}^2 \geq \frac{1}{2} |\mathbf{v}|_{1,\Omega}^2 \quad \forall \mathbf{v} \in \mathbf{H}_0^1(\Omega), \quad (4.32)$$

where (4.32) is the well known Korn inequality (see [128, Theorem 10.1]).

### 4.3.2 Well-posedness of the uncoupled problems

We begin by establishing a result that provides conditions under which the operator  $\mathbf{S}$  in (4.24) is well-defined, or equivalently, the problem (4.25) is well-posed.

**Lemma 4.1.** *Assume that*

$$\kappa_1 \in \left(0, \frac{2\delta_1\mu_1}{\mu_2}\right), \quad \kappa_3 \in \left(0, 2\delta_2\left(\mu_1 - \frac{\kappa_1\mu_2}{2\delta_1}\right)\right), \quad \kappa_4 \in \left(0, 2\delta_3\kappa_3\left(1 - \frac{\delta_2}{2}\right)\right), \quad \text{and} \quad \kappa_2 > 0,$$

with  $\delta_1 \in \left(0, \frac{2}{\mu_2}\right)$ , and  $\delta_2, \delta_3 \in (0, 2)$ . Then, for each  $\phi \in H^1(\Omega)$ , the problem (4.25) has a unique solution  $(\underline{\mathbf{t}}, \mathbf{u}) := \mathbf{S}(\phi) \in \mathbb{H} \times \mathbf{H}_0^1(\Omega)$ . Moreover, there exists a constant  $c_{\mathbf{S}} > 0$ , independent of  $\phi$ , such that there holds

$$\|\mathbf{S}(\phi)\| = \|(\underline{\mathbf{t}}, \mathbf{u})\| \leq c_{\mathbf{S}} \|\mathbf{f}\|_{0,\Omega}. \quad (4.33)$$

*Proof.* For a given  $\phi \in H^1(\Omega)$ , we observe from (4.19) that  $\mathbf{A}_\phi$  is clearly a bilinear form. Also, from Cauchy–Schwarz inequality we deduce that there exists a positive constant, which we denote by  $\|\mathbf{A}_\phi\|$ , only depending on  $\kappa_1, \kappa_2, \kappa_3, \kappa_4$ , and  $\mu_2$  (cf. (4.10)), such that

$$\left| \mathbf{A}_\phi((\underline{\mathbf{t}}, \mathbf{u}), (\underline{\mathbf{r}}, \mathbf{v})) \right| \leq \|\mathbf{A}_\phi\| \|(\underline{\mathbf{t}}, \mathbf{u})\| \|(\underline{\mathbf{r}}, \mathbf{v})\|, \quad (4.34)$$

for all  $(\underline{\mathbf{t}}, \mathbf{u}), (\underline{\mathbf{r}}, \mathbf{v}) \in \mathbb{H} \times \mathbf{H}_0^1(\Omega)$ . It turn, we have from (4.19) that

$$\begin{aligned} \mathbf{A}_\phi((\underline{\mathbf{r}}, \mathbf{v}), (\underline{\mathbf{r}}, \mathbf{v})) &= \int_{\Omega} \mu(\phi) \mathbf{r} : \mathbf{r} - \kappa_1 \int_{\Omega} \mu(\phi) \mathbf{r} : \boldsymbol{\tau}^d + \kappa_1 \|\boldsymbol{\tau}^d\|_{0,\Omega}^2 + \kappa_2 \|\mathbf{div} \boldsymbol{\tau}\|_{0,\Omega}^2 + \kappa_3 \|\mathbf{e}(\mathbf{v})\|_{0,\Omega}^2 \\ &\quad - \kappa_3 \int_{\Omega} \mathbf{r} : \mathbf{e}(\mathbf{v}) + \kappa_4 \|\boldsymbol{\eta}\|_{0,\Omega}^2 - \kappa_4 \int_{\Omega} \left\{ \nabla \mathbf{v} - \mathbf{e}(\mathbf{v}) \right\} : \boldsymbol{\eta}. \end{aligned}$$

Hence, we proceed similarly to the proof of [26, Lemma 3.6], utilise the Cauchy–Schwarz and Young inequalities, apply the boundedness of  $\mu$  (cf. (4.10)), and the fact that

$$\|\nabla \mathbf{v} - \mathbf{e}(\mathbf{v})\|_{0,\Omega}^2 = |\mathbf{v}|_{1,\Omega}^2 - \|\mathbf{e}(\mathbf{v})\|_{0,\Omega}^2,$$

to obtain that for any  $\delta_1, \delta_2, \delta_3 > 0$ , and for all  $(\underline{\mathbf{r}}, \mathbf{v}) \in \mathbb{H} \times \mathbf{H}_0^1(\Omega)$ , there holds

$$\begin{aligned} \mathbf{A}_\phi((\underline{\mathbf{r}}, \mathbf{v}), (\underline{\mathbf{r}}, \mathbf{v})) &\geq \left\{ \left( \mu_1 - \frac{\kappa_1\mu_2}{2\delta_1} \right) - \frac{\kappa_3}{2\delta_2} \right\} \|\mathbf{r}\|_{0,\Omega}^2 + \kappa_1 \left( 1 - \frac{\mu_2\delta_1}{2} \right) \|\boldsymbol{\tau}^d\|_{0,\Omega}^2 + \kappa_2 \|\mathbf{div} \boldsymbol{\tau}\|_{0,\Omega}^2 \\ &\quad + \left\{ \kappa_3 \left( 1 - \frac{\delta_2}{2} \right) + \frac{\kappa_4}{2\delta_3} \right\} \|\mathbf{e}(\mathbf{v})\|_{0,\Omega}^2 - \frac{\kappa_4}{2\delta_3} |\mathbf{v}|_{1,\Omega}^2 + \kappa_4 \left( 1 - \frac{\delta_3}{2} \right) \|\boldsymbol{\eta}\|_{0,\Omega}^2, \end{aligned}$$

which, together with the Korn inequality (4.32), implies

$$\begin{aligned} \mathbf{A}_\phi((\underline{\mathbf{r}}, \mathbf{v}), (\underline{\mathbf{r}}, \mathbf{v})) &\geq \left\{ \left( \mu_1 - \frac{\kappa_1\mu_2}{2\delta_1} \right) - \frac{\kappa_3}{2\delta_2} \right\} \|\mathbf{r}\|_{0,\Omega}^2 + \kappa_1 \left( 1 - \frac{\mu_2\delta_1}{2} \right) \|\boldsymbol{\tau}^d\|_{0,\Omega}^2 + \kappa_2 \|\mathbf{div} \boldsymbol{\tau}\|_{0,\Omega}^2 \\ &\quad + \left\{ \frac{\kappa_3}{2} \left( 1 - \frac{\delta_2}{2} \right) - \frac{\kappa_4}{4\delta_3} \right\} |\mathbf{v}|_{1,\Omega}^2 + \kappa_4 \left( 1 - \frac{\delta_3}{2} \right) \|\boldsymbol{\eta}\|_{0,\Omega}^2. \end{aligned} \quad (4.35)$$

Then, assuming the stipulated hypotheses on  $\delta_1, \kappa_1, \kappa_3, \delta_2, \delta_3, \kappa_4$ , and  $\kappa_2$ , and applying the inequality (4.30), we can define the positive constants

$$\begin{aligned} \alpha_1(\Omega) &:= \left( \mu_1 - \frac{\kappa_1 \mu_2}{2\delta_1} \right) - \frac{\kappa_3}{2\delta_2}, \quad \alpha_2(\Omega) := \min \left\{ \kappa_1 \left( 1 - \frac{\mu_2 \delta_1}{2} \right), \frac{\kappa_2}{2} \right\}, \\ \alpha_3(\Omega) &:= \min \left\{ c_1(\Omega) \alpha_2(\Omega), \frac{\kappa_2}{2} \right\}, \quad \alpha_4(\Omega) := \frac{\kappa_3}{2} \left( 1 - \frac{\delta_2}{2} \right) - \frac{\kappa_4}{4\delta_3}, \quad \text{and} \quad \alpha_5(\Omega) := \kappa_4 \left( 1 - \frac{\delta_3}{2} \right), \end{aligned}$$

which allow us to deduce from (4.35) that

$$\mathbf{A}_\phi((\mathbf{r}, \mathbf{v}), (\mathbf{r}, \mathbf{v})) \geq \alpha(\Omega) \|(\mathbf{r}, \mathbf{v})\|^2 \quad \forall (\mathbf{r}, \mathbf{v}) \in \mathbb{H} \times \mathbf{H}_0^1(\Omega), \quad (4.36)$$

where

$$\alpha(\Omega) := \min \left\{ \alpha_1(\Omega), \alpha_3(\Omega), c_p \alpha_4(\Omega), \alpha_5(\Omega) \right\},$$

and  $c_p$  is the positive constant provided by Poincaré's inequality (see [140, Théorème 1.2-5]). In turn, concerning the linear functional  $\mathbf{F}$  and using the Cauchy–Schwarz inequality, we find that

$$\|\mathbf{F}\| \leq M_{\mathbf{S}} \|\mathbf{f}\|_{0,\Omega}, \quad (4.37)$$

where  $M_{\mathbf{S}} := (1 + \kappa_2^2)^{1/2}$ . We conclude by Lax–Milgram theorem (see, e.g., [81, Theorem 1.1]) that there is a unique solution  $(\mathbf{t}, \mathbf{u}) := \mathbf{S}(\phi) \in \mathbb{H} \times \mathbf{H}_0^1(\Omega)$  of (4.25), and the corresponding continuous dependence result together with the ellipticity constant  $\alpha(\Omega)$  and the estimate (4.37) imply (4.33) with the positive constant  $c_{\mathbf{S}} := M_{\mathbf{S}}/\alpha(\Omega)$ , which is clearly independent of  $\phi$ .  $\square$

On the other hand, again we use the Lax–Milgram theorem to establishes the well-posedness of problem (4.27), or equivalently, that the operator  $\tilde{\mathbf{S}}$  (cf. (4.26)) is well-defined.

**Lemma 4.2.** *Assume that  $\kappa_5 \in (0, 2\tilde{\delta})$ , with  $\tilde{\delta} \in (0, 2\kappa)$ , and  $\kappa_6, \kappa_7 > 0$ . Let  $\mathbf{w} \in \mathbf{H}_0^1(\Omega)$  such that  $\|\mathbf{w}\|_{1,\Omega} \leq \frac{\tilde{\alpha}(\Omega)}{2\kappa^{-1}(1 + \kappa_5^2)^{1/2}c(\Omega)}$ , where  $c(\Omega)$  is the constant in (4.15) and  $\tilde{\alpha}(\Omega)$  is the ellipticity constant of the bilinear form  $\tilde{\mathbf{A}}$  given below in (4.40). Then, there exist a unique  $(\mathbf{p}, \theta) := \tilde{\mathbf{S}}(\mathbf{w}) \in \mathbf{H}_{\Gamma_N}(\text{div}; \Omega) \times H^1(\Omega)$  solution of (4.27). Moreover, there exists a constant  $c_{\tilde{\mathbf{S}}} > 0$ , independent of  $\mathbf{w}$ , such that there holds*

$$\|\tilde{\mathbf{S}}(\mathbf{w})\| = \|(\mathbf{p}, \theta)\| \leq c_{\tilde{\mathbf{S}}} \left\{ \|g\|_{0,\Omega} + \|\theta_D\|_{0,\Gamma_D} + \|\theta_D\|_{1/2,\Gamma_D} \right\}. \quad (4.38)$$

*Proof.* For a given  $\mathbf{w} \in \mathbf{H}_0^1(\Omega)$  as stated, we observe from (4.20) and (4.21) that  $\tilde{\mathbf{A}} + \tilde{\mathbf{B}}_{\mathbf{w}}$  is clearly a bilinear form. Now, applying the Cauchy–Schwarz inequality and the estimate (4.15), we deduce that

$$\left| \tilde{\mathbf{A}}((\mathbf{p}, \theta), (\mathbf{q}, \psi)) \right| \leq \|\tilde{\mathbf{A}}\| \|(\mathbf{p}, \theta)\| \|(\mathbf{q}, \psi)\|$$

and

$$\left| \tilde{\mathbf{B}}_{\mathbf{w}}((\mathbf{p}, \theta), (\mathbf{q}, \psi)) \right| \leq \kappa^{-1}(1 + \kappa_5^2)^{1/2}c(\Omega) \|\mathbf{w}\|_{1,\Omega} \|\theta\|_{1,\Omega} \|(\mathbf{q}, \psi)\|, \quad (4.39)$$

for all  $(\mathbf{p}, \theta), (\mathbf{q}, \psi) \in \mathbf{H}_{\Gamma_N}(\text{div}; \Omega) \times H^1(\Omega)$ . Then, by gathering the foregoing inequalities, we find that there exists a positive constant, which we denote by  $\|\tilde{\mathbf{A}} + \tilde{\mathbf{B}}_{\mathbf{w}}\|$ , only depending on  $\kappa, \kappa_5, \kappa_6, \kappa_7, c(\Omega)$ , and the bound for  $\|\mathbf{w}\|_{1,\Omega}$  assumed here, such that

$$\left| (\tilde{\mathbf{A}} + \tilde{\mathbf{B}}_{\mathbf{w}})((\mathbf{p}, \theta), (\mathbf{q}, \psi)) \right| \leq \|\tilde{\mathbf{A}} + \tilde{\mathbf{B}}_{\mathbf{w}}\| \|(\mathbf{p}, \theta)\| \|(\mathbf{q}, \psi)\|,$$

for all  $(\mathbf{p}, \theta), (\mathbf{q}, \psi) \in \mathbf{H}_{\Gamma_N}(\text{div}; \Omega) \times H^1(\Omega)$ . In turn, from (4.20) we have that

$$\tilde{\mathbf{A}}((\mathbf{q}, \psi), (\mathbf{q}, \psi)) = \kappa^{-1} \|\mathbf{q}\|_{0,\Omega}^2 + \kappa_6 \|\text{div } \mathbf{q}\|_{0,\Omega}^2 - \kappa^{-1} \kappa_5 \int_{\Omega} \mathbf{q} \cdot \nabla \psi + \kappa_5 |\psi|_{1,\Omega}^2 + \kappa_7 \|\psi\|_{0,\Gamma_D}^2,$$

and hence, using the Cauchy–Schwarz and Young inequalities, we obtain that for any  $\tilde{\delta} > 0$  and for all  $(\mathbf{q}, \psi) \in \mathbf{H}_{\Gamma_N}(\text{div}; \Omega) \times H^1(\Omega)$ , there holds

$$\tilde{\mathbf{A}}((\mathbf{q}, \psi), (\mathbf{q}, \psi)) \geq \kappa^{-1} \left(1 - \frac{\kappa_5}{2\tilde{\delta}}\right) \|\mathbf{q}\|_{0,\Omega}^2 + \kappa_6 \|\text{div } \mathbf{q}\|_{0,\Omega}^2 + \kappa_5 \left(1 - \frac{\kappa^{-1}}{2}\tilde{\delta}\right) |\psi|_{1,\Omega}^2 + \kappa_7 \|\psi\|_{0,\Gamma_D}^2.$$

In this way, applying the inequality (4.31), we can define the constants

$$\tilde{\alpha}_1(\Omega) := \min \left\{ \kappa^{-1} \left(1 - \frac{\kappa_5}{2\tilde{\delta}}\right), \kappa_6 \right\} \quad \text{and} \quad \tilde{\alpha}_2(\Omega) := c_2(\Omega) \min \left\{ \kappa_5 \left(1 - \frac{\kappa^{-1}}{2}\tilde{\delta}\right), \kappa_7 \right\},$$

which are positive thanks to the hypotheses on  $\tilde{\delta}$ ,  $\kappa_5$ ,  $\kappa_6$ , and  $\kappa_7$ . In this way, it follows that

$$\tilde{\mathbf{A}}((\mathbf{q}, \psi), (\mathbf{q}, \psi)) \geq \tilde{\alpha}(\Omega) \|(\mathbf{q}, \psi)\|^2 \quad \forall (\mathbf{q}, \psi) \in \mathbf{H}_{\Gamma_N}(\text{div}; \Omega) \times H^1(\Omega), \quad (4.40)$$

with  $\tilde{\alpha}(\Omega) := \min \{\tilde{\alpha}_1(\Omega), \tilde{\alpha}_2(\Omega)\}$ , which shows that  $\tilde{\mathbf{A}}$  is elliptic. Therefore, combining now (4.39), (4.40), and the bound for  $\|\mathbf{w}\|_{1,\Omega}$  assumed here, we deduce that for all  $(\mathbf{q}, \psi) \in \mathbf{H}_{\Gamma_N}(\text{div}; \Omega) \times H^1(\Omega)$ , there holds

$$(\tilde{\mathbf{A}} + \tilde{\mathbf{B}}_{\mathbf{w}})((\mathbf{q}, \psi), (\mathbf{q}, \psi)) \geq \left\{ \tilde{\alpha}(\Omega) - \kappa^{-1}(1 + \kappa_5^2)^{1/2} c(\Omega) \|\mathbf{w}\|_{1,\Omega} \right\} \|(\mathbf{q}, \psi)\|^2 \geq \frac{\tilde{\alpha}(\Omega)}{2} \|(\mathbf{q}, \psi)\|^2, \quad (4.41)$$

which proves the ellipticity of  $\tilde{\mathbf{A}} + \tilde{\mathbf{B}}_{\mathbf{w}}$ , with constant  $\frac{\tilde{\alpha}(\Omega)}{2}$ , independent of  $\mathbf{w}$ . On the other hand, it is easy to see from (4.23), by using Cauchy–Schwarz’s inequality and the trace theorems in  $\mathbf{H}(\text{div}; \Omega)$  and  $H^1(\Omega)$ , whose boundedness constants are given by 1 and  $\|\gamma_0\|$ , respectively, that the functional  $\tilde{\mathbf{F}}$  is bounded with

$$\|\tilde{\mathbf{F}}\| \leq M_{\tilde{\mathbf{S}}} \left\{ \|g\|_{0,\Omega} + \|\theta_D\|_{0,\Gamma_D} + \|\theta_D\|_{1/2,\Gamma_D} \right\}, \quad (4.42)$$

where  $M_{\tilde{\mathbf{S}}} := \max \left\{ (1 + \kappa_6^2)^{1/2}, \kappa_7 \|\gamma_0\| \right\}$ . Summing up, and owing to the hypotheses on  $\kappa_5$ ,  $\kappa_6$  and  $\kappa_7$ , we have proved that for any sufficiently small  $\mathbf{w} \in \mathbf{H}_0^1(\Omega)$ , the bilinear form  $\tilde{\mathbf{A}} + \tilde{\mathbf{B}}_{\mathbf{w}}$  and the functional  $\tilde{\mathbf{F}}$  satisfy the hypotheses of the Lax–Milgram theorem (see, e.g., [81, Theorem 1.1]), which guarantees the well-posedness of (4.27) and the continuous dependence estimate (4.38) with  $c_{\tilde{\mathbf{S}}} := 2M_{\tilde{\mathbf{S}}}/\tilde{\alpha}(\Omega)$ .  $\square$

At this point we remark that the restriction on  $\|\mathbf{w}\|_{1,\Omega}$  in Lemma 4.2 could also have been taken as  $\|\mathbf{w}\|_{1,\Omega} \leq \omega \frac{\tilde{\alpha}(\Omega)}{\kappa^{-1}(1 + \kappa_5^2)^{1/2} c(\Omega)}$  with any  $\omega \in (0, 1)$ . However, we have chosen  $\omega = \frac{1}{2}$  for simplicity and because it yields a joint maximization of the ellipticity constant of  $\tilde{\mathbf{A}} + \tilde{\mathbf{B}}_{\mathbf{w}}$  and the upper bound for  $\|\mathbf{w}\|_{1,\Omega}$ . In addition, we also remark that the constants  $\alpha(\Omega)$  and  $\tilde{\alpha}(\Omega)$  yielding the ellipticity of  $\mathbf{A}_{\phi}$  and  $\tilde{\mathbf{A}} + \tilde{\mathbf{B}}_{\mathbf{w}}$ , respectively, can be maximized by taking the parameters  $\delta_1, \kappa_1, \delta_2, \kappa_3, \delta_3, \kappa_4, \tilde{\delta}$ , and  $\kappa_5$  as the middle points of their feasible ranges, and by choosing  $\kappa_2, \kappa_6$  and  $\kappa_7$  so that they maximize

the minima defining  $\alpha_2(\Omega)$ ,  $\tilde{\alpha}_1(\Omega)$ , and  $\tilde{\alpha}_2(\Omega)$ , respectively. More precisely, we simply take

$$\begin{aligned} \delta_1 &= \frac{1}{\mu_2}, \quad \kappa_1 = \frac{\delta_1 \mu_1}{\mu_2} = \frac{\mu_1}{\mu_2^2}, \quad \delta_2 = 1, \quad \kappa_3 = \delta_2 \left( \mu_1 - \frac{\kappa_1 \mu_2}{2\delta_1} \right) = \frac{\mu_1}{2}, \quad \delta_3 = 1, \\ \kappa_4 &= \delta_3 \kappa_3 \left( 1 - \frac{\delta_2}{2} \right) = \frac{\mu_1}{4}, \quad \kappa_2 = 2\kappa_1 \left( 1 - \frac{\mu_2 \delta_1}{2} \right) = \frac{\mu_1}{\mu_2^2}, \quad \tilde{\delta} = \kappa, \\ \kappa_5 &= \tilde{\delta} = \kappa, \quad \kappa_6 = \kappa^{-1} \left( 1 - \frac{\kappa_5}{2\tilde{\delta}} \right) = \frac{\kappa^{-1}}{2}, \quad \kappa_7 = \kappa_5 \left( 1 - \frac{\kappa^{-1}}{2} \tilde{\delta} \right) = \frac{\kappa}{2}, \end{aligned} \quad (4.43)$$

which yields

$$\begin{aligned} \alpha_1(\Omega) &= \frac{\mu_1}{4}, \quad \alpha_2(\Omega) = \frac{\mu_1}{2\mu_2^2}, \quad \alpha_3(\Omega) = \min \left\{ c_1(\Omega), 1 \right\} \frac{\mu_1}{2\mu_2^2}, \\ \alpha_4(\Omega) &= \frac{\mu_1}{16}, \quad \alpha_5(\Omega) = \frac{\mu_1}{8}, \quad \tilde{\alpha}_1(\Omega) = \frac{\kappa^{-1}}{2}, \quad \tilde{\alpha}_2(\Omega) = c_2(\Omega) \frac{\kappa}{2}, \end{aligned}$$

and hence

$$\alpha(\Omega) = \min \left\{ \min \left\{ c_1(\Omega), 1 \right\} \frac{\mu_1}{2\mu_2^2}, c_p \frac{\mu_1}{16}, \frac{\mu_1}{8} \right\}, \quad \text{and} \quad \tilde{\alpha}(\Omega) = \frac{1}{2} \min \left\{ \kappa^{-1}, c_2(\Omega) \kappa \right\}.$$

The explicit values of the stabilization parameters  $\kappa_i$ ,  $i \in \{1, \dots, 7\}$ , given in (4.43), will be employed in Section 4.5 for the corresponding numerical experiments.

### 4.3.3 Solvability analysis of the fixed-point equation

Having proved the well-posedness of the uncoupled problems (4.25) and (4.27), which ensures that the operators  $\mathbf{S}$ ,  $\tilde{\mathbf{S}}$  and  $\mathbf{T}$  are well defined, we now aim to establish the existence of a unique fixed point of the operator  $\mathbf{T}$ . For this purpose, in what follows we verify the hypothesis of the Schauder and Banach fixed-point theorems. We begin the analysis with the following straightforward consequence of Lemmas 4.1 and 4.2.

**Lemma 4.3.** *Suppose that the parameters  $\kappa_i$ ,  $i \in \{1, \dots, 7\}$ , satisfy the conditions required by Lemmas 4.1 and 4.2. Let  $\mathcal{W}$  be the closed and convex subset of  $H^1(\Omega)$  defined by*

$$\mathcal{W} := \left\{ \phi \in H^1(\Omega) : \quad \|\phi\|_{1,\Omega} \leq c_{\tilde{\mathbf{S}}} \left\{ \|g\|_{0,\Omega} + \|\theta_D\|_{0,\Gamma_D} + \|\theta_D\|_{1/2,\Gamma_D} \right\} \right\},$$

where  $c_{\tilde{\mathbf{S}}}$  is the constant given by (4.38). In addition, assume that the datum  $\mathbf{f}$  satisfy

$$c_{\mathbf{S}} \|\mathbf{f}\|_{0,\Omega} \leq \frac{\tilde{\alpha}(\Omega)}{2\kappa^{-1}(1 + \kappa_5^2)^{1/2} c(\Omega)}, \quad (4.44)$$

where  $c_{\mathbf{S}}$  is the constant given by (4.33). Then  $\mathbf{T}(\mathcal{W}) \subseteq \mathcal{W}$ .

*Proof.* Given  $\phi \in \mathcal{W}$ , we get from (4.33) (cf. Lemma 4.1) that

$$\|\mathbf{S}(\phi)\| = \|(\mathbf{t}, \mathbf{u})\| \leq c_{\mathbf{S}} \|\mathbf{f}\|_{0,\Omega},$$

and hence, thanks to the constraint (4.44), we observe that  $\mathbf{u} = \mathbf{S}_2(\phi)$  satisfies the hypotheses of Lemma 4.2. Moreover, the corresponding estimate (4.38) gives

$$\|\mathbf{T}(\phi)\|_{1,\Omega} = \|\tilde{\mathbf{S}}_2(\mathbf{u})\|_{1,\Omega} \leq c_{\tilde{\mathbf{S}}} \left\{ \|g\|_{0,\Omega} + \|\theta_D\|_{0,\Gamma_D} + \|\theta_D\|_{1/2,\Gamma_D} \right\},$$

which implies that  $\mathbf{T}(\phi) \in \mathcal{W}$ , thus finishing the proof.  $\square$

Next, we establish two lemmas that will be useful to derive conditions under which the operator  $\mathbf{T}$  is continuous and compact. To that end, and similarly as in [2, Section 3.3], we first introduce suitable regularity hypotheses on the operator  $\mathbf{S}$ , which will be employed later on. In fact, for the remainder of this chapter we proceed as in [2, eq. (3.22)], and suppose that  $\mathbf{f} \in \mathbf{H}^\delta(\Omega)$ , for some  $\delta \in (0, 1)$  (when  $n = 2$ ) or  $\delta \in (1/2, 1)$  (when  $n = 3$ ). Then, we assume that for each  $\phi \in H^1(\Omega)$  there holds  $\mathbf{S}(\phi) \in (\mathbb{H}^\delta(\Omega) \times (\mathbb{H}_0(\mathbf{div}; \Omega) \cap \mathbb{H}^\delta(\Omega)) \times \mathbb{H}^\delta(\Omega)) \times \mathbf{H}^{1+\delta}(\Omega)$ , with

$$\|\mathbf{S}_1^{\mathbf{t}}(\phi)\|_{\delta, \Omega} + \|\mathbf{S}_1^{\sigma}(\phi)\|_{\delta, \Omega} + \|\mathbf{S}_1^{\rho}(\phi)\|_{\delta, \Omega} + \|\mathbf{S}_2(\phi)\|_{1+\delta, \Omega} \leq \widehat{C}_{\mathbf{S}} \|\mathbf{f}\|_{\delta, \Omega}, \quad (4.45)$$

where  $\widehat{C}_{\mathbf{S}}$  is a positive constant independent of  $\phi$ . The reason of the stipulated ranges for  $\delta$  will be clarified in the forthcoming analysis (see below proof of Lemmas 4.4 and 4.7). More precisely, we remark in advance that the regularity estimate (4.45) is needed in the proof of Lemmas 4.4 and 4.7 to bound an expression of the form  $\|\mathbf{S}_1^{\mathbf{t}}(\phi)\|_{\mathbf{L}^{2p}(\Omega)}$  in terms of  $\|\mathbf{S}_1^{\mathbf{t}}(\phi)\|_{\delta, \Omega}$ , and hence of the data at the right-hand side of (4.45).

**Lemma 4.4.** *There exists a positive constant  $C_{\mathbf{S}}$ , depending on  $L_\mu$ , the parameter  $\kappa_1$ , the ellipticity constant  $\alpha(\Omega)$  of the bilinear form  $\mathbf{A}_\phi$  (cf. (4.36)), and  $\delta$  (cf. (4.45)), such that*

$$\|\mathbf{S}(\phi) - \mathbf{S}(\tilde{\phi})\| \leq C_{\mathbf{S}} \|\mathbf{S}_1^{\mathbf{t}}(\phi)\|_{\delta, \Omega} \|\phi - \tilde{\phi}\|_{\mathbf{L}^{n/\delta}(\Omega)} \quad \forall \phi, \tilde{\phi} \in H^1(\Omega). \quad (4.46)$$

*Proof.* We proceed as in [2, Lemma 3.9]. In fact, given  $\phi, \tilde{\phi} \in H^1(\Omega)$ , we let  $(\mathbf{t}, \mathbf{u}) := \mathbf{S}(\phi)$  and  $(\tilde{\mathbf{t}}, \tilde{\mathbf{u}}) := \mathbf{S}(\tilde{\phi})$  be the corresponding solutions of problem (4.25). Then, using the bilinearity of  $\mathbf{A}_\phi$  for any  $\phi$ , it follows easily from (4.25) that

$$\mathbf{A}_{\tilde{\phi}}((\mathbf{t}, \mathbf{u}) - (\tilde{\mathbf{t}}, \tilde{\mathbf{u}}), (\mathbf{r}, \mathbf{v})) = - \int_{\Omega} \left\{ \mu(\phi) - \mu(\tilde{\phi}) \right\} \mathbf{t} : \left\{ \mathbf{r} - \kappa_1 \boldsymbol{\tau}^{\mathbf{d}} \right\},$$

for all  $(\mathbf{r}, \mathbf{v}) \in \mathbb{H} \times \mathbf{H}_0^1(\Omega)$ . Hence, applying the ellipticity of  $\mathbf{A}_\phi$  (cf. (4.19)), Cauchy–Schwarz inequality, the Lipschitz-continuity assumption (4.9), and then Hölder inequality, we find that

$$\begin{aligned} \alpha(\Omega) \|(\mathbf{t}, \mathbf{u}) - (\tilde{\mathbf{t}}, \tilde{\mathbf{u}})\|^2 &\leq \mathbf{A}_{\tilde{\phi}}((\mathbf{t}, \mathbf{u}) - (\tilde{\mathbf{t}}, \tilde{\mathbf{u}}), (\mathbf{t}, \mathbf{u}) - (\tilde{\mathbf{t}}, \tilde{\mathbf{u}})) \\ &= - \int_{\Omega} \left\{ \mu(\phi) - \mu(\tilde{\phi}) \right\} \mathbf{t} : \left\{ (\mathbf{t} - \tilde{\mathbf{t}}) - \kappa_1 (\boldsymbol{\sigma}^{\mathbf{d}} - \tilde{\boldsymbol{\sigma}}^{\mathbf{d}}) \right\} \\ &\leq L_\mu (1 + \kappa_1^2)^{1/2} \|\mathbf{t}\|_{\mathbf{L}^{2p}(\Omega)} \|\phi - \tilde{\phi}\|_{\mathbf{L}^{2q}(\Omega)} \|(\mathbf{t}, \mathbf{u}) - (\tilde{\mathbf{t}}, \tilde{\mathbf{u}})\|, \end{aligned} \quad (4.47)$$

where  $p, q \in [1, +\infty)$  are such that  $1/p + 1/q = 1$ . Next, given the further regularity  $\delta$  assumed in (4.45), we recall that the Sobolev embedding theorem (cf. [1, Theorem 4.12], [139, Theorem 1.3.4]) establishes the continuous injection  $i_\delta : H^\delta(\Omega) \rightarrow L^{\delta^*}(\Omega)$  with boundedness constant  $C_\delta > 0$ , where

$$\delta^* := \begin{cases} \frac{2}{1-\delta} & \text{if } n = 2, \\ \frac{6}{3-2\delta} & \text{if } n = 3. \end{cases}$$

Thus, choosing  $p$  such that  $2p = \delta^*$  and recalling that  $\mathbf{t} := \mathbf{S}_1^{\mathbf{t}}(\phi)$ , we find that

$$\|\mathbf{t}\|_{\mathbf{L}^{2p}(\Omega)} = \|\mathbf{S}_1^{\mathbf{t}}(\phi)\|_{\mathbf{L}^{2p}(\Omega)} \leq C_\delta \|\mathbf{S}_1^{\mathbf{t}}(\phi)\|_{\delta, \Omega}. \quad (4.48)$$



In turn, according to the above choice of  $p$ , that is  $p = \delta^*/2$ , it readily follows that

$$2q := \frac{2p}{p-1} = \begin{cases} \frac{2}{\delta} & \text{if } n = 2 \\ \frac{3}{\delta} & \text{if } n = 3 \end{cases} = \frac{n}{\delta}. \quad (4.49)$$

Therefore, inequalities (4.47) and (4.48) together with identity (4.49) conclude (4.46) with constant  $C_S := L_\mu(1 + \kappa_1^2)^{1/2}C_\delta/\alpha(\Omega)$ .  $\square$

In turn, the following result establishes the Lipschitz-continuity of the operator  $\tilde{\mathbf{S}}$ .

**Lemma 4.5.** *There exists a positive constant  $C_{\tilde{\mathbf{S}}}$ , depending on  $\kappa$ , the parameter  $\kappa_5$ , the ellipticity constant  $\tilde{\alpha}(\Omega)$  of the bilinear form  $\tilde{\mathbf{A}}$  (cf. (4.40)), and the constant  $c(\Omega)$  (cf. (4.15)), such that for all  $\mathbf{w}, \tilde{\mathbf{w}} \in \mathbf{H}_0^1(\Omega)$  with  $\|\mathbf{w}\|_{1,\Omega}, \|\tilde{\mathbf{w}}\|_{1,\Omega} \leq \frac{\tilde{\alpha}(\Omega)}{2\kappa^{-1}(1 + \kappa_5^2)^{1/2}c(\Omega)}$ , there holds*

$$\|\tilde{\mathbf{S}}(\mathbf{w}) - \tilde{\mathbf{S}}(\tilde{\mathbf{w}})\| \leq C_{\tilde{\mathbf{S}}} \|\tilde{\mathbf{S}}_2(\mathbf{w})\|_{1,\Omega} \|\mathbf{w} - \tilde{\mathbf{w}}\|_{1,\Omega}. \quad (4.50)$$

*Proof.* It follows almost straightforwardly from a slight modification of the proof of [52, Lemma 3.7]. We omit further details.  $\square$

As a consequence of the previous lemmas we establish the following result providing an estimate needed to derive next the required continuity and compactness properties of the operator  $\mathbf{T}$ .

**Lemma 4.6.** *Let  $\mathcal{W} := \left\{ \phi \in H^1(\Omega) : \|\phi\|_{1,\Omega} \leq c_{\tilde{\mathbf{S}}} \left\{ \|g\|_{0,\Omega} + \|\theta_D\|_{0,\Gamma_D} + \|\theta_D\|_{1/2,\Gamma_D} \right\} \right\}$ , and assume that the datum  $\mathbf{f}$  satisfy (4.44). Then, there holds*

$$\|\mathbf{T}(\phi) - \mathbf{T}(\tilde{\phi})\|_{1,\Omega} \leq C_S C_{\tilde{\mathbf{S}}} \|\mathbf{T}(\phi)\|_{1,\Omega} \|\mathbf{S}_1^t(\phi)\|_{\delta,\Omega} \|\phi - \tilde{\phi}\|_{L^{n/\delta}(\Omega)}, \quad (4.51)$$

where  $C_S$  and  $C_{\tilde{\mathbf{S}}}$  are the constants given by (4.46) and (4.50), respectively.

*Proof.* It suffices to recall that  $\mathbf{T}(\phi) = \tilde{\mathbf{S}}_2(\mathbf{S}_2(\phi)) \quad \forall \phi \in H^1(\Omega)$  (cf. (4.28)), and then apply Lemmas 4.3, 4.4 and 4.5.  $\square$

Owing to the above analysis, we establish now the announced properties of the operator  $\mathbf{T}$ .

**Lemma 4.7.** *Let  $\mathcal{W} := \left\{ \phi \in H^1(\Omega) : \|\phi\|_{1,\Omega} \leq c_{\tilde{\mathbf{S}}} \left\{ \|g\|_{0,\Omega} + \|\theta_D\|_{0,\Gamma_D} + \|\theta_D\|_{1/2,\Gamma_D} \right\} \right\}$ , and assume that the datum  $\mathbf{f}$  satisfy (4.44). Then,  $\mathbf{T} : \mathcal{W} \rightarrow \mathcal{W}$  is continuous and  $\overline{\mathbf{T}(\mathcal{W})}$  is compact.*

*Proof.* The required result follows basically from (4.51), the Rellich–Kondrachov compactness Theorem (cf. [1, Theorem 6.3], [139, Theorem 1.3.5]), the specified range of the constant  $\delta$  involved in the further regularity assumptions given by (4.45), and the well-known fact that every bounded sequence in a Hilbert space has a weakly convergent subsequence. We omit further details and refer to [2, Lemma 3.12].  $\square$

Finally, the main result of this section is given as follows.

**Theorem 4.8.** *Suppose that the parameters  $\kappa_i$ ,  $i \in \{1, \dots, 7\}$ , satisfy the conditions required by Lemmas 4.1 and 4.2. Let  $\mathcal{W} := \left\{ \phi \in \mathbf{H}^1(\Omega) : \|\phi\|_{1,\Omega} \leq c_{\mathbf{S}} \left\{ \|g\|_{0,\Omega} + \|\theta_D\|_{0,\Gamma_D} + \|\theta_D\|_{1/2,\Gamma_D} \right\} \right\}$ , and assume that the datum  $\mathbf{f}$  satisfy (4.44). Then the augmented fully-mixed problem (4.18) has at least one solution  $(\mathbf{t}, \mathbf{u}, \mathbf{p}, \theta) \in \mathbb{H} \times \mathbf{H}_0^1(\Omega) \times \mathbf{H}_{\Gamma_N}(\text{div}; \Omega) \times \mathbf{H}^1(\Omega)$  with  $\theta \in \mathcal{W}$ , and there holds*

$$\|(\mathbf{t}, \mathbf{u})\| \leq c_{\mathbf{S}} \|\mathbf{f}\|_{0,\Omega}, \quad (4.52)$$

and

$$\|(\mathbf{p}, \theta)\| \leq c_{\mathbf{S}} \left\{ \|g\|_{0,\Omega} + \|\theta_D\|_{0,\Gamma_D} + \|\theta_D\|_{1/2,\Gamma_D} \right\}, \quad (4.53)$$

where  $c_{\mathbf{S}}$  and  $c_{\mathbf{S}}$  are the constants specified in Lemmas 4.1 and 4.2, respectively. Moreover, assume that the data  $\mathbf{f}$ ,  $g$  and  $\theta_D$  are sufficiently small so that, with the constants  $C_{\mathbf{S}}$ ,  $C_{\mathbf{S}}$  and  $\widehat{C}_{\mathbf{S}}$  from Lemmas 4.4 and 4.5, and estimate (4.45), respectively, and denoting by  $\widetilde{C}_{\delta}$  the boundedness constant of the continuous injection of  $\mathbf{H}^1(\Omega)$  into  $\mathbf{L}^{n/\delta}(\Omega)$ , there holds

$$\widetilde{C}_{\delta} \widehat{C}_{\mathbf{S}} C_{\mathbf{S}} C_{\mathbf{S}} c_{\mathbf{S}} \left\{ \|g\|_{0,\Omega} + \|\theta_D\|_{0,\Gamma_D} + \|\theta_D\|_{1/2,\Gamma_D} \right\} \|\mathbf{f}\|_{\delta,\Omega} < 1. \quad (4.54)$$

Then the solution  $\theta$  is unique in  $\mathcal{W}$ .

*Proof.* The equivalence between (4.18) and the fixed-point equation (4.29), together with Lemmas 4.3 and 4.7, confirm the existence of solution of (4.18) as a direct application of the Schauder fixed-point theorem [47, Theorem 9.12-1(b)]. In addition, it is clear that the estimates (4.52) and (4.53) follow straightforwardly from (4.33) and (4.38), respectively. Furthermore, given another solution  $\widetilde{\theta} \in \mathcal{W}$  of (4.29), the estimates  $\|\mathbf{T}(\theta)\|_{1,\Omega} = \|\theta\|_{1,\Omega} \leq c_{\mathbf{S}} \left\{ \|g\|_{0,\Omega} + \|\theta_D\|_{0,\Gamma_D} + \|\theta_D\|_{1/2,\Gamma_D} \right\}$ ,

$$\|\mathbf{S}_1^{\mathbf{t}}(\theta)\|_{\delta,\Omega} \leq \widehat{C}_{\mathbf{S}} \|\mathbf{f}\|_{\delta,\Omega},$$

and

$$\|\phi\|_{\mathbf{L}^{n/\delta}(\Omega)} \leq \widetilde{C}_{\delta} \|\phi\|_{1,\Omega} \quad \forall \phi \in \mathbf{H}^1(\Omega), \quad (4.55)$$

confirm (4.54) as a sufficient condition for concluding, together with (4.51), that  $\theta = \widetilde{\theta}$ . In other words, (4.54) constitutes the condition that makes the operator  $\mathbf{T}$  to become a contraction, thus yielding, thanks to the Banach fixed-point theorem, the existence of a unique fixed point of  $\mathbf{T}$  in  $\mathcal{W}$ .  $\square$

## 4.4 The Galerkin scheme

In this section we introduce and analyse the Galerkin scheme of the augmented fully-mixed formulation (4.18). We analyse its solvability by employing a discrete version of the fixed-point strategy developed in Sections 4.3.1 and 4.3.2. Finally, we derive the corresponding Céa estimate and rates of convergence of our Galerkin scheme.

### 4.4.1 Discrete setting

Let  $\mathcal{T}_h$  be a regular triangulation of  $\Omega$  made up of triangles  $K$  (when  $n = 2$ ) or tetrahedra  $K$  (when  $n = 3$ ) of diameter  $h_K$ , and define the meshsize  $h := \max \{ h_K : K \in \mathcal{T}_h \}$ . Then, for each  $K \in \mathcal{T}_h$

we set the local Raviart–Thomas space of order  $k$  as

$$\mathbf{RT}_k(K) := \mathbf{P}_k(K) \oplus \mathbf{P}_k(K)\mathbf{x},$$

where  $\mathbf{x} := (x_1, \dots, x_n)^\top$  is a generic vector of  $\mathbb{R}^n$ . Then, we introduce the finite element subspaces approximating the unknowns  $\mathbf{t}, \boldsymbol{\sigma}, \boldsymbol{\rho}, \mathbf{u}, \mathbf{p}$  and  $\theta$  as follows

$$\begin{aligned} \mathbb{H}_h^{\mathbf{t}} &:= \left\{ \mathbf{r}_h \in \mathbb{L}_{\text{tr}}^2(\Omega) : \quad \mathbf{r}_h|_K \in \mathbb{P}_k(K) \quad \forall K \in \mathcal{T}_h \right\}, \\ \mathbb{H}_h^{\boldsymbol{\sigma}} &:= \left\{ \boldsymbol{\tau}_h \in \mathbb{H}_0(\text{div}; \Omega) : \quad \mathbf{c}^\top \boldsymbol{\tau}_h|_K \in \mathbf{RT}_k(K) \quad \forall \mathbf{c} \in \mathbb{R}^n \quad \forall K \in \mathcal{T}_h \right\}, \\ \mathbb{H}_h^{\boldsymbol{\rho}} &:= \left\{ \boldsymbol{\eta}_h \in \mathbb{L}_{\text{skew}}^2(\Omega) : \quad \boldsymbol{\eta}_h|_K \in \mathbb{P}_k(K) \quad \forall K \in \mathcal{T}_h \right\}, \\ \mathbf{H}_h^{\mathbf{u}} &:= \left\{ \mathbf{v}_h \in \mathbf{C}(\overline{\Omega}) : \quad \mathbf{v}_h|_K \in \mathbf{P}_{k+1}(K) \quad \forall K \in \mathcal{T}_h, \quad \mathbf{v}_h = 0 \text{ on } \Gamma \right\}, \\ \mathbf{H}_h^{\mathbf{p}} &:= \left\{ \mathbf{q}_h \in \mathbf{H}_{\Gamma_N}(\text{div}; \Omega) : \quad \mathbf{q}_h|_K \in \mathbf{RT}_k(K) \quad \forall K \in \mathcal{T}_h \right\}, \\ \mathbf{H}_h^\theta &:= \left\{ \psi_h \in C(\overline{\Omega}) : \quad \psi_h|_K \in \mathbf{P}_{k+1}(K) \quad \forall K \in \mathcal{T}_h \right\}. \end{aligned} \tag{4.56}$$

In this way, by defining  $\underline{\mathbf{t}}_h := (\mathbf{t}_h, \boldsymbol{\sigma}_h, \boldsymbol{\rho}_h)$ ,  $\underline{\mathbf{r}}_h := (\mathbf{r}_h, \boldsymbol{\tau}_h, \boldsymbol{\eta}_h) \in \mathbb{H}_h := \mathbb{H}_h^{\mathbf{t}} \times \mathbb{H}_h^{\boldsymbol{\sigma}} \times \mathbb{H}_h^{\boldsymbol{\rho}}$ , the Galerkin scheme of (4.18) reads: Find  $(\underline{\mathbf{t}}_h, \mathbf{u}_h, \mathbf{p}_h, \theta_h) \in \mathbb{H}_h \times \mathbf{H}_h^{\mathbf{u}} \times \mathbf{H}_h^{\mathbf{p}} \times \mathbf{H}_h^\theta$  such that

$$\begin{aligned} \mathbf{A}_{\theta_h}((\underline{\mathbf{t}}_h, \mathbf{u}_h), (\underline{\mathbf{r}}_h, \mathbf{v}_h)) &= \mathbf{F}(\underline{\mathbf{r}}_h, \mathbf{v}_h) \quad \forall (\underline{\mathbf{r}}_h, \mathbf{v}_h) \in \mathbb{H}_h \times \mathbf{H}_h^{\mathbf{u}}, \\ \tilde{\mathbf{A}}((\mathbf{p}_h, \theta_h), (\mathbf{q}_h, \psi_h)) + \tilde{\mathbf{B}}_{\mathbf{u}_h}((\mathbf{p}_h, \theta_h), (\mathbf{q}_h, \psi_h)) &= \tilde{\mathbf{F}}(\mathbf{q}_h, \psi_h) \quad \forall (\mathbf{q}_h, \psi_h) \in \mathbf{H}_h^{\mathbf{p}} \times \mathbf{H}_h^\theta. \end{aligned} \tag{4.57}$$

Similarly to the continuous context, in order to analyse problem (4.57) we rewrite it equivalently as a fixed-point problem. Indeed, we firstly define  $\mathbf{S}_h : \mathbf{H}_h^\theta \rightarrow \mathbb{H}_h \times \mathbf{H}_h^{\mathbf{u}}$  by

$$\mathbf{S}_h(\phi_h) := (\mathbf{S}_{1,h}(\phi_h), \mathbf{S}_{2,h}(\phi_h)) = (\underline{\mathbf{t}}_h, \mathbf{u}_h) \quad \forall \phi_h \in \mathbf{H}_h^\theta, \tag{4.58}$$

where  $\mathbf{S}_{1,h}(\phi_h) := (\mathbf{S}_{1,h}^{\mathbf{t}}(\phi_h), \mathbf{S}_{1,h}^{\boldsymbol{\sigma}}(\phi_h), \mathbf{S}_{1,h}^{\boldsymbol{\rho}}(\phi_h))$  and  $(\underline{\mathbf{t}}_h, \mathbf{u}_h)$  is the unique solution of the discrete version of the problem (4.25): Find  $(\underline{\mathbf{t}}_h, \mathbf{u}_h) \in \mathbb{H}_h \times \mathbf{H}_h^{\mathbf{u}}$  such that

$$\mathbf{A}_{\phi_h}((\underline{\mathbf{t}}_h, \mathbf{u}_h), (\underline{\mathbf{r}}_h, \mathbf{v}_h)) = \mathbf{F}(\underline{\mathbf{r}}_h, \mathbf{v}_h) \quad \forall (\underline{\mathbf{r}}_h, \mathbf{v}_h) \in \mathbb{H}_h \times \mathbf{H}_h^{\mathbf{u}}, \tag{4.59}$$

where the bilinear form  $\mathbf{A}_{\phi_h}$  (with  $\phi_h$  in place of  $\phi$ ) and the functional  $\mathbf{F}$  are defined as in (4.19) and (4.22), respectively. Secondly, we define the operator  $\tilde{\mathbf{S}}_h : \mathbf{H}_h^{\mathbf{u}} \rightarrow \mathbf{H}_h^{\mathbf{p}} \times \mathbf{H}_h^\theta$  as

$$\tilde{\mathbf{S}}_h(\mathbf{w}_h) := (\tilde{\mathbf{S}}_{1,h}(\mathbf{w}_h), \tilde{\mathbf{S}}_{2,h}(\mathbf{w}_h)) = (\mathbf{p}_h, \theta_h) \quad \forall \mathbf{w}_h \in \mathbf{H}_h^{\mathbf{u}}, \tag{4.60}$$

where  $(\mathbf{p}_h, \theta_h)$  is the unique solution of the discrete version of the problem (4.27): Find  $(\mathbf{p}_h, \theta_h) \in \mathbf{H}_h^{\mathbf{p}} \times \mathbf{H}_h^\theta$  such that

$$\tilde{\mathbf{A}}((\mathbf{p}_h, \theta_h), (\mathbf{q}_h, \psi_h)) + \tilde{\mathbf{B}}_{\mathbf{w}_h}((\mathbf{p}_h, \theta_h), (\mathbf{q}_h, \psi_h)) = \tilde{\mathbf{F}}(\mathbf{q}_h, \psi_h) \quad \forall (\mathbf{q}_h, \psi_h) \in \mathbf{H}_h^{\mathbf{p}} \times \mathbf{H}_h^\theta, \tag{4.61}$$

where the bilinear form  $\tilde{\mathbf{A}}$  and the functional  $\tilde{\mathbf{F}}$  are defined as in (4.20) and (4.23), respectively, whereas,  $\tilde{\mathbf{B}}_{\mathbf{w}_h}$  is the bilinear form given by (4.21) (with  $\mathbf{w}_h$  instead of  $\mathbf{w}$ ). Finally, we introduce the operator  $\mathbf{T}_h : \mathbf{H}_h^\theta \rightarrow \mathbf{H}_h^\theta$  as

$$\mathbf{T}_h(\phi_h) := \tilde{\mathbf{S}}_{2,h}(\mathbf{S}_{2,h}(\phi_h)) \quad \forall \phi_h \in \mathbf{H}_h^\theta, \tag{4.62}$$

and realise that solving (4.57) is equivalent to seeking a fixed point of the operator  $\mathbf{T}_h$ , that is: Find  $\theta_h \in \mathbf{H}_h^\theta$  such that

$$\mathbf{T}_h(\theta_h) = \theta_h. \tag{4.63}$$

### 4.4.2 Solvability analysis

Now we establish the solvability of problem (4.57) by studying the equivalent fixed-point problem (4.63). To that end, first we guarantee that the discrete problems (4.59) and (4.61) are well-posed. Indeed, it is easy to see that the respective proofs are almost verbatim of the continuous analogues provided in Section 4.3.2, and hence we simply state the corresponding results as follows.

**Lemma 4.9.** *Assume that  $\kappa_i$ ,  $i \in \{1, \dots, 4\}$ , satisfy the conditions required by Lemma 4.1. Then, for each  $\phi_h \in \mathbf{H}_h^\theta$ , the problem (4.59) has a unique solution  $(\mathbf{t}_h, \mathbf{u}_h) := \mathbf{S}_h(\phi_h) \in \mathbb{H}_h \times \mathbf{H}_h^\mathbf{u}$ . Moreover, with the same constant  $c_{\mathbf{S}} > 0$  from (4.33), which is independent of  $\phi_h$ , there holds*

$$\|\mathbf{S}_h(\phi_h)\| = \|(\mathbf{t}_h, \mathbf{u}_h)\| \leq c_{\mathbf{S}} \|\mathbf{f}\|_{0,\Omega}. \quad (4.64)$$

**Lemma 4.10.** *Assume that  $\kappa_i$ ,  $i \in \{5, 6, 7\}$ , satisfy the conditions required by Lemma 4.2. Let  $\mathbf{w}_h \in \mathbf{H}_h^\mathbf{u}$  such that  $\|\mathbf{w}_h\|_{1,\Omega} \leq \frac{\tilde{\alpha}(\Omega)}{2\kappa^{-1}(1 + \kappa_5^2)^{1/2}c(\Omega)}$ , where  $c(\Omega)$  and  $\tilde{\alpha}(\Omega)$  are the positive constants provided by (4.15) and (4.40), respectively. Then, there exist a unique  $(\mathbf{p}_h, \theta_h) := \tilde{\mathbf{S}}_h(\mathbf{w}_h) \in \mathbf{H}_h^\mathbf{p} \times \mathbf{H}_h^\theta$  solution of (4.61). Moreover, with the same constant  $c_{\tilde{\mathbf{S}}} > 0$  from (4.38), which is independent of  $\mathbf{w}_h$ , there holds*

$$\|\tilde{\mathbf{S}}_h(\mathbf{w}_h)\| = \|(\mathbf{p}_h, \theta_h)\| \leq c_{\tilde{\mathbf{S}}} \left\{ \|g\|_{0,\Omega} + \|\theta_D\|_{0,\Gamma_D} + \|\theta_D\|_{1/2,\Gamma_D} \right\}. \quad (4.65)$$

We now proceed to analyse the fixed-point equation (4.63). More precisely, in what follows we verify the hypotheses of the Brouwer fixed-point theorem (cf. [47, Theorem 9.9-2]). We begin with the discrete version of Lemma 4.3. Its proof, being a simple translation of the arguments proving that lemma, is omitted.

**Lemma 4.11.** *Let  $\mathcal{W}_h := \left\{ \phi_h \in \mathbf{H}_h^\theta : \|\phi_h\|_{1,\Omega} \leq c_{\tilde{\mathbf{S}}} \left\{ \|g\|_{0,\Omega} + \|\theta_D\|_{0,\Gamma_D} + \|\theta_D\|_{1/2,\Gamma_D} \right\} \right\}$ , and assume that the datum  $\mathbf{f}$  satisfy (4.44). Then  $\mathbf{T}(\mathcal{W}_h) \subseteq \mathcal{W}_h$ .*

The discrete analogues of Lemma 4.4 is provided next. We notice in advance that, instead of the regularity assumptions employed in the proof of that result, which actually are not needed nor could be applied in the present discrete case, we simply utilise a  $L^4 - L^4 - L^2$  argument.

**Lemma 4.12.** *There exists a positive constant  $C_{\mathbf{S}_h}$ , depending on  $L_\mu, \kappa_1$ , and  $\alpha(\Omega)$ , such that*

$$\|\mathbf{S}_h(\phi_h) - \mathbf{S}_h(\tilde{\phi}_h)\| \leq C_{\mathbf{S}_h} \|\mathbf{S}_{1,h}^{\mathbf{t}}(\phi_h)\|_{\mathbf{L}^4(\Omega)} \|\phi_h - \tilde{\phi}_h\|_{\mathbf{L}^4(\Omega)} \quad \forall \phi_h, \tilde{\phi}_h \in \mathbf{H}_h^\theta. \quad (4.66)$$

*Proof.* Given  $\phi_h, \tilde{\phi}_h \in \mathbf{H}_h^\theta$ , we first let  $(\mathbf{t}_h, \mathbf{u}_h) := \mathbf{S}_h(\phi_h)$  and  $(\tilde{\mathbf{t}}_h, \tilde{\mathbf{u}}_h) := \mathbf{S}_h(\tilde{\phi}_h)$  be the corresponding solutions of problem (4.59). Next, we proceed analogously as in the proof of Lemma 4.4, except for the derivation of the discrete analogue of the right-hand side of (4.47), where, instead of choosing the values of  $p$  and  $q$  determined by the regularity parameter  $\delta$ , it suffices to take  $p = q = 2$  (see [2]), thus obtaining

$$\alpha(\Omega) \|(\mathbf{t}_h, \mathbf{u}_h) - (\tilde{\mathbf{t}}_h, \tilde{\mathbf{u}}_h)\|^2 \leq L_\mu (1 + \kappa_1^2)^{1/2} \|\mathbf{t}_h\|_{\mathbf{L}^4(\Omega)} \|\phi_h - \tilde{\phi}_h\|_{\mathbf{L}^4(\Omega)} \|(\mathbf{t}_h, \mathbf{u}_h) - (\tilde{\mathbf{t}}_h, \tilde{\mathbf{u}}_h)\|.$$

Then, the fact that the elements of  $\mathbb{H}_h^{\mathbf{t}}$  are piecewise polynomials insures that  $\|\mathbf{t}_h\|_{\mathbf{L}^4(\Omega)} < +\infty$ , and hence the foregoing equation yields (4.66) with  $C_{\mathbf{S}_h} := L_\mu (1 + \kappa_1^2)^{1/2} / \alpha(\Omega)$ . Further details are omitted.  $\square$

Next, we address the Lipschitz-continuity of  $\tilde{\mathbf{S}}_h$ , its proof is omitted since it is almost verbatim as that of the corresponding continuous estimate provided by Lemma 4.5.

**Lemma 4.13.** *Let  $C_{\tilde{\mathbf{S}}}$  be the constant provided by Lemma 4.5. Then, given  $\mathbf{w}_h, \tilde{\mathbf{w}}_h \in \mathbf{H}_h^{\mathbf{u}}$  such that  $\|\mathbf{w}_h\|_{1,\Omega}, \|\tilde{\mathbf{w}}_h\|_{1,\Omega} \leq \frac{\tilde{\alpha}(\Omega)}{2\kappa^{-1}(1+\kappa_5^2)^{1/2}c(\Omega)}$ , there holds*

$$\|\tilde{\mathbf{S}}_h(\mathbf{w}_h) - \tilde{\mathbf{S}}_h(\tilde{\mathbf{w}}_h)\| \leq C_{\tilde{\mathbf{S}}} \|\tilde{\mathbf{S}}_{2,h}(\mathbf{w}_h)\|_{1,\Omega} \|\mathbf{w}_h - \tilde{\mathbf{w}}_h\|_{1,\Omega}. \quad (4.67)$$

Now, utilising Lemmas 4.12 and 4.13, we can prove the discrete version of Lemma 4.6.

**Lemma 4.14.** *Let  $\mathcal{W}_h := \left\{ \phi_h \in \mathbf{H}_h^\theta : \|\phi_h\|_{1,\Omega} \leq c_{\tilde{\mathbf{S}}} \left\{ \|g\|_{0,\Omega} + \|\theta_D\|_{0,\Gamma_D} + \|\theta_D\|_{1/2,\Gamma_D} \right\} \right\}$ , and assume that the datum  $\mathbf{f}$  satisfy (4.44). Then, there holds*

$$\|\mathbf{T}_h(\phi_h) - \mathbf{T}_h(\tilde{\phi}_h)\|_{1,\Omega} \leq C_{\mathbf{S}_h} C_{\tilde{\mathbf{S}}} \|\mathbf{T}(\phi_h)\|_{1,\Omega} \|\mathbf{S}_{1,h}^{\mathbf{t}}(\phi_h)\|_{\mathbf{L}^4(\Omega)} \|\phi_h - \tilde{\phi}_h\|_{\mathbf{L}^4(\Omega)}, \quad (4.68)$$

where  $C_{\tilde{\mathbf{S}}}$  and  $C_{\mathbf{S}_h}$  are the constants provided by Lemmas 4.5 and 4.12, respectively.

Consequently, since the foregoing lemma and the continuous injection of  $\mathbf{H}^1(\Omega)$  into  $\mathbf{L}^4(\Omega)$  confirm the continuity of  $\mathbf{T}_h$ , we conclude, thanks to the Brouwer fixed-point theorem (cf. [47, Theorem 9.9-2]) and Lemmas 4.11 and 4.14, the main result of this section.

**Theorem 4.15.** *Suppose that the parameters  $\kappa_i, i \in \{1, \dots, 7\}$ , satisfy the conditions required by Lemmas 4.1 and 4.2. Let  $\mathcal{W}_h := \left\{ \phi_h \in \mathbf{H}_h^\theta : \|\phi_h\|_{1,\Omega} \leq c_{\tilde{\mathbf{S}}} \left\{ \|g\|_{0,\Omega} + \|\theta_D\|_{0,\Gamma_D} + \|\theta_D\|_{1/2,\Gamma_D} \right\} \right\}$ , and assume that the datum  $\mathbf{f}$  satisfy (4.44). Then the Galerkin scheme (4.57) has at least one solution  $(\underline{\mathbf{t}}_h, \mathbf{u}_h, \mathbf{p}_h, \theta_h) \in \mathbb{H}_h \times \mathbf{H}_h^{\mathbf{u}} \times \mathbf{H}_h^{\mathbf{p}} \times \mathbf{H}_h^\theta$  with  $\theta_h \in \mathcal{W}_h$ , and there holds*

$$\|(\underline{\mathbf{t}}_h, \mathbf{u}_h)\| \leq c_{\mathbf{S}} \|\mathbf{f}\|_{0,\Omega}, \quad (4.69)$$

and

$$\|(\mathbf{p}_h, \theta_h)\| \leq c_{\tilde{\mathbf{S}}} \left\{ \|g\|_{0,\Omega} + \|\theta_D\|_{0,\Gamma_D} + \|\theta_D\|_{1/2,\Gamma_D} \right\}, \quad (4.70)$$

where  $c_{\mathbf{S}}$  and  $c_{\tilde{\mathbf{S}}}$  are the constants provided by Lemmas 4.1 and 4.2, respectively.

We end this section by remarking that the lack of suitable estimates for  $\|\mathbf{S}_{1,h}^{\mathbf{t}}(\phi_h)\|_{\mathbf{L}^4(\Omega)}$  stops us of trying to use (4.68) to derive a contraction estimate for  $\mathbf{T}_h$ . This is the reason why in the foregoing Theorem 4.15 we are able only to guarantee existence, but no uniqueness, of a discrete solution.

#### 4.4.3 Convergence of the Galerkin scheme

Given  $(\underline{\mathbf{t}}, \mathbf{u}, \mathbf{p}, \theta) \in \mathbb{H} \times \mathbf{H}_0^1(\Omega) \times \mathbf{H}_{\Gamma_N}(\text{div}; \Omega) \times \mathbf{H}^1(\Omega)$  with  $\theta \in \mathcal{W}$ , and  $(\underline{\mathbf{t}}_h, \mathbf{u}_h, \mathbf{p}_h, \theta_h) \in \mathbb{H}_h \times \mathbf{H}_h^{\mathbf{u}} \times \mathbf{H}_h^{\mathbf{p}} \times \mathbf{H}_h^\theta$  with  $\theta_h \in \mathcal{W}_h$ , solutions of (4.18) and (4.57), respectively, we now aim to derive a corresponding a priori error estimate. For this purpose, we first observe from (4.18) and (4.57) that the above problems can be rewritten as two pairs of corresponding continuous and discrete formulations, namely

$$\begin{aligned} \mathbf{A}_\theta((\underline{\mathbf{t}}, \mathbf{u}), (\underline{\mathbf{r}}, \mathbf{v})) &= \mathbf{F}(\underline{\mathbf{r}}, \mathbf{v}) \quad \forall (\underline{\mathbf{r}}, \mathbf{v}) \in \mathbb{H} \times \mathbf{H}_0^1(\Omega), \\ \mathbf{A}_{\theta_h}((\underline{\mathbf{t}}_h, \mathbf{u}_h), (\underline{\mathbf{r}}_h, \mathbf{v}_h)) &= \mathbf{F}(\underline{\mathbf{r}}_h, \mathbf{v}_h) \quad \forall (\underline{\mathbf{r}}_h, \mathbf{v}_h) \in \mathbb{H}_h \times \mathbf{H}_h^{\mathbf{u}}, \end{aligned} \quad (4.71)$$

and

$$\begin{aligned}\tilde{\mathbf{A}}((\mathbf{p}, \theta), (\mathbf{q}, \psi)) + \tilde{\mathbf{B}}_{\mathbf{u}}((\mathbf{p}, \theta), (\mathbf{q}, \psi)) &= \tilde{\mathbf{F}}(\mathbf{q}, \psi) \quad \forall (\mathbf{q}, \psi) \in \mathbf{H}_{\Gamma_N}(\text{div}; \Omega) \times H^1(\Omega), \\ \tilde{\mathbf{A}}((\mathbf{p}_h, \theta_h), (\mathbf{q}_h, \psi_h)) + \tilde{\mathbf{B}}_{\mathbf{u}_h}((\mathbf{p}_h, \theta_h), (\mathbf{q}_h, \psi_h)) &= \tilde{\mathbf{F}}(\mathbf{q}_h, \psi_h) \quad \forall (\mathbf{q}_h, \psi_h) \in \mathbf{H}_h^{\mathbf{P}} \times H_h^{\theta}.\end{aligned}\tag{4.72}$$

Then, as suggested by the structure of the foregoing systems, in what follows we apply the well-known Strang lemma for elliptic variational problems (see, e.g., [141, Theorem 11.1]) to (4.71) and (4.72). This auxiliary result is stated first.

**Lemma 4.16.** *Let  $V$  be a Hilbert space,  $F \in V'$ , and  $A : V \times V \rightarrow \mathbb{R}$  be a bounded and  $V$ -elliptic bilinear form. In addition, let  $\{V_h\}_{h>0}$  be a sequence of finite dimensional subspaces of  $V$ , and for each  $h > 0$  consider a bounded bilinear form  $A_h : V_h \times V_h \rightarrow \mathbb{R}$  and a functional  $F_h \in V_h'$ . Assume that the family  $\{A_h\}_{h>0}$  is uniformly elliptic, that is, there exists a constant  $\tilde{\alpha} > 0$ , independent of  $h$ , such that*

$$A_h(v_h, v_h) \geq \tilde{\alpha} \|v_h\|_V^2 \quad \forall v_h \in V_h, \quad \forall h > 0.$$

*In turn, let  $u \in V$  and  $u_h \in V_h$  such that*

$$A(u, v) = F(v) \quad \forall v \in V \quad \text{and} \quad A_h(u_h, v_h) = F_h(v_h) \quad \forall v_h \in V_h.$$

*Then, for each  $h > 0$  there holds*

$$\begin{aligned}\|u - u_h\|_V \leq C_{\text{ST}} &\left\{ \sup_{\substack{w_h \in V_h \\ w_h \neq 0}} \frac{|F(w_h) - F_h(w_h)|}{\|w_h\|_V} \right. \\ &\left. + \inf_{\substack{v_h \in V_h \\ v_h \neq 0}} \left( \|u - v_h\|_V + \sup_{\substack{w_h \in V_h \\ w_h \neq 0}} \frac{|A(v_h, w_h) - A_h(v_h, w_h)|}{\|w_h\|_V} \right) \right\},\end{aligned}$$

where  $C_{\text{ST}} := \tilde{\alpha}^{-1} \max \{1, \|A\|\}$ .

In the sequel, for the sake of simplicity, we denote as usual

$$\text{dist} \left( (\underline{\mathbf{t}}, \mathbf{u}), \mathbb{H}_h \times \mathbf{H}_h^{\mathbf{u}} \right) := \inf_{(\underline{\mathbf{r}}_h, \mathbf{v}_h) \in \mathbb{H}_h \times \mathbf{H}_h^{\mathbf{u}}} \|(\underline{\mathbf{t}}, \mathbf{u}) - (\underline{\mathbf{r}}_h, \mathbf{v}_h)\|$$

and

$$\text{dist} \left( (\mathbf{p}, \theta), \mathbf{H}_h^{\mathbf{P}} \times H_h^{\theta} \right) := \inf_{(\mathbf{q}_h, \psi_h) \in \mathbf{H}_h^{\mathbf{P}} \times H_h^{\theta}} \|(\mathbf{p}, \theta) - (\mathbf{q}_h, \psi_h)\|.$$

The following Lemma provides a preliminary estimate for the error  $\|(\underline{\mathbf{t}}, \mathbf{u}) - (\underline{\mathbf{t}}_h, \mathbf{u}_h)\|$ .

**Lemma 4.17.** *Let  $C_{\text{ST}} := \frac{1}{\alpha(\Omega)} \max \{1, \|\mathbf{A}_{\theta}\|\}$ , where  $\alpha(\Omega)$  is the constant yielding the ellipticity of  $\mathbf{A}_{\phi}$  for any  $\phi \in H^1(\Omega)$  (cf. (4.36)). Then, there holds*

$$\begin{aligned}\|(\underline{\mathbf{t}}, \mathbf{u}) - (\underline{\mathbf{t}}_h, \mathbf{u}_h)\| &\leq C_{\text{ST}} \left\{ L_{\mu} (1 + \kappa_1^2)^{1/2} C_{\delta} \|\underline{\mathbf{t}}\|_{\delta, \Omega} \|\theta - \theta_h\|_{L^{n/\delta}(\Omega)} \right. \\ &\quad \left. + (1 + 2\|\mathbf{A}_{\theta}\|) \text{dist} \left( (\underline{\mathbf{t}}, \mathbf{u}), \mathbb{H}_h \times \mathbf{H}_h^{\mathbf{u}} \right) \right\}.\end{aligned}\tag{4.73}$$

*Proof.* We proceed similarly as in [2, Lemma 5.3]. In fact, from Lemmas 4.1 and 4.9, we have that the bilinear forms  $\mathbf{A}_\theta$  and  $\mathbf{A}_{\theta_h}$  are both bounded and elliptic with the same constants  $\|\mathbf{A}_\theta\|$  and  $\alpha(\Omega)$ , respectively. In addition,  $\mathbf{F}$  is a linear and bounded functional in  $\mathbb{H} \times \mathbf{H}_0^1(\Omega)$  and, in particular, in  $\mathbb{H}_h \times \mathbf{H}_h^\mathbf{u}$ . Then, by applying Lemma 4.16 to the context (4.71), we obtain

$$\begin{aligned} \|(\underline{\mathbf{t}}, \mathbf{u}) - (\underline{\mathbf{t}}_h, \mathbf{u}_h)\| &\leq C_{\text{ST}} \inf_{\substack{(\underline{\mathbf{r}}_h, \mathbf{v}_h) \in \mathbb{H}_h \times \mathbf{H}_h^\mathbf{u} \\ (\underline{\mathbf{r}}_h, \mathbf{v}_h) \neq \mathbf{0}}} \left\{ \|(\underline{\mathbf{t}}, \mathbf{u}) - (\underline{\mathbf{r}}_h, \mathbf{v}_h)\| \right. \\ &\quad \left. + \sup_{\substack{(\underline{\mathbf{s}}_h, \mathbf{w}_h) \in \mathbb{H}_h \times \mathbf{H}_h^\mathbf{u} \\ (\underline{\mathbf{s}}_h, \mathbf{w}_h) \neq \mathbf{0}}} \frac{|\mathbf{A}_\theta((\underline{\mathbf{r}}_h, \mathbf{v}_h), (\underline{\mathbf{s}}_h, \mathbf{w}_h)) - \mathbf{A}_{\theta_h}((\underline{\mathbf{r}}_h, \mathbf{v}_h), (\underline{\mathbf{s}}_h, \mathbf{w}_h))|}{\|(\underline{\mathbf{s}}_h, \mathbf{w}_h)\|} \right\}. \end{aligned} \quad (4.74)$$

In turn, in order to estimate the supremum in (4.74), we add and subtract suitable terms to write

$$\begin{aligned} \mathbf{A}_\theta((\underline{\mathbf{r}}_h, \mathbf{v}_h), (\underline{\mathbf{s}}_h, \mathbf{w}_h)) - \mathbf{A}_{\theta_h}((\underline{\mathbf{r}}_h, \mathbf{v}_h), (\underline{\mathbf{s}}_h, \mathbf{w}_h)) &= \mathbf{A}_\theta((\underline{\mathbf{r}}_h, \mathbf{v}_h) - (\underline{\mathbf{t}}, \mathbf{u}), (\underline{\mathbf{s}}_h, \mathbf{w}_h)) \\ &\quad + (\mathbf{A}_\theta - \mathbf{A}_{\theta_h})((\underline{\mathbf{t}}, \mathbf{u}), (\underline{\mathbf{s}}_h, \mathbf{w}_h)) + \mathbf{A}_{\theta_h}((\underline{\mathbf{t}}, \mathbf{u}) - (\underline{\mathbf{r}}_h, \mathbf{v}_h), (\underline{\mathbf{s}}_h, \mathbf{w}_h)), \end{aligned}$$

whence, applying the boundedness (4.34) to the first and third terms on the right-hand side of the foregoing equation, and proceeding analogously as for the derivation of (4.47) with the second one, we find that

$$\begin{aligned} \sup_{\substack{(\underline{\mathbf{s}}_h, \mathbf{w}_h) \in \mathbb{H}_h \times \mathbf{H}_h^\mathbf{u} \\ (\underline{\mathbf{s}}_h, \mathbf{w}_h) \neq \mathbf{0}}} \frac{|\mathbf{A}_\theta((\underline{\mathbf{r}}_h, \mathbf{v}_h), (\underline{\mathbf{s}}_h, \mathbf{w}_h)) - \mathbf{A}_{\theta_h}((\underline{\mathbf{r}}_h, \mathbf{v}_h), (\underline{\mathbf{s}}_h, \mathbf{w}_h))|}{\|(\underline{\mathbf{s}}_h, \mathbf{w}_h)\|} \\ \leq L_\mu(1 + \kappa_1^2)^{1/2} C_\delta \|\underline{\mathbf{t}}\|_{\delta, \Omega} \|\theta - \theta_h\|_{L^{n/\delta}(\Omega)} + 2\|\mathbf{A}_\theta\| \|(\underline{\mathbf{t}}, \mathbf{u}) - (\underline{\mathbf{r}}_h, \mathbf{v}_h)\|. \end{aligned} \quad (4.75)$$

Finally, by replacing the inequality (4.75) into (4.74), we get (4.73), which ends the proof.  $\square$

Next, we have the following result concerning  $\|(\mathbf{p}, \theta) - (\mathbf{p}_h, \theta_h)\|$ .

**Lemma 4.18.** *Let  $\tilde{C}_{\text{ST}} := \frac{2}{\tilde{\alpha}(\Omega)} \max\{1, \|\tilde{\mathbf{A}} + \tilde{\mathbf{B}}_\mathbf{u}\|\}$ , where  $\tilde{\alpha}(\Omega)$  is the constant yielding the ellipticity of both  $\tilde{\mathbf{A}}$  and  $\tilde{\mathbf{A}} + \tilde{\mathbf{B}}_\mathbf{w}$ , for any  $\mathbf{w} \in \mathbf{H}_0^1(\Omega)$  (cf. (4.40) and (4.41)). Then, there holds*

$$\begin{aligned} \|(\mathbf{p}, \theta) - (\mathbf{p}_h, \theta_h)\| &\leq \tilde{C}_{\text{ST}} \left\{ \kappa^{-1}(1 + \kappa_5^2)^{1/2} c(\Omega) \|\theta\|_{1, \Omega} \|\mathbf{u} - \mathbf{u}_h\|_{1, \Omega} \right. \\ &\quad \left. + \left(1 + \kappa^{-1}(1 + \kappa_5^2)^{1/2} c(\Omega) \|\mathbf{u} - \mathbf{u}_h\|_{1, \Omega}\right) \text{dist}\left((\mathbf{p}, \theta), \mathbf{H}_h^\mathbf{p} \times \mathbf{H}_h^\theta\right) \right\}. \end{aligned} \quad (4.76)$$

*Proof.* It follows almost straightforwardly from a slight modification of the proof of [52, Lemma 5.3]. We omit further details.  $\square$

We now combine the inequalities provided by Lemmas 4.17 and 4.18 to derive the a priori estimate for the total error  $\|(\underline{\mathbf{t}}, \mathbf{u}, \mathbf{p}, \theta) - (\underline{\mathbf{t}}_h, \mathbf{u}_h, \mathbf{p}_h, \theta_h)\|$ . Indeed, by gathering together the estimates (4.73) and (4.76), it follows that

$$\begin{aligned} \|(\underline{\mathbf{t}}, \mathbf{u}, \mathbf{p}, \theta) - (\underline{\mathbf{t}}_h, \mathbf{u}_h, \mathbf{p}_h, \theta_h)\| &\leq \tilde{C}_{\text{ST}} \kappa^{-1}(1 + \kappa_5^2)^{1/2} c(\Omega) \|\theta\|_{1, \Omega} \|\mathbf{u} - \mathbf{u}_h\|_{1, \Omega} \\ &\quad + C_{\text{ST}} L_\mu(1 + \kappa_1^2)^{1/2} C_\delta \|\underline{\mathbf{t}}\|_{\delta, \Omega} \|\theta - \theta_h\|_{L^{n/\delta}(\Omega)} + C_{\text{ST}}(1 + 2\|\mathbf{A}_\theta\|) \text{dist}\left((\underline{\mathbf{t}}, \mathbf{u}), \mathbb{H}_h \times \mathbf{H}_h^\mathbf{u}\right) \\ &\quad + \tilde{C}_{\text{ST}} \left(1 + \kappa^{-1}(1 + \kappa_5^2)^{1/2} c(\Omega) \|\mathbf{u} - \mathbf{u}_h\|_{1, \Omega}\right) \text{dist}\left((\mathbf{p}, \theta), \mathbf{H}_h^\mathbf{p} \times \mathbf{H}_h^\theta\right). \end{aligned}$$

Then, by noting that  $\theta \in \mathcal{W}$ , using the estimate (4.45) to bound  $\|\mathbf{t}\|_{\delta,\Omega}$ , and recalling that  $\tilde{C}_\delta$  is the boundedness constant of the continuous injection of  $H^1(\Omega)$  into  $L^{n/\delta}(\Omega)$  (cf. (4.55)), from the latter inequality we find that

$$\begin{aligned} \|(\underline{\mathbf{t}}, \mathbf{u}, \mathbf{p}, \theta) - (\underline{\mathbf{t}}_h, \mathbf{u}_h, \mathbf{p}_h, \theta_h)\| &\leq \mathbf{C}(\mathbf{f}, g, \theta_D) \|(\underline{\mathbf{t}}, \mathbf{u}, \mathbf{p}, \theta) - (\underline{\mathbf{t}}_h, \mathbf{u}_h, \mathbf{p}_h, \theta_h)\| \\ &+ C_{\text{ST}}(1 + 2\|\mathbf{A}_\theta\|) \text{dist}\left((\underline{\mathbf{t}}, \mathbf{u}), \mathbb{H}_h \times \mathbf{H}_h^{\mathbf{u}}\right) \\ &+ \tilde{C}_{\text{ST}} \left(1 + \kappa^{-1}(1 + \kappa_5^2)^{1/2} c(\Omega) \|\mathbf{u} - \mathbf{u}_h\|_{1,\Omega}\right) \text{dist}\left((\mathbf{p}, \theta), \mathbf{H}_h^{\mathbf{p}} \times \mathbf{H}_h^\theta\right), \end{aligned} \quad (4.77)$$

where

$$\mathbf{C}(\mathbf{f}, g, \theta_D) := \max \left\{ \mathbf{C}_1(\mathbf{f}, g, \theta_D), \mathbf{C}_2(\mathbf{f}, g, \theta_D) \right\},$$

with

$$\mathbf{C}_1(\mathbf{f}, g, \theta_D) := \tilde{C}_{\text{ST}} \kappa^{-1} (1 + \kappa_5^2)^{1/2} c(\Omega) c_{\tilde{\mathbf{S}}} \left\{ \|g\|_{0,\Omega} + \|\theta_D\|_{0,\Gamma_D} + \|\theta_D\|_{1/2,\Gamma_D} \right\}$$

and

$$\mathbf{C}_2(\mathbf{f}, g, \theta_D) := C_{\text{ST}} L_\mu (1 + \kappa_1^2)^{1/2} C_\delta \hat{C}_{\mathbf{S}} \tilde{C}_\delta \|\mathbf{f}\|_{\delta,\Omega}.$$

Consequently, we can establish the following result providing the complete Céa estimate.

**Theorem 4.19.** *Assume that the data  $\mathbf{f}, g$  and  $\theta_D$  satisfy:*

$$\mathbf{C}_i(\mathbf{f}, g, \theta_D) \leq \frac{1}{2} \quad \forall i \in \{1, 2\}. \quad (4.78)$$

*Then, there exists a positive constant  $C$ , depending only on parameters, data and other constants, all of them independent of  $h$ , such that*

$$\|(\underline{\mathbf{t}}, \mathbf{u}, \mathbf{p}, \theta) - (\underline{\mathbf{t}}_h, \mathbf{u}_h, \mathbf{p}_h, \theta_h)\| \leq C \left\{ \text{dist}\left((\underline{\mathbf{t}}, \mathbf{u}), \mathbb{H}_h \times \mathbf{H}_h^{\mathbf{u}}\right) + \text{dist}\left((\mathbf{p}, \theta), \mathbf{H}_h^{\mathbf{p}} \times \mathbf{H}_h^\theta\right) \right\}. \quad (4.79)$$

*Proof.* From (4.77) and (4.78), it follows that

$$\begin{aligned} \|(\underline{\mathbf{t}}, \mathbf{u}, \mathbf{p}, \theta) - (\underline{\mathbf{t}}_h, \mathbf{u}_h, \mathbf{p}_h, \theta_h)\| &\leq 2C_{\text{ST}}(1 + 2\|\mathbf{A}_\theta\|) \text{dist}\left((\underline{\mathbf{t}}, \mathbf{u}), \mathbb{H}_h \times \mathbf{H}_h^{\mathbf{u}}\right) \\ &+ 2\tilde{C}_{\text{ST}} \left(1 + \kappa^{-1}(1 + \kappa_5^2)^{1/2} c(\Omega) \|\mathbf{u} - \mathbf{u}_h\|_{1,\Omega}\right) \text{dist}\left((\mathbf{p}, \theta), \mathbf{H}_h^{\mathbf{p}} \times \mathbf{H}_h^\theta\right), \end{aligned}$$

and then, the rest of the proof reduces to employ the triangle inequality on the term  $\|\mathbf{u} - \mathbf{u}_h\|_{1,\Omega}$  and use that both  $\|\mathbf{u}\|_{1,\Omega}$  and  $\|\mathbf{u}_h\|_{1,\Omega}$  are bounded by  $c_{\mathbf{S}}\|\mathbf{f}\|_{0,\Omega}$  (cf. Lemmas 4.1 and 4.9).  $\square$

Now, in order to approximate the polymeric and solvent parts of the extra-stress tensor, as well as the pressure, we propose, motivated by (4.6), (4.12), and the fifth equation of (4.8), the expressions

$$\tilde{\sigma}_{\text{P},h} = 2\mu_{\text{P}}(\theta_h) \underline{\mathbf{t}}_h, \quad \sigma_{\text{N},h} = 2\epsilon\mu_{\text{N}}(\theta_h) \underline{\mathbf{t}}_h, \quad \hat{\sigma}_{\text{P},h} = \sigma_h^{\text{d}} - \sigma_{\text{N},h}, \quad \text{and} \quad p_h = -\frac{1}{n} \text{tr} \sigma_h, \quad (4.80)$$

respectively, with  $(\underline{\mathbf{t}}_h, \mathbf{u}_h, \mathbf{p}_h, \theta_h) \in \mathbb{H}_h \times \mathbf{H}_h^{\mathbf{u}} \times \mathbf{H}_h^{\mathbf{p}} \times \mathbf{H}_h^\theta$  being the unique solution of the discrete problem (4.57). The corresponding error estimates are established in the following lemma.



**Lemma 4.20.** *Assume that the hypotheses of Theorem 4.19 hold. Let  $(\mathbf{t}, \mathbf{u}, \mathbf{p}, \theta) \in \mathbb{H} \times \mathbf{H}_0^1(\Omega) \times \mathbf{H}_{\Gamma_N}(\text{div}; \Omega) \times H^1(\Omega)$  and  $(\mathbf{t}_h, \mathbf{u}_h, \mathbf{p}_h, \theta_h) \in \mathbb{H}_h \times \mathbf{H}_h^{\mathbf{u}} \times \mathbf{H}_h^{\mathbf{p}} \times H_h^\theta$  be the unique solutions of the continuous and discrete problems (4.18) and (4.57), respectively. Then, there exists a positive constant  $C$ , depending only on parameters, data and other constants, all of them independent of  $h$ , such that*

$$\|p - p_h\|_{0,\Omega} + \|\sigma_N - \sigma_{N,h}\|_{0,\Omega} + \|\sigma_P - \tilde{\sigma}_{P,h}\|_{0,\Omega} \leq C \left\{ \text{dist} \left( (\mathbf{t}, \mathbf{u}), \mathbb{H}_h \times \mathbf{H}_h^{\mathbf{u}} \right) + \text{dist} \left( (\mathbf{p}, \theta), \mathbf{H}_h^{\mathbf{p}} \times H_h^\theta \right) \right\}.$$

*Proof.* From (4.6) and (4.80), adding and subtracting  $2\mu_P(\theta_h)\mathbf{t}$ , it is clear that

$$\sigma_P - \tilde{\sigma}_{P,h} = 2(\mu_P(\theta) - \mu_P(\theta_h))\mathbf{t} + 2\mu_P(\theta_h)(\mathbf{t} - \mathbf{t}_h).$$

Next, employing the triangle and Hölder inequalities, the estimate (4.45) to bound  $\|\mathbf{t}\|_{\delta,\Omega}$ , the continuous injection of  $H^1(\Omega)$  into  $L^{n/\delta}(\Omega)$ , and the Lipschitz-continuity assumption (4.4), it is not difficult to see that there exist a positive constant  $c$ , depending only on data and other constants, all of them independent of  $h$ , such that

$$\|\sigma_P - \tilde{\sigma}_{P,h}\|_{0,\Omega} \leq c \left\{ \|\mathbf{t} - \mathbf{t}_h\|_{0,\Omega} + \|\theta - \theta_h\|_{1,\Omega} \right\}.$$

In this way, following similar arguments for the solvent part of the extra-stress tensor  $\sigma_N$  (cf. (4.80)), we obtain

$$\|p - p_h\|_{0,\Omega} + \|\sigma_N - \sigma_{N,h}\|_{0,\Omega} + \|\sigma_P - \tilde{\sigma}_{P,h}\|_{0,\Omega} \leq C \left\{ \|\mathbf{t} - \mathbf{t}_h\|_{0,\Omega} + \|\sigma - \sigma_h\|_{\text{div};\Omega} + \|\theta - \theta_h\|_{1,\Omega} \right\}.$$

Then, the result is a direct application of Theorem 4.19. Observe that the proof is also valid if we consider  $\hat{\sigma}_{P,h}$  in place of  $\tilde{\sigma}_{P,h}$ .  $\square$

Finally, we complete our a priori error analysis with the following results which provides the corresponding rate of convergence of our Galerkin scheme (4.57).

**Theorem 4.21.** *In addition to the hypotheses of Theorems 4.8, 4.15 and 4.19, assume that there exists  $s > 0$  such that  $\mathbf{t} \in \mathbb{H}^s(\Omega)$ ,  $\sigma \in \mathbb{H}^s(\Omega)$ ,  $\text{div} \sigma \in \mathbf{H}^s(\Omega)$ ,  $\rho \in \mathbb{H}^s(\Omega)$ ,  $\mathbf{u} \in \mathbf{H}^{s+1}(\Omega)$ ,  $\mathbf{p} \in \mathbf{H}^s(\Omega)$ ,  $\text{div} \mathbf{p} \in \mathbf{H}^s(\Omega)$ , and  $\theta \in H^{s+1}(\Omega)$ , and that the finite element subspaces are defined by (4.56). Then, there exist  $C > 0$ , independent of  $h$ , such that*

$$\begin{aligned} \|(\mathbf{t}, \mathbf{u}, \mathbf{p}, \theta) - (\mathbf{t}_h, \mathbf{u}_h, \mathbf{p}_h, \theta_h)\| &\leq Ch^{\min\{s, k+1\}} \left\{ \|\mathbf{t}\|_{s,\Omega} + \|\sigma\|_{s,\Omega} + \|\text{div} \sigma\|_{s,\Omega} + \|\rho\|_{s,\Omega} \right. \\ &\quad \left. + \|\mathbf{u}\|_{s+1,\Omega} + \|\mathbf{p}\|_{s,\Omega} + \|\text{div} \mathbf{p}\|_{s,\Omega} + \|\theta\|_{s+1,\Omega} \right\}. \end{aligned} \quad (4.81)$$

*Proof.* It follows directly from the Céa estimate (4.79) and the well-known approximation properties of the discrete spaces  $\mathbb{H}_h^{\mathbf{t}}, \mathbb{H}_h^{\sigma}, \mathbb{H}_h^{\rho}, \mathbf{H}_h^{\mathbf{u}}, \mathbf{H}_h^{\mathbf{p}}$ , and  $H_h^\theta$  (cf. [19, 47]).  $\square$

Consequently, from Lemma 4.20 and Theorem 4.21 we obtain the optimal convergence of the post-processed unknowns introduced in (4.80).

**Lemma 4.22.** *Let  $(\mathbf{t}, \mathbf{u}, \mathbf{p}, \theta) \in \mathbb{H} \times \mathbf{H}_0^1(\Omega) \times \mathbf{H}_{\Gamma_N}(\text{div}; \Omega) \times H^1(\Omega)$  be the unique solutions of the continuous problem (4.18), and let  $\sigma_P$ ,  $\sigma_N$ , and  $p$  given by (4.6) and the fifth equation of (4.8). In addition, let  $\tilde{\sigma}_{P,h}$  (or  $\hat{\sigma}_{P,h}$ ),  $\sigma_{N,h}$ , and  $p_h$  be the discrete counterparts introduced in (4.80). Assume that hypotheses of Theorem 4.21 hold. Then, there exist  $C > 0$ , independent of  $h$ , such that*

$$\begin{aligned} \|p - p_h\|_{0,\Omega} + \|\sigma_N - \sigma_{N,h}\|_{0,\Omega} + \|\sigma_P - \tilde{\sigma}_{P,h}\|_{0,\Omega} &\leq Ch^{\min\{s, k+1\}} \left\{ \|\mathbf{t}\|_{s,\Omega} + \|\sigma\|_{s,\Omega} + \|\text{div} \sigma\|_{s,\Omega} \right. \\ &\quad \left. + \|\rho\|_{s,\Omega} + \|\mathbf{u}\|_{s+1,\Omega} + \|\mathbf{p}\|_{s,\Omega} + \|\text{div} \mathbf{p}\|_{s,\Omega} + \|\theta\|_{s+1,\Omega} \right\}. \end{aligned}$$

## 4.5 Numerical results

In this section we present some examples illustrating the performance of our augmented fully-mixed finite element scheme (4.57), and confirming the rates of convergence provided by Theorem 4.21 and Lemma 4.22. Our implementation is based on a FreeFem++ code [111], in conjunction with the direct linear solver UMFPACK [62]. A Picard algorithm with a fixed tolerance  $\text{tol} = 1E - 8$  has been used for the corresponding fixed-point problem (4.63) and the iterations are terminated once the relative error of the entire coefficient vectors between two consecutive iterates is sufficiently small, i.e.,

$$\frac{\|\text{coeff}^{m+1} - \text{coeff}^m\|_{l^2}}{\|\text{coeff}^{m+1}\|_{l^2}} \leq \text{tol},$$

where  $\|\cdot\|_{l^2}$  is the standard  $l^2$ -norm in  $\mathbb{R}^N$ , with  $N$  denoting the total number of degrees of freedom defining the finite element subspaces  $\mathbb{H}_h^{\mathbf{t}}, \mathbb{H}_h^{\boldsymbol{\sigma}}, \mathbb{H}_h^{\boldsymbol{\rho}}, \mathbf{H}_h^{\mathbf{u}}, \mathbf{H}_h^{\mathbf{p}}$ , and  $\mathbf{H}_h^{\theta}$ . As usual, the individual errors are denoted by:

$$\begin{aligned} \mathbf{e}(\mathbf{t}) &:= \|\mathbf{t} - \mathbf{t}_h\|_{0,\Omega}, & \mathbf{e}(\boldsymbol{\sigma}) &:= \|\boldsymbol{\sigma} - \boldsymbol{\sigma}_h\|_{\text{div};\Omega}, & \mathbf{e}(\boldsymbol{\rho}) &:= \|\boldsymbol{\rho} - \boldsymbol{\rho}_h\|_{0,\Omega}, & \mathbf{e}(\mathbf{u}) &:= \|\mathbf{u} - \mathbf{u}_h\|_{1,\Omega}, \\ \mathbf{e}(\mathbf{p}) &:= \|\mathbf{p} - \mathbf{p}_h\|_{\text{div};\Omega}, & \mathbf{e}(\theta) &:= \|\theta - \theta_h\|_{1,\Omega}, & \mathbf{e}(p) &:= \|p - p_h\|_{0,\Omega}, \\ \mathbf{e}(\boldsymbol{\sigma}_N) &:= \|\boldsymbol{\sigma}_N - \boldsymbol{\sigma}_{N,h}\|_{0,\Omega}, & \mathbf{e}(\tilde{\boldsymbol{\sigma}}_P) &:= \|\boldsymbol{\sigma}_P - \tilde{\boldsymbol{\sigma}}_{P,h}\|_{0,\Omega}, & \mathbf{e}(\hat{\boldsymbol{\sigma}}_P) &:= \|\boldsymbol{\sigma}_P - \hat{\boldsymbol{\sigma}}_{P,h}\|_{0,\Omega}. \end{aligned}$$

In addition, we let  $r(\cdot)$  be the experimental rate of convergence given by

$$r(\%) := \frac{\log(\mathbf{e}(\%)/\mathbf{e}'(\%))}{\log(h/h')} \quad \text{for each } \% \in \{\mathbf{t}, \boldsymbol{\sigma}, \boldsymbol{\rho}, \mathbf{u}, \mathbf{p}, \theta, p, \boldsymbol{\sigma}_N, \tilde{\boldsymbol{\sigma}}_P, \hat{\boldsymbol{\sigma}}_P\},$$

where  $\mathbf{e}$  and  $\mathbf{e}'$  denote errors computed on two consecutive meshes of sizes  $h$  and  $h'$ , respectively.

The examples to be considered in this section are described next. In all of them, as in [56, Section 2], we choose the coefficients of the polymer and solvent viscosity  $a_1, b_1, a_2$  and  $b_2$  (cf. (4.2)) as follow:

$$b_1 = b_2 = \frac{\Delta E}{R}, \quad a_2 = \exp\left(\frac{-\Delta E}{R\theta_R}\right), \quad \text{and} \quad a_1 = (1 - \epsilon)a_2,$$

where  $\Delta E$  is the activation energy,  $R$  is the ideal gas constant, and  $\theta_R$  is a reference temperature of the fluid. Note that the constraint (4.3) will be satisfied as long as the temperature of the system stays above  $\theta_R$ . In turn, we consider  $\kappa = 1$ ,  $\epsilon = 0.01$ , and according to (4.43), the stabilization parameters are taken as  $\kappa_1 = \mu_1/\mu_2^2$ ,  $\kappa_2 = \kappa_1$ ,  $\kappa_3 = \mu_1/2$ ,  $\kappa_4 = \mu_1/4$ ,  $\kappa_5 = \kappa$ ,  $\kappa_6 = \kappa^{-1}/2$ , and  $\kappa_7 = \kappa/2$ . In addition, the conditions  $\int_{\Omega} \text{tr } \boldsymbol{\sigma}_h = 0$  is imposed via a penalization strategy.

In our first example we illustrate the accuracy of our method in 2D by considering the square domain  $\Omega := (0, 1)^2$ , the boundary  $\Gamma = \bar{\Gamma}_D \cup \bar{\Gamma}_N$ , with  $\Gamma_D := \{0\} \times (0, 1)$  and  $\Gamma_N := \Gamma \setminus \bar{\Gamma}_D$ . The following viscosity parameters correspond to polystyrene [118, Section 4.2]:

$$\frac{\Delta E}{R} = 14500, \quad \theta_R = 538.$$

The data  $\mathbf{f}$ ,  $g$ , and  $\theta_D$  are chosen so that the exact solution is given by

$$\begin{aligned} \mathbf{u}(\mathbf{x}) &:= \begin{pmatrix} \pi x_1^2 (x_1 - 1)^2 \sin(2\pi x_2) \\ -2x_1(x_1 - 1)(2x_1 - 1) \sin(\pi x_2)^2 \end{pmatrix}, \\ p(\mathbf{x}) &:= \cos(\pi x_1) \sin(\pi x_2), \\ \theta(\mathbf{x}) &:= 10(x_1 - 1)^2 \sin(\pi x_2)^2 + 540 \quad \forall \mathbf{x} := (x_1, x_2) \in \Omega. \end{aligned}$$

In our second example we consider a four-to-one contraction domain  $\Omega := (0, 2) \times (0, 1) \setminus (1, 2) \times (0.25, 1)$ , the boundary  $\Gamma = \bar{\Gamma}_D \cup \bar{\Gamma}_N$ , with  $\Gamma_D := \{0\} \times (0, 1)$  and  $\Gamma_N := \Gamma \setminus \bar{\Gamma}_D$ . The following viscosity parameters correspond to Nylon-6,6 [118, Section 4.2]:

$$\frac{\Delta E}{R} = 6600, \quad \theta_R = 563.$$

The data  $\mathbf{f}$ ,  $g$ , and  $\theta_D$  are chosen so that the exact solution is given by

$$\begin{aligned} \mathbf{u}(\mathbf{x}) &:= \begin{pmatrix} 2x_1^2x_2(x_1-1)^2(x_1-2)^2(x_2-1)(4x_2-1)(12x_2^2-10x_2+1) \\ -2x_1x_2^2(x_1-1)(x_1-2)(3x_1^2-6x_1+2)(x_2-1)^2(4x_2-1)^2 \end{pmatrix}, \\ p(\mathbf{x}) &:= (x_1 - 0.5) \cos(4\pi x_2), \\ \theta(\mathbf{x}) &:= x_1(2x_1^2 - 9x_1 + 12) \sin(2\pi x_2)^2 + 580 \quad \forall \mathbf{x} := (x_1, x_2) \in \Omega. \end{aligned}$$

In our third example we illustrate the accuracy of our method in 3D by considering the cube domain  $\Omega := (0, 1)^3$ , the boundary  $\Gamma = \bar{\Gamma}_D \cup \bar{\Gamma}_N$ , with  $\Gamma_D := (0, 1)^2 \times \{0\}$  and  $\Gamma_N := \Gamma \setminus \bar{\Gamma}_D$ . The viscosity parameters are the same as in the first example and the data  $\mathbf{f}$ ,  $g$ , and  $\theta_D$  are chosen so that the exact solution is given by

$$\begin{aligned} \mathbf{u}(\mathbf{x}) &:= \begin{pmatrix} 8x_1^2x_2x_3(x_1-1)^2(x_2-1)(x_3-1)(x_2-x_3) \\ -8x_1x_2^2x_3(x_1-1)(x_2-1)^2(x_3-1)(x_1-x_3) \\ 8x_1x_2x_3^2(x_1-1)(x_2-1)(x_3-1)^2(x_1-x_2) \end{pmatrix}, \\ p(\mathbf{x}) &:= (x_1 - 0.5)^3 \sin(x_2 + x_3), \\ \theta(\mathbf{x}) &:= 10 \sin(\pi x_1)^2 \sin(\pi x_2)^2 (x_3 - 1)^2 + 540 \quad \forall \mathbf{x} := (x_1, x_2, x_3) \in \Omega. \end{aligned}$$

Finally, in our fourth example we illustrate the accuracy of the 3D version of the four-to-one domain  $\Omega := (0, 2) \times (0, 1)^2 \setminus (1, 2) \times (0.25, 1)^2$ , the boundary  $\Gamma = \bar{\Gamma}_D \cup \bar{\Gamma}_N$ , with  $\Gamma_D := \{0\} \times (0, 1)^2$  and  $\Gamma_N := \Gamma \setminus \bar{\Gamma}_D$ . The viscosity parameters are the same as in the second example and the data  $\mathbf{f}$ ,  $g$ , and  $\theta_D$  are chosen so that the exact solution is given by

$$\begin{aligned} \mathbf{u}(\mathbf{x}) &:= \begin{pmatrix} 4x_1^2(x_1-1)^2(x_1-2)^2x_2(x_2-1)(2x_2-1)x_3(x_3-1)(4x_3-1)(12x_3^2-10x_3+1) \\ 4x_1(x_1-1)(x_1-2)(3x_1^2-6x_1+2)x_2^2(x_2-1)^2x_3(x_3-1)(4x_3-1)(12x_3^2-10x_3+1) \\ -8x_1(x_1-1)(x_1-2)(3x_1^2-6x_1+2)x_2(x_2-1)(2x_2-1)x_3^2(4x_3-1)^2(x_3-1)^2 \end{pmatrix}, \\ p(\mathbf{x}) &:= (x_1 - 0.5)(x_2 - 0.5) \cos(4\pi x_3), \\ \theta(\mathbf{x}) &:= x_1(2x_1^2 - 9x_1 + 12) \sin(\pi x_2)^2 \sin(2\pi x_3)^2 + 570 \quad \forall \mathbf{x} := (x_1, x_2, x_3) \in \Omega. \end{aligned}$$

We remark that in all the examples, the temperature is given as a function  $\hat{\theta}(\mathbf{x})$  plus a big constant chosen such that  $c > \theta_R$ , that is,  $\theta(\mathbf{x}) := \hat{\theta}(\mathbf{x}) + c$ . Then, the heat-flux vector is compute as:

$$\mathbf{p}(\mathbf{x}) = \kappa \nabla \hat{\theta}(\mathbf{x}) - \hat{\theta}(\mathbf{x}) \mathbf{u}(\mathbf{x}) - c \mathbf{u}(\mathbf{x}),$$

which implies that the errors of  $\mathbf{p}$  are influenced for  $c$ , and then they are higher than in the other unknowns as we will see below.

In Tables 4.1, 4.2, 4.3, 4.4, 4.5 and 4.6, we summarise the convergence history for a sequence of quasi-uniform triangulations, considering the finite element spaces introduced in Section 4.4.1, which required around four fixed-point iterations. In particular, for the 2D examples in Tables 4.1, 4.2, 4.3, and 4.4, we observe that the rate of convergence  $O(h^{k+1})$  predicted by Theorem 4.21 and Lemma 4.22 (when  $s = k + 1$ ) is attained in all the variables (with  $k = 0$  and  $k = 1$ ). Notice that the higher the order of the finite element chosen the lower the number of iterations. In turn, in Tables 4.5 and 4.6 we observe that optimal rates of convergence are also obtained (with  $k = 0$ ) for our 3D examples. On the other hand, some components of the approximate solutions for the four examples are displayed in Figures 4.1, 4.2, 4.3, and 4.4. All the figures were built using the  $\mathbb{P}_0 - \mathbb{RT}_0 - \mathbb{P}_0 - \mathbf{P}_1 - \mathbf{RT}_0 - \mathbf{P}_1$  approximation with 353853, 430221, 3314052, and 4148740 degrees of freedom for the Examples 1, 2, 3, and 4, respectively. In particular, we can observe in Figure 4.1 that the temperature is higher in the left side and then it dissipates to the others sides meanwhile in Figure 4.2 the temperature is lightly higher in the right side. Next, analogously to Figures 4.1 and 4.2, in Figures 4.3 and 4.4 we can observe that the temperature is higher in the bottom of the cube and in the left side of the four-to-one domain and then it dissipates to the others sides, respectively. Moreover, it can be seen that the velocity streamlines of the fluid are higher inside of the domain and lower close to the boundary as expected.

| N      | $h$   | $e(t)$ | $r(t)$ | $e(\sigma)$ | $r(\sigma)$ | $e(\rho)$ | $r(\rho)$ | $e(u)$ | $r(u)$ | $e(p)$  | $r(p)$ |
|--------|-------|--------|--------|-------------|-------------|-----------|-----------|--------|--------|---------|--------|
| 1467   | 0.196 | 0.1540 | –      | 1.2323      | –           | 0.2549    | –         | 0.2609 | –      | 18.7854 | –      |
| 5631   | 0.097 | 0.0759 | 1.002  | 0.6258      | 0.961       | 0.1452    | 0.784     | 0.1266 | 1.025  | 9.6388  | 0.946  |
| 22131  | 0.048 | 0.0376 | 0.995  | 0.3099      | 0.993       | 0.0799    | 0.844     | 0.0618 | 1.014  | 4.7401  | 1.003  |
| 87837  | 0.025 | 0.0189 | 1.031  | 0.1564      | 1.024       | 0.0396    | 1.052     | 0.0311 | 1.026  | 2.4056  | 1.015  |
| 353853 | 0.013 | 0.0092 | 1.096  | 0.0768      | 1.090       | 0.0193    | 1.103     | 0.0155 | 1.072  | 1.1875  | 1.082  |

| $e(\theta)$ | $r(\theta)$ | $e(p)$ | $r(p)$ | $e(\sigma_N)^*$ | $r(\sigma_N)$ | $e(\tilde{\sigma}_P)$ | $r(\tilde{\sigma}_P)$ | $e(\hat{\sigma}_P)$ | $r(\hat{\sigma}_P)$ | iter |
|-------------|-------------|--------|--------|-----------------|---------------|-----------------------|-----------------------|---------------------|---------------------|------|
| 3.6159      | –           | 0.1322 | –      | 0.3557          | –             | 0.3521                | –                     | 0.3095              | –                   | 5    |
| 1.4896      | 1.257       | 0.0677 | 0.949  | 0.1717          | 1.033         | 0.1700                | 1.033                 | 0.1493              | 1.033               | 5    |
| 0.6674      | 1.135       | 0.0325 | 1.039  | 0.0830          | 1.026         | 0.0822                | 1.026                 | 0.0727              | 1.018               | 4    |
| 0.3326      | 1.042       | 0.0150 | 1.154  | 0.0417          | 1.031         | 0.0413                | 1.031                 | 0.0361              | 1.047               | 4    |
| 0.1631      | 1.093       | 0.0073 | 1.105  | 0.0201          | 1.119         | 0.0199                | 1.119                 | 0.0175              | 1.111               | 4    |

Table 4.1: EXAMPLE 1, Degrees of freedom, mesh sizes, errors, rates of convergence, and number of iterations for the fully-mixed  $\mathbb{P}_0 - \mathbb{RT}_0 - \mathbb{P}_0 - \mathbf{P}_1 - \mathbf{RT}_0 - \mathbf{P}_1$  approximation of the non-isothermal Oldroyd–Stokes equations (\* errors divided by  $\epsilon = 0.01$ ).

| N      | $h$   | $e(t)$ | $r(t)$ | $e(\sigma)$ | $r(\sigma)$ | $e(\rho)$ | $r(\rho)$ | $e(u)$ | $r(u)$ | $e(p)$ | $r(p)$ |
|--------|-------|--------|--------|-------------|-------------|-----------|-----------|--------|--------|--------|--------|
| 3666   | 0.196 | 0.0264 | –      | 0.1535      | –           | 0.0227    | –         | 0.0370 | –      | 2.4423 | –      |
| 14076  | 0.097 | 0.0063 | 2.037  | 0.0374      | 2.002       | 0.0056    | 1.987     | 0.0086 | 2.073  | 0.5847 | 2.027  |
| 55326  | 0.048 | 0.0015 | 2.045  | 0.0089      | 2.024       | 0.0013    | 2.048     | 0.0020 | 2.065  | 0.1379 | 2.041  |
| 219591 | 0.025 | 0.0004 | 1.989  | 0.0023      | 2.037       | 0.0003    | 1.998     | 0.0005 | 1.986  | 0.0357 | 2.024  |
| 884631 | 0.013 | 0.0001 | 2.187  | 0.0006      | 2.153       | 0.0001    | 2.196     | 0.0001 | 2.195  | 0.0088 | 2.148  |

| $e(\theta)$ | $r(\theta)$ | $e(p)$ | $r(p)$ | $e(\sigma_N)^*$ | $r(\sigma_N)$ | $e(\tilde{\sigma}_P)$ | $r(\tilde{\sigma}_P)$ | $e(\hat{\sigma}_P)$ | $r(\hat{\sigma}_P)$ | iter |
|-------------|-------------|--------|--------|-----------------|---------------|-----------------------|-----------------------|---------------------|---------------------|------|
| 0.2957      | –           | 0.0155 | –      | 0.0455          | –             | 0.0450                | –                     | 0.0861              | –                   | 4    |
| 0.0692      | 2.060       | 0.0041 | 1.899  | 0.0107          | 2.049         | 0.0106                | 2.049                 | 0.0177              | 2.246               | 4    |
| 0.0154      | 2.119       | 0.0010 | 1.965  | 0.0025          | 2.039         | 0.0025                | 2.039                 | 0.0041              | 2.063               | 4    |
| 0.0039      | 2.047       | 0.0003 | 2.074  | 0.0007          | 2.006         | 0.0007                | 2.006                 | 0.0011              | 2.018               | 4    |
| 0.0010      | 2.133       | 0.0001 | 2.138  | 0.0002          | 2.185         | 0.0002                | 2.185                 | 0.0003              | 2.198               | 4    |

Table 4.2: EXAMPLE 1, Degrees of freedom, mesh sizes, errors, rates of convergence, and number of iterations for the fully-mixed  $\mathbb{P}_1 - \mathbb{RT}_1 - \mathbb{P}_1 - \mathbf{P}_2 - \mathbf{RT}_1 - \mathbf{P}_2$  approximation of the non-isothermal Oldroyd–Stokes equations (\* errors divided by  $\epsilon = 0.01$ ).

| N      | $h$   | $e(t)$ | $r(t)$ | $e(\sigma)$ | $r(\sigma)$ | $e(\rho)$ | $r(\rho)$ | $e(u)$ | $r(u)$ | $e(p)$  | $r(p)$ |
|--------|-------|--------|--------|-------------|-------------|-----------|-----------|--------|--------|---------|--------|
| 1803   | 0.190 | 0.1627 | –      | 2.3476      | –           | 0.1990    | –         | 0.2346 | –      | 91.0099 | –      |
| 6987   | 0.103 | 0.0872 | 1.017  | 1.1683      | 1.139       | 0.1209    | 0.814     | 0.1138 | 1.181  | 43.1779 | 1.217  |
| 27345  | 0.049 | 0.0432 | 0.953  | 0.5758      | 0.959       | 0.0650    | 0.841     | 0.0553 | 0.978  | 21.7689 | 0.929  |
| 107985 | 0.026 | 0.0219 | 1.052  | 0.2936      | 1.040       | 0.0326    | 1.066     | 0.0279 | 1.058  | 10.9728 | 1.059  |
| 430221 | 0.013 | 0.0108 | 1.062  | 0.1449      | 1.062       | 0.0168    | 0.996     | 0.0136 | 1.076  | 5.4528  | 1.051  |

| $e(\theta)$ | $r(\theta)$ | $e(p)$ | $r(p)$ | $e(\sigma_N)^*$ | $r(\sigma_N)$ | $e(\tilde{\sigma}_P)$ | $r(\tilde{\sigma}_P)$ | $e(\hat{\sigma}_P)$ | $r(\hat{\sigma}_P)$ | iter |
|-------------|-------------|--------|--------|-----------------|---------------|-----------------------|-----------------------|---------------------|---------------------|------|
| 10.2650     | –           | 0.2544 | –      | 0.2532          | –             | 0.2507                | –                     | 0.2724              | –                   | 5    |
| 4.4925      | 1.348       | 0.1108 | 1.356  | 0.1339          | 1.040         | 0.1325                | 1.040                 | 0.1387              | 1.101               | 4    |
| 2.1518      | 0.998       | 0.0495 | 1.092  | 0.0668          | 0.942         | 0.0662                | 0.942                 | 0.0702              | 0.924               | 4    |
| 1.0794      | 1.066       | 0.0230 | 1.185  | 0.0339          | 1.051         | 0.0335                | 1.051                 | 0.0349              | 1.078               | 3    |
| 0.5271      | 1.077       | 0.0112 | 1.085  | 0.0167          | 1.060         | 0.0166                | 1.060                 | 0.0171              | 1.072               | 3    |

Table 4.3: EXAMPLE 2, Degrees of freedom, mesh sizes, errors, rates of convergence, and number of iterations for the fully-mixed  $\mathbb{P}_0 - \mathbb{RT}_0 - \mathbb{P}_0 - \mathbf{P}_1 - \mathbf{RT}_0 - \mathbf{P}_1$  approximation of the non-isothermal Oldroyd–Stokes equations (\* errors divided by  $\epsilon = 0.01$ ).

| N       | $h$   | $e(\mathbf{t})$ | $r(\mathbf{t})$ | $e(\boldsymbol{\sigma})$ | $r(\boldsymbol{\sigma})$ | $e(\boldsymbol{\rho})$ | $r(\boldsymbol{\rho})$ | $e(\mathbf{u})$ | $r(\mathbf{u})$ | $e(\mathbf{p})$ | $r(\mathbf{p})$ |
|---------|-------|-----------------|-----------------|--------------------------|--------------------------|------------------------|------------------------|-----------------|-----------------|-----------------|-----------------|
| 4506    | 0.190 | 0.0357          | –               | 0.4304                   | –                        | 0.0318                 | –                      | 0.0504          | –               | 16.7122         | –               |
| 17466   | 0.103 | 0.0085          | 2.334           | 0.1039                   | 2.319                    | 0.0073                 | 2.397                  | 0.0117          | 2.386           | 4.0081          | 2.330           |
| 68361   | 0.049 | 0.0021          | 1.906           | 0.0247                   | 1.946                    | 0.0018                 | 1.927                  | 0.0028          | 1.938           | 1.0104          | 1.868           |
| 269961  | 0.026 | 0.0005          | 2.096           | 0.0064                   | 2.087                    | 0.0005                 | 2.097                  | 0.0007          | 2.095           | 0.2605          | 2.095           |
| 1075551 | 0.013 | 0.0001          | 2.131           | 0.0016                   | 2.117                    | 0.0001                 | 2.125                  | 0.0002          | 2.136           | 0.0627          | 2.141           |

| $e(\theta)$ | $r(\theta)$ | $e(p)$ | $r(p)$ | $e(\boldsymbol{\sigma}_N)^*$ | $r(\boldsymbol{\sigma}_N)$ | $e(\tilde{\boldsymbol{\sigma}}_P)$ | $r(\tilde{\boldsymbol{\sigma}}_P)$ | $e(\hat{\boldsymbol{\sigma}}_P)$ | $r(\hat{\boldsymbol{\sigma}}_P)$ | iter |
|-------------|-------------|--------|--------|------------------------------|----------------------------|------------------------------------|------------------------------------|----------------------------------|----------------------------------|------|
| 1.9318      | –           | 0.0741 | –      | 0.0509                       | –                          | 0.0504                             | –                                  | 0.0911                           | –                                | 4    |
| 0.4124      | 2.520       | 0.0152 | 2.582  | 0.0122                       | 2.325                      | 0.0121                             | 2.325                              | 0.0238                           | 2.191                            | 3    |
| 0.1039      | 1.869       | 0.0033 | 2.055  | 0.0030                       | 1.909                      | 0.0030                             | 1.909                              | 0.0056                           | 1.952                            | 3    |
| 0.0264      | 2.115       | 0.0087 | 2.087  | 0.0008                       | 2.097                      | 0.0008                             | 2.097                              | 0.0015                           | 2.089                            | 3    |
| 0.0065      | 2.097       | 0.0002 | 2.148  | 0.0002                       | 2.131                      | 0.0002                             | 2.131                              | 0.0003                           | 2.156                            | 3    |

Table 4.4: EXAMPLE 2, Degrees of freedom, mesh sizes, errors, rates of convergence, and number of iterations for the fully-mixed  $\mathbb{P}_1 - \mathbb{RT}_1 - \mathbb{P}_1 - \mathbf{P}_2 - \mathbf{RT}_1 - \mathbf{P}_2$  approximation of the non-isothermal Oldroyd–Stokes equations (\* errors divided by  $\epsilon = 0.01$ ).

| N       | $h$   | $e(\mathbf{t})$ | $r(\mathbf{t})$ | $e(\boldsymbol{\sigma})$ | $r(\boldsymbol{\sigma})$ | $e(\boldsymbol{\rho})$ | $r(\boldsymbol{\rho})$ | $e(\mathbf{u})$ | $r(\mathbf{u})$ | $e(\mathbf{p})$ | $r(\mathbf{p})$ |
|---------|-------|-----------------|-----------------|--------------------------|--------------------------|------------------------|------------------------|-----------------|-----------------|-----------------|-----------------|
| 7028    | 0.354 | 0.0149          | –               | 0.1252                   | –                        | 0.0181                 | –                      | 0.0259          | –               | 23.7426         | –               |
| 53604   | 0.177 | 0.0082          | 0.862           | 0.0644                   | 0.959                    | 0.0119                 | 0.606                  | 0.0139          | 0.899           | 12.3360         | 0.945           |
| 419012  | 0.088 | 0.0042          | 0.970           | 0.0324                   | 0.994                    | 0.0068                 | 0.812                  | 0.0070          | 0.979           | 6.2286          | 0.986           |
| 3314052 | 0.044 | 0.0021          | 0.995           | 0.0162                   | 1.001                    | 0.0036                 | 0.927                  | 0.0035          | 0.998           | 3.1220          | 0.997           |

| $e(\theta)$ | $r(\theta)$ | $e(p)$ | $r(p)$ | $e(\boldsymbol{\sigma}_N)^*$ | $r(\boldsymbol{\sigma}_N)$ | $e(\tilde{\boldsymbol{\sigma}}_P)$ | $r(\tilde{\boldsymbol{\sigma}}_P)$ | $e(\hat{\boldsymbol{\sigma}}_P)$ | $r(\hat{\boldsymbol{\sigma}}_P)$ | iter |
|-------------|-------------|--------|--------|------------------------------|----------------------------|------------------------------------|------------------------------------|----------------------------------|----------------------------------|------|
| 5.1532      | –           | 0.0170 | –      | 0.0328                       | –                          | 0.0325                             | –                                  | 0.0312                           | –                                | 4    |
| 2.8687      | 0.845       | 0.0096 | 0.817  | 0.0194                       | 0.758                      | 0.0192                             | 0.758                              | 0.0187                           | 0.736                            | 3    |
| 1.4810      | 0.954       | 0.0046 | 1.055  | 0.0103                       | 0.908                      | 0.0102                             | 0.908                              | 0.0103                           | 0.868                            | 3    |
| 0.7470      | 0.987       | 0.0022 | 1.076  | 0.0053                       | 0.966                      | 0.0052                             | 0.966                              | 0.0054                           | 0.938                            | 3    |

Table 4.5: EXAMPLE 3, Degrees of freedom, mesh sizes, errors, rates of convergence, and number of iterations for the fully-mixed  $\mathbb{P}_0 - \mathbb{RT}_0 - \mathbb{P}_0 - \mathbf{P}_1 - \mathbf{RT}_0 - \mathbf{P}_1$  approximations of the non-isothermal Oldroyd–Stokes equations (\* errors divided by  $\epsilon = 0.01$ ).

| N       | $h$   | $e(\mathbf{t})$ | $r(\mathbf{t})$ | $e(\boldsymbol{\sigma})$ | $r(\boldsymbol{\sigma})$ | $e(\boldsymbol{\rho})$ | $r(\boldsymbol{\rho})$ | $e(\mathbf{u})$ | $r(\mathbf{u})$ | $e(\mathbf{p})$ | $r(\mathbf{p})$ |
|---------|-------|-----------------|-----------------|--------------------------|--------------------------|------------------------|------------------------|-----------------|-----------------|-----------------|-----------------|
| 8884    | 0.354 | 0.0657          | –               | 1.0895                   | –                        | 0.0705                 | –                      | 0.1070          | –               | 120.9619        | –               |
| 67396   | 0.177 | 0.0414          | 0.667           | 0.6751                   | 0.691                    | 0.0478                 | 0.559                  | 0.0711          | 0.590           | 55.2472         | 1.131           |
| 525316  | 0.088 | 0.0227          | 0.865           | 0.3443                   | 0.971                    | 0.0290                 | 0.723                  | 0.0376          | 0.917           | 28.2498         | 0.968           |
| 4148740 | 0.044 | 0.0116          | 0.966           | 0.1727                   | 0.995                    | 0.0157                 | 0.882                  | 0.0189          | 0.992           | 14.2047         | 0.992           |

| $e(\theta)$ | $r(\theta)$ | $e(p)$ | $r(p)$ | $e(\boldsymbol{\sigma}_N)^*$ | $r(\boldsymbol{\sigma}_N)$ | $e(\tilde{\boldsymbol{\sigma}}_P)$ | $r(\tilde{\boldsymbol{\sigma}}_P)$ | $e(\hat{\boldsymbol{\sigma}}_P)$ | $r(\hat{\boldsymbol{\sigma}}_P)$ | iter |
|-------------|-------------|--------|--------|------------------------------|----------------------------|------------------------------------|------------------------------------|----------------------------------|----------------------------------|------|
| 7.6590      | –           | 0.1087 | –      | 0.1318                       | –                          | 0.1305                             | –                                  | 0.1300                           | –                                | 3    |
| 6.1383      | 0.319       | 0.0755 | 0.525  | 0.0793                       | 0.732                      | 0.0785                             | 0.732                              | 0.0810                           | 0.683                            | 3    |
| 3.2313      | 0.926       | 0.0337 | 1.165  | 0.0443                       | 0.841                      | 0.0439                             | 0.841                              | 0.0463                           | 0.806                            | 3    |
| 1.6359      | 0.982       | 0.0144 | 1.224  | 0.0233                       | 0.926                      | 0.0231                             | 0.926                              | 0.0244                           | 0.926                            | 3    |

Table 4.6: EXAMPLE 4, Degrees of freedom, mesh sizes, errors, rates of convergence, and number of iterations for the fully-mixed  $\mathbb{P}_0 - \mathbb{RT}_0 - \mathbb{P}_0 - \mathbf{P}_1 - \mathbf{RT}_0 - \mathbf{P}_1$  approximations of the non-isothermal Oldroyd–Stokes equations (\* errors divided by  $\epsilon = 0.01$ ).

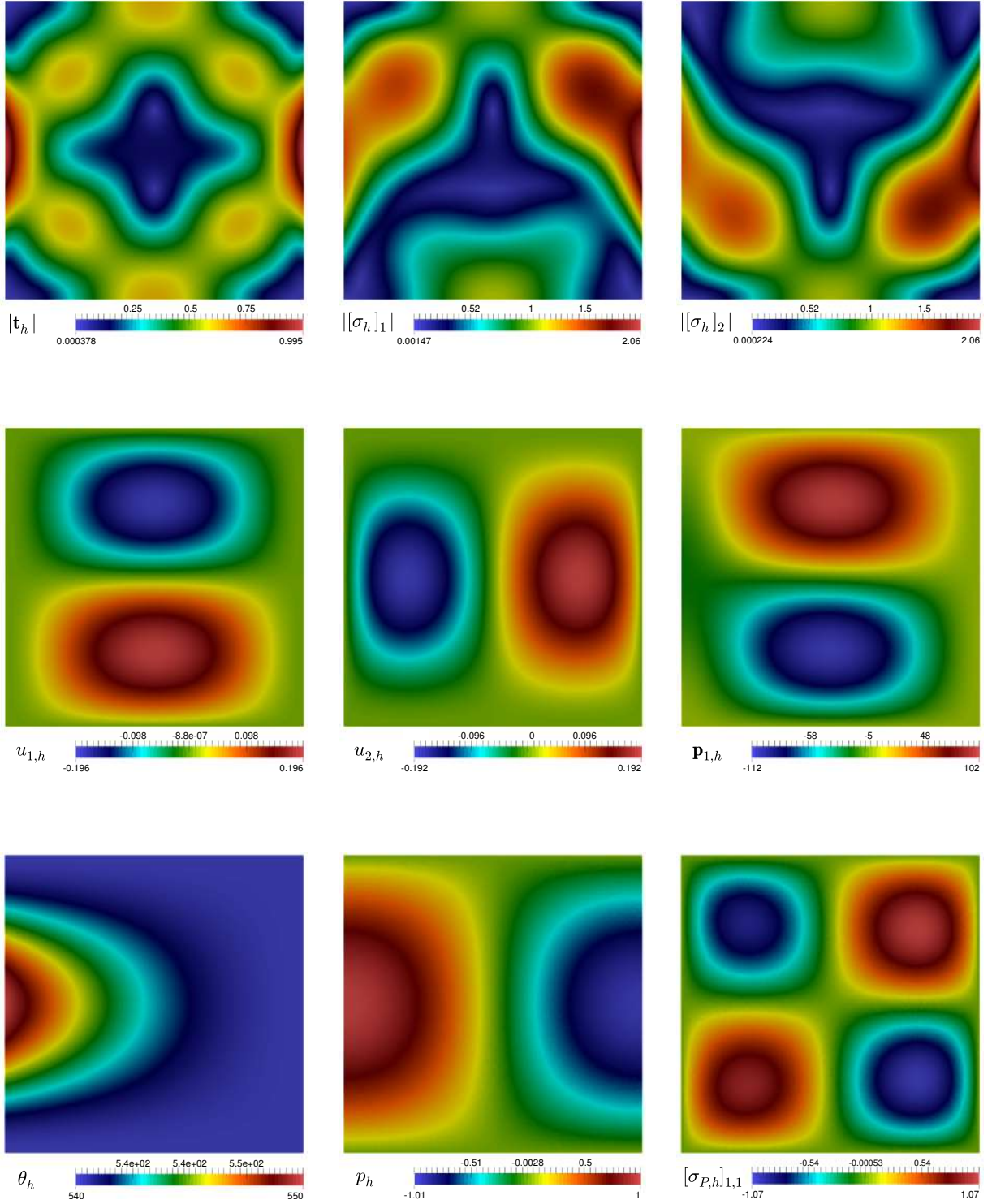


Figure 4.1: Example 1:  $\mathbb{P}_0 - \mathbb{RT}_0 - \mathbb{P}_0 - \mathbf{P}_1 - \mathbf{RT}_0 - \mathbf{P}_1$  approximated spectral norm of strain tensor and the stress tensor components (top panels), velocity and heat flux vector components (centre panels), and temperature and pressure fields, and polymeric part of the extra-stress tensor component (bottom row).



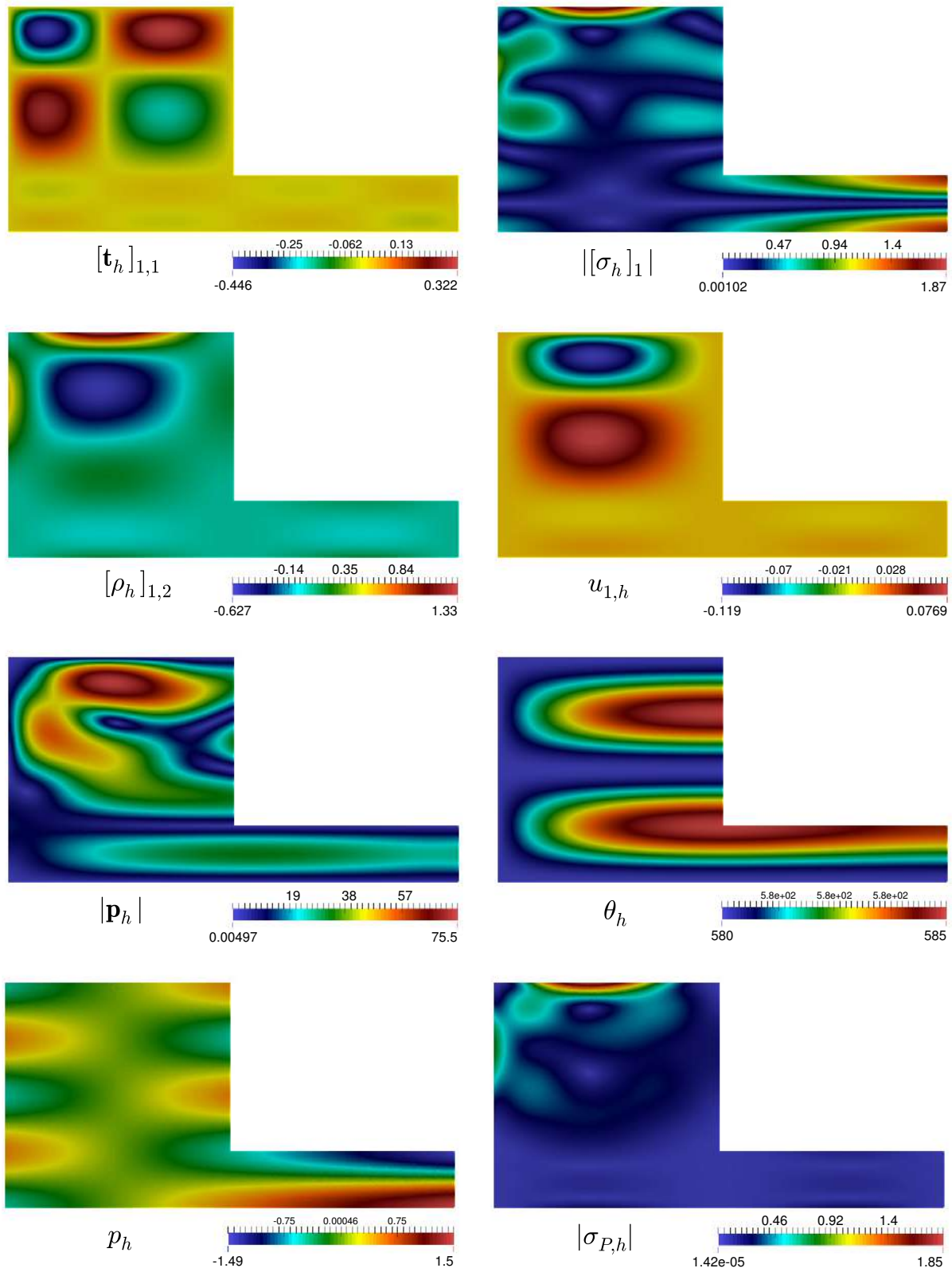


Figure 4.2: Example 2:  $\mathbb{P}_0 - \mathbf{RT}_0 - \mathbb{P}_0 - \mathbf{P}_1 - \mathbf{RT}_0 - \mathbf{P}_1$  approximation of some components of the approximate solutions.

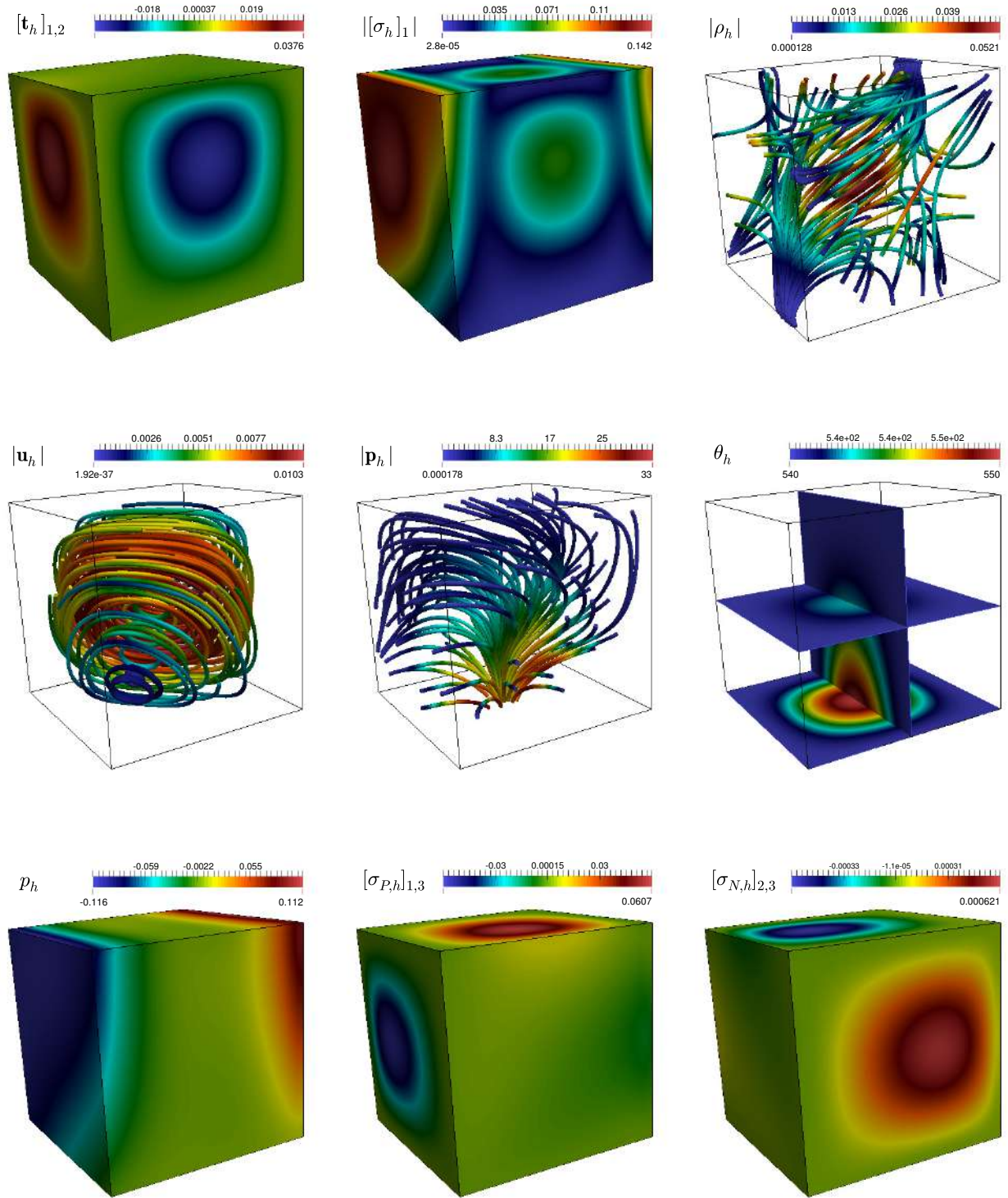


Figure 4.3: Example 3:  $\mathbb{P}_0 - \mathbf{RT}_0 - \mathbb{P}_0 - \mathbf{P}_1 - \mathbf{RT}_0 - \mathbf{P}_1$  approximation of the strain tensor component, approximated spectral norm of the stress tensor component, and vorticity streamlines (top panels), velocity streamlines, heat flux streamlines, and temperature field (centre panels), and pressure field, polymeric part and solvent part of the extra-stress tensor component (bottom row).

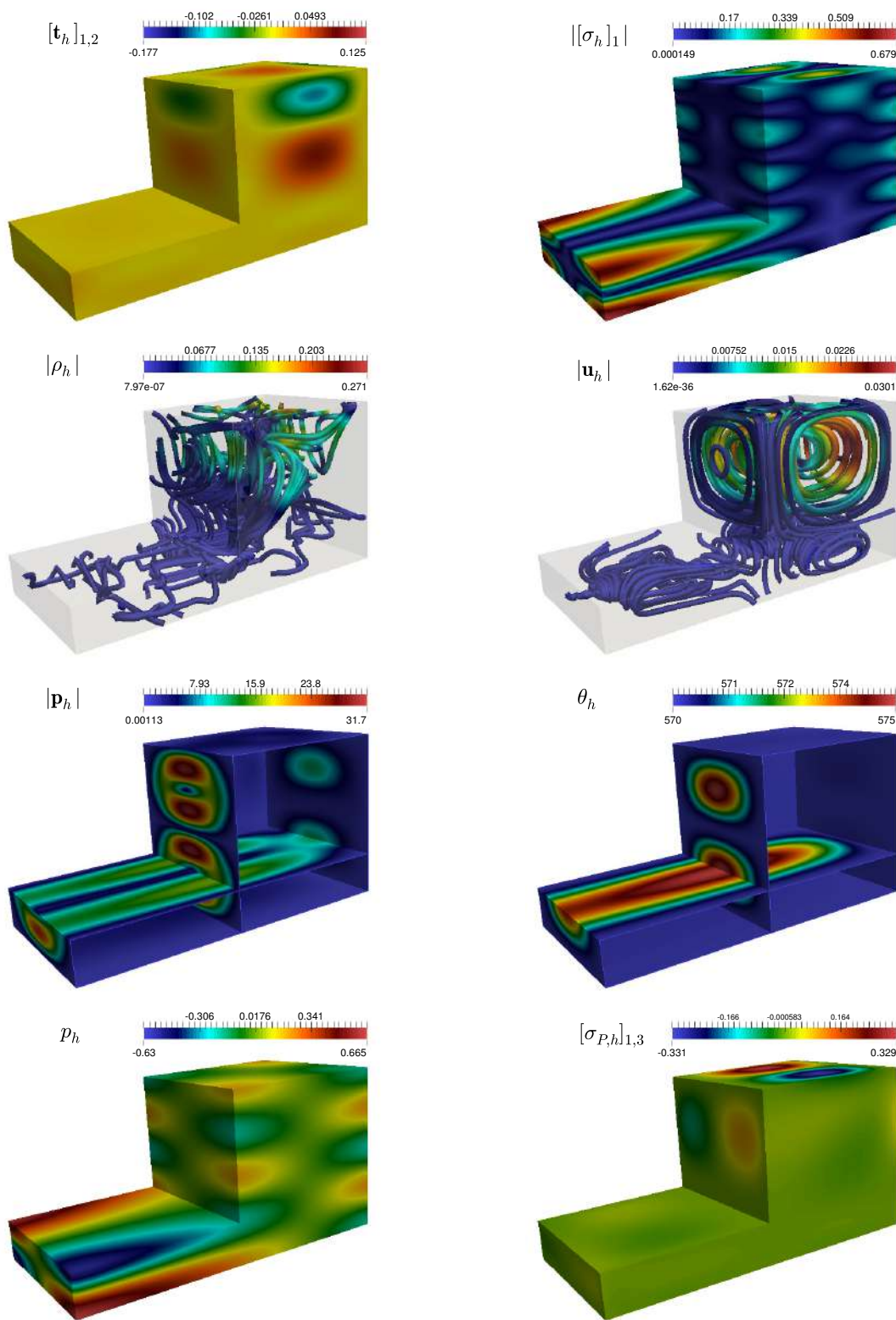


Figure 4.4: Example 4:  $\mathbb{P}_0 - \mathbf{RT}_0 - \mathbb{P}_0 - \mathbf{P}_1 - \mathbf{RT}_0 - \mathbf{P}_1$  approximation of some components of the approximate solutions.

## CHAPTER 5

---

### A posteriori error analysis of an augmented fully-mixed formulation for the non-isothermal Oldroyd–Stokes problem

---

In this chapter we develop an a posteriori error analysis for the variational formulation described in Chapter 4 for the 2D and 3D versions of the associated mixed finite element scheme. We derive two reliable and efficient residual-based a posteriori error estimators on arbitrary (convex or non-convex) polygonal and polyhedral regions.

#### 5.1 Introduction

We have recently introduced in Chapter 4, an augmented-mixed finite element method to numerically approximate the flow patterns of a non-isothermal incompressible viscoelastic fluid described by the non-isothermal Oldroyd–Stokes equations. The underlying model consists of the Stokes-type equation for Oldroyd viscoelasticity, coupled with the heat equation through a convective term and the viscosity of the fluid. The original unknowns are the polymeric part of the extra-stress tensor, the velocity, the pressure, and the temperature of the fluid. In turn, for convenience of the analysis, the strain tensor, the vorticity, and the stress tensor are introduced as further unknowns. This allows to join the polymeric and solvent viscosities in an adimensional viscosity, and to eliminate the polymeric part of the extra-stress tensor and the pressure from the system, which, together with the solvent part of the extra-stress tensor, can anyway be approximated later on by postprocessed. In this way, a fully mixed approach is applied, in which the heat flux vector is incorporated as an additional unknown as well. Since the convective term in the heat equation forces both the velocity and the temperature to live in  $H^1$  instead of  $L^2$  as usual, we proceed as for the Boussinesq model in [51, 50, 52] and augment the variational formulation with suitable Galerkin type expressions arising from the constitutive and equilibrium equations, the relation defining the strain and vorticity tensors, and the Dirichlet boundary condition on the temperature. The resulting augmented scheme is then written equivalently as a fixed-point equation, so that the well-known Schauder and Banach theorems, combined with the Lax–Milgram theorem and certain regularity assumptions, are applied to prove the unique solvability of the continuous system. As for the associated Galerkin scheme, whose solvability is established similarly to the continuous case by using the Brouwer fixed-point and Lax–Milgram theorems, we employ Raviart–Thomas approximations of order  $k$  for the stress tensor and the heat flux vector, continuous piecewise



polynomials of order  $\leq k + 1$  for velocity and temperature, and piecewise polynomials of order  $\leq k$  for the strain tensor and the vorticity. Optimal a priori error estimates were also derived.

Now, it is well known that under the eventual presence of singularities or high gradients of the solution, most of the standard Galerkin procedures such as finite element and mixed finite element methods inevitably lose accuracy, and hence one usually tries to recover it by applying an adaptive algorithm based on a posteriori error estimates. For example, residual-based a posteriori error analyses for the aforementioned Boussinesq model have been developed in [54] and [53] for the associated mixed-primal and fully-mixed formulations, respectively. In fact, standard arguments relying on duality techniques, suitable decompositions and classical approximation properties, are combined there with corresponding small data assumptions to derive the reliability of the estimators. In turn, inverse inequalities and the usual localisation technique based on bubble functions are employed in both works to prove the corresponding efficiency estimates. On the other hand, and concerning isothermal viscoelastic flows, not much has been done and we just refer to [71, 131, 137] for the steady-state case and [75, 76] for the time dependent case, where different contributions addressing this interesting issue can be found. In particular, a fully local a posteriori error estimator for a simplified Oldroyd-B model without convective terms in a convex polygonal domain was obtained in [137]. The main unknowns are given by the velocity, the extra-stress and the pressure of the fluid, whereas continuous piecewise linear finite elements together with a Galerkin Least Square (GLS) approach are used for the associated discrete scheme. In turn, a fully local residual-based a posteriori error estimator for the velocity-pressure-stress formulation of a more general model, namely the Giesekus and Oldroyd-B type differential constitutive laws in 2D and 3D, was derived in [71]. In this case, the discrete spaces employed are the Hood–Taylor pair for the velocity and the pressure, and continuous piecewise linear elements for the viscoelastic stress component. Furthermore, and up to the authors’ knowledge, the first work dealing with high gradients of the solution for the non-isothermal Oldroyd–Stokes problem is [57]. An optimal control technique is proposed and analysed there for a four-to-one contraction domain, where a vortex is generated near the corner region of the contraction. However, we remark that this work does not consider an adaptive algorithm.

According to the above discussion, and in order to complement the study started in Chapter 4 for the non-isothermal Oldroyd–Stokes problem, in this chapter we proceed similarly to [3, 54, 53, 97], and develop two reliable and efficient residual-based a posteriori error estimators for the augmented-mixed finite element method studied in Chapter 4. This means that our analysis begins by applying the uniform ellipticity of the bilinear form defining the continuous formulation. Next, we apply suitable Helmholtz decompositions, local approximation properties of the Clément and Raviart–Thomas interpolants, and known estimates from [85, 91], to prove the reliability of a residual-based estimator. In turn, the efficiency estimate is consequence of standard arguments such as inverse inequalities, the localization technique based on bubble functions, and other known results to be specified later on in Section 5.3.4. Alternative, a second reliable and efficient residual-based a posteriori error estimator not making use of any Helmholtz decomposition is also proposed.

We have organised the contents of this chapter as follows. In Section 5.2 we recall from Chapter 4 the model problem and its continuous and discrete augmented fully-mixed variational formulations. Next, in Section 5.3 we consider the 2D case, introduce two a posteriori error indicators, and assuming small data and certain regularity assumptions, we derive the corresponding theoretical bounds yielding

reliability and efficiency of each estimator. The analysis and results from Section 5.3 are then extended to the 3D case in Section 5.4. Finally, some numerical results illustrating the good performance and good effectivity indexes of both error estimators under diverse scenarios in 2D and 3D, and confirming the satisfactory behaviour of the corresponding adaptive refinement strategies, are presented in Section 5.5.

## 5.2 The non-isothermal Oldroyd–Stokes problem

In this section we recall from Chapter 4 the non-isothermal Oldroyd–Stokes model, its fully-mixed variational formulation, the associated Galerkin scheme, and the main results concerning the corresponding solvability analysis.

### 5.2.1 The model problem

The non-isothermal Oldroyd–Stokes problem consists of a system of equations where the Stokes equation for the Oldroyd viscoelastic model introduced in [14], is coupled with the heat equation through a convective term and the viscosity of the fluid (cf. [56, 73]). More precisely, given a body force  $\mathbf{f}$ , and a heat source  $g$ , the aforementioned system of equations is given by

$$\begin{aligned} \boldsymbol{\sigma}_P - 2\mu_P(\theta)\mathbf{e}(\mathbf{u}) &= \mathbf{0} \quad \text{in } \Omega, \quad -\operatorname{div}(\boldsymbol{\sigma}_P + 2\epsilon\mu_N(\theta)\mathbf{e}(\mathbf{u})) + \nabla p = \mathbf{f} \quad \text{in } \Omega, \\ \operatorname{div} \mathbf{u} &= 0 \quad \text{in } \Omega, \quad -\operatorname{div}(\kappa \nabla \theta) + \mathbf{u} \cdot \nabla \theta = g \quad \text{in } \Omega, \\ \mathbf{u} &= \mathbf{0} \quad \text{on } \Gamma, \quad \theta = \theta_D \quad \text{on } \Gamma_D, \quad \kappa \nabla \theta \cdot \mathbf{n} = 0 \quad \text{on } \Gamma_N \quad \text{and} \quad \int_{\Omega} p = 0, \end{aligned} \quad (5.1)$$

where the unknowns are the polymeric part of the extra-stress tensor  $\boldsymbol{\sigma}_P$ , the velocity  $\mathbf{u}$ , the pressure  $p$ , and the temperature  $\theta$  of a fluid occupying the region  $\Omega$ . In addition,  $\mathbf{e}(\mathbf{u}) := \frac{1}{2}\{\nabla \mathbf{u} + (\nabla \mathbf{u})^t\}$  stands for the strain tensor of small deformations,  $\kappa$  is the thermal conductivity coefficient,  $\mu_P$  and  $\mu_N$  are the polymeric and solvent (or newtonian) viscosities, respectively, which are given by the following Arrhenius relationship:

$$\mu_P(\theta) = a_1 \exp\left(\frac{b_1}{\theta}\right), \quad \mu_N(\theta) = a_2 \exp\left(\frac{b_2}{\theta}\right), \quad (5.2)$$

where the coefficients  $a_1, b_1, a_2$ , and  $b_2$  are defined so that

$$0 < \mu_P(s) \leq 1, \quad 0 < \mu_N(s) \leq 1 \quad \forall s \geq 0. \quad (5.3)$$

Furthermore, we assume that both the polymeric and solvent viscosities are Lipschitz continuous and bounded from above and from below, that is,

$$|\mu_P(s) - \mu_P(t)| \leq L_{\mu_P}|s - t|, \quad |\mu_N(s) - \mu_N(t)| \leq L_{\mu_N}|s - t| \quad \forall s, t \geq 0, \quad (5.4)$$

and

$$\mu_{1,P} \leq \mu_P(s) \leq \mu_{2,P}, \quad \mu_{1,N} \leq \mu_N(s) \leq \mu_{2,N} \quad \forall s \geq 0. \quad (5.5)$$

Note that a small real parameter  $\epsilon > 0$  on the second equation of (5.1) is introduced to make the effect of the solvent viscosity much smaller than that of the polymeric part.

Now, in order to derive our mixed approach (see [37, Section 2.1] for details), we begin by introducing the strain tensor as an additional unknown  $\mathbf{t} := \mathbf{e}(\mathbf{u})$ , whence the polymeric and solvent parts of the extra-stress tensor can be written, respectively, as

$$\boldsymbol{\sigma}_P = 2\mu_P(\theta)\mathbf{t} \quad \text{and} \quad \boldsymbol{\sigma}_N = 2\epsilon\mu_N(\theta)\mathbf{t} \quad \text{in } \Omega. \quad (5.6)$$

Next, defining the dimensionless effective viscosity as in [73], that is

$$\mu(\theta) := 2\mu_P(\theta) + 2\epsilon\mu_N(\theta), \quad (5.7)$$

and adopting the approach from [91] and [73] (see also [26, 51, 52]), we include as auxiliary variables the vorticity tensor  $\boldsymbol{\rho}$ , the stress tensor  $\boldsymbol{\sigma}$ , and the heat-flux vector  $\mathbf{p}$ , respectively, by

$$\boldsymbol{\rho} := \nabla \mathbf{u} - \mathbf{e}(\mathbf{u}), \quad \boldsymbol{\sigma} := \mu(\theta)\mathbf{t} - p\mathbb{I}, \quad \text{and} \quad \mathbf{p} := \kappa \nabla \theta - \theta \mathbf{u} \quad \text{in } \Omega.$$

In this way, utilising the incompressibility condition  $\operatorname{div} \mathbf{u} = \operatorname{tr}(\mathbf{e}(\mathbf{u})) = 0$  in  $\Omega$  and the homogeneous Dirichlet boundary condition  $\mathbf{u} = \mathbf{0}$  on  $\Gamma$ , the equations in (5.1) can be rewritten, equivalently, as

$$\begin{aligned} \mathbf{t} + \boldsymbol{\rho} &= \nabla \mathbf{u} \quad \text{in } \Omega, \quad \boldsymbol{\sigma}^d = \mu(\theta)\mathbf{t} \quad \text{in } \Omega, \quad -\operatorname{div} \boldsymbol{\sigma} = \mathbf{f} \quad \text{in } \Omega, \\ p &= -\frac{1}{n} \operatorname{tr} \boldsymbol{\sigma} \quad \text{in } \Omega, \quad \kappa^{-1} \mathbf{p} + \kappa^{-1} \theta \mathbf{u} = \nabla \theta \quad \text{in } \Omega, \quad -\operatorname{div} \mathbf{p} = g \quad \text{in } \Omega, \\ \mathbf{u} &= \mathbf{0} \quad \text{on } \Gamma, \quad \theta = \theta_D \quad \text{on } \Gamma_D, \quad \mathbf{p} \cdot \mathbf{n} = 0 \quad \text{on } \Gamma_N \quad \text{and} \quad \int_{\Omega} \operatorname{tr} \boldsymbol{\sigma} = 0. \end{aligned} \quad (5.8)$$

Note that the fourth equation in (5.8) allows us to eliminate the pressure  $p$  from the system and compute it as a simple post-process of  $\boldsymbol{\sigma}$ . In addition, it easy to see from (5.4) and (5.5) that the fluid viscosity  $\mu$  (cf. (5.7)) is Lipschitz continuous and bounded from above and from below, that is, there exist constants  $L_\mu > 0$  and  $\mu_1, \mu_2 > 0$ , such that

$$|\mu(s) - \mu(t)| \leq L_\mu |s - t| \quad \forall s, t \geq 0, \quad (5.9)$$

and

$$\mu_1 \leq \mu(s) \leq \mu_2 \quad \forall s \geq 0. \quad (5.10)$$

We end this section emphasizing from (5.6) that we can recover the polymeric and solvent parts of the extra-stress tensor as a simple post-process of  $\theta$  and  $\mathbf{t}$ , whereas from the fourth equation of (5.8) we can compute the pressure in terms of  $\boldsymbol{\sigma}$  conserving the same rate of convergence of the solution as we show theoretical and numerically in [37, Lemma 4.14 and Section 5], respectively. However, for the sake of simplicity and physical interest, in Section 5.5 we will focus only on the formulae suggested for the polymeric part of the extra-stress tensor and the pressure.

### 5.2.2 The fully-mixed variational formulation

In this section we recall from [37, Section 2.2] the weak formulation of the coupled problem given by (5.8). To this end, let us first group appropriately some of the unknowns and spaces as follows:

$$\underline{\mathbf{t}} := (\mathbf{t}, \boldsymbol{\sigma}, \boldsymbol{\rho}) \in \mathbb{H} := \mathbb{L}_{\operatorname{tr}}^2(\Omega) \times \mathbb{H}_0(\operatorname{div}; \Omega) \times \mathbb{L}_{\operatorname{skew}}^2(\Omega),$$

where  $\mathbb{H}$  is endowed with the norm

$$\|\underline{\mathbf{r}}\|_{\mathbb{H}}^2 := \|\mathbf{r}\|_{0,\Omega}^2 + \|\boldsymbol{\tau}\|_{\text{div};\Omega}^2 + \|\boldsymbol{\eta}\|_{0,\Omega}^2 \quad \forall \underline{\mathbf{r}} := (\mathbf{r}, \boldsymbol{\tau}, \boldsymbol{\eta}) \in \mathbb{H}.$$

Hence, the augmented fully-mixed variational formulation for the non-isothermal Oldroyd–Stokes problem reads: Find  $(\underline{\mathbf{t}}, \mathbf{u}, \mathbf{p}, \theta) \in \mathbb{H} \times \mathbf{H}_0^1(\Omega) \times \mathbf{H}_{\Gamma_N}(\text{div}; \Omega) \times H^1(\Omega)$  such that

$$\begin{aligned} \mathbf{A}_\theta((\underline{\mathbf{t}}, \mathbf{u}), (\underline{\mathbf{r}}, \mathbf{v})) &= \mathbf{F}(\underline{\mathbf{r}}, \mathbf{v}) \quad \forall (\underline{\mathbf{r}}, \mathbf{v}) \in \mathbb{H} \times \mathbf{H}_0^1(\Omega), \\ \tilde{\mathbf{A}}((\mathbf{p}, \theta), (\mathbf{q}, \psi)) + \tilde{\mathbf{B}}_{\mathbf{u}}((\mathbf{p}, \theta), (\mathbf{q}, \psi)) &= \tilde{\mathbf{F}}(\mathbf{q}, \psi) \quad \forall (\mathbf{q}, \psi) \in \mathbf{H}_{\Gamma_N}(\text{div}; \Omega) \times H^1(\Omega), \end{aligned} \quad (5.11)$$

where, given  $(\phi, \mathbf{w}) \in H^1(\Omega) \times \mathbf{H}_0^1(\Omega)$ ,  $\mathbf{A}_\phi$ ,  $\tilde{\mathbf{A}}$ , and  $\tilde{\mathbf{B}}_{\mathbf{w}}$  are the bilinear forms defined, respectively, as

$$\begin{aligned} \mathbf{A}_\phi((\underline{\mathbf{t}}, \mathbf{u}), (\underline{\mathbf{r}}, \mathbf{v})) &:= \int_{\Omega} \mu(\phi) \mathbf{t} : \left\{ \mathbf{r} - \kappa_1 \boldsymbol{\tau}^{\text{d}} \right\} + \int_{\Omega} \boldsymbol{\sigma}^{\text{d}} : \left\{ \kappa_1 \boldsymbol{\tau}^{\text{d}} - \mathbf{r} \right\} + \int_{\Omega} \mathbf{t} : \boldsymbol{\tau}^{\text{d}} \\ &+ \int_{\Omega} \left\{ \mathbf{u} + \kappa_2 \text{div} \boldsymbol{\sigma} \right\} \cdot \text{div} \boldsymbol{\tau} - \int_{\Omega} \mathbf{v} \cdot \text{div} \boldsymbol{\sigma} + \int_{\Omega} \boldsymbol{\rho} : \boldsymbol{\tau} - \int_{\Omega} \boldsymbol{\sigma} : \boldsymbol{\eta} \\ &+ \kappa_3 \int_{\Omega} \left\{ \mathbf{e}(\mathbf{u}) - \mathbf{t} \right\} : \mathbf{e}(\mathbf{v}) + \kappa_4 \int_{\Omega} \left( \boldsymbol{\rho} - \left\{ \nabla \mathbf{u} - \mathbf{e}(\mathbf{u}) \right\} \right) : \boldsymbol{\eta}, \end{aligned} \quad (5.12)$$

$$\begin{aligned} \tilde{\mathbf{A}}((\mathbf{p}, \theta), (\mathbf{q}, \psi)) &:= \kappa^{-1} \int_{\Omega} \mathbf{p} \cdot \left\{ \mathbf{q} - \kappa_5 \nabla \psi \right\} + \int_{\Omega} \left\{ \theta + \kappa_6 \text{div} \mathbf{p} \right\} \text{div} \mathbf{q} - \int_{\Omega} \psi \text{div} \mathbf{p} \\ &+ \kappa_5 \int_{\Omega} \nabla \theta \cdot \nabla \psi + \kappa_7 \int_{\Gamma_D} \theta \psi, \end{aligned} \quad (5.13)$$

and

$$\tilde{\mathbf{B}}_{\mathbf{w}}((\mathbf{p}, \theta), (\mathbf{q}, \psi)) := \kappa^{-1} \int_{\Omega} \theta \mathbf{w} \cdot \left\{ \mathbf{q} - \kappa_5 \nabla \psi \right\}, \quad (5.14)$$

for all  $(\underline{\mathbf{t}}, \mathbf{u}), (\underline{\mathbf{r}}, \mathbf{v}) \in \mathbb{H} \times \mathbf{H}_0^1(\Omega)$  and for all  $(\mathbf{p}, \theta), (\mathbf{q}, \psi) \in \mathbf{H}_{\Gamma_N}(\text{div}; \Omega) \times H^1(\Omega)$ . In turn,  $\mathbf{F}$  and  $\tilde{\mathbf{F}}$  are the bounded linear functionals given by

$$\mathbf{F}(\underline{\mathbf{r}}, \mathbf{v}) := \int_{\Omega} \mathbf{f} \cdot \left\{ \mathbf{v} - \kappa_2 \text{div} \boldsymbol{\tau} \right\}, \quad (5.15)$$

for all  $(\underline{\mathbf{r}}, \mathbf{v}) \in \mathbb{H} \times \mathbf{H}_0^1(\Omega)$  and

$$\tilde{\mathbf{F}}(\mathbf{q}, \psi) := \langle \mathbf{q} \cdot \mathbf{n}, \theta_D \rangle_{\Gamma_D} + \int_{\Omega} g \left\{ \psi - \kappa_6 \text{div} \mathbf{q} \right\} + \kappa_7 \int_{\Gamma_D} \theta_D \psi, \quad (5.16)$$

for all  $(\mathbf{q}, \psi) \in \mathbf{H}_{\Gamma_N}(\text{div}; \Omega) \times H^1(\Omega)$ . Notice that  $\kappa_i, i \in \{1, \dots, 7\}$ , are positive parameters to be specified next in Theorem 5.1. Indeed, the following result taken from [37] establishes the well-posedness of (5.11).

**Theorem 5.1.** *Assume that*

$$\kappa_1 \in \left( 0, \frac{2\delta_1 \mu_1}{\mu_2} \right), \quad \kappa_3 \in \left( 0, 2\delta_2 \left( \mu_1 - \frac{\kappa_1 \mu_2}{2\delta_1} \right) \right), \quad \kappa_4 \in \left( 0, 2\delta_3 \kappa_3 \left( 1 - \frac{\delta_2}{2} \right) \right), \quad \kappa_5 \in (0, 2\tilde{\delta}),$$

and  $\kappa_2, \kappa_6, \kappa_7 > 0$ , with  $\delta_1 \in \left( 0, \frac{2}{\mu_2} \right)$ ,  $\delta_2, \delta_3 \in (0, 2)$ , and  $\tilde{\delta} \in (0, 2\kappa)$ . Let

$$\mathcal{W} := \left\{ \phi \in H^1(\Omega) : \quad \|\phi\|_{1,\Omega} \leq c_{\mathcal{S}} \left\{ \|g\|_{0,\Omega} + \|\theta_D\|_{0,\Gamma_D} + \|\theta_D\|_{1/2,\Gamma_D} \right\} \right\},$$



and assume that the datum  $\mathbf{f}$  satisfy

$$c_{\mathbf{S}} \|\mathbf{f}\|_{0,\Omega} \leq \frac{\tilde{\alpha}(\Omega)}{2\kappa^{-1}(1 + \kappa_5^2)^{1/2} c(\Omega)}, \quad (5.17)$$

where  $c(\Omega)$  is the constant in [37, eq. (2.15)],  $\tilde{\alpha}(\Omega)$  is the ellipticity constant of the bilinear form  $\tilde{\mathbf{A}}$  (cf. [37, eq. (3.17)]), and  $c_{\mathbf{S}}$  and  $c_{\tilde{\mathbf{S}}}$  are the positive constants, independent of the data, provided by [37, Lemmas 3.1 and 3.2], respectively. Then the augmented fully-mixed problem (5.11) has at least one solution  $(\underline{\mathbf{t}}, \mathbf{u}, \mathbf{p}, \theta) \in \mathbb{H} \times \mathbf{H}_0^1(\Omega) \times \mathbf{H}_{\Gamma_N}(\text{div}; \Omega) \times H^1(\Omega)$  with  $\theta \in \mathcal{W}$ , and there holds

$$\|(\underline{\mathbf{t}}, \mathbf{u})\| \leq c_{\mathbf{S}} \|\mathbf{f}\|_{0,\Omega} \quad \text{and} \quad \|(\mathbf{p}, \theta)\| \leq c_{\tilde{\mathbf{S}}} \left\{ \|g\|_{0,\Omega} + \|\theta_D\|_{0,\Gamma_D} + \|\theta_D\|_{1/2,\Gamma_D} \right\}. \quad (5.18)$$

Moreover, if the data  $\mathbf{f}$ ,  $g$  and  $\theta_D$  are sufficiently small so that, with the constants  $C_{\mathbf{S}}$ ,  $C_{\tilde{\mathbf{S}}}$  and  $\hat{C}_{\mathbf{S}}$  from [37, Lemmas 3.4 and 3.5, and eq. (3.22)], respectively, and denoting by  $\tilde{C}_\delta$  the boundedness constant of the continuous injection of  $H^1(\Omega)$  into  $L^{n/\delta}(\Omega)$ , with  $\delta \in (0, 1)$  (when  $n = 2$ ) or  $\delta \in (1/2, 1)$  (when  $n = 3$ ), there holds

$$\tilde{C}_\delta \hat{C}_{\mathbf{S}} C_{\mathbf{S}} C_{\tilde{\mathbf{S}}} c_{\tilde{\mathbf{S}}} \left\{ \|g\|_{0,\Omega} + \|\theta_D\|_{0,\Gamma_D} + \|\theta_D\|_{1/2,\Gamma_D} \right\} \|\mathbf{f}\|_{\delta,\Omega} < 1. \quad (5.19)$$

Then the solution  $\theta$  is unique in  $\mathcal{W}$ .

*Proof.* See [37, Theorem 3.8] for details.  $\square$

### 5.2.3 The fully-mixed finite element method

Let  $\mathcal{T}_h$  be a regular triangulation of  $\Omega$  made up of triangles  $T$  (when  $n = 2$ ) or tetrahedra  $T$  (when  $n = 3$ ) of diameter  $h_T$ , and define the meshsize  $h := \max \{h_T : T \in \mathcal{T}_h\}$ . Then, given an integer  $k \geq 0$ , we set for each  $T \in \mathcal{T}_h$  the local Raviart–Thomas space of order  $k$  as

$$\mathbf{RT}_k(T) := \mathbf{P}_k(T) \oplus \mathbf{P}_k(T)\mathbf{x},$$

where  $\mathbf{x} := (x_1, \dots, x_n)^t$  is a generic vector of  $\mathbb{R}^n$ . Then, we introduce the finite element subspaces approximating the unknowns  $\mathbf{t}, \boldsymbol{\sigma}, \boldsymbol{\rho}, \mathbf{u}, \mathbf{p}$  and  $\theta$  as follows

$$\begin{aligned} \mathbb{H}_h^{\mathbf{t}} &:= \left\{ \mathbf{r}_h \in \mathbb{L}_{\text{tr}}^2(\Omega) : \quad \mathbf{r}_h|_T \in \mathbf{P}_k(T) \quad \forall T \in \mathcal{T}_h \right\}, \\ \mathbb{H}_h^{\boldsymbol{\sigma}} &:= \left\{ \boldsymbol{\tau}_h \in \mathbb{H}_0(\text{div}; \Omega) : \quad \mathbf{c}^t \boldsymbol{\tau}_h|_T \in \mathbf{RT}_k(T) \quad \forall \mathbf{c} \in \mathbb{R}^n \quad \forall T \in \mathcal{T}_h \right\}, \\ \mathbb{H}_h^{\boldsymbol{\rho}} &:= \left\{ \boldsymbol{\eta}_h \in \mathbb{L}_{\text{skew}}^2(\Omega) : \quad \boldsymbol{\eta}_h|_T \in \mathbf{P}_k(T) \quad \forall T \in \mathcal{T}_h \right\}, \\ \mathbf{H}_h^{\mathbf{u}} &:= \left\{ \mathbf{v}_h \in \mathbf{C}(\bar{\Omega}) : \quad \mathbf{v}_h|_T \in \mathbf{P}_{k+1}(T) \quad \forall T \in \mathcal{T}_h, \quad \mathbf{v}_h = 0 \text{ on } \Gamma \right\}, \\ \mathbf{H}_h^{\mathbf{p}} &:= \left\{ \mathbf{q}_h \in \mathbf{H}_{\Gamma_N}(\text{div}; \Omega) : \quad \mathbf{q}_h|_T \in \mathbf{RT}_k(T) \quad \forall T \in \mathcal{T}_h \right\}, \\ \mathbb{H}_h^{\theta} &:= \left\{ \psi_h \in C(\bar{\Omega}) : \quad \psi_h|_T \in \mathbf{P}_{k+1}(T) \quad \forall T \in \mathcal{T}_h \right\}. \end{aligned} \quad (5.20)$$

In this way, by defining  $\underline{\mathbf{t}}_h := (\mathbf{t}_h, \boldsymbol{\sigma}_h, \boldsymbol{\rho}_h)$ ,  $\underline{\mathbf{r}}_h := (\mathbf{r}_h, \boldsymbol{\tau}_h, \boldsymbol{\eta}_h) \in \mathbb{H}_h := \mathbb{H}_h^{\mathbf{t}} \times \mathbb{H}_h^{\boldsymbol{\sigma}} \times \mathbb{H}_h^{\boldsymbol{\rho}}$ , the Galerkin scheme of (5.11) reads: Find  $(\underline{\mathbf{t}}_h, \mathbf{u}_h, \mathbf{p}_h, \theta_h) \in \mathbb{H}_h \times \mathbf{H}_h^{\mathbf{u}} \times \mathbf{H}_h^{\mathbf{p}} \times \mathbf{H}_h^{\theta}$  such that

$$\begin{aligned} \mathbf{A}_{\theta_h}((\underline{\mathbf{t}}_h, \mathbf{u}_h), (\underline{\mathbf{r}}_h, \mathbf{v}_h)) &= \mathbf{F}(\underline{\mathbf{r}}_h, \mathbf{v}_h) \quad \forall (\underline{\mathbf{r}}_h, \mathbf{v}_h) \in \mathbb{H}_h \times \mathbf{H}_h^{\mathbf{u}}, \\ \tilde{\mathbf{A}}((\mathbf{p}_h, \theta_h), (\mathbf{q}_h, \psi_h)) + \tilde{\mathbf{B}}_{\mathbf{u}_h}((\mathbf{p}_h, \theta_h), (\mathbf{q}_h, \psi_h)) &= \tilde{\mathbf{F}}(\mathbf{q}_h, \psi_h) \quad \forall (\mathbf{q}_h, \psi_h) \in \mathbf{H}_h^{\mathbf{p}} \times \mathbf{H}_h^{\theta}. \end{aligned} \quad (5.21)$$

The following theorem, also taken from [37], provides the well-posedness of (5.21), the associated C ea estimate, and the corresponding theoretical rate of convergence.

**Theorem 5.2.** *Assume that the conditions on  $\kappa_i$ ,  $i \in \{1, \dots, 7\}$ , required by Theorem 5.1, hold. Let*

$$\mathcal{W}_h := \left\{ \phi_h \in \mathbf{H}_h^{\theta} : \|\phi_h\|_{1,\Omega} \leq c_{\mathbf{S}} \left\{ \|g\|_{0,\Omega} + \|\theta_D\|_{0,\Gamma_D} + \|\theta_D\|_{1/2,\Gamma_D} \right\} \right\},$$

and assume that the datum  $\mathbf{f}$  satisfy (5.17). Then the Galerkin scheme (5.21) has at least one solution  $(\underline{\mathbf{t}}_h, \mathbf{u}_h, \mathbf{p}_h, \theta_h) \in \mathbb{H}_h \times \mathbf{H}_h^{\mathbf{u}} \times \mathbf{H}_h^{\mathbf{p}} \times \mathbf{H}_h^{\theta}$  with  $\theta_h \in \mathcal{W}_h$ , and there holds

$$\|(\underline{\mathbf{t}}_h, \mathbf{u}_h)\| \leq c_{\mathbf{S}} \|\mathbf{f}\|_{0,\Omega} \quad \text{and} \quad \|(\mathbf{p}_h, \theta_h)\| \leq c_{\mathbf{S}} \left\{ \|g\|_{0,\Omega} + \|\theta_D\|_{0,\Gamma_D} + \|\theta_D\|_{1/2,\Gamma_D} \right\}. \quad (5.22)$$

In addition, there exists  $C_1 > 0$ , independent of  $h$ , such that

$$\|(\underline{\mathbf{t}}, \mathbf{u}, \mathbf{p}, \theta) - (\underline{\mathbf{t}}_h, \mathbf{u}_h, \mathbf{p}_h, \theta_h)\| \leq C_1 \left\{ \text{dist} \left( (\underline{\mathbf{t}}, \mathbf{u}), \mathbb{H}_h \times \mathbf{H}_h^{\mathbf{u}} \right) + \text{dist} \left( (\mathbf{p}, \theta), \mathbf{H}_h^{\mathbf{p}} \times \mathbf{H}_h^{\theta} \right) \right\}.$$

Assume further that there exists  $s > 0$  such that  $\mathbf{t} \in \mathbb{H}^s(\Omega)$ ,  $\boldsymbol{\sigma} \in \mathbb{H}^s(\Omega)$ ,  $\text{div } \boldsymbol{\sigma} \in \mathbf{H}^s(\Omega)$ ,  $\boldsymbol{\rho} \in \mathbb{H}^s(\Omega)$ ,  $\mathbf{u} \in \mathbf{H}^{s+1}(\Omega)$ ,  $\mathbf{p} \in \mathbf{H}^s(\Omega)$ ,  $\text{div } \mathbf{p} \in \mathbf{H}^s(\Omega)$ , and  $\theta \in \mathbf{H}^{s+1}(\Omega)$ , and that the finite element subspaces are defined by (5.20). Then, there exist  $C_2 > 0$ , independent of  $h$ , such that

$$\begin{aligned} \|(\underline{\mathbf{t}}, \mathbf{u}, \mathbf{p}, \theta) - (\underline{\mathbf{t}}_h, \mathbf{u}_h, \mathbf{p}_h, \theta_h)\| &\leq C_2 h^{\min\{s,k+1\}} \left\{ \|\mathbf{t}\|_{s,\Omega} + \|\boldsymbol{\sigma}\|_{s,\Omega} + \|\text{div } \boldsymbol{\sigma}\|_{s,\Omega} + \|\boldsymbol{\rho}\|_{s,\Omega} \right. \\ &\quad \left. + \|\mathbf{u}\|_{s+1,\Omega} + \|\mathbf{p}\|_{s,\Omega} + \|\text{div } \mathbf{p}\|_{s,\Omega} + \|\theta\|_{s+1,\Omega} \right\}. \end{aligned}$$

*Proof.* We refer the reader to [37, Theorems 4.7, 4.11, and 4.13] for details.  $\square$

## 5.3 A posteriori error analysis: the 2D-case

In this section we proceed analogously to [97, Section 3] and derive two reliable and efficient residual based a posteriori error estimators for the two-dimensional version of (5.21). The corresponding a posteriori error analysis for the 3D case, which follows from minor modifications of the one to be presented next, will be addressed in Section 5.4.

### 5.3.1 Preliminaries

We start by introducing a few useful notations for describing local information on elements and edges. Let  $\mathcal{E}_h$  be the set of all edges of  $\mathcal{T}_h$ , and  $\mathcal{E}(T)$  denotes the set of edges of a given  $T \in \mathcal{T}_h$ . Then  $\mathcal{E}_h = \mathcal{E}_h(\Omega) \cup \mathcal{E}_h(\Gamma_D) \cup \mathcal{E}_h(\Gamma_N)$ , where  $\mathcal{E}_h(\Omega) := \{e \in \mathcal{E}_h : e \subseteq \Omega\}$ ,  $\mathcal{E}_h(\Gamma_D) := \{e \in \mathcal{E}_h : e \subseteq \Gamma_D\}$ , and  $\mathcal{E}_h(\Gamma_N) := \{e \in \mathcal{E}_h : e \subseteq \Gamma_N\}$ . Moreover,  $h_e$  stands for the length of a given edge  $e$ . Also for each

edge  $e \in \mathcal{E}_h$  we fix a unit normal vector  $\mathbf{n}_e := (n_1, n_2)^t$ , and let  $\mathbf{s}_e := (-n_2, n_1)^t$  be the corresponding fixed unit tangential vector along  $e$ . However, when no confusion arises, we simply write  $\mathbf{n}$  and  $\mathbf{s}$  instead of  $\mathbf{n}_e$  and  $\mathbf{s}_e$ , respectively. Now, let  $\mathbf{v} \in \mathbf{L}^2(\Omega)$  such that  $\mathbf{v}|_T \in \mathbf{C}(T)$  on each  $T \in \mathcal{T}_h$ . Then, given  $T \in \mathcal{T}_h$  and  $e \in \mathcal{E}(T) \cap \mathcal{E}_h(\Omega)$ , we denote by  $\llbracket \mathbf{v} \cdot \mathbf{s} \rrbracket$  the tangential jump of  $\mathbf{v}$  across  $e$ , that is,  $\llbracket \mathbf{v} \cdot \mathbf{s} \rrbracket := (\mathbf{v}|_T - \mathbf{v}|_{T'})|_e \cdot \mathbf{s}$ , where  $T$  and  $T'$  are the triangles of  $\mathcal{T}_h$  having  $e$  as a common edge. Similar definitions hold for the tangential jumps of scalar and tensor fields  $\phi \in L^2(\Omega)$  and  $\boldsymbol{\tau} \in \mathbb{L}^2(\Omega)$ , respectively, such that  $\phi|_T \in C(T)$  and  $\boldsymbol{\tau}|_T \in \mathbb{C}(T)$  on each  $T \in \mathcal{T}_h$ . In addition, given scalar, vector and matrix valued fields  $\phi$ ,  $\mathbf{v} = (v_1, v_2)^t$  and  $\boldsymbol{\tau} = (\tau_{i,j})_{1 \leq i,j \leq 2}$ , respectively, we set

$$\begin{aligned} \mathbf{curl}(\phi) &:= \begin{pmatrix} \frac{\partial \phi}{\partial x_2} \\ -\frac{\partial \phi}{\partial x_1} \end{pmatrix}, \quad \underline{\mathbf{curl}}(\mathbf{v}) := \begin{pmatrix} \mathbf{curl}(v_1)^t \\ \mathbf{curl}(v_2)^t \end{pmatrix}, \\ \mathbf{rot}(\mathbf{v}) &= \frac{\partial v_2}{\partial x_1} - \frac{\partial v_1}{\partial x_2}, \quad \text{and} \quad \mathbf{rot}(\boldsymbol{\tau}) = \begin{pmatrix} \frac{\partial \tau_{12}}{\partial x_1} - \frac{\partial \tau_{11}}{\partial x_2}, \frac{\partial \tau_{22}}{\partial x_1} - \frac{\partial \tau_{21}}{\partial x_2} \end{pmatrix}^t, \end{aligned}$$

where the derivatives involved are taken in the distributional sense.

Let us now  $\Pi_h : \mathbf{H}^1(\Omega) \rightarrow \mathbf{H}_h^{\mathbf{P}}$  (cf. (5.20)) be the Raviart–Thomas interpolation operator, which, according to its characterisation properties (see, e.g., [81, Section 3.4.1]), verifies

$$\operatorname{div}(\Pi_h \mathbf{v}) = \mathcal{P}_h(\operatorname{div} \mathbf{v}) \quad \forall \mathbf{v} \in \mathbf{H}^1(\Omega), \quad (5.23)$$

where  $\mathcal{P}_h$  is the  $L^2(\Omega)$ -orthogonal projector onto the piecewise polynomials of degree  $\leq k$ . A tensor version of  $\Pi_h$ , say  $\mathbf{\Pi}_h : \mathbb{H}^1(\Omega) \rightarrow \mathbb{H}_h^\sigma$ , which is defined row-wise by  $\Pi_h$ , and a vector version of  $\mathcal{P}_h$ , say  $\mathbf{P}_h$ , which is the  $\mathbf{L}^2(\Omega)$ -orthogonal projector onto the piecewise polynomial vectors of degree  $\leq k$ , might also be required. The local approximation properties of  $\Pi_h$  (and hence of  $\mathbf{\Pi}_h$ ) are established in what follows. For the corresponding proof we refer to [81, Lemmas 3.16 and 3.18] (see also [19]).

**Lemma 5.3.** *There exist constants  $c_1, c_2 > 0$ , independent of  $h$ , such that for all  $\mathbf{v} \in \mathbf{H}^1(\Omega)$  there hold*

$$\|\mathbf{v} - \Pi_h \mathbf{v}\|_{0,T} \leq c_1 h_T \|\mathbf{v}\|_{1,T} \quad \forall T \in \mathcal{T}_h,$$

and

$$\|\mathbf{v} \cdot \mathbf{n} - \Pi_h \mathbf{v} \cdot \mathbf{n}\|_{0,e} \leq c_2 h_e^{1/2} \|\mathbf{v}\|_{1,T_e} \quad \forall e \in \mathcal{E}_h,$$

where  $T_e$  is a triangle of  $\mathcal{T}_h$  containing the edge  $e$  on its boundary.

In turn, let  $I_h : H^1(\Omega) \rightarrow H_h^1(\Omega)$  be the Cl  ment interpolation operator, where

$$H_h^1(\Omega) := \left\{ v \in C(\overline{\Omega}) : v|_T \in P_1(T) \quad \forall T \in \mathcal{T}_h \right\}.$$

The local approximation properties of this operator are established in the following lemma (see [49]).

**Lemma 5.4.** *There exist constants  $c_3, c_4 > 0$ , independent of  $h$ , such that for all  $v \in H^1(\Omega)$  there holds*

$$\|v - I_h v\|_{0,T} \leq c_3 h_T \|v\|_{1,\Delta(T)} \quad \forall T \in \mathcal{T}_h,$$

and

$$\|v - I_h v\|_{0,e} \leq c_4 h_e^{1/2} \|v\|_{1,\Delta(e)} \quad \forall e \in \mathcal{E}_h,$$

where

$$\Delta(T) := \cup \left\{ T' \in \mathcal{T}_h : T' \cap T \neq \emptyset \right\} \quad \text{and} \quad \Delta(e) := \cup \left\{ T' \in \mathcal{T}_h : T' \cap e \neq \emptyset \right\}.$$

In what follows, a vector version of  $I_h$ , say  $\mathbf{I}_h : \mathbf{H}^1(\Omega) \rightarrow \mathbf{H}_h^1(\Omega)$ , which is defined component-wise by  $I_h$ , will be needed as well. For the forthcoming analysis we will also utilise a couple of results providing stable Helmholtz decompositions for  $\mathbb{H}_0(\mathbf{div}; \Omega)$  and  $\mathbf{H}_{\Gamma_N}(\mathbf{div}; \Omega)$ . In this regard, we remark in advance that the decomposition for  $\mathbf{H}_{\Gamma_N}(\mathbf{div}; \Omega)$  will require the boundary  $\Gamma_N$  to lie in a “convex part” of  $\Omega$ , which means that there exists a convex domain containing  $\Omega$ , and whose boundary contains  $\Gamma_N$ . More precisely, we have the following lemma.

**Lemma 5.5.**

(a) For each  $\boldsymbol{\tau} \in \mathbb{H}_0(\mathbf{div}; \Omega)$  there exist  $\mathbf{z} \in \mathbf{H}^2(\Omega)$  and  $\boldsymbol{\varphi} \in \mathbf{H}^1(\Omega)$  such that

$$\boldsymbol{\tau} = \nabla \mathbf{z} + \mathbf{curl} \boldsymbol{\varphi} \quad \text{in } \Omega \quad \text{and} \quad \|\mathbf{z}\|_{2,\Omega} + \|\boldsymbol{\varphi}\|_{1,\Omega} \leq C \|\boldsymbol{\tau}\|_{\mathbf{div};\Omega}, \quad (5.24)$$

where  $C$  is a positive constant independent of all the foregoing variables.

(b) Assume that there exists a convex domain  $\Xi$  such that  $\bar{\Omega} \subseteq \Xi$  and  $\Gamma_N \subseteq \partial\Xi$ . Then, for each  $\mathbf{q} \in \mathbf{H}_{\Gamma_N}(\mathbf{div}; \Omega)$  there exist  $\boldsymbol{\zeta} \in \mathbf{H}^1(\Omega)$  and  $\chi \in H_{\Gamma_N}^1(\Omega)$  such that

$$\mathbf{q} = \boldsymbol{\zeta} + \mathbf{curl} \chi \quad \text{in } \Omega \quad \text{and} \quad \|\boldsymbol{\zeta}\|_{1,\Omega} + \|\chi\|_{1,\Omega} \leq C \|\mathbf{q}\|_{\mathbf{div};\Omega}, \quad (5.25)$$

where  $C$  is a positive constant independent of all the foregoing variables, and

$$H_{\Gamma_N}^1(\Omega) := \left\{ \eta \in H^1(\Omega) : \eta = 0 \quad \text{on } \Gamma_N \right\}.$$

*Proof.* For the proof of (a) we refer to [97, Lemma 3.7], whereas (b) follows from [3, Lemma 3.9]. We omit further details.  $\square$

### 5.3.2 The main result

In what follows we assume that the hypotheses of Theorems 5.1 and 5.2, hold and let  $(\mathbf{t}, \mathbf{u}, \mathbf{p}, \theta) \in \mathbb{H} \times \mathbf{H}_0^1(\Omega) \times \mathbf{H}_{\Gamma_N}(\mathbf{div}; \Omega) \times H^1(\Omega)$  and  $(\mathbf{t}_h, \mathbf{u}_h, \mathbf{p}_h, \theta_h) \in \mathbb{H}_h \times \mathbf{H}_h^{\mathbf{u}} \times \mathbf{H}_h^{\mathbf{p}} \times H_h^{\theta}$  be the unique solutions of problems (5.11) and (5.21), respectively. Then, we define for each  $T \in \mathcal{T}_h$  the local a posteriori error indicators

$$\begin{aligned} \tilde{\Theta}_{1,T}^2 := & \left\| \boldsymbol{\sigma}_h^d - \mu(\theta_h) \mathbf{t}_h \right\|_{0,T}^2 + \|\mathbf{f} + \mathbf{div} \boldsymbol{\sigma}_h\|_{0,T}^2 + \|\boldsymbol{\sigma}_h - \boldsymbol{\sigma}_h^t\|_{0,T}^2 \\ & + \|\mathbf{t}_h - \mathbf{e}(\mathbf{u}_h)\|_{0,T}^2 + \|\boldsymbol{\rho}_h - (\nabla \mathbf{u}_h - \mathbf{e}(\mathbf{u}_h))\|_{0,T}^2 + \|g + \mathbf{div} \mathbf{p}_h\|_{0,T}^2 \end{aligned} \quad (5.26)$$

$$\begin{aligned} & + \|\nabla \theta_h - (\kappa^{-1} \mathbf{p}_h + \kappa^{-1} \theta_h \mathbf{u}_h)\|_{0,T}^2 + \sum_{e \in \mathcal{E}(T) \cap \mathcal{E}_h(\Gamma_D)} \|\theta_D - \theta_h\|_{0,e}^2, \\ \Theta_{1,T}^2 := & \tilde{\Theta}_{1,T}^2 + \|\nabla \mathbf{u}_h - (\mathbf{t}_h + \boldsymbol{\rho}_h)\|_{0,T}^2, \end{aligned} \quad (5.27)$$

and

$$\begin{aligned} \Theta_{2,T}^2 := & \tilde{\Theta}_{1,T}^2 + \|\mathbf{f} - \mathbf{P}_h(\mathbf{f})\|_{0,T}^2 + \|g - \mathcal{P}_h(g)\|_{0,T}^2 + h_T^2 \|\nabla \mathbf{u}_h - (\mathbf{t}_h + \boldsymbol{\rho}_h)\|_{0,T}^2 \\ & + h_T^2 \|\mathbf{rot}(\mathbf{t}_h + \boldsymbol{\rho}_h)\|_{0,T}^2 + h_T^2 \|\mathbf{rot}(\kappa^{-1} \mathbf{p}_h + \kappa^{-1} \theta_h \mathbf{u}_h)\|_{0,T}^2 \\ & + \sum_{e \in \mathcal{E}(T)} h_e \|\llbracket (\mathbf{t}_h + \boldsymbol{\rho}_h) \mathbf{s} \rrbracket\|_{0,e}^2 + \sum_{e \in \mathcal{E}(T) \cap \mathcal{E}_h(\Omega)} h_e \|\llbracket (\kappa^{-1} \mathbf{p}_h + \kappa^{-1} \theta_h \mathbf{u}_h) \cdot \mathbf{s} \rrbracket\|_{0,e}^2 \\ & + \sum_{e \in \mathcal{E}(T) \cap \mathcal{E}_h(\Gamma_D)} h_e \left\| \frac{d\theta_D}{ds} - (\kappa^{-1} \mathbf{p}_h + \kappa^{-1} \theta_h \mathbf{u}_h) \cdot \mathbf{s} \right\|_{0,e}^2, \end{aligned} \quad (5.28)$$

so that the global a posteriori error estimators are given, respectively, by

$$\Theta_1 := \left\{ \sum_{T \in \mathcal{T}_h} \Theta_{1,T}^2 + \|\theta_D - \theta_h\|_{1/2, \Gamma_D}^2 \right\}^{1/2} \quad \text{and} \quad \Theta_2 := \left\{ \sum_{T \in \mathcal{T}_h} \Theta_{2,T}^2 \right\}^{1/2}. \quad (5.29)$$

Note that the last term defining  $\Theta_{2,T}$  (cf. (5.28)) requires that  $\frac{d\theta_D}{ds}\big|_e \in L^2(e)$  for each  $e \in \mathcal{E}_h(\Gamma_D)$ . This is ensured below by assuming that  $\theta_D \in H^1(\Gamma_D)$ .

The main goal of the present Section 5.3 is to establish, under suitable assumptions, the existence of positive constants  $C_{\text{rel}}, C_{\text{eff}}, \tilde{C}_{\text{rel}}$ , and  $\tilde{C}_{\text{eff}}$ , independent of the meshsizes and the continuous and discrete solutions, such that

$$C_{\text{eff}}\Theta_1 \leq \|(\mathbf{t}, \mathbf{u}, \mathbf{p}, \theta) - (\mathbf{t}_h, \mathbf{u}_h, \mathbf{p}_h, \theta_h)\| \leq C_{\text{rel}}\Theta_1, \quad (5.30)$$

and

$$\tilde{C}_{\text{eff}}\Theta_2 \leq \|(\mathbf{t}, \mathbf{u}, \mathbf{p}, \theta) - (\mathbf{t}_h, \mathbf{u}_h, \mathbf{p}_h, \theta_h)\| \leq \tilde{C}_{\text{rel}}\Theta_2. \quad (5.31)$$

The upper and lower bounds in (5.30) and (5.31), which are known as the reliability and efficiency of the estimators  $\Theta_1$  and  $\Theta_2$ , are derived below in Section 5.3.4 and 5.3.5, respectively, under the assumption that  $\theta_D$  is piecewise polynomials on the induced triangulation on  $\Gamma_D$ . Otherwise, higher order terms arising from polynomial approximations of these functions would appear in (5.30) and (5.31).

At this point we remark that for the derivation of the first a posteriori error estimator we will use the fact that  $\mathbf{u} \in \mathbf{H}_0^1(\Omega)$  and  $\theta \in H^1(\Omega)$ , so that we can integrate some terms by parts in the whole domain  $\Omega$ . In turn, for the second estimator we exploit the properties of the Helmholtz decompositions (cf. Lemma 5.5) jointly with the Clément and Raviart–Thomas operators, whence new terms capturing the jumps across the sides/edges of the triangulation appear.

### 5.3.3 A general a posteriori error estimate

In order to establish the reliability estimates of the a posteriori error estimators  $\Theta_1$  and  $\Theta_2$ , that is the upper bounds in (5.30) and (5.31), we first bound the unknowns related to the fluid and the heat by applying the uniform ellipticity of the bilinear forms of the continuous formulation, and then we conclude a preliminary upper bound for the total error by assuming that the data are small enough. More precisely, we begin with the following auxiliary result.

**Lemma 5.6.** *There exists  $C > 0$ , independent of  $h$ , such that*

$$\begin{aligned} \|(\mathbf{t}, \mathbf{u}) - (\mathbf{t}_h, \mathbf{u}_h)\| &\leq C \left\{ \left\| \boldsymbol{\sigma}_h^d - \mu(\theta_h)\mathbf{t}_h \right\|_{0,\Omega} + \|\mathbf{f} + \mathbf{div}\boldsymbol{\sigma}_h\|_{0,\Omega} + \|\boldsymbol{\sigma}_h - \boldsymbol{\sigma}_h^t\|_{0,\Omega} \right. \\ &\quad \left. + \|\mathbf{t}_h - \mathbf{e}(\mathbf{u}_h)\|_{0,\Omega} + \|\boldsymbol{\rho}_h - (\nabla\mathbf{u}_h - \mathbf{e}(\mathbf{u}_h))\|_{0,\Omega} + \|\mathcal{R}_f\|_{\mathbb{H}_0(\mathbf{div};\Omega)'} \right\} \\ &\quad + \frac{2}{\alpha(\Omega)} L_\mu (1 + \kappa_1^2)^{1/2} \hat{C}_S C_\delta \tilde{C}_\delta \|\mathbf{f}\|_{\delta,\Omega} \|\theta - \theta_h\|_{1,\Omega}, \end{aligned} \quad (5.32)$$

where  $\mathcal{R}_f : \mathbb{H}_0(\text{div}; \Omega) \rightarrow \mathbb{R}$  is the functional defined by

$$\begin{aligned} \mathcal{R}_f(\boldsymbol{\tau}) := & -\kappa_1 \int_{\Omega} \left\{ \boldsymbol{\sigma}_h^d - \mu(\theta_h) \mathbf{t}_h \right\} : \boldsymbol{\tau}^d - \kappa_2 \int_{\Omega} \left\{ \mathbf{f} + \text{div} \boldsymbol{\sigma}_h \right\} \cdot \text{div} \boldsymbol{\tau} \\ & - \int_{\Omega} (\mathbf{t}_h + \boldsymbol{\rho}_h) : \boldsymbol{\tau}^d - \int_{\Omega} \mathbf{u}_h \cdot \text{div} \boldsymbol{\tau}, \end{aligned} \quad (5.33)$$

which satisfies

$$\mathcal{R}_f(\boldsymbol{\tau}_h) = 0 \quad \forall \boldsymbol{\tau}_h \in \mathbb{H}_h^{\boldsymbol{\sigma}}. \quad (5.34)$$

*Proof.* According to [37, Lemma 3.1], we have that the bilinear form  $\mathbf{A}_{\theta}$  is uniformly elliptic on  $\mathbb{H} \times \mathbf{H}_0^1(\Omega)$  with a positive constant  $\alpha(\Omega)$ . This implies that

$$\alpha(\Omega) \|(\underline{\mathbf{t}}, \mathbf{u}) - (\underline{\mathbf{t}}_h, \mathbf{u}_h)\| \leq \sup_{\substack{(\underline{\mathbf{r}}, \mathbf{v}) \in \mathbb{H} \times \mathbf{H}_0^1(\Omega) \\ (\underline{\mathbf{r}}, \mathbf{v}) \neq \mathbf{0}}} \frac{\mathbf{A}_{\theta}((\underline{\mathbf{t}}, \mathbf{u}) - (\underline{\mathbf{t}}_h, \mathbf{u}_h), (\underline{\mathbf{r}}, \mathbf{v}))}{\|(\underline{\mathbf{r}}, \mathbf{v})\|}. \quad (5.35)$$

In turn, in order to estimate the right-hand side in (5.35), we first add and subtract suitable terms to write

$$\begin{aligned} & \mathbf{A}_{\theta}((\underline{\mathbf{t}}, \mathbf{u}) - (\underline{\mathbf{t}}_h, \mathbf{u}_h), (\underline{\mathbf{r}}, \mathbf{v})) \\ &= \mathbf{F}(\underline{\mathbf{r}}, \mathbf{v}) - \mathbf{A}_{\theta_h}((\underline{\mathbf{t}}_h, \mathbf{u}_h), (\underline{\mathbf{r}}, \mathbf{v})) - (\mathbf{A}_{\theta} - \mathbf{A}_{\theta_h})((\underline{\mathbf{t}}_h, \mathbf{u}_h), (\underline{\mathbf{r}}, \mathbf{v})), \end{aligned}$$

and then proceed similarly to [3, eq. (3.15)]. Indeed, from the definitions of  $\mathbf{A}_{\theta}$  and  $\mathbf{F}$  (cf. (5.12) and (5.15), respectively), and employing the Cauchy–Schwarz inequality, the estimate given by [37, eq. (3.24)] for  $|(\mathbf{A}_{\theta} - \mathbf{A}_{\theta_h})(\cdot, (\underline{\mathbf{r}}, \mathbf{v}))|$ , and the regularity assumption [37, eq. (3.22)], we deduce that

$$\begin{aligned} & \frac{|\mathbf{A}_{\theta}((\underline{\mathbf{t}}, \mathbf{u}) - (\underline{\mathbf{t}}_h, \mathbf{u}_h), (\underline{\mathbf{r}}, \mathbf{v}))|}{\|(\underline{\mathbf{r}}, \mathbf{v})\|} \leq C \left\{ \left\| \boldsymbol{\sigma}_h^d - \mu(\theta_h) \mathbf{t}_h \right\|_{0,\Omega} + \|\mathbf{f} + \text{div} \boldsymbol{\sigma}_h\|_{0,\Omega} \right. \\ & + \left\| \boldsymbol{\sigma}_h - \boldsymbol{\sigma}_h^t \right\|_{0,\Omega} + \|\mathbf{t}_h - \mathbf{e}(\mathbf{u}_h)\|_{0,\Omega} + \|\boldsymbol{\rho}_h - (\nabla \mathbf{u}_h - \mathbf{e}(\mathbf{u}_h))\|_{0,\Omega} + \|\mathcal{R}_f\|_{\mathbb{H}_0(\text{div}; \Omega)'} \Big\} \\ & + 2L_{\mu}(1 + \kappa_1^2)^{1/2} \widehat{C}_{\mathbf{S}} C_{\delta} \widetilde{C}_{\delta} \|\mathbf{f}\|_{\delta, \Omega} \|\theta - \theta_h\|_{1, \Omega}, \end{aligned} \quad (5.36)$$

where  $\widehat{C}_{\mathbf{S}}$ ,  $C_{\delta}$ , and  $\widetilde{C}_{\delta}$  are the constants provided by [37, eqs. (3.22), (3.25), and (3.32)], respectively. In this way, replacing the inequality (5.36) into (5.35), we get (5.32). Moreover, using the fact that

$$\mathbf{F}(\underline{\mathbf{r}}_h, \mathbf{v}_h) - \mathbf{A}_{\theta_h}((\underline{\mathbf{t}}_h, \mathbf{u}_h), (\underline{\mathbf{r}}_h, \mathbf{v}_h)) = 0 \quad \forall (\underline{\mathbf{r}}_h, \mathbf{v}_h) \in \mathbb{H}_h \times \mathbf{H}_h^{\mathbf{u}},$$

and taking in particular  $\underline{\mathbf{r}}_h = (\mathbf{0}, \boldsymbol{\tau}_h, \mathbf{0})$  and  $\mathbf{v}_h = \mathbf{0}$ , we get (5.34), which completes the proof.  $\square$

Next, we derive an analogous preliminary bound for the error associated to the heat variables.

**Lemma 5.7.** *There exists  $C > 0$ , independent of  $h$ , such that*

$$\begin{aligned} \|(\mathbf{p}, \theta) - (\mathbf{p}_h, \theta_h)\| &\leq C \left\{ \|g + \text{div} \mathbf{p}_h\|_{0,\Omega} + \|\nabla \theta_h - (\kappa^{-1} \mathbf{p}_h + \kappa^{-1} \theta_h \mathbf{u}_h)\|_{0,\Omega} \right. \\ &+ \left. \|\theta_D - \theta_h\|_{0, \Gamma_D} + \|\mathcal{R}_h\|_{\mathbf{H}_{\Gamma_N}(\text{div}; \Omega)'} \right\} + \frac{2}{\widetilde{\alpha}(\Omega)} \kappa^{-1} (1 + \kappa_5^2)^{1/2} c(\Omega) \|\theta_h\|_{1, \Omega} \|\mathbf{u} - \mathbf{u}_h\|_{1, \Omega}, \end{aligned} \quad (5.37)$$

where  $\mathcal{R}_h : \mathbf{H}_{\Gamma_N}(\text{div}; \Omega) \rightarrow \mathbb{R}$  is the functional defined by

$$\mathcal{R}_h(\mathbf{q}) := -\kappa_6 \int_{\Omega} \left\{ g + \text{div} \mathbf{p}_h \right\} \text{div} \mathbf{q} - \int_{\Omega} \left\{ \kappa^{-1} \mathbf{p}_h + \kappa^{-1} \theta_h \mathbf{u}_h \right\} \cdot \mathbf{q} - \int_{\Omega} \theta_h \text{div} \mathbf{q} + \langle \mathbf{q} \cdot \mathbf{n}, \theta_D \rangle_{\Gamma_D}, \quad (5.38)$$

which satisfies

$$\mathcal{R}_h(\mathbf{q}_h) = 0 \quad \forall \mathbf{q}_h \in \mathbf{H}_h^{\mathbf{P}}. \quad (5.39)$$

*Proof.* According to [37, Lemma 3.2] and using the fact that  $\|\mathbf{u}\|_{1,\Omega} \leq c_{\mathbf{S}}\|\mathbf{f}\|_{0,\Omega}$  (cf. (5.18)), we have that the bilinear form  $\tilde{\mathbf{A}} + \tilde{\mathbf{B}}_{\mathbf{u}}$  is uniformly elliptic on  $\mathbf{H}_{\Gamma_N}(\text{div}; \Omega) \times \mathbf{H}^1(\Omega)$  with a positive constant  $\tilde{\alpha}(\Omega)/2$ . This implies that

$$\frac{\tilde{\alpha}(\Omega)}{2} \|(\mathbf{p}, \theta) - (\mathbf{p}_h, \theta_h)\| \leq \sup_{\substack{(\mathbf{q}, \psi) \in \mathbf{H}_{\Gamma_N}(\text{div}; \Omega) \times \mathbf{H}^1(\Omega) \\ (\mathbf{q}, \psi) \neq \mathbf{0}}} \frac{(\tilde{\mathbf{A}} + \tilde{\mathbf{B}}_{\mathbf{u}})((\mathbf{p}, \theta) - (\mathbf{p}_h, \theta_h), (\mathbf{q}, \psi))}{\|(\mathbf{q}, \psi)\|}. \quad (5.40)$$

In turn, in order to estimate the right-hand side in (5.40), we add and subtract suitable terms to write

$$\begin{aligned} & (\tilde{\mathbf{A}} + \tilde{\mathbf{B}}_{\mathbf{u}})((\mathbf{p}, \theta) - (\mathbf{p}_h, \theta_h), (\mathbf{q}, \psi)) \\ &= \tilde{\mathbf{F}}(\mathbf{q}, \psi) - (\tilde{\mathbf{A}} + \tilde{\mathbf{B}}_{\mathbf{u}_h})((\mathbf{p}_h, \theta_h), (\mathbf{q}, \psi)) - \tilde{\mathbf{B}}_{\mathbf{u}-\mathbf{u}_h}((\mathbf{p}_h, \theta_h), (\mathbf{q}, \psi)), \end{aligned}$$

whence, using the definitions of  $\tilde{\mathbf{A}}$ ,  $\tilde{\mathbf{B}}_{\mathbf{w}}$ , and  $\tilde{\mathbf{F}}$  (cf. (5.13), (5.14), and (5.16), respectively), the continuity of  $\tilde{\mathbf{B}}_{\mathbf{u}-\mathbf{u}_h}$  (see [37, eq. (3.16)]), and the Cauchy–Schwarz inequality, we find that

$$\begin{aligned} & \left| \frac{(\tilde{\mathbf{A}} + \tilde{\mathbf{B}}_{\mathbf{u}})((\mathbf{p}, \theta) - (\mathbf{p}_h, \theta_h), (\mathbf{q}, \psi))}{\|(\mathbf{q}, \psi)\|} \right| \leq C \left\{ \|g + \text{div } \mathbf{p}_h\|_{0,\Omega} + \|\nabla \theta_h - (\kappa^{-1} \mathbf{p}_h + \kappa^{-1} \theta_h \mathbf{u}_h)\|_{0,\Omega} \right. \\ & \left. + \|\theta_D - \theta_h\|_{0,\Gamma_D} + \|\mathcal{R}_h\|_{\mathbf{H}_{\Gamma_N}(\text{div}; \Omega)'} \right\} + \kappa^{-1} (1 + \kappa_5^2)^{1/2} c(\Omega) \|\theta_h\|_{1,\Omega} \|\mathbf{u} - \mathbf{u}_h\|_{1,\Omega}, \end{aligned} \quad (5.41)$$

where  $c(\Omega)$  is the constant in [37, eq. (2.15)]. Then, replacing the inequality (5.41) into (5.40), we obtain (5.37). Finally, using the fact that

$$\tilde{\mathbf{F}}(\mathbf{q}_h, \psi_h) - (\tilde{\mathbf{A}} + \tilde{\mathbf{B}}_{\mathbf{u}_h})((\mathbf{p}_h, \theta_h), (\mathbf{q}_h, \psi_h)) = 0 \quad \forall (\mathbf{q}_h, \psi_h) \in \mathbf{H}_h^{\mathbf{P}} \times \mathbf{H}_h^{\theta},$$

and taking in particular  $\psi_h = 0$ , we arrive at (5.39), which completes the proof.  $\square$

We now combine the inequalities provided by Lemmas 5.6 and 5.7 to derive a preliminary upper bound for the total error  $\|(\mathbf{t}, \mathbf{u}, \mathbf{p}, \theta) - (\mathbf{t}_h, \mathbf{u}_h, \mathbf{p}_h, \theta_h)\|$ . Indeed, by gathering together the estimates (5.32) and (5.37), and noting the fact that  $\theta_h \in \mathcal{W}_h$ , it follows that

$$\begin{aligned} & \|(\mathbf{t}, \mathbf{u}, \mathbf{p}, \theta) - (\mathbf{t}_h, \mathbf{u}_h, \mathbf{p}_h, \theta_h)\| \leq \mathbf{C}(\mathbf{f}, g, \theta_D) \|(\mathbf{t}, \mathbf{u}, \mathbf{p}, \theta) - (\mathbf{t}_h, \mathbf{u}_h, \mathbf{p}_h, \theta_h)\| \\ & + C \left\{ \left\| \boldsymbol{\sigma}_h^d - \mu(\theta_h) \mathbf{t}_h \right\|_{0,\Omega} + \|\mathbf{f} + \text{div } \boldsymbol{\sigma}_h\|_{0,\Omega} + \|\boldsymbol{\sigma}_h - \boldsymbol{\sigma}_h^t\|_{0,\Omega} + \|\mathbf{t}_h - \mathbf{e}(\mathbf{u}_h)\|_{0,\Omega} \right. \\ & + \|\boldsymbol{\rho}_h - (\nabla \mathbf{u}_h - \mathbf{e}(\mathbf{u}_h))\|_{0,\Omega} + \|g + \text{div } \mathbf{p}_h\|_{0,\Omega} + \|\nabla \theta_h - (\kappa^{-1} \mathbf{p}_h + \kappa^{-1} \theta_h \mathbf{u}_h)\|_{0,\Omega} \\ & \left. + \|\theta_D - \theta_h\|_{0,\Gamma_D} + \|\mathcal{R}_f\|_{\mathbb{H}_0(\text{div}; \Omega)'} + \|\mathcal{R}_h\|_{\mathbf{H}_{\Gamma_N}(\text{div}; \Omega)'} \right\}, \end{aligned} \quad (5.42)$$

where

$$\mathbf{C}(\mathbf{f}, g, \theta_D) := \max \left\{ \mathbf{C}_1(\mathbf{f}, g, \theta_D), \mathbf{C}_2(\mathbf{f}, g, \theta_D) \right\},$$

with

$$\mathbf{C}_1(\mathbf{f}, g, \theta_D) := \frac{2}{\tilde{\alpha}(\Omega)} \kappa^{-1} (1 + \kappa_5^2)^{1/2} c(\Omega) c_{\mathbf{S}} \left\{ \|g\|_{0,\Omega} + \|\theta_D\|_{0,\Gamma_D} + \|\theta_D\|_{1/2,\Gamma_D} \right\}$$

and

$$\mathbf{C}_2(\mathbf{f}, g, \theta_D) := \frac{2}{\alpha(\Omega)} L_\mu (1 + \kappa_1^2)^{1/2} \widehat{C}_S C_\delta \widetilde{C}_\delta \|\mathbf{f}\|_{\delta, \Omega}.$$

Consequently, we can establish the following preliminary upper bound for the total error.

**Lemma 5.8.** *Assume that the data  $\mathbf{f}, g$  and  $\theta_D$  satisfy:*

$$\mathbf{C}_i(\mathbf{f}, g, \theta_D) \leq \frac{1}{2} \quad \forall i \in \{1, 2\}. \quad (5.43)$$

*Then, there exists  $C > 0$ , depending only on parameters, data and other constants, all of them independent of  $h$ , such that*

$$\begin{aligned} \|(\underline{\mathbf{t}}, \mathbf{u}, \mathbf{p}, \theta) - (\underline{\mathbf{t}}_h, \mathbf{u}_h, \mathbf{p}_h, \theta_h)\| &\leq C \left\{ \left\| \boldsymbol{\sigma}_h^d - \mu(\theta_h) \mathbf{t}_h \right\|_{0, \Omega} + \|\mathbf{f} + \mathbf{div} \boldsymbol{\sigma}_h\|_{0, \Omega} \right. \\ &+ \left\| \boldsymbol{\sigma}_h - \boldsymbol{\sigma}_h^t \right\|_{0, \Omega} + \|\mathbf{t}_h - \mathbf{e}(\mathbf{u}_h)\|_{0, \Omega} + \|\boldsymbol{\rho}_h - (\nabla \mathbf{u}_h - \mathbf{e}(\mathbf{u}_h))\|_{0, \Omega} + \|g + \mathbf{div} \mathbf{p}_h\|_{0, \Omega} \\ &\left. + \left\| \nabla \theta_h - (\kappa^{-1} \mathbf{p}_h + \kappa^{-1} \theta_h \mathbf{u}_h) \right\|_{0, \Omega} + \|\theta_D - \theta_h\|_{0, \Gamma_D} + \|\mathcal{R}_f\|_{\mathbb{H}_0(\mathbf{div}; \Omega)'} + \|\mathcal{R}_h\|_{\mathbf{H}_{\Gamma_N}(\mathbf{div}; \Omega)'} \right\}. \end{aligned} \quad (5.44)$$

*Proof.* It follows from a direct application of the assumption (5.43) in the inequality (5.42).  $\square$

We end this section with equivalent definitions of the functionals  $\mathcal{R}_f$  and  $\mathcal{R}_h$ . In fact, noting that  $\mathbf{t}_h : \mathbb{I} = \text{tr } \mathbf{t}_h = 0$  and  $\boldsymbol{\rho}_h : \mathbb{I} = 0$ , we first observe that

$$\int_{\Omega} (\mathbf{t}_h + \boldsymbol{\rho}_h) : \boldsymbol{\tau}^d = \int_{\Omega} (\mathbf{t}_h + \boldsymbol{\rho}_h)^d : \boldsymbol{\tau} = \int_{\Omega} (\mathbf{t}_h + \boldsymbol{\rho}_h) : \boldsymbol{\tau}.$$

In this way, given  $\boldsymbol{\tau} \in \mathbb{H}_0(\mathbf{div}; \Omega)$ , we integrate by parts the expression  $\int_{\Omega} \mathbf{u}_h \cdot \mathbf{div} \boldsymbol{\tau}$  and use the homogeneous Dirichlet boundary condition on  $\Gamma$  of  $\mathbf{u}_h \in \mathbf{H}_h^u$  (cf. (5.20)), to find that

$$\mathcal{R}_f(\boldsymbol{\tau}) = -\kappa_1 \int_{\Omega} \left\{ \boldsymbol{\sigma}_h^d - \mu(\theta_h) \mathbf{t}_h \right\} : \boldsymbol{\tau} - \kappa_2 \int_{\Omega} \left\{ \mathbf{f} + \mathbf{div} \boldsymbol{\sigma}_h \right\} \cdot \mathbf{div} \boldsymbol{\tau} + \int_{\Omega} \left\{ \nabla \mathbf{u}_h - (\mathbf{t}_h + \boldsymbol{\rho}_h) \right\} : \boldsymbol{\tau}. \quad (5.45)$$

Analogously, given  $\mathbf{q} \in \mathbf{H}_{\Gamma_N}(\mathbf{div}; \Omega)$ , we integrate by parts the expression  $\int_{\Omega} \theta_h \mathbf{div} \mathbf{q}$  and use now the homogeneous Neumann boundary condition of  $\mathbf{q}$  on  $\Gamma_N$ , to arrive at

$$\mathcal{R}_h(\mathbf{q}) = -\kappa_6 \int_{\Omega} \left\{ g + \mathbf{div} \mathbf{p}_h \right\} \mathbf{div} \mathbf{q} + \int_{\Omega} \left\{ \nabla \theta_h - (\kappa^{-1} \mathbf{p}_h + \kappa^{-1} \theta_h \mathbf{u}_h) \right\} \cdot \mathbf{q} + \langle \mathbf{q} \cdot \mathbf{n}, \theta_D - \theta_h \rangle_{\Gamma_D}. \quad (5.46)$$

### 5.3.4 Reliability of the a posteriori error estimators

We now proceed to bound the norms of the functionals  $\mathcal{R}_f$  and  $\mathcal{R}_h$  appearing on the right-hand side of (5.44), by conveniently considering either their original definitions or the new expressions (5.45) and (5.46), respectively. This task is actually performed in two different ways, which leads to the reliability of the a posteriori error estimators  $\Theta_1$  and  $\Theta_2$ . We begin with  $\Theta_1$ .

**Theorem 5.9.** *Assume that the data  $\mathbf{f}, g$  and  $\theta_D$  satisfy (5.43). Then there exist  $C_{\text{rel}} > 0$ , independent of  $h$ , such that*

$$\|(\underline{\mathbf{t}}, \mathbf{u}, \mathbf{p}, \theta) - (\underline{\mathbf{t}}_h, \mathbf{u}_h, \mathbf{p}_h, \theta_h)\| \leq C_{\text{rel}} \Theta_1. \quad (5.47)$$



*Proof.* We first observe that, employing Cauchy–Schwarz inequality and recalling that  $\langle \cdot, \cdot \rangle_{\Gamma_D}$  stands for the duality pairing between  $\mathbf{H}^{-1/2}(\Gamma_D)$  and  $\mathbf{H}^{1/2}(\Gamma_D)$ , we deduce from (5.45) and (5.46) that

$$\|\mathcal{R}_f\|_{\mathbb{H}_0(\mathbf{div};\Omega)'} \leq c_1 \left\{ \left\| \boldsymbol{\sigma}_h^d - \mu(\theta_h) \mathbf{t}_h \right\|_{0,\Omega} + \|\mathbf{f} + \mathbf{div} \boldsymbol{\sigma}_h\|_{0,\Omega} + \|\nabla \mathbf{u}_h - (\mathbf{t}_h + \boldsymbol{\rho}_h)\|_{0,\Omega} \right\} \quad (5.48)$$

and

$$\|\mathcal{R}_h\|_{\mathbf{H}_{\Gamma_N}(\mathbf{div};\Omega)'} \leq c_2 \left\{ \|g + \mathbf{div} \mathbf{p}_h\|_{0,\Omega} + \|\nabla \theta_h - (\kappa^{-1} \mathbf{p}_h + \kappa^{-1} \theta_h \mathbf{u}_h)\|_{0,\Omega} + \|\theta_D - \theta_h\|_{1/2,\Gamma_D} \right\}, \quad (5.49)$$

respectively. In this way, the proof follows straightforwardly from the definition of  $\Theta_1$  (cf. (5.27)), Lemma 5.8, and inequalities (5.48) and (5.49).  $\square$

Having proved Theorem 5.9, we now aim to establish the reliability of  $\Theta_2$  (cf. (5.28)), which is accomplished by applying the Helmholtz decompositions provided by Lemma 5.5 to bound  $\|\mathcal{R}_f\|_{\mathbb{H}_0(\mathbf{div};\Omega)'}$  and  $\|\mathcal{R}_h\|_{\mathbf{H}_{\Gamma_N}(\mathbf{div};\Omega)'}$ . Actually, in what follows we provide the details only for  $\mathcal{R}_f$  since those for  $\mathcal{R}_h$  follow analogously. In fact, given  $\boldsymbol{\tau} \in \mathbb{H}_0(\mathbf{div};\Omega)$ , and thanks to part (a) of Lemma 5.5, we first let  $\mathbf{z} \in \mathbf{H}^2(\Omega)$  and  $\boldsymbol{\varphi} \in \mathbf{H}^1(\Omega)$  be such that  $\boldsymbol{\tau} = \nabla \mathbf{z} + \mathbf{curl} \boldsymbol{\varphi}$  in  $\Omega$ , and

$$\|\mathbf{z}\|_{2,\Omega} + \|\boldsymbol{\varphi}\|_{1,\Omega} \leq C \|\boldsymbol{\tau}\|_{\mathbf{div};\Omega}, \quad (5.50)$$

and then define  $\boldsymbol{\tau}_h := \boldsymbol{\Pi}_h(\nabla \mathbf{z}) + \mathbf{curl}(\mathbf{I}_h \boldsymbol{\varphi}) + c\mathbb{I}$ , where  $c \in \mathbb{R}$  is chosen so that  $\boldsymbol{\tau}_h$  belongs to  $\mathbb{H}_h^\sigma$  (cf. Section 5.3.1). Hence, employing from (5.34) that  $\mathcal{R}_f(\boldsymbol{\tau}_h) = 0$ , it readily follows from the foregoing expressions that  $\mathcal{R}_f(\boldsymbol{\tau})$  can be decomposed as

$$\mathcal{R}_f(\boldsymbol{\tau}) = \mathcal{R}_f(\boldsymbol{\tau} - \boldsymbol{\tau}_h) = \mathcal{R}_f(\nabla \mathbf{z} - \boldsymbol{\Pi}_h(\nabla \mathbf{z})) + \mathcal{R}_f(\mathbf{curl}(\boldsymbol{\varphi} - \mathbf{I}_h \boldsymbol{\varphi})). \quad (5.51)$$

Consequently, we now require to bound the terms on the right-hand side of (5.51), which is done in the following two lemmas.

**Lemma 5.10.** *There exists  $C > 0$ , independent of  $h$ , such that for each  $\mathbf{z} \in \mathbf{H}^2(\Omega)$  there holds*

$$\left| \mathcal{R}_f(\nabla \mathbf{z} - \boldsymbol{\Pi}_h(\nabla \mathbf{z})) \right| \leq C \left\{ \sum_{T \in \mathcal{T}_h} \tilde{\Theta}_{f,T}^2 \right\}^{1/2} \|\mathbf{z}\|_{2,\Omega},$$

where

$$\tilde{\Theta}_{f,T}^2 = h_T^2 \left\| \boldsymbol{\sigma}_h^d - \mu(\theta_h) \mathbf{t}_h \right\|_{0,T}^2 + \|\mathbf{f} - \mathbf{P}_h(\mathbf{f})\|_{0,T}^2 + h_T^2 \|\nabla \mathbf{u}_h - (\mathbf{t}_h + \boldsymbol{\rho}_h)\|_{0,T}^2. \quad (5.52)$$

*Proof.* Using the alternative definition of the functional  $\mathcal{R}_f$  (cf. (5.45)), the proof follows from a slight modification of that of [97, Lemma 3.10]. We omit further details.  $\square$

**Lemma 5.11.** *There exists  $C > 0$ , independent of  $h$ , such that for each  $\boldsymbol{\varphi} \in \mathbf{H}^1(\Omega)$  there holds*

$$\left| \mathcal{R}_f(\mathbf{curl}(\boldsymbol{\varphi} - \mathbf{I}_h \boldsymbol{\varphi})) \right| \leq C \left\{ \sum_{T \in \mathcal{T}_h} \hat{\Theta}_{f,T}^2 \right\}^{1/2} \|\boldsymbol{\varphi}\|_{1,\Omega},$$

where

$$\hat{\Theta}_{f,T}^2 = \left\| \boldsymbol{\sigma}_h^d - \mu(\theta_h) \mathbf{t}_h \right\|_{0,T}^2 + h_T^2 \|\mathbf{rot}(\mathbf{t}_h + \boldsymbol{\rho}_h)\|_{0,T}^2 + \sum_{e \in \mathcal{E}(T)} h_e \|\llbracket (\mathbf{t}_h + \boldsymbol{\rho}_h) \mathbf{s} \rrbracket\|_{0,e}^2. \quad (5.53)$$

*Proof.* Given  $\varphi \in \mathbf{H}^1(\Omega)$ , we first notice from the original definition (5.33) of  $\mathcal{R}_f$  that there holds

$$\mathcal{R}_f(\underline{\mathbf{curl}}(\varphi - \mathbf{I}_h\varphi)) = -\kappa_1 \int_{\Omega} \left\{ \boldsymbol{\sigma}_h^d - \mu(\theta_h)\mathbf{t}_h \right\} : \underline{\mathbf{curl}}(\varphi - \mathbf{I}_h\varphi) - \int_{\Omega} (\mathbf{t}_h + \boldsymbol{\rho}_h) : \underline{\mathbf{curl}}(\varphi - \mathbf{I}_h\varphi). \quad (5.54)$$

Then, for estimating the first term on the right-hand side of (5.54) we proceed as in the proof of [97, Lemma 3.9] and apply the boundedness of  $\mathbf{I}_h : \mathbf{H}^1(\Omega) \rightarrow \mathbf{H}^1(\Omega)$  ([69, Lemma 1.127, pag. 69]), as well as the Cauchy–Schwarz and triangle inequalities, to obtain

$$\left| \kappa_1 \int_{\Omega} \left\{ \boldsymbol{\sigma}_h^d - \mu(\theta_h)\mathbf{t}_h \right\} : \underline{\mathbf{curl}}(\varphi - \mathbf{I}_h\varphi) \right| \leq C \left\{ \sum_{T \in \mathcal{T}_h} \left\| \boldsymbol{\sigma}_h^d - \mu(\theta_h)\mathbf{t}_h \right\|_{0,T}^2 \right\}^{1/2} \|\varphi\|_{1,\Omega}. \quad (5.55)$$

Next, analogously to the proof of [97, Lemma 3.9], we decompose the second term on the right-hand side of (5.54) according to the triangulation  $\mathcal{T}_h$ , and integrate by parts on each  $T \in \mathcal{T}_h$  to obtain

$$\int_{\Omega} (\mathbf{t}_h + \boldsymbol{\rho}_h) : \underline{\mathbf{curl}}(\varphi - \mathbf{I}_h\varphi) = \sum_{T \in \mathcal{T}_h} \int_T \mathbf{rot}(\mathbf{t}_h + \boldsymbol{\rho}_h) \cdot (\varphi - \mathbf{I}_h\varphi) - \sum_{e \in \mathcal{E}_h} \int_e [(\mathbf{t}_h + \boldsymbol{\rho}_h)\mathbf{s}] \cdot (\varphi - \mathbf{I}_h\varphi).$$

In this way, applying the Cauchy–Schwarz inequality, the approximation properties of the Clément interpolator  $\mathbf{I}_h$  (cf. Lemma 5.4), and the fact that the number of triangles of the macro-elements  $\Delta(T)$  and  $\Delta(e)$  are uniformly bounded, we deduce that

$$\begin{aligned} & \left| \int_{\Omega} (\mathbf{t}_h + \boldsymbol{\rho}_h) : \underline{\mathbf{curl}}(\varphi - \mathbf{I}_h\varphi) \right| \\ & \leq C \sum_{T \in \mathcal{T}_h} \left\{ h_T^2 \|\mathbf{rot}(\mathbf{t}_h + \boldsymbol{\rho}_h)\|_{0,T}^2 + \sum_{e \in \mathcal{E}(T)} h_e \|[(\mathbf{t}_h + \boldsymbol{\rho}_h)\mathbf{s}]\|_{0,e}^2 \right\}^{1/2} \|\varphi\|_{1,\Omega}. \end{aligned} \quad (5.56)$$

Finally, by replacing the inequalities (5.55) and (5.56) into (5.54) we conclude the proof.  $\square$

As a direct consequence of Lemmas 5.10 and 5.11, and the stability estimate (5.50) for the Helmholtz decomposition, we obtain the following upper bound for  $\|\mathcal{R}_f\|_{\mathbb{H}_0(\mathbf{div};\Omega)'}.$

**Lemma 5.12.** *There exists  $C > 0$ , independent of  $h$ , such that*

$$\|\mathcal{R}_f\|_{\mathbb{H}_0(\mathbf{div};\Omega)'} \leq C \left\{ \sum_{T \in \mathcal{T}_h} \Theta_{f,T}^2 \right\}^{1/2},$$

where

$$\begin{aligned} \Theta_{f,T}^2 := & \left\| \boldsymbol{\sigma}_h^d - \mu(\theta_h)\mathbf{t}_h \right\|_{0,T}^2 + \|\mathbf{f} - \mathbf{P}_h(\mathbf{f})\|_{0,T}^2 + h_T^2 \|\nabla \mathbf{u}_h - (\mathbf{t}_h + \boldsymbol{\rho}_h)\|_{0,T}^2 \\ & + h_T^2 \|\mathbf{rot}(\mathbf{t}_h + \boldsymbol{\rho}_h)\|_{0,T}^2 + \sum_{e \in \mathcal{E}(T)} h_e \|[(\mathbf{t}_h + \boldsymbol{\rho}_h)\mathbf{s}]\|_{0,e}^2. \end{aligned} \quad (5.57)$$

*Proof.* It suffices to see that the first term defining  $\tilde{\Theta}_{f,T}^2$  (cf. (5.52) in Lemma 5.10) is dominated by the first term of  $\hat{\Theta}_{f,T}^2$  (cf. (5.53) in Lemma 5.11), which explains the subtraction of the former in the original definition of  $\Theta_{f,T}^2$ .  $\square$

Finally, the corresponding estimate for  $\mathcal{R}_h$  is given by the following lemma.

**Lemma 5.13.** *Assume that there exists a convex domain  $\Xi$  such that  $\bar{\Omega} \subseteq \Xi$  and  $\Gamma_N \subseteq \partial\Xi$ . Assume further that  $\theta_D \in H^1(\Gamma_D)$ . Then there exists  $C > 0$ , independent of  $h$ , such that*

$$\|\mathcal{R}_h\|_{\mathbf{H}_{\Gamma_N}(\text{div}; \Omega)'} \leq C \left\{ \sum_{T \in \mathcal{T}_h} \Theta_{h,T}^2 \right\},$$

where

$$\begin{aligned} \Theta_{h,T}^2 := & \|g - \mathcal{P}_h(g)\|_{0,T}^2 + h_T^2 \|\nabla \theta_h - (\kappa^{-1} \mathbf{p}_h + \kappa^{-1} \theta_h \mathbf{u}_h)\|_{0,T}^2 \\ & + h_T^2 \|\text{rot}(\kappa^{-1} \mathbf{p}_h + \kappa^{-1} \theta_h \mathbf{u}_h)\|_{0,T}^2 + \sum_{e \in \mathcal{E}(T) \cap \mathcal{E}_h(\Omega)} h_e \left\| [(\kappa^{-1} \mathbf{p}_h + \kappa^{-1} \theta_h \mathbf{u}_h) \cdot \mathbf{s}] \right\|_{0,e}^2 \\ & + \sum_{e \in \mathcal{E}(T) \cap \mathcal{E}_h(\Gamma_D)} h_e \left\{ \left\| \frac{d\theta_D}{ds} - (\kappa^{-1} \mathbf{p}_h + \kappa^{-1} \theta_h \mathbf{u}_h) \cdot \mathbf{s} \right\|_{0,e}^2 + \|\theta_D - \theta_h\|_{0,e}^2 \right\}. \end{aligned} \quad (5.58)$$

*Proof.* The result follows analogously to the proof of Lemma 5.12 (see also [53, Lemma 3.8]), taking into account now the Helmholtz decomposition provided by part (b) of Lemma 5.5 and the fact that  $\mathcal{R}_h(\mathbf{q}_h) = 0 \quad \forall \mathbf{q}_h \in \mathbf{H}_h^P$  (cf. (5.39)). In particular, using the alternative definition of  $\mathcal{R}_h$  (cf. (5.46)) and proceeding similarly to Lemma 5.10, we find the first, second and last term of the local estimator (5.58). On the other hand, considering the original definition (5.38) of  $\mathcal{R}_h$ , noting that  $\frac{d\theta_D}{ds} \in L^2(\Gamma_D)$ , applying the integration by parts formula on  $\Gamma_D$  given by (cf. [67, Lemma 3.5, eq. (3.34)])

$$\langle \text{curl } \chi \cdot \mathbf{n}, \theta_D \rangle_{\Gamma_D} = - \left\langle \frac{d\theta_D}{ds}, \chi \right\rangle_{\Gamma_D} \quad \forall \chi \in H^1(\Omega), \quad (5.59)$$

and proceeding analogously to Lemma 5.11 (see also [53, Lemma 3.7]), we obtain the remaining terms of (5.58). Further details are omitted.  $\square$

The reliability estimate for  $\Theta_2$  is stated now.

**Theorem 5.14.** *Assume that the data  $\mathbf{f}, g$  and  $\theta_D$  satisfy (5.43). Assume further that  $\theta_D \in H^1(\Gamma_D)$ . Then there exist  $\tilde{C}_{\text{rel}} > 0$ , independent of  $h$ , such that*

$$\|(\underline{\mathbf{t}}, \mathbf{u}, \mathbf{p}, \theta) - (\underline{\mathbf{t}}_h, \mathbf{u}_h, \mathbf{p}_h, \theta_h)\| \leq \tilde{C}_{\text{rel}} \Theta_2. \quad (5.60)$$

*Proof.* It is a straightforward consequence of the definition of  $\Theta_2$  (cf. (5.28)), Lemmas 5.8, 5.12, and 5.13, and the fact that the terms  $h_T^2 \|\nabla \theta_h - (\kappa^{-1} \mathbf{p}_h + \kappa^{-1} \theta_h \mathbf{u}_h)\|_{0,T}^2$  and  $h_e \|\theta_D - \theta_h\|_{0,e}^2$ , which form part of  $\Theta_{h,T}^2$  (cf. (5.58)), are dominated by  $\|\nabla \theta_h - (\kappa^{-1} \mathbf{p}_h + \kappa^{-1} \theta_h \mathbf{u}_h)\|_{0,T}^2$  and  $\|\theta_D - \theta_h\|_{0,e}^2$ , respectively.  $\square$

### 5.3.5 Efficiency of the a posteriori error estimators

We now aim to establish the lower bounds in (5.30) and (5.31). For this purpose, we will make extensive use of the original system of equations given by (5.8), which is recovered from the augmented-mixed continuous formulation (5.11) by choosing suitable test functions and then integrating by parts backwardly the corresponding equations.

We begin with the efficiency estimate for  $\Theta_1$ .

**Theorem 5.15.** *There exists  $C_{\text{eff}} > 0$ , independent of  $h$ , such that*

$$C_{\text{eff}}\Theta_1 \leq \|(\mathbf{t}, \mathbf{u}, \mathbf{p}, \theta) - (\mathbf{t}_h, \mathbf{u}_h, \mathbf{p}_h, \theta_h)\|. \quad (5.61)$$

*Proof.* We first introduce the identity  $\boldsymbol{\sigma}^d - \mu(\theta)\mathbf{t} = 0$  (cf. (5.8)), that is,

$$\boldsymbol{\sigma}_h^d - \mu(\theta_h)\mathbf{t}_h = \left(\boldsymbol{\sigma}_h^d - \boldsymbol{\sigma}^d\right) + \mu(\theta_h)(\mathbf{t} - \mathbf{t}_h) + (\mu(\theta) - \mu(\theta_h))\mathbf{t},$$

which, proceeding as in [37, Lemma 3.4], and noting that  $\|\boldsymbol{\tau}^d\|_{0,\Omega} \leq \|\boldsymbol{\tau}\|_{0,\Omega}$  for each  $\boldsymbol{\tau} \in \mathbb{L}^2(\Omega)$ , yields

$$\left\|\boldsymbol{\sigma}_h^d - \mu(\theta_h)\mathbf{t}_h\right\|_{0,\Omega}^2 \leq 3\left\{\mu_2^2\|\mathbf{t} - \mathbf{t}_h\|_{0,\Omega}^2 + \|\boldsymbol{\sigma} - \boldsymbol{\sigma}_h\|_{0,\Omega}^2 + L_\mu^2\|\mathbf{t}\|_{\delta,\Omega}^2\|\theta - \theta_h\|_{L^{n/\delta}(\Omega)}^2\right\}.$$

Recall here from [37] that  $\delta \in (0, 1)$  (when  $n = 2$ ) or  $\delta \in (1/2, 1)$  (when  $n = 3$ ) stands for the extra regularity that we need to assume for the solution of (5.11). In turn, employing the estimate [37, eq. (3.22)] to bound  $\|\mathbf{t}\|_{\delta,\Omega}$ , and the continuous injection of  $H^1(\Omega)$  into  $L^{n/\delta}(\Omega)$ , whose boundedness constant is  $\tilde{C}_\delta$  (cf. Theorem 5.1), it is not difficult to see that there exist a positive constant  $c_1$ , depending only on data and other constants, all of them independent of  $h$ , such that

$$\left\|\boldsymbol{\sigma}_h^d - \mu(\theta_h)\mathbf{t}_h\right\|_{0,\Omega}^2 \leq c_1\left\{\|\mathbf{t} - \mathbf{t}_h\|_{0,\Omega}^2 + \|\boldsymbol{\sigma} - \boldsymbol{\sigma}_h\|_{0,\Omega}^2 + \|\theta - \theta_h\|_{1,\Omega}^2\right\}. \quad (5.62)$$

Analogously, by considering the identity  $\nabla\theta - (\kappa^{-1}\mathbf{p} + \kappa^{-1}\theta\mathbf{u}) = 0$  (cf. (5.8)), we have

$$\nabla\theta_h - (\kappa^{-1}\mathbf{p}_h + \kappa^{-1}\theta_h\mathbf{u}_h) = \nabla(\theta_h - \theta) + \kappa^{-1}(\mathbf{p} - \mathbf{p}_h) + \kappa^{-1}(\theta\mathbf{u} - \theta_h\mathbf{u}_h),$$

where the last term of the right-hand side can be rewritten as  $\theta\mathbf{u} - \theta_h\mathbf{u}_h = \theta(\mathbf{u} - \mathbf{u}_h) + (\theta - \theta_h)\mathbf{u}_h$ , and then it can be bounded by

$$\|\theta\mathbf{u} - \theta_h\mathbf{u}_h\|_{0,\Omega} \leq \|\theta\|_{L^4(\Omega)}\|\mathbf{u} - \mathbf{u}_h\|_{L^4(\Omega)} + \|\mathbf{u}_h\|_{L^4(\Omega)}\|\theta - \theta_h\|_{L^4(\Omega)}.$$

Therefore, using the fact that  $H^1(\Omega)$  is continuously embedded into  $L^4(\Omega)$ ,  $\theta$  lives in the ball  $\mathcal{W}$ , and the estimate  $\|\mathbf{u}_h\|_{1,\Omega} \leq c_S\|\mathbf{f}\|_{0,\Omega}$  holds (cf. (5.22)), we obtain

$$\|\nabla\theta_h - (\kappa^{-1}\mathbf{p}_h + \kappa^{-1}\theta_h\mathbf{u}_h)\|_{0,\Omega}^2 \leq c_2\|(\mathbf{u}, \mathbf{p}, \theta) - (\mathbf{u}_h, \mathbf{p}_h, \theta_h)\|^2, \quad (5.63)$$

with  $c_2$  a positive constant independent of  $h$ . On the other hand, it is readily seen from (5.8) that

$$\begin{aligned} \|\mathbf{f} + \mathbf{div}\boldsymbol{\sigma}_h\|_{0,\Omega}^2 &\leq \|\mathbf{div}(\boldsymbol{\sigma} - \boldsymbol{\sigma}_h)\|_{0,\Omega}^2, \\ \|g + \mathbf{div}\mathbf{p}_h\|_{0,\Omega}^2 &\leq \|\mathbf{div}(\mathbf{p} - \mathbf{p}_h)\|_{0,\Omega}^2, \\ \|\boldsymbol{\sigma}_h - \boldsymbol{\sigma}_h^t\|_{0,\Omega}^2 &\leq 4\|\boldsymbol{\sigma} - \boldsymbol{\sigma}_h\|_{0,\Omega}^2, \\ \|\mathbf{t}_h - \mathbf{e}(\mathbf{u}_h)\|_{0,\Omega}^2 &\leq 2\left\{\|\mathbf{t} - \mathbf{t}_h\|_{0,\Omega}^2 + \|\mathbf{u} - \mathbf{u}_h\|_{1,\Omega}^2\right\}, \\ \|\boldsymbol{\rho}_h - (\nabla\mathbf{u}_h - \mathbf{e}(\mathbf{u}_h))\|_{0,\Omega}^2 &\leq 2\left\{\|\boldsymbol{\rho} - \boldsymbol{\rho}_h\|_{0,\Omega}^2 + \|\mathbf{u} - \mathbf{u}_h\|_{1,\Omega}^2\right\}, \\ \|\nabla\mathbf{u}_h - (\mathbf{t}_h + \boldsymbol{\rho}_h)\|_{0,\Omega}^2 &\leq 3\left\{\|\mathbf{t} - \mathbf{t}_h\|_{0,\Omega}^2 + \|\boldsymbol{\rho} - \boldsymbol{\rho}_h\|_{0,\Omega}^2 + \|\mathbf{u} - \mathbf{u}_h\|_{1,\Omega}^2\right\}, \\ \|\theta_D - \theta_h\|_{0,\Gamma_D}^2 &\leq c_3\|\theta - \theta_h\|_{1,\Omega}^2, \end{aligned} \quad (5.64)$$

and

$$\|\theta_D - \theta_h\|_{1/2, \Gamma_D}^2 \leq c_4 \|\theta - \theta_h\|_{1, \Omega}^2, \quad (5.65)$$

where the last two inequalities make use of the trace inequalities in  $L^2(\Gamma_D)$  and  $H^{1/2}(\Gamma_D)$ , respectively. In this way, the required efficiency estimate (5.61) follows straightforwardly from the definition of  $\Theta_1$  (cf. (5.27)) and the inequalities (5.62)–(5.65).  $\square$

Next, we continue with the derivation of the efficiency estimate of  $\Theta_2$ .

**Lemma 5.16.** *There hold*

- (a)  $\|\mathbf{f} - \mathbf{P}_h(\mathbf{f})\|_{0,T} \leq 2\|\mathbf{div}(\boldsymbol{\sigma} - \boldsymbol{\sigma}_h)\|_{0,T} \quad \forall T \in \mathcal{T}_h,$
- (b)  $\|g - \mathcal{P}_h(g)\|_{0,T} \leq 2\|\mathbf{div}(\mathbf{p} - \mathbf{p}_h)\|_{0,T} \quad \forall T \in \mathcal{T}_h,$

and there exist  $c_1, c_2 > 0$ , independent of  $h$ , such that

- (c)  $h_T^2 \|\mathbf{rot}(\mathbf{t}_h + \boldsymbol{\rho}_h)\|_{0,T}^2 \leq c_1 \left\{ \|\mathbf{t} - \mathbf{t}_h\|_{0,T}^2 + \|\boldsymbol{\rho} - \boldsymbol{\rho}_h\|_{0,T}^2 \right\} \quad \forall T \in \mathcal{T}_h,$
- (d)  $h_e \|\llbracket (\mathbf{t}_h + \boldsymbol{\rho}_h) \mathbf{s} \rrbracket\|_{0,e}^2 \leq c_2 \left\{ \|\mathbf{t} - \mathbf{t}_h\|_{0,\omega_e}^2 + \|\boldsymbol{\rho} - \boldsymbol{\rho}_h\|_{0,\omega_e}^2 \right\} \quad \forall e \in \mathcal{E}_h,$

where the set  $\omega_e$  is given by  $\omega_e := \cup \{T' \in \mathcal{T}_h : e \in \mathcal{E}(T')\}$ .

*Proof.* For (a) and (b) we refer to [97, Lemma 3.18]. In turn, since  $\mathbf{rot}(\mathbf{t} + \boldsymbol{\rho}) = \mathbf{rot}(\nabla \mathbf{u}) = \mathbf{0}$ , we find that the proof of (c) and (d) follows after a straightforward application of [15, Lemmas 4.3 and 4.4], respectively.  $\square$

The corresponding bounds for the remaining terms defining  $\Theta_2$  are given next.

**Lemma 5.17.** *There exist  $c_1, c_2 > 0$ , independent of  $h$ , such that*

- (a)  $\sum_{T \in \mathcal{T}_h} h_T^2 \|\mathbf{rot}(\kappa^{-1} \mathbf{p}_h + \kappa^{-1} \theta_h \mathbf{u}_h)\|_{0,T}^2 \leq c_1 \|(\mathbf{u}, \mathbf{p}, \theta) - (\mathbf{u}_h, \mathbf{p}_h, \theta_h)\|^2,$
- (b)  $\sum_{e \in \mathcal{E}_h(\Omega)} h_e \|\llbracket (\kappa^{-1} \mathbf{p}_h + \kappa^{-1} \theta_h \mathbf{u}_h) \cdot \mathbf{s} \rrbracket\|_{0,e}^2 \leq c_2 \|(\mathbf{u}, \mathbf{p}, \theta) - (\mathbf{u}_h, \mathbf{p}_h, \theta_h)\|^2.$

In addition, under the assumption that  $\theta_D \in H^1(\Gamma_D)$ , there exists  $c_3 > 0$ , independent of  $h$ , such that

- (c)  $\sum_{e \in \mathcal{E}_h(\Gamma_D)} h_e \left\| \frac{d\theta_D}{ds} - (\kappa^{-1} \mathbf{p}_h + \kappa^{-1} \theta_h \mathbf{u}_h) \cdot \mathbf{s} \right\|_{0,e}^2 \leq c_3 \|(\mathbf{u}, \mathbf{p}, \theta) - (\mathbf{u}_h, \mathbf{p}_h, \theta_h)\|^2.$

*Proof.* It follows almost straightforwardly from a slight modification of the proof of [53, Lemma 3.11]. We omit further details.  $\square$

As a consequence of Theorem 5.15 and Lemmas 5.16 and 5.17, we are now in position to state the efficiency of  $\Theta_2$ .

**Theorem 5.18.** *Assume that  $\theta_D \in H^1(\Gamma_D)$ . Then, there exists  $\tilde{C}_{\text{eff}} > 0$ , independent of  $h$ , such that*

$$\tilde{C}_{\text{eff}} \Theta_2 \leq \|(\mathbf{t}, \mathbf{u}, \mathbf{p}, \theta) - (\mathbf{t}_h, \mathbf{u}_h, \mathbf{p}_h, \theta_h)\|. \quad (5.66)$$

## 5.4 A posteriori error analysis: the 3D-case

In this section we extend the results from Section 5.3 to the three-dimensional version of (5.21). Similarly as in the previous section, given a tetrahedron  $T \in \mathcal{T}_h$ , we let  $\mathcal{E}(T)$  be the set of its faces, and let  $\mathcal{E}_h$  be the set of all faces of the triangulation  $\mathcal{T}_h$ . Then, we write  $\mathcal{E}_h = \mathcal{E}_h(\Omega) \cup \mathcal{E}_h(\Gamma_D) \cup \mathcal{E}_h(\Gamma_N)$ , where  $\mathcal{E}_h(\Omega) := \{e \in \mathcal{E}_h : e \subseteq \Omega\}$ ,  $\mathcal{E}_h(\Gamma_D) := \{e \in \mathcal{E}_h : e \subseteq \Gamma_D\}$ , and  $\mathcal{E}_h(\Gamma_N) := \{e \in \mathcal{E}_h : e \subseteq \Gamma_N\}$ . Also, for each face  $e \in \mathcal{E}_h$  we fix a unit normal  $\mathbf{n}_e$  to  $e$ , so that given  $\boldsymbol{\tau} \in \mathbb{L}^2(\Omega)$  such that  $\boldsymbol{\tau}|_T \in \mathbb{C}(T)$  on each  $T \in \mathcal{T}_h$ , and given  $e \in \mathcal{E}_h(\Omega)$ , we let  $\llbracket \boldsymbol{\tau} \times \mathbf{n}_e \rrbracket$  be the corresponding jump of the tangential traces across  $e$ , that is  $\llbracket \boldsymbol{\tau} \times \mathbf{n}_e \rrbracket := (\boldsymbol{\tau}|_T - \boldsymbol{\tau}|_{T'})|_e \times \mathbf{n}_e$ , where  $T$  and  $T'$  are the elements of  $\mathcal{T}_h$  having  $e$  as a common face. In what follows, when no confusion arises, we simply write  $\mathbf{n}$  instead of  $\mathbf{n}_e$ .

Now, we recall that the curl of a 3D vector  $\mathbf{v} := (v_1, v_2, v_3)$  is the 3D vector

$$\text{curl}(\mathbf{v}) = \nabla \times \mathbf{v} := \left( \frac{\partial v_3}{\partial x_2} - \frac{\partial v_2}{\partial x_3}, \frac{\partial v_1}{\partial x_3} - \frac{\partial v_3}{\partial x_1}, \frac{\partial v_2}{\partial x_1} - \frac{\partial v_1}{\partial x_2} \right),$$

and that, given a tensor function  $\boldsymbol{\tau} := (\tau_{ij})_{3 \times 3}$ , the operator  $\underline{\text{curl}}(\boldsymbol{\tau})$  is the  $3 \times 3$  tensor whose rows are given by

$$\underline{\text{curl}}(\boldsymbol{\tau}) := \begin{pmatrix} \text{curl}(\tau_{11}, \tau_{12}, \tau_{13}) \\ \text{curl}(\tau_{21}, \tau_{22}, \tau_{23}) \\ \text{curl}(\tau_{31}, \tau_{32}, \tau_{33}) \end{pmatrix}.$$

In addition,  $\boldsymbol{\tau} \times \mathbf{n}$  stands for the  $3 \times 3$  tensor whose rows are given by the tangential components of each row of  $\boldsymbol{\tau}$ , that is,

$$\boldsymbol{\tau} \times \mathbf{n} := \begin{pmatrix} (\tau_{11}, \tau_{12}, \tau_{13}) \times \mathbf{n} \\ (\tau_{21}, \tau_{22}, \tau_{23}) \times \mathbf{n} \\ (\tau_{31}, \tau_{32}, \tau_{33}) \times \mathbf{n} \end{pmatrix}.$$

Having introduced these notations, we now set for each  $T \in \mathcal{T}_h$  the local a posteriori error indicators  $\tilde{\Theta}_{1,T}^2$  and  $\Theta_{1,T}^2$  (exactly as in (5.26) and (5.27), respectively), and define

$$\begin{aligned} \Theta_{2,T}^2 &:= \tilde{\Theta}_{1,T}^2 + \|\mathbf{f} - \mathbf{P}_h(\mathbf{f})\|_{0,T}^2 + \|g - \mathcal{P}_h(g)\|_{0,T}^2 + h_T^2 \|\nabla \mathbf{u}_h - (\mathbf{t}_h + \boldsymbol{\rho}_h)\|_{0,T}^2 \\ &+ h_T^2 \|\underline{\text{curl}}(\mathbf{t}_h + \boldsymbol{\rho}_h)\|_{0,T}^2 + h_T^2 \|\text{curl}(\kappa^{-1} \mathbf{p}_h + \kappa^{-1} \theta_h \mathbf{u}_h)\|_{0,T}^2 \\ &+ \sum_{e \in \mathcal{E}(T)} h_e \|\llbracket (\mathbf{t}_h + \boldsymbol{\rho}_h) \times \mathbf{n} \rrbracket\|_{0,e}^2 + \sum_{e \in \mathcal{E}(T) \cap \mathcal{E}_h(\Omega)} h_e \|\llbracket (\kappa^{-1} \mathbf{p}_h + \kappa^{-1} \theta_h \mathbf{u}_h) \times \mathbf{n} \rrbracket\|_{0,e}^2 \\ &+ \sum_{e \in \mathcal{E}(T) \cap \mathcal{E}_h(\Gamma_D)} h_e \|\nabla \theta_D \times \mathbf{n} - (\kappa^{-1} \mathbf{p}_h + \kappa^{-1} \theta_h \mathbf{u}_h) \times \mathbf{n}\|_{0,e}^2. \end{aligned} \quad (5.67)$$

In this way, the corresponding global a posteriori error estimators are defined as in (5.29), that is

$$\Theta_1 := \left\{ \sum_{T \in \mathcal{T}_h} \Theta_{1,T}^2 + \|\theta_D - \theta_h\|_{1/2, \Gamma_D}^2 \right\}^{1/2} \quad \text{and} \quad \Theta_2 := \left\{ \sum_{T \in \mathcal{T}_h} \Theta_{2,T}^2 \right\}^{1/2},$$

and the main estimates, which are the analogue of Theorems 5.9 and 5.14, are as follows.

**Theorem 5.19.** *Assume that the data  $\mathbf{f}, g$  and  $\theta_D$  satisfy (5.43). Assume further that  $\theta_D \in H^1(\Gamma_D)$ . Then, there exist positive constants  $C_{\text{rel}}, C_{\text{eff}}, \tilde{C}_{\text{rel}}$ , and  $\tilde{C}_{\text{eff}}$ , independent of  $h$ , such that*

$$C_{\text{eff}} \Theta_1 \leq \|(\mathbf{t}, \mathbf{u}, \mathbf{p}, \theta) - (\mathbf{t}_h, \mathbf{u}_h, \mathbf{p}_h, \theta_h)\| \leq C_{\text{rel}} \Theta_1$$

and

$$\tilde{C}_{\text{eff}} \Theta_2 \leq \|(\mathbf{t}, \mathbf{u}, \mathbf{p}, \theta) - (\mathbf{t}_h, \mathbf{u}_h, \mathbf{p}_h, \theta_h)\| \leq \tilde{C}_{\text{rel}} \Theta_2.$$

The proof of Theorem 5.19 follows very closely the analysis of Section 5.3, except a few issues to be described throughout the following discussion. Indeed, we first observe that the general a posteriori error estimate given by Lemma 5.8 is also valid in 3D, and that the corresponding upper bounds of  $\|\mathcal{R}_f\|_{\mathbb{H}_0(\mathbf{div}; \Omega)'} and  $\|\mathcal{R}_h\|_{\mathbf{H}_{\Gamma_N}(\mathbf{div}; \Omega)'}$  yielding the reliability of  $\Theta_1$  are the same as those given in (5.48) and (5.49), respectively.$

Now, for the reliability of  $\Theta_2$ , we need to use a 3D version of the stable Helmholtz decompositions provided by Lemma 5.5. These required results were established recently for arbitrary polyhedral domains in [82, Theorems 3.1 and 3.2]. Next, the associated discrete Helmholtz decompositions and the functionals  $\mathcal{R}_f$  and  $\mathcal{R}_h$  are set and rewritten exactly as in (5.45) and (5.46), respectively. Furthermore, in order to derive the new upper bound of  $\|\mathcal{R}_f\|_{\mathbb{H}_0(\mathbf{div}; \Omega)'}$  and  $\|\mathcal{R}_h\|_{\mathbf{H}_{\Gamma_N}(\mathbf{div}; \Omega)'}$ , we now need the 3D analogue of the integration by parts formula on the boundary given by (5.59). In fact, by applying the identities from [100, Chapter I, eq. (2.17) and Theorem 2.11], we deduce that in this case there holds

$$\langle \text{curl } \boldsymbol{\chi} \cdot \mathbf{n}, \theta_D \rangle_{\Gamma_D} = - \langle \nabla \theta_D \times \mathbf{n}, \boldsymbol{\chi} \rangle_{\Gamma_D} \quad \forall \boldsymbol{\chi} \in \mathbf{H}^1(\Omega).$$

In addition, the integration by parts formula on each tetrahedron  $T \in \mathcal{T}_h$ , which is employed in the proof of the 3D analogue of Lemma 5.11, becomes (cf. [100, Chapter I, Theorem 2.11])

$$\int_T \text{curl } \mathbf{q} \cdot \boldsymbol{\chi} - \int_T \mathbf{q} \cdot \text{curl } \boldsymbol{\chi} = \langle \mathbf{q} \times \mathbf{n}, \boldsymbol{\chi} \rangle_{\partial T} \quad \forall \mathbf{q} \in \mathbf{H}(\text{curl}; \Omega), \quad \forall \boldsymbol{\chi} \in \mathbf{H}^1(\Omega),$$

where  $\langle \cdot, \cdot \rangle_{\partial T}$  is the duality pairing between  $\mathbf{H}^{-1/2}(\partial T)$  and  $\mathbf{H}^{1/2}(\partial T)$ , and, as usual,  $\mathbf{H}(\text{curl}; \Omega)$  is the space of vectors in  $\mathbf{L}^2(\Omega)$  whose curl lie also in  $\mathbf{L}^2(\Omega)$ . Note that the foregoing identities explain the appearing of the expressions  $(\mathbf{t}_h + \boldsymbol{\rho}_h) \times \mathbf{n}$ ,  $(\kappa^{-1} \mathbf{p}_h + \kappa^{-1} \theta_h \mathbf{u}_h) \times \mathbf{n}$ , and  $\nabla \theta_D \times \mathbf{n} - (\kappa^{-1} \mathbf{p}_h + \kappa^{-1} \theta_h \mathbf{u}_h) \times \mathbf{n}$  in the 3D definitions of  $\Theta_{2,T}^2$  (cf. (5.67)). The rest of the proof of the reliability of  $\Theta_2$  and the entire analysis yielding the efficiency of both  $\Theta_1$  and  $\Theta_2$  proceed as in Sections 5.3.4 and 5.3.5, respectively, taking into account that the proof of the 3D version of the Lemma 5.17 follows almost straightforwardly from a slight modification of the proof of [53, Lemma 4.2].

## 5.5 Numerical results

This section serves to illustrate the performance and accuracy of the proposed augmented finite element scheme along with the properties of the a posteriori error estimators  $\Theta_1$  and  $\Theta_2$ , in 2D and 3D domains, derived in Sections 5.3 and 5.4, respectively. In this regard, we remark that for purposes of adaptivity, which requires to have locally computable indicators, we use that

$$\|\theta_D - \theta_h\|_{1/2, \Gamma_D}^2 \leq c_D \|\theta_D - \theta_h\|_{1, \Gamma_D}^2 = c_D \sum_{e \in \mathcal{E}_h(\Gamma_D)} \|\theta_D - \theta_h\|_{1,e}^2,$$

and redefine  $\Theta_1$  as

$$\Theta_1 := \left\{ \sum_{T \in \mathcal{T}_h} \Theta_{1,T}^2 \right\}^{1/2},$$

where

$$\begin{aligned} \Theta_{1,T}^2 := & \left\| \boldsymbol{\sigma}_h^d - \mu(\theta_h) \mathbf{t}_h \right\|_{0,T}^2 + \|\mathbf{f} + \mathbf{div} \boldsymbol{\sigma}_h\|_{0,T}^2 + \|\boldsymbol{\sigma}_h - \boldsymbol{\sigma}_h^t\|_{0,T}^2 + \|\mathbf{t}_h - \mathbf{e}(\mathbf{u}_h)\|_{0,T}^2 \\ & + \|\boldsymbol{\rho}_h - (\nabla \mathbf{u}_h - \mathbf{e}(\mathbf{u}_h))\|_{0,T}^2 + \|\nabla \mathbf{u}_h - (\mathbf{t}_h + \boldsymbol{\rho}_h)\|_{0,T}^2 + \|g + \mathbf{div} \mathbf{p}_h\|_{0,T}^2 \\ & + \|\nabla \theta_h - (\kappa^{-1} \mathbf{p}_h + \kappa^{-1} \theta_h \mathbf{u}_h)\|_{0,T}^2 + \sum_{e \in \mathcal{E}(T) \cap \mathcal{E}_h(\Gamma_D)} \|\theta_D - \theta_h\|_{1,e}^2. \end{aligned}$$

Under this redefinition  $\Theta_1$  is certainly still reliable, but efficient only up to all its terms, except for the last one, associated to the boundary  $\Gamma_D$ . Nevertheless, the numerical results to be displayed below allow us to conjecture that this modified  $\Theta_1$  actually verifies both properties.

Our implementation is based on the public domain finite element software **FreeFem++** [111] which provides for both 2D and 3D domains the automatic adaptation procedure tools **adaptmesh** and **msh-met**, respectively. A Picard algorithm with a fixed tolerance  $\text{tol} = 1E - 6$  has been used for the corresponding fixed-point problem (5.21) and the iterations are terminated once the relative error of the entire coefficient vectors between two consecutive iterates is sufficiently small, i.e.,

$$\frac{\|\text{coeff}^{m+1} - \text{coeff}^m\|_{l^2}}{\|\text{coeff}^{m+1}\|_{l^2}} \leq \text{tol},$$

where  $\|\cdot\|_{l^2}$  is the standard  $l^2$ -norm in  $\mathbb{R}^N$ , with  $N$  denoting the total number of degrees of freedom defining the finite element subspaces  $\mathbb{H}_h^{\mathbf{t}}, \mathbb{H}_h^{\boldsymbol{\sigma}}, \mathbb{H}_h^{\boldsymbol{\rho}}, \mathbb{H}_h^{\mathbf{u}}, \mathbb{H}_h^{\mathbf{p}}$ , and  $\mathbb{H}_h^{\theta}$ . As usual, the individual errors are denoted by:

$$\begin{aligned} \mathbf{e}(\mathbf{t}) &:= \|\mathbf{t} - \mathbf{t}_h\|_{0,\Omega}, & \mathbf{e}(\boldsymbol{\sigma}) &:= \|\boldsymbol{\sigma} - \boldsymbol{\sigma}_h\|_{\text{div};\Omega}, & \mathbf{e}(\boldsymbol{\rho}) &:= \|\boldsymbol{\rho} - \boldsymbol{\rho}_h\|_{0,\Omega}, \\ \mathbf{e}(\mathbf{u}) &:= \|\mathbf{u} - \mathbf{u}_h\|_{1,\Omega}, & \mathbf{e}(\mathbf{p}) &:= \|\mathbf{p} - \mathbf{p}_h\|_{\text{div};\Omega}, & \mathbf{e}(\theta) &:= \|\theta - \theta_h\|_{1,\Omega}, \\ \mathbf{e}(\boldsymbol{\sigma}_P) &:= \|\boldsymbol{\sigma}_P - \boldsymbol{\sigma}_{P,h}\|_{0,\Omega}, & \mathbf{e}(p) &:= \|p - p_h\|_{0,\Omega}, \end{aligned}$$

where  $\boldsymbol{\sigma}_{P,h}$  and  $p_h$  are the postprocessed polymeric part of the extra-stress tensor and the pressure, respectively, given by

$$\boldsymbol{\sigma}_{P,h} := 2\mu_P(\theta_h) \mathbf{t}_h \quad \text{and} \quad p_h := -\frac{1}{n} \text{tr} \boldsymbol{\sigma}_h \quad \text{in } \Omega.$$



In turn, the global error is computed as

$$\mathbf{e} := \left\{ \mathbf{e}(\mathbf{t})^2 + \mathbf{e}(\boldsymbol{\sigma})^2 + \mathbf{e}(\boldsymbol{\rho})^2 + \mathbf{e}(\mathbf{u})^2 + \mathbf{e}(\mathbf{p})^2 + \mathbf{e}(\theta)^2 \right\}^{1/2},$$

whereas the effectivity index with respect to  $\Theta_i$ ,  $i \in \{1, 2\}$  is given by

$$\text{eff}(\Theta_i) := \frac{\mathbf{e}}{\Theta_i}.$$

In addition, we define the experimental rates of convergence

$$r(\diamond) := \frac{\log(\mathbf{e}(\diamond)/\mathbf{e}'(\diamond))}{\log(h/h')} \quad \text{for each } \diamond \in \{\mathbf{t}, \boldsymbol{\sigma}, \boldsymbol{\rho}, \mathbf{u}, \mathbf{p}, \theta, \boldsymbol{\sigma}_P, p\},$$

where  $\mathbf{e}$  and  $\mathbf{e}'$  denote errors computed on two consecutive meshes of sizes  $h$  and  $h'$ , respectively. However, when the adaptive algorithm is applied, the expression  $\log(h/h')$  appearing in the computation of the above rates is replaced by  $-\frac{1}{n} \log(\mathbf{N}/\mathbf{N}')$  with  $n = 2$  (in 2D domains) or  $n = 3$  (in 3D domains), where  $\mathbf{N}$  and  $\mathbf{N}'$  denote the corresponding degrees of freedom of each triangulation.

The examples to be considered in this section are described next. In all of them, as in [56, Section 2], we choose the coefficients of the polymer and solvent viscosity  $a_1, b_1, a_2$  and  $b_2$  (cf. (5.2)) as follow:

$$b_1 = b_2 = \frac{\Delta E}{R}, \quad a_2 = \exp\left(\frac{-\Delta E}{R\theta_R}\right), \quad \text{and} \quad a_1 = (1 - \epsilon)a_2,$$

where  $\Delta E$  is the activation energy,  $R$  is the ideal gas constant, and  $\theta_R$  is a reference temperature of the fluid. Note that the constraint (5.3) will be satisfied as long as the temperature of the system stays above  $\theta_R$ . In turn, we consider  $\kappa = 1$ ,  $\epsilon = 0.01$ , and according to [37, eq. (3.20)], the stabilization parameters are taken as  $\kappa_1 = \mu_1/\mu_2^2$ ,  $\kappa_2 = \kappa_1$ ,  $\kappa_3 = \mu_1/2$ ,  $\kappa_4 = \mu_1/4$ ,  $\kappa_5 = \kappa$ ,  $\kappa_6 = \kappa^{-1}/2$ , and  $\kappa_7 = \kappa/2$ . In addition, the condition  $\int_{\Omega} \text{tr } \boldsymbol{\sigma}_h = 0$  is imposed via a penalization strategy.

**Example 1.** In our first example we concentrate on the accuracy of the augmented method. We consider the square domain  $\Omega := (0, 1)^2$ , the boundary  $\Gamma = \bar{\Gamma}_D \cup \bar{\Gamma}_N$ , with  $\Gamma_D := \{0\} \times (0, 1)$  and  $\Gamma_N := \Gamma \setminus \bar{\Gamma}_D$ . The following viscosity parameters correspond to polystyrene [118, Section 4.2]:

$$\frac{\Delta E}{R} = 14500, \quad \theta_R = 538.$$

The data  $\mathbf{f}$ ,  $g$ , and  $\theta_D$  are chosen so that a manufactured solution of (5.8) is given by the smooth functions

$$\begin{aligned} \mathbf{u}(\mathbf{x}) &:= \begin{pmatrix} 2\pi x_1^2(x_1 - 1)^2 \cos(\pi x_2) \sin(\pi x_2) \\ -2x_1(x_1 - 1)(2x_1 - 1) \sin(\pi x_2)^2 \end{pmatrix}, \\ p(\mathbf{x}) &:= \cos(\pi x_1) \cos(\pi x_2), \\ \theta(\mathbf{x}) &:= 10(x_1 - 1)^2 \sin(\pi x_2)^2 + 540 \quad \forall \mathbf{x} := (x_1, x_2) \in \Omega. \end{aligned}$$

The results reported in Tables 5.1 and 5.2 are in accordance with the theoretical bounds established in Theorem 5.2. In addition, we also compute the global a posteriori error indicators  $\Theta_1, \Theta_2$  and measure their reliability and efficiency with the effectivity index. For the two orders tested, these estimators remain always bounded.

**Example 2.** Our second example is aimed at testing the features of adaptive mesh refinement after the a posteriori error estimators  $\Theta_1$  and  $\Theta_2$ . We consider a four-to-one contraction domain  $\Omega := (0, 2) \times (0, 1) \setminus (1, 2) \times (0.25, 1)$ , the boundary  $\Gamma = \bar{\Gamma}_D \cup \bar{\Gamma}_N$ , with  $\Gamma_D := \{0\} \times (0, 1)$  and  $\Gamma_N := \Gamma \setminus \bar{\Gamma}_D$ . The following viscosity parameters correspond to Nylon-6,6 [118, Section 4.2]:

$$\frac{\Delta E}{R} = 6600, \quad \theta_R = 563.$$

The data  $\mathbf{f}$ ,  $g$ , and  $\theta_D$  are chosen so that the exact solution is given by

$$\begin{aligned} \mathbf{u}(\mathbf{x}) &:= \begin{pmatrix} x_2(x_2 - 1)(x_2 - 0.25)(3x_2^2 - 2.5x_2 + 0.25) \sin(\pi x_1)^2 \\ -\pi x_2^2(x_2 - 1)^2(x_2 - 0.25)^2 \cos(\pi x_1) \sin(\pi x_1) \end{pmatrix}, \\ p(\mathbf{x}) &:= \frac{10(x_2 - 0.25)}{(x_1 - 1.02)^2 + (x_2 - 0.27)^2} + p_0, \\ \theta(\mathbf{x}) &:= \frac{4(x_1 - 1)(x_2 - 0.25)}{(x_1 - 1.02)^2 + (x_2 - 0.27)^2} + 570 \quad \forall \mathbf{x} := (x_1, x_2) \in \Omega. \end{aligned}$$

The constant  $p_0$  is such that  $\int_{\Omega} p = 0$ . Notice that both the pressure and the temperature exhibit high gradients near the vertex  $(1, 0.25)$ . Notice also that the only difference with respect to (5.8) is a non-homogeneous heat flux  $\mathbf{p} \cdot \mathbf{n} = f_N$  imposed on  $\Gamma_N$ , where  $f_N$  is manufactured according to the above solution. Therefore, the local estimators  $\Theta_{1,T}$  and  $\Theta_{2,T}$  have to be modified by adding the term

$$\sum_{e \in \mathcal{E}(T) \cap \mathcal{E}_h(\Gamma_N)} h_e \|f_N - \mathbf{p}_h \cdot \mathbf{n}\|_{0,e}^2,$$

whose estimation from below and above follows in a straightforward manner.

Tables 5.3, 5.4, and 5.5 along with Figure 5.1, summarizes the convergence history of the method applied to a sequence of quasi-uniformly and adaptively refined triangulation of the domain. Sub-optimal rates are observed in the first case, whereas adaptive refinement according to either a posteriori error indicator yield optimal convergence and stable effectivity indexes. On the other hand, approximate solutions builded using the augmented  $\mathbb{P}_0 - \mathbf{RT}_0 - \mathbb{P}_0 - \mathbf{P}_1 - \mathbf{RT}_0 - \mathbf{P}_1$  scheme with 562743 degrees of freedom (via the indicator  $\Theta_1$ ) are shown in Figure 5.2. In particular, we observe in both the velocity and heat flux streamlines a vortex near the corner region of the four-to-one domain whereas both the pressure and temperature exhibit high gradients in the same region. In turn, examples of some adapted meshes generated using  $\Theta_1$  and  $\Theta_2$  are collected in Figure 5.3. We can observe a clear clustering of elements near the corner region of the contraction as we expected. Notice that the meshes obtained via the indicator  $\Theta_2$  are lightly more refined in the interior of the contraction domain than the meshes obtained via the indicator  $\Theta_1$ . This fact is justified by the terms that capture the jumps between triangles obtained in the Helmholtz decomposition.

**Example 3.** To conclude, we replicate the Example 2 in a three-dimensional setting. In fact, we consider the four-to-one domain  $\Omega := (0, 2) \times (0, 1)^2 \setminus (1, 2) \times (0.25, 1)^2$ , the boundary  $\Gamma = \bar{\Gamma}_D \cup \bar{\Gamma}_N$ , with  $\Gamma_D := \{0\} \times (0, 1)^2$  and  $\Gamma_N := \Gamma \setminus \bar{\Gamma}_D$ . The viscosity parameters are the same as in the second example. However, this time the manufactured exact solutions adopt the form

$$\mathbf{u}(\mathbf{x}) := \begin{pmatrix} -x_3(x_3 - 1)(x_3 - 0.25)(3x_3^2 - 2.5x_3 - \pi \cos(\pi x_2) + 0.25) \sin(\pi x_1)^2 \sin(\pi x_2) \\ x_3(x_3 - 1)(x_3 - 0.25)(3x_3^2 - 2.5x_3 - \pi \cos(\pi x_1) + 0.25) \sin(\pi x_1) \sin(\pi x_2)^2 \\ -\pi x_3^2(x_3 - 1)^2(x_3 - 0.25)^2 \sin(\pi x_1) \sin(\pi x_2)(\cos(\pi x_2) - \cos(\pi x_1)) \end{pmatrix},$$

$$p(\mathbf{x}) := \frac{10(x_3 - 0.25)}{(x_1 - 1.05)^2 + (x_3 - 0.3)^2} + p_0,$$

$$\theta(\mathbf{x}) := \frac{4(x_1 - 1)(x_3 - 0.25)}{(x_1 - 1.05)^2 + (x_3 - 0.3)^2} + 570 \quad \forall \mathbf{x} := (x_1, x_2, x_3) \in \Omega.$$

Similarly, Tables 5.6 and 5.7 along with the Figure 5.4 confirm a disturbed convergence under quasi-uniform refinement and an optimal convergence rates when using adaptive refinement guided by the a posteriori error estimator  $\Theta_1$ . In turn, some approximated solutions after four mesh refinement steps showing an analogous behaviour to its 2D counterpart are collected in Figure 5.5, whereas snapshots of the last three meshes via  $\Theta_1$  are shown in Figure 5.6.

| N      | $h$   | $e(\mathbf{t})$ | $r(\mathbf{t})$ | $e(\boldsymbol{\sigma})$ | $r(\boldsymbol{\sigma})$ | $e(\boldsymbol{\rho})$ | $r(\boldsymbol{\rho})$ | $e(\mathbf{u})$ | $r(\mathbf{u})$ | $e(p)$ | $r(p)$ |
|--------|-------|-----------------|-----------------|--------------------------|--------------------------|------------------------|------------------------|-----------------|-----------------|--------|--------|
| 1467   | 0.196 | 0.155           | –               | 1.246                    | –                        | 0.268                  | –                      | 0.264           | –               | 0.148  | –      |
| 5631   | 0.097 | 0.075           | 1.025           | 0.633                    | 0.960                    | 0.146                  | 0.859                  | 0.127           | 1.040           | 0.063  | 1.214  |
| 22131  | 0.048 | 0.038           | 0.979           | 0.310                    | 1.009                    | 0.080                  | 0.858                  | 0.062           | 1.018           | 0.031  | 0.995  |
| 87837  | 0.025 | 0.019           | 1.032           | 0.157                    | 1.018                    | 0.040                  | 1.045                  | 0.031           | 1.027           | 0.015  | 1.105  |
| 353853 | 0.013 | 0.009           | 1.093           | 0.077                    | 1.085                    | 0.020                  | 1.089                  | 0.015           | 1.072           | 0.007  | 1.111  |

| $e(\mathbf{p})$ | $r(\mathbf{p})$ | $e(\theta)$ | $r(\theta)$ | $e(\boldsymbol{\sigma}_P)$ | $r(\boldsymbol{\sigma}_P)$ | $e$    | $r$   | $\text{eff}(\Theta_1)$ | $\text{eff}(\Theta_2)$ | iter |
|-----------------|-----------------|-------------|-------------|----------------------------|----------------------------|--------|-------|------------------------|------------------------|------|
| 18.678          | –               | 3.265       | –           | 0.349                      | –                          | 19.007 | –     | 0.931                  | 0.183                  | 4    |
| 9.628           | 0.940           | 1.419       | 1.181       | 0.171                      | 1.017                      | 9.755  | 0.992 | 0.942                  | 0.180                  | 4    |
| 4.738           | 1.002           | 0.654       | 1.094       | 0.082                      | 1.027                      | 4.794  | 1.038 | 0.947                  | 0.178                  | 3    |
| 2.405           | 1.014           | 0.331       | 1.019       | 0.041                      | 1.035                      | 2.434  | 0.984 | 0.950                  | 0.176                  | 3    |
| 1.187           | 1.082           | 0.163       | 1.087       | 0.020                      | 1.117                      | 1.201  | 1.013 | 0.950                  | 0.176                  | 3    |

Table 5.1: EXAMPLE 1,  $\mathbb{P}_0 - \mathbb{RT}_0 - \mathbb{P}_0 - \mathbf{P}_1 - \mathbf{RT}_0 - \mathbf{P}_1$  scheme with quasi-uniform refinement.

| N      | $h$   | $e(\mathbf{t})$ | $r(\mathbf{t})$ | $e(\boldsymbol{\sigma})$ | $r(\boldsymbol{\sigma})$ | $e(\boldsymbol{\rho})$ | $r(\boldsymbol{\rho})$ | $e(\mathbf{u})$ | $r(\mathbf{u})$ | $e(p)$ | $r(p)$ |
|--------|-------|-----------------|-----------------|--------------------------|--------------------------|------------------------|------------------------|-----------------|-----------------|--------|--------|
| 3666   | 0.196 | 0.026           | –               | 0.151                    | –                        | 0.023                  | –                      | 0.037           | –               | 0.016  | –      |
| 14076  | 0.097 | 0.006           | 2.036           | 0.037                    | 2.002                    | 0.006                  | 1.986                  | 0.009           | 2.071           | 0.004  | 1.894  |
| 55326  | 0.048 | 0.001           | 2.044           | 0.009                    | 2.019                    | 0.001                  | 2.048                  | 0.002           | 2.065           | 0.001  | 1.998  |
| 219591 | 0.025 | 0.000           | 1.989           | 0.002                    | 2.040                    | 0.000                  | 1.998                  | 0.001           | 1.986           | 0.000  | 2.032  |
| 884631 | 0.013 | 0.000           | 2.186           | 0.000                    | 2.153                    | 0.000                  | 2.196                  | 0.000           | 2.195           | 0.000  | 2.167  |

| $e(\mathbf{p})$ | $r(\mathbf{p})$ | $e(\theta)$ | $r(\theta)$ | $e(\boldsymbol{\sigma}_P)$ | $r(\boldsymbol{\sigma}_P)$ | $e$   | $r$   | $\text{eff}(\Theta_1)$ | $\text{eff}(\Theta_2)$ | iter |
|-----------------|-----------------|-------------|-------------|----------------------------|----------------------------|-------|-------|------------------------|------------------------|------|
| 2.435           | –               | 0.296       | –           | 0.045                      | –                          | 2.458 | –     | 0.951                  | 0.114                  | 3    |
| 0.584           | 2.024           | 0.069       | 2.060       | 0.011                      | 2.048                      | 0.590 | 2.122 | 0.953                  | 0.116                  | 3    |
| 0.138           | 2.041           | 0.015       | 2.120       | 0.003                      | 2.039                      | 0.139 | 2.111 | 0.951                  | 0.115                  | 3    |
| 0.036           | 2.023           | 0.004       | 2.047       | 0.001                      | 2.006                      | 0.036 | 1.961 | 0.956                  | 0.115                  | 3    |
| 0.009           | 2.148           | 0.001       | 2.133       | 0.000                      | 2.185                      | 0.009 | 2.011 | 0.957                  | 0.115                  | 3    |

Table 5.2: EXAMPLE 1,  $\mathbb{P}_1 - \mathbf{RT}_1 - \mathbb{P}_1 - \mathbf{P}_2 - \mathbf{RT}_1 - \mathbf{P}_2$  scheme with quasi-uniform refinement.

| N      | $h$   | $e(\mathbf{t})$ | $r(\mathbf{t})$ | $e(\boldsymbol{\sigma})$ | $r(\boldsymbol{\sigma})$ | $e(\boldsymbol{\rho})$ | $r(\boldsymbol{\rho})$ | $e(\mathbf{u})$ | $r(\mathbf{u})$ | $e(p)$ | $r(p)$ |
|--------|-------|-----------------|-----------------|--------------------------|--------------------------|------------------------|------------------------|-----------------|-----------------|--------|--------|
| 1803   | 0.190 | 1.651           | –               | 485.735                  | –                        | 2.078                  | –                      | 2.717           | –               | 11.050 | –      |
| 6987   | 0.103 | 0.692           | 1.285           | 540.574                  | –                        | 1.742                  | 0.260                  | 3.783           | –               | 11.448 | –      |
| 27345  | 0.049 | 1.409           | –               | 384.144                  | 0.501                    | 1.410                  | 0.310                  | 1.625           | 1.238           | 6.920  | 0.738  |
| 107985 | 0.026 | 1.135           | 0.315           | 231.471                  | 0.738                    | 0.932                  | 0.603                  | 0.673           | 1.285           | 2.842  | 1.296  |
| 430221 | 0.013 | 0.646           | 0.817           | 123.634                  | 0.907                    | 0.558                  | 0.742                  | 0.208           | 1.698           | 1.205  | 1.242  |

| $e(\mathbf{p})$ | $r(\mathbf{p})$ | $e(\theta)$ | $r(\theta)$ | $e(\boldsymbol{\sigma}_P)$ | $r(\boldsymbol{\sigma}_P)$ | $e$     | $r$   | $\text{eff}(\Theta_1)$ | $\text{eff}(\Theta_2)$ | iter |
|-----------------|-----------------|-------------|-------------|----------------------------|----------------------------|---------|-------|------------------------|------------------------|------|
| 260.136         | –               | 82.410      | –           | 5.521                      | –                          | 557.149 | –     | 1.010                  | 0.701                  | 8    |
| 453.925         | –               | 105.853     | –           | 6.172                      | –                          | 713.786 | –     | 1.013                  | 0.712                  | 6    |
| 338.485         | 0.430           | 31.700      | 1.767       | 4.031                      | 0.624                      | 512.982 | 0.484 | 1.002                  | 0.708                  | 5    |
| 221.602         | 0.617           | 10.676      | 1.585       | 1.674                      | 1.280                      | 320.629 | 0.684 | 1.001                  | 0.707                  | 4    |
| 125.639         | 0.821           | 2.834       | 1.919       | 0.970                      | 0.789                      | 176.293 | 0.865 | 1.000                  | 0.707                  | 3    |

Table 5.3: EXAMPLE 2,  $\mathbb{P}_0 - \mathbb{RT}_0 - \mathbb{P}_0 - \mathbf{P}_1 - \mathbf{RT}_0 - \mathbf{P}_1$  scheme with quasi-uniform refinement.

| N      | $e(\mathbf{t})$ | $r(\mathbf{t})$ | $e(\boldsymbol{\sigma})$ | $r(\boldsymbol{\sigma})$ | $e(\boldsymbol{\rho})$ | $r(\boldsymbol{\rho})$ | $e(\mathbf{u})$ | $r(\mathbf{u})$ | $e(p)$ | $r(p)$ |
|--------|-----------------|-----------------|--------------------------|--------------------------|------------------------|------------------------|-----------------|-----------------|--------|--------|
| 1803   | 1.651           | –               | 485.735                  | –                        | 2.078                  | –                      | 2.717           | –               | 11.050 | –      |
| 2793   | 1.152           | 1.645           | 477.153                  | 0.042                    | 0.887                  | 3.893                  | 2.440           | 0.491           | 5.918  | 2.854  |
| 3969   | 1.353           | –               | 233.594                  | 3.936                    | 0.604                  | 2.188                  | 0.715           | 6.984           | 3.017  | 3.834  |
| 6465   | 1.108           | 0.818           | 95.506                   | 3.515                    | 0.503                  | 0.751                  | 0.524           | 1.274           | 2.464  | 0.829  |
| 12177  | 0.985           | 0.372           | 52.350                   | 2.003                    | 0.435                  | 0.460                  | 0.425           | 0.665           | 2.127  | 0.466  |
| 24309  | 0.789           | 0.641           | 35.354                   | 1.156                    | 0.358                  | 0.558                  | 0.286           | 1.139           | 1.696  | 0.655  |
| 42405  | 0.612           | 0.913           | 26.435                   | 1.043                    | 0.284                  | 0.830                  | 0.173           | 1.822           | 1.213  | 1.204  |
| 78363  | 0.507           | 0.615           | 19.354                   | 1.030                    | 0.238                  | 0.581                  | 0.126           | 1.033           | 0.957  | 0.772  |
| 148599 | 0.337           | 1.276           | 14.094                   | 1.012                    | 0.173                  | 1.004                  | 0.067           | 1.976           | 0.668  | 1.123  |
| 286053 | 0.268           | 0.702           | 10.136                   | 0.989                    | 0.138                  | 0.682                  | 0.047           | 1.045           | 0.513  | 0.807  |
| 562743 | 0.172           | 1.313           | 7.245                    | 1.008                    | 0.089                  | 1.287                  | 0.025           | 1.904           | 0.324  | 1.358  |

| $e(\mathbf{p})$ | $r(\mathbf{p})$ | $e(\theta)$ | $r(\theta)$ | $e(\boldsymbol{\sigma}_P)$ | $r(\boldsymbol{\sigma}_P)$ | $e$     | $r$   | $\text{eff}(\Theta_1)$ | iter |
|-----------------|-----------------|-------------|-------------|----------------------------|----------------------------|---------|-------|------------------------|------|
| 260.136         | –               | 82.410      | –           | 5.521                      | –                          | 557.149 | –     | 1.010                  | 8    |
| 410.800         | –               | 57.315      | 1.659       | 3.435                      | 2.169                      | 632.238 | –     | 1.005                  | 5    |
| 218.748         | 3.587           | 20.780      | 5.775       | 2.067                      | 2.891                      | 320.704 | 3.863 | 1.003                  | 5    |
| 86.491          | 3.804           | 19.236      | 0.317       | 1.540                      | 1.207                      | 130.284 | 3.693 | 1.014                  | 5    |
| 42.241          | 2.264           | 17.562      | 0.288       | 1.316                      | 0.496                      | 69.531  | 1.984 | 1.042                  | 5    |
| 28.680          | 1.120           | 13.182      | 0.830       | 1.069                      | 0.601                      | 47.403  | 1.108 | 1.052                  | 4    |
| 21.095          | 1.104           | 10.129      | 0.947       | 0.789                      | 1.093                      | 35.311  | 1.058 | 1.053                  | 3    |
| 15.621          | 0.978           | 8.060       | 0.744       | 0.642                      | 0.670                      | 26.151  | 0.978 | 1.061                  | 3    |
| 11.037          | 1.086           | 3.787       | 2.361       | 0.440                      | 1.184                      | 18.302  | 1.116 | 1.025                  | 3    |
| 8.051           | 0.963           | 2.458       | 1.320       | 0.352                      | 0.680                      | 13.179  | 1.003 | 1.020                  | 3    |
| 5.615           | 1.065           | 0.981       | 2.716       | 0.228                      | 1.289                      | 9.221   | 1.056 | 1.007                  | 3    |

Table 5.4: EXAMPLE 2,  $\mathbb{P}_0 - \mathbb{RT}_0 - \mathbb{P}_0 - \mathbf{P}_1 - \mathbf{RT}_0 - \mathbf{P}_1$  scheme with adaptive refinement via  $\Theta_1$ .

| N      | e(t)  | r(t)  | e( $\sigma$ ) | r( $\sigma$ ) | e( $\rho$ ) | r( $\rho$ ) | e(u)  | r(u)  | e(p)   | r(p)  |
|--------|-------|-------|---------------|---------------|-------------|-------------|-------|-------|--------|-------|
| 1803   | 1.651 | –     | 485.735       | –             | 2.078       | –           | 2.717 | –     | 11.050 | –     |
| 3177   | 1.161 | 1.242 | 479.666       | 0.044         | 0.910       | 2.914       | 2.499 | 0.295 | 8.074  | 1.108 |
| 4395   | 1.358 | –     | 233.586       | 4.434         | 0.720       | 1.447       | 0.688 | 7.946 | 2.966  | 6.170 |
| 6987   | 1.041 | 1.147 | 92.836        | 3.981         | 0.438       | 2.147       | 0.453 | 1.804 | 2.021  | 1.655 |
| 12759  | 0.953 | 0.230 | 51.210        | 1.976         | 0.374       | 0.518       | 0.404 | 0.384 | 1.785  | 0.413 |
| 24789  | 0.715 | 0.864 | 34.828        | 1.161         | 0.347       | 0.224       | 0.227 | 1.732 | 1.333  | 0.878 |
| 42729  | 0.576 | 0.793 | 26.799        | 0.963         | 0.258       | 1.091       | 0.152 | 1.481 | 1.070  | 0.807 |
| 81009  | 0.435 | 0.879 | 18.989        | 1.077         | 0.218       | 0.526       | 0.095 | 1.469 | 0.865  | 0.666 |
| 151581 | 0.319 | 0.993 | 14.100        | 0.950         | 0.157       | 1.055       | 0.055 | 1.719 | 0.607  | 1.131 |
| 297489 | 0.233 | 0.924 | 9.898         | 1.050         | 0.121       | 0.757       | 0.037 | 1.191 | 0.444  | 0.924 |
| 577731 | 0.162 | 1.093 | 7.223         | 0.949         | 0.078       | 1.342       | 0.020 | 1.901 | 0.304  | 1.140 |

| e(p)    | r(p)  | e( $\theta$ ) | r( $\theta$ ) | e( $\sigma_P$ ) | r( $\sigma_P$ ) | e       | r     | eff( $\Theta_2$ ) | iter |
|---------|-------|---------------|---------------|-----------------|-----------------|---------|-------|-------------------|------|
| 260.136 | –     | 82.410        | –             | 5.521           | –               | 557.149 | –     | 0.701             | 8    |
| 408.119 | –     | 57.796        | 1.253         | 3.587           | 1.523           | 632.447 | –     | 0.709             | 5    |
| 214.041 | 3.977 | 19.688        | 6.637         | 2.312           | 2.707           | 317.437 | 4.248 | 0.708             | 5    |
| 84.584  | 4.005 | 17.847        | 0.424         | 1.442           | 2.038           | 126.858 | 3.957 | 0.712             | 5    |
| 41.294  | 2.381 | 17.352        | 0.093         | 1.301           | 0.342           | 68.044  | 2.069 | 0.723             | 4    |
| 28.423  | 1.125 | 12.086        | 1.089         | 0.955           | 0.930           | 46.558  | 1.143 | 0.720             | 4    |
| 20.719  | 1.161 | 7.255         | 1.874         | 0.751           | 0.885           | 34.649  | 1.085 | 0.715             | 3    |
| 15.350  | 0.938 | 4.951         | 1.195         | 0.565           | 0.889           | 24.919  | 1.031 | 0.709             | 3    |
| 10.830  | 1.113 | 2.240         | 2.532         | 0.422           | 0.930           | 17.923  | 1.052 | 0.704             | 3    |
| 7.893   | 0.938 | 1.568         | 1.060         | 0.313           | 0.883           | 12.760  | 1.008 | 0.699             | 3    |
| 5.517   | 1.079 | 0.641         | 2.697         | 0.214           | 1.150           | 9.113   | 1.014 | 0.699             | 3    |

Table 5.5: EXAMPLE 2,  $\mathbb{P}_0 - \mathbb{RT}_0 - \mathbb{P}_0 - \mathbf{P}_1 - \mathbf{RT}_0 - \mathbf{P}_1$  scheme with adaptive refinement via  $\Theta_2$ .

| N       | $h$   | $e(\mathbf{t})$ | $r(\mathbf{t})$ | $e(\boldsymbol{\sigma})$ | $r(\boldsymbol{\sigma})$ | $e(\boldsymbol{\rho})$ | $r(\boldsymbol{\rho})$ | $e(\mathbf{u})$ | $r(\mathbf{u})$ | $e(p)$ | $r(p)$ |
|---------|-------|-----------------|-----------------|--------------------------|--------------------------|------------------------|------------------------|-----------------|-----------------|--------|--------|
| 8884    | 0.354 | 2.808           | –               | 202.828                  | –                        | 3.755                  | –                      | 2.133           | –               | 13.714 | –      |
| 67396   | 0.177 | 2.070           | 0.451           | 196.015                  | 0.051                    | 3.701                  | 0.021                  | 2.435           | –               | 8.711  | 0.672  |
| 525316  | 0.088 | 1.703           | 0.285           | 134.581                  | 0.549                    | 2.871                  | 0.371                  | 1.288           | 0.930           | 4.323  | 1.024  |
| 4148740 | 0.044 | 1.168           | 0.548           | 79.625                   | 0.762                    | 1.811                  | 0.669                  | 0.524           | 1.307           | 2.078  | 1.063  |

| $e(\mathbf{p})$ | $r(\mathbf{p})$ | $e(\theta)$ | $r(\theta)$ | $e(\boldsymbol{\sigma}_P)$ | $r(\boldsymbol{\sigma}_P)$ | $e$     | $r$   | $\text{eff}(\Theta_1)$ | iter |
|-----------------|-----------------|-------------|-------------|----------------------------|----------------------------|---------|-------|------------------------|------|
| 160.643         | –               | 74.310      | –           | 5.237                      | –                          | 269.247 | –     | 1.040                  | 7    |
| 180.583         | –               | 68.476      | 0.121       | 3.958                      | 0.415                      | 275.218 | –     | 1.037                  | 6    |
| 121.390         | 0.580           | 33.893      | 1.027       | 3.120                      | 0.347                      | 184.416 | 0.585 | 1.020                  | 5    |
| 73.642          | 0.726           | 12.062      | 1.500       | 1.933                      | 0.695                      | 109.150 | 0.761 | 1.007                  | 4    |

Table 5.6: EXAMPLE 3,  $\mathbb{P}_0 - \mathbb{RT}_0 - \mathbb{P}_0 - \mathbf{P}_1 - \mathbf{RT}_0 - \mathbf{P}_1$  scheme with quasi-uniform refinement.

| N       | $e(\mathbf{t})$ | $r(\mathbf{t})$ | $e(\boldsymbol{\sigma})$ | $r(\boldsymbol{\sigma})$ | $e(\boldsymbol{\rho})$ | $r(\boldsymbol{\rho})$ | $e(\mathbf{u})$ | $r(\mathbf{u})$ | $e(p)$ | $r(p)$ |
|---------|-----------------|-----------------|--------------------------|--------------------------|------------------------|------------------------|-----------------|-----------------|--------|--------|
| 8884    | 2.808           | –               | 202.828                  | –                        | 3.755                  | –                      | 2.133           | –               | 13.714 | –      |
| 16760   | 2.912           | –               | 195.934                  | 0.163                    | 3.105                  | 0.898                  | 1.136           | 2.978           | 10.403 | 1.306  |
| 121932  | 1.913           | 0.635           | 135.452                  | 0.558                    | 1.815                  | 0.812                  | 1.051           | 0.118           | 5.117  | 1.073  |
| 782480  | 1.197           | 0.757           | 72.896                   | 1.000                    | 1.078                  | 0.841                  | 0.390           | 1.598           | 2.536  | 1.133  |
| 4282528 | 0.649           | 1.081           | 36.213                   | 1.235                    | 0.601                  | 1.031                  | 0.161           | 1.561           | 1.246  | 1.255  |

| $e(\mathbf{p})$ | $r(\mathbf{p})$ | $e(\theta)$ | $r(\theta)$ | $e(\boldsymbol{\sigma}_P)$ | $r(\boldsymbol{\sigma}_P)$ | $e$     | $r$   | $\text{eff}(\Theta_1)$ | iter |
|-----------------|-----------------|-------------|-------------|----------------------------|----------------------------|---------|-------|------------------------|------|
| 160.643         | –               | 74.310      | –           | 5.237                      | –                          | 269.247 | –     | 1.040                  | 7    |
| 163.159         | –               | 32.320      | 3.935       | 3.794                      | 1.524                      | 257.051 | 0.219 | 1.007                  | 6    |
| 120.935         | 0.453           | 27.820      | 0.227       | 2.455                      | 0.658                      | 183.724 | 0.508 | 1.009                  | 5    |
| 66.899          | 0.955           | 9.073       | 1.808       | 1.422                      | 0.881                      | 99.370  | 0.992 | 1.004                  | 5    |
| 33.902          | 1.200           | 3.302       | 1.784       | 0.741                      | 1.151                      | 49.724  | 1.222 | 1.006                  | 4    |

Table 5.7: EXAMPLE 3,  $\mathbb{P}_0 - \mathbb{RT}_0 - \mathbb{P}_0 - \mathbf{P}_1 - \mathbf{RT}_0 - \mathbf{P}_1$  scheme with adaptive refinement via  $\Theta_1$ .

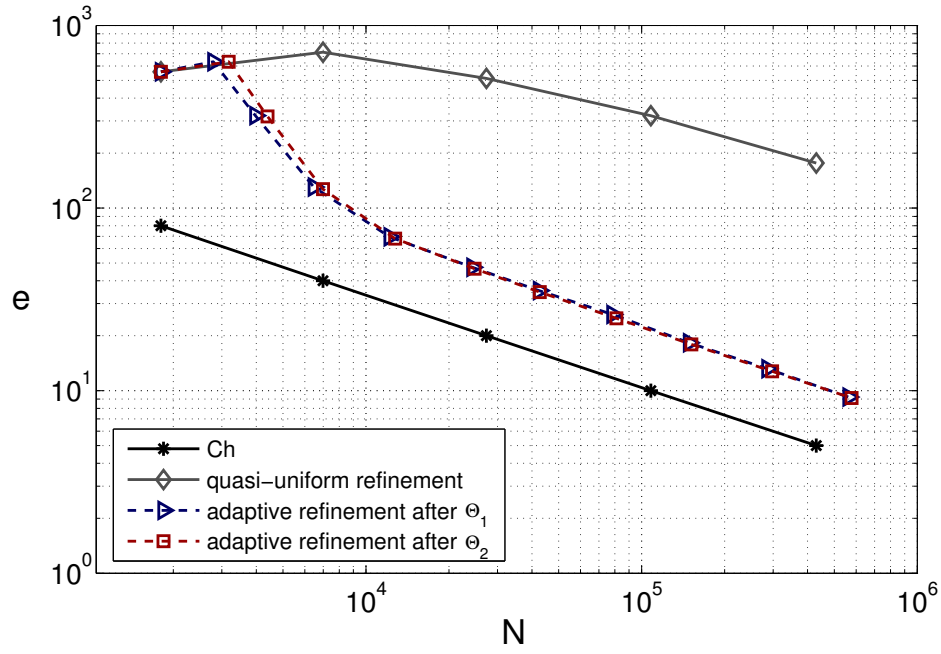
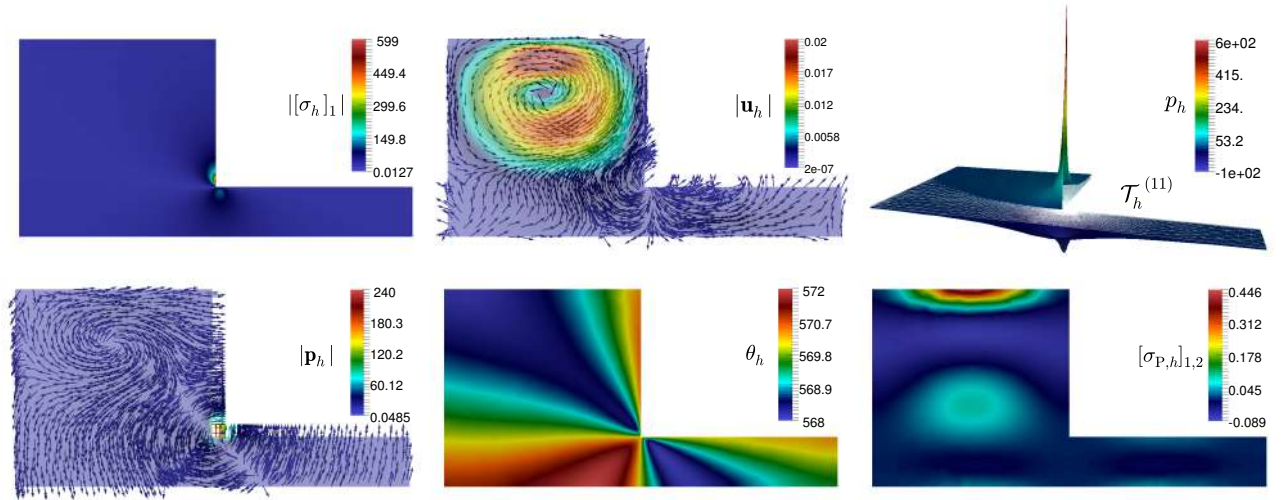
Figure 5.1: Example 2,  $e$  vs.  $N$  for quasi-uniform/adaptive schemes.

Figure 5.2: Example 2, approximated spectral norm of the stress tensor component, velocity streamlines, and pressure field (top panels), heat flux streamlines, temperature field, and polymeric part of the extra-stress tensor component (bottom panels).

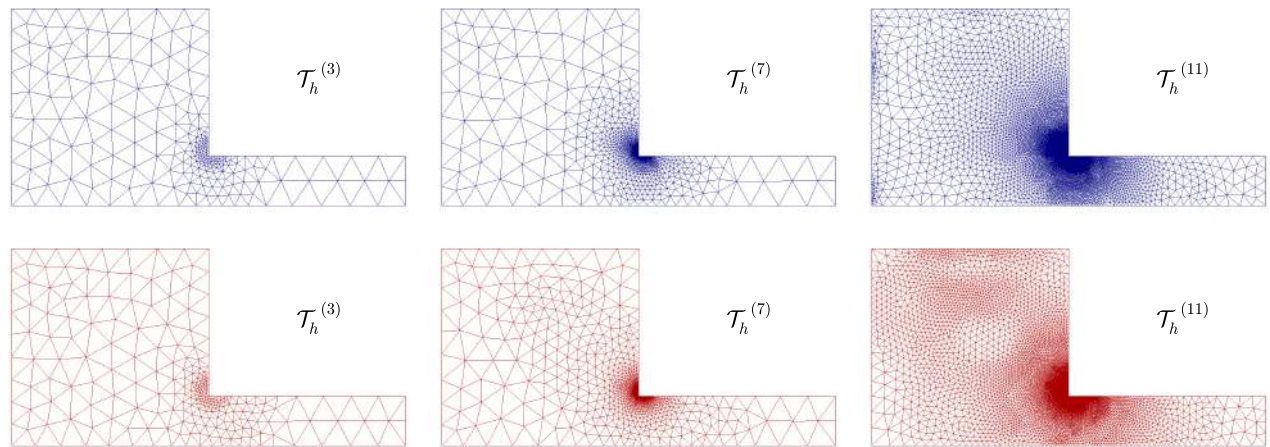


Figure 5.3: Example 2, three snapshots of adapted meshes according to the indicators  $\Theta_1$  and  $\Theta_2$  (top and bottom panels, respectively).

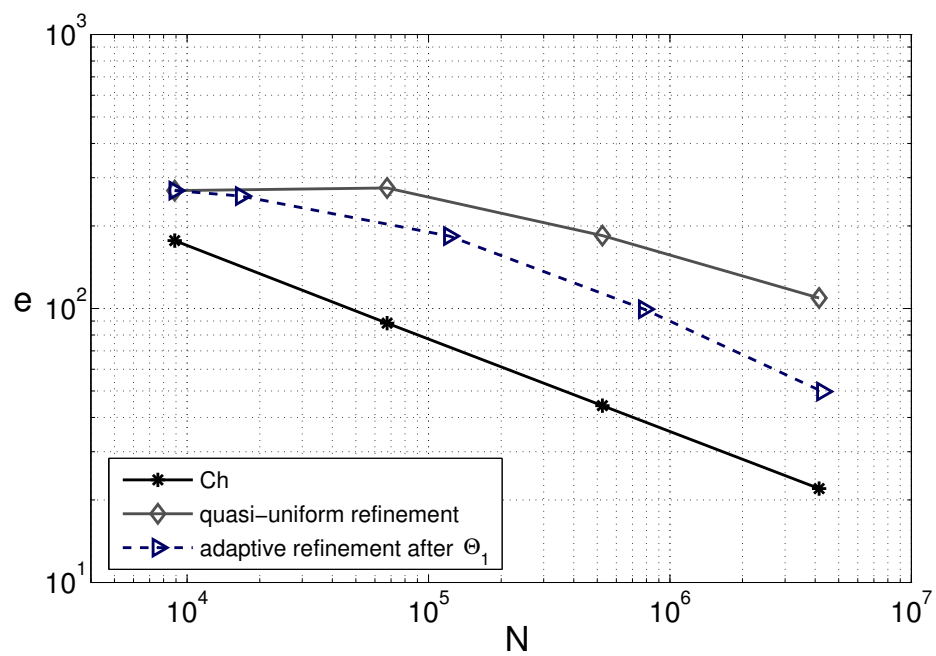


Figure 5.4: Example 3,  $e$  vs.  $N$  for quasi-uniform/adaptive scheme via  $\Theta_1$ .



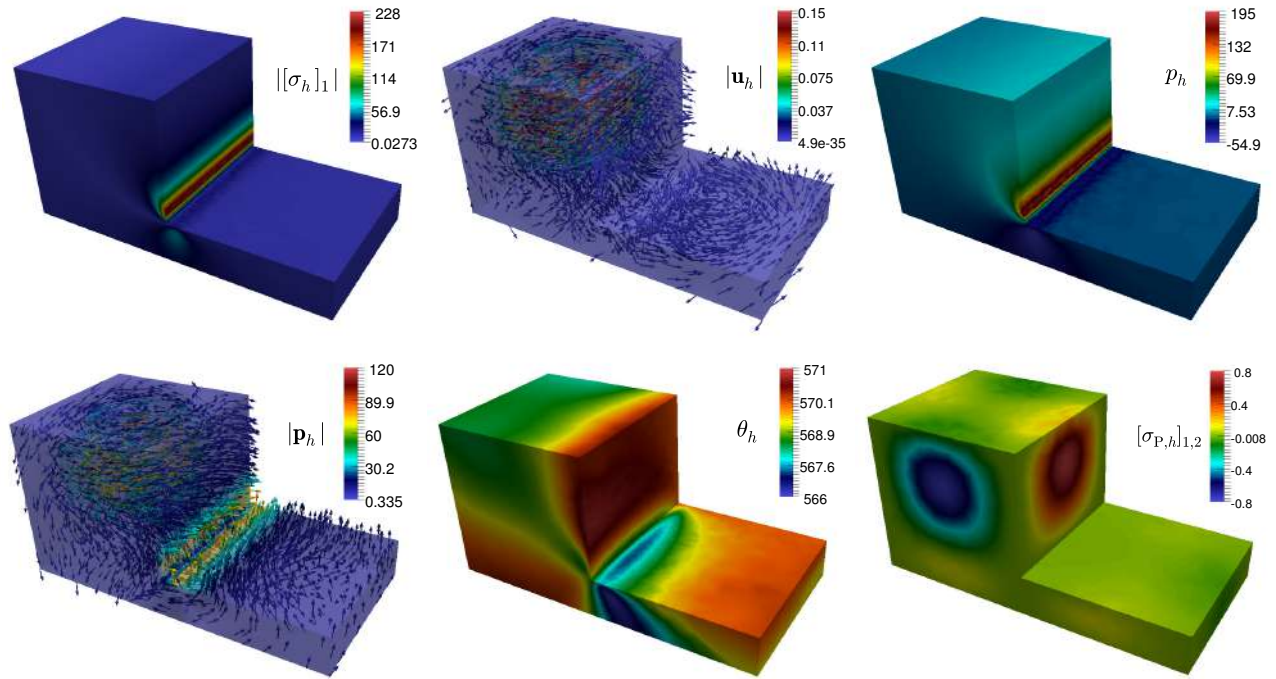


Figure 5.5: Example 3, approximated spectral norm of the stress tensor component, velocity streamlines, and pressure field (top panels), heat flux streamlines, temperature field, and polymeric part of the extra-stress tensor component (bottom panels).

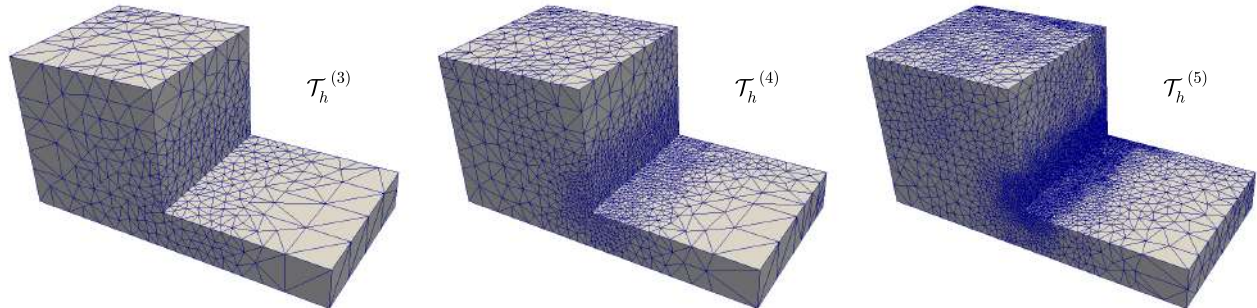


Figure 5.6: Example 3, three snapshots of adapted meshes according to the indicators  $\Theta_1$ .

### Conclusions

In this thesis we develop mixed finite element methods for a set of partial differential equations of physical interest in fluid mechanics, more precisely, linear and nonlinear coupled problems in porous media and non-isothermal flows. We have proved solvability of both continuous and discrete problems as well as their convergence, all illustrated by means of examples and numerical simulations. The main conclusions of this work are:

1. We introduced a fully-mixed finite element method for the Navier–Stokes/Darcy coupled problem with nonlinear viscosity. The original problem was reformulated by an augmented variational approach in the incompressible viscous fluid modelled by the Navier–Stokes equations (with nonlinear viscosity) coupled with a mixed formulation for the flow in a porous medium described by the linear Darcy equations. Then, through a fixed-point strategy together with sufficiently small data assumptions, the corresponding solvability analysis was developed. Consequently, an augmented fully-mixed finite element method was derived for arbitrary spaces, and then we showed it is well-posed. In particular, for Raviart–Thomas spaces in 2D and 3D convergence of the method was proved. Finally, several numerical experiments were reported in order to validate the good performance of the method and confirm the corresponding order of convergence.
2. We established the a posteriori error analysis for the fully-mixed finite element method associated to the Navier–Stokes/Darcy coupled problem with nonlinear viscosity. We derive a reliable and efficient residual-based a posteriori error estimator for that scheme. In addition, several numerical results were provided in order to illustrate the reliability and efficiency of the estimator, together with the expected behavior of the associated adaptive algorithm.
3. We developed a mixed finite element method for the Navier–Stokes/Darcy–Forchheimer coupled problem with constant viscosity and density. By means of a fixed-point strategy, classical results on nonlinear monotone operators, and small data assumptions, we developed the corresponding solvability analysis of both the continuous and discrete problems. In particular, we considered the discrete spaces of Bernardi–Raugel for the velocity in the fluid, Raviart–Thomas elements of lowest order for the filtration velocity in the porous medium, piecewise constants with null mean value for the pressures, and piecewise constants elements for the Lagrange multiplier on the interface. Theoretical and numerically we obtained sub-optimal and optimal order of convergence, respectively.

4. We introduced a new fully-mixed finite element method for the non-isothermal Oldroyd-Stokes problem. For convenience of the analysis, we introduced the strain tensor, vorticity, and stress as additional unknowns (besides the polymeric part of the extra-stress tensor, the velocity, the pressure, and the temperature of the fluid). Which allow us to join the polymeric and solvent viscosities in a dimensionless viscosity, and to eliminate the polymeric part of the extra-stress tensor and the pressure from the system, which, together with the solvent part of the extra-stress tensor, were recovered through of an appropriate postprocessing formula. In this sense, a fully-mixed approximation was applied, in which the heat-flux vector was incorporated as an additional unknown. We prove solvability of both the continuous and discrete problems as well as its corresponding a priori estimate.
5. We established the a posteriori error analysis for the fully-mixed finite element method associated to the non-isothermal Oldroyd-Stokes problem. We derived two reliable and efficient residual-based a posteriori error estimators.

## Future works

The methods developed and the results obtained in this thesis have motivated to several ongoing and future projects. Some of them are described below:

1. **A posteriori error analysis for the Navier-Stokes/Darcy-Forchheimer coupled problem.**

As a natural continuation, we are interested in carrying out an a posteriori error analysis for the coupled problem studied in Chapter 3 to improve its robustness in the context of problems involving complex geometries or solutions with high gradients.

2. **Analysis of an augmented mixed-primal formulation for the non-isothermal Oldroyd-Stokes problem.**

As a complement and alternative to our fully-mixed method presented in Chapter 4, we are interested in studying a formulation that is mixed in the fluid but without considering the vorticity as an unknown of the system as in [29] and primal in the heat as in [50]. Consequently, this approach allows us to eliminate two unknowns from the system (vorticity and heat-flux) and several redundant Galerkin terms associated with them.

3. **Development of new mixed finite element methods for the non-isothermal Stokes-Darcy coupled problem.**

In accordance with the theoretical and numerical techniques applied to coupled problems in porous media and non-isothermal flows developed in this thesis. We are interested in extend our study to the non-isothermal Stokes-Darcy coupled problem proposed in [55], in order to model the movement of a non-isothermal quasi-Newtonian viscous fluid that occupies the region  $\Omega_S$  (modelled by the Stokes equation with temperature-dependent viscosity) which flows towards and from a porous medium  $\Omega_D$  through  $\Sigma$ , where  $\Omega_D$  is saturated with the same fluid (modelled by the Darcy equation with temperature-dependent viscosity and permeability).

4. **Development of new mixed finite element methods for the double-diffusive non-linear convection problem through a porous medium.**

Finally, another future goal is to analyse the problem of double-diffusive non-linear convection through a porous medium based upon the Brinkman–Forchheimer model proposed in [119]:

$$\begin{aligned} -\mu_0 D_a \Delta \mathbf{u} + \mathbf{M}\mathbf{u} + \sigma D_a R_\theta |\mathbf{u}| \mathbf{u} + \nabla p &= \mathbf{f}(\theta, S) \quad \text{in } \Omega, \quad \operatorname{div} \mathbf{u} = 0 \quad \text{in } \Omega, \\ -\operatorname{div}(\mathbf{N} \nabla \theta) + R_\theta \mathbf{u} \cdot \nabla \theta &= 0 \quad \text{in } \Omega, \quad -\operatorname{div}(\mathbf{Q} \nabla S) + \tau R_S \mathbf{u} \cdot \nabla S = 0 \quad \text{in } \Omega, \\ \mathbf{u} &= \mathbf{u}_D \quad \text{on } \partial\Omega, \quad \theta = \theta_D \quad \text{on } \partial\Omega, \quad S = S_D \quad \text{on } \partial\Omega, \end{aligned}$$

where  $\mathbf{u}$  is the filtration velocity,  $p$  is the pressure,  $\theta$  is the temperature, and  $S$  is the concentration of a fluid occupying the region  $\Omega$ . In addition,  $\mathbf{M}$ ,  $\mathbf{N}$ , and  $\mathbf{Q}$  are the permeability, thermal diffusion and concentration diffusion tensors, respectively, meanwhile  $R_\theta, R_S, D_a, \sigma, \tau$ , and  $\mu_0$  are physical constants. According to the mathematical structure of this model, the study carried out in Chapter 3 for porous media modelled by the Darcy–Forchheimer equation and the theory for non-isothermal fluids developed in Chapters 4 and 5, we plan to extend our technical and numerical techniques to this model, considering an approach based on mixed-primal and fully-mixed finite element methods, as well as their corresponding adaptive algorithms. We advance that by introducing the tensor  $\mathbf{T} := \mu_0 D_a \nabla \mathbf{u} - p \mathbb{I}$ , the first two equations of the system can be rewritten as:

$$\frac{1}{\mu_0 D_a} \mathbf{T}^d = \nabla \mathbf{u} \quad \text{in } \Omega, \quad -\operatorname{div}(\mathbf{T}) + \mathbf{M}\mathbf{u} + \sigma D_a R_\theta |\mathbf{u}| \mathbf{u} = \mathbf{f}(\theta, S) \quad \text{in } \Omega,$$

where the pressure  $p = -\frac{1}{n} \operatorname{tr}(\mathbf{T})$  in  $\Omega$ , it has been removed from the system and can be recovered by post-processing. This approach motivates the study of a mixed formulation for the Brinkman–Forchheimer equations.

### Conclusiones

En esta tesis desarrollamos métodos de elementos finitos mixtos para un conjunto de ecuaciones diferenciales parciales de interés físico en mecánica de fluidos, más precisamente, problemas lineales y no lineales acoplados en medios porosos y flujos no isotérmicos. Hemos demostrado solubilidad de los problemas continuo y discreto, así como su convergencia, todo ilustrado mediante ejemplos y simulaciones numéricas. Las principales conclusiones de este trabajo son:

1. Introdujimos un método de elementos finitos completamente mixto para el problema acoplado de Navier–Stokes/Darcy con viscosidad no lineal. El problema original fue reformulado mediante un enfoque variacional aumentado para el fluido viscoso incompresible modelado por las ecuaciones de Navier–Stokes (con viscosidad no lineal) acoplado con una formulación mixta para el flujo en el medio poroso descrito por las ecuaciones de Darcy lineal. Seguidamente, a través de una estrategia de punto fijo junto con supuestos de datos suficientemente pequeños, fue desarrollado el análisis de solubilidad correspondiente. Consecuentemente, se derivó un método de elementos completamente mixto aumentado para espacios genéricos, y luego se probó que el mismo estaba bien puesto. En particular, para espacios de Raviart–Thomas en 2D y 3D se demostró convergencia del método. Finalmente, se reportaron varios experimentos numéricos que validaron el buen desempeño del método y que confirmaron los órdenes de convergencia correspondientes.
2. Establecimos el análisis de error a posteriori para el método de elementos finitos completamente mixto aumentado asociado al problema acoplado de Navier–Stokes/Darcy con viscosidad no lineal. Derivamos un estimador de error a posteriori confiable y eficiente de tipo residual para dicho esquema. Además, se proporcionaron varios resultados numéricos que ilustraron la confiabilidad y la eficiencia del estimador, junto con el comportamiento esperado del algoritmo adaptativo asociado.
3. Desarrollamos un método de elementos finitos mixto para el problema acoplado de Navier–Stokes/Darcy–Forchheimer con viscosidad y densidad constantes. Por medio de una estrategia de punto fijo, resultados clásicos de operadores monótonos no lineales, y supuestos de dato pequeño, desarrollamos el análisis de solubilidad para los problemas continuo y discreto. En particular, consideramos espacios de Bernardi–Raugel para la velocidad en el fluido, elementos de Raviart–Thomas de bajo orden para la velocidad de filtración en el medio poroso, constantes a trozos con medida nula para la presiones, y constantes a trozos para el multiplicador de Lagrange sobre

la interfaz. Teóricamente y numéricamente obtuvimos órdenes de convergencia sub-óptimos y óptimos, respectivamente.

4. Introdujimos un nuevo método de elementos finitos completamente mixto para el problema de Oldroyd–Stokes no isotérmico. Por conveniencia del análisis, introdujimos el tensor de pequeñas deformaciones, la vorticidad, y el esfuerzo como incógnitas adicionales (además de la parte polimérica del tensor de extra-esfuerzo, la velocidad, la presión, y la temperatura del fluido). Lo que nos permitió unir las viscosidades polimérica y solvente en una viscosidad adimensional, y eliminar del sistema la parte polimérica del tensor de extra-esfuerzo y la presión, las que, junto con la parte solvente del tensor de extra-esfuerzo, fueron recuperadas a través de una fórmula de postproceso adecuada. En este sentido, una aproximación completamente mixta fué aplicada, en la que el vector de flujo de calor se incorporó como una incógnita adicional. Demostramos solubilidad de los problemas continuo y discreto, con su estimación a priori correspondiente.
5. Establecimos el análisis de error a posteriori para el método de elementos finitos completamente mixto aumentado asociado al problema de Oldroyd–Stokes no isotérmico. Derivamos dos estimadores de error a posteriori confiables y eficientes de tipo residual para dicho esquema.

## Trabajos futuros

Los métodos desarrollados y los resultados obtenidos en esta tesis han motivado varios proyectos en proceso y a futuro. Algunos de ellos son descritos a continuación:

1. **Análisis de error a posteriori para el problema acoplado de Navier–Stokes/Darcy–Forchheimer.**

Como una continuación natural, estamos interesados en llevar a cabo un análisis de error a posteriori para el problema acoplado estudiado en el Capítulo 3 para mejorar su robustez ante problemas en los cuales se involucran geometrías complejas o soluciones con altos gradientes.

2. **Análisis de una nueva formulación mixta-primal aumentada para el problema de Oldroyd–Stokes no isotérmico.**

Como complemento y alternativa a nuestro método completamente mixto presentado en el Capítulo 4, nos interesa estudiar una formulación que sea mixta en el fluido pero sin considerar la vorticidad como incógnita del sistema al igual que en [29] y primal en el calor como en [50]. En consecuencia, este enfoque nos permite eliminar dos incógnitas de sistema (la vorticidad y el flujo de calor) y varios términos de Galerkin asociados a ellos.

3. **Desarrollo de nuevos métodos de elementos finitos mixtos para el problema acoplado de Stokes–Darcy no isotérmico.**

Acorde a las técnicas teóricas y numéricas aplicadas a problemas acoplados en medios porosos y flujos no isotérmicos desarrolladas en esta tesis. Estamos interesados en extender nuestro estudio al problema acoplado de Stokes–Darcy no isotérmico propuesto en [55], el cual modela el movimiento de un fluido viscoso cuasi-Newtoniano no isotérmico que ocupa el dominio  $\Omega_S$  (modelado por la ecuación de Stokes con viscosidad dependiente de la temperatura) y que fluye hacia y desde el dominio  $\Omega_D$  a través de la interfaz  $\Sigma$ , donde  $\Omega_D$  está saturado con el mismo

fluido (modelado por la ecuación de Darcy con viscosidad y permeabilidad dependiente de la temperatura).

4. **Desarrollo de nuevos métodos de elementos finitos mixtos para el problema de convección no lineal doble-difusivo a través de un medio poroso.**

Finalmente, otro objetivo a futuro es analizar el problema de convección no lineal doble-difusivo a través de un medio poroso modelado por las ecuaciones de Brinkman–Forchheimer propuesto en [119]:

$$\begin{aligned} -\mu_0 D_a \Delta \mathbf{u} + \mathbf{M} \mathbf{u} + \sigma D_a R_\theta |\mathbf{u}| \mathbf{u} + \nabla p &= \mathbf{f}(\theta, S) \quad \text{en } \Omega, \quad \operatorname{div} \mathbf{u} = 0 \quad \text{en } \Omega, \\ -\operatorname{div}(\mathbf{N} \nabla \theta) + R_\theta \mathbf{u} \cdot \nabla \theta &= 0 \quad \text{en } \Omega, \quad -\operatorname{div}(\mathbf{Q} \nabla S) + \tau R_S \mathbf{u} \cdot \nabla S = 0 \quad \text{en } \Omega, \\ \mathbf{u} &= \mathbf{u}_D \quad \text{sobre } \partial\Omega, \quad \theta = \theta_D \quad \text{sobre } \partial\Omega, \quad S = S_D \quad \text{sobre } \partial\Omega, \end{aligned}$$

donde  $\mathbf{u}$  es la velocidad de filtración,  $p$  es la presión,  $\theta$  es la temperatura, y  $S$  es la concentración del fluido que ocupa la región  $\Omega$ . Además,  $\mathbf{M}$ ,  $\mathbf{N}$ , y  $\mathbf{Q}$  son los tensores de permeabilidad, de difusión térmica, y de difusión de la concentración, respectivamente, mientras que  $R_\theta$ ,  $R_S$ ,  $D_a$ ,  $\sigma$ ,  $\tau$ , y  $\mu_0$  son constantes físicas. Acorde a la estructura matemática de este modelo, el estudio realizado en el Capítulo 3 para medios porosos modelados por la ecuación de Darcy–Forchheimer y la teoría para fluidos no isotérmicos desarrollada en los Capítulos 4 y 5, pretendemos extender nuestras técnicas teóricas y numéricas a dicho modelo, considerando un enfoque basado en métodos de elementos finitos mixto-primal y completamente mixto, así como sus correspondientes algoritmos adaptativos. Adelantamos que al introducir el tensor  $\mathbf{T} := \mu_0 D_a \nabla \mathbf{u} - p \mathbb{I}$ , las dos primeras ecuaciones del sistema pueden ser reescritas como:

$$\frac{1}{\mu_0 D_a} \mathbf{T}^d = \nabla \mathbf{u} \quad \text{en } \Omega, \quad -\operatorname{div}(\mathbf{T}) + \mathbf{M} \mathbf{u} + \sigma D_a R_\theta |\mathbf{u}| \mathbf{u} = \mathbf{f}(\theta, S) \quad \text{en } \Omega,$$

donde la presión  $p = -\frac{1}{n} \operatorname{tr}(\mathbf{T})$  en  $\Omega$ , ha sido eliminada del sistema y puede ser recuperada por postproceso. Este enfoque, motiva el estudio de una formulación mixta para las ecuaciones de Brinkman–Forchheimer.

---

## References

---

- [1] R. A. ADAMS AND J. J. F. FOURNIER, *Sobolev Spaces*, Academic Press, Elsevier Ltd, 2003.
- [2] M. ALVAREZ, G. N. GATICA, AND R. RUIZ-BAIER, *An augmented mixed-primal finite element method for a coupled flow-transport problem*, ESAIM: Mathematical Modelling and Numerical Analysis, 49 (2015), pp. 1399–1427.
- [3] ———, *A posteriori error analysis for a viscous flow-transport problem*, ESAIM: Mathematical Modelling and Numerical Analysis, 50 (2016), pp. 1789–1816.
- [4] M. AMARA AND J. BARANGER, *An extra stress-vorticity formulation of Stokes problem for the Oldroyd viscoelastic model*, Numerische Mathematik, 94 (2003), pp. 603–622.
- [5] M. AMARA, D. CAPATINA, AND L. LIZAIK, *Coupling of Darcy–Forchheimer and compressible Navier–Stokes equations with heat transfer*, SIAM Journal on Scientific Computing, 31 (2008/09), pp. 1470–1499.
- [6] T. ARBOGAST AND D. S. BRUNSON, *A computational method for approximating a Darcy–Stokes system governing a vuggy porous medium*, Computational Geosciences, 11 (2007), pp. 207–218.
- [7] T. ARBOGAST AND H. L. LEHR, *Homogenization of a Darcy–Stokes system modeling vuggy porous media*, Computational Geosciences, 10 (2006), pp. 291–302.
- [8] M. M. ARZANFUDI, S. SAEID, R. AL-KHOURY, AND L. J. SLUYS, *Multidomain-staggered coupling technique for Darcy–Navier Stokes multiphase flow: An application to CO<sub>2</sub> geosequestration*, Finite Elements in Analysis and Design, 121 (2016), pp. 52–63.
- [9] K. AZIZ AND A. SETTARI, *Petroleum Reservoir Simulation*, Applied Science Publishers LTD, London, 1979.
- [10] I. BABUŠKA AND G. N. GATICA, *A residual-based a posteriori error estimator for the Stokes–Darcy coupled problem*, SIAM Journal on Numerical Analysis, 48 (2010), pp. 498–523.
- [11] L. BADEA, M. DISCACCIATI, AND A. QUARTERONI, *Numerical analysis of the Navier–Stokes/Darcy coupling*, Numerische Mathematik, 115 (2010), pp. 195–227.
- [12] A. BAGCHI AND F. A. KULACKI, *Natural Convection in Superposed Fluid-Porous Layers*, SpringerBriefs in Applied Sciences and Technology. Springer New York, 2014.
- [13] J. BARANGER, C. GUILLOPÉ, AND J.-C. SAUT, *Mathematical analysis of differential models for viscoelastic fluids*, Rheology Series, 5 (1996), pp. 199–236.



- [14] J. BARANGER AND D. SANDRI, *A formulation of Stokes's problem and the linear elasticity equations suggested by the Oldroyd model for viscoelastic flow*, RAIRO Modélisation Mathématique et Analyse Numérique, 26 (1992), pp. 331–345.
- [15] T. P. BARRIOS, G. N. GATICA, M. GONZÁLEZ, AND N. HEUER, *A residual based a posteriori error estimator for an augmented mixed finite element method in linear elasticity*, M2AN Mathematical Modelling and Numerical Analysis, 40 (2006), pp. 843–869.
- [16] G. S. BEAVERS AND D. D. JOSEPH, *Boundary conditions at a naturally permeable wall*, Journal of Fluid Mechanics, 30 (1967), pp. 197–207.
- [17] C. BERNARDI AND G. RAUGEL, *Analysis of some finite elements for the Stokes problem*, Mathematics of Computation, 44 (1985), pp. 71–79.
- [18] H. BREZIS AND P. MIRONESCU, *Gagliardo-Nirenberg, composition and products in fractional Sobolev spaces*, Journal of Evolution Equations, 1 (2001), pp. 387–404.
- [19] F. BREZZI AND M. FORTIN, *Mixed and Hybrid Finite Element Methods*, Springer Series in Computational Mathematics, 15. Springer-Verlag, New York, 1991.
- [20] F. BREZZI, M. FORTIN, AND L. D. MARINI, *Mixed finite element methods with continuous stresses*, Mathematical Models and Methods in Applied Sciences, 3 (1993), pp. 275–287.
- [21] A. BUFFA, M. COSTABEL, AND D. SHEEN, *On traces for  $\mathbf{H}(\mathbf{curl}, \Omega)$  in Lipschitz domains*, Journal of Mathematical Analysis and Applications, 276 (2002), pp. 845–867.
- [22] M. CAI, M. MU, AND J. XU, *Numerical solution to a mixed Navier–Stokes/Darcy model by the two-grid approach*, SIAM Journal on Numerical Analysis, 47 (2009), pp. 3325–3338.
- [23] Z. CAI, C. TONG, P. S. VASSILEVSKI, AND C. WANG, *Mixed finite element methods for incompressible flow: stationary Stokes equations*, Numerical Methods for Partial Differential Equations, 26 (2010), pp. 957–978.
- [24] Z. CAI, C. WANG, AND S. ZHANG, *Mixed finite element methods for incompressible flow: stationary Navier–Stokes equations*, SIAM Journal on Numerical Analysis, 48 (2010), pp. 79–94.
- [25] Z. CAI AND S. ZHANG, *Mixed methods for stationary Navier–Stokes equations based on pseudostress-pressure-velocity formulation*, Mathematics of Computation, 81 (2012), pp. 1903–1927.
- [26] J. CAMAÑO, G. N. GATICA, R. OYARZÚA, AND R. RUIZ-BAIER, *An augmented stress-based mixed finite element method for the steady state Navier–Stokes equations with nonlinear viscosity*, Numerical Methods for Partial Differential Equations, 33 (2017), pp. 1692–1725.
- [27] J. CAMAÑO, G. N. GATICA, R. OYARZÚA, R. RUIZ-BAIER, AND P. VENEGAS, *New fully-mixed finite element methods for the Stokes–Darcy coupling*, Computer Methods in Applied Mechanics and Engineering, 295 (2015), pp. 362–395.

- [28] J. CAMAÑO, G. N. GATICA, R. OYARZÚA, AND G. TIERRA, *An augmented mixed finite element method for the Navier–Stokes equations with variable viscosity*, SIAM Journal on Numerical Analysis, 54 (2016), pp. 1069–1092.
- [29] J. CAMAÑO, R. OYARZÚA, R. RUIZ-BAIER, AND G. TIERRA, *Error analysis of an augmented mixed method for the Navier–Stokes problem with mixed boundary conditions*, Preprint 2016–36, Centro de Investigación en Ingeniería Matemática (CI<sup>2</sup>MA), Universidad de Concepción, Chile, (2016).
- [30] J. CAMAÑO, R. OYARZÚA, AND G. TIERRA, *Analysis of an augmented mixed-FEM for the Navier–Stokes problem*, Mathematics of Computation, 86 (2017), pp. 589–615.
- [31] C. CANUTO AND F. CIMOLIN, *A sweating model for the internal ventilation of a motorcycle helmet*, Computers & Fluids, 43 (2011), pp. 29–37.
- [32] Y. CAO, Y. CHU, X. HE, AND M. WEI, *Decoupling the stationary Navier–Stokes–Darcy system with the Beavers–Joseph–Saffman interface condition*, Abstract and Applied Analysis, Art. ID 136483 (2013), p. 10.
- [33] A. E. CAOLA, Y. L. JOO, R. C. ARMSTRONG, AND R. A. BROWN, *Highly parallel time integration of viscoelastic flows*, Journal of Non-Newtonian Fluid Mechanics, 100 (2001), pp. 191–216.
- [34] C. CARSTENSEN, *A posteriori error estimate for the mixed finite element method*, Mathematics of Computation, 66 (1997), pp. 465–476.
- [35] E. CASTILLO AND R. CODINA, *Stabilized stress-velocity-pressure finite element formulations of the Navier–Stokes problem for fluids with non-linear viscosity*, Computer Methods in Applied Mechanics and Engineering, 279 (2014), pp. 554–578.
- [36] S. CAUCAO, M. DISCACCIATI, G. N. GATICA, AND R. OYARZÚA, *A conforming mixed finite element method for the Navier–Stokes/Darcy–Forchheimer coupled problem*, Preprint 2017–29, Centro de Investigación en Ingeniería Matemática (CI<sup>2</sup>MA), Universidad de Concepción, Chile, (2017).
- [37] S. CAUCAO, G. N. GATICA, AND R. OYARZÚA, *Analysis of an augmented fully-mixed formulation for the non-isothermal Oldroyd–Stokes problem*, Preprint 2017–21, Centro de Investigación en Ingeniería Matemática (CI<sup>2</sup>MA), Universidad de Concepción, Chile, (2017).
- [38] —, *A posteriori error analysis of a fully-mixed formulation for the Navier–Stokes/Darcy coupled problem with nonlinear viscosity*, Computer Methods in Applied Mechanics and Engineering, 315 (2017), pp. 943–971.
- [39] —, *A posteriori error analysis of an augmented fully-mixed formulation for the non-isothermal Oldroyd–Stokes problem*, Preprint 2017–25, Centro de Investigación en Ingeniería Matemática (CI<sup>2</sup>MA), Universidad de Concepción, Chile, (2017).
- [40] S. CAUCAO, G. N. GATICA, R. OYARZÚA, AND I. ŠEBESTOVÁ, *A fully-mixed finite element method for the Navier–Stokes/Darcy coupled problem with nonlinear viscosity*, Journal of Numerical Mathematics, 25 (2017), pp. 55–88.

- [41] S. CAUCAO, D. MORA, AND R. OYARZÚA, *A priori and a posteriori error analysis of a pseudostress-based mixed formulation of the Stokes problem with varying density*, IMA Journal of Numerical Analysis, 36 (2016), pp. 947–983.
- [42] A. ÇEŞMELIOĞLU, V. GIRAULT, AND B. RIVIÈRE, *Time-dependent coupling of Navier–Stokes and Darcy flows*, ESAIM: Mathematical Modelling and Numerical Analysis, 47 (2013), pp. 539–554.
- [43] A. ÇEŞMELIOĞLU AND B. RIVIÈRE, *Analysis of time-dependent Navier–Stokes flow coupled with Darcy flow*, Journal of Numerical Mathematics, 16 (2008), pp. 249–280.
- [44] W. CHEN AND Y. WANG, *A posteriori error estimate for the  $H(\text{div})$  conforming mixed finite element for the coupled Darcy–Stokes system*, Journal of Computational and Applied Mathematics, 255 (2014), pp. 502–516.
- [45] P. CHIDYAGWAI AND B. RIVIÈRE, *On the solution of the coupled Navier–Stokes and Darcy equations*, Computer Methods in Applied Mechanics and Engineering, 198 (2009), pp. 3806–3820.
- [46] T. CHINYOKA, *Modeling of cross-flow heat exchangers with viscoelastic fluids*, Nonlinear Analysis. Real World Applications, 10 (2009), pp. 3353–3359.
- [47] P. CIARLET, *Linear and Nonlinear Functional Analysis with Applications*, Society for Industrial and Applied Mathematics, Philadelphia, PA, 2013.
- [48] F. CIMOLIN AND M. DISCACCIATI, *Navier–Stokes/Forchheimer models for filtration through porous media*, Applied Numerical Mathematics, 72 (2013), pp. 205–224.
- [49] P. CLÉMENT, *Approximation by finite element functions using local regularisation*, RAIRO Modélisation Mathématique et Analyse Numérique, 9 (1975), pp. 77–84.
- [50] E. COLMENARES, G. N. GATICA, AND R. OYARZÚA, *Analysis of an augmented mixed-primal formulation for the stationary Boussinesq problem*, Numerical Methods for Partial Differential Equations, 32 (2016), pp. 445–478.
- [51] —, *Fixed point strategies for mixed variational formulations of the stationary Boussinesq problem*, Comptes Rendus Mathématique. Académie des Sciences. Paris, 354 (2016), pp. 57–62.
- [52] —, *An augmented fully-mixed finite element method for the stationary Boussinesq problem*, Calcolo, 54 (2017), pp. 167–205.
- [53] —, *A posteriori error analysis of an augmented fully-mixed formulation for the stationary Boussinesq model*, Preprint 2017–17, Centro de Investigación en Ingeniería Matemática (CI<sup>2</sup>MA), Universidad de Concepción, Chile, (2017).
- [54] —, *A posteriori error analysis of an augmented mixed-primal formulation for the stationary Boussinesq model*, Calcolo, 54 (2017), pp. 1055–1095.
- [55] L. CONSIGLIERI, *Heat-conducting viscous fluids over porous media*, Communications in Mathematical Sciences, 10 (2012), pp. 835–857.

- [56] C. COX, H. LEE, AND D. SZURLEY, *Finite element approximation of the non-isothermal Stokes–Oldroyd equations*, International Journal of Numerical Analysis and Modelling, 4 (2007), pp. 425–440.
- [57] ———, *Optimal control of non-isothermal viscous fluid flow*, Mathematical and Computer Modelling, 50 (2009), pp. 1142–1153.
- [58] M. CUI AND N. YAN, *A posteriori error estimate for the Stokes–Darcy system*, Mathematical Methods in the Applied Sciences, 34 (2011), pp. 1050–1064.
- [59] ———, *Residual based a posteriori error estimates for convex optimal control problems governed by Stokes–Darcy equations*, Numerical Mathematics. Theory, Methods and Applications, 5 (2012), pp. 602–634.
- [60] S. DAMAK AND C. GUILLOPÉ, *Non-isothermal flows of viscoelastic incompressible fluids*, Non-linear Analysis. Theory, Methods & Applications, 7 (2001), pp. 919–942.
- [61] M. DAUGE, *Stationary Stokes and Navier–Stokes systems on two- or three-dimensional domains with corners. I. linearized equations*, SIAM Journal on Mathematical Analysis, 20 (1989), pp. 74–97.
- [62] T. DAVIS, *Algorithm 832: UMFPACK V4.3 - an unsymmetric-pattern multifrontal method*, ACM Transactions on Mathematical Software, 30 (2004), pp. 196–199.
- [63] M. DISCACCIATI, *Domain Decomposition Methods for the Coupling of Surface and Groundwater Flows*, École Polytechnique Fédérale de Lausanne, Switzerland, 2004.
- [64] M. DISCACCIATI, E. MIGLIO, AND A. QUARTERONI, *Mathematical and numerical models for coupling surface and groundwater flows*, Applied Numerical Mathematics, 43 (2002), pp. 57–74.
- [65] M. DISCACCIATI AND R. OYARZÚA, *A conforming mixed finite element method for the Navier–Stokes/Darcy coupled problem*, Numerische Mathematik, 135 (2017), pp. 571–606.
- [66] M. DISCACCIATI AND A. QUARTERONI, *Navier–Stokes/Darcy coupling: modeling, analysis, and numerical approximation*, Revista Matemática Complutense, 22 (2009), pp. 315–426.
- [67] C. DOMÍNGUEZ, G. N. GATICA, AND S. MEDDAHI, *A posteriori error analysis of a fully-mixed finite element method for a two-dimensional fluid-solid interaction problem*, Journal of Computational Mathematics, 33 (2015), pp. 606–641.
- [68] J. DOUGLAS AND J. WANG, *An absolutely stabilized finite element method for the Stokes problem*, Mathematics of Computation, 52 (1989), pp. 495–508.
- [69] A. ERN AND J.-L. GUERMOND, *Theory and Practice of Finite Elements*, Applied Mathematical Sciences, 159. Springer–Verlag, New York, 2004.
- [70] V. J. ERVIN, E. W. JENKINS, AND S. SUN, *Coupled generalized nonlinear Stokes flow with flow through a porous medium*, SIAM Journal on Numerical Analysis, 47 (2009), pp. 929–952.

- [71] V. J. ERVIN AND L. N. NTASIN, *A posteriori error estimation and adaptive computation of viscoelastic fluid flow*, Numerical Methods for Partial Differential Equations, 21 (2005), pp. 297–322.
- [72] M. FARHLOUL, *A mixed finite element method for a nonlinear Dirichlet problem*, IMA Journal of Numerical Analysis, 18 (1998), pp. 121–132.
- [73] M. FARHLOUL AND A. ZINE, *A dual mixed formulation for non-isothermal Oldroyd–Stokes problem*, Mathematical Modelling of Natural Phenomena, 6 (2011), pp. 130–156.
- [74] J. FAULKNER, B. X. HU, S. KISH, AND F. HUA, *Laboratory analog and numerical study of groundwater flow and solute transport in a karst aquifer with conduit and matrix domains*, Journal of Contaminant Hydrology, 110 (2009), pp. 34–44.
- [75] J. R. FERNÁNDEZ AND P. HILD, *A priori and a posteriori error analyses in the study of viscoelastic problems*, Journal of Computational and Applied Mathematics, 225 (2009), pp. 569–580.
- [76] J. R. FERNÁNDEZ AND D. SANTAMARINA, *An a posteriori error analysis for dynamic viscoelastic problems*, ESAIM: Mathematical Modelling and Numerical Analysis, 45 (2011), pp. 925–945.
- [77] L. FIGUEROA, G. N. GATICA, AND A. MÁRQUEZ, *Augmented mixed finite element methods for the stationary Stokes equations*, SIAM Journal on Scientific Computing, 31 (2008/09), pp. 1082–1119.
- [78] L. P. FRANCA AND T. J. HUGHES, *Two classes of mixed finite element methods*, Computer Methods in Applied Mechanics and Engineering, 69 (1988), pp. 89–129.
- [79] L. P. FRANCA AND R. STENBERG, *Error analysis of Galerkin least squares methods for the elasticity equations*, SIAM Journal on Numerical Analysis, 28 (1991), pp. 1680–1697.
- [80] A. I. GARRALDA-GUILLÉM, G. N. GATICA, A. MÁRQUEZ, AND M. RUIZ-GALÁN, *A posteriori error analysis of twofold saddle point variational formulations for nonlinear boundary value problems*, IMA Journal of Numerical Analysis, 34 (2014), pp. 326–361.
- [81] G. N. GATICA, *A Simple Introduction to the Mixed Finite Element Method: Theory and Applications*, SpringerBriefs in Mathematics. Springer, Cham, 2014.
- [82] —, *A note on stable Helmholtz decompositions in 3D*, Preprint 2016–03, Centro de Investigación en Ingeniería Matemática (CI<sup>2</sup>MA), Universidad de Concepción, Chile, (2016).
- [83] G. N. GATICA, L. F. GATICA, AND F. SEQUEIRA, *A priori and a posteriori error analyses of a pseudostress-based mixed formulation for linear elasticity*, Computers and Mathematics with Applications, 71 (2016), pp. 585–614.
- [84] G. N. GATICA, N. HEUER, AND S. MEDDAHI, *On the numerical analysis of nonlinear twofold saddle point problems*, IMA Journal of Numerical Analysis, 23 (2003), pp. 301–330.
- [85] G. N. GATICA, G. C. HSIAO, AND S. MEDDAHI, *A residual-based a posteriori error estimator for a two-dimensional fluid-solid interaction problem*, Numerische Mathematik, 114 (2009), pp. 63–106.

- [86] ———, *A coupled mixed finite element method for the interaction problem between an electromagnetic field and an elastic body*, SIAM Journal on Numerical Analysis, 48 (2010), pp. 1338–1368.
- [87] G. N. GATICA, A. MÁRQUEZ, AND S. MEDDAHI, *Analysis of the coupling of primal and dual-mixed finite element methods for a two-dimensional fluid-solid interaction problem*, SIAM Journal on Numerical Analysis, 45 (2007), pp. 2072–2097.
- [88] G. N. GATICA, A. MÁRQUEZ, R. OYARZÚA, AND R. REBOLLEDO, *Analysis of an augmented fully-mixed approach for the coupling of quasi-Newtonian fluids and porous media*, Computer Methods in Applied Mechanics and Engineering, 270 (2014), pp. 76–112.
- [89] G. N. GATICA, A. MÁRQUEZ, AND W. RUDOLPH, *A priori and a posteriori error analyses of augmented twofold saddle point formulations for nonlinear elasticity problems*, Computer Methods in Applied Mechanics and Engineering, 264 (2013), pp. 23–48.
- [90] G. N. GATICA, A. MÁRQUEZ, AND M. A. SÁNCHEZ, *Analysis of a velocity-pressure-pseudostress formulation for the stationary Stokes equations*, Computer Methods in Applied Mechanics and Engineering, 199 (2010), pp. 1064–1079.
- [91] ———, *A priori and a posteriori error analyses of a velocity-pseudostress formulation for a class of quasi-Newtonian Stokes flows*, Computer Methods in Applied Mechanics and Engineering, 200 (2011), pp. 1619–1636.
- [92] G. N. GATICA, S. MEDDAHI, AND R. OYARZÚA, *A conforming mixed finite element method for the coupling of fluid flow with porous media flow*, IMA Journal of Numerical Analysis, 29 (2009), pp. 86–108.
- [93] G. N. GATICA, R. OYARZÚA, AND F.-J. SAYAS, *Analysis of fully-mixed finite element methods for the Stokes–Darcy coupled problem*, Mathematics of Computation, 80 (2011), pp. 1911–1948.
- [94] ———, *Convergence of a family of Galerkin discretizations for the Stokes–Darcy coupled problem*, Numerical Methods for Partial Differential Equations, 27 (2011), pp. 721–748.
- [95] ———, *A residual-based a posteriori error estimator for a fully-mixed formulation of the Stokes–Darcy coupled problem*, Computer Methods in Applied Mechanics and Engineering, 200 (2011), pp. 1877–1891.
- [96] ———, *A twofold saddle point approach for the coupling of fluid flow with nonlinear porous media flow*, IMA Journal of Numerical Analysis, 32 (2012), pp. 845–887.
- [97] G. N. GATICA, R. RUIZ-BAIER, AND G. TIERRA, *A posteriori error analysis of an augmented mixed method for the Navier–Stokes equations with nonlinear viscosity*, Computers and Mathematics with Applications, 72 (2016), pp. 2289–2310.
- [98] G. N. GATICA AND W. L. WENDLAND, *Coupling of mixed finite elements and boundary elements for linear and nonlinear elliptic problems*, Applicable Analysis, 63 (1996), pp. 39–75.
- [99] J. GENG,  *$W^{1,p}$  estimates for elliptic problems with Neumann boundary conditions in Lipschitz domains*, Advances in Mathematics, 229 (2012), pp. 2427–2448.

- [100] V. GIRAULT AND P.-A. RAVIART, *Finite Element Methods for Navier–Stokes Equations. Theory and Algorithms*, Springer Series in Computational Mathematics, 5. Springer–Verlag, Berlin, 1986.
- [101] V. GIRAULT AND B. RIVIÈRE, *DG approximation of coupled Navier–Stokes and Darcy equations by Beaver–Joseph–Saffman interface condition*, SIAM Journal on Numerical Analysis, 47 (2009), pp. 2052–2089.
- [102] V. GIRAULT AND M. F. WHEELER, *Numerical discretization of a Darcy–Forchheimer model*, Numerische Mathematik, 110 (2008), pp. 161–198.
- [103] R. GLOWINSKI AND A. MARROCO, *Sur l’approximation, par éléments finis d’ordre un, et la résolution, par pénalisation-dualité, d’une classe de problèmes de Dirichlet non linéaires*, Revue Française d’Automatique, Informatique et Recherche Opérationnelle Série Rouge. Analyse Numérique, 9 (1975), pp. 41–76.
- [104] P. GRISVARD, *Théorèmes de traces relatifs à un polyèdre*, C. R. Acad. Sci. Paris Sér. A, 278 (1974), pp. 1581–1583.
- [105] —, *Elliptic Problems in Nonsmooth Domains*, Monographs and Studies in Mathematics, 24. Pitman (Advanced Publishing Program), Boston, MA, 1985.
- [106] —, *Problèmes aux limites dans les polygones. Mode d’emploi. (French) [Boundary value problems in plane polygons. Instructions for use]*, Électricité de France. Bulletin de la Direction des Études et Recherches. Série C. Mathématiques. Informatique, 3 (1986), pp. 21–59.
- [107] J. K. GUEST AND J. H. PRÉVOST, *Topology optimization of creeping fluid flows using a Darcy–Stokes finite element*, International Journal for Numerical Methods in Engineering, 66 (2006), pp. 461–484.
- [108] M. L. HADJI, A. ASSALA, AND F. Z. NOURI, *A posteriori error analysis for Navier–Stokes equations coupled with Darcy problem*, Calcolo, 52 (2015), pp. 559–576.
- [109] P. HANSBO AND M. JUNTUNEN, *Weakly imposed Dirichlet boundary conditions for the Brinkman model of porous media flow*, Applied Numerical Mathematics, 59 (2009), pp. 1274–1289.
- [110] N. S. HANSPAL, A. N. WAGHODE, V. NASSEHI, AND R. J. WAKEMAN, *Numerical analysis of coupled Stokes/Darcy flows in industrial filtrations*, Transport in Porous Media, 64 (2006), pp. 73–101.
- [111] F. HECHT, *New development in FreeFem++*, Journal of Numerical Mathematics, 20 (2012), pp. 251–265.
- [112] R. HIPTMAIR, *Finite elements in computational electromagnetism*, Acta Numerica, 11 (2002), pp. 237–339.
- [113] B. HJERTAGER, *Multi-Fluid CFD Analysis of Chemical Reactors*, Multiphase reacting flows: modelling and simulation, 125–179, CISM Courses and Lectures, 492, SpringerWienNewYork, Vienna, 2007.

- [114] C. O. HORGAN, *Korn's inequalities and their applications in continuum mechanics*, SIAM Review, 37 (1995), pp. 491–511.
- [115] J. S. HOWELL, *Dual-mixed finite element approximation of Stokes and nonlinear Stokes problems using trace-free velocity gradients*, Journal of Computational and Applied Mathematics, 231 (2009), pp. 780–792.
- [116] J. S. HOWELL AND N. J. WALKINGTON, *Dual-mixed finite element methods for the Navier–Stokes equations*, ESAIM: Mathematical Modelling and Numerical Analysis, 47 (2013), pp. 789–805.
- [117] W. JÄGER AND A. MIKELIĆ, *On the interface boundary condition of Beavers, Joseph, and Saffman*, SIAM Journal on Applied Mathematics, 60 (2000), pp. 1111–1127.
- [118] Y. L. JOO, J. SUN, M. D. SMITH, R. C. ARMSTRONG, R. A. BROWN, AND R. A. ROSS, *Two-dimensional numerical analysis of non-isothermal melt spinning with and without phase transition*, Journal of Non-Newtonian Fluid Mechanics, 102 (2002), pp. 37–70.
- [119] P. N. KALONI AND J. GUO, *Steady nonlinear double-diffusive convection in a porous medium based upon the Brinkman–Forchheimer model*, Journal of Mathematical Analysis and Applications, 204 (1996), pp. 138–155.
- [120] F. KHANI, M. T. DARVISHI, AND R. GORLA, *Analytical investigation for cooling turbine disks with a non-Newtonian viscoelastic fluid*, Computers and Mathematics with Applications, 61 (2011), pp. 1728–1738.
- [121] L. I. G. KOVASZNAY, *Laminar flow behind a two-dimensional grid*, Mathematical Proceedings of the Cambridge Philosophical Society, 44 (1948), pp. 58–62.
- [122] A. KUFNER, O. JHON, AND S. FUČÍK, *Function Spaces. Monographs and Textbooks on Mechanics of Solids and Fluids; Mechanics: Analysis*, Noordhoff International Publishing, Leyden; Academia, Prague, 1977.
- [123] K. KUNISCH AND X. MARDUEL, *Optimal control of non-isothermal viscoelastic fluid flow*, Journal of Non-Newtonian Fluid Mechanics, 88 (2000), pp. 261–301.
- [124] W. L. LAYTON, F. SCHIEWECK, AND I. YOTOV, *Coupling fluid flow with porous media flow*, SIAM Journal on Numerical Analysis, 40 (2003), pp. 2195–2218.
- [125] H. MANOUZI AND M. FARHLOUL, *Mixed finite element analysis of a non-linear three-fields Stokes model*, IMA Journal of Numerical Analysis, 21 (2001), pp. 143–164.
- [126] A. MÁRQUEZ, S. MEDDAHI, AND F. J. SAYAS, *Strong coupling of finite element methods for the Stokes–Darcy problem*, IMA Journal of Numerical Analysis, 35 (2015), pp. 969–988.
- [127] I. MARTINI, G. ROZZA, AND B. HAASDONK, *Reduced basis approximation and a-posteriori error estimation for the coupled Stokes–Darcy system*, Advances in Computational Mathematics, 41 (2015), pp. 1131–1157.



- [128] W. MCLEAN, *Strongly Elliptic Systems and Boundary Integral Equations*, Cambridge University Press, Cambridge, 2000.
- [129] M. MORAITI, *On the quasistatic approximation in the Stokes–Darcy model of groundwater-surface water flows*, Journal of Mathematical Analysis and Applications, 394 (2012), pp. 796–808.
- [130] Y. MU, G. ZHAO, X. WU, L. HANG, AND H. CHU, *Continuous modeling and simulation of flow-swell-crystallization behaviors of viscoelastic polymer melts in the hollow profile extrusion process*, Applied Mathematical Modelling, 39 (2015), pp. 1352–1368.
- [131] K. NAJIB, D. SANDRI, AND A.-M. ZINE, *On a posteriori estimates for a linearized Oldroyd’s problem*, Journal of Computational and Applied Mathematics, 167 (2004), pp. 345–361.
- [132] V. NASSEHI, *Modelling of combined Navier–Stokes and Darcy flows in crossflow membrane filtration*, Chemical Engineering Science, 53 (1998), pp. 1253–1265.
- [133] S. NICAISE, B. AHOUNOU, AND W. HOUEDANOU, *Residual-based a posteriori error estimates for a nonconforming finite element discretization of the Stokes–Darcy coupled problem: isotropic discretization*, Afrika Matematika, 27 (2016), pp. 701–729.
- [134] R. OYARZÚA, T. QIN, AND D. SCHÖTZAU, *An exactly divergence-free finite element method for a generalized Boussinesq problem*, IMA Journal of Numerical Analysis, 34 (2014), pp. 1104–1135.
- [135] H. PAN AND H. RUI, *Mixed element method for two-dimensional Darcy–Forchheimer model*, Journal of Scientific Computing, 52 (2012), pp. 563–587.
- [136] G. W. M. PETERS AND F. P. T. BAAIJENS, *Modelling of non-isothermal viscoelastic flows*, Journal of Non-Newtonian Fluid Mechanics, 68 (1997), pp. 205–224.
- [137] M. PICASSO AND J. RAPPAZ, *Existence, a priori and a posteriori error estimates for a nonlinear three-field problem arising from Oldroyd-B viscoelastic flows*, M2AN Mathematical Modelling and Numerical Analysis, 35 (2001), pp. 879–897.
- [138] C. POZRIKIDIS AND D. A. FARROW, *A model of fluid flow in solid tumors*, Annals of Biomedical Engineering, 31 (2003), pp. 181–194.
- [139] A. QUARTERONI AND A. VALLI, *Numerical Approximation of Partial Differential Equations*, Springer Series in Computational Mathematics, 23. Springer–Verlag, Berlin, 1994.
- [140] P.-A. RAVIART AND J. M. THOMAS, *A mixed finite element method for 2nd order elliptic problems*, Mathematical aspects of finite element methods (Proc. Conf., Consiglio Naz. delle Ricerche (C.N.R.), Rome, 1975). Lecture Notes in Math., 606 (1977), pp. 292–315.
- [141] J. E. ROBERTS AND J.-M. THOMAS, *Mixed and Hybrid Methods*, Handbook of Numerical Analysis, Vol. II, 523–639, Handb. Numer. Anal., II, North-Holland, Amsterdam, 1991.
- [142] D. RUTH AND H. MA, *On the derivation of the Forchheimer equation by means of the averaging theorem*, Transport in Porous Media, 7 (1992), pp. 255–264.

- [143] P. SAFFMAN, *On the boundary condition at the interface of a porous medium*, Studies in Applied Mathematics, 50 (1971), pp. 77–84.
- [144] B. SCHEURER, *Existence et approximation de points selles pour certains problèmes non linéaires*, RAIRO Modélisation Mathématique et Analyse Numérique, 11 (1977), pp. 369–400.
- [145] R. E. SHOWALTER, *Monotone Operators in Banach Space and Nonlinear Partial Differential Equations*, Mathematical Surveys and Monographs, 49. American Mathematical Society, Providence, RI, 1997.
- [146] M. SUGIHARA-SEKI AND B. M. FU, *Blood flow and permeability in microvessels*, Fluid Dynamics Research, 37 (2005), pp. 82–132.
- [147] T. TANG, Z. LI, J. M. McDONOUGH, AND P. D. HISLOP, *Numerical investigation of the “poor man’s Navier–Stokes equations” with Darcy and Forchheimer terms*, International Journal of Bifurcation and Chaos in Applied Sciences and Engineering, 26 (2016), pp. 1650086, 19.
- [148] R. TEMAM, *Navier–Stokes Equations. Theory and Numerical Analysis*, Studies in Mathematics and its Applications, Vol. 2. North-Holland Publishing Co., Amsterdam-New York-Oxford, 1977.
- [149] R. VERFÜRTH, *A Review of A-Posteriori Error Estimation and Adaptive Mesh-Refinement Techniques*, Wiley Teubner, Chichester, 1996.
- [150] ———, *A Posteriori Error Estimation Techniques for Finite Element Methods*, Numerical Mathematics and Scientific Computation. Oxford University Press, Oxford, 2013.
- [151] W. WANG AND C. XU, *A posteriori error estimation of spectral and spectral element methods for the Stokes/Darcy coupled problem*, Journal of Mathematical Study, 47 (2014), pp. 85–110.
- [152] L. ZUO AND Y. HOU, *Numerical analysis for the mixed Navier–Stokes and Darcy problem with the Beavers–Joseph interface condition*, Numerical Methods for Partial Differential Equations, 31 (2015), pp. 1009–1030.